



ISTANBUL
UNIVERSITY
PRESS

Indexed in
Web of Science



Istanbul Journal of Pharmacy

Original Articles

Evaluation of drug-drug interactions and their clinical importance in a pediatric hematopoietic stem cell transplantation unit
Nesligül Özdemir, Ayçe Çeliker, Bülent Barış Kuşkonmaz, Duygu Uçkan Çetinkaya

Alpha lipolic acid bioequivalence study redesigned: a candidate for highly variable drugs
Burcu Bulut, Nagehan Sarraçoğlu, Onur Pinarbaşı

Development and validation an HPLC - UV method for determination of esomeprazole and pifenidone simultaneously in rat plasma: application to a drug monitoring study
Emrah Dural, Sema Tülay Köz, Süleyman Köz

Preparation and *in vitro* studies of fixed-dose tablet combination of repaglinide and metformin
Sinem Şahin, Burcu Mesut, M. Ezgi Durgun, Esher Özçelik, Yıldız Özsoy

The formulation and characterization of water-soluble snakehead fish (*Ophiocephalus striatus*) dry extract in nanoemulsion using permeation and *in vivo* study
Robert Tungadi, Widysusanti Abdulkadir, Munafri Tahir

Pseudo ternary phase diagrams: a practical approach for the area and centroid calculation of stable microemulsion regions
Murat Sami Berkman, Kadri Güleç

Rational design and synthesis of quinazoline derivatives
Fatimah AlKharaz, Zead Abudayah, Qais Abualassal, Loay Hassouneh

Molecular and crystal structure of 1-methyl-5-trifluoromethoxy-1*H*-indole-2,3-dione 3-[4-(4-methoxyphenyl)thiosemicarbazone]
Özge Soylu Eter, Zeliha Atioğlu, Mehmet Akkurt, Cem Cüneyt Ersanlı, Nilgün Karalı

Synthesis, characterization and antibacterial evaluation of new pyridyl-thiazole hybrids of sulfonamides
Zafer Şahin, Sevd Nur Biltekin, Leyla Yurttaş, Şeref Demirayak

The effects of vanadyl sulfate on glutathione, lipid peroxidation and nonenzymatic glycosylation levels in various tissues in experimental diabetes
Sevim Tunali, Refiye Yanardağ

Short-term adaptive metabolic response of *Escherichia coli* to ciprofloxacin exposure
Engin Koçak, Ceren Özkul

***In vitro* urease and trypsin inhibitory activities of some sulfur compounds**
Eda Dağsuyu, Refiye Yanardağ

Quality of turmeric powder in herbal stores: pharmacognostical investigations on turmeric powders obtained from herbal stores in Istanbul, Turkey
Ebru Kuruldak, Fatmanur Yılmaz, Gizem Gülsoy Toplan, Berna Özbek Çelik, Afife Mat

Isolation of potential liver x receptor alpha agonist and antioxidant compounds from *Hypericum microcalycinum* Boiss. & Heldr.
Seçil Sarıkaya Aydın, Vahap Murat Kutluay, Toshiaki Makino, Makoto Inoue, Ümmühan Şebnem Harput, İclal Saraçoğlu

***In vitro* evaluation of antimicrobial activity of *Distemonanthus benthamianus* chewing stick mouthwash**
Mbang Nyong Femi-Oyewo, Olutayo Ademola Adeleye, Caroline Olufunke Babalola, Olufemi Babatunde Banjo, Modupe Nofisat Adebawale, Florence Olubola Odeleye

Phytochemical screening, phenolic content and antioxidant activity of *Lavandula* species extracts from Algeria
Farah Haddouchi, Tarik Mohammed Chaouche, Meriem Saker, Imane Ghellai, Ouhiba Boudjemai

Antimicrobial activities of some narrow endemic gypsophyte
Esmâ Ocak, Şule İnci, Derviş Öztürk, Sanem Akdeniz Şafak, Ebru Özdeniz, Sevdâ Kirbağ, Ahmet Harun Evren, Latif Kurt

***Chelidonium majus* L. (Papaveraceae) morphology, anatomy and traditional medicinal uses in Turkey**
Golshan Zare, Nezha Yağmur Diker, Zekiye Ceren Arıtuluk, İffet İrem Tatlı Çankaya

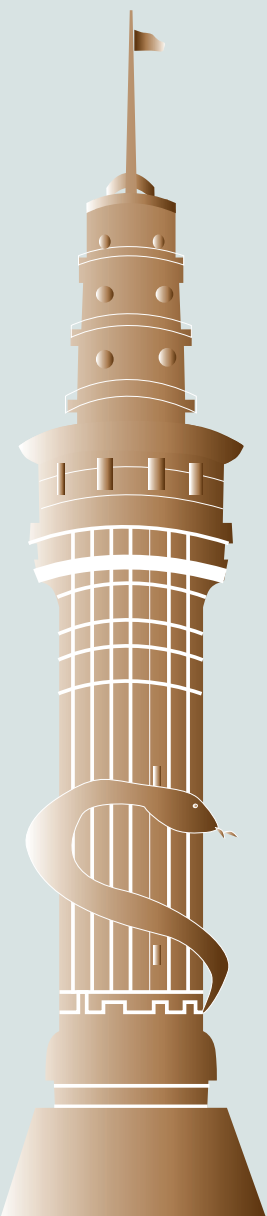
The anatomical properties of endemic *Hypericum kotschyannum* Boiss.
Onur Altınbaşak, Gülay Ecevit Genç, Şükran Kültür

Review Articles

Fungal homoserine transacetylase: a potential antifungal target
Esra Seyran

Bioavailability of berberine: challenges and solutions
Asha Thomas, Seema Kamble, Sanjeevani Deshkar, Lata Kothapalli, Sohan Chittlange

Evaluation of toxic effects of statins and their possible role in treatment of cancer
Aysun Ökçesiz, Ülkü Ündeşer Bucurğat





Istanbul Journal of Pharmacy

INDEXING AND ABSTRACTING

Web of Science - Emerging Sources Citation Index (ESCI)

TÜBİTAK-ULAKBİM TR Index



Istanbul Journal of Pharmacy

OWNER

Prof. Dr. Erdal CEVHER

Istanbul University, Faculty of Pharmacy, Department of Pharmaceutical Technology, İstanbul, Turkey

RESPONSIBLE MANAGER

Asst. Prof. Bahar GÜRDAL ABAMOR

Istanbul University, Faculty of Pharmacy, Department of Pharmaceutical Botany, İstanbul, Turkey

CORRESPONDENCE ADDRESS

Istanbul University, Faculty of Pharmacy,
Department of Pharmaceutical Botany,
Beyazit, 34116, Fatih / İstanbul, Turkey

Phone: +90 212 440 02 75

Fax: +90 212 440 02 52

E-mail: akaline@istanbul.edu.tr

<https://dergipark.org.tr/tr/pub/iujp>

<https://iupress.istanbul.edu.tr/tr/journal/ijp/home>

PUBLISHER

Istanbul University Press

Istanbul University Central Campus,
34452 Beyazit, Fatih / İstanbul, Turkey

Phone: +90 212 440 00 00

Authors bear responsibility for the content of their published articles.

The publication languages of the journal is English.

This is a scholarly, international, peer-reviewed and open-access journal published triannually in April, August and December.

Publication Type: Periodical



Istanbul Journal of Pharmacy

EDITORIAL MANAGEMENT

Editor-in-Chief

Prof. Dr. Emine AKALIN

Istanbul University, Faculty of Pharmacy, Department of Pharmaceutical Botany, İstanbul, Turkey – akaline@istanbul.edu.tr

Co-Editors in Chief

Prof. Dr. B. Sönmez UYDEŞ DOĞAN

Istanbul University, Faculty of Pharmacy, Department of Pharmacology, İstanbul, Turkey – sonmezdo@istanbul.edu.tr

Prof. Dr. Nilgün KARALI

Istanbul University, Faculty of Pharmacy, Department of Pharmaceutical Chemistry, İstanbul, Turkey – karalin@istanbul.edu.tr

Section Editors

Prof. Dr. Nuriye AKEV

Istanbul University, Faculty of Pharmacy, Department of Biochemistry, İstanbul, Turkey – nakevi@istanbul.edu.tr

Prof. Dr. Nilgün KARALI

Istanbul University, Faculty of Pharmacy, Department of Pharmaceutical Chemistry, İstanbul, Turkey – karalin@istanbul.edu.tr

Prof. Dr. B. Sönmez UYDEŞ DOĞAN

Istanbul University, Faculty of Pharmacy, Department of Pharmacology, İstanbul, Turkey – sonmezdo@istanbul.edu.tr

Prof. Dr. Sevgi GÜNGÖR

Istanbul University, Faculty of Pharmacy, Department of Pharmaceutical Technology, İstanbul, Turkey – sgungori@istanbul.edu.tr

Asst. Prof. Bahar GÜRDAL ABAMOR

Istanbul University, Faculty of Pharmacy, Department of Pharmaceutical Botany, İstanbul, Turkey – bahar.gurdal@istanbul.edu.tr

Language Editors

Elizabeth Mary EARL

Istanbul University, Department of Foreign Languages, İstanbul, Turkey – elizabeth.earl@istanbul.edu.tr

Alan James NEWSON

Istanbul University, Department of Foreign Languages, İstanbul, Turkey – alan.newson@istanbul.edu.tr

Statistics Editor

Prof. Dr. Abdülbari BENER

Istanbul University-Cerrahpasa, Cerrahpasa Faculty of Medicine, Department of Biostatistics and Medical Informatics, İstanbul, Turkey – abdulbari.bener@iuc.edu.tr

Scientific Secretariat

Asst. Prof. Gülsev ÖZEN

Istanbul University Faculty of Pharmacy, Department of Pharmacology, İstanbul, Turkey – gulsevozen@istanbul.edu.tr



Istanbul Journal of Pharmacy

EDITORIAL BOARD

Afife MAT

Istanbul University, Faculty of Pharmacy, Department of Pharmacognosy, İstanbul, Turkey – afifemat@gmail.com

Berna ÖZBEK-ÇELİK

Istanbul University, Faculty of Pharmacy, Department of Pharmaceutical Microbiology, İstanbul, Turkey – berna.ozbek@istanbul.edu.tr

Bilge ŞENER

Gazi University, Faculty of Pharmacy, Department of Pharmacognosy, Ankara, Turkey – bilgesener11@gmail.com

Carsten EHRHARDT

Trinity College Dublin, School of Pharmacy and Pharmaceutical Sciences and Trinity Biomedical Sciences Institute, Dublin, Ireland – ehrhards@tcd.ie

Claudio T. SUPURAN

University of Florence, Section of Pharmaceutical and Nutriceutical Sciences, Neurofarba Department, Florence, Italy – claudio.supuran@unifi.it

Domenico Vittorio DELFINO

University of Perugia, Department of Medicine and Surgery, Perugia, Italy – domenico.delfino@unipg.it

Erden BANOĞLU

Gazi University, Faculty of Pharmacy, Department of Pharmaceutical Chemistry, Ankara, Turkey – banoglu@gazi.edu.tr

Fatma AKAR

Gazi University, Faculty of Pharmacy, Department of Pharmacology, Ankara, Turkey – fakar@gazi.edu.tr

Giannantonio DOMINA

University of Palermo, Food and Forest Sciences, Department of Agricultural, Palermo, Italy – giannantonio.domina@unipa.it

İlkay KÜÇÜKGÜZEL

Marmara University, Faculty of Pharmacy, Department of Pharmaceutical Chemistry, İstanbul, Turkey – ikucukguzel@marmara.edu.tr

Johan Van de VOORDE

Ghent University, Department of Pharmacology, Gent, Belgium – johan.vandevoorde@ugent.be

Melih ALTAN

Bezmialem University, Faculty of Pharmacy, Department of Pharmacology, İstanbul, Turkey – vmaltan@bezmialem.edu.tr

Meral ÖZALP

Hacettepe University, Faculty of Pharmacy, Department of Pharmaceutical Microbiology, Ankara, Turkey – mozalp@hacettepe.edu.tr

Müberra KOŞAR

Eastern Mediterranean University, Faculty of Pharmacy, Department of Pharmacognosy, Famagusta, Northern Cyprus – muberra.kosar@emu.edu.tr

Nilüfer YÜKSEL

Ankara University, Faculty of Pharmacy, Department of Pharmaceutical Technology, Ankara, Turkey – nyuksel@pharmacy.ankara.edu.tr

Nurşen BAŞARAN

Hacettepe University, Faculty of Pharmacy, Department of Pharmaceutical Toxicology, Ankara, Turkey – nbasaran@hacettepe.edu.tr

Oya ALPAR

Altınbaş University, Faculty of Pharmacy, Department of Pharmaceutical Technology, İstanbul, Turkey and Department of Pharmaceutical Technology, UCL, UK – oya.alpar@altinbas.edu.tr

Özlem Nazan ERDOĞAN

Istanbul University, Faculty of Pharmacy, Department of Pharmacy Management, İstanbul, Turkey – nazan.erdogan@istanbul.edu.tr

Sıdıka TOKER

Istanbul University, Faculty of Pharmacy, Department of Analytical Chemistry, İstanbul, Turkey – serturk@istanbul.edu.tr

Sibel ÖZDEN

Istanbul University, Faculty of Pharmacy, Department of Pharmaceutical Toxicology, İstanbul, Turkey – stopuz@istanbul.edu.tr

Stephen R. DOWNIE

University of Illinois, Department of Plant Biology, Urbana, Illinois, USA – sdownie@illinois.edu

Tao CHEN

Medical College of Soochow University, School of Public Health, Department of Toxicology, Suzhou, China – tchen@suda.edu.cn

Ufuk KOLAK

Istanbul University, Faculty of Pharmacy, Department of Analytical Chemistry, İstanbul, Turkey – kolak@istanbul.edu.tr

Zeliha YAZICI

Biruni University, Faculty of Medicine, Department of Medical Pharmacology, İstanbul, Turkey – zyazici@biruni.edu.tr



Istanbul Journal of Pharmacy

AIMS AND SCOPE

Istanbul Journal of Pharmacy (Istanbul J Pharm) is an international, scientific, open access periodical published in accordance with independent, unbiased, and double-blinded peer-review principles. The journal is the official publication of İstanbul University Faculty of Pharmacy and it is published triannually on April, August, and December. The publication language of the journal is English.

Istanbul Journal of Pharmacy (Istanbul J Pharm) aims to contribute to the literature by publishing manuscripts at the highest scientific level on all fields of pharmaceutical sciences. The journal publishes original articles, short reports, letters to the editor and reviews.

The target audience of the journal includes specialists and professionals working and interested in all disciplines of pharmaceutical, also medicinal, biological and chemical sciences.

The editorial and publication processes of the journal are shaped in accordance with the guidelines of the International Committee of Medical Journal Editors (ICMJE), World Association of Medical Editors (WAME), Council of Science Editors (CSE), Committee on Publication Ethics (COPE), European Association of Science Editors (EASE), and National Information Standards Organization (NISO). The journal is in conformity with the Principles of Transparency and Best Practice in Scholarly Publishing (doaj.org/bestpractice).

Istanbul Journal of Pharmacy is currently indexed in Web of Science-Emerging Sources Citation Index, TUBITAK ULAKBIM TR Index and CAS database.

Processing and publication are free of charge with the journal. No fees are requested from the authors at any point throughout the evaluation and publication process. All manuscripts must be submitted via the online submission system, which is available at <http://dergipark.gov.tr/iujp>. The journal guidelines, technical information, and the required forms are available on the journal's web page.

All expenses of the journal are covered by the İstanbul University Faculty of Pharmacy. Potential advertisers should contact the Editorial Office. Advertisement images are published only upon the Editor-in-Chief's approval.

Statements or opinions expressed in the manuscripts published in the journal reflect the views of the author(s) and not the opinions of the İstanbul University Faculty of Pharmacy, editors, editorial board, and/or publisher; the editors, editorial board, and publisher disclaim any responsibility or liability for such materials.

Istanbul Journal of Pharmacy is an open access publication and the journal's publication model is based on Budapest Open Access Initiative (BOAI) declaration. Journal's archive is available online, free of charge at <http://ijp.istanbul.edu.tr>. İstanbul Journal of Pharmacy's content is licensed under a Creative Commons Attribution-NonCommercial 4.0 International License.



Editor in Chief: (Prof. Dr.) Emine AKALIN

Address: İstanbul University, Faculty of Pharmacy, Department of Pharmaceutical Botany, Beyazıt, 34116, Fatih İstanbul

Phone: +90 212 440 02 75

Fax: +90 212 440 02 52

E-mail: akaline@istanbul.edu.tr

Publisher: İstanbul University Press

Address: İstanbul University Central Campus, 34452 Beyazıt, Fatih / İstanbul - Turkey

Phone: +90 212 440 00 00



INSTRUCTIONS TO AUTHORS

Context

Istanbul Journal of Pharmacy (Istanbul J Pharm) is an international, scientific, open access periodical published in accordance with independent, unbiased, and double-blinded peer-review principles. The journal is the official publication of İstanbul University Faculty of Pharmacy and it is published triannually on April, August, and December. The publication language of the journal is English.

Istanbul Journal of Pharmacy (Istanbul J Pharm) aims to contribute to the literature by publishing manuscripts at the highest scientific level on all fields of pharmaceutical sciences. The journal publishes original articles, short reports, letters to the editor and reviews.

Editorial Policy

The editorial and publication processes of the journal are shaped in accordance with the guidelines of the International Council of Medical Journal Editors (ICMJE), the World Association of Medical Editors (WAME), the Council of Science Editors (CSE), the Committee on Publication Ethics (COPE), the European Association of Science Editors (EASE), and National Information Standards Organization (NISO). The journal conforms to the Principles of Transparency and Best Practice in Scholarly Publishing (doaj.org/bestpractice).

Originality, high scientific quality, and citation potential are the most important criteria for a manuscript to be accepted for publication. Manuscripts submitted for evaluation should not have been previously presented or already published in an electronic or printed medium. The journal should be informed of manuscripts that have been submitted to another journal for evaluation and rejected for publication. The submission of previous reviewer reports will expedite the evaluation process. Manuscripts that have been presented in a meeting should be submitted with detailed information on the organization, including the name, date, and location of the organization.

Peer-Review Policy

Manuscripts submitted to İstanbul Journal of Pharmacy will go through a double-blind peer-review process. Each submission will be reviewed by at least two external, independent peer reviewers who are experts in their fields in order to ensure an unbiased evaluation process. The

editorial board will invite an external and independent editor to manage the evaluation processes of manuscripts submitted by editors or by the editorial board members of the journal. The Editor in Chief is the final authority in the decision-making process for all submissions.

Ethical Principles

An approval of research protocols by the Ethics Committee in accordance with international agreements (World Medical Association Declaration of Helsinki "Ethical Principles for Medical Research Involving Human Subjects," amended in October 2013, www.wma.net) is required for experimental, clinical, and drug studies. If required, ethics committee reports or an equivalent official document will be requested from the authors. For manuscripts concerning experimental research on humans, a statement should be included that shows that written informed consent of patients and volunteers was obtained following a detailed explanation of the procedures that they may undergo. For studies carried out on animals, the measures taken to prevent pain and suffering of the animals should be stated clearly. Information on patient consent, the name of the ethics committee, and the ethics committee approval number should also be stated in the Materials and Methods section of the manuscript. It is the authors' responsibility to carefully protect the patients' anonymity. For photographs that may reveal the identity of the patients, signed releases of the patient or of their legal representative should be enclosed.

Plagiarism

All submissions are screened by a similarity detection software (iThenticate by CrossCheck) at any point during the peer-review or production process. Even if you are the author of the phrases or sentences, the text should not have unacceptable similarity with the previously published data.

When you are discussing others' (or your own) previous work, please make sure that you cite the material correctly in every instance.

In the event of alleged or suspected research misconduct, e.g., plagiarism, citation manipulation, and data falsification/fabrication, the Editorial Board will follow and act in accordance with COPE guidelines



Authorship

Each individual listed as an author should fulfill the authorship criteria recommended by the International Committee of Medical Journal Editors (ICMJE - www.icmje.org). The ICMJE recommends that authorship be based on the following 4 criteria:

1. Substantial contributions to the conception or design of the work; or the acquisition, analysis, or interpretation of data for the work; AND
2. Drafting the work or revising it critically for important intellectual content; AND
3. Final approval of the version to be published; AND
4. Agreement to be accountable for all aspects of the work in ensuring that questions related to the accuracy or integrity of any part of the work are appropriately investigated and resolved.

In addition to being accountable for the parts of the work he/she has done, an author should be able to identify which co-authors are responsible for specific other parts of the work. In addition, authors should have confidence in the integrity of the contributions of their co-authors.

All those designated as authors should meet all four criteria for authorship, and all who meet the four criteria should be identified as authors. Those who do not meet all four criteria should be acknowledged in the title page of the manuscript.

Istanbul Journal of Pharmacy requires corresponding authors to submit a signed and scanned version of the authorship contribution form (available for download through <http://ijp.istanbul.edu.tr/en/>) during the initial submission process in order to act appropriately on authorship rights and to prevent ghost or honorary authorship. If the editorial board suspects a case of "gift authorship," the submission will be rejected without further review. As part of the submission of the manuscript, the corresponding author should also send a short statement declaring that he/she accepts to undertake all the responsibility for authorship during the submission and review stages of the manuscript.

Conflict of Interest

Istanbul Journal of Pharmacy requires and encourages

the authors and the individuals involved in the evaluation process of submitted manuscripts to disclose any existing or potential conflicts of interests, including financial, consultant, and institutional, that might lead to potential bias or a conflict of interest. Any financial grants or other support received for a submitted study from individuals or institutions should be disclosed to the Editorial Board. To disclose a potential conflict of interest, the ICMJE Potential Conflict of Interest Disclosure Form should be filled in and submitted by all contributing authors. Cases of a potential conflict of interest of the editors, authors, or reviewers are resolved by the journal's Editorial Board within the scope of COPE and ICMJE guidelines.

The Editorial Board of the journal handles all appeal and complaint cases within the scope of COPE guidelines. In such cases, authors should get in direct contact with the editorial office regarding their appeals and complaints. When needed, an ombudsperson may be assigned to resolve cases that cannot be resolved internally. The Editor in Chief is the final authority in the decision-making process for all appeals and complaints.

Copyright and Licensing

Istanbul Journal of Pharmacy requires each submission to be accompanied by a Copyright Agreement Form (available for download at <http://ijp.istanbul.edu.tr/en/>). When using previously published content, including figures, tables, or any other material in both print and electronic formats, authors must obtain permission from the copyright holder. Legal, financial and criminal liabilities in this regard belong to the author(s). By signing the Copyright Agreement Form, authors agree that the article, if accepted for publication by the Istanbul Journal of Pharmacy, will be licensed under a Creative Commons Attribution-NonCommercial 4.0 International License (CC-BY-NC).

Disclaimer

Statements or opinions expressed in the manuscripts published in Istanbul Journal of Pharmacy reflect the views of the author(s) and not the opinions of the editors, the editorial board, or the publisher; the editors, the editorial board, and the publisher disclaim any responsibility or liability for such materials. The final responsibility in regard to the published content rests with the authors.



MANUSCRIPT PREPARATION

The manuscripts should be prepared in accordance with ICMJE-Recommendations for the Conduct, Reporting, Editing, and Publication of Scholarly Work in Medical Journals (updated in December 2015 - <http://www.icmje.org/icmje-recommendations.pdf>). Authors are required to prepare manuscripts in accordance with the CONSORT guidelines for randomized research studies, STROBE guidelines for observational original research studies, STARD guidelines for studies on diagnostic accuracy, PRISMA guidelines for systematic reviews and meta-analysis, ARRIVE guidelines for experimental animal studies, and TREND guidelines for non-randomized public behavior.

Manuscripts can only be submitted through the journal's online manuscript submission and evaluation system, available at <http://ijp.istanbul.edu.tr/en/>. Manuscripts submitted via any other medium will not be evaluated.

Manuscripts submitted to the journal will first go through a technical evaluation process where the editorial office staff will ensure that the manuscript has been prepared and submitted in accordance with the journal's guidelines. Submissions that do not conform to the journal's guidelines will be returned to the submitting author with technical correction requests.

Authors are required to submit the following:

- Copyright Agreement Form
- Author Form
- Title Page

during the initial submission.

The manuscript should be prepared in MS Word format by using Times New Roman font (12 pt) and double-spaced on one side of the paper with adequate margins (2.5 cm).

Preparation of the Manuscript

Title page: A separate title page should be submitted with all submissions and this page should include:

- The full title of the manuscript as well as a short title (running head) of no more than 50 characters,

- Name(s), affiliations, and highest academic degree(s) and ORCID ID(s) of the author(s),
- Grant information and detailed information on the other sources of support,
- Name, address, telephone (including the mobile phone number) and fax numbers, and email address of the corresponding author,
- Acknowledgment of the individuals who contributed to the preparation of the manuscript but who do not fulfill the authorship criteria.

Abstract: An structured abstract should be submitted with Original Articles (Background and Aims, Methods, Results, Conclusion). Please check Table 1 below for word count specifications.

Keywords: Each submission must be accompanied by a minimum of three to a maximum of six keywords for subject indexing at the end of the abstract. The keywords should be listed in full without abbreviations. The keywords should be selected from the National Library of Medicine, Medical Subject Headings database (<https://www.nlm.nih.gov/mesh/MBrowser.html>).

Manuscript Types

Original Articles: This is the most important type of article since it provides new information based on original research. The main text of original articles should be structured with Introduction, Materials and Methods, Results, Discussion, and Conclusion subheadings. Results and Discussion sections can be combined under "Result and Discussion" heading. Please check Table 1 for the limitations for Original Articles.

Statistical analysis to support conclusions is usually necessary. Statistical analyses must be conducted in accordance with international statistical reporting standards (Altman DG, Gore SM, Gardner MJ, Pocock SJ. Statistical guidelines for contributors to medical journals. *Br Med J* 1983; 7; 1489-93). Information on statistical analyses with specified statistical software and descriptive details of the chemical used should be provided with a separate subheading under the Materials and Methods section.

Units should be prepared in accordance with the International System of Units (SI).



Editorial Comments: Editorial comments aim to provide a brief critical commentary by reviewers with expertise or with high reputation in the topic of the research article published in the journal. Authors are selected and invited by the journal to provide such comments. Abstract, Keywords, and Tables, Figures, Images, and other media are not included.

Review Articles: Reviews prepared by authors who have extensive knowledge on a particular field and whose scientific background has been translated into a high volume of publications with a high citation potential are welcomed. These authors may even be invited by the journal. Reviews should describe, discuss, and evaluate the current level of knowledge of a topic in clinical practice and should guide future studies. Please check Table 1 for the limitations for Review Articles.

Short Papers: Please check Table 1 for the limitations for Short Papers.

Letters to the Editor: This type of manuscript discusses important parts, overlooked aspects, or lacking parts of a previously published article. Articles on subjects within the scope of the journal that might attract the readers' attention, particularly educative cases, may also be submitted in the form of a "Letter to the Editor." Readers can also present their comments on the published manuscripts in the form of a "Letter to the Editor." Abstract, Keywords, and Tables, Figures, Images, and other media should not be included. The text should be unstructured. The manuscript that is being commented on must be properly cited within this manuscript.

Tables

Tables should be included in the main document, pre-

ented after the reference list, and they should be numbered consecutively in the order they are referred to within the main text. A descriptive title must be placed above the tables. Abbreviations used in the tables should be defined below the tables by footnotes (even if they are defined within the main text). Tables should be created using the "insert table" command of the word processing software and they should be arranged clearly to provide easy reading. Data presented in the tables should not be a repetition of the data presented within the main text but should be supporting the main text.

Figures and Figure Legends

Figures, graphics, and photographs should be submitted as separate files (in TIFF or JPEG format) through the submission system. The files should not be embedded in a Word document or the main document. When there are figure subunits, the subunits should not be merged to form a single image. Each subunit should be submitted separately through the submission system. Images should not be labeled (a, b, c, etc.) to indicate figure subunits. Thick and thin arrows, arrowheads, stars, asterisks, and similar marks can be used on the images to support figure legends. Like the rest of the submission, the figures too should be blind. Any information within the images that may indicate an individual or institution should be blinded. The minimum resolution of each submitted figure should be 300 DPI. To prevent delays in the evaluation process, all submitted figures should be clear in resolution and large in size (minimum dimensions: 100 × 100 mm). Figure legends should be listed at the end of the main document.

All acronyms, abbreviations, and symbols used in the manuscript must follow international rules and should be defined at first use, both in the abstract and in the

Table 1. Limitations for each manuscript type

Type of manuscript	Word limit	Abstract word limit	Table limit	Figure limit
Original Article	3500	250 (Structured)	6	7 or total of 15 images
Review Article	5000	250 (Unstructured)	6	10 or total of 20 images
Short Paper	1000	200	No tables	10 or total of 20 images
Letter to the Editor	500	No abstract	No tables	No media



main text. The abbreviation should be provided in parentheses following the definition.

For plant materials, herbarium name (or acronym), number, name and surname of the person who identified the plant materials should be indicated in the Materials and Methods section of the manuscript.

When a drug, product, hardware, or software program is mentioned within the main text, product information, including the name of the product, the producer of the product, and city and the country of the company (including the state if in USA), should be provided in parentheses in the following format: "Discovery St PET/CT scanner (General Electric, Milwaukee, WI, USA)"

All references, tables, and figures should be referred to within the main text, and they should be numbered consecutively in the order they are referred to within the main text. Limitations, drawbacks, and the shortcomings of original articles should be mentioned in the Discussion section before the conclusion paragraph.

REFERENCES

Reference Style and Format

Istanbul Journal of Pharmacy complies with APA (American Psychological Association) style 6th Edition for referencing and quoting. For more information:

- American Psychological Association. (2010). Publication manual of the American Psychological Association (6th ed.). Washington, DC: APA.
- <http://www.apastyle.org>

Accuracy of citation is the author's responsibility. All references should be cited in text. Reference list must be in alphabetical order. Type references in the style shown below

Citations in the Text

Citations must be indicated with the author surname and publication year within the parenthesis.

If more than one citation is made within the same parenthesis, separate them with (;).

Samples:

More than one citation;

(Esin et al., 2002; Karasar, 1995)

Citation with one author;

(Akyolcu, 2007)

Citation with two authors;

(Sayiner & Demirci, 2007)

Citation with three, four, five authors;

First citation in the text: (Ailen, Ciambune, & Welch, 2000) Subsequent citations in the text: (Ailen et al., 2000)

Citations with more than six authors;

(Çavdar et al., 2003)

Citations in the Reference

All the citations done in the text should be listed in the References section in alphabetical order of author surname without numbering. Below given examples should be considered in citing the references.

Basic Reference Types

Book

a) Turkish Book

Karasar, N. (1995). *Araştırmalarda rapor hazırlama* (8th ed.) [Preparing research reports]. Ankara, Turkey: 3A Eğitim Danışmanlık Ltd.

b) Book Translated into Turkish

Mucchielli, A. (1991). *Zihniyetler* [Mindsets] (A. Kotil, Trans.). İstanbul, Turkey: İletişim Yayınları.

c) Edited Book

Ören, T., Üney, T., & Çölkesen, R. (Eds.). (2006). *Türkiye bilişim ansiklopedisi* [Turkish Encyclopedia of Informatics]. İstanbul, Turkey: Papatya Yayıncılık.

d) Turkish Book with Multiple Authors

Tonta, Y., Bitirim, Y., & Sever, H. (2002). *Türkçe arama motorlarında performans değerlendirme* [Performance evaluation in Turkish search engines]. Ankara, Turkey: Total Bilişim.

e) Book in English

Kamien R., & Kamien A. (2014). *Music: An appreciation*. New York, NY: McGraw-Hill Education.

f) Chapter in an Edited Book

Bassett, C. (2006). Cultural studies and new media. In G. Hall & C. Birchall (Eds.), *New cultural studies: Adventures in theory* (pp. 220-237). Edinburgh, UK: Edinburgh University Press.



g) Chapter in an Edited Book in Turkish

Erkmen, T. (2012). Örgüt kültürü: Fonksiyonları, öğeleri, işletme yönetimi ve liderlikteki önemi [Organization culture: Its functions, elements and importance in leadership and business management]. In M. Zencirkıran (Ed.), *Örgüt sosyolojisi* [Organization sociology] (pp. 233–263). Bursa, Turkey: Dora Basım Yayın.

h) Book with the same organization as author and publisher

American Psychological Association. (2009). *Publication manual of the American psychological association* (6th ed.). Washington, DC: Author.

Article

a) Turkish Article

Mutlu, B., & Savaşer, S. (2007). Çocuğu ameliyat sonrası yoğun bakımda olan ebeveynlerde stres nedenleri ve azaltma girişimleri [Source and intervention reduction of stress for parents whose children are in intensive care unit after surgery]. *Istanbul University Florence Nightingale Journal of Nursing*, 15(60), 179–182.

b) English Article

de Cillia, R., Reisigl, M., & Wodak, R. (1999). The discursive construction of national identity. *Discourse and Society*, 10(2), 149–173. <http://dx.doi.org/10.1177/0957926599010002002>

c) Journal Article with DOI and More Than Seven Authors

Lal, H., Cunningham, A. L., Godeaux, O., Chlibek, R., Diez-Domingo, J., Hwang, S.-J. ... Heineman, T. C. (2015). Efficacy of an adjuvanted herpes zoster subunit vaccine in older adults. *New England Journal of Medicine*, 372, 2087–2096. <http://dx.doi.org/10.1056/NEJMoa1501184>

d) Journal Article from Web, without DOI

Sidani, S. (2003). Enhancing the evaluation of nursing care effectiveness. *Canadian Journal of Nursing Research*, 35(3), 26–38. Retrieved from <http://cjr.mcgill.ca>

e) Journal Article with DOI

Turner, S. J. (2010). Website statistics 2.0: Using Google Analytics to measure library website effectiveness. *Technical Services Quarterly*, 27, 261–278. <http://dx.doi.org/10.1080/07317131003765910>

f) Advance Online Publication

Smith, J. A. (2010). Citing advance online publication: A review. *Journal of Psychology*. Advance online publication. <http://dx.doi.org/10.1037/a45d7867>

g) Article in a Magazine

Henry, W. A., III. (1990, April 9). Making the grade in today's schools. *Time*, 135, 28–31.

Doctoral Dissertation, Master's Thesis, Presentation, Proceeding

a) Dissertation/Thesis from a Commercial Database

Van Brunt, D. (1997). *Networked consumer health information systems* (Doctoral dissertation). Available from ProQuest Dissertations and Theses database. (UMI No. 9943436)

b) Dissertation/Thesis from an Institutional Database

Yaylı-Yıldız, B. (2014). *University campuses as places of potential publicness: Exploring the political, social and cultural practices in Ege University* (Doctoral dissertation). Retrieved from Retrieved from: <http://library.iyte.edu.tr/tr/hizli-erisim/iyte-tez-portali>

c) Dissertation/Thesis from Web

Tonta, Y. A. (1992). *An analysis of search failures in online library catalogs* (Doctoral dissertation, University of California, Berkeley). Retrieved from <http://yunus.hacettepe.edu.tr/~tonta/yayinlar/phd/ickapak.html>

d) Dissertation/Thesis abstracted in Dissertations Abstracts International

Appelbaum, L. G. (2005). Three studies of human information processing: Texture amplification, motion representation, and figure-ground segregation. *Dissertation Abstracts International: Section B. Sciences and Engineering*, 65(10), 5428.

e) Symposium Contribution

Krinsky-McHale, S. J., Zigman, W. B., & Silverman, W. (2012, August). Are neuropsychiatric symptoms markers of prodromal Alzheimer's disease in adults with Down syndrome? In W. B. Zigman (Chair), *Predictors of mild cognitive impairment, dementia, and mortality in adults with Down syndrome*. Symposium conducted at the meeting of the American Psychological Association, Orlando, FL.

f) Conference Paper Abstract Retrieved Online

Liu, S. (2005, May). *Defending against business crises with the help of intelligent agent based early warning solutions*. Paper presented at the Seventh



International Conference on Enterprise Information Systems, Miami, FL. Abstract retrieved from http://www.iceis.org/iceis2005/abstracts_2005.htm

g) Conference Paper - In Regularly Published Proceedings and Retrieved Online

Herculano-Houzel, S., Collins, C. E., Wong, P., Kaas, J. H., & Lent, R. (2008). The basic nonuniformity of the cerebral cortex. *Proceedings of the National Academy of Sciences*, 105, 12593–12598. <http://dx.doi.org/10.1073/pnas.0805417105>

h) Proceeding in Book Form

Parsons, O. A., Pryzwansky, W. B., Weinstein, D. J., & Wiens, A. N. (1995). Taxonomy for psychology. In J. N. Reich, H. Sands, & A. N. Wiens (Eds.), *Education and training beyond the doctoral degree: Proceedings of the American Psychological Association National Conference on Postdoctoral Education and Training in Psychology* (pp. 45–50). Washington, DC: American Psychological Association.

i) Paper Presentation

Nguyen, C. A. (2012, August). *Humor and deception in advertising: When laughter may not be the best medicine*. Paper presented at the meeting of the American Psychological Association, Orlando, FL.

Other Sources

a) Newspaper Article

Browne, R. (2010, March 21). This brainless patient is no dummy. *Sydney Morning Herald*, 45.

b) Newspaper Article with no Author

New drug appears to sharply cut risk of death from heart failure. (1993, July 15). *The Washington Post*, p. A12.

c) Web Page/Blog Post

Bordwell, D. (2013, June 18). David Koepf: Making the world movie-sized [Web log post]. Retrieved from <http://www.davidbordwell.net/blog/page/27/>

d) Online Encyclopedia/Dictionary

Ignition. (1989). In *Oxford English online dictionary* (2nd ed.). Retrieved from <http://dictionary.oed.com>

Marcoux, A. (2008). Business ethics. In E. N. Zalta (Ed.). *The Stanford encyclopedia of philosophy*. Retrieved from <http://plato.stanford.edu/entries/ethics-business/>

e) Podcast

Dunning, B. (Producer). (2011, January 12). *inFact: Conspiracy theories* [Video podcast]. Retrieved from <http://itunes.apple.com/>

f) Single Episode in a Television Series

Egan, D. (Writer), & Alexander, J. (Director). (2005). Failure to communicate. [Television series episode]. In D. Shore (Executive producer), *House*; New York, NY: Fox Broadcasting.

g) Music

Fuchs, G. (2004). Light the menorah. On *Eight nights of Hanukkah* [CD]. Brick, NJ: Kid Kosher.

REVISIONS

When submitting a revised version of a paper, the author must submit a detailed “Response to the reviewers” that states point by point how each issue raised by the reviewers has been covered and where it can be found (each reviewer’s comment, followed by the author’s reply and line numbers where the changes have been made) as well as an annotated copy of the main document. Revised manuscripts must be submitted within 30 days from the date of the decision letter. If the revised version of the manuscript is not submitted within the allocated time, the revision option may be cancelled. If the submitting author(s) believe that additional time is required, they should request this extension before the initial 30-day period is over.

Accepted manuscripts are copy-edited for grammar, punctuation, and format. Once the publication process of a manuscript is completed, it is published online on the journal’s webpage as an ahead-of-print publication before it is included in its scheduled issue. A PDF proof of the accepted manuscript is sent to the corresponding author and their publication approval is requested within 2 days of their receipt of the proof.

Editor in Chief: Emine AKALIN

Address: İstanbul University Faculty of Pharmacy, İstanbul, Turkey

Phone: +90 212 440 02 75

Fax: +90 212 440 02 52

E-mail: jfacpharm@istanbul.edu.tr

Publisher: İstanbul University Press

Address: İstanbul University Central Campus, 34452 Beyazıt, Fatih / İstanbul - Turkey

Phone: +90 212 440 00 00



CONTENTS

ORIGINAL ARTICLES

- Evaluation of drug-drug interactions and their clinical importance in a pediatric hematopoietic stem cell transplantation unit 1
Nesligül Özdemir, Ayçe Çeliker, Bülent Barış Kuşkonmaz, Duygu Uçkan Çetinkaya
- Alpha lipoic acid bioequivalence study redesigned: a candidate for highly variable drugs 8
Burcu Bulut, Nagehan Sarraçoğlu, Onur Pınarbaşı
- Development and validation an HPLC - UV method for determination of esomeprazole and pirfenidone simultaneously in rat plasma: application to a drug monitoring study 16
Emrah Dural, Sema Tülay Köz, Süleyman Köz
- Preparation and *in vitro* studies of fixed-dose tablet combination of repaglinide and metformin 26
Sinem Şahin, Burcu Mesut, M. Ezgi Durgun, Esher Özçelik, Yıldız Özsoy
- The formulation and characterization of water-soluble snakehead fish (*Ophiocephalus striatus*) dry extract in nanoemulsion using permeation and *in vivo* study 35
Robert Tungadi, Widysusanti Abdulkadir, Munafri Tahir
- Pseudo ternary phase diagrams: a practical approach for the area and centroid calculation of stable microemulsion regions 42
Murat Sami Berkman, Kadri Güleç
- Rational design and synthesis of quinazoline derivatives 50
Fatimah AlKharaz, Zead Abudayeh, Qais Abualassal, Loay Hassouneh
- Molecular and crystal structure of 1-methyl-5-trifluoromethoxy-1*H*-indole-2,3-dione 3-[4-(4-methoxyphenyl)thiosemicarbazone] 59
Özge Soylu Eter, Zeliha Atioğlu, Mehmet Akkurt, Cem Cüneyt Ersanlı, Nilgün Karalı
- Synthesis, characterization and antibacterial evaluation of new pyridyl-thiazole hybrids of sulfonamides 67
Zafer Şahin, Sevede Nur Biltekin, Leyla Yurttaş, Şeref Demirayak
- The effects of vanadyl sulfate on glutathione, lipid peroxidation and nonenzymatic glycosylation levels in various tissues in experimental diabetes 73
Sevim Tunalı, Refiye Yanardağ
- Short-term adaptive metabolic response of *Escherichia coli* to ciprofloxacin exposure 79
Engin Koçak, Ceren Özkul
- In vitro* urease and trypsin inhibitory activities of some sulfur compounds 85
Eda Dağsuyu, Refiye Yanardağ
- Quality of turmeric powder in herbal stores: pharmacognostical investigations on turmeric powders obtained from herbal stores in Istanbul, Turkey 92
Ebru Kuruldak, Fatmanur Yılmaz, Gizem Gülsoy Toplan, Berna Özbek Çelik, Afife Mat



CONTENTS



ORIGINAL ARTICLES

- Isolation of potential liver x receptor alpha agonist and antioxidant compounds from *Hypericum microcalycinum* Boiss. & Heldr.**98
Seçil Sarıkaya Aydın, Vahap Murat Kutluay, Toshiaki Makino, Makoto Inoue, Ümmühan Şebnem Harput, İclal Saraçoğlu
- In vitro* evaluation of antimicrobial activity of *Distemonanthus benthamianus* chewing stick extract mouthwash**..... 105
Mbang Nyong Femi-Oyewo, Olutayo Ademola Adeleye, Caroline Olufunke Babalola, Olufemi Babatunde Banjo, Modupe Nofisat Adebowale, Florence Olubola Odeleye
- Phytochemical screening, phenolic content and antioxidant activity of *Lavandula* species extracts from Algeria**.....111
Farah Haddouchi, Tarik Mohammed Chaouche, Meriem Saker, Imane Ghellai, Ouhiba Boudjemai
- Antimicrobial activities of some narrow endemic gypsopyhte**.....118
Esmâ Ocak, Şule İnci, Derviş Öztürk, Sanem Akdeniz Şafak, Ebru Özdeniz, Sevda Kırbağ, Ahmet Harun Evren, Latif Kurt
- Chelidonium majus* L. (Papaveraceae) morphology, anatomy and traditional medicinal uses in Turkey**.....123
Golshan Zare, Neziha Yağmur Diker, Zekiye Ceren Arıtuluk, İffet İrem Tatlı Çankaya
- The anatomical properties of endemic *Hypericum kotschyanum* Boiss.**133
Onur Altınbaşak, Gülay Ecevit Genç, Şükran Kültür

REVIEW ARTICLES

- Fungal homoserine transacetylase: A potential antifungal target**137
Esra Seyran
- Bioavailability of berberine: challenges and solutions**141
Asha Thomas, Seema Kamble, Sanjeevani Deshkar, Lata Kothapalli, Sohan Chitlange
- Evaluation of toxic effects of statins and their possible role in treatment of cancer**154
Aysun Ökçesiz, Ülkü Ündeğer Bucurgat

Evaluation of drug-drug interactions and their clinical importance in a pediatric hematopoietic stem cell transplantation unit

Nesligül Özdemir¹ , Ayçe Çeliker¹ , Bülent Barış Kuşkonmaz² , Duygu Uçkan Çetinkaya² 

¹Hacettepe University, Faculty of Pharmacy, Department of Clinical Pharmacy, Ankara, Turkey

²Hacettepe University, Faculty of Medicine, Department of Pediatric Hematology, Ankara, Turkey

ORCID IDs of the authors: N.Ö. 0000-0003-2551-9549; A.Ç. 0000-0001-6753-6844; B.B.K. 0000-0002-1207-4205; D.U.Ç. 0000-0003-3593-6493

Cite this article as: Ozdemir, N., Celiker, A., Kuskonmaz, B. B., & Uckan, Cetinkaya, D. (2021). Evaluation of drug-drug interactions and their clinical importance in a pediatric hematopoietic stem cell transplantation unit. *Istanbul Journal of Pharmacy*, 51 (1), 1-7.

ABSTRACT

Background and Aims: Many drugs with narrow therapeutic range and high toxicity risk are used in hematopoietic stem cell transplantation (HSCT) Units. The increase in the number of drugs raises the likelihood of interactions. This is particularly important in pediatric patients and may adversely affect the treatment process. In this study, we aimed to determine the potential drug interactions and to evaluate the clinical significance of them in terms of physician's and pharmacist's perceptions.

Methods: The study was conducted as a prospective descriptive study over a six-month period in a tertiary care hospital's Pediatric HSCT Unit. A pharmacist evaluated inpatients' drugs for drug interactions by using a drug interaction checker program and the clinical significance of the interactions were evaluated by the physician and the pharmacist separately.

Results: Drugs used in 20 patients (median age= 8 years, range= 0.6-17 years) were evaluated. A total of 525 potential drug-drug interactions were identified. Two hundred and forty seven interactions (47.05%) were major; 238 (45.33%) were moderate; 23 (4.38%) were contraindicated. The number of the interactions considered "clinically significant" by the pharmacist and "clinically insignificant" by the physician at the preparative regimen and post-transplant period were 15 (35.7%) and 37 (29.4%), respectively.

Conclusion: The management of drug interactions is important in pediatric HSCT patients as a vulnerable group. Drug interactions should be interpreted according to the patient's clinical presentation, not only theoretically. Cooperation between physicians and pharmacists in the management of interactions will contribute to optimize the patient's treatment.

Keywords: Drug interactions, pediatric patients, hematopoietic stem cell transplantation

INTRODUCTION

Drug interactions, one of the drug-related problems, are an important issue for both adult and pediatric patients. In particular, the intensive care unit, hematology, oncology, and hematopoietic stem cell transplantation (HSCT) are fields where multiple drugs are used and complex treatment strategies are required (Marcath, Coe, Hoylman, Redman, & Hertz, 2018; Metzke et al., 2012; Aljadani & Aseari, 2018; Rodrigues et al., 2017; Sanchez, Bacle, Lamy, & Le-Corre, 2019). Many drugs with a narrow therapeutic index are used before and after transplantation. Thus drug interactions appear to be an important factor that may affect the success of the treatment (Trevisan, Silva, Oliveira, Secoli, & Lima, 2015). Especially in patients who undergo allogeneic HSCT, which constitute a high-risk group, may develop clinically important drug interactions due to the large number of drugs used to prevent marrow rejection and immunological complications (Prot-Labarthe, Therrien, Demanche, Larocque, & Bussieres, 2008).

Address for Correspondence:

Nesligül ÖZDEMİR, e-mail: nesliozdmr@hotmail.com

This work is licensed under a Creative Commons Attribution 4.0 International License.



Submitted: 30.04.2020
Revision Requested: 26.08.2020
Last Revision Received: 30.08.2020
Accepted: 29.09.2020

Preparative regimens including high-dose chemotherapy drugs, medications used for prophylaxis of veno-occlusive disease (VOH), immunosuppressive drugs given to prevent the development of graft versus host disease (GVHD) after transplantation, and supportive therapies applied to prevent infections are related to the possible drug interactions and may affect the results of the treatment (Deeg, 2005). Alkylating drugs with narrow therapeutic index, especially busulfan and cyclophosphamide, which are included in the preparative regimens, interact with each other and with many other drugs due to their metabolization pathways (Myers et al., 2017). The blood level of cyclosporine, one of the drugs most frequently used for prophylaxis of GVHD, may vary due to interactions with many drugs such as azole antifungals, clarithromycin, phenobarbital, metronidazole, corticosteroids and etc. (Campana, Regazzi, Buggia, & Molinaro, 1996; Sadaba, Lopez-de-Ocariz, Azanza, Quiroga, & Cienfuegos, 1998). Supportive therapies to prevent complications include a large number of drug groups such as antimicrobials, antihypertensives, analgesics, mucosal protective drugs, anticoagulants, antiemetics and diuretics, and this situation possess a significant risk for drug interactions (Glottzbecker, Duncan, Alyea, Campbell, & Soiffer, 2012).

The aim of this study is to determine the potential drug interactions of pediatric patients in a pediatric HSCT unit by a clinical pharmacist during transplantation periods and to evaluate the clinical significance of the interactions according to the physician's and the pharmacist's perceptions.

MATERIALS AND METHODS

The study was conducted as a prospective descriptive study between October 1st, 2015 and May 1st 2016 in a tertiary care hospital's pediatric HSCT Unit inpatient service. The study was considered ethically appropriate with regards to GO 15 / 596-04 dated 21.10.2015 by Hacettepe University Non-Interventional Clinical Research Ethics Committee.

Patients aged 0-18 years who were admitted to the HSCT unit for transplantation were included in the study. Informed consent was obtained from the patients and their relatives. The demographic data of the patients were collected from the patient files and the medication data were obtained from the hospital's electronic patient medication system by the clinical pharmacist. The potential interactions for each patient during the preparative regimen and post-transplantation periods were recorded daily. The clinical pharmacist participated in the physicians' morning rounds every day and examined and recorded every patient's drug orders before the visits. After the visits, every patient's drugs were checked in terms of potential drug interactions. If a new drug had been started at the weekend and/or out of working hours of the clinical pharmacist, the orders were examined retrospectively and detected interactions were recorded. This process continued until the patient was discharged. For every patient, the number of potential drug interactions was recorded but not calculated daily, it was calculated after the preparative regimen and the post-transplantation period had finished. For example, if there was a potential drug interaction during one or more days at

any point of the transplantation period, it was calculated as "one potential drug interaction" at the end of the transplantation period. A current and scientific online database namely, Micromedex Solutions[®], which is one of the databases having high specificity, was used to detect drug interactions. The interactions in the Micromedex Solutions[®] database were categorized into four categories: "contraindicated, major, moderate, and minor". In this database contraindicated interaction means "The drugs are contraindicated for concurrent use". Major interaction means "The interaction may be life-threatening and/or require medical intervention to minimize or prevent serious adverse effects". Moderate interaction means "The interaction may result in exacerbation of the patient's condition and/or require an alteration in therapy". Minor interaction means "The interaction would have limited clinical effects; manifestations may include an increase in the frequency or severity of the side effects but generally would not require a major alteration in therapy". The clinical pharmacist verbally reported the identified interactions to the physician. In order to prevent an interaction, it was recommended to reduce the dose of the drug, to discontinue the drug or to select a drug that does not interact.

At the end of the study, a list showing the separate drug interactions detected in the preparative regimen and in the post-transplantation period was formed. When interactions that may lead to serious adverse events or adversely affect the treatment of HSCT occurred, they were classified as "clinically significant interactions". Interactions that have a tolerable adverse effect on the patient or that can be managed with drug dose adjustment or have an adverse effect that can be prevented by supportive treatments or is unlikely to occur are accepted as "clinically insignificant interactions". A physician with >20 years' experience and a pharmacist who was a clinical pharmacist in-training each examined the formed list and rated the drug interactions individually as mentioned above.

IBM SPSS[®] version 22 program was used for statistical analysis of the data in the study. Distribution of data was identified by descriptive statistics (number and percentages). The number and the percentages of the interaction types and the clinically significant and clinically insignificant interactions were calculated.

RESULTS

During the study period, a total of 20 patients were followed up from hospital admission to discharge and potential drug interactions were detected. The patients' median age was 8 years (0.6–17 years). The demographic data of the patients are summarized in Table 1.

A total of 525 potential drug interactions were identified in 20 patients during the study. Two hundred and forty seven interactions (47.05%) were major; 238 (45.33%) were moderate; 23 (4.38%) were contraindicated and 17 (3.24%) were classified as minor according to the Micromedex Solutions[®] drug interaction checker program. It was found that 75.42% (n=396) of the potential interactions were caused by drugs

Table 1. Demographic data of the patients.

	n (%)
Gender	
Female	4 (20.0)
Male	16 (80.0)
Total	20 (100.0)
Diagnosis	
ALL	5 (25.0)
Thalassemia major	3 (15.0)
WAS	2 (10.0)
Fanconi anemia	3 (15.0)
Others*	7 (35.0)
Type of transplantation	
Allogeneic	19 (95.0)
Autologous	1 (5.0)
Stem cell source	
Peripheral blood stem cell	4 (20.0)
Bone marrow	16 (80.0)
Type of Preparative regimes	
Myeloablative	16 (80.0)
Reduced intensity/nonmyeloablative	4 (20.0)

ALL; Acute Lymphoblastic Leukemia, WAS; Wiskott Aldrich Syndrome. Others*: osteopetrosis, neuroblastoma, congenital neutropenia, adrenoleuchodystrophy, LRBA (lipopolysaccharide - responsive beige - like anchor) gene defect - immunodeficiency and juvenile myelomonocytic leukemia (JMML); There was one patient with each diagnosis.

used for HSCT treatment protocols (chemotherapeutics, immunosuppressants, antimicrobial prophylaxis). The most observed potential drug interaction (in 75% of the patients) was cyclosporine-fluconazole (major interaction).

Table 2 summarizes the distributions of the potential drug interactions detected in the preparative regimen and post-transplantation periods separately. During the preparative regimen period, 42 different drug pairs showed a total of 144 potential drug interactions. After transplantation, 126 different drug pairs showed a total of 381 potential drug interactions. One hundred and thirty seven of 381 interactions detected after transplantation were due to cyclosporine interactions with 22

different drugs. Nine of them were major; 13 were moderate. The drugs with the highest interaction rate with cyclosporine were fluconazole, methylprednisolone (MPZ), methotrexate (MTX), metronidazole, amikacin, ciprofloxacin and furosemide, respectively.

The data of major interactions detected during the preparative regimen period are summarized in Figure 1. The moderate interactions are given in the Figure 2.

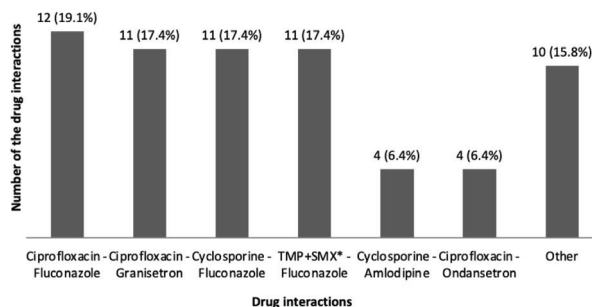


Figure 1. Distribution of major interactions detected at the preparative regimen period (n=63).

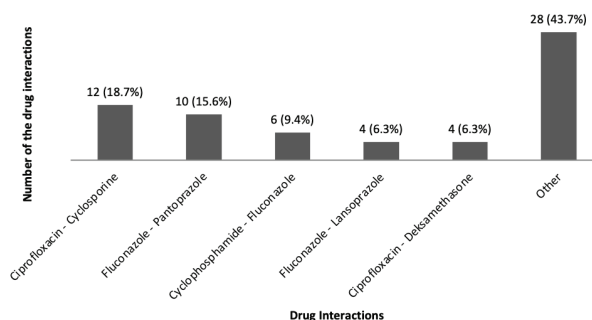


Figure 2. Distribution of moderate interactions detected at the preparative regimen period (n=64).

Seventy five percent of the contraindicated interactions (n= 12) were fluconazole-granisetron; 18.7% (n= 3) were fluconazole-ondansetron and 6.3% (n= 1) were calcium gluconate-ceftriaxone interactions in the preparative regimen period. The only minor interaction detected during the preparative regime was the interaction between amikacin and piperacillin/tazobactam.

Table 2. Distribution of drug interactions detected at preparative regimen and post-transplantation period according to the interaction degree.

	Major interaction	Moderate interaction	Minor interaction	Contraindicated interaction	Total
	n (%)	n (%)	n (%)	n (%)	
Preparative regimen period	63 (43.75)	64 (44.40)	1 (0.70)	16 (11.15)	144
Post-transplantation period	184 (48.30)	174 (45.70)	16 (4.20)	7 (3.90)	381

The data of major interactions and moderate interactions detected at the post-transplantation period are summarized in Figures 3 and 4, respectively.

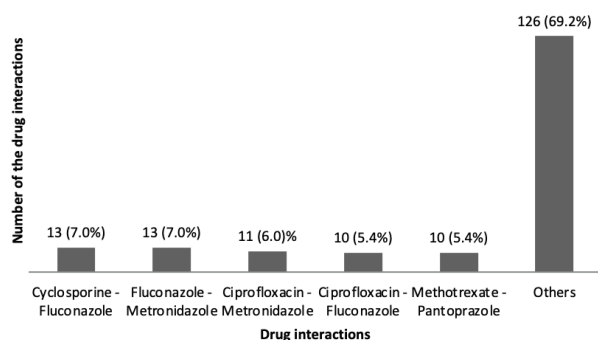


Figure 3. Distribution of the major interactions detected at the post-transplantation period (n=184).

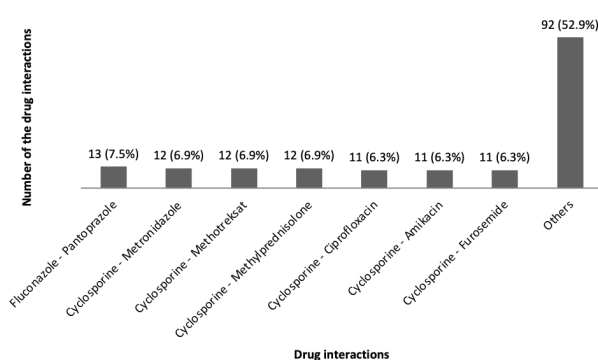


Figure 4. Distribution of the moderate interactions detected at the post-transplantation period (n=174).

The number and percentages of contraindicated drug interactions detected at the post-transplantation period were fluconazole-granisetron; 3 (42.8%), fluconazole-ondansetron; 3 (42.8%) and clarithromycin-fluconazole; 1 (14.4%).

The number and percentages of minor interactions detected at the post-transplantation period were amikacin-piperacillin/tazobactam; 10 (58.89%), folic acid-MTX; 2 (11.6%), furosemide-phenytoin; 1 (5.8%), ferro glycol sulfate-sodium bicarbonate; 1 (5.8%), clarithromycin-lansoprazole; 1 (5.89%) and calcium carbonate-ferro glycol sulfate; 1 (5.8%).

Table 3 summarizes the data of the drug interactions' clinical significance determined by the pharmacist and physician sep-

arately. Forty-two drug interactions in the preparative regimen period and 126 drug interactions in the post-transplantation period were evaluated in terms of clinical significance. In the preparative regimen period, 15 (35.7%) interactions were defined as "clinically significant" by the pharmacist, and as "clinically insignificant" by the physician. Two (4.8%) interactions were considered as "clinically insignificant" by the pharmacist and as "clinically significant" by the physician. While, 7 (16.6%) interactions were considered as "clinically significant", 18 (42.9%) interactions were considered as "clinically insignificant" by both clinical pharmacist and physician.

In the post-transplantation period 37 (29.4%) interactions were defined as "clinically significant" by the pharmacist, and as "clinically insignificant" by the physician. Two (1.6%) interactions were considered as "clinically insignificant" by the pharmacist and as "clinically significant" by the physician. While, 29 (23.0%) interactions were considered as "clinically significant", 58 (46.0%) interactions were considered as "clinically insignificant" by both the clinical pharmacist and the physician.

DISCUSSION

Many drugs are used for different purposes in HSCT. The majority of these drugs have a narrow therapeutic index and are highly toxic. The rise in the number of drugs taken by a patient increases the probability of interaction occurrence (Leather, 2004). Drug interactions are one of the major drug-related problems that have the potential to adversely affect the treatment process in both adult and pediatric patients. There are a limited number of studies evaluating drug interactions in pediatric hematology-oncology and HSCT patients (Tavousi, Sadeghi, Darakhshandeh, & Moghaddas, 2019; Balk et al., 2017). In these studies, only the interactions of the drugs used specifically for stem cell transplantation were evaluated, not all the drugs including the ones used for other indications (Valenzuela et al., 2017; Bernard, Goutelle, Bertrand, & Bleyzac, 2014). Apart from HSCT specific drugs, the use of non-immunosuppressant and non-chemotherapeutic drugs are common in pediatric HSCT patients and these drugs may interact with each other or with the HSCT specific drugs (Eldesouky, Li, Abutaleb, Mohammad, & Seleem, 2018). In Turkey, there have been no studies that evaluate these drug interactions in the pediatric HSCT patient population.

Trevisan et al. evaluated the prevalence of potential drug interactions of the drugs received on the day of transplantation by the HSCT patients (Trivesan et al., 2015). Interactions were ana-

Table 3. Distribution of the clinical importance of drug interactions detected during the pre-transplantation (n=42) and post-transplantation period (n=126) according to pharmacist and physician.

	Preparative regimen period		Post-transplantation period	
	Clinically significant interactions n (%)	Clinically insignificant interactions n (%)	Clinically significant interactions n (%)	Clinically insignificant interactions n (%)
Clinical pharmacist	22 (52.3)	20 (47.7)	66 (52.3)	60 (47.6)
Physician	9 (21.4)	33 (78.6)	31 (24.6)	95 (75.4)

lyzed by an interaction program called DRUG-REAX®. At least one clinically significant interaction was detected in 82.5% of 40 patients and 80.9% of the detected interactions were classified as major interactions.

In a retrospective study, Gholaminezhad et al. (2014) evaluated potential drug interactions before and after transplantation in adolescent and adult HSCT patients (Gholaminezhad et al., 2014). Drug interactions were classified by using the Lexi-Interact® interaction program. Minor interactions and intravenous drug incompatibilities were excluded; only moderate and major interactions were reported. All patients had at least one interaction and a total of 13,600 potential drug interactions were detected in 384 patients. Almost 82% of the interactions were ranked as moderate. The most common interaction was the interaction between trimethoprim/sulfamethoxazole and fluconazole. Granisetron-fluconazole and fluconazole-phenytoin interactions followed them. Sixty one point five percent of interactions were due to HSCT-related drugs (preparation regimen drugs, immunosuppressants and antimicrobials).

In the present study, 525 potential drug interactions were detected in 20 patients. Forty seven percent of the interactions were classified as major interaction and 45.33% were classified as moderate interaction. The number of major and moderate interactions were close to each other. This finding highlighted that the interactions occurring in pediatric HSCT patients may lead to more serious consequences if not prevented or controlled. In our study, the rate of HSCT specific drug interactions was lower (75.42%) than Gholaminezhad et al. (2014)'s study. This finding was associated with the possibility of more drug use in adult patients. The most frequent interaction observed was between cyclosporine and fluconazole, fluconazole being incriminated in both studies. The widespread use of both drugs in HSCT and their high interaction potential may have contributed to this result.

In this study, of the 381 interactions detected after transplantation, 35.9% were cyclosporine interactions with other drugs. Cyclosporine is frequently used in allogeneic transplantations other than autologous transplantations. Cyclosporine blood levels should be kept within the ideal range in order to prevent both stem cell rejection and the development of GVHD (Zeighami et al., 2014). The cyclosporine blood level may increase or decrease due to its interaction with other drugs. Therefore, strict monitoring of the blood level is necessary and adjusting of the dose of cyclosporine is important for the success of HSCT. The fact that cyclosporine was responsible for one third of the interactions detected in the post-transplantation period supports that all drugs used concurrently with cyclosporine should be evaluated carefully in terms of interaction.

The detected interactions were potential interactions and it was difficult to distinguish the clinical outcomes of them in practice. Some specific drug interaction effects, such as increase in liver transaminases (cyclosporine-caspofungin) and creatinine levels (cyclosporine-nephrotoxic drugs), were seen clinically.

The long and complex HSCT process and polypharmacy increase the probability of drug interactions. Prevention of interactions is often possible by selecting the drugs that do not interact, or removing one of the drugs that display interaction. Therefore, the interaction probability needs to be carefully evaluated. In order to guide the treatment process correctly, determining the clinical significance of potential drug interactions will be a valuable support for the physicians. All interactions detected through drug interaction checker programs may not be clinically important (Ament, Bertolino, & Liszewski, 2000). In a study by Chan et al. (2009) in which the interactions between oral anticancer and non-cancer drugs were evaluated in terms of clinical significance, 41 different drug interactions were detected through the Drugdex® database (Chan, Tan, Wong, Yap, & Ko, 2009). Nine pharmacists evaluated all the interactions and 17.1% of the interactions were not considered clinically important by all the pharmacists.

In our study, approximately half of the interactions detected during the preparation regimen and after the transplantation were found to be clinically important by the pharmacist. Unlike the studies in the literature, the proportion of clinically insignificant interactions was found to be higher. Firstly, only one clinical pharmacist's evaluation of the interactions may have led to this discrepancy. Secondly, while only anticancer drugs were evaluated in the study of Chan et al., all drugs' interactions were evaluated in our study. While anticancer drugs have a high potential of clinically significant interactions, drugs used for supportive treatment may have clinically less important interactions.

In this study, the pharmacist and physician's interpretations of clinical interactions were also compared. The rate of the clinically significant interactions, both in the pre- and post-transplantation periods, evaluated by the physician was lower than that of the pharmacist. In our study, concomitant use of cyclosporine with another drug that has a nephrotoxic effect was considered clinically significant interaction by the physicians. If the adverse event due to drug interaction can be controlled by supportive treatments or monitoring of the drug level, then, that interaction is considered as less clinically important by the physician. This indicates that physicians pay regard to the benefit/harm relationship in the treatment of critically important patients such as HSCT patients and take into account the interactions with only very serious results as a general approach.

The number of interactions determined as clinically significant was higher in the post transplantation period than the preparative regimen period for both pharmacist and physician evaluations. The post transplantation period is a critical and complex period because of engraftment expectation and possibility of GVHD. Therefore, it has a burden of polypharmacy. The drugs used after transplantation are the drugs that have a high possibility of adverse effect and drug interactions. Both the pharmacist and physician who consider these post transplantation drugs were more alert to prevent undesired effects of these drugs. As a consequence, the number of clinically significant interactions was found to be higher than that of the preparative regimen period that had a lower drug burden.

Considering factors such as concomitant drug administration, drug administration site and age of the patient, the interaction as assumed “clinically insignificant” by the clinicians if it was unlikely to occur even if it was theoretically a major interaction or contraindicated. For example, calcium gluconate-ceftriaxone is an age specific (for neonates) contraindicated interaction but both pharmacist and physician determined it as “clinically insignificant” in the HSCT service, which had no neonate patients. Besides, the minor drug interactions (e.g., amikacin and piperacillin/tazobactam, clarithromycin and lansoprazole, furosemide and phenytoin) were determined “clinically insignificant” by both the pharmacist and physician. At this point, the importance and the difference of the drug interaction checker programs’ theoretical data and the practice experience of the clinicians gained more value.

This study is the first one to evaluate drug interactions in pediatric HSCT patients in Turkey. Although there are lots of studies about drug interactions in adult patients, these studies cannot adequately guide the clinicians that work in the pediatric services due to pharmacokinetic differences between pediatric and adult subjects. Therefore, this study will be beneficial for clinicians to manage the treatment of pediatric HSCT patients when they encounter drug interactions.

This study’s limitations are, the evaluation of the clinical significance of the interactions was performed by only one pharmacist and one physician, it was a short-term study and it had a limited number of patients for evaluation.

CONCLUSION

Drug interactions in areas where polypharmacy can be encountered frequently may be an obstacle for giving an optimal treatment regimen. Pediatric stem cell transplantation units are among the areas where polypharmacy is common. Although pediatric patients are exposed to less polypharmacy than adults, management of drug interactions is important due to pediatric patients vulnerability. Not only chemotherapeutic and immunosuppressant drugs but also other drugs used for antimicrobial prophylaxis and supportive therapies may have important interactions. Drug interaction databases are frequently used in clinical practice and guide clinicians for the regulation of treatments. However, the clinical significance of drug interactions detected in databases can be interpreted differently by the physicians and clinical pharmacists. Drug interactions should be evaluated according to the patient’s clinical situation, not just as the theoretical information. The cooperation of physicians and clinical pharmacists will contribute to optimizing the treatment of the patient and the management of drug interactions.

Ethics Committee Approval: The study was considered ethically appropriate with regards to GO 15 / 596-04 dated 21.10.2015 by Hacettepe University Non-Interventional Clinical Research Ethics Committee.

Informed Consent: Written consent was obtained from the participants.

Peer-review: Externally peer-reviewed.

Author Contributions: Conception/Design of Study- N.Ö., A.Ç., D.U.Ç.; Data Acquisition- N.Ö., D.U.Ç.; Data Analysis/Interpretation- N.Ö., A.Ç., B.B.K., D.U.Ç.; Drafting Manuscript- N.Ö., A.Ç.; Critical Revision of Manuscript- A.Ç., B.B.K., D.U.Ç.; Final Approval and Accountability- N.Ö., A.Ç., B.B.K., D.U.Ç.; Technical or Material Support- D.U.Ç.; Supervision- A.Ç., B.B.K., D.U.Ç.

Conflict of Interest: The authors have no conflict of interest to declare.

Financial Disclosure: Authors declared no financial support.




Acknowledgement: The authors would like to thank Assoc. (MD) Prof. Fatma Visal Okur, Coordinator of Nurses Nevin Cetin and Head Nurse Fatma Kirac for supporting clinical activities and Pharmacist Anna Maria Kuyumcu for English editing.

REFERENCES

- Aljadani, R., & Aseeri, M. (2018). Prevalence of drug-drug interactions in geriatric patients at an ambulatory care pharmacy in a tertiary care teaching hospital. *BMC Research Notes*, 11(1). <http://dx.doi.org/10.1186/s13104-018-3342-5>
- Ament, P. W., Bertolino, J.G., & Liszewski, J.L. (2000). Clinically significant drug interactions. *American Family Physician*, 61(6), 1745–1754.
- Balk, T. E., Van-der-Sijts, I. H., Van-Gelder, T., Janssen, J. J. B., Van-der Sluis IM, Van-Leeuwen, R. W. F., & Engels, F. K. (2017). Drug-drug interactions in pediatric oncology patients. *Pediatric Blood Cancer*. 64(7). <https://doi.org/10.1002/pbc.26410>
- Bernard, E., Goutelle, S., Bertrand, Y., & Bleyzac, N. (2014). Pharmacokinetic drug-drug interaction of calcium channel blockers with cyclosporine in hematopoietic stem cell transplant children. *Annals of Pharmacotherapy*, 48(12), 1580–1584. <https://doi.org/10.1177/1060028014550644>
- Campana, C., Regazzi, M. B, Buggia, I., & Molinaro, M. (1996). Clinically significant drug interactions with cyclosporin - An update. *Clinical Pharmacokinetics*, 30(2), 141–179.
- Chan, A., Tan, S. H., Wong, C. M., Yap, K. Y., & Ko, Y. (2009). Clinically significant drug-drug interactions between oral anticancer agents and nonanticancer agents: a Delphi survey of oncology pharmacists. *Clinical Therapeutics*, 31(2), 2379–2386. <https://doi.org/10.1016/j.clinthera.2009.11.008>
- Deeg, H. J. (2005). Optimization of transplant regimens for patients with myelodysplastic syndrome (MDS). *Hematology American Society of Hematology Education Program*, 167–173.
- Eldesouky, H. E., Li, X., Abutaleb, N. S., Mohammad, H., & Seleem, M. N. (2018). Synergistic interactions of sulfamethoxazole and azole antifungal drugs against emerging multidrug-resistant *Candida auris*. *International Journal of Antimicrobial Agents*, 52(6), 754–761. <https://doi.org/10.1016/j.ijantimicag.2018.08.016>
- Gholaminezhad, S., Hadjibabaie, M., Gholami, K., Javadi, M. R., Radfar, M., Karimzadeh, I., & Ghavamzadeh, A. (2014). Pattern and associated factors of potential drug-drug interactions in both pre- and early post-hematopoietic stem cell transplantation stages at a referral center in the Middle East. *Annals of Hematology*, 93(11), 1913–1922.
- Glantzbecker, B., Duncan, C., Alyea, E., Campbell, B., & Soiffer, R. (2012). Important drug interactions in hematopoietic stem cell transplantation: what every physician should know. *Biology of Blood and Marrow Transplantation*, 18(7), 989–1006. <https://doi.org/10.1016/j.bbmt.2011.11.029>
- Leather, H. L. (2004). Drug interactions in the hematopoietic stem cell transplant (HSCT) recipient: what every transplant needs to know. *Bone Marrow Transplantation*, 33(2), 137–152.

- Marcat, L. A., Coe, T. D., Hoylman, E. K., Redman, B. G., & Hertz, D. L. (2018). Prevalence of drug-drug interactions in oncology patients enrolled on National Clinical Trials Network oncology clinical trials. *BMC Cancer*, 18(1), 1155-1163. <http://dx.doi.org/10.1186/s12885-018-5076-0>
- Metzke, B., Hug, M. J., Fink, G., Hieke, S., Jung, M., & Engelhardt, M. (2012). Drug-drug interactions in the hematology and oncology department: a real-life assessment of frequency and severity. *Blood*, 120(21), 4250-4250. Retrieved from <https://www.researchgate.net/publication>
- Myers, A. L., Kawedia, J. D., Champlin, R. E., Kramer, M. A., Nieto, Y., Ghose, R., & Andersson, B. S. (2017). Clarifying busulfan metabolism and drug interactions to support new therapeutic drug monitoring strategies: a comprehensive review. *Expert Opinion on Drug Metabolism & Toxicology*, 13(9), 901-923. <https://doi.org/10.1080/17425255.2017.1360277>
- Prot-Labarthe, S., Therrien, R., Demanche, C., Larocque, D., & Bussieres, J. F. (2008). Pharmaceutical care in an inpatient pediatric hematopoietic stem cell transplant service. *Journal of Oncology Pharmacy Practice*, 14(3), 147-152. <https://doi.org/10.1177/1078155208093929>
- Rodrigues, A. T., Stahlschmidt, R., Granja, S., Pilger, D., Falcao, A. L. E., & Mazzola, P. G. (2017). Prevalence of potential drug-drug interactions in the intensive care unit of a Brazilian teaching hospital. *Brazilian Journal of Pharmaceutical Science*, 53(1), e16109- e16117. <https://doi.org/10.1590/s2175-97902017000116109>
- Sadaba, B., Lopez-de-Ocariz, A., Azanza, J. R., Quiroga, J., & Cienfuegos, J. A. (1998). Concurrent clarithromycin and cyclosporin A treatment. *Journal of Antimicrobial Chemotherapy*, 42(3), 393-395.
- Sanchez, L., Bacle, A., Lamy, T., & Le-Corre, P. (2019). Potential drug-drug interactions and nephrotoxicity in hematopoietic stem cell transplant adult recipients during bone marrow transplantation unit stay. *Cancer Chemotherapy and Pharmacology*, 83(5), 827-835. <https://doi.org/10.1007/s00280-019-03791-9>.
- Tavousi, F., Sadeghi, A., Darakhshandeh, A., & Moghaddas, A. (2019). Potential drug-drug interactions at a referral pediatric oncology ward in Iran: A cross-sectional study. *Journal of Pediatric Hematology Oncology*, 41(3), e146-e151. <https://doi.org/10.1097/MPH.0000000000001346>
- Trevisan, D. D., Silva, J. B., Oliveira, H. C., Secoli, S. R., & Lima, M. H. (2015). Prevalence and clinical significance of potential drug-drug interaction in hematopoietic stem cell transplantation. *Cancer Chemotherapy and Pharmacology*, 75(2), 393-400. <https://doi.org/10.1007/s00280-014-2657-8>
- Valenzuela, R., Torres, J. P., Salas, C., Gajardo, I., Palma, J., Catalan, P. ... Morales, J. (2017). Drug interaction of voriconazole-cyclosporine in children undergoing hematopoietic stem cell transplantation (2013-2014). *Revista Chilena de Infectologia*, 34(1), 14-18. <https://doi.org/10.4067/s0716-10182017000100002>
- Zeighami, S., Hadjibabaie, M., Ashouri, A., Sarayani, A., Khoei, S. H., Mousavi, S. ... Ghavamzadeh, A. (2014). Assessment of cyclosporine serum concentrations on the incidence of acute graft versus host disease post hematopoietic stem cell transplantation. *Iranian Journal of Pharmaceutical Research*, 13(1), 305-312.

Alpha lipoic acid bioequivalence study redesigned: a candidate for highly variable drugs

Burcu Bulut¹ , Nagehan Sarraçoğlu¹ , Onur Pınarbaşlı¹ 

¹Ilko Pharmaceuticals, Research and Development Center, Ankara, Turkey

ORCID IDs of the authors: B.B. 0000-0002-9726-8577; N.S. 0000-0002-1222-7339; O.P. 0000-0001-7091-683X

Cite this article as: Bulut, B., Sarracoglu, N., & Pinarbasli, O. (2021). Alpha lipoic acid bioequivalence study redesigned: A candidate for highly variable drugs. *Istanbul Journal of Pharmacy*, 51(1), 8-15.

ABSTRACT

Background and Aims: Alpha lipoic acid 600 mg HR film tablet showed high intra-subject variabilities in bioequivalence studies. In this regard, this study aims to determine whether Alpha lipoic acid 600 mg HR film coated tablet is a highly variable drug.

Methods: First, a randomized, open-label, balanced, two-treatment, two-period, two-sequence, single-dose, two-way crossover oral bioequivalence study comparing the test product (Alpha lipoic acid HR film tablet - ILKO Pharmaceuticals, Turkey) with the reference product (Thioctacid® - Meda Pharma, Germany) was conducted in normal, healthy, adult human subjects under fasting conditions (Study 1). Secondly, a randomized, open-label, balanced, two-treatment, four-period, two-sequence, single-dose, fully replicate crossover oral bioequivalence study was conducted in normal, healthy, adult human subjects under fasting conditions (Study 2).

Results: Study 1 failed. It had a 90% confidence interval for LnC_{max} (ng/mL) value between 79.69% - 138.98% with a high intra-subject coefficient of variability (ISCV=57.5%). In study 2 a 90% confidence interval for LnC_{max} (ng/mL) was found between 88.40% - 129.81% while the ISCV value for LnC_{max} was 64.5%.

Conclusion: The findings suggest that bioequivalence study for Alpha lipoic acid HR film tablet should be redesigned since this is a highly variable drug. Therefore, conventional bioequivalence acceptable limits (80.0%-125.0%) should be adjusted to 69.84% - 143.19% for alpha lipoic acid.

Keywords: Alpha lipoic acid, bioequivalence, highly variable drugs, intra-subject variability, replicate design

INTRODUCTION

Alpha lipoic acid (ALA), also known as thioctic acid, serves as a cofactor of mitochondrial respiratory enzymes, catalyzing oxidative decarboxylation reactions. ALA has been shown to possess antioxidant, cardiovascular, cognitive, anti-aging, detoxifying, anti-inflammatory, anti-cancer, and neuroprotective pharmacological properties. At present, it is mostly used for its antioxidant function (Ghelani, Razmovski-Naumovski, & Nammi, 2017) and, in particular, it is widely used as a dietary supplement by the older adult population (Keith et al., 2012). ALA has two optical isomers, specifically R-ALA and S-ALA, and is commonly used in racemic mixture (R,S-ALA) (Mignini, Streccioni, Tomassoni, Traini, & Amenta, 2007). It is readily absorbed following oral administration and is rapidly converted to dihydrolipoic acid (DHLA), its primary metabolite. ALA and its primary metabolite DHLA can directly regenerate ascorbic acid from dehydroascorbic acid and indirectly regenerate vitamin E. ALA also increases intracellular glutathione and coenzyme Q10 levels (Amenta, Traini, Tomassoni, & Mignini, 2008).

In clinical trials alpha-lipoic acid has mainly been used in the treatment of symptomatic peripheral (sensorimotor) diabetic polyneuropathy. The reference product Thioctacid® (alpha lipoic acid) 600 mg HR (High Release) film coated tablet is manufactured by Meda

Address for Correspondence:

Onur PINARBAŞLI, e-mail: opinarbasli@ilko.com.tr

Submitted: 09.03.2020
Revision Requested: 18.05.2020
Last Revision Received: 10.11.2020
Accepted: 02.12.2020

This work is licensed under a Creative Commons Attribution 4.0 International License.



Pharma, Germany. The pharmacokinetic parameters of the reference product evaluated in healthy volunteers under fasting condition are as follows: median time for peak absorption (T_{max}): 88.1 min; area under the curve from time zero to the time of last measurable concentration (AUC_t): 3270.9 ng x h/g; peak plasma concentration (C_{max}): 1266.2 ng/g (Amenta et al., 2008).

The United States Food and Drug Administration (FDA) defines bioequivalence as 'the absence of a significant difference in the rate and extent to which the active ingredient or active moiety in pharmaceutical equivalents or pharmaceutical alternatives becomes available at the site of drug action when administered at the same molar dose under similar conditions in an appropriately designed study' (US FDA Code of Federal Regulations, 2019). For systemically available drug products, classical single-dose, two-period, two-sequence, and crossover RT/TR designs are used, wherein the reference product is denoted as R and the test product as T. In this design, subjects receive a single test product dose and a reference product dose at randomly assigned times (Kang & Vahl, 2017; Lohar et al., 2012). In some cases, the drugs studied can be highly variable according to their pharmacokinetic properties. As the subject is exposed to two doses of the same formulation at two different times in one study, the variability measured from the same subject is considered as intra-subject variability (Thota et al., 2013).

Highly variable drugs are commonly known to have an intra-subject (within-subject) coefficient of variability (ISCV) equal to or greater than 30% in terms of AUC or C_{max} (Kang & Vahl, 2017; Knahl, Lang, Fleischer, & Kieser, 2018). Intra-subject variability can be estimated from study designs with more than two periods (Knahl et al., 2018). High intra-subject variability makes it difficult to obtain 90% confidence interval (CI 90%) of the ratio between the test and reference products for log-transformed data in the acceptable bioequivalence interval (80.0%-125.0%) (Fagiolino, González, Vázquez, & Eiraldi, 2007; Kang & Vahl, 2017; Li et al., 2017). This may result in non-bioequivalence even with the same product due to the variability within it (Lohar et al., 2012). As a striking example, Siewert and coworkers (1990) could not demonstrate the bioequivalence of the product in a bioequivalence study conducted with 16 volunteers using the same product containing 80 mg immediate-release verapamil (Blume et al., 1994). According to David et al.'s review study of the FDA's Office of Generic Drugs from 2003 to 2005, 31% of the bioequivalence studies conducted with 180 drugs were highly variable (Lohar et al., 2012; Molins, Cobo, & Ocaña, 2017). At that time, the standard 2-way cross-over study designs could not be used for proving bioequivalence. Designs with more subjects and more periods, such as three- and four-period designs were needed to give an estimation of the relevant variability. Full-replicate designs such as TRTR/RTTR or partial-replicate designs such as TRR/RTR/RRT were developed (Knahl et al., 2018). The main requirement for developing replicate crossover designs in highly variable drugs was to enable subjects to receive at least one of the drug products more than once (Kang & Vahl, 2017).

In the literature, some technical limitations are mentioned for oral formulations of alpha lipoic acid because of low solubility,

short blood half-life, elevated systemic elimination, and first-pass hepatic metabolism (Mignini, Nasuti, Gioventu, Napolioni, & Martino, 2012). The absolute bioavailability of alpha lipoic acid is around 30% (Brufani & Figliola, 2014). However, in addition to the lack of product-specific FDA and EMA guidelines including Alpha lipoic acid 600 mg HR tablet, there is no information available in the literature about the highly variable properties of this product. Therefore, researchers or generic drug development companies have to design a bioequivalence study for this product according to the general rules of the FDA and EMA bioequivalence guidance. If there is no special information about the highly variable properties, two-period, two-sequence, crossover RT/TR designs are generally used for classical single-dose products which is not suitable for this product. This study assesses bioequivalence of the test product (ILKO Pharmaceuticals) with the registered reference drug (Thioctacid® 600 mg HR film coated tablet) in order to determine whether alpha lipoic acid in high release tablet dosage form is a highly variable drug product.

MATERIALS AND METHODS

API grade alpha lipoic acid active substance was obtained from Olon SPA Company (Milano-Italy) in racemic form. Low-substituted hydroxypropyl cellulose (Shin-Etsu Chemical Co. – Japan), hydroxypropyl cellulose (Nippon Soda Co. – Japan), magnesium stearate (FACI SPA – Spain), and hypromellose based coating materials (Colorcon, Inc. – England) were used as inactive ingredients in formulations. Analytical grades of potassium dihydrogen phosphate (Merck, Germany), phosphoric acid (ortho-phosphoric acid 85%, Merck, Germany), methanol (J.T. Baker, Poland) and acetonitrile (J.T. Baker, Poland) were used in HPLC analysis. Quantitative stability indicating HPLC test methods were performed on Waters Alliance HPLC System equipped with the 2695 Separations Module (Waters, Milford, MA, USA) with variable wavelength UV-Detector and run with Empower-2 Software. Ultrapure deionized water was obtained from a Millipore water purification system (Millipore Corp., Bedford, MA, USA).

In all studies, the test product (T) alpha lipoic acid 600 mg HR film coated tablet manufactured by ILKO Pharmaceuticals, Turkey (Lot: 1305119001) and the reference product (R) Thioctacid® (racemic alpha lipoic acid) 600 mg HR film coated tablet manufactured by Meda Pharma, Germany (Lot: 3741051) were used (Table 1).

EXPERIMENTAL

Analytical methods

Dissolved alpha lipoic acid content at *in vitro* condition was determined spectrophotometrically by a validated HPLC method at 215 nm using a Waters 2695 separation module (Waters, Milford, MA, USA). Separation was achieved on a C18 ACE 5 μ m column (4.6 mm x 250 mm) using a mobile phase of buffer: methanol : acetonitrile (350:350:300). The buffer was prepared by dissolving 680 mg of potassium dihydrogen phosphate in 1 L of deionized water and adjusted to pH 3.0 with phosphoric acid. The flow rate was 1.2 mL/min, and the signal was monitored at a wavelength of 214 nm. The analytical method

Table 1. Active substance and excipients of test product (T) Alpha lipoic acid 600 mg HR film tablet and reference product (R) Thioctacid® 600 mg HR film coated tablet.

	Test Product (T) Alpha Lipoic Acid 600 mg HR Film Tablet	Reference Product (R) Thioctacid® 600 mg HR Film Coated Tablet
Active substance	- Alpha lipoic acid 600 mg	- Alpha lipoic acid 600 mg
Excipients	Core Tablet	Core Tablet
	- Poly (0-2-hydroxypropyl) cellulose	- Poly (0-2-hydroxypropyl) cellulose
	- Magnesium stearate	- Magnesium stearate
	- Hydroxypropyl cellulose	- Hydroxypropyl cellulose
	- HPMC based film coating agents	- HPMC based film coating agents

of alpha lipoic acid was validated for specificity, selectivity, sensitivity, linearity, recovery, accuracy and precision parameters.

All the plasma samples from all subjects of *in vivo* bioequivalence study were assayed as per protocol criteria for alpha lipoic acid using a validated LC-MS/MS method. Nineteen (19) blood samples were collected from each subject during each period. The venous blood samples (0.5 mL per sample) were withdrawn at pre-dose [(0.00) (within 2.00 hours prior to dosing)] and at 0.083, 0.167, 0.25, 0.33, 0.50, 0.67, 0.83, 1.00, 1.25, 1.50, 1.75, 2.00, 2.50, 3.00, 4.00, 5.00, 6.00 and 8.00 hours post-dose. Samples from those subjects who completed at least two clinical study periods and who received test and reference products at least once were assayed. Plasma samples were assayed for alpha lipoic acid using Liquid Chromatography Tandem Mass Spectrometry (LC-MS/MS) method.

The method was developed and validated in-house with Guidance on Bioanalytical Method Validation by EMEA. This method for alpha lipoic acid was validated by solid phase extraction method for its selectivity, sensitivity, accuracy, precision and other parameters. Calibration curve standards were prepared by spiking known concentration of analyte into screened and pooled biological matrix.

In vitro dissolution study

Before the *in vivo* study, an *in vitro* dissolution study was conducted comparing the dissolution behavior of the test product (T) and reference product (R) to verify the similarity of the products. *In vitro* dissolution testing was performed using USP type II paddle apparatus at 75 rpm at 10, 15, 20, 30, 45 and 60 min using 900 mL of deionized water, 0.1 N HCl, pH 4.5 acetate buffer and pH 6.8 phosphate buffer dissolution media. The conditional release profiles of the test product and reference product were plotted as the cumulative percent of drug dissolved vs. time.

The dissolution profiles were compared; the dissolution profiles obtained were evaluated by similarity factor (f_2) (Helmy & Bedaiwy, 2013). According to the EMEA and FDA Guidelines, dissolution similarity may be determined using the f_2 statistic as follows:

$$f_2 = 50 \cdot \log \left[\frac{100}{1 + \frac{\sum_{t=1}^n [R(t) - T(t)]^2}{n}} \right] \quad \text{Eq.1}$$

In this equation (Eq.1) f_2 is the similarity factor, n is the number of time points, R(t) is the mean percent reference drug dissolved at time t after initiation of the study; T(t) is the mean percent test drug dissolved at time t after initiation of the study. For both the reference and test formulations, percent dissolution should be determined. An f_2 value between 50 and 100 suggests that the two dissolution profiles are similar (EMA Guideline on the Investigation of Bioequivalence, 2010).

In vivo bioequivalence study

Initially, a randomized, two-period, single-dose, two-way crossover oral bioequivalence study comparing the test product (T) and reference product (R) was conducted in normal, healthy, adult human subjects under fasting conditions (indicated below as Study 1). According to the results, this study failed with a high ISCV value, and then it was decided to repeat the study with a full replicate study design proposed for highly variable products (indicated below as Study 2). The details of the two studies are presented below.

Ethics statement

The study protocol was approved by the Kavach Ethics Committee (ethics committee registration no: ECR/96/Indt/AP/2013) from Drugs Control General of India (DCGI) on December 12, 2014 (approval number: T-BE-5341/14). The study was conducted in compliance with the approved protocols, ethical principles laid down in the Declaration of Helsinki, and Good Practice Guidelines issued under the applicable regulations. A written informed consent of volunteers was obtained following a detailed explanation of the procedures that they may undergo.

Study subjects

Adult, healthy, male volunteers between 22 to 45 years of age with a body mass index (BMI) between 18.5–30.0 kg/m² and a mean body weight of 45 kg were enrolled as the study subjects. Before the study, medical and surgical histories of the volunteers were determined by general clinical examinations and laboratory tests. The clinical phase of the study lasted 20 days.

The subjects maintained 10.00 hours of overnight fasting before the scheduled dosing time. According to the randomization schedule, each subject was administered either a single dose of the test product (T) or reference product (R) with 240±5 mL of water in a standing position at ambient temperature (23±4°C). The subjects were instructed not to chew or crush the tablet but to consume it as a whole. They were

instructed to maintain an upright posture (sitting) for the first two hours after dosing in each period except when a change of posture was clinically indicated or necessary.

Study design

Study 1: A randomized, open-label, balanced, two-treatment, two-period, two-sequence, single-dose, two-way crossover oral bioequivalence study comparing the test product (T) and reference product (R) in 24 normal, healthy, adult human subjects under fasting conditions.

Study 2: A randomized, open-label, balanced, two-treatment, four-period, two-sequence, single-dose, fully replicate crossover oral bioequivalence study comparing the test product (T) and reference product (R) in 28 normal, healthy, adult human subjects under fasting conditions.

The randomization for the bioequivalence studies was generated using statistical software SAS® Version 9.4. Eighteen blood samples of 0.5 mL each were collected in vacutainers containing K₂EDTA from each subject during each period at pre-dose [(0.00) within 2.00 hours prior to dosing] and at 0.083, 0.167, 0.25, 0.33, 0.50, 0.67, 0.83, 1.00, 1.25, 1.50, 1.75, 2.00, 2.50, 3.00, 4.00, 5.00 and 6.00 hours post-dose. Plasma samples taken from the subjects who completed all clinical phases were analyzed. Quantification was performed with LC-MS/MS using solid-phase extraction method.

Pharmacokinetic analysis

Based on the plasma concentrations of alpha lipoic acid, pharmacokinetic parameters (C_{max} , AUC_{0-t} , $AUC_{0-\infty}$, T_{max} , K_{el} , and $t_{1/2}$) were calculated using "Non-compartmental model" for test and reference treatments. All pharmacokinetic analyses were carried out using WinNonlin Professional Software Version 5.4 (Pharsight Corporation, USA).

Pharmacokinetic parameters are summarized as follows: C_{max} [ng/mL] is the observed maximum concentration in ng/mL, AUC_{0-t} [ngxh/mL] is the area under the plasma concentration vs. time curve in ngxh/mL, $AUC_{0-\infty}$ [ngxh/mL] is the area under the plasma concentration vs time curve, T_{max} [h] is the time observed to reach C_{max} , and $t_{1/2}$ (λ) [h] is the terminal half-life calculated from λ according to $t_{1/2} = \ln(2)/\lambda$.

Statistical analysis

Descriptive statistics (such as mean, minimum, maximum, standard deviation, standard error, median, CV% geometric mean and coefficient of variation) were calculated for plasma concentrations of alpha lipoic acid at several time points as well as for the pharmacokinetic parameters C_{max} and AUC_{0-t} of the test and reference treatments.

Statistical analyses were performed on the pharmacokinetic parameters using the SAS Statistical Software Version 9.4 or higher, SAS Institute, Inc., CARY, USA. ANOVA, and two one-sided t-tests, 90% confidence intervals, ratio analysis for Ln transformed C_{max} and AUC_{0-t} were calculated for the test and reference formulations.

If the intra-subject variability of the reference is $\leq 30\%$ for C_{max} , then the 90% confidence intervals for the difference between

treatments and least-squares means will be calculated for Ln-transformed C_{max} and AUC_{0-t} .

If the intra-subject variability of the reference is $> 30\%$ for C_{max} (not resulting from outliers), then the 90% CI will be calculated according to the formula $[U, L] = \exp [\pm k \cdot SWR]$, where U is the upper limit of the acceptance range, L is the lower limit of the acceptance range, k is the regulatory constant set to 0.760 and SWR is the within-subject standard deviation of the log-transformed values of C_{max} of the reference product.

The test and reference products showed similar relative bioavailability if the difference between compared parameters was found to be statistically insignificant ($p > 0.05$) and the 90% CI for these parameters was found to be within 80% to 125%. The acceptance range for C_{max} may be wider than that for AUC, particularly for drugs having highly variable peak concentrations; in such situations, the recommended range for C_{max} is 69.84% to 143.19% (Helmy & Bedaiwy, 2013).

Safety assessment

The safety assessments included monitoring of adverse events comprising adverse drug reactions, periodic physical examination, vital signs at regular predetermined intervals and those determined by the principal investigator. Pre-study 12-lead ECG, chest X-ray, urine analysis, and serology were conducted for screening of volunteers. Pre-study hematology and serum chemistry assessments were done to select participants with baseline values within reference ranges or clinically non-significant values if outside the reference range. These were repeated in post-study stage to determine any clinically significant abnormality.

Urine drug screening and alcohol breath test were done during the enrollment period of the study to detect participants for any recent substance abuse. A clinical assessment, which includes general and systemic examination, was conducted initially during the pre-study screening and finally during the post-study examination. Blood glucose monitoring was done at 01.00 and 03.00 hours post-dose (within ± 30 minutes of scheduled time) in each period or whenever the physician felt necessary during the conduct of the study.

RESULTS AND DISCUSSION

Validation of analytical methods

Analytical method for estimation of dissolved alpha lipoic acid in *in vitro* analysis was developed and validated using HPLC. Calibration curve for alpha lipoic acid ranged from 0.135 mg/mL to 0.812 mg/mL; correlation coefficient between concentrations and areas was higher than 0.99 ($r^2 > 0.99$); recovery of analyte was 100.4%.

Analytical method for estimation of alpha lipoic acid in human plasma was developed and validated using LC-MS/MS. The validated analytical method was used for analysis of plasma samples. Calibration curve for alpha lipoic acid ranged from 20.006 to 16004.569 ng/mL; linear relationship between concentration and signal intensity were obtained ($r^2 > 0.99$); the limit of quantitation (LOQ) was 20.006 ng/mL; precision values were 2.5%, 3.9%, 3.2% and 4.0% at 9653.792 ng/mL, 6564.578

ng/mL, 1641.145 ng/mL and 50.875 ng/mL concentrations, respectively; accuracy values were 90.0%, 92.6%, 96.0% and 95.0% at 9653.792 ng/mL, 6564.578 ng/mL, 1641.145 ng/mL and 50.875 ng/mL concentrations, respectively; recovery of analyte was 97.37%.

In vitro dissolution study results

The results obtained confirmed that there were acceptable similarities between the test and reference products for various dissolution media (deionized water, 0.1 N HCl, pH 4.5 acetate buffer and pH 6.8 phosphate buffer) under comparison; as a result, *f*₂ values of all dissolution media are higher than 50. The results of *in vitro* tests confirm acceptable similarity between the test and reference products at different dissolution media such as deionized water, 0.1 N HCl, pH 4.5 acetate buffer and pH 6.8 phosphate buffer (Figure 1) having similarity factors (*f*₂) 60.1, 60.0, 64.6 and 70.7, respectively.

Safety results

As for these bioequivalence studies, the drugs were well tolerated upon single-dose administration to normal, healthy, adult, human subjects. No serious adverse events occurred during the conduct of these studies.

Pharmacokinetic and statistical analysis results

Pharmacokinetic parameters and statistical analyses of the test and reference products after administration to healthy vol-

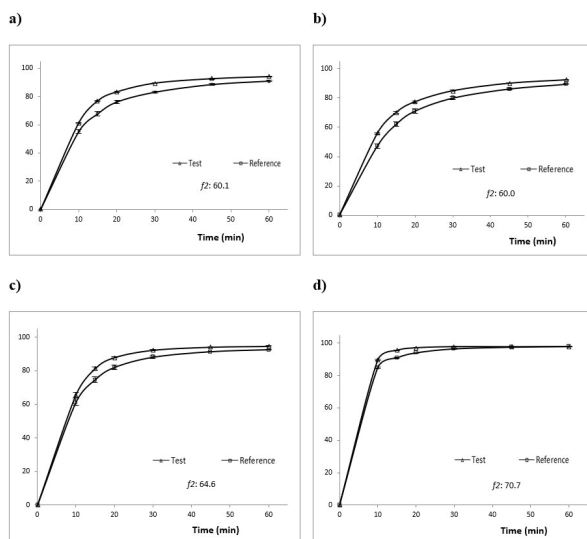


Figure 1. *In vitro* % released alpha lipoic acid vs. time profiles from the test and reference products in four different conditions. a) deionized water; b) 0.1 N HCl; c) pH 4.5 acetate buffer; d) pH 6.8 phosphate buffer. The data represent mean±standard error (n=12).

unteers are summarized in Tables 2, 3 and 4, for both Study 1 and Study 2. For Study 1, the plan was for twenty-four healthy, adult, human subjects to take part, but only twenty-two completed the study. On the other hand, for Study 2, twenty-eight

Table 2. Pharmacokinetic parameters of alpha lipoic acid with the test (T) and reference (R) product for Study 1.

Pharmacokinetic Parameters			Test (T)	Reference (R)
Study 1	C _{max} (ng/mL)	Mean	5852.0	5049.6
		Min - Max	1085.7 - 19504.2	1680.3 - 13827.8
		Median	4514.2	3493.6
		SD	4722.7	3819.1
		CV%	80.7	75.6
	AUC _{0-t} (ng . h/mL)	Mean	3933.9	3815.6
		Min - Max	1604.1 - 7903.2	1819.1 - 8139.7
		Median	3769.8	3493.6
		SD	1685.0	1473.6
		CV%	42.8	38.6
	AUC _{0-∞} (ng . h/mL)	Mean	3998.3	3845.0
		Min - Max	1691.5 - 7934.8	1857.3 - 8156.2
		Median	3795.6	3531.1
		SD	1689.5	1473.9
		CV%	42.3	38.3
	T _{max} (h)	Mean	0.98	0.82
		Median	0.50	0.59
		SD	0.77	0.68
CV%		78.4	83.5	
K _{el} (1/h)	Mean	1.3	1.7	
	SD	0.59	0.54	
	CV%	44.5	32.5	
t _{1/2} (h)	Mean	0.66	0.47	
	SD	0.36	0.17	
	CV%	54.2	36.8	

Table 3. Pharmacokinetic parameters of alpha lipoic acid with the test (T) and reference (R) product for Study 2 - replicate design.

Pharmacokinetic Parameters			Test (T)	Reference (R)
Study 2	C_{max} (ng/mL)	Mean	5215.8	4873.7
		Min - Max	592.4 - 19039.3	803.1 - 11791.0
		Median	4021.0	3655.0
		SD	3669.7	3131.6
		CV%	70.4	64.3
	AUC_{0-t} (ng · h/mL)	Mean	3648.7	3383.6
		Min - Max	1263.4 - 9755.7	803.1 - 11791.0
		Median	3244.8	3232.0
		SD	1745.7	1406.9
		CV%	47.8	41.6
	$AUC_{0-\infty}$ (ng · h/mL)	Mean	3710.6	3413.5
		Min - Max	1275.0 - 9786.7	1301.2 - 7455.6
		Median	3307.2	3285.8
		SD	1746.7	1398.7
		CV%	47.1	41.0
	T_{max} (h)	Mean	0.96	0.98
		Median	0.59	0.67
		SD	0.80	0.69
		CV%	83.7	70.2
	K_{el} (1/h)	Mean	1.76	1.82
		SD	0.54	0.62
CV%		30.8	33.8	
$t_{1/2}$ (h)	Mean	0.44	0.45	
	SD	0.20	0.23	
	CV%	45.6	50.9	

Table 4. Statistical analysis for Log transformed C_{max} , AUC_{0-t} , $AUC_{0-\infty}$ data for test (T) and reference (R) product.

Pharmacokinetic Parameters		Statistical Analysis						
		Least Square Geometric Mean		T/R	90% C.I.		ISCV** %	Power
		Reference	Test		Lower	Upper		
Study 1	LnC_{max} (ng/mL)	4216.5	4006.6	105.2%	79.7%	139.0%	57.5%	37.1%
	$LnAUC_{0-t}$ (ng · h/mL)	3602.0	3580.8	100.6%	89.7%	112.8%	22.3%	94.2%
	$LnAUC_{0-\infty}$ (ng · h/mL)	3668.3	3612.0	101.6%	91.1%	113.2%	21.1%	95.8%
Study 2	LnC_{max} (ng/mL)	4056.1	3786.4	107.1%	88.4%	129.8%	64.5%	60.6%
	$LnAUC_{0-t}$ (ng · h/mL)	3266.2	364.2	106.6%	99.5%	114.7%	22.2%	100.0%
	$LnAUC_{0-\infty}$ (ng · h/mL)	3312.3	3102.0	106.8%	101.3%	116.2%	21.2%	100.0%

* C.I: Confidence Interval; ** ISCV: Intra-Subject Coefficient of Variability

healthy, adult, human subjects were enrolled and initially dosed at the beginning of the study. Twenty-two subjects completed four periods of the study, and twenty-eight subjects who completed at least two periods dosed with T and R were considered for pharmacokinetic and statistical analysis for alpha lipoic acid.

According to the results of Study 1, two-way crossover design study, the test product could not be considered to be bioequivalent to the reference product as the 90% confidence interval for $\text{Ln}C_{\text{max}}$ (ng/mL) was 79.69% – 138.98% (ISCV=57.5%). However, according to Study 2, a fully replicate design study, the test product was bioequivalent in terms of LnAUC_{0-t} (ng · h/mL) and $\text{LnAUC}_{0-\infty}$ (ng · h/mL), but for $\text{Ln}C_{\text{max}}$ (ng/mL) the 90% confidence intervals (88.40% – 129.81%) were slightly higher than acceptable limits (80.0%-125.0%). When the intra-subject variations were considered, a moderately variable LnAUC_{0-t} and $\text{LnAUC}_{0-\infty}$ having ISCV 22.2% and 21.2% respectively, and a highly variable $\text{Ln}C_{\text{max}}$ (ISCV=64.5%) which is much higher than 30% were found. Therefore, intra-subject variabilities showed that alpha lipoic acid is a highly variable drug.

Mean plasma concentration vs. time profiles from 0 to 6 h obtained after administration of the test product and the reference product are shown in Figure 2. The curves after administration of the test or reference products are similar for alpha lipoic acid, especially for Study 2, a full replicate design study.

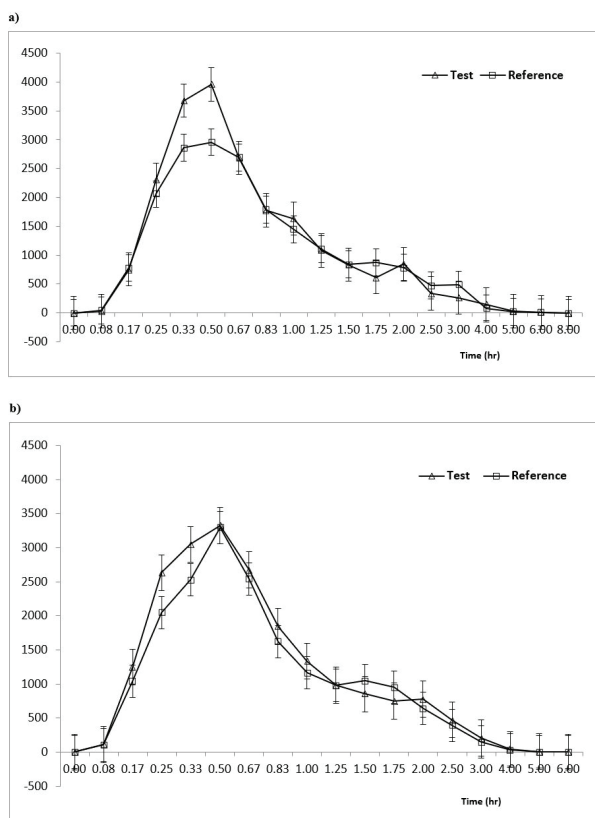


Figure 2. Mean \pm standard error (SE) plasma concentration vs. time profile of alpha lipoic acid following single oral dose administration of test (T) and reference (R) product in healthy, adult, male volunteers under fasting condition. (a) Study 1 (n=22); (b) Study 2 Replicate design study (n=28).

CONCLUSION

Alpha lipoic acid meets the criteria for a highly variable drug with respect to replicate design bioequivalence study results (Study 2). Alpha lipoic acid 600 mg HR film tablet, which does not have product-specific FDA and EMA bioequivalence guidance, has been shown to have high intra-subject variabilities. Therefore, conventional bioequivalence acceptable limits (80.0%-125.0%) should be adjusted to 69.84%-143.19% for alpha-lipoic acid. This study will contribute greatly to the literature and especially to pharmaceutical companies that develop generic products while designing the bioequivalence study.

Acknowledgement: The authors would like to thank to the colleagues at Ilko Pharmaceutical R&D Center for their contributions to this research.

Peer-review: Externally peer-reviewed.

Author Contributions: Conception/Design of Study- B.B., O.P.; Data Acquisition- B.B., O.P.; Data Analysis/Interpretation- B.B., O.P., N.S.; Drafting Manuscript- N.S.; Critical Revision of Manuscript- B.B., O.P., N.S.; Final Approval and Accountability- B.B., O.P., N.S.

Conflict of Interest: The authors have no conflict of interest to declare.



Financial Disclosure: This work was supported by Ilko Pharmaceuticals.

REFERENCES

- Amenta, F., Traini, E., Tomassoni, D., & Mignini, F. (2008). Pharmacokinetics of different formulations of tiotic (alpha-lipoic) acid in healthy volunteers. *Clinical and Experimental Hypertension*, 30(8), 767–775. <https://doi.org/10.1080/10641960802563568>
- Blume, H., Zhong, D., Elze, M., Wendt, G., Schug, B., Scheidel, B. ... Hagenlocher, M. (1994). Advantages of a steady-state crossover design in assessment of bioequivalence of highly variable drugs: propafenone. *European Journal of Pharmaceutical Sciences*, 2(5-6), 385-393. [https://doi.org/10.1016/0928-0987\(94\)00068-9](https://doi.org/10.1016/0928-0987(94)00068-9)
- Brufani, M., & Figliola, R. (2014). (R)- α -lipoic acid oral liquid formulation: pharmacokinetic parameters and therapeutic efficacy. *Acta Bio-Medica: Atenei Parmensis*, 85(2), 108-115. Retrieved from <https://www.mattioli1885journals.com/index.php/actabiomedica/article/view/3800>
- Fagiolino, P., González, N., Vázquez, M., & Eiraldi, R. (2007). Itraconazole Bioequivalence Revisited: Influence of Gender on Highly Variable Drugs. *The Open Drug Metabolism Journal*, 1, 7-13. <http://dx.doi.org/10.2174/1874073100701010007>
- Ghelani, H., Razmovski-Naumovski, V., & Nammi, S. (2017). Chronic treatment of (R)- α -lipoic acid reduces blood glucose and lipid levels in high-fat diet and low-dose streptozotocin-induced metabolic syndrome and type 2 diabetes in Sprague-Dawley rats. *Pharmacology Research & Perspectives*, 5(3). <https://doi.org/10.1002/prp2.306>
- Helmy, S. A., & El Bedaiwy, H. M. (2013). Comparative in vitro dissolution and in vivo bioavailability of diflunisal/naproxen fixed-dose combination tablets and concomitant administration of diflunisal and naproxen in healthy adult subjects. *Drug Research*, 63(3), 150–158. <http://dx.doi.org/10.1055/s-0033-1333768>
- Kang, Q., & Vahl, C. I. (2017). Testing for bioequivalence of highly variable drugs from TR-RT crossover designs with heterogeneous residual variances. *Pharmaceutical Statistics*, 16(5), 361–377. <http://doi.org/10.1002/pst.1816>

- Keith, D. J., Butler, J. A., Bemer, B., Dixon, B., Johnson, S., Garrard, M. ... Hagen, T. M. (2012). Age and gender dependent bioavailability of R- and R,S- α -lipoic acid: A pilot study. *Pharmacological Research*, 66(3), 199–206. <http://doi.org/10.1016/j.phrs.2012.05.002>
- Knahl, S. I., Lang, B., Fleischer, F., & Kieser, M. (2018). A comparison of group sequential and fixed sample size designs for bioequivalence trials with highly variable drugs. *European Journal of Clinical Pharmacology*, 74(5), 549–559. <https://doi.org/10.1007/s00228-018-2415-7>
- Li, C., Xu, J., Zheng, Y., Chen, G., Wang, J., Ma, L. ... Ding, Y. (2017). Bioequivalence and Pharmacokinetic Profiles of Agomelatine 25-mg Tablets in Healthy Chinese Subjects: A Four-Way Replicate Crossover Study Demonstrating High Intra- and Inter-Individual Variations. *Chemical & Pharmaceutical Bulletin*, 65(6), 524–529. <https://doi.org/10.1248/cpb.c16-00866>
- Lohar, V., Patel, H., Rathore, A. S., Singhal, S., Sharma, A. K., & Sharma, P. (2012). Bioequivalence and highly variable drugs: an overview. *International Journal of Current Research and Review*, 04(08), 124–146. Retrieved from https://www.ijcrr.com/uploads/1853_pdf.pdf
- Mignini, F., Streccioni, V., Tomassoni, D., Traini, E., & Amenta, F. (2007). Comparative Crossover, Randomized, Open-Label Bioequivalence Study on the Bioequivalence of Two Formulations of Thiocctic Acid in Healthy Volunteers. *Clinical and Experimental Hypertension*, 29(8), 575–586. <http://dx.doi.org/10.1080/10641960701744111>
- Mignini, F., Nasuti, C., Gioventu, G., Napolioni, V., & Martino, P. D. (2012). Human Bioavailability and Pharmacokinetic Profile of Different Formulations Delivering Alpha Lipoic Acid. *Open Access Scientific Reports*, 1(8), 418. <http://dx.doi.org/10.4172/scientificreports.418>
- Molins, E., Cobo, E., & Ocaña, J. (2017). Two-stage designs versus European scaled average designs in bioequivalence studies for highly variable drugs: Which to choose? *Statistics in Medicine*, 36(30), 4777–4788. <https://doi.org/10.1002/sim.7452>
- Thota, S., Khan, S. M., Tippabhotla, S. K., Battula, R., Gadiko, C., & Vobalaboina, V. (2013). Bioequivalence of two lansoprazole delayed release capsules 30 mg in healthy male volunteers under fasting, fed and fasting-applesauce conditions: A partial replicate crossover study design to estimate the pharmacokinetics of highly variable drugs. *Drug Research*, 63(11), 551–557. <http://dx.doi.org/10.1055/s-0033-1347236>
- US FDA Code of Federal Regulations. (2019, April). Title 21, Section 314.3 Definitions. Retrieved from <https://www.accessdata.fda.gov/scripts/cdrh/cfdocs/cfcfr/CFRSearch.cfm?fr=314.3>

Development and validation an HPLC - UV method for determination of esomeprazole and pirfenidone simultaneously in rat plasma: application to a drug monitoring study

Emrah Dural¹ , Sema Tülay Köz^{2,3} , Süleyman Köz^{4,5} 

¹Sivas Cumhuriyet University, Faculty of Pharmacy, Department of Pharmaceutical Toxicology, Sivas, Turkey

²Sivas Cumhuriyet University, Faculty of Medicine, Department of Physiology, Sivas, Turkey

³Bahçeşehir University, Faculty of Medicine, Department of Physiology, İstanbul, Turkey

⁴Sivas Cumhuriyet University, Faculty of Medicine, Department of Nefrology, Sivas, Turkey

⁵Medipol Health Group, Department of Nefrology, İstanbul, Turkey

ORCID IDs of the authors: E.D. 0000-0002-9320-8008; S.T.K. 0000-0002-3809-1070; S.K. 0000-0001-5036-0475

Cite this article as: Dural, E., Koz, S. T., & Koz, S. (2021). Development and validation an HPLC - UV method for determination of esomeprazole and pirfenidone simultaneously in rat plasma: Application to a drug monitoring study. *İstanbul Journal of Pharmacy*, 51(1), 16-25.

ABSTRACT

Background and Aims: It has been observed that the combined treatment of esomeprazole and pirfenidone provides increased efficacy in the treatment of pulmonary fibrosis disease, recently. The aim of this study is to develop a simple, sensitive, and reliable high-performance liquid chromatography method to be used in drug monitoring to increase the effectiveness of esomeprazole and pirfenidone in treatment and to reduce their adverse effects.

Methods: Separation was conducted with a C18 reverse-phase column (4.6 mm x 250 mm, 5 µm) used as a mobile phase prepared with the phosphate buffer (10 mM KH₂PO₄ and 10 mM K₂HPO₄) and acetonitrile (60:40, v/v) by an isocratic flow (1 mL/min). Mobile phase pH was adjusted to 3.0. Ultraviolet detection was accomplished at 305 nm. The column oven was held at 35°C to ensure an efficient analytical separation.

Results: Analytical recovery of esomeprazole was between 92.43 and 105.36% and for pirfenidone it was found between 89.56 and 104.32%. Accuracy values of esomeprazole and pirfenidone were determined between (-2.90) - 4.22 and (-4.45) - 5.78, respectively. Precision (RSD%) was ≤7.89. The quantification limit was determined as 0.58 and 0.36 ng/mL. Plasma esomeprazole and pirfenidone levels were found as 0.87-8296.87 ng/mL (612.99±2212.20, mean ± standard deviation) and 0.45-238.60 ng/mL (61.44±76.35, mean ± standard deviation), respectively.

Conclusion: Unexpectedly high RSD values were observed in both plasma (360.88%) and dose-rated results (89.61%) of esomeprazole, and pirfenidone were thought to be related to individual metabolism differences.

Keywords: Esomeprazole, pirfenidone, rat plasma, method validation, HPLC-UV

Address for Correspondence:

Emrah DURAL, e-mail: emrahdural@cumhuriyet.edu.tr

Submitted: 18.09.2020

Revision Requested: 18.11.2020

Last Revision Received: 17.12.2020

Accepted: 21.12.2020

This work is licensed under a Creative Commons Attribution 4.0 International License.



INTRODUCTION

Esomeprazole, 6-methoxy-2-[(S)-(4-methoxy-3,5-dimethylpyridin-2-yl)methylsulfinyl]-1H-benzimidazole (Figure 1a), is a part of the novel gastric proton pump inhibitors (Liu et al., 2017; Sebaiy, Hassan, & Elhennawy, 2019). It provides decreased stomach acid secretion through inhibition of the H⁺/K⁺-ATPase in the parietal cells of the stomach. It has better oral bioavailability than S-enantiomer. Esomeprazole is widely used in the treatment of many acid-related disorders such as peptic disease, gastroesophageal reflux, and in the prevention of the adverse reactions of non-steroidal anti-inflammatory drugs (Çelebi et al., 2016; Franke, Hepp, Harder, Beglinger, & Singer, 2008; Johnson, 2003; Liu et al., 2017). In addition, remarkable results have been reported in various studies showing that its anti-fibrotic activities for both liver and lung recently (Eltahir & Nazmy, 2018; Ghebre & Raghu, 2016; Ghebremariam et al., 2015). Pulmonary fibrosis disease has a prevalence of 494.5 cases per 100,000 and an incidence of 93.7 cases per 100,000 (Raghu et al., 2014). Although this disease often occurs over the age of 60, it may occur at earlier ages in familial idiopathic pulmonary fibrosis patients (Hodgson, Laitinen, & Tukiainen, 2002; Marshall, Puddicombe, Cookson, & Laurent, 2000; Nadrous, Myers, Decker, & Ryu, 2005). The median survival rate is only 3-4 years from the time of diagnosis (Raghu et al., 2014).

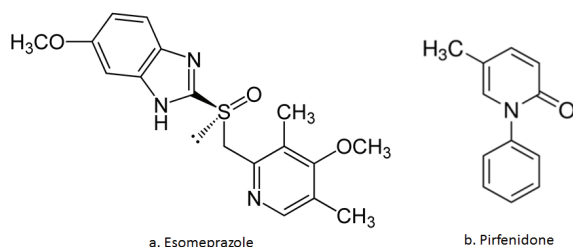


Figure 1. Chemical structures of esomeprazole (a) and pirfenidone (b).

Pirfenidone is a novel agent, 5-methyl-1-phenylpyridin-2-(1H)-one, approved for mild to moderate idiopathic pulmonary fibrosis by FDA in 2014. It is a non-peptide, orally active small molecule (185.22 g/mol) that is in use also as an antioxidant and anti-inflammatory agent. It is an orphan drug in Europe and Japan (Parmar, Desai, & Vaja, 2014). A study which conducted a phase III multi-national clinical trial has shown that it has beneficial effects on patients with various stages of idiopathic pulmonary fibrosis disease. It has been reported that this agent could reduce lung fibrosis in drug-fibrotic *in vivo* studies, including the pirfenidone-hamster and the cyclophosphamide-mouse models (Iyer et al., 1995; Kehrer & Margolin, 1997). Although it is a commonly well-tolerated agent and has a favourable benefit-risk profile, gastrointestinal problems, photosensitivity reactions and rashes are its important adverse reactions that have been seen commonly (Khan, Shirkhedkar, Chaudhari, & Pawara, 2019).

In this study, we aimed to develop a high performance liquid chromatography (HPLC) method for the monitoring of these agents from rat plasma based on solid phase extraction pretreatment due to the anti-fibrotic effects of esomeprazole and

pirfenidone detected in both combined and individual treatments (Ghebremariam et al., 2015). There are some analytical methods developed for the determination of esomeprazole from different matrices in the literature. These are based on spectrophotometric (Prabu et al., 2008), capillary electrophoresis (Estevez, Flor, Boscolo, Tripodi, & Lucangioli, 2014), gas chromatography (Raman, Reddy, Prasad, & Ramakrishna, 2008), and liquid chromatography that coupled with an ultraviolet detector (Jain, Jain, Charde, & Jain, 2011; Kayesh & Sultan, 2015; Talaat, 2017), photodiode array detector (Sebaiy et al., 2019), and tandem mass spectrometry (Gopinath, Kumar, Shankar, & Danabal, 2013). Also, some analytical methods were reported for the determination of pirfenidone from the different matrix which includes pharmaceutical dosage forms and plasma. These are spectrophotometric (Thorat, Padmane, Tajne, & Ittadwar, 2016), spectrofluorometric (Sambhani & Biju, 2018), capillary electrophoresis (Sotgia et al., 2020), high-performance thin layer chromatography (Thorat et al., 2016), gas chromatography (Ma et al., 2017), and HPLC with an ultraviolet detector (Bodempudi, Babur, & Reddy, 2015; Parmar et al., 2014; Ravisankar, Anusha Rani, Devadasu, & Devala Rao, 2014; Thorat et al., 2016), a photodiode array detector (Bodempudi et al., 2015) and a mass spectrometry detector (Tong et al., 2010; Wen et al., 2014) methods.

However, long analysis times, complex sample preparation protocols, and high sample quantities needed for analysis limit their use. At the same time low sensitivity, precision and accuracy of these methods may cause restriction of their use in the analyses. Although several liquid chromatographic methods were established for the determination of esomeprazole and pirfenidone, according to our investigation, there is no study that includes the simultaneous analysis of esomeprazole and pirfenidone by HPLC in rat plasma in the literature.

The aim of this study is to develop a simple, rapid and reliable HPLC analysis method for determination of esomeprazole and pirfenidone and to validate it in terms of linearity, repeatability, sensitivity, recovery, and robustness according to ICH Q2(R1) guidelines (ICH, 2005). This simple reproducible, efficient extraction method provided the determination of esomeprazole and pirfenidone levels from rat plasma without any process of the deproteinization and derivatization. It was used in the study of simultaneous monitoring of esomeprazole and pirfenidone levels in plasma samples from 14 rats treated by oral gavage. In addition, our study aimed to determine the plasma esomeprazole and pirfenidone concentrations of rats simultaneously by the chromatographic method to be developed. Also, it was aimed to analyze the relationship between drug doses and blood results statistically.

MATERIAL AND METHODS

Chemicals and reagents

Esomeprazole (Figure 1a) and pirfenidone (Figure 1b) analytical standards were purchased from Shandong Zhi Shang Chemical Co. Ltd. (Jinan, China) and Wuhan Benjamin Pharmaceutical Chemical Co. Ltd. (Wuhan, China), respectively. The Sep-Pac® Vac 1 cc (100 mg) solid-phase C18 cartridge was obtained from Waters (Dublin, Ireland). Ultragradient grade acetonitrile,

ethanol and methanol were bought from Carlo-Ebra (Val-de-Reuil, France). Triethylamine ($\geq 99\%$) was purchased from Sigma-Aldrich (Brussels, Belgium). Orthophosphoric acid (H_3PO_4), sodium hydroxide (NaOH), sodium chloride (NaCl), potassium chloride (KCl), disodium hydrogen phosphate (Na_2HPO_4), dipotassium hydrogen phosphate (K_2HPO_4) and potassium dihydrogen phosphate (KH_2PO_4) which are analytical grade were bought from Merck (Darmstadt, Germany). Carboxymethyl cellulose was purchased from Biokim & Wenda Chemicals (İzmir, Turkey). Bovine serum albumin was purchased from Solarbio Life Science (Beijing, China). Polytetrafluoroethylene (PTFE) membrane filter (47 mm diameter, 0.45 μm pore size) was obtained from Millipore (Massachusetts, USA). An MRC ultrasonic bath (Harlow, UK), ACP-250H model, was used for the preparation of the mobile phase. Elga Purelab Water Purification System (Lane End, UK) was employed to supply ultra-pure water.

Instrumentation and chromatographic parameters

Agilent (Hewlett-Packard) 1100 series (California, USA) HPLC system equipped with a degasser (G1322A), a gradient-quad pump (G1311A), a manual injector (Rheodyne, 7725i) with a 20 μL loop volume, a column thermostat (G1316A, Colcom), and an UV detector (G1314A, VWD) was used for separation and quantification of esomeprazole and pirfenidone in rat plasma. The system control and integration of the produced chromatographic data was achieved by a Chemstation 08.03 software (Palo Alto, USA). A stainless steel end-cap C18 reverse-phase (RP) analytical column (4.6 mm x 250 mm i.d., 5 μm p.s.) (USA) was successfully employed for the separation and quantitation of esomeprazole and pirfenidone.

Chromatographic conditions were determined after optimization studies on the analytical column, column thermostat temperature, mobile phase content and detector wavelength selection. The best analytical separation result was achieved from the C18 RP ACE-3 column (4.6 mm x 250 mm i.d., 5 μm p.s.) out of 3 tested columns which were the RP-C18 Waters column (4.6 mm x 250 mm i.d., 5 μm p.s.) and the RP-C18 Zorbax column (4.6 mm x 150 mm i.d., 3 μm p.s.).

The minimum column back pressure (≤ 95 bar) and enough peak resolution were gained after the oven temperature was set at 35°C. Although different wavelengths (220, 246, 254, 270 and 294 nm) were tested for the determination of esomeprazole and pirfenidone in plasma, the highest peak sharpness and lowest matrix interference were obtained from 305 nm. The UV spectrums of esomeprazole and pirfenidone were given in Figure 2.

The mobile phase buffer was prepared with KH_2PO_4 (10 mM) and K_2HPO_4 (10 mM) containing 0.1% triethylamine, then the pH was set at 3.0 by orthophosphoric acid (0.1 M) and then filtered by a PTFE membrane. Then, this solution was mixed with acetonitrile (60:40, v/v) and then it was degassed with an ultrasonic bath, for 30 mins. The mobile phase was applied isocratically to the column with 1.0 mL/min constant flow. Determination of analytes concentration in the quality control and rat blood samples were carried out using linear regression of response esomeprazole and pirfenidone peak area versus to their concentrations with the ultraviolet detector set at 305 nm.

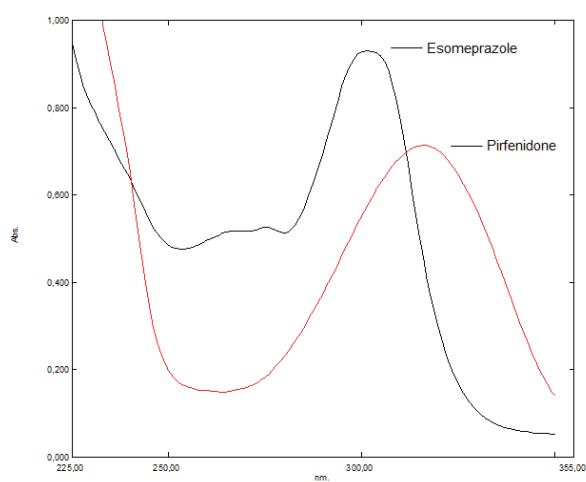


Figure 2. Overlapping UV spectra of esomeprazole and pirfenidone (200 $\mu\text{g}/\text{mL}$) that are between 255 and 355 nm.

Preparation of stock standard solutions and working standards

Simulated plasma was used in all stages during the development of the solid-phase extraction (SPE) procedure and optimization and validation of this analytical method. It was prepared as follows: 20 mg of KCl , 0.8 g of NaCl , 20 mg of KH_2PO_4 , 135 mg of Na_2HPO_4 and 4 g of bovine serum albumin were weighed and dissolved in 100 mL of ultrapure water. The final pH was adjusted to 7.4 with 1 M NaOH or 1 M orthophosphoric acid solutions (Mercolini, Mandrioli, Amore, & Raggi, 2008). It was stored as 500 μL in a 1.5 mL micro tube at -18 °C until use. The stock solution of esomeprazole and pirfenidone was prepared in methanol as 1 mg/mL and stored at -18°C until use. It has been observed to be chemically stable for at least 1 month. Working solutions of esomeprazole and pirfenidone were prepared weekly from the main stock solution in methanol as 0.25, 0.50, 1.00, 2.00 and 5.00 $\mu\text{g}/\text{mL}$ concentrations. Working standards were prepared daily, and they were used to add to simulated plasma samples prior to analysis. Quality control samples of esomeprazole and pirfenidone were freshly prepared in simulated plasma samples to provide concentrations of 25, 50, 100, 200 and 500 ng/mL. Likewise, plasma quality control standards spiked with 25, 100 and 500 ng/mL of esomeprazole and pirfenidone were prepared to measure the repeatability values of the method. Also, the same protocol was used in the preparation of limit of detection (LOD), limit of detection (LOQ), recovery and robustness test samples.

Preparation of quality control samples and real plasma samples

Simulated plasma samples have been used in the forming of the quality control samples used during the development and validation process of this method. The collected real rat blood centrifuged at 4000 rpm for 5 mins to separate the plasma. Quality control plasma and real patient plasma samples were stored at -20°C until the analyses were carried out. Working solutions were checked chromatographically for purity before experiments, were utilized as quality control specimens and were checked for the stability before and after the injections of every sample set.

The extraction procedure was carried out with a glass solid-phase apparatus (12 wells) coupled with the vacuum pump according to the following steps:

- i. In the initial step, the cartridge was conditioned with 1 mL acetonitrile;
- ii. Equilibrium was achieved with 1 mL water and 1 mL methanol;
- iii. The sample constituted 0.5 μ L plasma with 10 μ L ISTD (1 mg/mL) and 10 μ L esomeprazole and pirfenidone STDs (for quality control samples) was applied to the cartridge;
- iv. The cartridge adsorbent was washed with 1 mL (two times) water;
- v. The eluting was carried out with 1 mL acetonitrile (two times) for 5 mins at 75 kPa. All liquid in the cartridge was completely collected with a constant flow;

Finally, the collected extraction liquid (approximately 2 mL) was evaporated under nitrogen. The remains, after being reconstituted in 200 μ L of the mobile phase, were injected into the analysis system as a volume of 20 μ L.

Validation of the analysis method

The developed analytical method was validated in relation to its specificity and selectivity, linearity, accuracy and precision, sensitivity (LOD and LOQ), recovery and robustness. Intraday and inter-day validation protocol were applied considering reproducibility of the method to obtain accurate and precise measurements in accordance with ICH Q2R1 guidelines (ICH, 2005),

Specificity and selectivity

The method showed excellent chromatographic specificity without any endogenous interference in the retention times of esomeprazole and pirfenidone (4.2 and 6.1 mins, respectively) in simulated plasma. Blank (Figure 3a), spiked (Figure 3b) and real sample (Figure 3c), chromatograms were exhibited a high chromatographic resolution that conducted in 7.0 mins.

Linearity

After chromatographic conditions were established, matrix-based calibration curves of esomeprazole and pirfenidone were plotted concentrations over the concentration range 25-500 ng/mL versus peak-area of them. The calibration points (n=5), which were 25, 50, 100, 200 and 500 ng/mL composed of 3 individual replicates and were prepared by a standard addition method in simulated plasma and injected to HPLC.

Accuracy and precision

The accuracy defined as the relative error (RE%) was calculated as the percentage difference between the added and found esomeprazole and pirfenidone quantity by 5 individual replicates both intraday and inter-day. The precision, which is defined as relative standard deviation (RSD%), was calculated by five separate replicates of esomeprazole and pirfenidone both intraday and inter-day. Five replicated spiked samples were assayed intraday and inter-day at the three different concentrations (25, 100 and 500 ng/mL).

Robustness

The robustness test was performed with 200 ng/mL of esomeprazole and pirfenidone, which is the approximate medium concentration of the calibration interval. The response of the method over the changes in UV wavelength (± 3 nm) value, mobile phase flow rate (± 0.1 mL/min), mobile phase solvent content ($\pm 5\%$) and, column temperature ($\pm 5^\circ\text{C}$) was evaluated.

Sensitivity

LOD and LOQ were calculated according to the ICH recommendations based on the standard deviation of the response, and the slope of the calibration graph. 25 ng/mL was used as the lowest calibration point in a sensitivity test of esomeprazole and pirfenidone.

$\text{LOD} = 3.3 \frac{\sigma}{S}$; $\text{LOQ} = 10 \frac{\sigma}{S}$ (σ : The standard deviation of the response; S: The slope of the calibration curve).

Recovery

The recovery of the extraction procedure was calculated by comparing the results obtained from the extracted samples with the results of the unextracted samples which were directly prepared. This test was performed by adding 5 individual replicates of spiked samples at low, middle and high concentrations (25, 100 and 500 ng/mL, respectively) of esomeprazole and pirfenidone. The extraction procedure was carried out as described before in the sample preparation step.

Collection of plasma samples

Approximately 1 mL of femoral vein blood sample was taken from Wistar Albino rat 2 hrs before the Wistar Albino rat whose plasma had a steady state concentration was put down. The rats included in this study were treated with esomeprazole (50 mg/kg/day) and pirfenidone (100 mg/kg/day) by oral gavage prepared in 1 mL solution which has agents (esomeprazole and pirfenidone) dissolved in 1% carboxymethyl cellulose and 10% ethanol. In this study, 14 blood samples were obtained from 14 individual rats involved in this research.

The rats in this study were treated by oral gavage with 1 mL of solution containing agents (esomeprazole and pirfenidone) dissolved in 1% carboxymethyl and 10% ethanol. One mL rats whole blood sample was put in a vacuum tube (BD Vacutainer®) which contains K₂EDTA (5.4 mg) and was centrifuged at 3000 rpm for 10 mins on the same day. Then, the obtained plasma that had at least has 0.5 mL volume was transferred in a micro experiment tube and it was stored in a freezer at -86 C until the analysis. Plasma samples were analysed in less than 1 month.

Ethics committee approval: The ethical decision of this research was approved by the Animal Experiments Local Ethics Committee of Sivas Cumhuriyet University, with the 2016-03 decision number, dated on 14 January 2016. The research was conducted in accordance with the Declaration of Helsinki and its subsequent revisions.

Statistical analysis: All statistical analyses performed using the IBM Statistical Package for the Social Sciences (SPSS) 23.0. The Spearman non-parametric test was used to determine correlation.

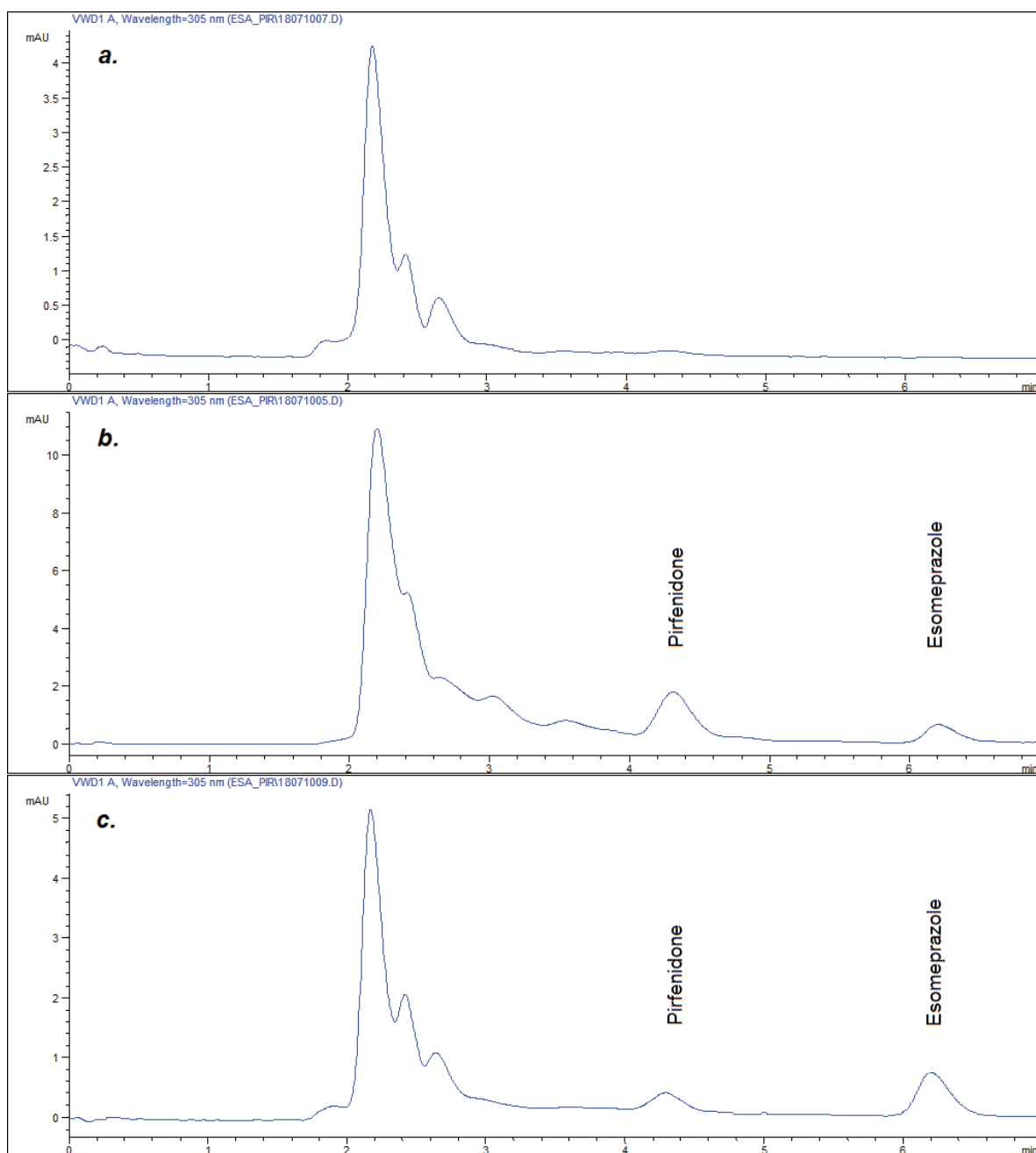


Figure 3. a. A chromatogram which belongs to blank-simulated plasma employed to prepare the quality control standards in all validation tests. b. A chromatogram sample containing 200 ng/mL esomeprazole and pirfenidone standards prepared with the standard addition method used as a quality control sample. c. A sample chromatogram belongs to a real plasma obtained from a rat treated with esomeprazole and pirfenidone.

RESULTS AND DISCUSSION

Method validation

Validation procedures were conducted considering ICH-Q2(R1) guidelines during the all of the test steps (ICH, 2005)

Linearity

The calibration curves of the esomeprazole and pirfenidone were constructed with excellent determination coefficient values which are $r^2 \geq 0.9986$ at 5 points ($n=3$) separately between 25 and 500 ng/mL concentrations by the standard addition method.

The correlation values of the method observed at the individual different 5 calibration points was quite good. The wide linear range has also had a positive effect on the use of the method. Since the obtained real blood results were shown very high standard deviation.

System suitability parameters showed that the method has a good resolution (R_s), selectivity (α), capacity factor (k') and theoretical plate number (N) for the determination of esomeprazole and pirfenidone successfully from rat plasma as it can see in Table 1. The column dead time was obtained by dividing

Table 1. Chromatographic characteristics, system suitability parameters and sensitivity values of the developed method.

Analyte	Retention time (min, t_R)	Linear range (ng/mL)	Calibration equation	Determination coefficient (r^2)	Capacity factor (k')	Theoretical plate number (N)	Specificity factor (α)	Resolution (R_s)	T_f	LOD (ng/mL)	LOQ (ng/mL)
Esomeprazole	4.2	25 - 500	$y = 226.69x + 95.92$	0.9986	1.91	7079.19	7.64	12.00	1.046	0.19	0.58
Pirfenidone	6.1	25 - 500	$y = 220.55x + 11.238$	0.9997	1.0	5831.41	4.00	7.16	1.125	0.12	0.36

Equations: Capacity factor (k') = $\frac{t_R - t_0}{t_0}$; Theoretical plate number (N) = $16 \left(\frac{t_R}{W_t} \right)^2$; Resolution (R_s) = $\frac{\sqrt{N} (\alpha - 1)}{4 \alpha} \frac{k}{(k+1)}$; Specificity factor (α) = $\frac{k_2}{k_1}$; Peak symmetry (T_f) = $\frac{a+b}{2a}$
 Abbreviations: t_R : retention time of the analyte peak; t_0 : retention time of mobile phase peak; W_t : peak width; a : the distance from the leading edge of the peak to the peak midpoint; b : The distance from the back edge of the peak to the peak midpoint

the packed column volume by the flow rate (Column Spacing/ Dwell Time) and is given in Table 1 in minutes.

Sensitivity

The results of LOD and LOQ values, which were obtained from the measurement of individual 10 quality control (QC) samples, were demonstrated in Table 1. It was observed that the sensitivity values, especially LOQs, covered all the real plasma sample esomeprazole and pirfenidone results. Although the minimum concentrations of esomeprazole and pirfenidone determined from plasma were 0.19 and 0.12 ng/mL, it was observed that the LOQ values were determined as 0.58 and 0.36 ng/mL, respectively. Therefore, the method is suitable for reliable analyzes for low concentrations of esomeprazole and pirfenidone.

Precision and accuracy

The data obtained from the accuracy and precision tests, performed in intraday and inter-day with quality control standards established in the blank plasma samples by standard addition method, showed low RSD% values ≤ 7.59 and $\leq 7.89\%$ for interday and intraday respectively. Also low RE% average values were observed between (-4.45)–5.78% for inter-day and (-2.05)–5.69% for intraday test values (Table 2). The obtained repeatability results showed that the method has excellent precision and accuracy values not only for intraday but also for inter-day analyses.

Recovery

Recovery test results which are done at 25, 100 and 500 ng/mL were between 89.56 and 105.36% with the results given in Table 2. The method has a highly successful analytical result with the average recovery values at 97.44 and 93.83% for esomeprazole and pirfenidone, respectively. Recovery values obtained in the extraction procedure have demonstrated excellent efficiency. It was observed that the extraction procedure was not complicated and had no need for sophisticated instruments.

Robustness

No significant changes in the analytical signals were observed upon changing the UV wavelength value (± 3 nm), mobile phase flow rate (± 0.1 mL/min), mobile phase organic solvent ingredient ($\pm 5\%$), and column temperature ($\pm 5^\circ\text{C}$). All robustness results were given on Table 3. In addition to that, change of analysts, columns, sources of chemicals and/or solvents did not lead to significant changes in chromatographic signals and results, either.

Stability

The stability of quality control (QC) simulated plasma samples (25, 100 and 500 ng/mL) prepared with a standard addition method and esomeprazole and pirfenidone analytes in stock solutions under several conditions were assessed. The stability of the stock solutions at room temperature was evaluated during 1, 2, 3 and 4 week periods. The stability test of freeze-thaw was carried out by three QC samples after operating five repeated freeze-thaw periods. The stability test in the long-term was carried out for 1, 2 and 3 months using QC samples maintained at -20°C . Neither significant decrease related to analytes peak area nor degradation which could be seen in chromatograms were observed in the concentration of esomeprazole and pirfenidone in three different conditions. The relative standard deviations which were observed in all sample results were less than 6.8%.

These investigations have shown that there is not an investigation study in which esomeprazole and pirfenidone were simultaneously analyzed by a validated HPLC-UV method which has a solid phase extraction method in the literature. However, studies in the literature focusing separately on the analysis of esomeprazole and pirfenidone by HPLC are summarized below.

In Jain et al (2011) study, an HPLC method was developed for the determination of esomeprazole. Analytical separation was achieved by a C18 (4.6 mm x 150 mm i.d., 5 μm) column at

Table 2. Confidence parameters that include intraday, inter-day precision and accuracy and recovery values. These results were obtained from individual samples (n=5) formed in simulated plasma. Intraday reproducibility experiments were performed sequentially on the same day. Inter-day repeatability experiments were performed sequentially on consecutive 5 days.

Analytes	Expected concentration (ng/mL)	Intra-day repeatability			Inter-day repeatability			Recovery%
		Observed concentration \pm SD (ng/mL)	Precision (RSD%)	Accuracy (RE%)	Observed concentration \pm SD (ng/mL)	Precision (RSD%)	Accuracy (RE%)	
Esomeprazole	25	2.85 \pm 0.31	6.31	4.22	2.75 \pm 0.47	4.59	2.49	92.43
	100	4.49 \pm 0.92	4.48	- 2.05	4.37 \pm 1.53	7.43	- 2.90	94.54
	500	49.15 \pm 1.13	3.27	- 1.93	48.39 \pm 0.92	4.33	- 0.78	105.36
Pirfenidone	25	2.88 \pm 0.43	7.89	5.69	2.85 \pm 0.58	7.59	5.78	89.56
	100	5.59 \pm 1.56	5.53	3.65	4.37 \pm 1.53	6.43	- 3.82	104.32
	500	48.55 \pm 1.13	4.76	- 0.93	48.39 \pm 0.92	3.33	- 4.45	96.61

Table 3. Robustness data of the described method representing as the RSD% value. These results were obtained in the analysis of three variable points calculated by independent (n=5) analyzes.

Analytes	Mobile phases solvent content (\pm 5%)	UV wavelength (\pm 3 nm)	Flow rate (\pm 0.1 mL/min)	Column temperature (\pm 5 °C)
Esomeprazole	3.82 \pm 0.12	4.85 \pm 0.19	2.81 \pm 0.14	2.12 \pm 0.08
Pirfenidone	4.65 \pm 0.14	4.31 \pm 0.12	1.92 \pm 0.07	2.89 \pm 0.10

25°C. Acetonitrile and phosphate buffer (pH:7.0) in the ratio of 50:50 (v/v) was used as a mobile phase for HPLC. The flow rate was 0.5 mL/min. Quantitation was applied at 300 nm. Method was found to be linear ($r=0.998$) in the concentration range between 50 – 250 μ g/mL. The retention time was 5.661 min. Mean recovery was 97.75%. Accuracy was < 2.0 (RSD%) (Jain et al., 2011).

Kayesh and Sultan (2015) established an HPLC-ion pair method to determine esomeprazol in pharmaceutical formulation. As a mobile phase, tetrabutylammonium hydroxide (7.7 mM) and n-heptane sulfonic acid-Na salt (20 mM), acetonitrile and methanol (3:1:1, v/v) was isocratically applied to a C18 octadecyl-silica column (4.6 mm x 250 mm i.d., 5 μ m p.s.) (Kayesh & Sultan, 2015).

Sebaiy et al. (2019) developed a method for esomeprazole in human plasma. Protein precipitation was used for preparation of samples. Separation was carried out on a C18 column (4.6 mm x 150 mm i.d., 5 μ m p.s.). Acetonitrile and 25 mM KH_2PO_4 (25:75, v/v) was used as a mobile phase. LOD was 40 ng/mL and LOQ was found as 130 μ g/mL. A DAD detector was set at 230 nm. An aliquot of 200 μ L plasma was precipitated MeOH. Then, the mixture was centrifuged at 5500 rpm for 15 mins. The obtained supernatant liquid was fitted with a 0.45 μ m PTFE filter. Then, it was applied to the analytical system.

Method was found to be linear between 0.5 μ g/mL to 50 μ g/mL ($r=1$) concentrations. Recovery was between 98.38% and 101.14%. Accuracy was observed as -5.27 %. Precision (RSD%) was observed between 0.78 and 15.79% (Sebaiy et al., 2019).

Talaat (2017) established a micellar HPLC-UV method employing a VP-ODS column (4.6 mm x 150 mm i.d.) in separation. The mobile phase consisted of 0.1 M sodium dodecyl sulfate, 10% n-propanol, 0.3% triethylamine in 0.02 M orthophosphoric acid (pH 3.5). The flow rate was 1.0 mL/min. The method was found to be linear between 1 and 20 μ g/mL. The UV detector was set at 280 nm (Talaat, 2017).

Ravisankar et al. (2014) established a RP-HPLC method to determine pirfenidone in pharmaceutical dosage forms. Separation was carried out on a C18 column (4.6 mm x 250 mm i.d., 5 μ m p.s.). The mobile phase was composed of acetonitrile: water (50:50, v/v). The flow rate was 1.0 mL/min and UV detection was accomplished at 315 nm. The method was found linear ($r=0.999$) in the range of 2-10 μ g/mL. Recovery was found to be 99.60% to 99.80%. Precision (RSD%) was less than 2% (Ravisankar et al., 2014).

Parmar et al. (2014) developed an HPLC method for determination of pirfenidone from its pharmaceutical formulations. The separation was achieved isocratically on a reversed-phase C18

column with a mobile phase consisting of acetonitrile: water (35:65, v/v) at a flow rate of 0.7 mL/min. The UV detector was set at 317 nm. The method was found linear between 0.2 and 5.0 µg/mL. Recovery was in the range of 98 and 102% and precision was found < 2% (RSD%) (Parmar et al., 2014).

In Bodempudi et al. (2015) study, an HPLC based chromatographic method was developed for the determination of pirfenidone in the drug substance. Separation was achieved with a C18 column (4.6 mm x 250 mm i.d., 5 µm p.s.) using 0.02 M KH₂PO₄ buffer and acetonitrile as mobile phase. The flow was 1.0 mL/min and detection was achieved at 220 nm. The method was found linear (r²=0.9985) between 47 and 382 ng/mL. LOD was found 14 ng/mL and LOQ was calculated as 9.4 µg/mL (Bodempudi et al., 2015).

In the study of Thorat et al. (2016) an HPLC method for the determination of pirfenidone from tablet dosage form was established. Analytical separation was carried out using an isocratic technique on a reversed phase C18 column (4.6 mm x 150 mm i.d., 5 µm p.s.), with phosphate buffer: acetonitrile (pH 3.5) 72:28 v/v as a mobile phase at flow rate 1 mL/min. The method was linear (r=0.9964) between 5-70 µg/mL. Recovery was between 99.2 and 101.3%. Precision was found as ≤0.6751 (RSD%) (Thorat et al., 2016).

Wang et al. (2006) established an HPLC method for determination of pirfenidone as an analytical reagent in rat plasma. Rat plasma samples (150 µL) were precipitated with 10% (v/v) perchloric acid solution, then centrifuged. Obtained supernatant was applied to HPLC. This method was found to be linear between 0.15 and 76.67 µg/mL. The separation was carried out on a C18 column (4.6 mm x 250 mm i.d., 5 µm p.s.) using acetonitrile – water containing 0.2% acetic acid (23:77, v/v) as a mobile phase at 1 mL/min flow-rate. Detection was performed at 310 nm. The accuracy (RE%) was observed in ranges from (-2.6) to 7.9% and the precision (coefficient of variation) was found ≤ 4.5% (Wang et al., 2006).

In More et al. (2019) study, an HPLC analysis method for determination of pirfenidone was developed. The flow rate was 1 mL/min. The method was found linear (r=0.9989) over the range of 5-25 µg/mL. Recovery was between 98 to 100%. The separation was applied with a C18 column (4.6 mm x 250 mm i.d., 5 µm p.s.) at 30 °C and a photodiode array detector was set at 317 nm. Intraday and interday precision were found ≤ 0.65% (More, Dalwate, Chandramore, Jadhav, & Jain, 2019).

Measurement of esomeprazole and pirfenidone levels in rat plasma samples

The developed HPLC method was employed for monitorization of the esomeprazole and pirfenidone levels in plasma samples belong to 14 rats that were treated with esomeprazole (50 mg/kg/day) and pirfenidone (100 mg/kg/day). The esomeprazole and pirfenidone dose values to be applied to rats were determined according to the results of the previous studies in our laboratory.

Plasma samples were treated with the solid-phase extraction method described in Section 2.4 and made ready for HPLC

analysis. No problem was observed in the samples for the quantification of the analytes. Additionally, peak purity showed that no analytical interference was encountered in the endogenous substances. The daily used esomeprazole and pirfenidone amounts, both their plasma levels and their dose-proportional plasma levels with the descriptive statistical analysis results for the obtained data were given in Table 4.

Table 4. Sample results which involved rat plasma esomeprazole and pirfenidone concentrations that are unrevised and dose-proportional.

Sample number	Esomeprazole (50 mg/kg/day)		Pirfenidone (100 mg/kg/day)	
	Plasma concentration (ng/mL)	Plasma concentration /Dose (ng/mL/mg)	Plasma concentration (ng/mL)	Plasma concentration /Dose (ng/mL/mg)
S.01	27.89	0.56	4.08	0.04
S.02	3.49	0.07	1.36	0.01
S.03	8296.87	165.94	-	-
S.04	202.21	4.04	4.08	0.04
S.05	6.97	0.14	39.84	0.40
S.06	7.85	0.16	45.28	0.45
S.07	5.23	0.11	3.62	0.04
S.08	1.74	0.04	1.81	0.02
S.09	2.62	0.05	0.45	0.01
S.10	0.87	0.02	53.43	0.53
S.11	9.59	0.19	129.04	1.29
S.12	12.20	0.24	122.70	1.22
S.13	1.74	0.04	238.60	2.39
S.14	2.62	0.05	154.39	1.54
Mean (x̄)	612.99	12.26	3.75	0.61
SD (σ)	2212.19	44.24	11.14	0.76
RSD%	360.89	360.89	297.48	124.27

Abbreviations: SD stands for "Standard Deviation"; RSD is "Relative Standard Deviation".

In this study, it was aimed to establish a method by focusing especially on the expected esomeprazole and pirfenidone concentrations in rat plasma. Therefore, these concentrations were taken into account in establishing the method and performing validation tests. For this purpose, in our study, a narrow linear range of 5 and 50 ng/mL was preferred for esomeprazole and pirfenidone, and a strong determination coefficient (r≥0.9986) was obtained in both analytes. The LOQ obtained was found to be the lowest value (≤ 0.58 ng/mL) detected in the literature. Chromatographic analysis was completed in 7 mins total without any endogenous intervention into the plasma sample. The value obtained from the precision test as ≤7.89% during the

day and between days is compatible with the literature. Nice values between (-4.45) and 5.78 (RE%) were obtained from intraday and inter-day accuracy tests. The average recovery values from the application of the preferred solid-phase extraction in preparing the samples for HPLC analysis were 93.83 to 97.44% for esomeprazole and pirfenidone, respectively. The data obtained from the robustness test carried out according to the change in mobile phase content, mobile phase flow rate, column temperature and UV value was ≤ 4.85 (RSD%).

Obtained plasma esomeprazole and pirfenidone and their dose rated results were statistically analyzed with Spearman non-parametric test. The results showed that there was no statistically significant relationship between the analyzed results ($p>0.05$).

CONCLUSION

We strongly recommend this validated method to be used in routine therapeutic drug analysis of esomeprazole and pirfenidone. Also, it can be adapted to human plasma for monitoring overdose/poisoning caused by these drugs. Furthermore, since the method is established in the range of 25 to 500 ng/mL, it can be used in case of compliance problems with these drugs. The proposed method can be easily applied in routine therapeutic drug monitoring (TDM) studies of esomeprazole and pirfenidone. Also, it can be preferred in bioequivalence, pharmacovigilance and pharmacokinetics studies.

In this study, it was observed that both plasma-esomeprazole levels and plasma-esomeprazole concentration corrected according to daily drug doses ($\mu\text{g}/\text{mL}/\text{mg}$) has very high RSD% value which is 360.89%. In addition, both plasma-esomeprazole levels and plasma-esomeprazole corrected according to daily drug doses ($\mu\text{g}/\text{mL}/\text{mg}$) had significantly high RSD% results which were 297.48 and 124.27%, respectively. These results are both pharmacologically and toxicologically significant, and indicate that the potential to cause serious health problems for esomeprazole treatment.

Since these observed unexpected plasma esomeprazole and pirfenidone concentrations are thought to be related to the polymorphism of the CYP2C19 and CYP2A1 enzymes which are responsible for the biotransformation of esomeprazole and pirfenidone, the polymorphisms of the respective enzymes in the collected blood samples and its relationship with the plasma results obtained are planned to be investigated.

Acknowledgement: Authors would like to thank Sivas Cumhuriyet University, Faculty of Medicine Scientific Research Centre abbreviated as CÜTFAM for the invaluable open collaboration shown during this research.

Peer-review: Externally peer-reviewed.

Author contributions: Conception/Design of Study- E.D., S.T.K., S.K.; Data Acquisition- E.D., S.T.K.; Data Analysis/Interpretation- E.D.; Drafting Manuscript- E.D., S.T.K., S.K.; Critical Revision of Manuscript- E.D.; Final Approval and Accountability- E.D., S.T.K., S.K..

Conflict of Interest: The authors have no conflict of interest to declare.



Financial Disclosure: This research was supported by The Scientific Research Projects Support Programme of Sivas Cumhuriyet University (CÜBAP) under project number T-684.

REFERENCES

- Bodempudi, S.B., Babur, R., & Reddy, K.S. (2015). Development and substantiation of a RP-HPLC method for monitoring of impurities in pirfenidone drug substance. *American Journal of Analytical Chemistry*, 06(13), 1019–1029.
- Çelebi, A., Aydın, D., Kocaman, O., Konduk, B.T., Şentürk, Ö., & Hül-agü, S. (2016). Comparison of the effects of esomeprazole 40 mg, rabeprazole 20 mg, lansoprazole 30 mg, and pantoprazole 40 mg on intragastric pH in extensive metabolizer patients with gastro-esophageal reflux disease. *The Turkish Journal of Gastroenterology*, 27(5), 408–414.
- Eltahir, H.M., & Nazmy, M.H. (2018). Esomeprazole ameliorates CCl4 induced liver fibrosis in rats via modulating oxidative stress, inflammatory, fibrogenic and apoptotic markers. *Biomedicine and Pharmacotherapy*, 97, 1356–1365.
- Estevez, P., Flor, S., Boscolo, O., Tripodi, V., & Lucangioli, S. (2014). Development and validation of a capillary electrophoresis method for determination of enantiomeric purity and related substances of esomeprazole in raw material and pellets. *Electrophoresis*, 35(6), 804–810.
- Franke, A., Hepp, C., Harder, H., Beglinger, C., & Singer, M. V. (2008). Esomeprazole reduces gastroesophageal reflux after beer consumption in healthy volunteers. *Scandinavian Journal of Gastroenterology*, 43(12), 1425–1431.
- Ghebre, Y.T., & Raghu, G. (2016). Idiopathic pulmonary fibrosis: Novel concepts of proton pump inhibitors as antifibrotic drugs. *American Journal of Respiratory and Critical Care Medicine*, 193(12), 1345–1352.
- Ghebremariam, Y.T., Cooke, J.P., Gerhart, W., Griego, C., Brower, J.B., Doyle-Eisele, M., ... Rosen, G.D. (2015). Pleiotropic effect of the proton pump inhibitor esomeprazole leading to suppression of lung inflammation and fibrosis. *Journal of Translational Medicine*, 13(1), 1–20.
- Gopinath, S., Kumar, R.S., Shankar, M.B., & Danabal, P. (2013). Development and validation of a sensitive and high-throughput LC-MS/MS method for the simultaneous determination of esomeprazole and naproxen in human plasma. *Biomedical Chromatography*, 27(7), 894–899.
- Hodgson, U., Laitinen, T., & Tukiainen, P. (2002). Nationwide prevalence of sporadic and familial idiopathic pulmonary fibrosis: evidence of founder effect among multiplex families in Finland. *Thorax*, 57(4), 338–342.
- ICH, I. (2005). Q2 (R1): Validation of analytical procedures: Text and methodology. In *International Conference on Harmonization, Geneva*.
- Iyer, S. N., Wild, J. S., Schiedt, M. J., Hyde, D.M., Margolin, S. B., & Giri, S. N. (1995). Dietary intake of pirfenidone ameliorates bleomycin-induced lung fibrosis in hamsters. *The Journal of Laboratory and Clinical Medicine*, 125(6), 779–785.
- Jain, D. K., Jain, N., Charde, R., & Jain, N. (2011). The RP-HPLC method for simultaneous estimation of esomeprazole and naproxen in binary combination. *Pharmaceutical Methods*, 2(3), 167–172.
- Johnson, D. A. (2003). Review of esomeprazole in the treatment of acid disorders. *Expert Opinion on Pharmacotherapy*, 4(2), 253–264.
- Kayesh, R., & Sultan, M. Z. (2015). A novel ion-pair RP-HPLC method for simultaneous quantification of naproxen and esomeprazole in pharmaceutical formulations. *Journal of Chromatographic Science*, 53(5), 687–693.

- Kehrer, J.P., & Margolin, S.B. (1997). Pirfenidone diminishes cyclophosphamide-induced lung fibrosis in mice. *Toxicology Letters*, 90(2-3), 125-132.
- Liu, R., Li, P., Xiao, J., Yin, Y., Sun, Z., Bi, K., & Li, Q. (2017). A fast, sensitive, and high throughput method for the determination of esomeprazole in dog plasma by UHPLC-MS/MS: Application to formulation development of the compound preparation of esomeprazole. *Journal of Chromatography B: Analytical Technologies in the Biomedical and Life Sciences*, 1068-1069, 352-357.
- Ma, J., Sun, F., Chen, B., Tu, X., Peng, X., Wen, C. . . Wang, X. (2017). Tissue metabolic changes for effects of pirfenidone in rats of acute paraquat poisoning by GC-MS. *Toxicology and Industrial Health*, 33(12), 887-900.
- Marshall, R.P., Puddicombe, A., Cookson, W.O., & Laurent, G.J. (2000). Adult familial cryptogenic fibrosing alveolitis in the United Kingdom. *Thorax*, 55(2), 143-146.
- Micolini, L., Mandrioli, R., Amore, M., & Raggi, M. A. (2008). Separation and HPLC analysis of 15 benzodiazepines in human plasma. *Journal of Separation Science*, 31(14), 2619-2626.
- More, S., Dalwate, S., Chandramore, N., Jadhav, V., & Jain, A. (2019). Development of chromatographic method and validation for estimation of pirfenidone in bulk and pharmaceutical dosage form. *International Research Journal of Pharmacy*, 10(7), 45-50.
- Khan, M.M.G., Shirkhedkar, A., Chaudhari, P., & Pawara, P.I. (2019). Analytical techniques for pirfenidone and terizidone: a review. *International Journal of Pharmaceutical Chemistry and Analysis*, 6(1), 1-5.
- Nadrous, H.F., Myers, J.L., Decker, P.A., & Ryu, J.H. (2005). Idiopathic pulmonary fibrosis in patients younger than 50 years. *Mayo Clinic Proceedings*, 80(1), 37-40.
- Parmar, V.K., Desai, S.B., & Vaja, T. (2014). RP-HPLC and UV spectrophotometric methods for estimation of pirfenidone in pharmaceutical formulations. *Indian Journal of Pharmaceutical Sciences*, 76(3), 225-229.
- Prabu, S.L., Shirwaikar, A., Shirwaikar, A., Kumar, C.D., Joseph, A., & Kumar, R. (2008). Simultaneous estimation of esomeprazole and domperidone by UV spectrophotometric method. *Indian Journal of Pharmaceutical Sciences*, 70(1), 128-131.
- Raghu, G., Chen, S.-Y., Yeh, W.-S., Maroni, B., Li, Q., Lee, Y.-C., & Colvard, H. R. (2014). Idiopathic pulmonary fibrosis in US Medicare beneficiaries aged 65 years and older: incidence, prevalence, and survival, 2001-11. *The Lancet. Respiratory Medicine*, 2(7), 566-572.
- Raman, N.V.V.S.S., Reddy, K.R., Prasad, A.V.S.S., & Ramakrishna, K. (2008). Development and validation of a GC-MS method for the determination of methyl and ethyl camphorsulfonates in esomeprazole magnesium. *Chromatographia*, 68(7), 675-678.
- Ravisankar, P., Anusha Rani, K., Devadasu, C., & Devala Rao, G. (2014). A novel validated RP-HPLC method for the determination of pirfenidone in pharmaceutical dosage forms. *Der Pharmacia Lettre*, 6(5), 19-29.
- Sambhani, N.G., & Biju, V.M.N. (2018). A micelle-enhanced spectrofluorimetric determination of pirfenidone: application to content uniformity testing and human urine. *Journal of Fluorescence*, 28(4), 951-957.
- Sebaiy, M.M., Hassan, W.S., & Elhennawy, M.E. (2019). Developing a high-performance liquid chromatography (HPLC) method for simultaneous determination of oxytetracycline, tinidazole and esomeprazole in human plasma. *Journal of Chromatographic Science*, 57(8), 724-729.
- Sotgia, S., Fois, A.G., Sotgiu, E., Zinellu, A., Paliogiannis, P., Mangoni, A.A., & Carru, C. (2020). Micellar electrokinetic capillary chromatographic determination of pirfenidone and 5-carboxy-pirfenidone by direct injection of plasma from patients receiving treatment for idiopathic pulmonary fibrosis (IPF). *Microchemical Journal*, 154, 104536.
- Talaat, W. (2017). Bioanalytical method for the estimation of co-administered esomeprazole, leflunomide and ibuprofen in human plasma and in pharmaceutical dosage forms using micellar liquid chromatography. *Biomedical Chromatography*, 31(5).
- Thorat, S.G., Padmane, S.P., Tajne, M.R., & Ittadwar, A.M. (2016). Development and validation of simple, rapid and sensitive UV, HPLC and HPTLC methods for the estimation of pirfenidone in tablet dosage form. *Journal of the Chilean Chemical Society*, 61(2), 2978-2981.
- Tong, S., Wang, X., Jiang, H., Xu, X., Pan, Y., Chen, K. . . Hu, G. (2010). Determination of pirfenidone in rat plasma by LC-MS-MS and its application to a pharmacokinetic study. *Chromatographia*, 71(7), 709-713.
- Wang, Y., Zhao, X., Zhong, J., Chen, Y., Liu, X., & Wang, G. (2006). Simple determination of pirfenidone in rat plasma via high-performance liquid chromatography. *Biomedical Chromatography*, 20(12), 1375-1379.
- Wen, Y.-G., Liu, X., He, X.-L., Shang, D.-W., Ni, X.-J., Zhang, M. . . Qiu, C. (2014). Simultaneous determination of pirfenidone and its metabolite in human plasma by liquid chromatography-tandem mass spectrometry: application to a pharmacokinetic study. *Journal of Analytical Toxicology*, 38(9), 645-652.

Preparation and *in vitro* studies of fixed-dose tablet combination of repaglinide and metformin

Sinem Şahin¹ , Burcu Mesut² , M. Ezgi Durgun² , Esher Özçelik³ , Yıldız Özsoy² 

¹Onko Koçsel Pharmaceuticals, Kocaeli, Turkey

²Istanbul University, Faculty of Pharmacy, Pharmaceutical Technology Department, Istanbul, Turkey

³Cibali Health and Social Security Center, Istanbul, Turkey

ORCID IDs of the authors: S.Ş. 0000-0002-0377-2757; B.M. 0000-0003-2838-1688; M.E.D. 0000-0001-5724-9809; E.Ö. 0000-0002-5611-1143; Y.Ö. 0000-0002-9110-3704

Cite this article as: Sahin, S., Mesut, B., Durgun, M.E., Ozcelik, E., & Ozsoy, Y. (2021). Preparation and *in vitro* studies of fixed-dose tablet combination of repaglinide and metformin. *Istanbul Journal of Pharmacy*, 51 (1), 26-34.

ABSTRACT

Background and Aims: The study aimed to design a Fixed-dose tablet formulation of Metformine and Repaglinide.

Methods: Wet granulation method was used to prepare tablet formulations. Characterization studies and dissolution studies were performed.

Results: A stable formulation was developed according to the requirements of the pharmacopoeia criteria. This new formulation dissolution results showed that Repaglinide and Metformin HCl dissolved more than 85% from film tablets at 15 minutes.

Conclusion: Thus, an alternative product to the market product was developed.

Keywords: Fixed-Dose Tablet, Metformin, Repaglinide

INTRODUCTION

Life expectancy is an average statistical data that indicates how long a newborn will live, assuming that death rates remain constant from the moment it is born. It is rapidly increasing worldwide thanks to factors such as the advancement of technology, development in new and effective treatment methods, improving the quality of care services, and facilitating individuals' access to care services. Since individuals' daily lives are directly affected by the socioeconomic status of the society they live in and the living standards offered by that country, life expectancy is calculated specifically for each country. The life expectancy of western countries is higher all around the world. As life expectancy increases, the prevalence of non-communicable chronic diseases (NCDs) such as cardiovascular, metabolic, and respiratory diseases may increase. Also, the changes in eating habits and the spread of fast-food-style nutrition throughout the world and the widespread of a sedentary lifestyle have a negative effect on individuals' metabolism. Thus, the diseases that are expected to be seen in the elderly population can be encountered at a younger age, even in the adolescent period.

Diabetes Mellitus (DM) is a metabolic disorder that causes hyperglycemia with impaired insulin production and/or function (Maffi & Secchi, 2017; Spampinato, Caruso, De Pasquale, Sortino, & Merlo, 2020). The American Diabetes Association (ADA) classified DM into two primary classes, types 1 and 2 (American Diabetes Association, 2015). In type 1 diabetes, insulin insufficiency occurs due to the destruction of the β -cells of the pancreas, where insulin is secreted. Type 2 diabetes is characterized by insulin resistance due to progressive insulin secretion defects. Type 2 DM usually occurs concerning age (Longo et al., 2019). A rapid

Address for Correspondence:

Yıldız ÖZSOY, e-mail: yozsoy@istanbul.edu.tr

Submitted: 13.07.2020
Revision Requested: 30.07.2020
Last Revision Received: 03.09.2020
Accepted: 14.10.2020

This work is licensed under a Creative Commons Attribution 4.0 International License.



increase in its prevalence was observed with prolonged life expectancy. The World Health Organization (WHO) reported that more than 425 million people worldwide live with diabetes, and more than 1.6 million deaths are directly related to diabetes (Rachdaoui, 2020; World Health Organization, 2020). Also, contrary to popular belief, Type 2 DM can be seen during childhood and adolescence (American Diabetes Association, 2000). Obesity, mainly due to changes in dietary and lifestyle habits, increased the prevalence of type 2 DM among children as well as adults. DM may destroy the vascular and neurological system due to hyperglycemia (Malone, 2016). Thus, different cases of NCDs are also seen in DM patients who cannot be treated efficiently. Problems in controlling the DM and accompanying other diseases seriously reduce the quality of life of the patient and his/her family and increase the costs of hospitalization (Riddle & Herman, 2018; Young-Hyman et al., 2016). One of the approaches developed in the treatment of Type 2 DM is to combine drugs to eliminate all the problems (Massi-Benedetti & Orsini-Federici, 2008).

Combine drug therapy is the combined usage of active pharmaceutical ingredient (API) that has successful results with different action mechanisms in the treatment of a single disease. If a more effective and/or faster treatment process is desired, combined therapy can be preferred. Studies have shown that combined therapy with additional APIs in the treatment of chronic diseases is five times effective than increasing the dose of the drug used in single therapy by two times (Tsioufis & Thomopoulos, 2017). In cases where hyperglycemia can not be controlled in type 2 DM patients with a single treatment agent, combined therapy is started (Massi-Benedetti & Orsini-Federici, 2008). Considering the damage caused by hyperglycemia on the vascular and neural system, the combined treatment approach seems to be a clinical requirement rather than an option. Despite these significant advantages, combine treatment has two main disadvantages. One of these disadvantages is since the increasing number of drugs that the patient will take in one time, the patient's compliance may decrease. Increasing health care costs is the other one. To overcome this situation, fixed-dose combinations (FDCs) have been developed. FDCs are pharmaceutical dosage forms prepared by combining two or more APIs in a single formulation (Gautam & Saha, 2008; Godman, McCabe, & D Leong, 2020; Tangalos & Zarowitz, 2005). Owing to FDCs, patient compliance may increase as it will use fewer drugs at one time and achieve a more therapeutic effect. Also, since the therapeutic effect will be increased, the dose of each APIs can be reduced. Thus systemic side effects can be reduced.

Metformin, a biguanide drug, is a first option in the treatment of type 2 DM patients who cannot be controlled with lifestyle changes (Lefèbvre & Scheen, 1992; Sanchez-Rangel & Inzucchi, 2017). It is used safely in Europe since 1957 and in America since 1995 (Pernicova & Korbonits, 2014). It increases the effect of insulin in the liver and decreases hepatic glucose production (Natali & Ferrannini, 2006). Although it has little impact on the absorption of glucose in the gastrointestinal tract, it can delay the absorption of glucose (Czyzyk, Tawecki, Sadowski, Ponikowska, & Szczepanik, 1968; Pernicova & Korbonits, 2014).

The most significant advantage of metformin is that it does not cause hypoglycemia while reducing the blood glucose level (Nasri & Rafeian-Kopaei, 2014). As a medicine that has been used for years, the therapeutic safety is quite high. It is indicated for use in gestational diabetes, polycystic ovarian syndrome, metabolic syndrome or prediabetes period, as well as type 2 DM (Cicero, Tartagni, & Ertek, 2012; Hostalek, Gwilt, & Hildemann, 2015). Metformin is used single or combined with other antidiabetes agents in the treatment of type 2 DM (Sanchez-Rangel & Inzucchi, 2017).

Repaglinide, a derivative of carbamoylbenzoic acid, enhances insulin secretion from pancreatic β -cells by closing ATP-sensitive potassium (KATP) channels in the plasma membrane (Johansen & Birkeland, 2007; Scott, 2012). It has a short duration of action (Abbink, van der Wal, Sweep, Smits, & Tack, 2004). It can be used primarily in type 2 DM patients with renal insufficiency since the kidneys do not perform its metabolism and elimination (Hasslacher, 2003). There are also studies showing that pharmacokinetic data in individuals with renal impairment can be safely used by kidney patients, although some studies have demonstrated minor differences to healthy individuals (Marbury, 2000; Schumacher et al., 2001; Scott, 2012).

The combined therapy of type 2 DM with repaglinide and metformin was approved in the USA in 1997 and in Europe in 1998. Since repaglinide, which provides insulin secretion, has a short-term effect, when used with metformin, the secreted insulin has the highest possible effect. Also, the fact that this combination does not have a negative effect on hepatic β -cells provides safe control of hyperglycemia for a long time (Kawamori et al., 2014).

In this study, stable fixed-dose combinations of Repaglinide and Metformin HCl with rapid drug release profiles were developed.

MATERIALS AND METHODS

Materials

Repaglinide (Polpharma, Poland), Metformin HCl (Aarti Drugs Limited, India), Povidone (PVP K25) (BASF), Microcrystalline Cellulose Types 101 and 102 (Vivapur 101 and Vivapur 102) (JRS Pharma), Sorbitol (Roquette), Polyethylene Glycol 6000 (Magrogol 6000) (Clariant), Poloxamer 188 (BASF), Meglumine (Merck), Polacriline potassium (Amberlite IRP88) (DOW), Ethanol (JT Baker), Magnesium stearate (FACI SpA), Opadry Pink 03B240027 (Colorcon). All other chemicals were analytical grade.

Methods

Active ingredients and excipients compatibility studies

Excipients that are included in the composition of repaglinide / metformin HCl 2 mg / 500 mg film tablet are defined in international pharmacopoeias. Also, in the literature for the reference product PrandiMet (repaglinide/metformin HCl) Tablet 2 mg / 500 mg, the excipients found in the content of the product were identified and mostly the same excipients were used in the developed formulation. To decide the

appropriate excipients compatibility tests were performed. The samples were stored for 30 days at different ratios and in different environments (2-8°C, 25°C±2°C; 60%±5% RH and 40°C±2°C; 75%±5% RH) and their compatibilities were examined after 30 days. DSC thermal analysis methodology was used to evaluate the compatibility. The tests were performed by using approximately 5 mg sample in a hermetic aluminum sample holder and heated from 35°C to 350°C at a heating rate of 10°C/min, an empty pan was used as the reference, the details of the studies are given in Table 1.

Preformulation studies

Preformulation studies were carried out to determine the quantitative composition of the formulation of the film tablets to be prepared. As a result of these studies, the physical parameters of the core tablets (hardness, disintegration, friability) were evaluated and film coating of the formulations closest to the physical parameters of the reference product was prepared, and the dissolution tests of this formulations were performed and compared with the reference product.

Table 1. Active ingredients and excipients compatibility studies details.

No	Mixture	Mixture ratio	2-8°C 30 day		25°C±2°C, 60%±5% RH 30 day		40°C±2°C, 75%±5% RH 30 day	
			*p	*p	**UP	*p	**UP	
1	Metformin HCl	-	+	+	+	+	+	+
2	Repaglinide	-	+	+	+	+	+	+
3	Metformin HCl+ Repaglinide	20:1	+	+	+	+	+	+
4	(Metformin HCl+ Repaglinide)***+ PVP K25	10:1	+	+	+	+	+	+
5	(Metformin HCl+ Repaglinide)***+Poloxamer 188	20:1	+	+	+	+	+	+
6	(Metformin HCl+ Repaglinide)***+ Meglumin	20:1	+	+	+	+	+	+
7	(Metformin HCl+ Repaglinide)***+ MCC tip 101	5:1	+	+	+	+	+	+
8	(Metformin HCl+ Repaglinide)***+ Sorbitol	10:1	+	+	+	+	+	+
9	(Metformin HCl+ Repaglinide)***+ Magrogol 6000	20:1	+	+	+	+	+	+
10	(Metformin HCl+ Repaglinide)***+ Polakrilin potasyum (Amberlite IRP88)	10:1	+	+	+	+	+	+
11	(Metformin HCl+ Repaglinide)***+ Akdisol	10:1	+	+	+	+	+	+
12	(Metformin HCl+ Repaglinide)***+ Starch 1500	10:1	+	+	+	+	+	+
13	(Metformin HCl+ Repaglinide)***+ Magnezyum stearat	20:1	+	+	+	+	+	+
14	(Metformin HCl+ Repaglinide)***+ Opadry II 85F240049 Pink	20:1	+	+	+	+	+	+
15	(Metformin HCl+ Repaglinide)***+ Opadry II 85F220124 Yellow	20:1	+	+	+	+	+	+
16	(Metformin HCl+ Repaglinide)***+ Opadry 03B240027 Pink	20:1	+	+	+	+	+	+
17	(Metformin HCl+ Repaglinide)***+ Opadry 03B220042 Yellow	20:1	+	+	+	+	+	+

*Packaged; **Unpackaged; ***The Metformin HCl + Repaglinide mixture was prepared in a 20:1 ratio.

Pilot scale batch production

Pilot productions were prepared by using the wet granulation method. Firstly, Repaglinide granule mixture and Metformin HCl granule mixture were prepared and dried in the oven at 50°C until to obtain well-dried granules to a loss of drying value is less than 2%. Dried granules were blended with external granular phase excipients. Three series of pilot production was carried out by using the unit formula and the production method determined based on the results of the *in vitro* dissolution test performed at zero time and after waiting for one month at 40°C±2°C; 75%±5% RH of the pre-formulation studies.

The tablet serial size prepared for pilot production was 100,000 and serial numbers were P001, P002 and P0003, respectively.

Physicochemical properties and dissolution tests

Physical tests (weight variation, hardness, diameter, thickness, water content), assay, content uniformity and dissolution tests were performed on the tablets prepared in the preformulation studies on the tablets in the pilot product series.

Tablet weight variation tests were performed according to the EP 6 section 2.9.5. Uniformity of Mass of Single-Dose (European Pharmacopeia, 2008). Twenty tablets were taken and weighed individually using digital analytical balance (Sartorius BP 3105, Germany). The results were recorded.

Tablet hardness test was performed by using Erweka hardness test equipment (D63150, Germany). 10 tablets were tested and the average hardness value (N) was recorded.

Disintegration test was performed according to USP <701> Disintegration test (2019). 6 tablets were checked (Erweka ZT304, Germany) and their disintegration times (min.) were recorded.

Friability % test was performed using Erweka TAR 220 (Germany) friability tester in accordance with USP <1216> Tablet Friability (2019). Weight loss % was calculated.

The analysis of Metformin HCl and Repaglinide were performed by using different system. To analyse Metformin HCl, HPLC system was used and the system was operated at 40°C at a flow rate of 1 mL/min and 240 nm. The injection volume was 10 µL. To analyse Repaglinide, UPLC system was used and the system was operated at 25°C at a flow rate of 0.3 mL/min and 240 nm. The injection volume was 10 µL.

The Repaglinide/Metformine HCl tablet dissolution test method was performed according to the FDA dissolution method (FDA, 2009). USP apparatus II with the paddle method was used at 37°C±0.5 at 50 rpm and the medium was pH 5.0 citric acid/phosphate buffer. The samples were taken from the dissolution medium at the determined time intervals 5, 10, 15, 20, 30, 45 and 60 minutes.

The dissolution rate test was performed on the film tablets obtained as a result of pilot productions and the reference tablet (PrandiMet Tablets 2 mg / 500 mg) in the pH 5.0 citric acid/phosphate buffer. *In vitro* dissolution tests were performed

to the pilot production series and to the reference product at three different pHs (1.2, 4.5 and 6.8) of the gastrointestinal tract recommended by the EMA guidelines and f2 similarity factors were calculated. An f2 value greater than 50 to be taken here shows the similarity between the two formulations (EMA, 2010).

Stability studies

The prepared tablets were put in the final packing and kept for stability studies. The stability studies were carried out in accordance with the storage conditions specified in the ICH Q1A (R2) guide of the three pilot production series produced. According to the ICH Q1A (R2) (2003) guidelines (ICH, 2003), long-term stability operating conditions are 25°C±2°C / 60%±5% RH and accelerated stability conditions are 40°C±2°C / 75%±5% RH. During stability, at different time intervals, the tablets were tested for its physicochemical parameters which include appearance, weight average, hardness, assay, dissolution and impurities.

RESULTS AND DISCUSSION

Active ingredients and excipients compatibility test results

It was seen that all the samples in different storage conditions (2-8°C, 25°C±2°C; 60%±5% RH and 40°C±2°C / 75%±5% RH) of the mixtures prepared with all excipients were found suitable. There was any inconsistency in the graphics of the studies. The DSC graphic showing 10:1 active ingredients (Metformin HCl and Repaglinide) / Starch 1500 mixtures is given in Figure 1.

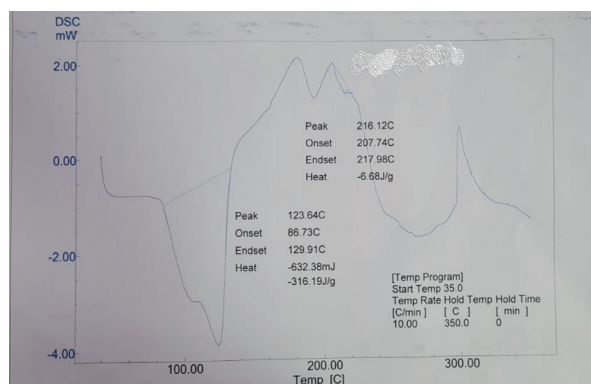


Figure 1. Active ingredients (Metformin HCl and Repaglinide):Starch 1500 mixture (10:1) DSC graphic under 25°C±2°C / 60%±5% RH condition after 30 days.

Preformulation studies

Preformulation studies were performed, the Components of D001 and D002 formulations and the detected quantitative amounts are given in Tables 2 and 3.

The unit formula of the optimum formula determined as a result of the tests made on the tablets obtained by the preformulation studies is given in Table 4.

Physicochemical properties and dissolution tests

Physicochemical test results of the formulations D001 and D002 prepared in the preformulation studies are given in the

Table 2. Unit formula of Repaglinide / Metformin HCl 2 mg / 500 mg film tablets coded D001.

Active Ingredient and excipients	Unit formula (mg/tablet)
Repaglinide Granule	
Repaglinide	2.00
Povidone (PVP K25)	0.572
Poloksamer 188	0.572
Meglumine	1.00
Microcrystalline cellulose 101 (Vivapur 101)	44.00
Deionized water	qs.
Metformin HCl Granule	
Metformin HCl	500.00
Povidone (PVP K25)	20.00
Sorbitol	10.00
Polyethylene glycol (Magrogol 6000)	5.00
Deionized water	qs.
External Phase	
Microcrystalline cellulose 112 (Vivapur 112)	20.00
Polacrillin potassium (Amberlite IRP88)	18.76
Magnesium stearate	3.10
Core tablet weight	625.00
Opadry 3B240027 Pink	15.00
Deionized water	135.00
Film tablet weight	640.00

Table 3. Unit formula of Repaglinide / Metformin HCl 2 mg / 500 mg film tablets coded D002.

Active Ingredient and excipients	Unit formula (mg/tablet)
Internal Phase	
Repaglinide	2.00
Metformin HCl	500.00
Poloksamer 188	0.572
Meglumine	1.00
Microcrystalline cellulose 101 (Vivapur 101)	44.00
Povidone (PVP K25)	20.572
Sorbitol	10.00
Polyethylene glycol (Magrogol 6000)	5.00
Ethanol	qs.
Deionized water	qs.
External Phase	
Microcrystalline cellulose 102 (Vivapur 112)	20.00
Polacrillin potassium (Amberlite IRP88)	18.76
Magnesium stearate	3.10
Core tablet weight	625.00
Opadry 3B240027 Pink	15.00
Deionized water	135.00
Film tablet weight	640.00

Table 4. Unit formula of the optimised formulation.

Active Ingredient and excipients	Unit formula (mg/tablet)
Internal Phase	
Repaglinide	2.00
Metformin HCl	500.00
Poloksamer 188	0.572
Meglumine	1.00
Microcrystalline cellulose 101 (Vivapur 101)	44.00
Povidone (PVP K25)	20.572
Sorbitol	10.00
Polyethylene glycol (Magrogol 6000)	5.00
Ethanol	qs.
Deionized water	qs.
External Phase	
Microcrystalline cellulose 102 (Vivapur 112)	20.00
Polacrillin potassium (Amberlite IRP88)	18.76
Magnesium stearate	3.10
Core tablet weight	625.00
Opadry 3B240027 Pink	15.00
Deionized water	135.00
Film tablet weight	640.00

Table 5. Physicochemical test results of formulations D001 and D002.

Tests	D001	D002
Appearance	White or whitish oblong, biconvex tablet White or whitish oblong, biconvex tablet	White or whitish oblong, biconvex tablet White or whitish oblong, biconvex tablet
Average tablet weight (mg)	623.5	624.2
Hardness (N)	130	120
Disintegration time (min.)	4	2
Friability (%)	0.1	0.2
Loss of Water Content (%)	2.28	2.11

Table 5. There was no significant difference in the test results obtained from the D001 and D002 formulations.

Consequently, the calibration curves used to analyze the concentration of Metformin HCl and Repaglinide showed good linear relationship over the concentration range 139,71 -399,385 µg/mL and 1,80 – 8,03 µg/mL. The correlation coefficient values were above then >0,99 and precise (intra- and inter-day variation <2%) and accurate (mean recovery>98 %).

The LOD and LOQ values of Metformin HCl were 18,67 µg/mL and 56,58 µg/mL, respectively. And, The LOD and LOQ values of Repaglinide were 0,80 and 1,68 µg/mL, respectively.

The findings of the dissolution study of pilot production tablets and commercial product in pH 5.0 environment are given in Figure 2. At the end of 15 minutes, it was observed that both repaglinide and metformin dissolved above 85% in all formulations.

The dissolution data's of pilot production series (P001 and P002) and commercial product in different pH's 1.2, 4.5 and 6.8 are given in Figures 3, 4 and 5, respectively. As a result of dissolution studies conducted in different environments, it was observed that the active substances dissolved above 85% after 15 minutes.

When *in vitro* dissolution rate test data were examined, it was determined that the amount of active substances released from

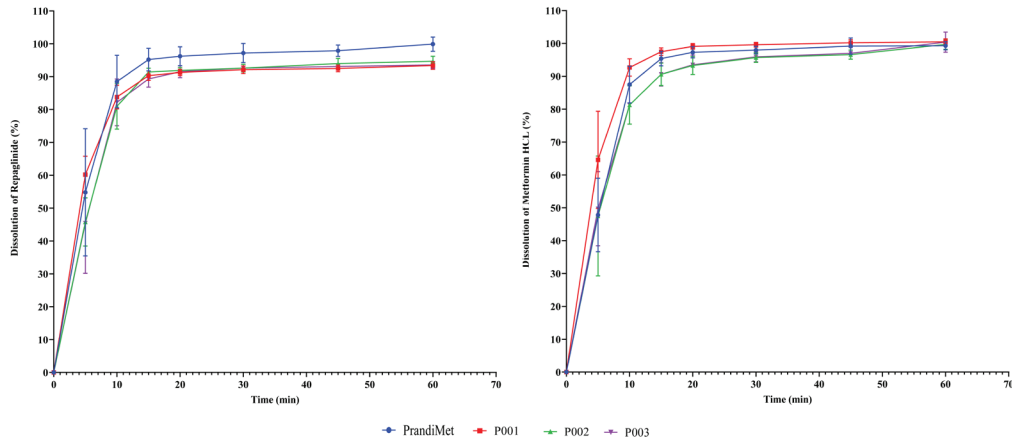


Figure 2. Pilot production formulations and the commercial product dissolution study results in pH 5.0.

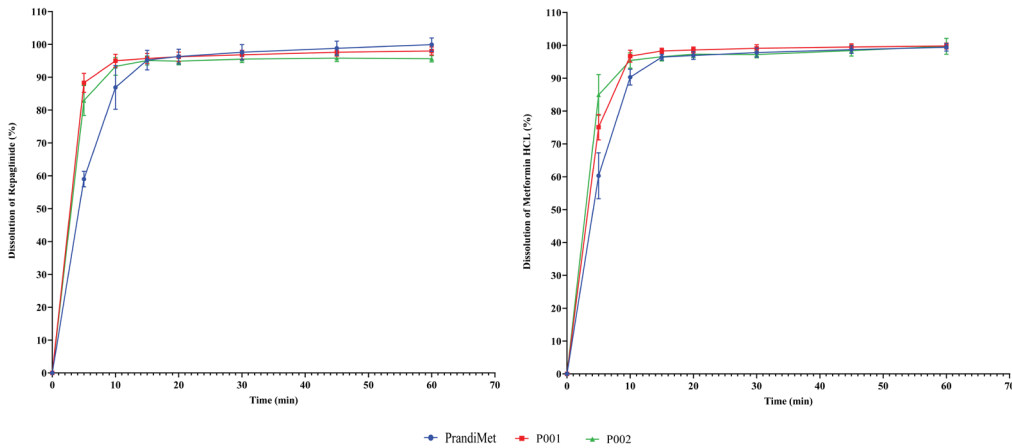


Figure 3. The dissolution profile of the commercial product and pilot production series (P001 and P002) in pH 1.2 buffer.

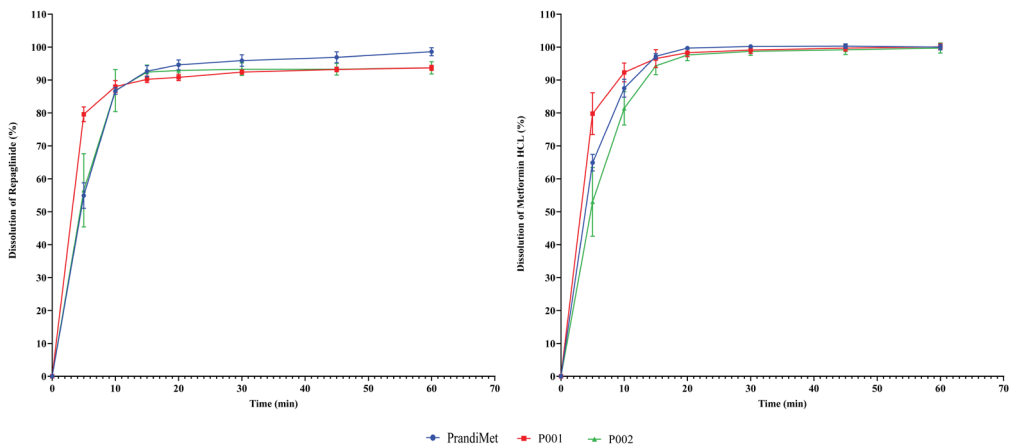


Figure 4. The dissolution profile of the commercial product and pilot production series (P001 and P002) in pH 4.5 buffer.

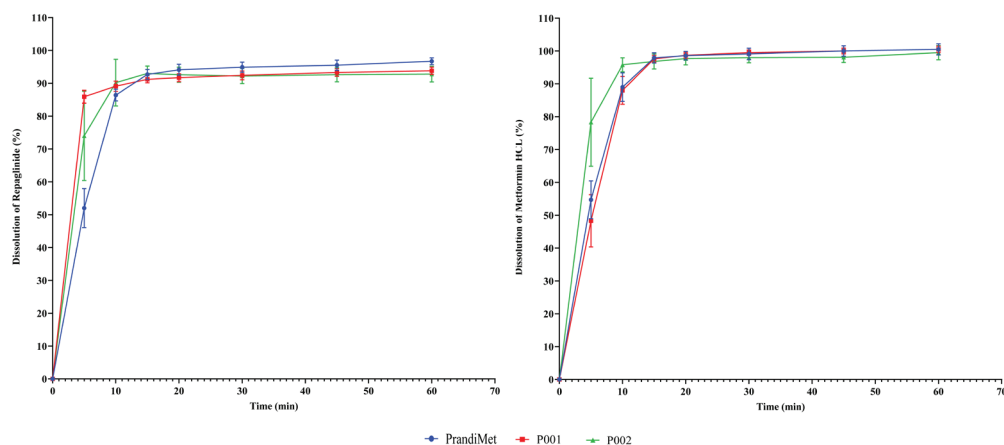


Figure 5. The dissolution profile of the commercial product and pilot production series (P001 and P002) in pH 6.8 buffer.

tablets in all 3 environments was more than 85% in 15 minutes. For this reason, it was found that they are equivalent according to EMA criteria and there is no need to perform f_2 similarity test.

Stability studies

The stability studies are very important to provide the evidence about the quality of the tablet formulation that chang-

es with time through environmental aspects. Prepared tablets were kept in stability cabins for 6 months for accelerated stability studies ($40^{\circ}\text{C}\pm 2^{\circ}\text{C}$ / $75\%\pm 5\%$ RH) and 24 months for long term stability studies ($25^{\circ}\text{C}\pm 2^{\circ}\text{C}$ / $60\%\pm 5\%$ RH). The samples analyzed at the end. As a result of the findings of all physico-chemical tests, assay analysis and impurity analysis, both long

Table 6. Stability test results of pilot production tablets.

Specifications	P001		P002	
	Long Term* (24 Month)	Accelerated** (6 Month)	Long Term* (24 Month)	Accelerated** (6 Month)
Appearance	Suitable	Suitable	Suitable	Suitable
Average weight 640.0 mg \pm 5.0 (608.0 mg - 672.0 mg)	638.6 mg	640.5 mg	638.3 mg	644.98 mg
Hardness (for information)	169 N	158 N	167 N	102 N
Disintegration (max. 30 min.)	3 min.	3 min.	3 min.	3 min.
Water content (KF) (Max. 6 %)	2.04%	1.78%	2.01%	2.50%
Assay (HPLC)				
<i>Metformin HCl</i> 500.0 mg/tb (%90-%105) (450.0-525.0) mg/tb	497.9 mg/tb (99.6%)	486.3 mg/tb (97.3%)	497.3 mg/tb (99.5%)	488.4 mg/tb (97.7%)
<i>Repaglinide</i> 2.00 mg/tb (%90-%105) (1.80-2.10) mg/tb	1.98 mg/tb (99.0%)	1.97 mg/tb (98.5%)	1.99 mg/tb (99.5%)	1.92 mg/tb (96.0%)
Dissolution				
<i>Metformin HCl</i> Min 85 % (30. min) (Q=80)	98.4%	98.5%	95.9%	94.3%
<i>Repaglinide</i> Min 75 % (30. min) (Q=70)	92.9%	92.2%	92.7%	89.0%
Impurities				
<i>Metformin HCl</i>				
Unknown imp. % 0.1 max.	0.03%	0.01%	0.03%	0.03%
<i>Repaglinide</i>				
Unknown imp. % 0.2 max.	0.06%	0.13%	0.08%	0.04%
Related imp. A % 0.5 max.	N.D.	N.D.	N.D.	N.D.
Related imp. C % 0.5 max.	0.21%	N.D.	0.20%	0.01%
Total imp. % 1.0 max.	0.42%	0.32%	0.40%	0.14%

*Long term: $25^{\circ}\text{C}\pm 2^{\circ}\text{C}$; $60\%\pm 5\%$ RH; **Accelerated: $40^{\circ}\text{C}\pm 2^{\circ}\text{C}$; $75\%\pm 5\%$ RH; ND: Not detected

and accelerated stability findings were found within the limit. The details of the analysis are given in Table 6.

CONCLUSION

The tablet formulation containing Fixed-Dose Metformin and Repaglinide was developed and compared to the commercial product available in the market. The characterization studies and the dissolution rate tests were carried out and compared with the commercial product. In dissolution studies at pH 1.2, 4.5 and 6.8, over 85% data were obtained in 15 minutes. It was seen that it could be an alternative product to market preparation.

Peer-review: Externally peer-reviewed.

Author Contributions: Conception/Design of Study- S.Ş., Y.Ö.; Data Acquisition- S.Ş., B.M., M.E.D., E.Ö.; Data Analysis/Interpretation- S.Ş., Y.Ö., B.M., M.E.D., E.Ö.; Drafting Manuscript- S.Ş., B.M., M.E.D., E.Ö.; Critical Revision of Manuscript- S.Ş., B.M., M.E.D.; Final Approval and Accountability- S.Ş., B.M., M.E.D., E.Ö., Y.Ö.

Conflict of Interest: The authors have no conflict of interest to declare.


Financial Disclosure: Authors declared no financial support.

REFERENCES

- Abbink, E. J., van der Wal, P. S., Sweep, C. G. J. (Fred), Smits, P., & Tack, C. J. (2004). Compared to glibenclamide, repaglinide treatment results in a more rapid fall in glucose level and beta-cell secretion after glucose stimulation. *Diabetes/Metabolism Research and Reviews*, 20(6), 466–471. <https://doi.org/10.1002/dmrr.474>
- American Diabetes Association. (2000). Type 2 Diabetes in children and adolescents. *Pediatrics*, 105(3), 671–680. <https://doi.org/10.1542/peds.105.3.671>
- American Diabetes Association. (2015). Classification and diagnosis of diabetes. *Diabetes Care*, 38(Supplement_1), S8–S16. <https://doi.org/10.2337/dc15-S005>
- Cicero, A. F. G., Tartagni, E., & Ertek, S. (2012). Mini-Special issue paper management of diabetic patients with hypoglycemic agents metformin and its clinical use: new insights for an old drug in clinical practice. *Archives of Medical Science*, 5, 907–917. <https://doi.org/10.5114/aoms.2012.31622>
- Czyzyk, A., Tawecki, J., Sadowski, J., Ponikowska, I., & Szczepanik, Z. (1968). Effect of biguanides on intestinal absorption of glucose. *Diabetes*, 17(8), 492–498. <https://doi.org/10.2337/diab.17.8.492>
- EMA. (2010). Guideline on the investigation of bioequivalence. Retrieved from https://www.ema.europa.eu/en/documents/scientific-guideline/guideline-investigation-bioequivalence-rev1_en.pdf
- European Pharmacopeia 6. <2.9.5.> Uniformity of mass of single-dose preparations. Retrieved from %2020907e.pdf
- FDA. 2009. Dissolution methods. Retrieved from https://www.accessdata.fda.gov/scripts/cder/dissolution/dsp_getalldata.cfm
- Gautam, C. S., & Saha, L. (2008). Fixed dose drug combinations (FDCs): rational or irrational: a view point. *British Journal of Clinical Pharmacology*, 65(5), 795–796. <https://doi.org/10.1111/j.1365-2125.2007.03089.x>
- Godman, B., McCabe, H., & D Leong, T. (2020). Fixed dose drug combinations – are they pharmacoeconomically sound? Findings and implications especially for lower- and middle-income countries. *Expert Review of Pharmacoeconomics & Outcomes Research*, 20(1), 1–26. <https://doi.org/10.1080/14737167.2020.1734456>
- Hasslacher, C. (2003). Safety and efficacy of repaglinide in type 2 diabetic patients with and without impaired renal function. *Diabetes Care*, 26(3), 886–891. <https://doi.org/10.2337/diacare.26.3.886>
- Hostalek, U., Gwilt, M., & Hildemann, S. (2015). Therapeutic use of metformin in prediabetes and diabetes prevention. *Drugs*, 75(10), 1071–1094. <https://doi.org/10.1007/s40265-015-0416-8>
- ICH. (2003). Stability testing of new drug substances and products Q1A(R2). Retrieved from https://database.ich.org/sites/default/files/Q1A%28R2%29_Guideline.pdf
- Johansen, O. E., & Birkeland, K. I. (2007). Defining the role of repaglinide in the management of type 2 diabetes mellitus. *American Journal of Cardiovascular Drugs*, 7(5), 319–335. <https://doi.org/10.2165/00129784-200707050-00002>
- Kawamori, R., Kaku, K., Hanafusa, T., Oikawa, T., Kageyama, S., & Hotta, N. (2014). Effect of combination therapy with repaglinide and metformin hydrochloride on glycemic control in Japanese patients with type 2 diabetes mellitus. *Journal of Diabetes Investigation*, 5(1), 72–79. <https://doi.org/10.1111/jdi.12121>
- Lefèbvre, P. J., & Scheen, A. J. (1992). Management of non-insulin-dependent diabetes mellitus. *Drugs*, 44(Supplement 3), 29–38. <https://doi.org/10.2165/00003495-199200443-00005>
- Longo, M., Bellastella, G., Maiorino, M. I., Meier, J. J., Esposito, K., & Giugliano, D. (2019). Diabetes and aging: From treatment goals to pharmacologic therapy. *Frontiers in Endocrinology*, 10. <https://doi.org/10.3389/fendo.2019.00045>
- Maffi, P., & Secchi, A. (2017). *The Burden of Diabetes: Emerging Data*. <https://doi.org/10.1159/000459641>
- Malone, J. I. (2016). Diabetic central neuropathy: CNS damage related to hyperglycemia. *Diabetes*, 65(2), 355–357. <https://doi.org/10.2337/dbi15-0034>
- Marbury, T. (2000). Pharmacokinetics of repaglinide in subjects with renal impairment. *Clinical Pharmacology & Therapeutics*, 67(1), 7–15. <https://doi.org/10.1067/mcp.2000.103973>
- Massi-Benedetti, M., & Orsini-Federici, M. (2008). Treatment of type 2 diabetes with combined therapy: What are the pros and cons? *Diabetes Care*, 31(Supplement 2), S131–S135. <https://doi.org/10.2337/dc08-s233>
- Nasri, H., & Rafieian-Kopaei, M. (2014). Metformin: Current knowledge. *J Res Med Sci*, 19(7), 658–664.
- Natali, A., & Ferrannini, E. (2006). Effects of metformin and thiazolidinediones on suppression of hepatic glucose production and stimulation of glucose uptake in type 2 diabetes: a systematic review. *Diabetologia*, 49(3), 434–441. <https://doi.org/10.1007/s00125-006-0141-7>
- Pernicova, I., & Korbonits, M. (2014). Metformin—mode of action and clinical implications for diabetes and cancer. *Nature Reviews Endocrinology*, 10(3), 143–156. <https://doi.org/10.1038/nrendo.2013.256>
- Rachdaoui, N. (2020). Insulin: The friend and the foe in the development of type 2 diabetes mellitus. *International Journal of Molecular Sciences*, 21(5), 1770. <https://doi.org/10.3390/ijms21051770>
- Riddle, M. C., & Herman, W. H. (2018). The cost of diabetes care—An elephant in the room. *Diabetes Care*, 41(5), 929–932. <https://doi.org/10.2337/dci18-0012>
- Sanchez-Rangel, E., & Inzucchi, S. E. (2017). Metformin: clinical use in type 2 diabetes. *Diabetologia*, 60(9), 1586–1593. <https://doi.org/10.1007/s00125-017-4336-x>
- Schumacher, S., Abbasi, I., Weise, D., Hatorp, V., Sattler, K., Sieber, J., & Hasslacher, C. (2001). Single- and multiple-dose pharmacokinetics of repaglinide in patients with type 2 diabetes and renal impairment. *European Journal of Clinical Pharmacology*, 57(2), 147–152. <https://doi.org/10.1007/s002280100280>
- Scott, L. J. (2012). Repaglinide. *Drugs*, 72(2), 249–272. <https://doi.org/10.2165/11207600-000000000-00000>

- Spampinato, S. F., Caruso, G. I., De Pasquale, R., Sortino, M. A., & Merlo, S. (2020). The treatment of impaired wound healing in diabetes: Looking among old drugs. *Pharmaceuticals*, 13(4), 60. <https://doi.org/10.3390/ph13040060>
- Tangalos, E. G., & Zarowitz, B. J. (2005). Combination drug therapy. *Journal of the American Medical Directors Association*, 6(6), 406–409. <https://doi.org/10.1016/j.jamda.2005.04.013>
- The United States Pharmacopeia (USP), <701> Disintegration, 2019. Retrieved from https://www.usp.org/sites/default/files/usp/document/harmonization/gen-method/q02_pf_ira_31_2_2005.pdf
- The United States Pharmacopeia (USP), <1216> Tablet Friability, 2019. Retrieved from https://www.usp.org/sites/default/files/usp/document/harmonization/gen-chapter/g06_pf_ira_32_2_2006.pdf
- Tsioufis, C., & Thomopoulos, C. (2017). Combination drug treatment in hypertension. *Pharmacological Research*, 125, 266–271. <https://doi.org/10.1016/j.phrs.2017.09.011>
- World Health Organization. 2020. Diabetes. Retrieved from <https://www.who.int/news-room/fact-sheets/detail/diabetes>
- Young-Hyman, D., de Groot, M., Hill-Briggs, F., Gonzalez, J. S., Hood, K., & Peyrot, M. (2016). Psychosocial care for people with diabetes: A position statement of the American Diabetes Association. *Diabetes Care*, 39(12), 2126–2140. <https://doi.org/10.2337/dc16-2053>

The formulation and characterization of water-soluble snakehead fish (*Ophiocephalus striatus*) dry extract in nanoemulsion using permeation and *in vivo* study

Robert Tungadi¹ , Widysusanti Abdulkadir¹ , Munafri Tahir¹ 

¹State University of Gorontalo, Faculty of Sport and Health, Department of Pharmacy, Gorontalo, Indonesia

ORCID IDs of the authors: R.T. 0000-0003-2141-2402; W.A. 0000-0002-8975-134X; M.T. 0000-0002-9351-2843

Cite this article as: Tungadi, R., Abdulkadir, W., & Tahir, M. (2021). The formulation and characterization of water-soluble snakehead fish (*Ophiocephalus striatus*) dry extract in nanoemulsion using permeation and *in vivo* study. *Istanbul Journal of Pharmacy*, 51(1), 35-41.

ABSTRACT

Background and Aims: The study was conducted to determine the optimal concentration of water-soluble snakehead fish dry extract (SFDE) in nanoemulsion and the amount of albumin required to penetrate the skin in order to accelerate the wound healing process.

Methods: The snakehead fish (SF) was extracted using an atomizer while the nanoemulsion basis was optimized using oleic acid, Tween 80, and propylene glycol. The developed SFDE in nanoemulsion was characterized based on droplet size, PDI, and zeta potential. The ability of the mixture to penetrate the snakeskin was tested using Franz diffusion cells. The effectiveness of the nanoemulsion was evaluated by dividing the rabbits used for experiment into 6 treatment groups including SFDE F1 0.25%, F2 0.5%, F3 1%, F4 SF 2% cream, F5 nanoemulsion basis, and F6 no treatment.

Results: The SFDE nanoemulsion produced a particle size of 147.5 nm with acceptable PDI (0.23) and zeta potential (+13.38 mV). The most effective SFDE to accelerate the healing of open wounds in rabbits was a concentration of 1%, which was found to have dried and closed the wound on the 3rd day.

Conclusion: The permeation study and the effectiveness test showed the 1% SFDE nanoemulsion is the best concentration in accelerating the wound healing process and ensuring the highest albumin penetration into the skin.

Keywords: Snakehead fish, nanoemulsion, albumin, wound, water-soluble, rabbit

INTRODUCTION

Snakehead fish (SF) (*Ophiocephalus striatus*) is an economically valuable fish widely used for processed products. According to Suprayitno (2003), it has a protein content estimated to be 25.1% compared to the 6.224% found in albumin and is higher than the values obtained from other animal sources used for patients with hypoalbuminemia (i.e. low albumin) and wounds. This is important because albumin has been discovered in medical science to have the ability of accelerating the recovery of broken body cell tissues due to surgery (Suprayitno, 2003; Ulandari, Kurniawan, & Putri, 2011).

Albumin is the largest type of protein in plasma with 60% content and also has the ability to synergize with zinc mineral needed for the development and formation of new cell tissues in wounds. Zinc has been reported to have the ability to functions as an antioxidant to protect cells, accelerate the wound healing process, and regulate expression of lymphocytes and proteins (Mustafa, Widodo, & Kristianto, 2012; Maryanto, 2004). Moreover, the chemical compounds of Snakehead fish dry extract (SFDE), including albumin and amino acids (glycine and lysine), have been discovered to be soluble in water based on chemical analysis tests from

Address for Correspondence:

Robert TUNGADI, e-mail: robert.tungadi@ung.ac.id

Submitted: 10.05.2020
Revision Requested: 06.07.2020
Last Revision Received: 02.09.2020
Accepted: 21.09.2020

This work is licensed under a Creative Commons Attribution 4.0 International License.



LIPI conducted using spectrophotometry and HPLC methods. It is, therefore, the mix of these elements with nanoemulsion (NE) that is needed to obtain a homogenous system through the emulsification method (Zhang, Zhang, Fan, Liu, & Meng, 2019).

According to Tungadi, Susanty, Wicita, & Pido (2018), snake-head fish with 2% cream was found to have accelerated the healing process of rabbit skin's open wound in an *in vivo* study, but the cream was observed to be physically unstable after 3 months of storage. This was associated with the mixture of snakehead fish dry extract (SFDE) with macro emulsion, which causes effortless damage due to the strength of oil and water phase and storage temperature. A solution has, however, been reported which involves reducing the particle size of snake-head fish dry extract and stabilizer using nanoemulsion formulation through appropriate utilization of surface-active agents, co-surfactant, and oil (Tungadi, 2011; Devarajan, & Ravichandran, 2011). It is also possible to formulate the SFDE into the emulsion because it contains hydrophilic and hydrophobic compounds with the nanoemulsion discovered to be useful for transdermal drug delivery such as the penetration of active compounds due to stratum corneum deformability (Tungadi, Susanty, Wicita, & Pido, 2018).

Meanwhile, Tungadi, R. (2016) showed snakehead fish cream containing only 50% albumin has the ability to penetrate the skin membrane using penetrant enhancers such as propylene glycol. This, according to an *in vivo* study, has been reported to accelerate the healing of open wounds (treatment group) due to the increase in the rate of diffusing albumin into the stratum corneum. However, a low percentage of albumin is produced without the use of a penetrant enhancer (Tungadi & Hasan, 2016).

This shows a nanoemulsion system is suitable for the drug delivery through the skin due to its large surface area, which makes the penetration of active substances faster. It is also useful because its manufacturing process is very easy and efficient (Chuesiang, Siripatrawan, Sanguandeekul, McLandsborough, & McClements, 2018; Laxmi, Bhardwaj, Mehta, & Mehta, 2015) as observed in the formation of SFDE into dosage forms in Winda's research. This involved the optimization of nanoemulsion basis as a carrier for SF nanoemulsion preparation and later characterization by particle size, polydispersity index, and zeta potential with the results found to be 147.5 nm, 0.234, and +13.38 mV respectively (Tungadi, Moo, & Mozin, 2017). Therefore, this current study was conducted to determine the effectiveness of different concentrations of SFDE at 0.25, 0.5, and 1% in accelerating the healing of open wounds on rabbits dorsum and the amount of albumin required to penetrate their skin using the Franz diffusion cell.

MATERIALS AND METHODS

Materials

Snakehead fish dry extract was obtained from PT. Ismut Medical Pharmaceutical, Indonesia. The Rabbits were purchased from the animal market. The nanoemulsion basis (tween 80, propylene glycol, and oleic acid) was purchased from PT. Brataco Chemical. Other materials, such as propylparaben,

methylparaben, isopropyl myristate, lanolin, cetyl alcohol, paraffin liquid, and BHT were purchased from PT. Sentana Chemical. A UV-Vis Spectrophotometer (USA), Delsa™ Nano (UK), pH meter (Systronics model EQMK), sonicator (Specta Lab), hot air oven (Mettler), and the Franz diffusion cell (Intalab) were used.

Albino rabbits (2 kg) were obtained from the animal laboratory center of LIPI, Serpong, Indonesia. The experimental procedure was conducted according to the Institutional Animal Ethics Committee based on the recommendations of the Health Ethics Committee, The Faculty of Medicine, Hasanuddin University, Indonesia Government with registration No. UH08060042

The optimization and characterization of SFDE nanoemulsion basis

The nanoemulsion basis was optimized by comparing different concentrations of oil (oleic acid), co-surfactant (propylene glycol), and surfactant (Tween 80) using five formulas including F1 (1:2:4), F2 (1:3:4), F3 (1:3:5), F4 (1:3:6), and F5 (1:3:7). The Tween 80 and propylene glycol were mixed collectively using a magnetic stirrer for 30 minutes at 250 rpm. For the first mixture, the oleic acid was introduced during the stirring process. Water containing 0.25%, 0.5%, and 1% of SFDE was added drop by drop then other adjuvants, such as methylparabens and propylparabens (preservatives) as well as BHT (antioxidant) were added. After that, sonication of the mixtures at 20 KHz was performed for 10 minutes at 25°C to complete the process. The same procedure was performed for all the formulations with different concentrations of Tween 80, propylene glycol, and oleic acid. All formulations were characterized using a particle size analyzer to measure the size of droplets, zeta potential, and PDI.

Permeation study

In vitro permeation, conducted using Franz diffusion cell, has been described as a dependable technique to predict the transport of drugs in the skin (Zhu et al., 2009) and, for this study, an excised python skin (*Python reticulatus*) was used.

This process involved the separation of the skin from abundant fats and the elimination of connective tissue using a scalpel. The excised skin was washed with NaCl 0.9% and examined for integrity before it was hooked up on the diffusion cell with an effective diffusion area. Moreover, the stratum corneum facet was focused on the donor while the dermal layer was on the receiver compartment consisting of 47 ml phosphate buffer of pH 7.4 as the receptor fluid agitated at 100 rpm and maintained at 37±0.5°C during the experiments with 1 g of the nanoemulsion used in every diffusion cell. Approximately 2 ml of the samples were withdrawn for evaluation at 0, 30, 60, 90, 120, 150, 180, 210, and 240 min after the experiment has commenced and changed immediately with an equal volume of fresh diffusion medium (Tungadi et al., 2018).

Skin irritation study

Skin inflammation was evaluated using 12 healthy rabbits without any injuries or skin disorders. They were grouped into three with n=3 of albino male rabbits weighing 1.5-2 kg; positive control (2% w/w SFDE, commercial product), and negative control (nanoemulsion basis) also with n=3 on the 2 cm² dor-

sal facet of the shaven skin of the rabbits. The treatment was eliminated after 72 h to check for any symptoms of erythema and edema (Tungadi et al., 2018; Barot, Parejiya, Patel, Mehta, & Shelat, 2012; Lala, & Awari, 2014). Undesirable skin changes such as coloration and morphology were examined at 1h, 24 h, 48 h, and 72 h intervals. The reactions obtained were recorded and compared with a control group (n=3).

Effectiveness of the SFDE *in vivo* study

Preparation and grouping of test animals

The implementation stage started with the preparation of 12 male white rabbits randomly divided into 6 groups of treatments, each consisting of 2 rabbits, each of which were placed in individual cages and acclimated for 5 days. The Treatment Group contained SFDE varied at G1 0.25%, G2 0.5% and G3 1% of SFDE.

Testing of SFDE on test animals

The dorsal back of each test animal was shaved and cleaned with 70% alcohol after which they were locally anesthetized with 0.2 mL lidocaine and the wounds created by slicing off 4 cm² of skin and smearing the wounds with the SFDE treatments. The average change in length and the condition of the wounds were observed and documented every day for 10 days.

Measurement of the open wound area

The average length of the open wound was calculated using a ruler while pictures were also taken from day 0 to 10 to determine the healing process. The values measured in each day were converted to amount of contraction to determine the reduction effect of SFDE in different concentrations.

Statistical analysis

All the experimental measurements were recorded in triplicate and the final values were expressed as mean value±standard deviation (SD). The statistical evaluation of the permeation *in vitro* for the predetermined intervals was conducted using One-way ANOVA SPSS 16 with a degree of significance of P cost <0.05* and <0.01**.

RESULTS AND DISCUSSION

The formulation and optimization of nanoemulsion basis

There are several challenges to the application of nanoemulsion as a transdermal system to successfully deliver drugs via the skin (Kong, Chen, Kweon, & Park, 2011) and some of the important ones include the small particle-sized formulation and rheology properties. Therefore, it is necessary to understand the best formula to improve the introduction of snakehead fish dry extract (SFDE) into nanoemulsion using appropriate oil, surfactant, and co-surfactant (Tungadi et al., 2018).

The best optimization for nanoemulsion basis was found to be Formula 5 (F5) with oleic acid, tween eighty and propylene glycol (1:10) based on its viscosity, clarity, and stability as shown in Table 1.

Formula 5 was also observed to be physically stable by not segregating after being centrifuged at 3800 rpm for 5 hours while Formulas 1 to 4 produced a cloudy appearance and segregated. The stability was associated with the use of Tween 80 as a nonionic surfactant considering its excessive hydrophilic and lipophilic balance estimated at 15 which made it steady in an emulsion formulation with oil in water (Brandelero, Yamashita, & Grossmann, 2010).

Surfactant plays important roles in the nanoemulsion basis due to the fact it has a large surface area to decrease interfacial and surface tension, which further leads to its absorption in the interface phase. This means it has the ability to reduce the surface free energy by disintegrating a globule into smaller parts (Natalia, 2012). However, most surfactants are unable to decrease interfacial tension in the emulsion. Therefore, there is a need to add co-surfactant such a propylene glycol to improve the solubility of nonpolar agencies (Swarbrick, 2007), intensify the flexibility of surfactant film and fluidity of the emulsion phase to shield compounds from adverse environmental conditions, and enhance their balance (Madene, Jacquot, Scher, & Desobry, 2006; Kumar, Bishnoi, Shukla, & Jain, 2019).

Table 1. The optimization of nanoemulsion basis.

Materials	Formula %				
	F1 1:2:4	F2 1:3:4	F3 1:3:5	F4 1:3:6	F5 1:3:7
Oleic acid	5	5	5	5	5
Tween 80	18	20	23	25	27.5
Propylene glycol	12	15	17	20	22.5
Distilled water	100	100	100	100	100
Observation	cloudy	cloudy	cloudy	cloudy	clear
Stability tests:					
pH	6.5±0.3	6.2±0.5	6.0±0.7	5.8±0.2	5.5±0.1
Viscosity (cP)	385.6±1.3	267.8±2.5	200.3±2.1	187.5±3.2	178.2±1.4
Transmittance (%)	75.65±1.5	82.34±0.9	87.35±1.1	90.58±1.8	98.75±0.8

Characterization of snakehead fish nanoemulsion

Nanoemulsion systems can be used to deliver drugs through trans-mucosal and transdermal routes and this means they have the ability to effectively enhance bioavailability (Kumar et al., 2019; Rehman et al., 2017). The polydispersity index (PDI) of the SFDE produced good results in the three replications, 0.205, 0.215, and 0.284 respectively, and the 147.5 nm average droplet size shown in Table 2.

Sample	Particle size (nm)	Average of Size (nm)	Zeta potential (mV)	Polydispersity index (PDI)	Average of PDI
1% SFDE	111 ± 0.2	147.5 ± 0.53	+ 13.38	0.205 ± 0.1	0.23 ± 0.26
	233 ± 0.5			0.215 ± 0.2	
	98.6 ± 0.9			0.284 ± 0.5	

As shown in Table 2, the average size of the droplet of SFDE nanoemulsion was 147.5 nm showing that SFDE meets the criteria of nanostructures, which require a particle size range between 1 – 100 nm or 2 – 500 nm (Shah, Bhalodia, & Shelat, 2011). Meanwhile, the zeta potential value was +13.38 mV and this indicates it has a good degree of stability. This is associated with the standard that nanoparticles with values above or below ± 30 mV indicate a physically stable colloidal system due to their ability to ensure the magnitude of the charged particle prevents particle aggregation (Singh, & Lillard, 2014; Hadian, Sahari, & Moghimi, 2014). Meanwhile, smaller values have been reported to cause particles to aggregate and flocculate due to van der Waals attractive forces acting on them, thereby, leading to physical instability. Furthermore, the average polydispersity index was recorded to be 0.234 and this means SFDE has a uniform particle size and homogeneous dispersion because this value is below 0.25 (Winterhalter, & Lasic, 2013).

The solubility of active compounds is very important in drug formulation due to its ability to increase bioavailability through oral, topical, and parenteral formulations. SFDE contains water-soluble active compounds such as albumin and amino acids and water-insoluble ones such as polyunsaturated fatty acids, vitamins, and amino acids. This study made use of only the albumin and amino acid contents to ensure easy formulation into the nanoemulsion. Therefore, solubility is one of the important parameters to achieve the appropriate concentration of drug in systemic circulation and appropriate pharmacological response (Vemula, Lagishetty, & Lingala, 2010).

Permeation study of SFDE in nanoemulsion

Ex vivo permeation studies were also conducted using snake-skin as the membrane and the drugs from G1 (0.25% SFDE), G2 (0.5% SFDE), G3 (1% SFDE), and G4 (2% SF cream; commercial product) were found have produced $62.80 \pm 1.45\%$, $69.30 \pm 2.34\%$, $72.30 \pm 1.22\%$, and $50.80 \pm 0.50\%$ permeation, respectively in 4h as shown in Figure 1.

Figure 1 shows 2% SF cream had the lowest percentage of albumin permeation into the skin with approximately 50.80%

compared to all other concentrations and this is associated with the formulation of SFDE containing albumin into cream o/w to produce the big particle size in SF cream due to the macroemulsion. Its introduction to nanoemulsion produced a small particle size estimated to be 147.5 nm and water-soluble compounds with the ability to increase the loading capacity of albumin to penetrate the skin easily. This is consistent with the findings of previous research on the formulation of SFDE into

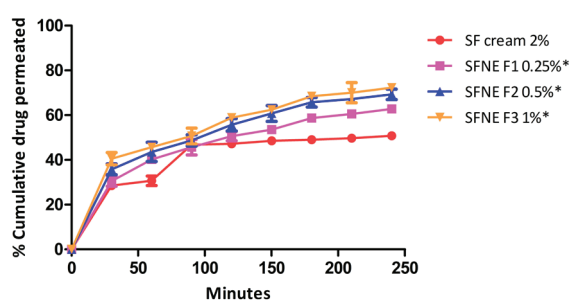


Figure 1. The amount of albumin penetrated into the skin in 4 h; * $P < 0.05$; One Way Anova Test.

liposome which showed solubility and particle size to be the most important factors to increase the loading capacity and bioavailability of drugs. SFDE into liposome was discovered to have a smaller particle size, 121 nm, compared to nanoemulsion and this led to the production of the highest entrapment efficiency of albumin recorded to be 85.75% (Tungadi, Abdulkadir, Ischak, & Rahim, 2019).

The biggest impediment to the transdermal drug transport is usually associated with the stratum corneum as observed in the 10-20 μm thick tissue layer which has a remarkably composed lipid/protein matrix structure (Ceve, 2004). According to Tungadi (2011), a study of SFDE cream containing penetrant enhancer such as propylene glycol is expected to accelerate the wound healing process through skin permeation, but the cumulative albumin penetration into rat skin membrane was recorded to be 50%. This study found SFDE nanoemulsion to have the ability to enhance the permeation of drug through the skin as observed from the cumulative percentage of SFDE permeation of F3 which was found to be the highest with $72.30 \pm 1.22\%$ using a snakeskin membrane while the positive control, SF cream 2%, had $50.80 \pm 0.50\%$. This, therefore, means nanoemulsion formulation acts as drug reservoirs in the transdermal delivery systems affecting the release of drugs from the inner to the outer phase and similarly to the skin (Tungadi

et al., 2018; Mou et al., 2008). These release mechanisms, however, rely on the composition of the network surfactant chains and the Crosslink density (Tungadi et al., 2018; Bernard, 2012). Moreover, the capacity of a drug to penetrate the skin and release the therapeutic agent effectively is affected by its affinity to diffuse out from the vehicle and permeate through the barrier (Tungadi et al., 2018; Alves, Scarrone, Santos, Pohlmann, & Guterren 2007).

In the current permeation study using Franz diffusion cell, *Phyton* snakeskin was used as a membrane to facilitate the penetration of the test substances compared to the use of extracts of stratum corneum isolated from the skins. This method was used in the study by Lin and colleagues (1992) and the permeability values in snakeskin (*Phyton molurus*) were found to be 2 to 4 times higher than in isolated stratum corneum for sodium diclophenate, theophylline, and benzoic acid (2 mg/mL or 0.2% in aqueous solution). The use of *phyton* snakeskin in studying SFDE nanoemulsion as a promoter of skin penetration for hydrophilic substances such as albumin required the consideration of the lower permeability coefficient (3.3 to 6.1 times) of these membranes for such compounds, thereby, causing an extension of the time needed for the experiments. Meanwhile, lipophilic compounds have been reported to have permeability coefficients close to those obtained from human skin membranes (0.9 to 1.8 times and 3.3 to 6.1 times) (Tungadi et al., 2019).

Skin irritation test of snakehead fish nanoemulsion

The results from the skin irritation study including erythema and edema on the rabbit skin after 1 h, 24 h, 48 h, and 72 h post-treatment of positive control, negative control, F1, F2, and F3 are represented in Table 3. The results showed no proof of inflammation, erythema, or edema; based on visible inspection after the application of all formulations of nanoemulsion on the rabbit skin during the three days of observation. This, therefore, means they were all non-sensitizing and safe for topical use.

Percentage of wound contraction on rabbit's skin

Based on observations, on the 3rd, 6th, and 10th-day, the open wound on the rabbit in group I (F1 0.25% SFDE) was found to have wound contraction percentages between 90% and 46% as shown in Figures 2-6 with the physical appearance marked by the presence of fibrin yarns protecting the open wound as presented in Figures 3-6. In group II (F2 0.5%), the reduction

was found to be 100% to 42% and was discovered to be drying in contrast to the observation made for group I. The results of group III (F3 1%) showed a substantial contraction from 100% to 25% compared to the negative control, which was observed to be faster. This change was characterized by the production of new granulation tissue on the side of the open wound and the fact that it was already dry on the third day. Furthermore, the positive control (F4) containing snakehead fish cream 2% had the change of wound contraction from 100% to 56%. The negative control F5 with nanoemulsion basis and F6 without treatment had the slowest healing process of approximately 15 days and a marked wound contraction exchange from 100% to 75-77% (Figures 2, 3-6).

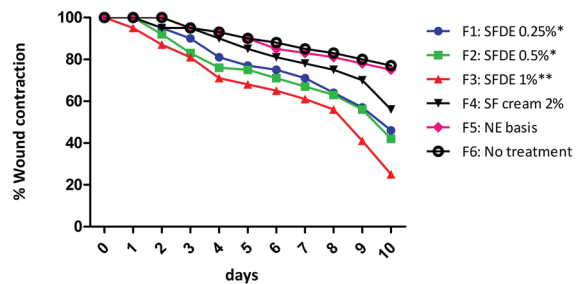


Figure 2. Percentage of wound contraction on rabbit's skin *P<0.05; **P<0.01; One Way Anova Test.

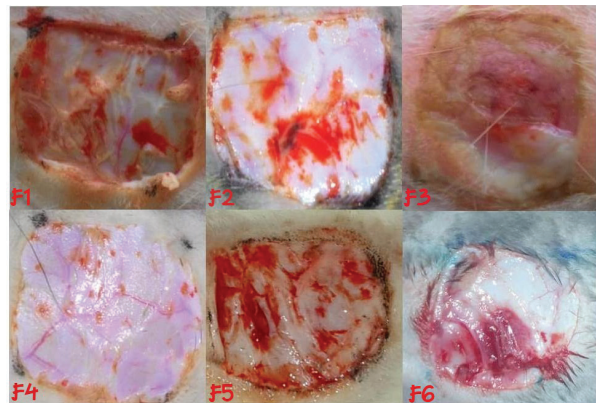


Figure 3. The observation of wound area on the first day, F1: NE 0.25% of SFDE; F2: NE 0.5%; F3: NE 1%; F4: 2% of SF cream; F5: NE basis; F6: no treatment.

	1 h		24 h		48 h		72 h	
	Erythema	Edema	Erythema	Edema	Erythema	Edema	Erythema	Edema
G1 0.25%	0	0	0	0	0	0	0	0
G2 0.5%	0	0	0	0	0	0	0	0
G3 1%	0	0	0	0	0	0	0	0
Positive Control	0	0	0	0	0	0	0	0
Negative Control	0	0	0	0	0	0	0	0

Positive control: SF cream 2% (w/w); commercial product, negative control: nanoemulsion basis; Erythema scale: 0= none, 1=slight, 2= well-defined, 3= moderate, and 4= scar formation; Edema scale: 0= none, 1= slight, 2= well-defined, 3= moderate, and 4= severe

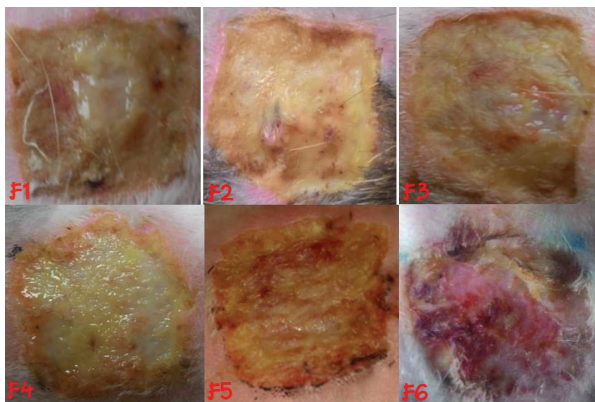


Figure 4. The observation of wound area on the third day, F1: NE 0.25% of SFDE; F2: NE 0.5%; F3: NE 1%; F4: 2% of SF cream; F5: NE basis; F6: no treatment.

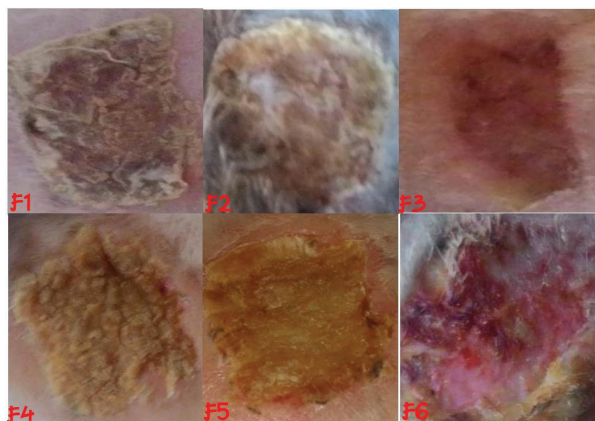


Figure 5. The observation of wound area on the sixth day, F1: NE 0.25% of SFDE; F2: NE 0.5%; F3: NE 1%; F4: 2% of SF cream; F5: NE basis; F6: no treatment.

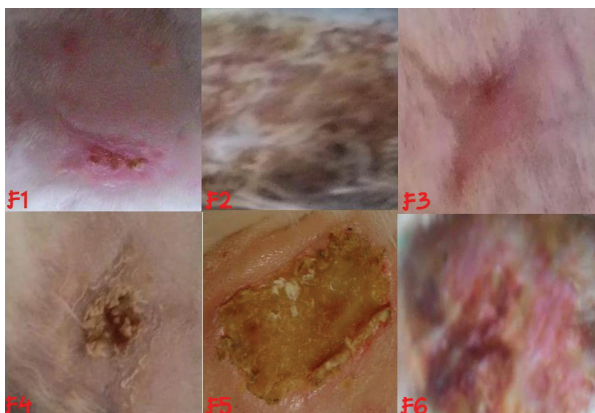


Figure 6. The observation of wound area on the ninth day, F1: NE 0.25% of SFDE; F2: NE 0.5%; F3: NE 1%; F4: 2% of SF cream; F5: NE basis; F6: no treatment.

The One-Way ANOVA analysis showed the P or Sig value was $0.022 < 0.05$ and 0.01 . This means there was a significant difference between the averages of open wound contraction for all treatment and control groups. However, observation data indicated NE 1% of SFDE had a faster wound area reduction compared to 0.25% and 0.5% nanoemulsion preparations and 2% SF cream.

Effectiveness of the SFDE *in vivo* study

F3 was found to be the best formula of SFDE nanoemulsion in this *in vivo* study functioning as a transdermal delivery system to ensure a controlled release of substances over a period and improve patient comfort during dosage preparation. Meanwhile, the small droplet size has been reported to have the ability to absorb albumin containing large molecules following the spontaneous size of the globule and surroundings (Lovelyn & Attama, 2011). The percentage of the albumin penetration and wound contraction of F3 were estimated at 72.30% and 25% on the 10th day. This was associated with the particle size and zeta potential of SFDE nanoemulsion because its small size of droplets increases the diffusion rate of albumin compared to micro or macro emulsion while the significant stability was due to the PDI and zeta potential.

The SFDE in nanoemulsion was able to accelerate the wound healing process due to the nutritional contents of snakehead fish including 0.003% Zn, 30.2% albumin, and 0.001% glycine (Mansyur, 2010) triggering the formation of Endothelial Progenitor Cells (EPC). The Zn plays a key role and has also been reported to be an important mineral in the structure and function of cell membranes by limiting the damage caused by free radicals during inflammation. Furthermore, it is also involved in the immune system, the defense of the skin, and the regulation of genes in lymphocytes (Tungadi et al., 2019; gawhirunpat, Panomsuk, Opanasopit, Rojanata, & Hatanaka, 2006; Tungadi, & Wicita, 2020).

CONCLUSION

It is possible to formulate water-soluble snakehead fish dry extract into nanoemulsion with small particles to increase the loading capacity of albumin in penetrating the skin. The permeation study and the effectiveness test showed the 1% SFDE in nanoemulsion is the best concentration compared to others in accelerating the wound healing process and ensuring the highest albumin penetration into the skin.

Acknowledgments: The authors are thankful to the Ministry of Research, Technology, and Higher Education of Indonesia, which has funded this research by grant competition (decentralization grant) and are also thankful to PT. Ismut, Pharmaceuticals, Indonesia, for providing snakehead fish powder for this work and PT. NanoTech Herbal Indonesia, LIPI Serpong, Indonesia which has given technical supports. Besides that, the authors also thanks the native proofreading service (NPS) for improving the quality of this paper.

Peer-review: Externally peer-reviewed.

Author Contributions: Conception/Design of Study- R.T.; Data Acquisition- R.T., W.A.; Data Analysis/Interpretation- R.T., W.A., M.T.; Drafting Manuscript- R.T., W.A., M.T.; Critical Revision of Manuscript- R.T., W.A.; Final Approval and Accountability- R.T., W.A., M.T.

Conflict of Interest: The authors have no conflict of interest to declare.

Financial Disclosure: Authors declare having received financial support from The Ministry of Research and Technology (DIKTI).

REFERENCES

- Alves, M. P., Scarrone, A. L., Santos, M., Pohlmann, A. R., & Guterren S. S. (2007). Human skin penetration and distribution of nimesulide from hydrophilic gels. *International Journal of Pharmaceutics*, 314(1-2), 215-220.
- Barot, B. S., Parejiya, P. B., Patel, H. K., Mehta D. M., & Shelat, P. K. (2012). Microemulsion-based antifungal gel delivery to nail for the treatment of onychomycosis: Formulation, optimization, and efficacy studies. *Drug Delivery and Translational Research*, 2(6), 463-476.
- Bernard, P. B. (2012). *Modern Aspects of Emulsion Science, Emulsions-Recent Advances in Understanding*. UK: Royal Science of Chemistry.
- Brandelero, R. P. H., Yamashita, F., & Grossmann, M. V. E. (2010). The effect of surfactant Tween 80 on the hydrophilic water vapor permeation, and the mechanical properties of cassava starch and poly (butylenes adipate-co-terephthalate) (pbat) blend films. *Carbohydrate Polymers*, 82, 1102-1109.
- Ceve, G. (2004). Lipid vesicles and other colloids as drug carriers on the skin. *Advanced Drug Delivery Review*, 56(5), 675-711.
- Chuesiang, P., Siripatrawan, U., Sanguandeeikul, R., McLandsborough, L., & McClements, D. J. (2018). Optimization of cinnamon oil nanoemulsions using phase inversion temperature method: Impact of oil phase composition and surfactant concentration. *Journal of Colloid and Interface Science*, 514, 208-216.
- Devarajan, V., & Ravichandran, V. (2011). Nanoemulsions: As modified drug delivery tool. *International Journal of Comprehensive Pharmacy*, 2, 1-5.
- Hadian, Z., Sahari, M. A., & Moghimi, H. R. (2014). Formulation, characterization and optimization of liposomes containing EPA and DHA; A methodology approach. *Iranian Journal of Pharmaceutical Research*, 13(2), 393-404.
- Kong, M., Chen, X. G., Kweon, D. K., & Park, H. J. (2011). Investigation on skin hyaluronic acid based nanoemulsion as transdermal carrier. *Carbohydrate Polymers*, 86(2), 837-843.
- Kumar, M., Bishnoi, R. S., Shukla, A. K., & Jain, P. (2019). Techniques for formulation of nanoemulsion drug delivery system: A review. *Preventive Nutrition and Food Science*, 24(3), 225-234.
- Lala, R., & Awari, N. (2014). Nanoemulsion-based gel formulations of COX-2 inhibitors for enhanced efficacy in inflammatory conditions. *Applied Nanoscience*, 4, 143-151.
- Laxmi, M., Bhardwaj, A., Mehta, S., & Mehta, A. (2015). Development and characterization of nanoemulsion as carrier for the enhancement of bioavailability of artemether. *Artificial Cells Nanomedicine and Biotechnology*, 43(5), 334-344.
- Lovelyn, C., & Attama, A. A. (2011). Current state of nanoemulsions in drug delivery. *Journal of Biomaterials and Nanobiotechnology*, 2(5), 626-639.
- Madene, A., Jacquot, M., Scher, J., & Desobry, S. (2006). Flavour encapsulation and controlled release - a review. *International Journal of Food Science and Technology*, 41, 1-21.
- Mansyur. (2010, July 15). Analysis of snakehead fish dry extract. Indonesian Institute of Sciences Biotechnology Research Center. Retrieved from <https://worldwidescience.org/topicpages/s/snakehead+fish+channa.html>
- Maryanto, A. (2004, June 18). The impact of albumin serum on length of postoperative wound healing process, Faculty of Medicine, University of Gadjah Mada. Retrieved from http://etd.repository.ugm.ac.id/home/detail_pencarian/25247
- Mou, D., Chen, H., Du, D., Mao, C., Wan, J., Xu, H., & Yang, X. (2008). Hydrogel thickened nanoemulsion system for topical delivery of lipophilic drugs. *International Journal of Pharmaceutics*, 353(1-2), 270-276.
- Mustafa, A., Widodo, A., & Kristianto, Y. (2012). Albumin and zinc content of snakehead fish extract and its role in health. *International Journal of Science and Technology*, 1, 1-8.
- Natalia, M. (2012). The stability and antibacterial activity test of black cumin oil (*nigella sativa l.*) nano-emulsion gel (nano-emulgel). (Master's thesis). Retrieved from <http://lib.ui.ac.id/file?file=digital/20309121-543091-Uji%20stabilitas.pdf>
- Ngawhirunpat, T., Panomsuk, S., Opanasopit, P., Rojanata, T., & Hatanaka, T. (2006). Comparison of the percutaneous absorption of hydrophilic and lipophilic compounds in shed snake skin and human skin. *Pharmazie*, 61(4), 331-335.
- Rehman, F. U., Shah, K. U., Shah, S. U., Khan, I. U., Khan, G. M., & Khan, A. (2017). From nanoemulsions to self-nanoemulsions, with recent advances in self-nanoemulsifying drug delivery systems (SNEDDS). *Expert Opinion on Drug Delivery*, 14(11), 1325-1340.
- Shah, P., Bhalodia, D., & Shelat, P. (2011). Nanoemulsion : A pharmaceutical review. *Systematic Reviews in Pharmacy*, 1, 24-32.
- Singh, R., & Lillard, J. W. (2014). Nanoparticle-based targeted drug delivery. *Experimental Molecular and Pathology*, 86(3), 215-223.
- Suprayitno, E. (2003). Snakehead Fish (*Ophiocephalus striatus*) albumin as functional food to overcome future nutrition problems. *Faculty of Fisheries, Brawijaya University*, 5(3), 32-36.
- Swarbrick, J. (2007). *Encyclopedia of pharmaceutical technology*. New York: Informa Healthcare USA Press, pp 1548-1565.
- Tungadi, R. (2011). The acceleration of wound healing of snakehead fish cream towards rabbit's skin wound histopathologically. *Indonesian Pharmaceutical Journal*, 9, 91-97.
- Tungadi, R., & Hasan, A. M. (2016). The effect of penetrant enhancer combination towards the diffusion rate of snakehead fish (*Ophiocephalus striatus*) cream in vitro and vivo. *International Journal of PharmTech Research*, 9(6), 508-13.
- Tungadi, R., Moo, D. R., & Mozin, W. R. (2017). Characterization and physical stability evaluation of snakehead fish (*Ophiocephalus striatus*) powder nanoemulsion. *International Journal of Pharmaceutical Sciences and Research*, 8(6), 2720-4.
- Tungadi, R., Susanty, W., Wicita, P., & Pido, E. (2018). Transdermal delivery of snakehead fish (*Ophiocephalus striatus*) nanoemulgel containing hydrophobic powder for burn wound. *Pharmaceutical Sciences*, 24(4), 313-323.
- Tungadi, R. (2019). Potential of snakehead fish (*Ophiocephalus striatus*) in accelerating wound healing. *Universal Journal of Pharmaceutical Research*, 4(5), 40-44.
- Tungadi, R., Abdulkadir, W., Ischak, N. I., & Rahim, B. R. (2019). Liposomal formulation of snakehead fish (*Ophiocephalus striatus*) powder and toxicity study in zebrafish (*Danio rerio*) model. *Pharmaceutical Sciences*, 25(2), 145-153.
- Tungadi, R., & Wicita, P. (2020). Formulation, optimization, and characterization of snakehead fish (*Ophiocephalus striatus*) powder nanoemulgel. *Brazilian Journal of Pharmaceutical Sciences*, 56, 1-8.
- Ulandari, A., Kurniawan, D., & Putri, A. S. (2011). Potential of snakehead fish protein in preventing kwashiorkor in toddlers in Jambi Province. Faculty of Medicine, Jambi University. Retrieved from <https://adoc.pub/potensi-protein-ikan-gabus-dalam-mencegah-kwashiorkor-pada-b.html>
- Vemula, V. R., Lagishetty, V., & Lingala, S. (2010). Solubility enhancement techniques. *International Journal of Pharmaceutical Science Review and Research*, 5(1), 41-51.
- Winterhalter, M., & Lasic, D. D. (2013). Liposome stability and formation: experimental parameters and theories on the size distribution. *Chemistry and Physics of Lipids*, 64, 35-37.
- Zhang, L., Zhang, F., Fan, Z., Liu, B., & Meng, X. (2019). DHA and EPA nanoemulsion prepared by the low-energy emulsification method: process factors influencing droplet size physicochemical stability. *Food Research International*, 121(7), 359-366.
- Zhu, W., Guo, C., Yu, A., Gao, Y., Cao, F., & Zhai, G. (2009). Microemulsion-based Hydrogel Formulation of penciclovir for topical delivery. *International Journal of Pharmaceutics*, 378(1-2), 152-158.

Pseudo ternary phase diagrams: a practical approach for the area and centroid calculation of stable microemulsion regions

Murat Sami Berkman¹ , Kadri Güleç² 

¹Anadolu University, Faculty of Pharmacy, Department of Pharmaceutical Technology, Eskişehir, Turkey

²Anadolu University, Faculty of Pharmacy, Department of Analytical Chemistry, Eskişehir, Turkey

ORCID IDs of the authors: M.S.B. 0000-0003-3722-4166; K.G. 0000-0002-1392-8276

Cite this article as: Berkman, M. S., & Gulec, K. (2021). Pseudo ternary phase diagrams: A practical approach for the area and centroid calculation of stable microemulsion regions. *Istanbul Journal of Pharmacy*, 51(1), 42-49.

ABSTRACT

Background and Aims: This study aims to develop and evaluate a practical approach for the complicated area and centroid calculation of stable microemulsion regions. Pseudo ternary phase diagrams are used to determine the region of microemulsion existence. The effect of various surfactant/co-surfactant weight ratios on the extent of a stable microemulsion area can easily be observed with these diagrams. Furthermore, the optimum formulations are selected using the centroid of the microemulsion region.

Methods: Microemulsion formulations were prepared by changing the weight ratios of the components. The titration method was used at a constant temperature. A pseudo ternary phase diagram was constructed using the spots of the stable microemulsion formulations.

Results: The area and centroid of the stable microemulsion region were calculated by using the formulas manually and the macro edited for Microsoft® Excel. Both results were the same. The macro was user-friendly, easy to use, and worked well in Microsoft® Excel.

Conclusion: Definitions, formulas, algorithms, and calculations used in this research will be constructive for everyone interested in this field and can be modified very easily in every different case.

Keywords: Microemulsion, pseudo ternary phase diagram, coordinate geometry, algorithm, Microsoft® Excel macro

INTRODUCTION

The theoretical existence of microscopic emulsion-like structures in transparent mixtures of water, cationic soap, oil, and alcohol was first put forward by Hoar and Schulman in 1943. These structures were defined as "soluble oil" and "oleopathic hydro-micelle" due to a lack of terminology (Hoar & Schulman, 1943). In 1959, the term 'microemulsion' was used for the first time by Shulman et al. after electron microscopy visualization of an oil phase stained and solidified system (Schulman, Stoeckenius, & Prince, 1959; Kreilgaard, 2002). Since then, microemulsions have been found in various applications such as the paint, cosmetic, agriculture, and beverage industries (Spernath & Aserin, 2006). Microemulsions have also proven themselves as useful drug vehicles for transdermal, dermal, topical, oral, nasal, ocular, and parenteral routes of administration (Fanun, Papadimitriou, & Xenakis, 2011) as they can confer higher water solubility and bioavailability of drugs (Hathout & Woodman, 2012).

Microemulsions are thermodynamically stable, isotropic, and transparent dispersions, consisting of an oil and water phase, stabilized by an interfacial surfactant molecular film, usually in conjunction with a cosurfactant (Zhang, Cui, Zhu, Feng, & Zheng,

Address for Correspondence:

Murat Sami BERKMAN, e-mail: muratsb@anadolu.edu.tr

Submitted: 17.09.2020

Accepted: 10.12.2020

This work is licensed under a Creative Commons Attribution 4.0 International License.



2010). Even there are many more formulation components; it is more convenient to assume the microemulsions as oil/surfactant/water ternary systems (Burguera & Burguera, 2012). Development of microemulsion-based formulations requires techniques that force the researcher to analyze the microstructure and formation conditions (including analysis of ternary phase diagrams, particle size, and hydration effects, etc.) (Hickey, Hagan, Kudryashov, & Buckin, 2010). Constructing ternary phase diagrams is a time-consuming process; nevertheless, it is the most important and essential step in the preparation of microemulsion formulation. These diagrams are used to find the region of the microemulsion existence and study the effect of different surfactant/co-surfactant weight ratios on the extent of a stable microemulsion area (Sahoo, Pani, & Sahoo, 2014). One of the simplest and preferred methods for the ternary phase diagram is to organize and plot the experimental data as oil/water/surfactant percentages. After this step, the optimum formulation is selected using the centroid of the largest microemulsion region. Various Microsoft® Excel templates for the area calculation can be found on the web, but their reliability is suspicious, or the percentage values of the components can be transferred to graph paper to achieve the diagram. However, it is not possible to get the exact results by using this second method because to draw the graph, you need to round a few numbers.

Basic concepts

Ternary phase diagrams used in microemulsion systems are called ‘pseudo ternary phase diagrams’ (Schmidts et al., 2009). These are equilateral triangles, and the corners typically represent a binary mixture of two components, such as surfactant/ cosurfactant, water/drug, or oil/drug if the formulation components are more than three (Lawrence & Rees, 2000). However, generally, each side of the triangle corresponds to one component (oil, surfactant, or water) and is divided into 100 equal parts. Thus, to plot a ternary blend, the mass fraction of the components should be calculated as a percentage by weight (Das et al., 2020).

Two alternative presentations can be used on a ternary phase diagram to identify the component fractions of microemulsion systems. Every spot on the diagram represents a different composition of ternary components, and the mass fractions are read off through the sides of the triangle. The grey arrows show the correct directions to the corresponding component of spot A (40% oil, 20% surfactant, and 40% water) in Figure 1a. If a straight line is parallel to the base of the diagram, it is located opposite to the apex of the triangle. There is only one component at each corner, while the other two do not exist. Parallel lines like B and C are opposite to the apex, where the oil fraction is 100%. Although these lines cut both the oil and surfactant sides, the oil side is the one to be considered. Thus, parallel lines B and C indicate 90% and 70% of oil fraction respectively, not the surfactant fraction. The sum of surfactant and water percentage is always 10% on any point of line B because the sum of the three is always 100%. The main mistake in this stage is the incorrect drawn parallel lines or not to form 120° angles between the lines. The mass fractions of the components can also be determined by drawing perpen-

dicular lines, as shown in Figure 1b. The shortest distance from any interior spot to each of the three sides is always achieved by a perpendicular line. Viviani’s theorem states that ‘the sum of these distances equals to the length of altitude in equilateral triangles’ (Abboud, 2010).

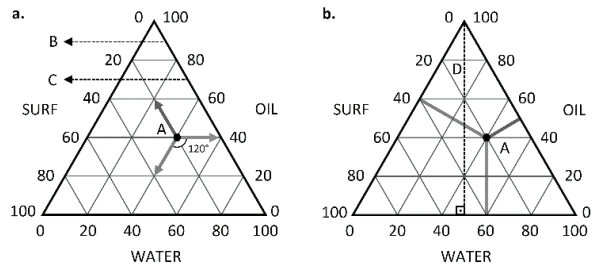


Figure 1. Reading values on a ternary phase diagram. a. component fractions by parallel lines; b. component fractions by perpendicular lines

Furthermore, the black dashed line D is the altitude and represents 100% of the oil component. Thus, the distances represented by the grey lines are once again the exact fractions of spot A (40% oil, 20% surfactant, and 40% water) and can easily be achieved.

Coordinate geometry

The percentages of the three components are useless for the area and centroid calculation unless they are represented in coordinate geometry. The problem starts at that point, as it is a hard step to transpose the spots into coordinates. In fact, the solution is very simple with the help of basic trigonometry knowledge. Although the oil, surfactant, and water percentages for spot A are known, what is the exact coordinate of this formulation on the x and y axes? Figure 2 provides a closer look at the situation and represents the phase diagram on coordinate geometry.

There is no need to rescale the triangle if 100 units of length are used on both axes. Thus, the base of the triangle is 100 units. A perpendicular line to the x-axis gives the x-coordinate as 60 units. Luckily, these phase diagrams are equilateral triangles with an interior angle of 60° in each corner. The cosine function can be used to achieve the y-coordinate because the cosine of an angle is the ratio of the length of the adjacent side (y) to the length of the hypotenuse, where it represents the oil percentage in Figure 2.

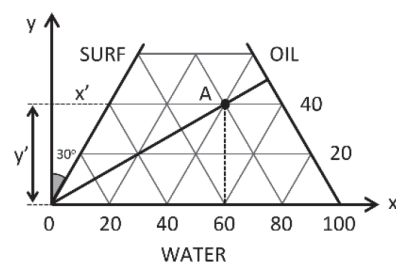


Figure 2. Pseudo ternary phase diagram on coordinate geometry.

$$y' = \text{hypotenuse} \times \cos(30^\circ) = 40 \times \cos(30^\circ) = 34.6410$$

Consequently, the exact coordinate of the spot is A(60.0000,34.6410). This approach is practical and works theoretically, but the x-coordinate is not always on the intersection of small triangles nor so easily readable. Actually, the fractions of the components obtained from experimental results are between the grey guidelines, as shown in Table 1.

Spots	Components (%)		
	Oil	Surfactant	Water
A	18	68	14
B	26	57	17
C	42	46	12
D	53	36	11
E	71	22	7

If all the formulation data are displayed on a ternary phase diagram, the location of the spots in the triangle can be observed clearly. This time the spots are not on the guidelines as shown in Figure 3.

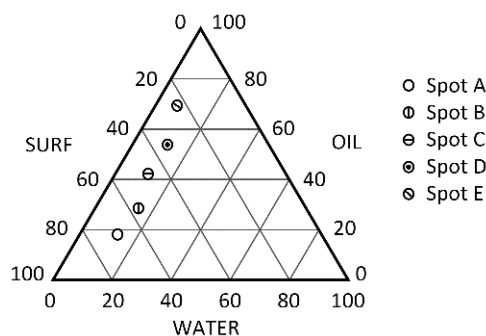


Figure 3. Plotting the spots on a pseudo ternary phase diagram.

After plotting spots A to E on the diagram, the same method with trigonometric functions can be used to define the coordinates. The first step to be done is to transpose the spots into coordinates. If the coordinates are carried out for spot A, then the formula can be used for the other spots as well. Therefore, a closer look at spot A will be useful, as in Figure 4.

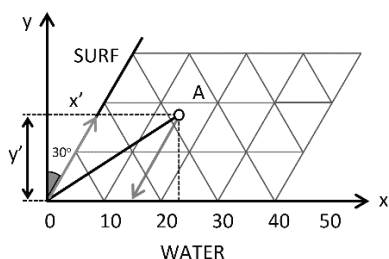


Figure 4. A closer look at a section of the pseudo ternary phase diagram.

Neither the x nor the y-coordinates can be read directly in Figure 4. The only known data are oil, surfactant, and water percentages, which are 18, 68, and 14, respectively. First, let us use the cosine function to achieve the y-coordinate (y'). As previously mentioned, note that the length of the hypotenuse (grey arrows) also represents the oil percentage in Figure 4.

$$y' = \text{hypotenuse} \times \cos(30^\circ) = 18 \times \cos(30^\circ) = 15.5885$$

$$y_A = 15.5885$$

Before finding the exact x-coordinate, the length of x' has to be calculated by using a similar equation to y' ;

$$x' = \text{hypotenuse} \times \sin(30^\circ) = 18 \times \sin(30^\circ) = 9.0000$$

The downward grey arrow in Figure 4 and also Figure 1a is used to detect the water percentage, and this line is parallel to the hypotenuse as well. Thus, the sum of water percentage and x' is equal to the x-coordinate (x_A) of the spot.

$$x_A = \text{water percentage} + x' = 14 + 9.0000 = 23.0000$$

The exact coordinate of the spot is A(23.0000,15.5885). Briefly, two general formulas can be used in every spot to determine the x and y-coordinates. These are

$$y_i = (\text{oil percentage}) \times \cos(30^\circ)$$

$$x_i = (\text{water percentage}) + \{(\text{oil percentage}) \times \sin(30^\circ)\}$$

If Microsoft® Excel is preferred instead of using a calculator, the following functions can be applied to the cells;

$$=(\text{COS}(\text{RADIANS}(30)) * (\text{OIL CELL})) \text{ for } y_i$$

$$=(\text{SIN}(\text{RADIANS}(30)) * (\text{OIL CELL})) + (\text{WATER CELL}) \text{ for } x_i$$

All the coordinates of spot A to E are given in Table 2, with the corresponding percentage of components.

Table 2. The coordinates of spots and the percentage of the components.

Spots	Coordinates	
	x_i	y_i
A	23.0000	15.5885
B	30.0000	22.5167
C	33.0000	36.3731
D	37.5000	45.8993
E	42.5000	61.4878

Creating a closed region

In order to select the optimum formulation and investigate the area and centroid, a closed region (Figure 5) in the ternary phase diagram should be defined. Thus, two straight lines are drawn from the corner to the opposite side, covering all the spots A to E (Yang, Kim, & Kim, 2002). The component on

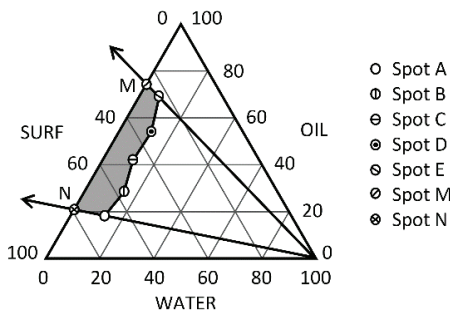


Figure 5. Stable microemulsion region on the pseudo ternary phase diagram.

the selected corner is called the formulation variable. If the microemulsion formulation is constructed by a water titration method, then the formulation variable is water (Liu et al., 2013).

When a closed region is formed with the boundary lines, two more spots must be considered. After these steps, there will be seven coordinated spots for the area calculation. Although the same methods are used for the coordinate calculation, the process is slightly more complicated. If the coordinates are carried out for spot N, then the formula can be used for spot M as well. Therefore, once again, a closer look at spot N will be useful, as in Figure 6a. If two straight lines are non-parallel on a two-dimensional space, they intersect at only one spot, which can be described by a single set of (x,y) coordinates (Figure 6b).

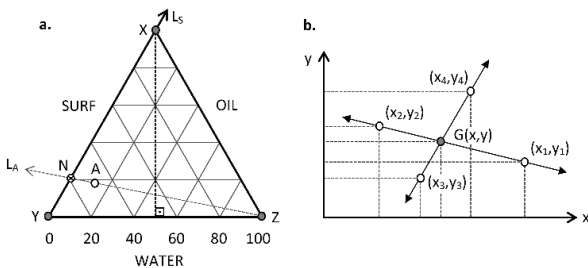


Figure 6. Position of spot N on pseudo ternary phase diagram. a. intersection of line L_A and L_S on coordinate geometry; b. the intersection of two straight lines.

Spot $N(x,y)$ is the intersection of line A (L_A) and the surfactant side of the triangle (L_S). Thus, to assign $N(x,y)$, each line has to be defined by two distinct spots with known coordinates, which may be as;

$$Z(x_1, y_1) = Z(100.0000, 0.0000) \text{ and}$$

$$A(x_2, y_2) = A(23.0000, 15.5885) \text{ for } L_A$$

$$Y(x_3, y_3) = Y(0.0000, 0.0000) \text{ and}$$

$$X(x_4, y_4) = X(50.0000, 86.6025) \text{ for } L_S$$

The intersection coordinate $G(x,y)$ of line L_A and L_S can be defined as;

$$x_G = \frac{(x_1 y_2 - y_1 x_2)(x_3 - x_4) - (x_1 - x_2)(x_3 y_4 - y_3 x_4)}{(x_1 - x_2)(y_3 - y_4) - (y_1 - y_2)(x_3 - x_4)}$$

$$y_G = \frac{(x_1 y_2 - y_1 x_2)(y_3 - y_4) - (y_1 - y_2)(x_3 y_4 - y_3 x_4)}{(x_1 - x_2)(y_3 - y_4) - (y_1 - y_2)(x_3 - x_4)}$$

After a series of laborious steps, the calculated intersection coordinate is;

$$N(x, y) = N(10.4651, 18.1261)$$

The usage of this formula is quite hard unless the data are transferred to Microsoft® Excel or any other calculus software. But there is quite a simple second way by using the previously mentioned equations and similarity.

Figure 7 represents two similar triangles with common sides. Thus, a simple proportion between them can be set;

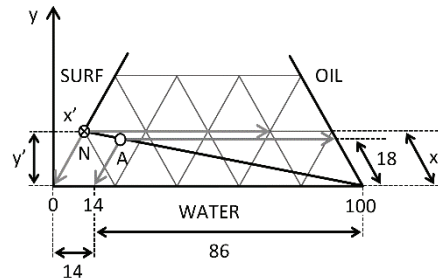


Figure 7. Position of spot N on pseudo ternary phase diagram by similarity.

$$\frac{86}{100} = \frac{18}{x} \quad x = 20.9302$$

This x value is the oil fraction of spot N, where the water fraction is zero. The exact coordinates of spot N can be achieved by using the previous equations, respectively.

$$y_N = 20.9302 \times \cos(30^\circ) = 18.1261$$

$$x_N = 20.9302 \times \sin(30^\circ) = 10.4651$$

The coordinates of the seventh spot, spot M, can be achieved as well with the same steps;

$$\frac{93}{100} = \frac{71}{x} \quad x = 76.3441$$

$$y_M = 76.3441 \times \cos(30^\circ) = 66.1159$$

$$x_M = 76.3441 \times \sin(30^\circ) = 38.1720$$

Area and centroid calculation

Calculating the area of a polygon is complicated. It can be verified by partitioning the polygon into smaller shapes, such as triangles or other quadrilaterals. Individual areas are calculated

and added together to find the entire polygon area. But the more numbers you deal with, the higher the chance of making mistakes. On the other hand, Gauss's area formula (Shoelace formula) and its mathematical algorithm offer a much easier way to determine the area (Lee, & Lim, 2017). Consider a non-self-intersecting closed polygon with n sides (Figure 8) and list the coordinates of each vertex clockwise or counterclockwise as you wish.

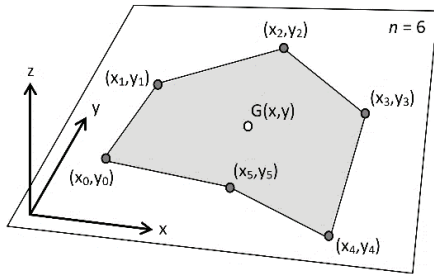


Figure 8. The coordinates of a closed polygon.

Notice that the polygon is closed. Thus, the last vertex (x_{n+1}, y_{n+1}) is the starting coordinate. The formula used is similar to a determinant function and can be expressed as below.

$$A = \frac{1}{2} \begin{vmatrix} x_1 & x_2 & \dots & x_n & x_1 \\ y_1 & y_2 & \dots & y_n & y_1 \end{vmatrix}$$

It is not literally a true determinant because the matrix is not square but can be evaluated like two by two determinants as well. Starting with x_1 , multiply the diagonal pairs and add them. Essentially, you get the sum of $x_1 y_2 + x_2 y_3 + \dots + x_n y_1$. Starting with y_1 , do the same calculations and get the sum of $y_1 x_2 + y_2 x_3 + \dots + y_n x_1$. The value of the determinant is the difference between these two terms, and if the result is negative, then use the absolute value. Multiply it by half to get the area. This formula can be used for any closed polygons and represented by the expression below.

$$A = \frac{1}{2} \left| \sum_{i=1}^{n-1} x_i y_{i+1} + x_n y_1 - \sum_{i=1}^{n-1} x_{i+1} y_i + x_1 y_n \right|$$

$$A = \frac{1}{2} |x_1 y_2 + x_2 y_3 + \dots + x_n y_1 - x_2 y_1 - \dots - x_1 y_n|$$

This formula can be simplified as;

$$A = \frac{1}{2} \left| \sum_{i=1}^n (x_i y_{i+1} - x_{i+1} y_i) \right|$$

Alternatively, the Trapezoid Rule can also be used to determine the area of polygons (Smith, Goodchild, & Longley, 2007). The area between the x-axis and the two vertical lines at x_1 and x_2 is simply the width between the two lines $(x_2 - x_1)$ times the average height of the two lines $(y_1 + y_2)/2$. If these operations are performed for all coordinates and the areas are added with positive and negative values, the total area of the polygon is obtained. In this case, the formula can be rearranged as;

$$A = \frac{1}{2} \left| \sum_{i=1}^n (x_{i+1} - x_i) (y_i + y_{i+1}) \right|$$

According to Green's Theorem (Green & Thomson, 1828; Soerjadi, 1968), if a curve C forms the boundary of a region D and F_n 's are the functions of (x,y) defined on an open region containing D with continuous partial derivatives there, then it states;

$$\oint_C F_1(x, y) dx + F_2(x, y) dy = \iint_D \left(\frac{\partial F_2}{\partial x} - \frac{\partial F_1}{\partial y} \right) dx dy$$

This theorem can only be used for the area calculation of a polygon in the following case;

$$\frac{\partial F_2}{\partial x} - \frac{\partial F_1}{\partial y} = 1$$

Choosing $F_1(x,y) = 0$ and $F_2(x,y) = x$ meets this requirement. Then, the area of the region can also be calculated by evaluating any of the following line integrals.

$$A = \oint_C x dy = - \oint_C y dx = \frac{1}{2} \oint_C (x dy - y dx)$$

Line integrals over the curves are additive over length, so;

$$A = \oint_C x dy = \int_{C_1} x dy + \int_{C_2} x dy + \dots + \int_{C_n} x dy$$

After the segment parametrisation from (x_i, y_i) to (x_{i+1}, y_{i+1}) and the integral substitution, the sum of all C_i gives the total area same as the Trapezoid Rule.

$$C_i: \vec{r} = ((x_{i+1} - x_i)t + x_i, (y_{i+1} - y_i)t + y_i), \quad 0 \leq t \leq 1$$

$$\begin{aligned} \int_{C_i} x dy &= (y_{i+1} - y_i) \int_0^1 ((x_{i+1} - x_i)t + x_i) dt \\ &= \frac{(x_i + x_{i+1})(y_{i+1} - y_i)}{2} \end{aligned}$$

$$A = \frac{1}{2} \left| \sum_{i=1}^n (x_i + x_{i+1})(y_{i+1} - y_i) \right|$$

After the area is calculated, one more parameter must be determined. The centroid of a non-self-intersecting closed polygon defined by n vertices $(x_1, y_1), (x_2, y_2), \dots, (x_n, y_n)$ is the point (G_x, G_y) , where;

$$G_x = \frac{1}{6A} \sum_{i=0}^{n-1} (x_i + x_{i+1}) (x_i y_{i+1} - x_{i+1} y_i)$$

$$G_y = \frac{1}{6A} \sum_{i=0}^{n-1} (y_i + y_{i+1}) (x_i y_{i+1} - x_{i+1} y_i)$$

Although these formulas are beneficial on their own, it is important to consider that this approach involves a lot of tedious arithmetic calculations. Thus, its main benefit arises when applied in a computer program as an algorithm.

Model optimization and algorithm

Microsoft® Excel is one of the most used software programs of all time. Millions of people around the world use this software to enter all sorts of data and perform financial, mathematical, or statistical calculations. It allows us to organize, format, and calculate data with formulas using a spreadsheet system. In addition to its standard calculation features, Excel also offers the ability to access data from external sources via Microsoft's Dynamic Data Exchange (DDE), programming support via Microsoft's Visual Basic for Applications (VBA), and extensive graphing and charting capabilities. Due to all these features, it can be said that this software is a very advanced calculator.

VBA is one of the most powerful features of Microsoft® Excel. It enables us to write functions and subroutines. A function returns a value to a cell in the same way as a worksheet function while a subroutine performs a process. Briefly, subroutines and functions are known as *macros*, and we need to use these user-defined functions (UDF) beside the built-in ones. If Microsoft® Excel has no built-in function, UDFs may be more convenient when we repeatedly need to perform a specific type of calculation (Liengme, 2016).

In order to work with the VBA editor, we shall need to have the Developer tab on the ribbon. If it is not present, right-click any of the tabs on the ribbon and select Customize Ribbon, and in the right-hand panel, enter a checkmark in the Developer box. Click the OK button to close the dialog.

The visual basic editor allows us to calculate the area and centroid of the stable microemulsion regions by using the formulas mentioned above. But first, we need to create an algorithm to make these operations simpler and write it into the relevant box. Open Microsoft® Excel, copy your data to the spreadsheet, and then use the command Developer / Code / Visual Basic (or the shortcut Alt+F1) to open the VBE. Use the command Insert / Module and add a module to the project tree. Click the module1 section and type or copy/paste the algorithm below. Do not forget to save your work as Macro-Enabled Workbook.

```
Function AREA(Coordinate)
mylast = Coordinate.Count / 2
Area1 = 0
For I = 1 To mylast
    xi = Coordinate(I, 1)
    yi = Coordinate(I, 2)
If I = mylast Then
    xk = Coordinate(1, 1)
    yk = Coordinate(1, 2)
Else
    xk = Coordinate(I + 1, 1)
```

```
    yk = Coordinate(I + 1, 2)
End If
    Formula = (xi * yk - xk * yi)
    Area1 = Area1 + Formula
Next I
    AREA = Abs(Area1 / 2)
End Function

Function GX(Coordinate)
mylast = Coordinate.Count / 2
Area1 = 0
Cx = 0
For I = 1 To mylast
    xi = Coordinate(I, 1)
    yi = Coordinate(I, 2)
If I = mylast Then
    xk = Coordinate(1, 1)
    yk = Coordinate(1, 2)
Else
    xk = Coordinate(I + 1, 1)
    yk = Coordinate(I + 1, 2)
End If
    Formula = (xi * yk - xk * yi)
    Area1 = Area1 + Formula
    Cx = Cx + (xi + xk) * Formula
Next I
    GX = Abs(Cx / (3 * Area1))
End Function

Function GY(Coordinate)
mylast = Coordinate.Count / 2
Area1 = 0
Cy = 0
For I = 1 To mylast
    xi = Coordinate(I, 1)
    yi = Coordinate(I, 2)
If I = mylast Then
    xk = Coordinate(1, 1)
    yk = Coordinate(1, 2)
Else
    xk = Coordinate(I + 1, 1)
    yk = Coordinate(I + 1, 2)
End If
    Formula = (xi * yk - xk * yi)
    Area1 = Area1 + Formula
    Cy = Cy + (yi + yk) * Formula
Next I
    GY = Abs(Cy / (3 * Area1))
End Function
```

If there is no problem, the macro is ready to use. Return to the Microsoft® Excel main page (you can click the Excel main file in the Windows taskbar or the Excel icon on the VBE toolbar) and just type the new function code as any of the built-in functions. Your new assigned functions are;

=AREA(x_i coordinates, y_i coordinates)

=GX(x_i coordinates, y_i coordinates)

=GY(x_i coordinates, y_i coordinates)

MATERIALS AND METHOD

This section provides details of the materials and methodology used to get the data needed for the calculations.

Materials

The following materials were used for the preparation of the microemulsion formulations. For the oil phase, isopropyl myristate (IPM), was provided by Merck Schuchardt OHG (Germany). The surfactants polyoxyethylene sorbitan monooleate (Tween® 80) and sorbitan monolaurate (Span® 20) were from Sigma-Aldrich (Germany). Ultrapure water (Millipore Milli-Q, USA) was used throughout the experiments as the hydrophilic phase. All chemicals were of pharmaceutical grade and used as received without any further purification.

Pseudo ternary phase diagram

A pseudo ternary phase diagram was constructed to find the area of microemulsion existence. Briefly, Tween® 80 and Span® 20 were blended in a 1:1 weight ratio and added into the oil phase. Ten grams of IPM and surfactant mixtures were prepared with various weight ratios from 1.0:9.0 to 9.0:1.0 in glass beakers. Ultrapure water was added dropwise to each oily mixture while stirring on a mechanical stirrer (200 rpm) at room temperature ($25 \pm 1^\circ\text{C}$). The titration was continued until the transparent and homogeneous dispersion turned turbid, which defined the transition point from microemulsion to coarse emulsion. The amount of water required to turn the mixture slightly turbid was then recorded. The samples were allowed to equilibrate at $25 \pm 1^\circ\text{C}$ for at least 24 h, and the transparent samples were considered as monophasic spots in the phase diagram (Figure 9).

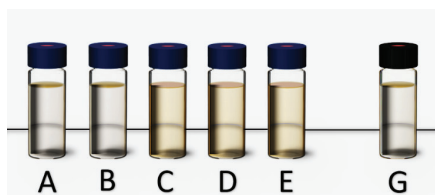


Figure 9. Transparent microemulsion samples (A-E) and the final formulation prepared from the G spot.

The mass fractions (oil, surfactants, and water) of each spot were calculated and plotted in the pseudo ternary phase diagram to find the stable microemulsion region. The percentages of the components and the coordinates of the spots are presented in Table 1, Table 2, and Figure 5 as well.

RESULTS AND DISCUSSION

The area and centroid of the stable microemulsion region were calculated using the formulas manually and the macro edited for Microsoft® Excel. Both results were the same.

The macro was super easy to use and available in the fx function menu too. We have worked very hard to make this algorithm user-friendly. The main problem in the development process was the desire to achieve results without the repetition of the last vertex because, as previously mentioned, (x_{n+1}, y_{n+1}) was the starting coordinate. In detail, the problem was solved, and unlike the formulas, you do not need to enter the first vertex again at the end, and you can go in either direction around the polygon. The internal programming of the calculator takes care of it all for you. A sample section of Microsoft® Excel interface while using the algorithm and the functions is present in Figure 10.

	B	C	D	E	F	G
1		x_i	y_i			
2		23.0000	15.5885		Area	556.5882
3		30.0000	22.5167		Gx	27.6889
4		33.0000	36.3731		=Gy	36.9646
5		37.5000	45.8993		fx GY	
6		42.5000	61.4878		fx GX	
7		38.1720	66.1159		fx AREA	
8		10.4651	18.1261			
9						

Figure 10. The area and centroid results in Microsoft® Excel.

The area of the stable microemulsion region was 556.5886 unit squared, and the centroid was on the G(27.6889,36.9646) spot, as seen in Figure 9 and 10. After this step, we needed a final calculation to find the percentage values of the components. The results were easily achieved by a reverse calculation specified at the beginning of the manuscript.

$$\text{oil percentage} = G_y / \cos(30^\circ)$$

$$= 36.9646 / \cos(30^\circ)$$

$$= 42.6830 \approx 43\%$$

$$\text{water percentage} = G_x - \{(\text{oil percentage}) \times \sin(30^\circ)\}$$

$$= 27.6889 - \{42.6830 \times \sin(30^\circ)\}$$

$$= 6.3474 \approx 6\%$$

$$\text{surfactants percentage} = 100 - (42.6830 + 6.3474)$$

$$= 50.9696 \approx 51\%$$

Remember that the surfactants were blended in a 1:1 weight ratio; therefore, the percentages of Tween® 80 and Span® 20 are both 25.5%.

In fact, the coordinate and percentage calculations could also be included in the algorithm. However, the locations of the components are interchangeable, and it was preferred to keep

it simple. This version of the algorithm could be used much more comfortably as a source code for Microsoft® Excel and all other platforms.

CONCLUSION

Microemulsion formulations were prepared by changing the weight ratios of the components. The titration method was used at a constant temperature. The pseudo ternary phase diagram was constructed using the spots of the stable microemulsion formulations. The region of microemulsion formation was assigned, then the area and centroid of the region were calculated. Formulas and the algorithm were used for all the calculations. A final formulation was prepared according to the percentages on the centroid and found to be stable as expected.

As a result, the macro was user-friendly, easy-to-use, and worked well in Microsoft® Excel. Definitions, formulas, and calculations used in this study will be very helpful for everyone interested in this field and can be modified very easily in every different case.

Acknowledgment: The authors thank the research assistant İsmail Terzi (Eskişehir Technical University, Department of Computer Engineering) for his valuable contributions to VBA and macro editing.

Peer-review: Externally peer-reviewed.

Author contributions: Conception/Design of Study- M.S.B., K.G.; Data Acquisition- M.S.B.; Data Analysis/Interpretation- M.S.B., K.G.; Drafting Manuscript-M.S.B., K.G.; Critical Revision of Manuscript- M.S.B.; Final Approval and Accountability- M.S.B., K.G.

Conflict of Interest: The authors have no conflict of interest to declare.

Financial Disclosure: Authors declared no financial support.

REFERENCES

- Abboud, E. (2010). Viviani's theorem and its extension. *The College Mathematics Journal*, 41(3), 203-211. <https://doi.org/10.4169/074683410X488683>
- Burguera, J. L., & Burguera, M. (2012). Analytical applications of emulsions and microemulsions. *Talanta*, 96, 11-20. <https://doi.org/10.1016/j.talanta.2012.01.030>
- Das, S., Lee, S. H., Chia, V. D., Chow, P. S., Macbeath, C., Liu, Y., & Shliout, G. (2020). Development of microemulsion based topical ivermectin formulations: pre-formulation and formulation studies. *Colloids and Surfaces B: Biointerfaces*, 189, 1-8. <https://doi.org/10.1016/j.colsurfb.2020.110823>
- Fanun, M., Papadimitriou, V., & Xenakis, A. (2011). Characterization of cephalixin loaded nonionic microemulsions. *Journal of Colloid and Interface Science*, 362(1), 115-121. <https://doi.org/10.1016/j.jcis.2011.05.042>
- Green, G., & Thomson, W. (1828). *An essay on the application of mathematical analysis to the theories of electricity and magnetism*. Nottingham: T Wheelhouse.
- Hathout, R. M., & Woodman, J. (2012). Applications of NMR in the characterization of pharmaceutical microemulsions. *Journal of Controlled Release*, 161(1), 62-72. <https://doi.org/10.1016/j.jconrel.2012.04.032>
- Hickey, S., Hagan, S. A., Kudryashov, E., & Buckin, V. (2010). Analysis of phase diagram and microstructural transitions in an ethyl oleate/water/Tween 80/Span 20 microemulsion system using high-resolution ultrasonic spectroscopy. *International Journal of Pharmaceutics*, 388(1-2), 213-222. <https://doi.org/10.1016/j.ijpharm.2009.12.003>
- Hoar, T. P., & Schulman, J. H. (1943). Transparent water in oil dispersions: oleopathic hydromicelle. *Nature*, 152, 102-103. <https://doi.org/10.1038/152102a0>
- Kreilgaard, M. (2002). Influence of microemulsions on cutaneous drug delivery. *Advanced Drug Delivery Reviews*, 54(1), 77-98. [https://doi.org/10.1016/S0169-409X\(02\)00116-3](https://doi.org/10.1016/S0169-409X(02)00116-3)
- Lawrence, M. J., & Rees, G. D. (2000). Microemulsion-based media as novel drug delivery systems. *Advanced Drug Delivery Reviews*, 45(1), 89-121. [https://doi.org/10.1016/S0169-409X\(00\)00103-4](https://doi.org/10.1016/S0169-409X(00)00103-4)
- Lee, Y., & Lim, W. (2017). Shoelace formula: connecting the area of a polygon with vector cross product. *The Mathematics Teacher*, 110(8), 631-636. <https://doi.org/10.5951/mathteacher.110.8.0631>
- Liengme, B. V. (2016). VBA user-defined functions. In B. V. Liengme (Ed.), *A guide to Microsoft Excel 2013 for scientists and engineers* (pp. 181-206). San Diego: Academic Press. <https://doi.org/10.1016/C2014-0-03421-1>
- Liu, D., Kobayashi, T., Russo, S., Li, F., Plevy, S. E., Gambling, T. M., Carson, J. L., & Mumper, R. J. (2013). *In vitro* and *in vivo* evaluation of a water-in-oil microemulsion system for enhanced peptide intestinal delivery. *The AAPS Journal*, 15(1), 288-298. <https://doi.org/10.1208/s12248-012-9441-7>
- Sahoo, S., Pani, N. R., & Sahoo, S. K. (2014). Microemulsion based topical hydrogel of sertaconazole: Formulation, characterization and evaluation. *Colloids and Surfaces B: Biointerfaces*, 120, 193-199. <https://doi.org/10.1016/j.colsurfb.2014.05.022>
- Schmidts, T., Nocker, P., Lavi, G., Khulman, J., Czermak, P., & Runkel, F. (2009). Development of an alternative, time and cost saving method of creating pseudoternary diagrams using the example of a microemulsion. *Colloids and Surfaces A: Physicochemical and Engineering Aspects*, 340(1-3), 187-192. <https://doi.org/10.1016/j.colsurfa.2009.03.029>
- Schulman, J. H., Stoeckenius, W., & Prince, L.M. (1959). Mechanism of formation and structure of microemulsions by electron microscopy. *The Journal of Physical Chemistry*, 63(10), 1677-1680. <https://doi.org/10.1021/j150580a027>
- Smith, M. J., Goodchild, M. F., & Longley, P. A. (2007). Building blocks of spatial analysis. In M. J. Smith, M. F. Goodchild & P. A. Longley (Eds.), *Geospatial analysis: A comprehensive guide to principles, techniques and software tools* (pp. 69-71). United Kingdom: Matador.
- Soerjadi, R. (1968). On the computation of the moments of a polygon, with some applications. *Heron*, 16(5), 43-58.
- Spernath, A., & Aserin, A. (2006). Microemulsions as carriers for drugs and nutraceuticals. *Advances in Colloid and Interface Science*, 128-130, 47-64. <https://doi.org/10.1016/j.jcis.2006.11.016>
- Yang, J. H., Kim, Y., & Kim, K. M. (2002). Preparation and evaluation of aceclofenac microemulsion for transdermal delivery system. *Archives of Pharmacal Research*, 25(4), 534-540. <https://doi.org/10.1007/BF02976614>
- Zhang, H., Cui, Y., Zhu, S., Feng, F., & Zheng, X. (2010). Characterization and antimicrobial activity of a pharmaceutical microemulsion. *International Journal of Pharmaceutics*, 395(1-2), 154-160. <https://doi.org/10.1016/j.ijpharm.2010.05.022>

Rational design and synthesis of quinazoline derivatives

Fatimah AlKharaz¹ , Zead Abudayeh¹ , Qais Abualassal¹ , Loay Hassouneh² 

¹Isra University, Faculty of Pharmacy, Department of Applied Pharmaceutical Sciences, Amman, Jordan

²Isra University, Faculty of Pharmacy, Department of Basic Pharmaceutical Sciences, Amman, Jordan

ORCID IDs of the authors: F.A. 0000-0001-9198-0603; Z.A. 0000-0003-4879-5634; Q.A. 0000-0002-6784-3147; L.H. 0000-0002-8278-7278

Cite this article as: AlKharaz, F., Abudayeh, Z., Abualassal, Q., & Hassouneh, L. (2021). Rational design and synthesis of quinazoline derivatives. *Istanbul Journal of Pharmacy*, 51(1), 50-58.

ABSTRACT

Background and Aims: Alzheimer's disease is a neurodegenerative disorder in which the death of brain cells causes memory loss and cognitive decline. It is one of the leading causes of mortality worldwide. Several different hallmarks of the disease have been reported such as low levels of acetylcholine, deposits of β -amyloid around neurons, hyperphosphorylated tau protein, oxidative stress, etc. Pharmacotherapy for this disease currently depends on using acetylcholinesterase inhibitors and *N*-methyl-D-aspartate receptor antagonists. They provide only symptomatic relief and mostly targets cognitive revival. Quinazoline derivatives were recently reported as being a valuable template in the treatment of many neurodegenerative disorders. Quinazoline based compounds were declared as being potential anti AD agents. This research focuses on the synthesis of novel quinazoline derivatives **3** and **4**.

Methods: Novel quinazoline derivatives **3** and **4** were synthesized starting from 2-(methylamino)benzamide by consecutive steps. The structures of these compounds have been characterized using different analytical and spectral methods: TLC, GC-MS, ¹H-NMR and ¹³C-NMR.

Results: This study revealed the synthesis of the novel compounds **3** and **4** with excellent yields equalling 97% and 73.1% respectively.

Conclusion: Novel quinazoline derivatives compounds **3** and **4** were obtained. These compounds might be promising lead compounds for potential poly-functional anti-Alzheimer's agents in future work.

Keywords: Quinazoline derivatives, Synthesis, Reaction conditions

INTRODUCTION

Alzheimer's disease (AD) is an age-related, gradual, and irreversible neurodegenerative disorder characterized by cognitive and memory failure, and it is the most common cause of dementia in elderly persons. Between 1997 and 2050, the older population, defined as adults 65 years of age and older, will increase from 63 to 137 million in the Americas, from 113 to 170 million in Europe, from 18 to 38 million in Africa and from 172 to 435 million in Asia. The estimated spread of this disease in 2015 was 44 million people all over the world and it is estimated that this number will double by 2050 and there are many studied defined risk factors for AD, age is the greatest leading factor for the AD (Apostolova, 2016; Hung & Fu, 2017). The likelihood of developing AD increases greatly with age. Gender can also change the prevalence of AD. Nearly two-thirds of all patients diagnosed with AD are women. General health status plays a role in AD: high blood cholesterol levels have been suggested as risk factors for AD and there is an association between high blood pressure and AD. However, this association is complex and differs with age. It has been shown that high blood pressure in middle age is associated with an increased risk of AD; while other studies found no association between hypertension in the older persons and dementia (Lazo-Porrás et al., 2017). Several studies linking obesity to increased cognitive decline and AD

Address for Correspondence:

Zead ABUDAYEH, e-mail: zead.abudayeh@iu.edu.jo

Submitted: 25.05.2020

Revision Requested: 26.06.2020

Last Revision Received: 09.09.2020

Accepted: 21.09.2020

This work is licensed under a Creative Commons Attribution 4.0 International License.



risk (Naderali, Ratcliffe, & Dale, 2009). Studies in both human and animal models suggest that particular dietary constituents may be important in modulating AD risk. For example, a high fatty acid diet is associated with obesity and thus with a higher risk of AD. It was recently reported that a high-fat diet causes damage similar to that noticed in Alzheimer's pathology. Type 2 diabetes mellitus is considered an independent risk factor for AD (Naderali et al., 2009; Bekris, Yu, Bird, & Tsuang, 2010; Panpalli, Karaman, Guntekin, & Ergun, 2016; Mendiola-Precoma, Berumen, Padilla, & Garcia-Alcocer, 2016; Lazo-Porras et al 2017; Tariq & Barber 2017; Kivimäki & Singh-Manoux, 2018; Benny & Thomas, 2019). Family history of sporadic AD is a well-established risk factor. Individuals who have a first-degree relative diagnosed with AD are more likely to develop the disease than those who do not (Bekris et al., 2010). Genetic makeup is not the only risk; shared environmental and lifestyle factors likely also play a role (Apostolova, 2016).

Cognition is the combination of two vital components, i.e., learning and memory. In many diseases like AD and dementia, the cognition is changed based on the severity of the disease. The concept of cognition and the function of central cholinergic transmission in the acquisition of cognitive roles has been recognized since the early sixties. Several neurotransmitters have role in the acquisition of learning and memory, but, the part of the cholinergic system is the most important role for neurological researchers (Benny & Thomas, 2019; Szeto, Simon, & Lewis, 2016).

The Cholinergic hypothesis was suggested thirty five years ago (Darras, Wehle, Huang, Sotriffer, & Decker, 2014). It revolutionized the area of AD research by transporting it from the field of descriptive neuropathology to the recent concept of synaptic neurotransmission. It is based on three fundamentals: the detection of depleted presynaptic cholinergic markers in the cerebral cortex; the finding that the neurons from the nucleus basalis of Meynert (NBM) in the basal forebrain, which are the origin of cortical cholinergic transmitters that undergo intense neurodegeneration in AD; and the confirmation that cholinergic antagonists decline memory whereas agonists have the counter effect. The hypothesis received compulsory validation when cholinesterase inhibitor drugs such as tacrine (Cognex, later disused because of harmful effects), donepezil (Aricept), galantamine (Reminyl), and rivastigmine (Exelon) were shown to produce significant symptomatic improvement in patients with AD. Although other pertinent pathophysiological mechanisms have got more research awareness in last years, treatments that improve cholinergic role remain definitive in the management of patients with AD. These compounds are usually prescribed at the early stages of AD when cognitive symptoms are light to moderate (Douchamps & Mathis, 2017; Hampel et al., 2018).

Benefits noticed as cognitive performances increase or at least stabilize, and there is an overall improvement in the activities of daily life. These drugs are the only ones approved so far as AD directed treatments, with the single exception of NMDA antagonist memantine (Olivares, et al., 2012; Douchamps & Mathis, 2017; Hampel et al., 2018).

Quinazoline is one of the benzodiazine family with its heteroatomic nitrogen located at 1- and 3-positions (Ajani, Ad-

erohunmu, Umeokoro, & Olomieja, 2016). These backbone structures were declared as potential anti AD agents and novel quinazoline-urea analogues were recently reported as being valuable templates in the treatment of many neurodegenerative disorders (Kamel, Zaghary, Al-Wabli, & Anwar, 2016; Park et al., 2017). Moderate or strong inhibitory effects of 3,4-dihydroquinazoline derivatives towards acetylcholinesterase enzyme (AChE) were also reported. Furthermore some new 2-(2-indolyl)-4(3H)-quinazoline derivatives were designed, synthesized and the biological evaluation of these new derivatives including anti AChE activity, kinetic analysis and molecular modeling of the AChE inhibition were investigated (Li et al., 2013). Many studies have highlighted 2,4-disubstituted quinazoline as cholinesterase inhibitors (Mohamed, Manna, & Rao, 2017; Mohamed & Rao, 2017). Based on the previously mentioned studies, we decided to synthesize new quinazoline derivatives as potential acetylcholinesterase enzyme inhibitor.

MATERIALS AND METHODS

Chemicals, instrumentation and analytical methods

N-Methylisatoic anhydride, lithium aluminium hydride (LiAlH₄), cycloheptanone, tetrahydrofuran (THF) anhydrous, trimethylsilyl chloride (TMSCl), all were purchased from Sigma Aldrich. Ammonia solution 32% from (ALPHA chemika company), ethyl acetate and n-hexane from (Tedia® HPLC/spectro), petroleum ether purchased from (Pharmaco), sodium hydroxide (NaOH) purchased from (Extra pure Sand C chemicals supply co chemicals laboratory chemicals), water (H₂O) HPLC grade and methanol GC grade, were in compliance to the specification of USP, BP, EP grades purchased from (Lab chem), toluene-4-sulfonic acid monohydrate, hydrochloric acid (HCl) 37%, sodium sulphate (Na₂SO₄) anhydrous and dichloromethane (DCM) all were purchased from (AZ Chem for chemicals), triethylamine (TEA) purchased from (Riedel-deHaen), acetonitrile purchased from (chem. lab. HPLC grade). All reagents and solvents were purchased from different commercial suppliers and utilized without any further modifications.

Thin-layer chromatography (TLC) plates (silica gel 60 coated with fluorescent indicator F254) were purchased from Sigma-Aldrich, which were visualized by exposing to iodine vapours and UV light. Mobile phase used was ethyl acetate: petroleum ether 1:1, v/v, for monitoring **2** synthesis and hexane: ethyl acetate 1:1, v/v used for **3** and **4** synthesis. Column dimension utilized (60 cm × 1 cm, or larger column based on the weight and the purity of sample), wet method was used for column packing with silica gel 60 Å (average particle size 63-200 µm, 60 g silica/1 g of product) loaded onto the top of the silica bed and the isocratic mobile phases used were ethyl acetate: petroleum ether (2:8) for purification of compound **2**, and DCM: ethyl acetate : TEA (160:40:4) v/v for the purification of compound **3**. Compounds were detected by a UV-light detector. Fractions possessing the same purity were collected together, concentrated using a rotary evaporator.

¹H NMR (500.13 MHz) and ¹³C NMR spectra (125.75 MHz) were recorded on a Bruker Avance NMR spectrometer (Bruker, Karlsruhe, Germany). Chemical shifts were recorded in ppm (δ) and were referenced to internal tetramethylsilane (TMS) and

coupling constants (J values) are expressed in Hz. To monitor the progress of reactions gas chromatography-mass spectrometer (GC-2010 plus Shimadzu) with flame ionization detector (FID) was used. GCMS real-time analysis software from Craig S Young, Sr. Technical Support. Shimadzu Scientific Instruments was used for data acquisition from the FID. The Perkin-Elmer column (25 m x 0.32 mm, 1.0 μ m film thickness) was utilized. Helium was used as the carrier gas (purity 99.995%) with a splitless injection (100:1). The splitless injector temperature was 250 °C and oven column temperature was 150 °C. Samples were dissolved in methanol (GC grade in compliance to the specification of USP, BP, EP grade. Lab chem).

Synthesis of target compounds 2-4

Synthesis of compound 2

2-(Methylamino)benzamide ($C_8H_{10}N_2O$) (2) was synthesized as previously reported

(Zhao, Wang, & Li, 2014) with slight modifications: *N*-Methylisatoic anhydride (5 g) was stirred with 125 ml ammonia aqueous solution in a 250 round bottom flask at 30 °C for 60 minutes. The mixture was cooled to room temperature and the solvent was removed in a vacuum. Then, the mixture was purified using column chromatography by elution solvent ethyl acetate: petroleum ether (2:8).

Synthesis of compound 3

The synthesis of compound 3 was achieved as previously reported method (Abualassal, Abudayeh, & Husien- Al-Ali, 2019) with some modifications: Toluene-4-sulfonic acid monohydrate 302 mg (0.13 eq) was stirred with 5 ml cycloheptanone followed by the addition 2.036 g (1 eq) of compound 2 previously prepared in methanol under reflux for 3 h. The reaction mixture was cooled to room temperature and thin stirred for 24 h. TLC and GC-MS revealed complete consumption of compound 2 with presence of our target product 3. The solvent in reaction mixture was removed under vacuum. The purification achieved using column chromatography with 160:40:4 DCM: ethyl acetate: TEA and recrystallized from methanol.

Synthesis of compound 4

Compound 4 was synthesized starting from the activation of amide group with TMSCl followed by reduction with $LiAlH_4$. This method permitted the target compound 4 to give an excellent yield (Scheme 1). The target compounds 2-4 were characterized by 1H NMR, ^{13}C NMR and GCMS methods.

Synthesis of 2-methylaminobenzamide (2).

%Yield (85.71%), color: white crystals, Rf : 0.5 (EtOAc/Petroleum ether = 2 : 8), MS m/z = 150. (Figure 1).

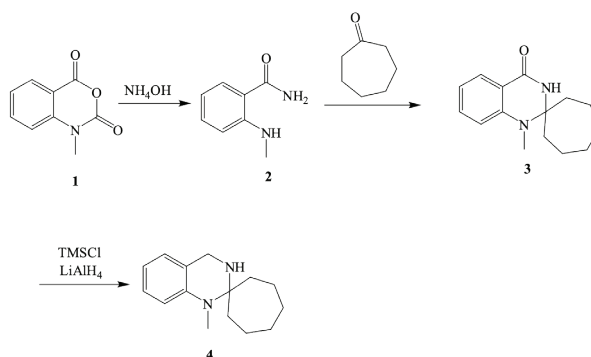
1H -NMR (500 MHz, DMSO): = 2.78 (d, 3H, J = 4.85 Hz, CH_3) 3.32 (s, 1H, NH), 6.52 (t, 1H, J = 7.45 Hz, ArH), 6.62 (d, 1H, J = 8.3 Hz, ArH), 7.28 (td, 1H, J_1 = 7.6 Hz, J_2 = 0.2 Hz, ArH), 7.59 (d, 1H, J = 7.8 Hz, ArH), 7.11, 7.88 (2br s, NH_2). (Figure 2).

1'-Methyl-1H'-spiro[cycloheptane-1,2'-quinazolin]-4'(3'H)-one (3).

%Yield: (98%), color: brown crystals, Rf : 0.7 (Hexane/EtOAc= 1:1), MS m/z = 244. (Figure 3).

1H -NMR (500 MHz, $CDCl_3$): δ = 1.56-1.99 (m, 12H, 2'-H2 - 7'-H2) 2.81 (s, 3H, CH_3), 6.63 (d, 1H, J = 8.2 Hz, ArH), 6.78 (dd, 1H, J_1 = 7.35 Hz, J_2 = 0.1 Hz, ArH), 7.34 (dd, 1H, J_1 = 7.8 Hz, J_2 = 0.35 Hz, ArH), 7.58 (s, 1H, NH), 7.89 (d, 1H, J = 7.45 Hz, 1H, ArH). (Figure 4).

^{13}C -NMR (125 Hz, $CDCl_3$): δ = 22.97, 30.46 (cyclohept.), 31.29 (NCH_3), 37.98 (cyclohept.),



Scheme 1. Synthesis of compound 2-4.

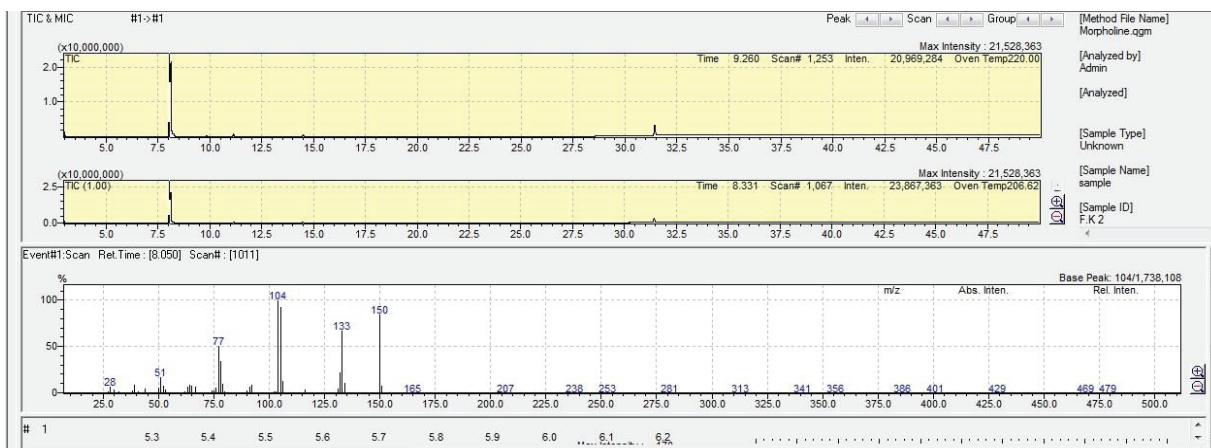


Figure 1. GC-MS spectrum of the compound 2.

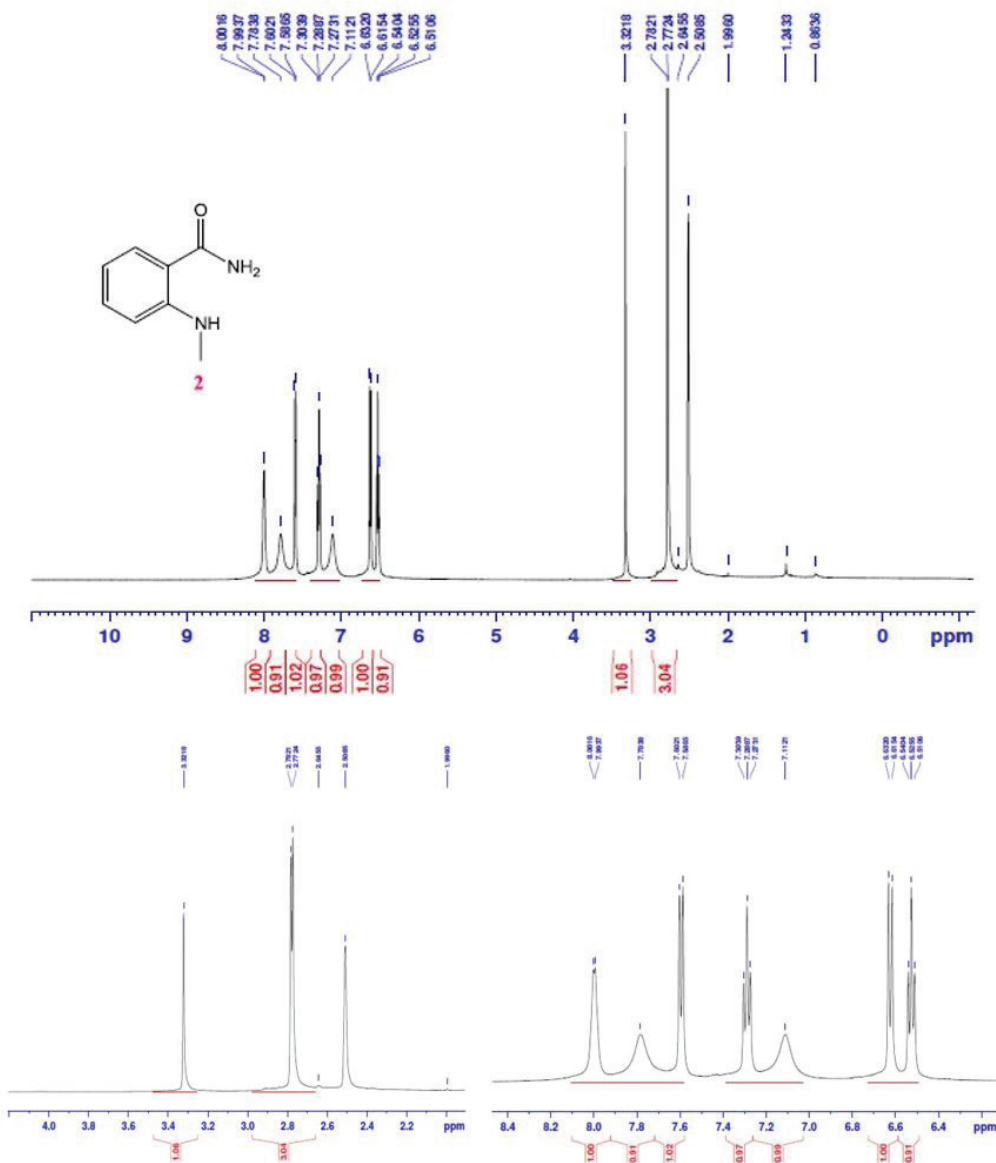


Figure 2. ¹H NMR spectrum for compound 2.

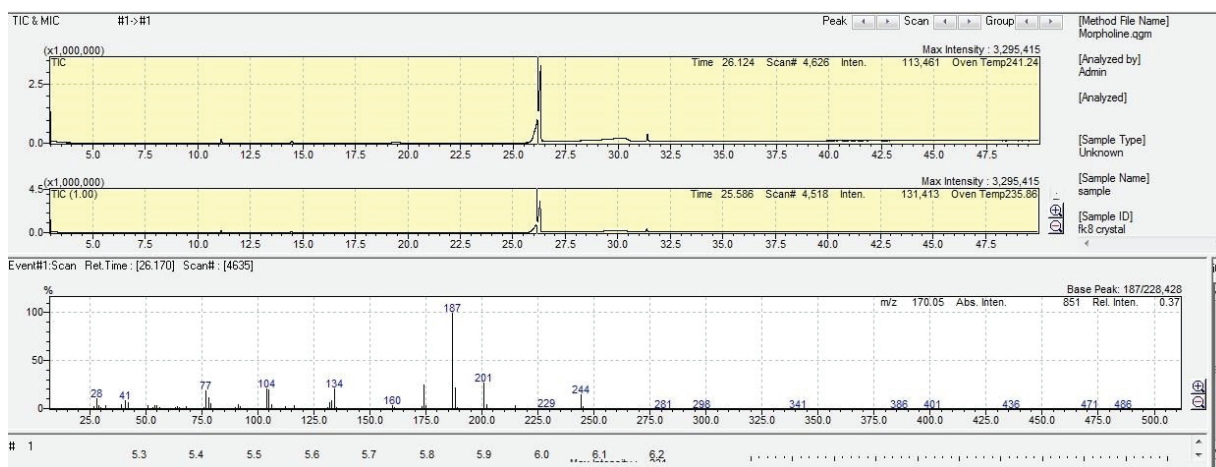


Figure 3. GC-MS spectrum for compound 3.

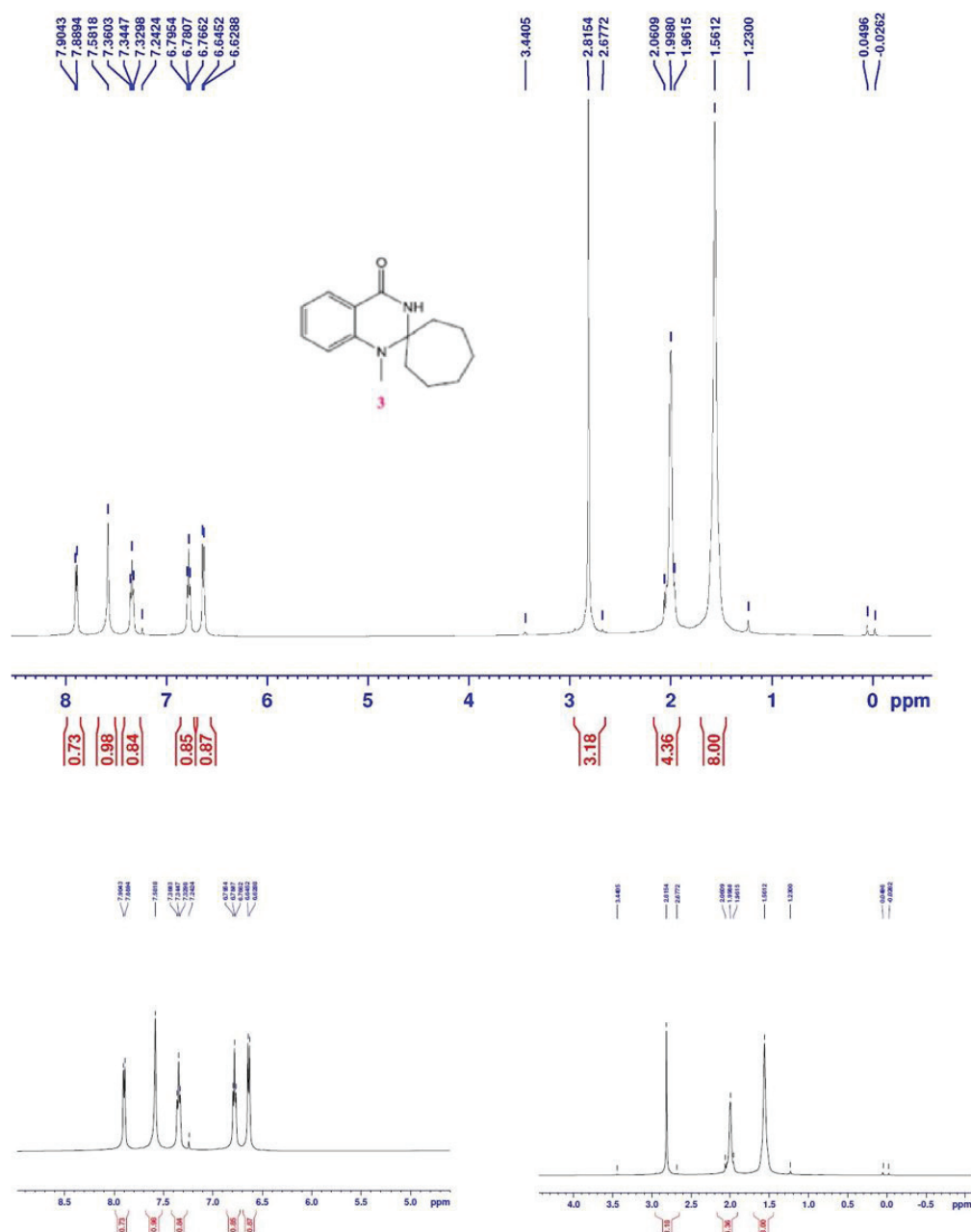


Figure 4. ^1H NMR spectrum for compound **3**.

77.08 (NCN), 112.62 (arom.), 116.72 (arom.), 117.59 (arom.), 128.13 (arom.), 134.01 (arom.), 148.14 (arom.), 164.51 (CO). (Figure 5).

1'-methyl-3',4'-dihydro-1'-H-spiro[cycloheptane-1,2'-quinazoline] (4).

%Yield: (97%), color: yellow oily liquid, Rf : 0.2 (Hexane /EtOAc = 1:1), MS m/z = 230. (Figure 6).

^1H -NMR (500 MHz, CDCl_3): δ = 1.40-1.98 (m, 12H, cycloheptyl), 2.75 (s, NH, brd), 2.90 (s, 3H, CH_3), 3.82 (s, 2H, CH_2), 6.6-6.9 (m, 2H, ArH), 7.08 (d, 1H, J = 7.1 Hz, ArH), 7.26 (dd, 1H, J_1 = 7.7 Hz, J_2 = 0.1 Hz, ArH). (Figure 7).

^{13}C -NMR (125 Hz, CDCl_3): δ = 23.11, 24.26, 28.71 (cyclohept.), 30.24 (CH_3), 34.87

(cyclohept.), 51.33 (CH_2N), 58.54 (NCN), 109.68 (arom.), 116.14 (arom.), 124.49 (arom.), 128.56 (arom.), 129.30 (arom.), 149.59 (arom.) (Figure 8).

RESULTS AND DISCUSSION

Compound **2** was synthesized through the reaction of compound **1** with NH_3 aqueous solution (32%) at 30 °C causing ring opening with liberation of carbon dioxide gas, affording the title compound with a good yield as previously confirmed in literature (Zhao et al., 2014).

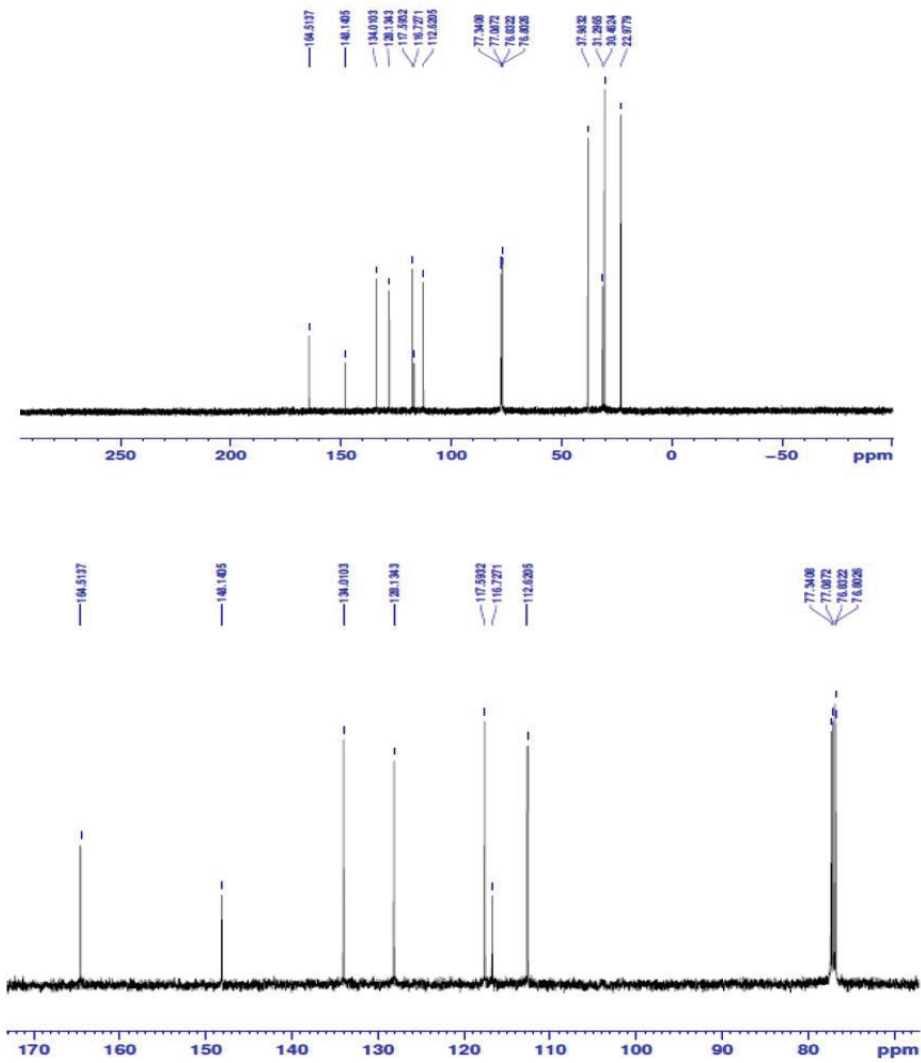


Figure 5. ¹³C NMR spectrum for compound 3.

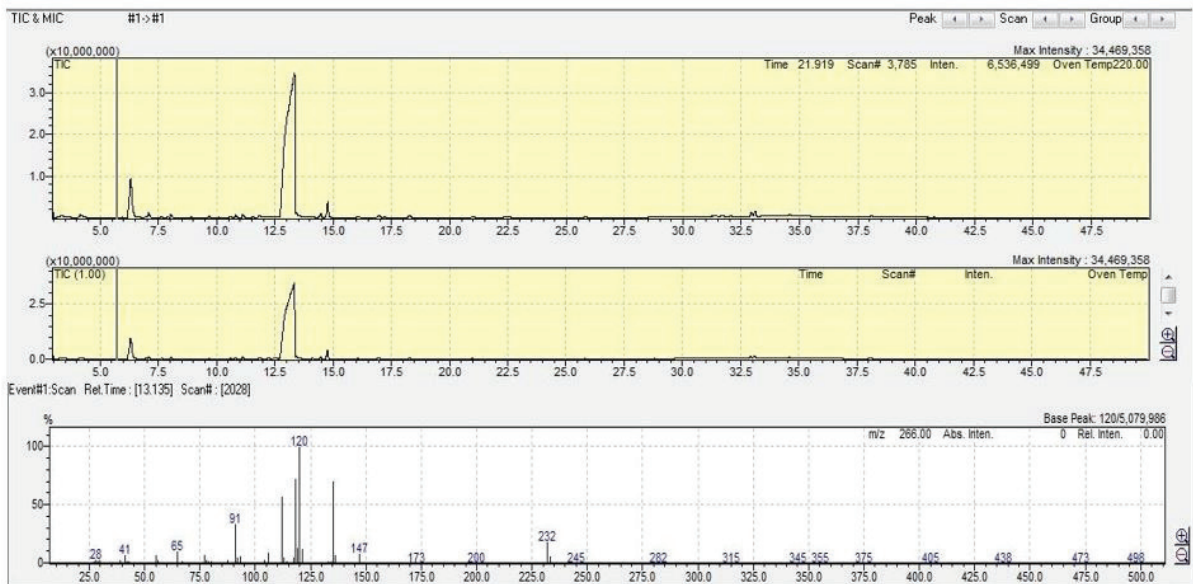


Figure 6. GC-MS spectrum for compound 4.

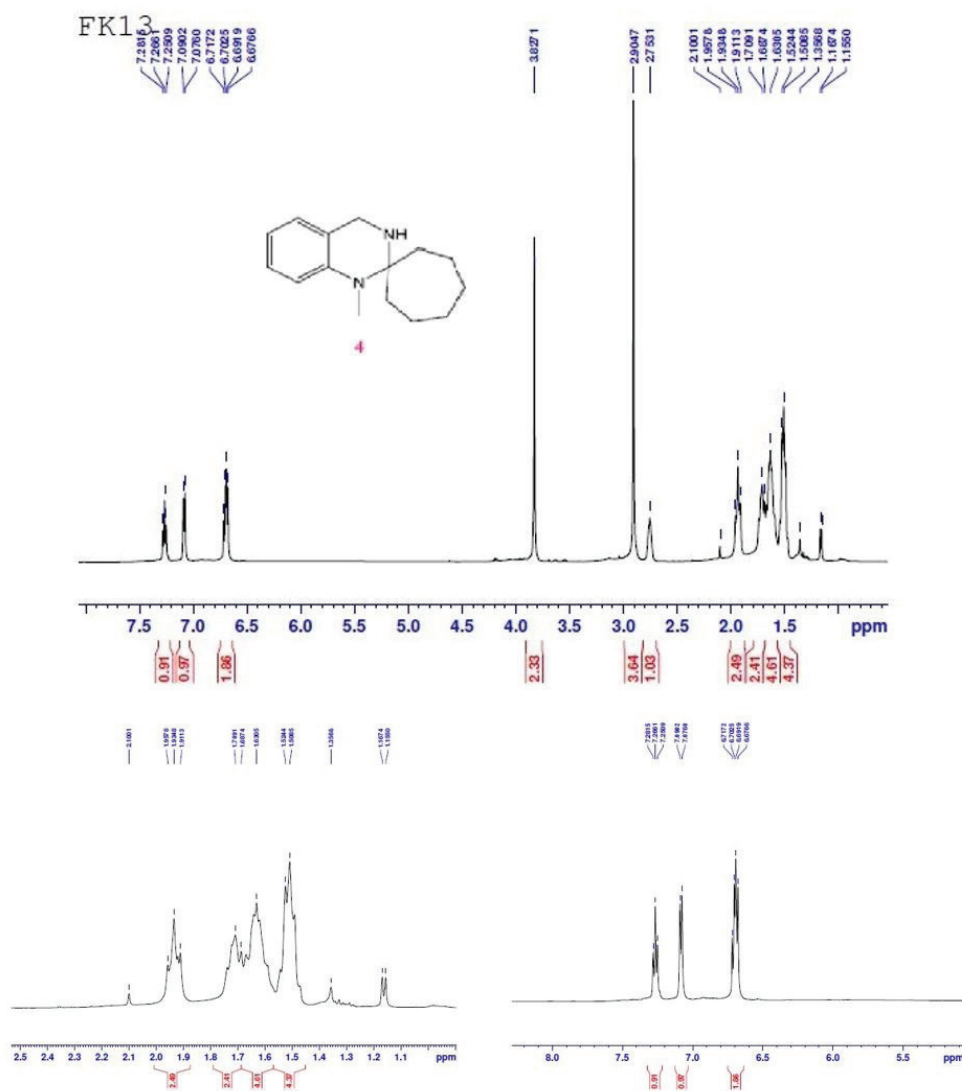


Figure 7. ^1H NMR spectrum for compound **4**.

To synthesize compound **3** toluene-4-sulfonic acid monohydrate was stirred with cycloheptanone and compound **2** in methanol under reflux for 3 hours. The reaction mixture was cooled to room temperature followed by stirring for 24 h. Pure crystals were obtained with insufficient yield so we decided to optimize the reaction conditions. Reaction runs with different equivalents of cycloheptanone and different equivalents of toluene-4-sulfonic acid monohydrate. The yield was increased from 50% to 98% when equivalents of cycloheptanone increased from 2 to 3 and toluene 4-sulfonic acid monohydrate from 0.09 to 0.13 but was no effect on reaction time. Reaction conditions used for the optimization of compound **3** synthesis are summarized in Table 1.

To prepare compound **4** an expeditious and practical method for the reduction of amides to amines was performed (Ravinder, Rajeswar, Panasa, & Rakeshwar, 2013). This method consists of activation of amides with TMSCl followed by reduction with LiAlH_4 . Various amides including hindered amides and secondary amides gave the corresponding amines in good to excel-

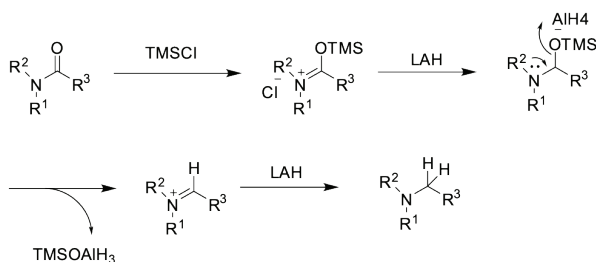
lent yields. Plausible mechanism for the amide reduction via activation with TMSCl illustrated in the following Scheme 2.

According to this Scheme, compound **4** was synthesized as the following: TMSCl dissolved in sufficient quantity of THF then compound **3** was added with continuous stirring for 2 hours to activate carbonyl carbon in the amide moiety. Subsequently LiAlH_4 was added to reduce activated carbonyl carbon and the progress of the reaction was monitored with TLC and GC-MS. When the reaction run with 2.5 eq of TMSCl and 3.5 eq of LiAlH_4 for 24 hours at room temperature TLC and GC-MS revealed no consumption of compound **3** and no product was formed, so we decide to optimize the reaction conditions. Reaction run again with 8.5 eq of LiAlH_4 this time, after 4 hour TLC and GC-MS revealed complete consumption of compound **3** with formation of mainly one product, product was extracted and % yield was calculated (good but insufficient). To maximize the reaction yield we decide to increase both eq of LiAlH_4 and eq of TMSCl, after 1 hour TLC and GC-MS revealed complete consumption of compound **3** with formation of mainly

Table 1. Reaction conditions used for optimization of compound 3 synthesis.

Compound2 (eq)	Temperature (°C)	Time	Catalyst (eq)	Cycloheptanone (eq)	Yield (%)
1	Under reflux for 3 hr then cooled to room temperature	24 hr	0.09	2	50
1	Under reflux for 3 hr then cooled to room temperature	24 hr	0.13	3	98

C: Toluene-4-sulfonic acid monohydrate.

**Scheme 2.** Amide activation with TMSCl followed by reduction with LAH.

one product, product was extracted and % yield was calculated. Maximum yield obtained (97%) with the shortening of reaction time. We concluded that the reaction needs different times to be done. Reaction optimization conditions are illustrated in Table 2.

Table 2. Reaction conditions used for optimization of compound 4 synthesis.

Compound3 (eq)	Temperature (°C)	Time	TMSCl (eq)	LiAlH ₄ (eq)	Yield (%)
1	Room temperature	24 hr	2.5	3.5	0
1	Room temperature	4 hr	2.5	8.5	60
1	Room temperature	1 hr	5	13.1	97

CONCLUSIONS

Novel quinazoline derivatives: 1'-methyl-1*H*-spiro[cycloheptane-1,2'-quinazolin]-4'(3*H*)-one (**3**) and 1'-methyl-3',4'-dihydro-1'*H*-spiro[cycloheptane-1,2'-quinazolin] (**4**) were synthesized. Furthermore, the reaction conditions were optimized for the synthesis of compounds **3** and **4** affording an excellent yield.

Peer-review: Externally peer-reviewed.

Author Contributions: Conception/Design of Study- Z.A., Q.A.; Data Acquisition- Z.A., Q.A., F.A., L.H.; Data Analysis/Interpretation- Z.A., Q.A., F.A., L.H.; Drafting Manuscript- Z.A., Q.A., F.A., L.H.; Critical Revision of Manuscript- Z.A., Q.A., F.A., L.H.; Final Approval and Accountability- Z.A., Q.A., F.A., L.H.

Conflict of Interest: The authors have no conflict of interest to declare.

Financial Disclosure: This work was supported Isra University, Faculty of Pharmacy.

REFERENCES

- Abualassal, Q., Abudayeh, Z., & Husien- Al-Ali, S. H. (2019). Synthesis of a Spiro Quinazoline Compound as Potential Drug Useful in the Treatment of Alzheimer's Disease. *Pharmakeftiki Journal*, 2(31), 60-68 Retrieved from https://www.hsmc.gr/wp-content/uploads/2015/12/ISSUE_2_2019.pdf
- Ajani, O. O., Aderohunmu, D. V., Umeokoro, E. N., & Olomieja, A. O. (2016). Quinazoline Pharmacophore in Therapeutic Medicine. *Bangladesh Journal of Pharmacology*, 11(3), 716-733. <https://doi.org/10.3329/bjpv11i3.25731>.
- Apostolova, L. G. (2016). Alzheimer Disease. *Continuum (Minneapolis, Minn)*, 22(2), 419-434. <https://doi.org/10.1212/CON.0000000000000307>.
- Bekris, L. M., Yu, C. E., Bird, T. D., & Tsuang, D. W. (2010). Genetics of Alzheimer Disease. *Journal of Geriatric Psychiatry and Neurology*, 23(4), 213-227. <https://doi.org/10.1177/0891988710383571>.
- Benny, A., & Thomas, J. (2019). Essential Oils as Treatment Strategy for Alzheimer's Disease: *Current and Future Perspectives. Planta Medica*, 85(03), 239-248. <https://doi.org/10.1055/a-0758-0188>.
- Darras, F. H., Wehle, S., Huang, G., Sotriffer, C. A., & Decker, M. (2014). Amine Substitution of Quinazolinones Leads to Selective Nanomolar AChE Inhibitors with 'Inverted' Binding Mode. *Bioorganic and Medicinal Chemistry*, 22(17), 4867-4881. <https://doi.org/10.1016/j.bmc.2014.06.045>.
- Douchamps, V., & Mathis, C. (2017). A Second Wind for the Cholinergic System in Alzheimer's Therapy. *Behavioural Pharmacology*, 28 (2 and 3-Spec Issue), 112-123. <https://doi.org/10.1097/FBP.0000000000000300>.
- Hampel, H., Mesulam, M. M., Cuello, A. C., Farlow, M. R., Giacobini, E., Grossberg, G. T., Khachaturian, A. S., Vergallo, A., Cavado, E., Snyder, P. J., & Khachaturian, Z. S. (2018). The Cholinergic System in the Pathophysiology and Treatment of Alzheimer's Disease. *Brain*, 141(7), 1917-1933. <https://doi.org/10.1093/brain/awy132>.
- Hung, S. Y., & Fu, W. M. (2017). Drug Candidates in Clinical Trials for Alzheimer's Disease. *Journal of Biomedical Science*, 24(1), 47. <https://doi.org/10.1186/s12929-017-0355-7>.
- Kamel M. M., Zaghary W. A., Al-Wabli R., & Anwar M. M. (2016). Synthetic Approaches and Potential Bioactivity of Different Functionalized Quinazoline and Quinazolinone Scaffolds. *Egyptian Pharmaceutical Journal*, 15(3), 98-131. <https://doi.org/10.4103/1687-4315.197580>.

- Kivimäki, M., & Singh-Manoux A. (2018). Prevention of Dementia by Targeting Risk Factors. *The Lancet*, 391(10130), 1574-1575. [https://doi.org/10.1016/S0140-6736\(18\)30578-6](https://doi.org/10.1016/S0140-6736(18)30578-6).
- Lazo-Porras, M., Ortiz-Soriano, V., Moscoso-Porras, M., Runzer-Colmenares, FM., Málaga, G., & Jaime Miranda, J. (2017). Cognitive Impairment and Hypertension in Older Adults Living in Extreme Poverty: A Cross-Sectional Study in Peru. *BMC Geriatric*, 17(1), 250-. <https://doi.org/10.1186/s12877-017-0628-8>.
- Li, Z., Wang, B., Hou, J. Q., Huang, S. L., Ou, T. M., Tan, J. H., An, L. K., Li, D., Gu, L. Q., & Huang, Z. S. (2013). 2-(2-indolyl)-4(3H)-quinazolines Derivates as New Inhibitors of AChE: Design, Synthesis, Biological Evaluation and Molecular Modelling. *Journal of Enzyme Inhibition and Medicinal Chemistry*, 28(3), 583-592. <https://doi.org/10.3109/14756366.2012.663363>.
- Mendiola-Precoma, J., Berumen L. C., Padilla, K., & Garcia-Alcocer, G. (2016). Therapies for Prevention and Treatment of Alzheimer's Disease. *BioMed Research International*, 2016(3), 1-17. <https://doi.org/10.1155/2016/2589276>.
- Mohamed, T., Manna, M. K., & Rao, P. P. N. (2017). Application of Quinazoline and Pyrido[3,2-d] Pyrimidine Templates to Design Multi-Targeting Agents in Alzheimer's Disease. *RSC Advances*, 7(36), 22360–22368. <https://doi.org/10.1039/c7ra02889j>.
- Mohamed, T., & Rao, P. P. N. (2017). 2,4-Disubstituted Quinazolines as Amyloid- β Aggregation Inhibitors with Dual Cholinesterase Inhibition and Antioxidant Properties: Development and Structure-Activity Relationship (SAR) Studies. *European Journal of Medicinal Chemistry*, 126, 823-843. <https://doi.org/10.1016/j.ejmech.2016.12.005>.
- Naderali, E. K., Ratcliffe, S. H., & Dale, M. C. (2009). Obesity and Alzheimer's Disease: A Link Between Body Weight and Cognitive Function in Old Age *American Journal of Alzheimer's Disease and Other Dementias*, 24(6), 445-449. <https://doi.org/10.1177/1533317509348208>.
- Olivares, D., Deshpande V. K., Shi, Y., Lahiri, D. K., Greig, N. H., Rogers, J. T., & Huang, X. (2012). N-methyl D-aspartate (NMDA) Receptor Antagonists and Memantine Treatment for Alzheimer's Disease, Vascular Dementia and Parkinson's Disease. *Current Alzheimer Research*, 9(6), 746-758. <https://doi.org/10.2174/156720512801322564>.
- Panpalli Ates, M., Karaman, Y., Guntekin, S., & Ergun, M.A. (2016). Analysis of Genetics and Risk Factors of Alzheimer's disease. *Neuroscience*, 14(325), 124-131. <https://doi.org/10.1016/j.Neuroscience.2016.03.051>.
- Park, B., Nam, J. H., Kim, J. H., Kim H. J., Onnis, V., Balboni, G., Lee K. T., Park, J. H., Catto, M., Carotti, A., & Lee, J. Y. (2017). 3,4-Dihydroquinazoline Derivatives Inhibit the Activities of Cholinesterase Enzymes. *Bioorganic & Medicinal Chemistry Letters*, 27(5), 1179-1185. <https://doi.org/10.1016/j.bmcl.2017.01.068>.
- Ravinder, B., Rajeswar, R. S., Panasa R. A., & Rakeshwar, B. (2013). Amide Activation by TMSCl: Reduction of Amides to Amines by LiAlH₄ under Mild Conditions. *Tetrahedron Letters*, 54(36), 4908-4913. <https://doi.org/10.1016/j.tetlet.2013.06.144>.
- Szeto, J.Y., Simon J.G., & Lewis, S.J.G (2016). Current Treatment Options for Alzheimer's Disease and Parkinson's Disease Dementia. *Current Neuropharmacology*, 14(4), 326–338. <https://doi.org/10.2174/1570159X14666151208112754>
- Tariq, S., & Barber, P. A. (2018). Dementia Risk and Prevention by Targeting Modifiable Vascular Risk Factors. *Journal of Neurochemistry*, 144(5), 565-581. <https://doi.org/10.1111/jnc.14132>.
- Zhao, D., Wang, T., & Li, J. X. (2014). Metal-Free Oxidative Synthesis of Quinazolinones via Dual Amination of sp³ C–H Bonds. *Chemical Communications*, 50(49), 6471-6474. <https://doi.org/10.1039/C4CC02648A>.

Molecular and crystal structure of 1-methyl-5-trifluoromethoxy-1*H*-indole-2,3-dione 3-[4-(4-methoxyphenyl)thiosemicarbazone]

Özge Soylu Eter^{1,2} , Zeliha Atioğlu³ , Mehmet Akkurt⁴ , Cem Cüneyt Ersanlı⁵ , Nilgün Karalı¹ 

¹Istanbul University, Faculty of Pharmacy, Department of Pharmaceutical Chemistry, Istanbul, Turkey

²Istanbul University, Institute of Health Sciences, Istanbul, Turkey

³Cappadocia University, The Medical Imaging Techniques Program, İlke Education and Health Foundation, Nevşehir, Turkey

⁴Erciyes University, Faculty of Sciences, Department of Physics, Kayseri, Turkey

⁵Sinop University, Faculty of Arts and Sciences, Department of Physics, Sinop, Turkey

ORCID IDs of the authors: Ö.S. 0000-0001-8875-3522; Z.A. 0000-0002-1141-5151; M.A. 0000-0003-2421-0929; C.C.E. 0000-0002-8113-5091; N.K. 0000-0002-6916-122X

Cite this article as: Soylu Eter, O., Atioğlu, Z., Akkurt, M., Ersanlı, C. C., & Karalı, N. (2021). Molecular and crystal structure of 1-methyl-5-trifluoromethoxy-1*H*-indole-2,3-dione 3-[4-(4-methoxyphenyl)thiosemicarbazone]. *Istanbul Journal of Pharmacy*, 51(1), 59-66.

ABSTRACT

Background and Aims: The main purpose of this study is to determine the molecular structure and isomers of the new 1-methyl-5-trifluoromethoxy-1*H*-indole-2,3-dione 3-[4-(4-methoxyphenyl)thiosemicarbazone] (**5**) and to prove the 3*Z*-conformer of the compound **5**.

Methods: The molecular structure of *E*- and *Z*-isomer mixture **5** was confirmed by analytical and spectral data (UV, IR, ¹H NMR, HSQC-2D and MS). The *Z*-conformer of compound **5** was characterized by NMR spectroscopy and X-ray single crystal diffraction analysis method (SC-XRD).

Results: The compound **5** was synthesized by condensation of 1-methyl-5-trifluoromethoxy-1*H*-indole-2,3-dione (**2**) with 4-(4-methoxyphenyl)thiosemicarbazide (**4**). The compound **5** was obtained in two separate forms, crystal and amorphous. It was proved by NMR data and X-ray diffraction findings that the crystal form is the *Z*-isomer and the amorphous form is a mixture of the *E*- and *Z*-isomers. The *E*- and *Z*-isomer ratios were determined by ¹H NMR spectroscopy. The crystal structure and molecular interactions of the *Z*-conformer were determined by X-ray single crystal diffraction analysis.

Conclusion: In the crystal, three intramolecular N-H...N, N-H...O and C-H...S hydrogen bonds provided isomer formation. Also, molecular packing was stabilized by intermolecular C-H...O hydrogen bonds, the π - π stacking interactions and weak CO... π (ring) contacts.

Keywords: Synthesis, molecular structure, isomerism, crystal structure, hydrogen bond, π - π stacking interaction

INTRODUCTION

1*H*-Indole-2,3-dione (isatin) is a natural product and important class of heterocyclic compounds. Isatin and its derivatives are in the spotlight of organic and medicinal chemistry as a consequence of having a wide range of biological and pharmacological activities especially as antiviral (Sadler, 1965), anti-inflammatory (Swathi & Sarangapani, 2014; Matheus, DeAlmeida Violante, Garden, Pinto, & Fernandes, 2007), antituberculosis (Pandeya, Sriram, Yogeewari, & Ananthan, 2001), antibacterial (Pandeya & Sriram, 1998) and anticancer activity (Ma *et al.*, 2015; Vine, Matesic, Locke, Ranson, & Skropeta, 2009). *N*-Methylisatin-3-thiosemicarbazone

Address for Correspondence:

Özge SOYLU ETER, e-mail: ozge.soylu@istanbul.edu.tr

Submitted: 12.08.2020

Revision Requested: 11.09.2020

Last Revision Received: 21.11.2020

Accepted: 04.12.2020

This work is licensed under a Creative Commons Attribution 4.0 International License.



(methisazone) was one of the Food and Drug Administration (FDA) approved first antiviral compounds used in clinical practice. This drug plays an important role as a prophylactic agent against several viral diseases. Also, *N*-methylisatin-3-(4,4-diethylthiosemicarbazone) inhibits reverse transcriptase (Ronen, Sherman, Bar-Nun, & Teitz, 1987). Isatin 3-thiosemicarbazone derivatives, which have anti-human immunodeficiency virus (HIV) effects, are used against smallpox and vaccinia viruses as prophylaxis (Hall *et al.*, 2009; Bal, Anand, Yogeewari, & Sriram, 2005). Anticancer activity has been observed significantly for *N*-substituted isatin 3-thiosemicarbazone derivatives in many studies (Pape *et al.*, 2016; Priyanka, Manasa, & Sammaiah, 2014; Hall *et al.*, 2011; Sabet, Mohammadpour, Sadeghi, & Fassihi, 2010). According to structure-activity relationship in 3-substituted 2-indolinone derivatives, it has been revealed that 3-thiosemicarbazone formation on the isatin moiety, aromatic/hydrophobic properties at the N_4 position of the thiosemicarbazone and introduction of electron-withdrawing groups on position 5 and alkylation on position 1 of isatin are required for anticancer activity (Hall *et al.*, 2011; Pervez, Saira, Iqbal, Yaqub, & Khan, 2011; Pervez *et al.*, 2010; Sabet *et al.*, 2010; Hall *et al.*, 2009; Güzel, Karalı, & Salman, 2008; Matesic *et al.*, 2008; Karalı *et al.*, 2007; Vine, Locke, Ranson, Pyne, & Bremner, 2007a; Vine, Locke, Ranson, Pyne, & Bremner, 2007b; Karalı, 2002). Additional studies infer that N_4 -phenyl substituted thiosemicarbazone derivatives have significantly higher activity than N_4 -alkyl, N_4 -cycloalkyl and N_4 -nonsubstituted thiosemicarbazone derivatives (Hall *et al.*, 2011; Hall *et al.*, 2009). The type and position of varied substituents on the phenyl ring linked to the N_4 position of the thiosemicarbazone part is much more important for activity (Pape *et al.*, 2016; Pervez, Chohan, Ramzan, Nasim, & Khan, 2009; Pervez *et al.*, 2008; Karalı *et al.*, 2007).

In studies in which isomer structures of isatin 3-thiosemicarbazone derivatives are examined, it has been noted that an intramolecular hydrogen bond may be formed between thioamide N_2 hydrogen and lactam oxygen of the indole ring, as well as between thioamide N_4 hydrogen and N_1 (Haribabu *et al.*, 2016; Muralisankar, Sujith, Bhuvanesh, & Sreekanth, 2016; Jakusová *et al.*, 2013; Kaynak, Özbey, & Karalı, 2013). There may be mention of the existence of intermolecular hydrogen bonds between the $N-H\cdots O$, $N-H\cdots S$ and $N-H\cdots N$ (Haribabu *et al.*, 2016; Jakusová *et al.*, 2013; Kaynak *et al.*, 2013; Bain *et al.*, 1997; Sadler, 1961). The proton acceptor OCF_3 , F, SO_3Na and NO_2 groups in the indole ring can form hydrogen bonds with the proton donor indole and thioamide N-H groups (Sakai *et al.*, 1998; Howard, Hoy, O'Hagan, & Smith, 1996; O'Sullivan, & Sadler, 1956). In a study examining the crystal structure and molecular interactions of 5-trifluoromethoxy-1*H*-indole-2,3-dione 3-(4-ethylthiosemicarbazone) derivative, the intramolecular and intermolecular interactions of proton donor groups are illuminated by dimer structure of the compound (Figure 1) (Kaynak *et al.*, 2013).

Anti (*E*) and sin (*Z*) isomers of 1*H*-indole-2,3-dione 3-thiosemicarbazone derivatives caused by $C=N_1$ bond were investigated in the aqueous solution. Theoretical and experimental studies have shown that *Z*-isomers are preferred and found at a higher rate compared to the *E*-isomers. It was determined that only the *Z*-configuration allowed the formation of the intramolecular hydrogen bond between the N_2 -H of the thioamide group

and the lactam oxygen of the indole ring. In these studies, the presence of two isomers formed by rotation around the thioamide N_2 -C bond of isatin-3-thiosemicarbazones have been reported. Geometric isomers have been reported to occur if free rotation around the thioamide N_2 -C bond is prevented (Figure 2) (DeSilva & Albu, 2007; Bain *et al.*, 1997).

In this study, the new (1-methyl-5-(trifluoromethoxy)-1*H*-indole-2,3-dione 3-[4-(4-methoxyphenyl)thiosemicarbazone] (**5**) was synthesized. The compound **5** was obtained in two separate forms, crystal (3*Z*-isomer) and amorphous (mixture of 3*E*- and 3*Z*-isomers). The structures of the 3*E* and 3*Z* isomers were determined by NMR data and X-ray diffraction findings.

MATERIALS AND METHODS

Synthesis

All the chemicals and reagents were purchased from Merck-Schuchardt and Sigma-Aldrich. The processes of the reactions

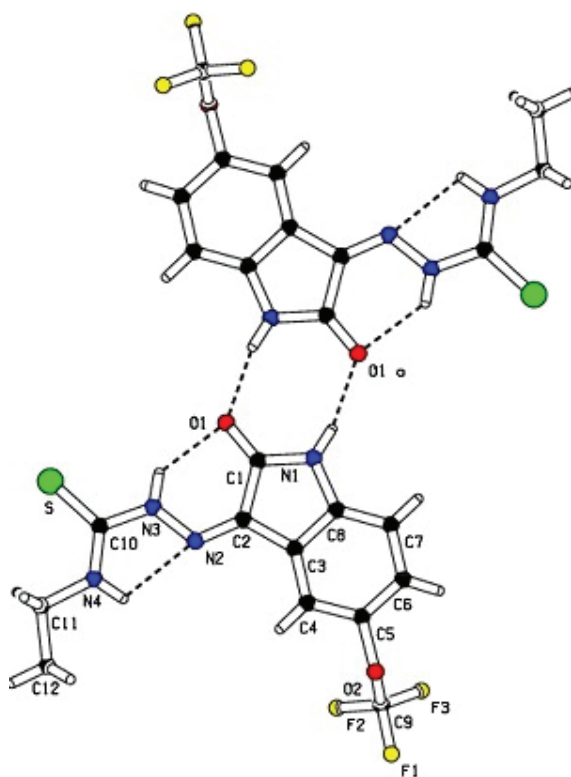


Figure 1. Crystal structure of 5-trifluoromethoxy-1*H*-indole-2,3-dione 3-(4-ethylthiosemicarbazone) (Kaynak *et al.*, 2013).

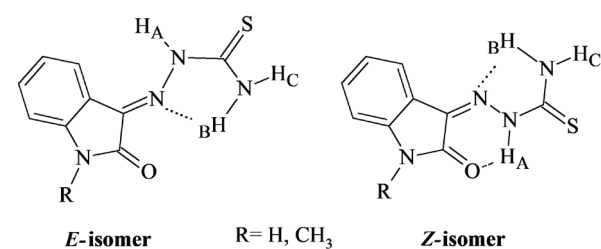


Figure 2. Possible *E*- and *Z*-conformers of 1*H*-indole-2,3-dione 3-thiosemicarbazone derivatives.

were monitored using thin layer chromatography (TLC). Silica gel 60 HF254 was used as the adsorbent and the solvent system was composed of ethylacetate:cyclohexane (50:50, v/v) for TLC. A UV lamp (Mineralight Lamp UVGL-58) was used at 254 nm for monitoring stains on the TLC plates after TLC was done.

The melting points of the compounds were estimated with a Buchi B-540 melting point apparatus in open capillary and was uncorrected. The UV spectra were obtained on Shimadzu UV-1800 spectrophotometer. The infrared (IR) spectra were recorded on a KBr disc, using a Shimadzu IR Affinity-1 FTIR spectrophotometer. ¹H Nuclear Magnetic Resonance (NMR) and Heteronuclear Single Quantum Coherence (HSQC-2D) spectra were procured on Varian UNITY INOVA 500 MHz, Varian Mercury (Agilent) 400 MHz and Oxford Pulsar 60 MHz NMR spectrophotometers dissolved in DMSO-*d*₆. The mass spectroscopy (MS) analysis was obtained on a Waters 2695 Alliance Micromass ZQ LC/MS spectrophotometer. The elemental analysis was performed on a Leco CHNS-932 elemental analyzer.

The synthesis of 1-methyl-5-trifluoromethoxy-1*H*-indole-2,3-dione (**2**)

Potassium carbonate (7 mmol) was added to a solution of 5-trifluoromethoxy-1*H*-indole-2,3-dione (**1**) (5 mmol) in dimethylformamide (5 mL), and stirred for 1 hour at room temperature. After the addition of iodomethane (15 mmol) and potassium iodide (1 mmol), the reaction mixture was refluxed for 3 h at 50–60°C. It was firstly evaporated to dryness under reduced pressure to obtain a crude product, which was poured into iced water and then filtered (Güzel *et al.*, 2008).

Red powder (yield 90%), M.p.: 110–112 °C. UV λ (250 mL EtOH+0.5 mL DMSO)_{max} nm (ε): 246.5 (42338), 252.3 (38906), 268.7 (13115), 295.0 (5270). IR (KBr) ν_{\max} (cm⁻¹): 3064, 3043 (aromatic C-H), 2951, 2889 (aliphatic C-H), 1737, 1716, 1687 (C=O), 1616, 1489, 1473 (C=C). ¹H NMR (60 MHz) (DMSO-*d*₆/TMS) δ (ppm): 3.31 (3H, s, indole N-CH₃), 7.34–7.61 (3H, m, indole C_{4,6,7}-H).

The synthesis of 4-(4-methoxyphenyl)thiosemicarbazide (**4**)

A suspension of 4-(methoxy)phenylisothiocyanate (**3**) (5 mmol) in ethanol (10 mL) was added dropwise with vigorous stirring to a solution of hydrazine hydrate (5 mmol) in ethanol (10 mL), and cooled in an ice bath. The mixture was allowed to stand overnight. The crystals formed were filtered off and recrystallized from ethanol (Tisler, 1956).

White powder (yield 70%), M.p.: 154 °C. UV λ (250 mL EtOH+0.5 mL DMSO)_{max} nm (ε): 242.5 (14084), 268.2 (9566). IR (KBr) ν_{\max} (cm⁻¹): 3319, 3273, 3163 (NH), 3045 (aromatic C-H), 2958, 2837 (aliphatic C-H), 1635, 1610, 1527, 1508 (C=C). ¹H NMR (400 MHz) (DMSO-*d*₆/TMS) δ (ppm): 3.73 (3H, s, OCH₃), 4.68 (2H, s, NH₂), 6.85 (2H, d, *J*: 9.0 Hz, phenyl C_{3,5}-H), 7.44 (2H, d, *J*: 9.0 Hz, phenyl C_{2,6}-H), 8.89 (1H, s, N₄-H), 9.42 (1H, s, N₂-H). ¹³C NMR (75 MHz) (DMSO-*d*₆/TMS) δ (ppm): 56.40 (OCH₃), 114.43 (phenyl C_{3,5}), 126.87 (phenyl C_{2,6}), 133.42 (phenyl C₁), 157.38 (phenyl C₄), 181.00 (C=S) (Huang *et al.*, 2010).

The synthesis of 1-methyl-5-trifluoromethoxy-1*H*-indole-2,3-dione 3-[4-(4-methoxyphenyl)thiosemicarbazone] (**5**)

A solution of 4-(4-methoxyphenyl)thiosemicarbazide (**4**) (2.5 mmol) in ethanol (10 mL) was added to a solution of 1-methyl-5-trifluoromethoxy-1*H*-indole-2,3-dione (**2**) (2.5 mmol) in ethanol (20 mL). Then 5–10 drops from trace amounts of concentrated sulfuric acid in ethanol (100 mL) were added to catalyze the reaction. The precipitated product was filtered after cooling and was washed with ethanol, and finally the isomer mixture of the compound **5** was obtained. Yellow-orange powder (yield 93%), M.p.: 185 °C (Karali *et al.*, 2020)

The *Z*-isomer was obtained by crystallizing the isomer mixture from ethanol.

The amorphous form (mixture of **3E** and **3Z** isomers) of 1-methyl-5-trifluoromethoxy-1*H*-indole-2,3-dione 3-[4-(4-methoxyphenyl)thiosemicarbazone] (**5**):

UV λ (250 mL EtOH+0.5 mL DMSO)_{max} nm (ε): 229.5 (26779), 259.0 (18800), 365.0 (30641). IR (KBr) ν_{\max} (cm⁻¹): 3307, 3219 (NH), 1693 (C=O), 1620, 1597, 1548, 1510 (C=N, C=C), 1163 (C=S). MS (ESI (+)) *m/z* (%): 425 ([M+H]⁺; 100); 260 (18); 302 (1). Anal. calcd. for C₁₈H₁₅F₃N₄O₃S: C, 50.94; H, 3.56; N, 13.20; S, 7.56(%) Found: C, 51.10; H, 3.94; N, 13.65; S, 9.25(%)

3Z-isomer, ¹H NMR (400 MHz) (DMSO-*d*₆/TMS) δ (ppm): 3.24 (3H, s, indole N-CH₃), 3.77 (3H, s, OCH₃), 6.98 (2H, d, *J*: 9.0 Hz, phenyl C_{3,5}-H), 7.25 (1H, d, *J*: 8.6 Hz, indole C₇-H), 7.44 (2H, d, *J*: 9.0 Hz, phenyl C_{2,6}-H), 7.44–7.47 (1H, m, indole C₆-H), 7.81 (1H, s, indole C₄-H), 10.81 (1H, s, N₄-H), 12.53 (1H, s, N₂-H) (The *E/Z* isomer ratio is 1:2) (Figure 3). ¹³C NMR (HSQC-2D) (125 MHz) (DMSO-*d*₆/TMS) δ (ppm): 26.40 (indole N-CH₃), 55.76 (OCH₃), 111.50 (indole C₇), 114.14 (phenyl C_{3,5}), 114.60 (indole C₄), 120.68 (q, *J*: 256.2 Hz, OCF₃), 121.26 (indole C_{3a}), 124.42 (indole C₆), 127.86 (phenyl C_{2,6}), 130.54 (indole C₃), 131.53 (phenyl C₁), 142.95 (indole C_{7a}), 144.46 (d, *J*: 1.9 Hz, indole C₅), 158.03 (phenyl C₄), 161.37 (indole C₂), 177.05 (C=S) (Figures 4–6).

3E-isomer, ¹H NMR (400 MHz) (DMSO-*d*₆/TMS) δ (ppm): 3.24 (3H, s, indole N-CH₃), 3.73 (3H, s, OCH₃), 6.88 (2H, d, *J*: 9.0 Hz, phenyl C_{3,5}-H), 7.25 (1H, d, *J*: 8.6 Hz, indole C₇-H), 7.35 (2H, d, *J*: 8.6 Hz, phenyl C_{2,6}-H), 7.44–7.47 (1H, m, indole C₆-H), 7.81 (1H, s, indole C₄-H), 9.52 (1H, s, N₄-H), 9.69 (1H, s, N₂-H) (The *E/Z* isomer ratio is 1:2) (Figure 3). ¹³C NMR (HSQC-2D) (125 MHz) (DM-

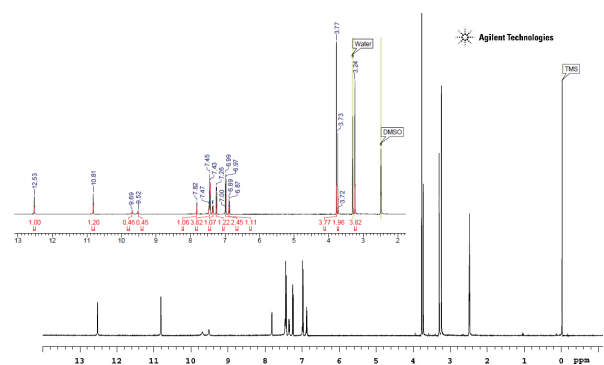


Figure 3. ¹H NMR (400 MHz, DMSO-*d*₆) spectra of *E*- and *Z*-isomer mixture of the compound **5**.

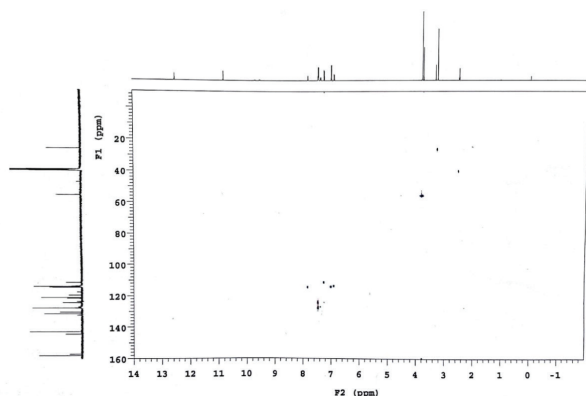


Figure 4. HSQC-2D NMR (500 MHz, DMSO- d_6) spectra of *E*- and *Z*-isomer mixture of the compound **5**.

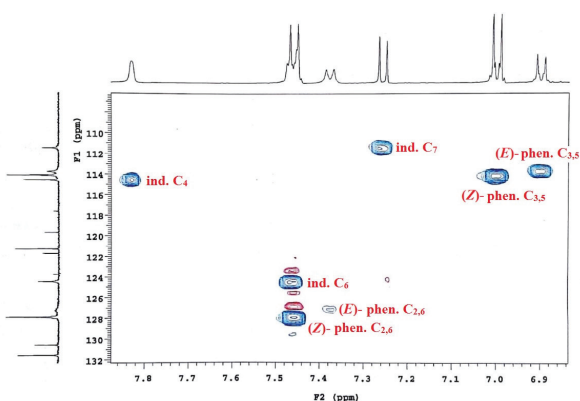


Figure 5. HSQC-2D NMR spectra of *E*- and *Z*-isomer mixture of the compound **5** (106-132 ppm).

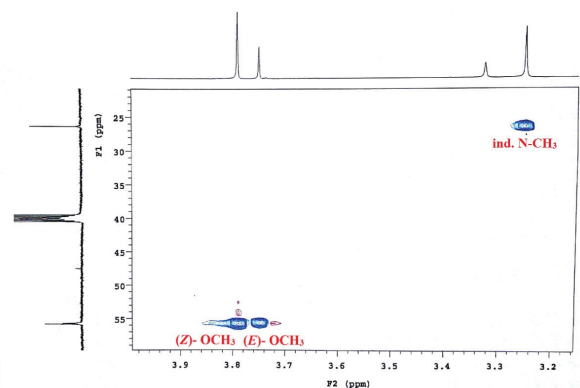


Figure 6. HSQC-2D NMR spectra of *E*- and *Z*-isomer mixture of the compound **5** (20-60 ppm).

SO- d_6 (TMS) δ (ppm): 26.40 (indole N-CH₃), 55.66 (OCH₃), 111.50 (indole C₇), 113.78 (phenyl C_{3,5}), 114.60 (indole C₄), 120.68 (q, *J*: 256.2 Hz, OCF₃), 121.26 (indole C_{3a}), 124.42 (indole C₆), 127.21 (phenyl C_{2,6}), 130.54 (indole C₃), 131.53 (phenyl C₁), 142.95 (indole C_{7a}), 144.46 (d, *J*: 1.9 Hz, indole C₅), 157.15 (phenyl C₄), 161.37 (indole C₂), 177.05 (C=S) (Figures 4-6).

(3Z)-1-methyl-5-trifluoromethoxy-1H-indole-2,3-dione 3-[4-(4-methoxyphenyl) thiosemicarbazone] (5): UV λ (250 mL EtOH+0.5 mL DMSO)_{max} nm (ϵ): 228.0 (63192), 258.5 (13580), 365.0 (20837). IR (KBr) ν_{max} (cm⁻¹): 3307, 3223 (NH), 1693 (C=O), 1620, 1597, 1548, 1510 (C=N, C=C), 1161 (C=S).

¹H NMR (400 MHz) (DMSO- d_6 /TMS) δ (ppm): 3.24 (3H, s, indole N-CH₃), 3.77 (3H, s, OCH₃), 6.98 (2H, d, *J*: 9.1 Hz, phenyl C_{3,5}-H), 7.24 (1H, d, *J*: 8.6 Hz, indole C₇-H), 7.44 (2H, d, *J*: 9.1 Hz, phenyl C_{2,6}-H), 7.44-7.47 (1H, m, indole C₆-H), 7.81 (1H, s, indole C₄-H), 10.82 (1H, s, N₄-H), 12.52 (1H, s, N₂-H) (Figure 7).

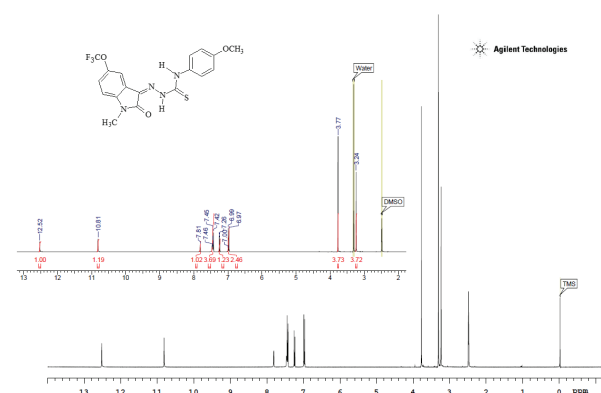


Figure 7. ¹H NMR (400 MHz, DMSO- d_6) spectra of *Z*-isomer of the compound **5**.

X-ray single crystal diffraction analysis (SC-XRD)

Crystal data, data collection and structure refinement details for 3*Z*-isomer of the compound **5** are summarized in Table 1.

RESULTS AND DISCUSSION

In this study, 1-methyl-5-trifluoromethoxy-1*H*-indole-2,3-dione (**2**) was reacted by 4-(4-methoxyphenyl)thiosemicarbazide (**4**) in ethanol to give 1-methyl-5-trifluoromethoxy-1*H*-indole-2,3-dione 3-[4-(4-methoxyphenyl)thiosemicarbazone] (**5**) (Scheme 1). The compound **5** was obtained in two separate forms, crystal and amorphous. It was proved by spectral and X-ray findings that the crystal form is the *Z*-isomer and the amorphous form are a mixture of the *E*- and *Z*-isomers. The mixture containing structures of *E*- and *Z*-isomers of the compound **5** were verified by elemental analysis and spectral data (UV, IR, ¹H NMR, HSQC-2D and MS). The 3*Z*-conformer of the compound **5** was further characterized by X-ray single crystal diffraction analysis method.

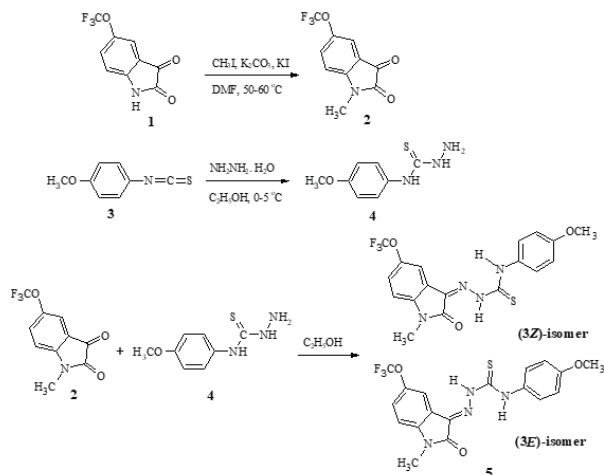
The ¹H NMR spectra of 3*Z*- and 3*E*-isomers of the compound **5** displayed OCH₃ (C18) protons at δ 3.77 and 3.73 ppm as singlets, respectively. The N₂ (N3) and N₄ (N4) protons of the thiosemicarbazone moiety showed an enormous change in the chemical shift of +2.83 and +1.30 ppm as a result of the intramolecular N3—H...O1 and N4—H...N2 hydrogen bonds in the 3*Z*-isomer. The phenyl protons of the thiosemicarbazone moiety of 3*Z*-isomer showed a change in the chemical shift of approximately +0.10 ppm. The spectra of 3*Z*- and 3*E*- isomers of the compound **5** showed the proton chemical shifts of a newer indole ring and N-CH₃ (C9). The carbon chemical shift values of 3*Z*- and 3*E*- isomers were established by HSQC-2D data of the compound **5**. The ortho (C13 and C17), meta (C14 and C16) and para (C15) carbons of phenyl were determined as changes in the chemical shift values of +0.65, +0.46 and +0.88 ppm, respectively. The change in the chemical shift value for OCH₃ (C18) was +0.10 ppm in 3*Z*-isomer. The chemical shifts of the other carbons were constant for the 3*Z*- and 3*E*- isomers.

Table 1. Experimental details of the 3*Z*-conformer of the compound 5.

Chemical formula	C ₁₈ H ₁₅ F ₃ N ₄ O ₃ S
M_r	424.40
Crystal system, space group	Monoclinic, <i>P</i> 2 ₁ / <i>n</i>
Temperature (K)	296
a, b, c (Å)	13.266 (2), 7.8433 (19), 18.667 (4)
β (°)	102.524 (7)
V (Å³)	1896.1 (7)
Z	4
Radiation type	Mo Kα
μ (mm⁻¹)	0.23
Crystal size (mm)	0.09 × 0.07 × 0.06
Diffractionmeter	Bruker APEX-II CCD diffractometer
Absorption correction	Multi-scan (SADABS; Bruker, 2007)
T_{min}, T_{max}	0.536, 0.746
No. of measured, independent and observed [I > 2σ(I)] reflections	54669, 4595, 3268
R_{int}	0.067
(sin θ/λ)_{max} (Å⁻¹)	0.670
R[F² > 2σ(F²)], wR(F²), S	0.075, 0.154, 1.18
No. of reflections	4595
No. of parameters	271
H-atom treatment	H atoms treated by a mixture of independent and constrained refinement
Δρ_{max}, Δρ_{min} (e Å⁻³)	0.30, -0.26
Computer programs: APEX2 and SAINT (Bruker, APEX2, SAINT and SADABS, Bruker AXS Inc., Madison, Wisconsin, USA), SHELXS97 (Sheldrick, 2008), SHELXL2014 (Sheldrick, 2015), WinGX (Farrugia, 2012) and PLATON (Spek, 2009).	

The 3*E*/3*Z* isomer ratio obtained from integral values was assigned as 1:2 in DMSO-*d*₆ at room temperature (Figure 3).

NMR studies were performed in order to better understand the molecular properties of the 1*H*-indole-2,3-dione 3-thiosemicarbazone derivatives. The calculated and experimental signals of the thiosemicarbazone residue NH protons were compared. It was determined that the thioamide N₂ (H_A) proton made the most prominent hydrogen bond with the lactam oxygen, and it was recorded that it was monitored over a wide chemical shift range (δ 12.4–14.2 ppm) due to this strong hydrogen bond. The thioamide NH signals of *Z*-isomers were observed at a lower area of about 1.00 ppm than the signals of the *E*-isomers. It has been determined that indole C₂, indole C₃ and C=S carbon resonances of *Z*-isomers give signals at a lower area than the *E*-isomers' resonances. The indole C₂ and C=S car-



Scheme 1. Synthesis of (3*E*/3*Z*)-1-methyl-5-trifluoromethoxy-1*H*-indole-2,3-dione 3-[4-(4-methoxyphenyl)thiosemicarbazone] (**5**).

bon resonances of (*Z*)-1*H*-indole-2,3-dione 3-(4,4'-dimethyl)thiosemicarbazone were observed at δ 162.86 and 182.12 ppm, respectively. Whereas, the indole C₂ and C=S carbon signals of the *E*-isomer were determined at δ 162.66 and 178.99 ppm, respectively (DeSilva & Albu, 2007). N₂ and N₄ proton signals of 1*H*-indole-2,3-dione 3-thiosemicarbazone derivatives, which have been proven to be in the form of *Z*-isomers, showed at δ 12.25–12.81 and 9.30–11.09 ppm, respectively (Haribabu *et al.*, 2016; Zhang *et al.*, 2015; Ali *et al.*, 2014; Kaynak *et al.*, 2013). In the study where the crystal structure and spectral findings of (*Z*)-5-fluoro-1-methyl-1*H*-indole-2,3-dione 3-[4-(methylthio)phenyl]thiosemicarbazone were determined, NCH₃, phenyl C_{3,5}, phenyl C_{2,6}, thiosemicarbazone N₄ and N₂ protons were recorded at δ 3.21, 7.30, 7.55, 10.81 and 12.56 ppm, respectively (Atioğlu, Sevinçli, Karalı, Akkurt, & Ersanlı, 2017a). The NMR findings of 1*H*-indole-2,3-dione 3-thiosemicarbazone derivatives given in the cited literatures confirmed the data of the compound **5**.

Figure 8 shows the molecular conformation of the 3*Z*-isomer of the compound **5**. A planar indole fused-ring (N1/C1–C8) [r.m.s deviation = 0.003 Å] made a dihedral angle of 4.13 (11)° with the benzene ring (C12–C17). The N—N—C S and N—N—C(S)—N torsion angles were -170.76(19) and 8.0 (3)°, respectively. All bond lengths and angles were within normal ranges and were in agreement with those reported for 2-(5-fluoro-1-methyl-2-oxindolin-3-ylidene)-*N*-[4-(methylsulfonyl)phenyl]hydrazine-1-carbothioamide (Atioğlu, *et al.*, 2017a), (*Z*)-2-(6-fluoro-3-methyl-2-oxo-2,3-dihydro-1*H*-inden-1-ylidene)-*N*-(3-fluorophenyl)hydrazine-1-carbothioamide (Atioğlu, Sevinçli, Karalı, Akkurt, & Ersanlı, 2017b), (3*E*)-3-[(4-butylphenyl)imino]-1,3-dihydro-2*H*-indol-2-one (Akkurt, Öztürk, Erçağ, Özgür, & Heinemann, 2003), *N'*-[(*ZZ*)-3-allyl-4-oxo-1,3-thiazolidin-2-ylidene]-5-fluoro-3-phenyl-1*H*-indole-2-carbohydrazide (Akkurt, Karaca, Cihan, Çapan, & Büyükgüngör, 2009) and 5-trifluoromethoxy-1*H*-indole-2,3-dione 3-thiosemicarbazone derivatives (Kaynak *et al.*, 2013).

As shown in Figure 8, in the crystal of (3*Z*)-1-methyl-5-trifluoromethoxy-1*H*-indole-2,3-dione 3-[4-(4-methoxyphenyl)thiosemicarbazone] (**5**), three intramolecular N—H...N, N—H...O

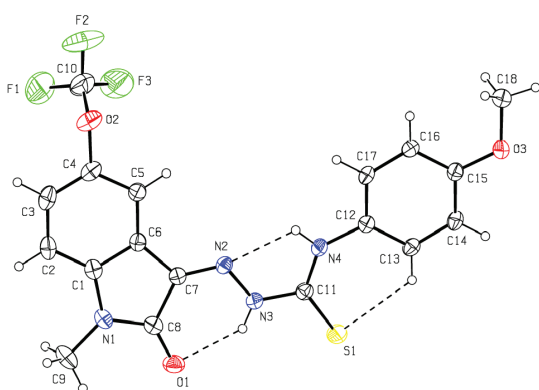


Figure 8. View of 3Z-isomer of the compound **5** with the atom numbering scheme. Displacement ellipsoids for non-H atoms are drawn at the 30% probability level.

and C—H...S hydrogen bonds generated S(5), S(6) and S(6) ring motifs, respectively (Table 2) (Bernstein, Davis, Shimoni, & Chang, 1995). H atoms attached to N atoms were localized in the difference Fourier map and refined freely with $U_{iso}(H) = 1.2U_{eq}(N)$. All C-bound H-atoms were included in the geometrically determined positions and refined using a riding model with C—H = 0.93 and 0.96 Å and $U_{iso}(H) = 1.2$ or $1.5 U_{eq}(C)$. In the crystal, the molecular packing was stabilized by intermolecular C—H...O hydrogen bonds (Figure 9; Table 2), the π - π stacking interactions [$Cg1 \cdots Cg3(1-x, 1-y, 1-z) = 3.6021(18)$ Å and $Cg2 \cdots Cg2(2-x, 1-y, 1-z) = 3.7250(19)$ Å; where $Cg1$, $Cg2$ and $Cg3$ are the centroids of the five-membered (N1/C1/C6–C8) and six-membered (C1–C6) of the 1,3-dihydro-2H-indol-2-one ring system, and the methoxyphenyl ring (C12–C17), respectively]. In addition, weak C O... π (ring) contacts between the molecules contributed to the stabilization of the crystal structure (Table 2). Figure 9a and 9c show the views of the hydrogen bonding, along the a, b and c axes of the crystal packing of the compound **5**, respectively.

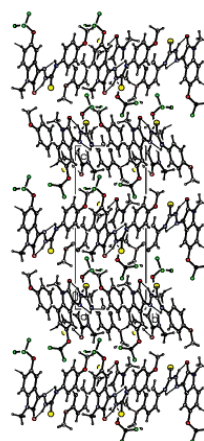
Table 2. Hydrogen-bond geometry (Å, °) of the 3Z-conformer of the compound 5.

D—H...A	D—H	H...A	D...A	D—H...A
N3—H3N...O1	0.86 (3)	2.08 (3)	2.749 (3)	134 (2)
N4—H4N...N2	0.86 (3)	2.14 (3)	2.611 (3)	114 (2)
C3—H3...O3 ⁱ	0.9300	2.4200	3.307 (4)	158.00
C13—H13...S1	0.9300	2.6100	3.262 (3)	128
C8—O1...Cg3 ⁱⁱ	1.223 (3)	3.675 (3)	3.424 (3)	68.62 (15)

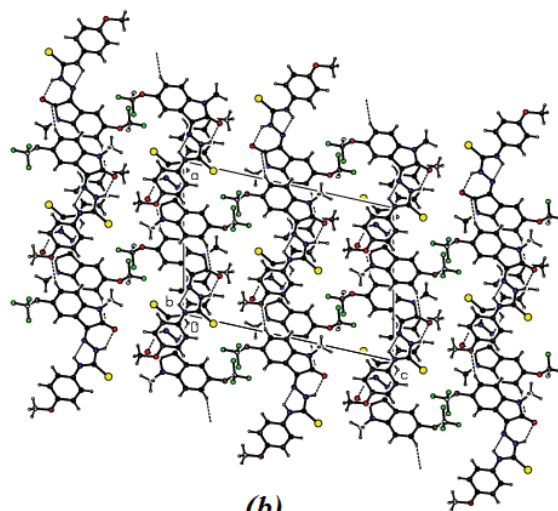
Symmetry codes: (i) $x+1, y+1, z$; (ii) $-x+1, -y+1, -z+1$.

CONCLUSION

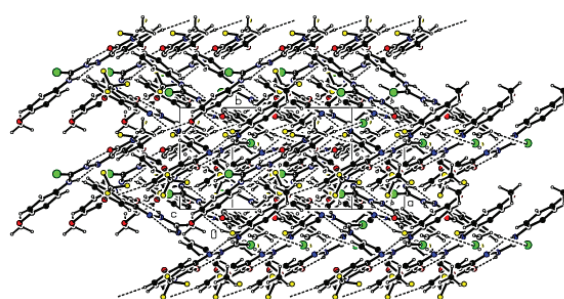
The structures of the *E*- and *Z*- isomers of the new 1-methyl-5-trifluoromethoxy-1*H*-indole-2,3-dione 3-[4-(4-methoxyph-



(a)



(b)



(c)

Figure 9. A view along the a axis (a), b axis (b), c axis (c) of the crystal packing and hydrogen bonding of 3Z-isomer of the compound **5**.

nyl)thiosemicarbazone] (**5**) were characterized by NMR data. The *Z*-conformer of the compound **5** was further confirmed by X-ray single crystal diffraction analysis technique. The intramolecular hydrogen bonds in the 3Z-isomer resulted in strong downfield shifts for the N₂-H and N₄-H protons of the thiosemicarbazone moiety. The conformation of the 3Z-isomer of the compound **5** was stabilized by three intramolecular N—H...N, N—H...O and C—H...S hydrogen bonds. Intermolecular C—H...O hydrogen bonds, π - π stacking interactions and weak C O... π (ring) contacts contributed to the stabilization of the crystal structure.

Acknowledgement: Authors acknowledge the Scientific and Technological Research Application and Research Center, Sinop University, Turkey, for the use of the Bruker D8 QUEST diffractometer.

Peer-review: Externally peer-reviewed.

Author Contributions: Conception/Design of Study- N.K., Ö.S.E.; Data Acquisition- Ö.S.E., Z.A.; Data Analysis/Interpretation- N.K., M.A., C.C.E., Ö.S.E., Z.A.; Drafting Manuscript- Ö.S.E., N.K., M.A.; Critical Revision of Manuscript- N.K., M.A., C.C.E., Z.A.; Final Approval and Accountability- N.K., M.A., C.C.E., Ö.S.E., Z.A.

Conflict of Interest: The authors have no conflict of interest to declare.

Financial Disclosure: This work was supported by The Scientific and Technological Research Council of Turkey (TUBITAK) [grant number 1003-215S011].

REFERENCES

- Akkurt, M., Karaca, S., Cihan, G., Çapan, G., & Büyükgüngör, O. (2009). *N'*-[(2*Z*)-3-Allyl-4-oxo-1,3-thiazolidin-2-ylidene]-5-fluoro-3-phenyl-1*H*-indole-2-carbohydrazide. *Acta Crystallographica Section E*, *65*, o1009-o1010. <https://doi.org/10.1107/S1600536809012677>
- Akkurt, M., Öztürk, S., Erçağ, A., Özgür, M. Ü., & Heinemann, F.W. (2003). (3*E*)-3-[(4-Butylphenyl)imino]-1,3-dihydro-2*H*-indol-2-one. *Acta Crystallographica Section E*, *59*, o780-o782. <https://doi.org/10.1107/S160053680300953X>
- Ali, A. Q., Teoh, S. G., Salhin, A., Eltayeb, N. E., Ahamed, M. B. K., & Majid, A. A. (2014). Synthesis of isatin thiosemicarbazones derivatives: in vitro anti-cancer, DNA binding and cleavage activities. *Spectrochimica Acta Part A: Molecular and Biomolecular Spectroscopy*, *125*, 440-448. <https://doi.org/10.1016/j.saa.2014.01.086>
- Atioğlu, Z., Sevinçli, Z. Ş., Karalı, N., Akkurt, M., & Ersanlı, C. C. (2017a). 2-(5-Fluoro-1-methyl-2-oxoindolin-3-ylidene)-*N*-[4-(methylsulfanyl)phenyl]hydrazine-1-carbothioamide. *IUCrData*, *2*, x170671. <https://doi.org/10.1107/S2414314617009002>
- Atioğlu, Z., Sevinçli, Z. Ş., Karalı, N., Akkurt, M., & Ersanlı, C. C. (2017b). (2*Z*)-2-(5-Fluoro-1-methyl-2-oxoindolin-3-ylidene)-*N*-(3-fluorophenyl)hydrazine-1-carbothioamide. *IUCrData*, *2*, x170900. <https://doi.org/10.1107/S2414314617009002>
- Bain, G. A., West, D. X., Krejci, J., Valdés-Martinez, J., Hernández-Ortega, S., & Toscano, R. A. (1997). Synthetic and spectroscopic investigations of *N*(4)-substituted isatin thiosemicarbazones and their copper (II) complexes. *Polyhedron*, *16*(5), 855-862. [https://doi.org/10.1016/S0277-5387\(96\)00323-3](https://doi.org/10.1016/S0277-5387(96)00323-3)
- Bal, T. R., Anand, B., Yogeewari, P., & Sriram, D. (2005). Synthesis and evaluation of anti-HIV activity of isatin beta-thiosemicarbazone derivatives. *Bioorganic & Medicinal Chemistry Letters*, *15*(20), 4451-4455. <https://doi.org/10.1016/j.bmcl.2005.07.046>
- Bernstein, J., Davis, R. E., Shimon, L., & Chang, N. L. (1995). Patterns in hydrogen bonding: functionality and graph set analysis in crystals. *Angewandte Chemie International Edition in English*, *34*, 1555-1573. <http://doi.org/10.1002/anie.199515551>
- DeSilva, N. W. S. V. N., & Albu, T. V. (2007). A theoretical investigation on the isomerism and the NMR properties of thiosemicarbazones. *Central European Journal of Chemistry*, *5*(2), 396-419. <https://doi.org/10.2478/s11532-007-0012-1>
- Farrugia, L. J. (2012). WinGX and ORTEP for Windows: an update. *Journal of Applied Crystallography*, *45*, 849-854. <https://doi.org/10.1107/S0021889812029111>
- Güzel, Ö., Karalı, N., & Salman, A. (2008). Synthesis and antituberculosis activity of 5-methyl/trifluoromethoxy-1*H*-indole-2,3-dione 3-thiosemicarbazone derivatives. *Bioorganic & Medicinal Chemistry*, *16*(19), 8976-8987. <https://doi.org/10.1016/j.bmc.2008.08.050>
- Hall, M.D., Brimacombe, K.R., Varonka, M.S., Pluchino, K.M., Monda, J.K., Li, J. ... Gottesman, M.M. (2011). Synthesis and structure-activity evaluation of isatin-β-thiosemicarbazones with improved selective activity towards multidrug-resistant cells expressing P-glycoprotein. *Journal of Medicinal Chemistry*, *54*(16), 5878-5889. <http://doi.org/10.1021/jm2006047>
- Hall, M.D., Salam, N.K., Hellawell, J.L., Fales, H.M., Kensler, C.B., Ludwig, J.A. ... Gottesman, M.M. (2009). Synthesis, activity, and pharmacophore development for isatin-β-thiosemicarbazones with selective activity toward multidrug-resistant cells. *Journal of Medicinal Chemistry*, *52*(10), 3191-3204. <http://doi.org/10.1021/jm800861c>
- Haribabu, J., Subhashree, G., Saranya, S., Gomathi, K., Karvembu, R., & Gayathri, D. (2016). Isatin based thiosemicarbazone derivatives as potential bioactive agents: Anti-oxidant and molecular docking studies. *Journal of Molecular Structure*, *1110*, 185-195. <https://doi.org/10.1016/j.molstruc.2016.01.044>
- Howard, J.A.K., Hoy, V.J., O'Hagan, D., & Smith, G.T. (1996). How good is fluorine as a hydrogen bond acceptor?. *Tetrahedron*, *52*(38), 12613-12622. [https://doi.org/10.1016/0040-4020\(96\)00749-1](https://doi.org/10.1016/0040-4020(96)00749-1)
- Huang, H., Chen, Q., Ku, X., Meng, L., Lin, L., Wang, X. ... Liu, H. (2010). A Series of α-Heterocyclic Carboxaldehyde Thiosemicarbazones Inhibit Topoisomerase IIa Catalytic Activity. *Journal of Medicinal Chemistry*, *53*(8), 3048-3064. <http://doi.org/10.1021/jm9014394>
- Jakusová, K., Gáplovský, M., Donovalová, J., Cigáň, M., Stankovičová, H. ... Anton, G. (2013). Effect of reactants' concentration on the ratio and yield of E, Z isomers of isatin-3-(4-phenyl)semicarbazone and *N*-methylisatin-3-(4-phenyl)semicarbazone. *Chemical Papers*, *67*(1), 117-126. <https://doi.org/10.2478/s11696-012-0248-x>
- Karalı, N. (2002). Synthesis and primary cytotoxicity evaluation of new 5-nitroindole-2,3-dione derivatives. *European Journal of Medicinal Chemistry*, *37*(11), 909-918. [https://doi.org/10.1016/S0223-5234\(02\)01416-2](https://doi.org/10.1016/S0223-5234(02)01416-2)
- Karalı, N., Gürsoy, A., Kandemirli, F., Shvets, N., Kaynak, F.B., Özbey, S. ... Dimoglo, A. (2007). Synthesis and structure-antituberculosis activity relationship of 1*H*-indole-2,3-dione derivatives. *Bioorganic & Medicinal Chemistry*, *15*(17), 5888-5904. <https://doi.org/10.1016/j.bmc.2007.05.063>
- Karalı, N., Soylu, Ö., Gül, A., Ozer, H., Erman, B., Hasanusta, B., Ersoy, B., 5-Fluoro(trifluoromethoxy)-2-indolinone derivatives. 11.02.2020 PCT/TR 2020/050401
- Kaynak, F.B., Özbey, S., & Karalı, N. (2013). Three Novel Compounds Of 5-Trifluoromethoxy-1*H*-Indole-2,3-Dione 3-Thiosemicarbazone: Synthesis, Crystal Structures And Molecular Interactions. *Journal of Molecular Structure*, *1049*, 157-164. <https://doi.org/10.1016/j.molstruc.2013.06.039>
- Ma, J., Bao, G., Wang, L., Li, W., Xu, B., Du, B. ... Gong, P. (2015). Design, synthesis, biological evaluation and preliminary mechanism study of novel benzothiazole derivatives bearing indole-based moiety as potent antitumor agents. *European Journal of Medicinal Chemistry*, *96*, 173-186. <http://doi.org/10.1016/j.ejmech.2015.04.018>
- Matesic, L., Locke, J., Bremner, J.B., Pyne, S.G., Skropeta, D., Ranson, M., & Vine, K.L. (2008). *N*-phenethyl and *N*-naphthylmethyl isatins and analogues as in vitro cytotoxic agents. *Bioorganic & Medicinal Chemistry*, *16*(6), 3118-3124. <https://doi.org/10.1016/j.bmc.2007.12.026>
- Matheus, M.E., DeAlmeida Violante, F., Garden, S.J., Pinto, A.C., & Fernandes, P.D. (2007). Isatins inhibit cyclooxygenase-2 and inducible nitric oxide synthase in a mouse macrophage cell line. *European Journal of Pharmacology*, *556*(1-3), 200-206. <https://doi.org/10.1016/j.ejphar.2006.10.057>

- Muralisankar, M., Sujith, S., Bhuvanesh, N.S.P., & Sreekanth, A. (2016). Synthesis and crystal structure of new monometallic and bimetallic copper (II) complexes with N-substituted isatin thiosemicarbazone ligands: Effects of the complexes on DNA/protein-binding property, DNA cleavage study and in vitro anticancer activity. *Polyhedron*, 118, 103-117. <https://doi.org/10.1016/j.poly.2016.06.017>
- O'Sullivan, D.G., & Sadler, P.W. (1956). The structure of isatin and substituted isatins. *Journal of the Chemical Society (Resumed)*, 0(0), 2202-2207. <https://doi.org/10.1039/JR9560002202>
- Pandeya, S.N., & Sriram, D. (1998). Synthesis and screening for antibacterial activity of Schiff's and Mannich bases of isatin and its derivatives. *Acta Pharmaceutica Turcica*, 40(1), 33-38.
- Pandeya, S.N., Sriram, D., Yogeewari, P., & Ananthan, S. (2001). Antituberculous activity of norfloxacin mannich bases with isatin derivatives. *Chemotherapy*, 47(4), 266-269. <https://doi.org/10.1159/000048533>
- Pape, V.F.S., Tóth, S., Füredi, A., Szebényi, K., Lovrics, A., Szabó, P. ... Szakács, G. (2016). Design, synthesis and biological evaluation of thiosemicarbazones, hydrazinobenzothiazoles and arylhydrazones as anticancer agents with a potential to overcome multidrug resistance. *European Journal of Medicinal Chemistry*, 117, 335-354. <https://doi.org/10.1016/j.ejmech.2016.03.078>
- Pervez, H., Saira, N., Iqbal, M.S., Yaqub, M., & Khan, K.M. (2011). Synthesis and toxicity evaluation of some new N₄-aryl substituted 5-trifluoromethoxyisatin-3-thiosemicarbazones. *Molecules*, 16(8), 6408-6421. <http://doi.org/10.3390/molecules16086408>
- Pervez, H., Manzoor, N., Yaqub, M., Khan, A., Khan, K.M., Nasim, F.H., & Choudhary, M.I. (2010). Synthesis and urease inhibitory properties of some new N₄-substituted 5-nitroisatin-3-thiosemicarbazones. *Letters in Drug Design & Discovery*, 7(2), 102-108. <https://doi.org/10.2174/157018010790225840>
- Pervez, H., Chohan, Z.H., Ramzan, M., Nasim, F.H., & Khan, K.M. (2009). Synthesis and biological evaluation of some new N4-substituted isatin-3-thiosemicarbazones. *Journal of Enzyme Inhibition and Medicinal Chemistry*, 24(2), 437-446. <http://doi.org/10.1080/14756360802188420>
- Pervez, H., Iqbal, M.S., Tahir, M.Y., Nasim, F.H., Choudhary, M.I., & Khan, K.M. (2008). In vitro cytotoxic, antibacterial, antifungal and urease inhibitory activities of some N 4-substituted isatin-3-thiosemicarbazones. *Journal of Enzyme Inhibition and Medicinal Chemistry*, 23(6), 848-854. <http://doi.org/10.1080/14756360701746179>
- Priyanka, K.B., Manasa, C., & Sammaiah, G. (2014). Synthesis and evaluation of new isatin derivatives for cytotoxic activity. *World Journal of Pharmaceutical Sciences*, 3, 2393-2242.
- Ronen, D., Sherman, L., Bar-Nun, S., & Teitz, Y. (1987). N-methylisatin-beta-4',4'-diethylthiosemicarbazone, an inhibitor of Moloney leukemia virus protein production: characterization and in vitro translation of viral Mrna. *Antimicrobial Agents and Chemotherapy*, 31(11), 1798-1802. <http://doi.org/10.1128/AAC.31.11.1798>
- Sabet, R., Mohammadpour, M., Sadeghi, A., & Fassihi, A. (2010). QSAR study of isatin analogues as in vitro anti-cancer agents. *European Journal of Medicinal Chemistry*, 45(3), 1113-1118. <https://doi.org/10.1016/j.ejmech.2009.12.010>
- Sadler, P. (1965). Antiviral chemotherapy with isatin-beta-thiosemicarbazone and its derivatives. *Annals of the New York Academy of Sciences*, 130(1), 71-79. <https://doi.org/10.1111/j.1749-6632.1965.tb12541.x>
- Sadler, P. (1961). Hydrogen bonding in some thiosemicarbazones and thioamides. *Journal of the Chemical Society (Resumed)*, 0(0), 957-960. <https://doi.org/10.1039/JR9610000957>
- Sakai, T., Miki, Y., Nakatani, M., Ema, T., Uneyama, K., & Utaka, M. (1998). Lipase-catalyzed kinetic resolution of 2-acyloxy-2-(pentafluorophenyl)acetonitrile. *Tetrahedron Letters*, 39(29), 5233-5236. [https://doi.org/10.1016/S0040-4039\(98\)01029-6](https://doi.org/10.1016/S0040-4039(98)01029-6)
- Sheldrick, G.M. (2015). Crystal structure refinement with SHELXL. *Acta Crystallographica Section C*, 71, 3-8. <https://doi.org/10.1107/S2053229614024218>
- Sheldrick, G.M. (2008). A short history of SHELX. *Acta Crystallographica Section A*, 64, 112-122. <https://doi.org/10.1107/S0108767307043930>
- Spek, A.L. (2009). Structure validation in chemical crystallography. *Acta Crystallographica Section D*, 65, 148-155. <https://doi.org/10.1107/S090744490804362X>
- Swathi, K., & Sarangapani, M. (2014). Synthesis and anti-inflammatory activity of a novel series of isatin hydrazone & isatin thiosemicarbazone derivatives. *World Journal of Pharmacy and Pharmaceutical Sciences*, 3(2), 2070-2078.
- Tisler, M. (1956). Syntheses in the 4-substituted thiosemicarbazide series. *Croatica Chemica Acta*, 28, 147-154.
- Vine, K.L., Matesic, L., Locke, J.M., Ranson, M., & Skropeta, D. (2009). Cytotoxic and anticancer activities of isatin and its derivatives: a comprehensive review from 2000-2008. *Anti-Cancer Agents in Medicinal Chemistry*, 9(4), 397-414. <https://doi.org/10.2174/1871520610909040397>
- Vine, K.L., Locke, J.M., Ranson, M., Pyne, S.G., & Bremner, J.B. (2007a). An investigation into the cytotoxicity and mode of action of some novel N-alkyl-substituted isatins. *Journal of Medicinal Chemistry*, 50(21), 5109-5117. <http://doi.org/10.1021/jm0704189>
- Vine, K.L., Locke, J.M., Ranson, M., Pyne, S.G., & Bremner, J.B. (2007b). In vitro cytotoxicity evaluation of some substituted isatin derivatives. *Bioorganic & Medicinal Chemistry*, 15(2), 931-938. <https://doi.org/10.1016/j.bmc.2006.10.035>
- Zhang, X-M., Guo, H., Li, Z-S., Song, F-H., Wang, W-M., Dai, H-Q. ... Wang, J-G. (2015). Synthesis and evaluation of isatin-beta-thiosemicarbazones as novel agents against antibiotic-resistant Gram-positive bacterial species. *European Journal of Medicinal Chemistry*, 101, 419-430. <https://doi.org/10.1016/j.ejmech.2015.06.047>

Synthesis, characterization and antibacterial evaluation of new pyridyl-thiazole hybrids of sulfonamides

Zafer Şahin¹ , Sevde Nur Biltekin² , Leyla Yurttaş³ , Şeref Demirayak¹ 

¹Istanbul Medipol University, School of Pharmacy, Department of Pharmaceutical Chemistry, İstanbul, Turkey

²Istanbul Medipol University, School of Pharmacy, Department of Pharmaceutical Microbiology, İstanbul, Turkey

³Anadolu University, Faculty of Pharmacy, Department of Pharmaceutical Chemistry, Eskişehir, Turkey

ORCID IDs of the authors: Z.Ş. 0000-0002-5976-676X; S.N.B. 0000-0003-1896-2729; L.Y. 0000-0002-0957-6044; Ş.D. 0000-0002-0841-1299

Cite this article as: Sahin, Z., Biltekin, S.N., Yurttaş, L., & Demirayak, S. (2021). Synthesis, characterization and antibacterial evaluation of new pyridyl-thiazole hybrids of sulfonamides. *Istanbul Journal of Pharmacy*, 51(1), 67-72.

ABSTRACT

Background and Aims: Sulfonamide drugs are a very old and noted group of small molecules, and are still one of the most important antimicrobial compounds. In this study, starting from sulfonamide drugs, new original compounds containing frequent and functional rings such as thiazole and pyridine were synthesized and their antimicrobial effects were evaluated.

Methods: Eighteen new compounds were synthesized by converting the 4-amino group of the sulfonamides to thiourea, and continued by thiazole ring closure. Characterization of the compounds was carried out by FT-IR, ¹H-NMR and ¹³C-NMR and HRMS. MIC values were obtained in antimicrobial activity studies, which were carried out by Broth Microdilution method.

Results: Compounds **3p-r** had an effect of 32 µg/ml against *B. spizizenii*. In addition, compounds **3d-f** and **3p-r** each showed effect against different gram-positive bacteria. Compound **3r** had an MIC of 128 µg/mL against gram-negative organisms. The rest of the series did not affect gram-negative bacteria. In the study, chloramphenicol and sulfamethoxazole were used as standards.

Conclusion: Sulfanilamide and sulfadiazine derivatives showed higher inhibitory effects compared to the rest of the series. **3d-f** and **3p-r** showed inhibitor activity against gram-positive bacteria, conversely to the standard drug sulfamethoxazole, which possibly means that the mechanism of action is not same.

Keywords: Sulfonamide, thiazole, antibacterial

INTRODUCTION

Infectious diseases have been an incessant problem for human over the years. Gram positive and gram negative bacteria cause diverse infectious reactions. Among the microbial strains, *E. coli* produce lethal toxins, which can be contaminated from unwashed foods (Donnenberg & Whittam, 2001). *P. aeruginosa* and *K. pneumoniae* cause respiratory diseases (Gellatly & Hancock, 2013; Bengoechea & Pessoa 2018; Russo & Marr 2019). *B. spizizenii* is a subspecies of the Bacillus family and may produce typical Bacillus infections (Drobniewski, 1993). *S. aureus*, *E. faecalis*, *S. epidermidis* and *vancomycin-resistant enterococcus* (VRE) are other pathogenic microorganisms involved in this study. Many drug classes and targets are identified for treatment of these diseases. One of the most important classes among them is the sulfonamides, with many drugs identified; sulfamethoxazole, sulfapyridine, sulfadiazine etc. (Supuran, 2017). Advances in the development of new drugs are dependent on synthesis of original molecules and evaluation of their activity on different microbial strains. Pyridine and thiazole are frequent rings used in approved and investigational drugs because they provide ionizable groups and/or good pharmacokinetical properties. Besides, pyridyle-

Address for Correspondence:

Zafer ŞAHİN, e-mail: zshahin@medipol.edu.tr

Submitted: 30.09.2020
Accepted: 14.10.2020

This work is licensed under a Creative Commons Attribution 4.0 International License.



thiazole analogs are an investigational pharmacophore against different targets. The feature for pyridyle-thiazole analogs is their potential for complex formation of cofactors as they are bearing close nitrogen atoms on related rings. (Kashyap et al., 2011; Hamada, 2018; Ertas et al., 2018) Similar sulfonamide derivatives have been reported in a variety of pharmacological activities such as sodium channel inhibitors, anticancer or anti-inflammatory properties in the literature (Sun et al. 2014; El-Sayed et al., 2010). In this study, we synthesized 18 novel pyridyle-thiazole sulfonamide hybrids to evaluate their antimicrobial properties.

MATERIALS AND METHODS

Chemistry

The reactants necessary for the synthesis process were purchased from Sigma Aldrich Chemical Corp. Melting point of title molecules were accomplished by a Stuart melting point apparatus and experiments performed in duplicate. Infra-red spectrums were recorded by Perkin Elmer Spectrom Two using attenuated total reflection (ATR) method. $^1\text{H-NMR}$ and $^{13}\text{C-NMR}$ spectrums were recorded in Bruker 300 MHz UltraShield NMR and Bruker 75 MHz UltraShield NMR, respectively. DMSO- d_6 was used as solvent and TMS was used as standard. High-resolution mass spectrums were recorded in Shimadzu 8,040 LC/MS/MS ITTOF system by the electron spray method (ESI).

Synthesis of sulfonamide-thioureas (1a-f)

Related sulfonamide drug (100 mmol), equal mole (100 mmol) ammonium thiocyanate was dissolved in distilled water by HCl

addition (Figure 1). The mixture was refluxed for 8 hours and then left to reach room temperature. The precipitation was collected and recrystallized from ethanol.

Synthesis of bromoacetylpyridines (2a-c)

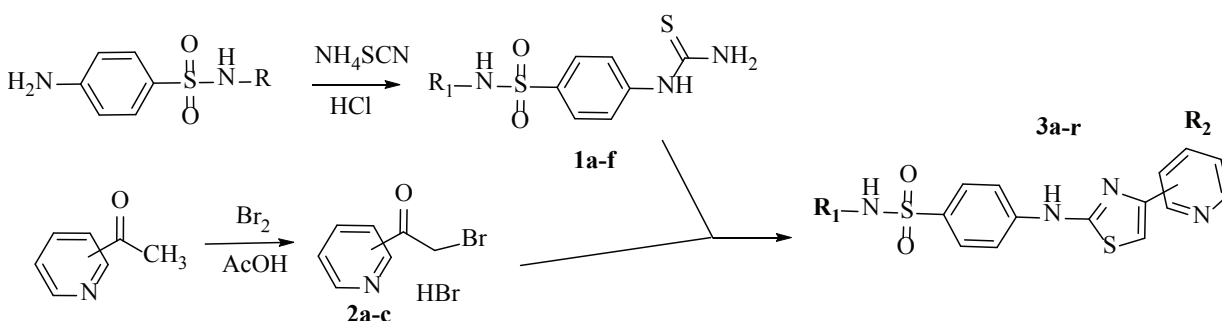
Acetyl pyridine derivatives were dissolved in hydrobromic acid solution (48%) and bromine added drop wise. The reaction mixture was stirred for 1 hour and the precipitation collected. It was crystallized from ethanol.

Synthesis of N-(pyridyle)thiazolyl sulfonamides (3a-r)

Equal moles (10 mmol) of bromoacetyl pyridine (2a-c) and sulfonamide thiourea (1a-f) derivatives were dissolved in ethanol and refluxed for 4 hours. The precipitated product was filtered, poured into water at room temperature and neutralized by sodium acetate. If precipitation did not occur, water was added to provide precipitation. The products were recrystallized from ethanol.

N-(4,6-dimethylpyrimidin-2-yl)-4-((4-(pyridine-2-yl)thiazol-2-yl)amino)benzene-sulfonamide (3a)

Yield: 77%, m.p. 253°C, IR $\bar{\nu}_{max}$ (cm^{-1}): 3351.25 (N-H), 3055.31 (N-H), 3005.95, 2927.74 (Ar C-H). $^1\text{H-NMR}$ (300 MHz, DMSO- d_6 , δ , ppm): 2.26 (6H, s, CH_3), 6.75 (1H, s, Ar), 7.31-7.35 (1H, m, Ar), 7.65 (1H, s, Ar), 7.84-7.92 (3H, m, Ar), 7.97 (2H, d, J : 8.89 Hz, Ar), 8.06 (2H, d, J : 7.93 Hz, Ar), 8.57-8.61 (1H, m, Ar), 10.75 (1H, s, NH), 11.46 (1H, s, NH). $^{13}\text{C-NMR}$ (75 MHz, DMSO- d_6 , δ , ppm): 23.45, 108.63, 116.15, 121.05, 123.27, 130.22, 132.45, 137.83, 144.92, 149.89, 150.87, 152.36, 156.83, 162.97 HR-MS (M+H): pred: 439.1005, found: 439.1002.



C	R1	R2	C	R1	R2
3a	3,5-Dimethylpyrimidine-2-yl	2-Pyridyle	3j	5-methylizoxazole-3-yl	2-Pyridyle
3b	3,5-Dimethylpyrimidine-2-yl	3-Pyridyle	3k	5-methylizoxazole-3-yl	3-Pyridyle
3c	3,5-Dimethylpyrimidine-2-yl	4-Pyridyle	3l	5-methylizoxazole-3-yl	4-Pyridyle
3d	Pyrimidine-2-yl	2-Pyridyle	3m	Thiazole-2-yl	2-Pyridyle
3e	Pyrimidine-2-yl	3-Pyridyle	3n	Thiazole-2-yl	3-Pyridyle
3f	Pyrimidine-2-yl	4-Pyridyle	3o	Thiazole-2-yl	4-Pyridyle
3g	Pyridine-2-yl	2-Pyridyle	3p	H	2-Pyridyle
3h	Pyridine-2-yl	3-Pyridyle	3q	H	3-Pyridyle
3i	Pyridine-2-yl	4-Pyridyle	3r	H	4-Pyridyle

Figure 1. Synthesis of compounds 3a-r.

N-(4,6-dimethylpyrimidin-2-yl)-4-((4-(pyridine-3-yl)thiazol-2-yl)amino)benzene-sulfonamide (3b)

Yield: 66%, m.p. 265°C, IR $\bar{\nu}_{max}$ (cm⁻¹): 3052.88 (N-H), 2925.56 (Ar C-H). ¹H-NMR (300 MHz, DMSO-*d*₆, δ , ppm): 2.25 (6H, s, CH₃), 6.75 (1H, s, Ar), 7.47-7.55 (1H, m, Ar), 7.65 (1H, s, Ar), 7.85 (2H, d, *J*: 8.62 Hz, Ar), 7.98 (2H, d, *J*: 8.93 Hz, Ar), 8.29 (1H, d, *J*: 8.07 Hz, Ar), 8.53 (1H, br. s, Ar), 9.17 (1H, br. s, Ar), 10.78 (1H, s, NH), 11.51 (1H, s, NH). ¹³C-NMR (75 MHz, DMSO-*d*₆, δ , ppm): 23.44, 106.43, 114.12, 116.19, 124.27, 130.25, 132.51, 133.41, 144.84, 147.50, 147.81, 149.03, 156.81, 163.20, 167.82. HR-MS (M+H): pred: 439.1005, found: 439.1002.

N-(4,6-dimethylpyrimidin-2-yl)-4-((4-(pyridine-4-yl)thiazol-2-yl)amino)benzene-sulfonamide (3c)

Yield: 60%, m.p. 266°C, IR $\bar{\nu}_{max}$ (cm⁻¹): 3264.27 (NH), 3185.09 (N-H), 3103.63 (Ar C-H). ¹H-NMR (300 MHz, DMSO-*d*₆, δ , ppm): 2.26 (6H, s, CH₃), 6.76 (1H, s, Ar), 7.87 (2H, d, *J*: 8.97 Hz, Ar), 7.98 (2H, d, *J*: 8.94 Hz, Ar), 8.17-8.29 (3H, m, Ar), 8.79-???? (2H, m, Ar), 10.93 (1H, s, NH), 11.55 (1H, s, NH). ¹³C-NMR (75 MHz, DMSO-*d*₆, δ , ppm): 23.44, 114.12, 116.44, 121.96, 130.21, 132.91, 144.52, 145.93, 156.79, 163.46. HR-MS (M+H): pred: 439.1005, found: 439.1001.

4-((4-(pyridine-2-yl)thiazol-2-yl)amino)-N-(pyrimidin-2-yl)benzenesulfonamide (3d)

Yield: 78%, m.p. 226°C, IR $\bar{\nu}_{max}$ (cm⁻¹): 3282.96 (NH), 3194.78 (N-H), 3083.00-2943.44 (Ar C-H). ¹H-NMR (300 MHz, DMSO-*d*₆, δ , ppm): 7.10 (1H, t, *J*: 4.84 Hz, Ar), 7.59 (1H, ddd, *J*: 7.63 Hz, 4.92 Hz, 1.00 Hz, Ar), 7.77 (1H, s, Ar), 7.94-8.05 (5H, m, Ar), 8.18 (1H, d, *J*: 8.33 Hz, Ar), 8.56 (2H, d, *J*: 4.80 Hz, Ar), 8.67 (1H, d, *J*: 4.68 Hz, Ar), 10.88 (1H, s, NH), 11.61 (1H, s, NH). ¹³C-NMR (75 MHz, DMSO-*d*₆, δ , ppm): 109.33, 116.22, 116.47, 121.35, 123.47, 129.81, 132.10, 138.49, 145.08, 149.32, 150.24, 151.79, 157.49, 158.82, 162.99. HR-MS (M+H): pred: 411.0692, found: 411.0690.

4-((4-(pyridine-3-yl)thiazol-2-yl)amino)-N-(pyrimidin-2-yl)benzenesulfonamide (3e)

Yield: 68%, m.p. 240.5°C, IR $\bar{\nu}_{max}$ (cm⁻¹): 2988.66-2734.87 (Ar C-H). ¹H-NMR (300 MHz, DMSO-*d*₆, δ , ppm): 7.04 (1H, t, *J*: 4.88 Hz, Ar), 7.59 (1H, dd, *J*: 9.48 Hz, 4.92 Hz, Ar), 7.72 (1H, s, Ar), 7.87-7.97 (4H, m, Ar), 8.42-8.51 (3H, m, Ar), 8.59 (1H, dd, *J*: 4.89 Hz, 1.45 Hz, Ar), 9.22 (1H, d, *J*: 1.74 Hz, Ar), 10.85 (1H, s, NH), 11.63 (1H, s, NH). ¹³C-NMR (75 MHz, DMSO-*d*₆, δ , ppm): 163.2318, 158.8155, 157.4858, 147.5972, 147.2030, 146.1180, 145.0079, 135.0453, 132.1740, 130.9313, 129.8394, 124.8952, 116.5137, 116.2106, 107.3003. HR-MS (M+H): pred: 411.0692, found: 411.0692.

4-((4-(pyridine-4-yl)thiazol-2-yl)amino)-N-(pyrimidin-2-yl)benzenesulfonamide (3f)

Yield: 80%, m.p. 283°C, IR $\bar{\nu}_{max}$ (cm⁻¹): 3609.64 (N-H), 2987.82-2871.18 (Ar C-H). ¹H-NMR (300 MHz, DMSO-*d*₆, δ , ppm): 7.04 (1H, t, *J*: 4.88 Hz, Ar), 7.84-8.01 (7H, m, Ar), 8.50 (2H, d, *J*: 4.86 Hz, Ar), 8.62 (2H, d, *J*: 5.76 Hz, Ar), 10.85 (1H, s, NH), 11.65 (1H, s, NH). ¹³C-NMR (75 MHz, DMSO-*d*₆, δ , ppm): 109.51, 116.22, 116.52, 120.54, 129.83, 132.21, 141.32, 144.98, 148.28, 150.62, 157.49, 158.82, 163.05. HR-MS (M+H): pred: 411.0692, found: 411.0694.

N-(pyridine-2-yl)-4-((4-(pyridine-2-yl)thiazol-2-yl)amino)benzenesulfonamide (3g)

Yield: 75%, m.p. 269°C, IR $\bar{\nu}_{max}$ (cm⁻¹): 3250.00 (N-H), 3112.13 (N-H), 3010.80-2810.35 (Ar C-H). ¹H-NMR (300 MHz, DMSO-*d*₆, δ ,

ppm): 6.81 (1H, d, *J*: 4.60 Hz, Ar), 7.24 (1H, d, *J*: 4.66 Hz, Ar), 7.33 (1H, ddd, *J*: 7.50 Hz, 4.80 Hz, 1.12 Hz, Ar), 7.64 (1H, s, Ar), 7.77-7.82 (2H, m, Ar), 7.84-7.96 (5H, m, Ar), 8.07 (1H, d, *J*: 7.89 Hz, Ar), 8.59-???? (1H, m, Ar), 10.73 (1H, s, NH), 12.63 (1H, s, NH). ¹³C-NMR (75 MHz, DMSO-*d*₆, δ , ppm): 108.42, 116.67, 121.08, 123.25, 124.84, 127.86, 134.54, 137.81, 144.46, 149.87, 150.89, 152.38, 163.02, 169.05. HR-MS (M+H): pred: 410.0740, found: 410.0734.

N-(pyridine-2-yl)-4-((4-(pyridine-3-yl)thiazol-2-yl)amino)benzenesulfonamide (3h)

Yield: 64%, m.p. 247.4°C, IR $\bar{\nu}_{max}$ (cm⁻¹): 3241.06 (N-H), 3100-2785 (Ar C-H). ¹H-NMR (300 MHz, DMSO-*d*₆, δ , ppm): 6.80 (1H, s, Ar), 7.24 (1H, br. s, Ar), 7.46 (1H, br. s, Ar), 7.61 (1H, br. s, Ar), 7.82-7.88 (6H, m, Ar), 8.31 (1H, m, Ar), 8.53 (1H, br. s, Ar), 9.18 (1H, d, *J*: 2.01 Hz, Ar), 10.77 (1H, s, NH), 12.63 (1H, s, NH). ¹³C-NMR (75 MHz, DMSO-*d*₆, δ , ppm): 106.28, 108.43, 115.96, 116.74, 123.92, 124.29, 124.84, 125.21, 127.11, 127.90, 128.85, 130.46, 133.58, 134.61, 144.40, 144.64, 147.39, 147.75, 148.88, 163.27, 169.06. HR-MS (M+H): pred: 410.0740, found: 410.0736.

N-(pyridine-2-yl)-4-((4-(pyridine-4-yl)thiazol-2-yl)amino)benzenesulfonamide (3i)

Yield: 70%, m.p. 281°C, IR $\bar{\nu}_{max}$ (cm⁻¹): 3251.75 (N-H), 3101.09 (N-H), 2922.97-2779.28 (Ar C-H). ¹H-NMR (300 MHz, DMSO-*d*₆, δ , ppm): 6.81 (1H, d, *J*: 4.54 Hz, Ar), 7.24 (1H, d, *J*: 4.71 Hz, Ar), 7.78-7.93 (9H, m, Ar), 8.63 (2H, d, *J*: 5.37 Hz, Ar), 10.79 (1H, s, NH), 12.63 (1H, s, NH). ¹³C-NMR (75 MHz, DMSO-*d*₆, δ , ppm): 108.44, 109.38, 116.77, 120.57, 124.85, 127.86, 134.72, 141.49, 144.29, 148.22, 150.48, 163.17, 169.06. HR-MS (M+H): pred: 410.0740, found: 410.0737.

N-(5-methylisoxazol-3-yl)-4-((4-(pyridine-2-yl)thiazol-2-yl)amino)benzenesulfonamide (3j)

Yield: 85%, m.p. 235°C, IR $\bar{\nu}_{max}$ (cm⁻¹): 3360.37 (N-H), 3223.83 (N-H), 3098.93-3005.34 (Ar C-H). ¹H-NMR (300 MHz, DMSO-*d*₆, δ , ppm): 2.29 (3H, s, Ar), 6.13 (1H, s, Ar), 7.59 (1H, t, *J*: 6.18 Hz, Ar), 7.84 (2H, d, *J*: 8.97 Hz, Ar), 7.94-7.98 (3H, m, Ar), 8.19 (1H, t, *J*: 8.26 Hz, Ar), 8.69 (1H, d, *J*: 5.16 Hz, Ar), 10.98 (1H, s, NH), 11.30 (1H, s, NH). ¹³C-NMR (75 MHz, DMSO-*d*₆, δ , ppm): 12.53, 95.83, 112.20, 117.14, 122.44, 124.29, 128.95, 130.89, 131.44, 141.43, 145.13, 146.94, 158.10, 163.34, 170.67. HR-MS (M+H): pred: 414.0689, found: 414.0695.

N-(5-methylisoxazol-3-yl)-4-((4-(pyridine-3-yl)thiazol-2-yl)amino)benzenesulfonamide (3k)

Yield: 80%, m.p. 254.5°C, IR $\bar{\nu}_{max}$ (cm⁻¹): 3439.15 (N-H), 3339.96 (NH), 3162.61-2875.16 (Ar C-H). ¹H-NMR (300 MHz, DMSO-*d*₆, δ , ppm): 2.29 (3H, s, Ar), 6.14 (1H, s, Ar), 7.47 (1H, dd, *J*: 6.09 Hz, 4.8 Hz, Ar), 7.66 (1H, s, Ar), 7.82-7.93 (4H, m, Ar), 8.31 (1H, dt, *J*: 8.05 Hz, 1.9 Hz, Ar), 8.53 (1H, dd, *J*: 4.56 Hz, 1.55 Hz, Ar), 9.17 (1H, d, *J*: 2.01 Hz, Ar), 10.88 (1H, s, NH), 11.28 (1H, s, NH). ¹³C-NMR (75 MHz, DMSO-*d*₆, δ , ppm): 170.6549, 163.0586, 158.1270, 149.0320, 147.8212, 147.4862, 145.3790, 133.5084, 131.1830, 130.3561, 129.0094, 124.2756, 116.9107, 106.6712, 95.8413, 95.8156, 12.5345 HR-MS (M+H): pred: 414.0689, found: 414.0697.

N-(5-methylisoxazol-3-yl)-4-((4-(pyridine-4-yl)thiazol-2-yl)amino)benzenesulfonamide (3l)

Yield: 65%, m.p. 290.5°C, IR $\bar{\nu}_{max}$ (cm⁻¹): 3320.74 (N-H), 3185.88 (N-H), 3114.95-2923.28 (Ar C-H). ¹H-NMR (300 MHz, DMSO-*d*₆, δ , ppm): 2.29 (3H, s, Ar), 6.14 (1H, s, Ar), 7.85-7.91 (7H, m, Ar), 8.63 (2H, d, *J*: 6.09 Hz, Ar), 10.90 (1H, s, NH), 11.29 (1H, s, NH). ¹³C-NMR

(75 MHz, DMSO- d_6 , δ , ppm): 12.54, 95.82, 109.60, 116.95, 120.52, 129.00, 131.29, 141.25, 145.30, 148.31, 150.68, 158.12, 162.99. HR-MS (M+H): pred: 414.0689, found: 414.0695.

4-((4-(pyridine-2-yl)thiazol-2-yl)amino)-N-(thiazol-2-yl)benzenesulfonamide (3m)

Yield: 72%, m.p. 266.8 °C, IR $\bar{\nu}_{max}$ (cm⁻¹): 3279.64 (N-H), 3149.35-2811.30 (Ar C-H). ¹H-NMR (300 MHz, DMSO- d_6 , δ , ppm): 6.81 (1H, d, *J*: 4.62 Hz, thiazole), 7.24 (1H, d, *J*: 4.62 Hz, thiazole), 7.3304-7.38 (1H, m, Ar), 7.66 (1H, s, Ar), 7.68-7.80 (2H, m, Ar), 7.85-7.95 (3H, m, Ar), 8.09 (1H, d, *J*: 7.89 Hz, Ar), 8.59-8.61 (1H, m, Ar) 10.74 (1H, s, NH), 12.64 (1H, s, NH). ¹³C-NMR (75 MHz, DMSO- d_6 , δ , ppm): 108.42, 108.73, 116.68, 121.20, 123.34, 124.82, 127.84, 134.56, 138.12, 144.42, 149.61, 150.57, 152.13, 163.05. HR-MS (M+H): pred: 416.0304, found: 416.0297.

4-((4-(pyridine-3-yl)thiazol-2-yl)amino)-N-(thiazol-2-yl)benzenesulfonamide (3n)

Yield: 75%, m.p. 292 °C, IR ($\bar{\nu}_{max}$ (cm⁻¹): 3217.14 (N-H), 3165.09 (N-H), 3029-2998 (Ar C-H). ¹H-NMR (300 MHz, DMSO- d_6 , δ , ppm): 6.82 (1H, d, *J*: 4.59 Hz, thiazole), 7.25 (1H, d, *J*: 4.62 Hz, thiazole), 7.79 (2H, d, *J*: 8.85 Hz, Ar), 7.91 (2H, d, *J*: 8.82 Hz, Ar), 7.98 (1H, s, thiazole), 8.05 (1H, dd, *J*: 9 Hz, 5.60 Hz, Ar), 8.82 (1H, d, *J*: 5.43 Hz, Ar), 8.99 (1H, d, *J*: 8.37 Hz, Ar), 9.40 (1H, s, NH), 10.95 (1H, s, NH). ¹³C-NMR (75 MHz, DMSO- d_6 , δ , ppm): 169.0689, 163.7379, 144.7641, 144.0954, 141.8711, 141.1882, 140.6548, 134.9036, 133.1460, 127.8172, 127.3908, 124.8855, 116.9819, 110.1459, 108.4805. HR-MS (M+H): pred: 416.0304, found: 416.0302.

4-((4-(pyridine-4-yl)thiazol-2-yl)amino)-N-(thiazol-2-yl)benzenesulfonamide (3o)

Yield: 90%, m.p. Decomposed, IR $\bar{\nu}_{max}$ (cm⁻¹): 3212.97 (N-H), 3157.92 (N-H), 3091.73-2780.85 (Ar C-H). ¹H-NMR (300 MHz, DMSO- d_6 , δ , ppm): 6.83 (1H, d, *J*: 4.62 Hz, thiazole), 7.25 (1H, d, *J*: 4.62 Hz, thiazole), 7.79 (2H, d, *J*: 8.82 Hz, Ar), 7.91 (2H, d, *J*: 8.79 Hz, Ar), 8.42 (1H, s, thiazole), 8.51 (2H, d, *J*: 6.45 Hz, Ar), 8.91 (2H, d, *J*: 6.63 Hz, Ar), 11.05 (1H, s, NH), 12.67 (1H, s, NH). ¹³C-NMR (75 MHz, DMSO- d_6 , δ , ppm): 169.0807, 163.6579, 148.8425, 145.8981, 143.9361, 142.9127, 135.1140, 127.8246, 124.8885, 122.8679, 117.0760, 108.5102. HR-MS (M+H): pred: 416.0304, found: 416.0299.

4-((4-(pyridine-2-yl)thiazol-2-yl)amino)benzenesulfonamide (3p)

Yield: 60%, m.p. 242 °C, IR $\bar{\nu}_{max}$ (cm⁻¹): 3340.25, 3269.36 (N-H), 3190.39 (N-H), 3123.55-3007.22 (Ar C-H). ¹H-NMR (300 MHz, DMSO- d_6 , δ , ppm): 7.23 (2H, s, SO₂NH₂), 7.31-7.36 (1H, m, Ar), 7.65 (1H, s, thiazole), 7.79-7.94 (5H, m, Ar), 8.07 (1H, d, *J*: 7.86 Hz, Ar), 8.59-8.61 (1H, m, Ar), 10.74 (1H, s, NH). ¹³C-NMR (75 MHz, DMSO- d_6 , δ , ppm): 163.1068, 152.3861, 150.8621, 149.9034, 144.2033, 137.8423, 136.5434, 127.6186, 123.2630, 121.0212, 116.6925, 108.4336. HR-MS (M+H): pred: 333.0474, found: 333.0470.

4-((4-(pyridine-3-yl)thiazol-2-yl)amino)benzenesulfonamide (3q)

Yield: 70%, m.p. 290 °C, IR $\bar{\nu}_{max}$ (cm⁻¹): 3380.7, 3309.18 (N-H), 3225.50 (N-H), 3126.74-2814.21 (Ar C-H). ¹H-NMR (300 MHz, DMSO- d_6 , δ , ppm): 7.24 (2H, s, SO₂NH₂), 7.48 (1H, dd, *J*: 8.01 Hz, 4.79 Hz, Ar), 7.64 (1H, s, thiazole), 7.79-7.87 (4H, m, Ar), 8.11 (1H,

d, *J*: 8.1 Hz, 1.95 Hz, Ar), 8.52-8.54 (1H, m, Ar), 9.17-???? (1H, m, Ar), 10.75 (1H, s, NH). ¹³C-NMR (75 MHz, DMSO- d_6 , δ , ppm): 106.24, 116.75, 124.29, 127.63, 130.44, 133.45, 136.63, 144.13, 147.47, 147.77, 149.00, 163.34. HR-MS (M+H): pred: 333.0474, found: 333.0466.

4-((4-(pyridine-4-yl)thiazol-2-yl)amino)benzenesulfonamide (3r)

Yield: 80%, m.p. 249.5 °C, IR $\bar{\nu}_{max}$ (cm⁻¹): 3332.95, 3299.27 (N-H), 3231.70 (NH), 3174.5-3007.22 (Ar C-H). ¹H-NMR (300 MHz, DMSO- d_6 , δ , ppm): 7.23 (2H, s, SO₂NH₂), 7.80-7.91 (4H, m, Ar), 8.03 (1H, s, thiazole), 8.11 (2H, d, *J*: 6.09 Hz, Ar), 8.73 (2H, d, *J*: 5.60 Hz, py 2,6-H), 10.87 (1H, s, NH). ¹³C-NMR (75 MHz, DMSO- d_6 , δ , ppm): 111.91, 116.91, 121.32, 127.62, 136.87, 143.93, 144.00, 147.42, 147.94. HR-MS (M+H): pred: 333.0474, found: 333.0478.

Antimicrobial activity

Minimum inhibitory concentration assay

Antimicrobial activity test was applied to various gram positive and gram negative bacteria strains including, *E. coli* (ATCC8739), *S. aureus* (ATCC6538), *B. spizizenii* (ATCC6633), *K. pneumoniae* (Clinical isolate), *P. aeruginosa* (ATCC9027), *E. faecalis* (ATCC29212), *S. epidermidis* (ATCC12228), *VRE* (Clinical isolate). These organisms were inoculated to mid-log phase in Muller Hinton Broth (MHB) at 37 °C. Broth microdilution procedure is a more user-friendly method that enables testing of multiple antimicrobial agents. The broth microdilution method was carried out in accordance with the relevant 2018 CLSI standard. Compounds were dissolved in DMSO below 1% concentration and were added to 96-well plates. These compounds were 2-fold serially diluted to make different concentrations, from 0.5 to 256 mM. Bacterial inoculum suspensions were prepared at a final concentration of 1x10⁵ cfu /ml and plates were incubated at 37 °C for 24 hours. Positive or negative controls were set to wells with and without bacteria, respectively. Sulfamethoxazole and chloramphenicol were used as standards. The MIC was determined by visual inspection after the change in turbidity. Experiments were performed in triplicate.

RESULTS AND DISCUSSION

Chemistry

Tested compounds were synthesized successfully by the proposed methods in 60 - 85% yield. NH stretchings were observed above 3.000 cm⁻¹ and C-H stretchings were observed between 2.800-3.100 cm⁻¹ in the IR spectra. All protons matched with the expectations in ¹H-NMR. NH protons for **3a-o** were observed as two separated singlet peaks around $\delta \sim 10.8$ and ~ 11.55 ppm. Supporting the literature information, SO₂NH₂ containing (**3p-r**) molecules NH stretchings were observed at $\delta \sim 10.8$ ppm and the other NH group stretchings observed at $\delta \sim 10.8$ ppm like the rest in the series (Gowda, Jyothi, & D'Souza, 2002; Bařar, Tunca, Bülbül, & Kaya, 2016). The hydrogen on the neighborhood of the pyridine nitrogen was observed approximately δ 8-9 ppm for pyridine/pyrimidine containing molecules as singlet or mixed by aromatic hydrogens as multiplet. Most of the single aromatic hydrogens at thiazole and/or isoxazole rings were observed around δ 8.2 and 6.2 ppm, respectively. Some of them were interfered by other aromatic peaks and observed as multiplet. Methyl groups on **1-3** and **10-12** were observed

around $\delta \sim 2.25$ ppm. In the ^{13}C NMR, methyl-containing compounds gave a $\delta \sim 20$ ppm peak. All other carbons were aromatics, thus were observed between d 120-160 ppm. Finally, HRMS results proved the structures of the molecules.

Antimicrobial activity

Antimicrobial activity of the tested compounds are given in Table 1. Among the series, 6 of the 18 compounds exhibited lower MIC values than 256 $\mu\text{g}/\text{mL}$. The MIC value of **3d**, sulfadiazine-thiazole 2-pyridyle derivative was 64 $\mu\text{g}/\text{mL}$ against *S. aureus*. The other sulfadiazine derivatives (**3e**, **3f**) were also found more active compared to the rest of the series. 3-pyridyle derivative (**3e**), exhibited 128 $\mu\text{g}/\text{mL}$ against *S. aureus* and *E. faecalis*. Compound **3e** also showed 32 $\mu\text{g}/\text{mL}$ against *S.epidermidis*. 4-pyridyle derivative of sulfadiazine (**3f**) exhibited 64 $\mu\text{g}/\text{mL}$ against *S.epidermidis*. Sulfanilamide derivatives (**3p-r**) exhibited 32 and 128 $\mu\text{g}/\text{mL}$ against *B.spizizenii* and *S.aureus*, respectively. Besides, **3q** exhibited 64 $\mu\text{g}/\text{mL}$ against VRE, as the only effective compound against this microorganism. **3r** exhibited 128 $\mu\text{g}/\text{mL}$ against *E.coli* and *Paeruginosa* as the only compound that showed inhibitory activity against gram-negative species along with **3q**. The standard drug sulfamethoxazole showed 4, 32 and 64 $\mu\text{g}/\text{mL}$ against *E.coli*, *Paeruginosa* and *S.aureus*, respectively. The other standard drug chloramphenicol showed 8-16 $\mu\text{g}/\text{mL}$ against all micro-

organisms as a wide spectrum antibiotic. None of the compounds showed inhibitory effect against *K.pneumoniae*, and there was only one compound (**3r**), which showed inhibition against gram-negative bacteria growth. The compounds were derived from two main parts; those which are sulfonamide derivatives and the position of pyridyl substitution. To point this out, 6 compounds seemed to be more effective compared to the rest of the series, and these 6 compounds were sulfanilamide and sulfadiazine derivatives. There was no significant data difference between 2, 3 or 4-pyridyl derivatives of each sulfonamide derivative. Considering these results, it was interpreted that activity was mainly related to the sulfonamide part. Besides, the pyridyl position did not make an important change in inhibition. High inhibitor potential (32 $\mu\text{g}/\text{mL}$) was provided by compound **3p-r**, which supports the SAR feature that an unsubstituted amine group is important for activity in sulfonamide derivatives.

Acknowledgements: Authors declare that there is no conflict of interest for this work.

Peer-review: Externally peer-reviewed.

Author Contributions: Conception/Design of Study- Z.Ş., Ş.D.; Data Acquisition- L.Y., Z.Ş., S.N.B.; Data Analysis/Interpretation- Z.Ş., S.N.B.; Drafting Manuscript- Z.Ş., S.N.B., L.Y.; Critical Revision of Manuscript-

Table 1. Screening for MIC of the compounds 3a-r using microdilution method.

Cpd.	Microorganisms and minimal inhibitory concentration ($\mu\text{g}/\text{mL}$)							
	Gram-Negative Bacteria				Gram-Positive Bacteria			
	<i>E.coli</i>	<i>P.aeruginosa</i>	<i>K.pneumoniae</i>	<i>B.spizizenii</i>	<i>S.aureus</i>	<i>E.faecalis</i>	<i>S.epidermidis</i>	VRE
3a	>256	>256	>256	>256	>256	>256	>256	>256
3b	>256	>256	>256	>256	>256	>256	>256	>256
3c	>256	>256	>256	>256	>256	>256	>256	>256
3d	>256	>256	>256	>256	>64	>256	>128	>256
3e	>256	>256	>256	>256	>128	>128	>32	>256
3f	>256	>256	>256	>256	>256	>256	>64	>256
3g	>256	>256	>256	>256	>256	>256	>256	>256
3h	>256	>256	>256	>256	>256	>256	>256	>256
3i	>256	>256	>256	>256	>256	>256	>256	>256
3j	>256	>256	>256	>256	>256	>256	>256	>256
3k	>256	>256	>256	>256	>256	>256	>256	>256
3l	>256	>256	>256	>256	>256	>256	>256	>256
3m	>256	>256	>256	>256	>256	>256	>256	>256
3n	>256	>256	>256	>256	>256	>256	>256	>256
3o	>256	>256	>256	>256	>256	>256	>256	>256
3p	>256	>256	>256	>32	>128	>256	>256	>256
3q	>256	>256	>256	>32	>128	>256	>256	>64
3r	>128	>128	>256	>32	>128	>256	>256	>128
C	>8	>16	>8	>16	>16	>8	>8	>16
S	>4	>32	>256	>256	>64	>256	>256	>256

C* Chloramphenicol S* Sulfamethoxazole

Z.Ş., Ş.D.; Final Approval and Accountability- Z.Ş., S.N.B., L.Y., Ş.D.; Technical or Material Support- L.Y., Z.Ş., S.N.B.; Supervision- Ş.D., L.Y.

Conflict of Interest: The authors have no conflict of interest to declare.

Financial Disclosure: Authors declared no financial support.

REFERENCES

- Başar, E., Tunca, E., Bülbül, M., & Kaya, M. (2016). Synthesis of novel sulfonamides under mild conditions with effective inhibitory activity against the carbonic anhydrase isoforms I and II. *Journal of Enzyme Inhibition and Medicinal Chemistry*, 31(6), 1356–1361.
- Bengoechea, J. A., & Pessoa, J. S. (2018). Klebsiella pneumoniae infection biology: living to counteract host defences. *FEMS Microbiology Reviews*, 43(2), 123-144.
- Donnenberg, M. S., & Whittam, T. S. (2001). Pathogenesis and evolution of virulence in enteropathogenic and enterohemorrhagic Escherichia coli. *Journal of Clinical Investigation*, 107(5), 539–548.
- Drobniowski, F. A. (1993). Bacillus cereus and related species. *Clinical Microbiology Reviews*, 6(4), 324–338.
- El-Sayed, A., Solimana, M., El-Zahar, I., El-Masry, A. H., Kamel, M., & Gohar, R. S. (2010). Synthesis and anticancer evaluation of novel tetrahydronaphthalen-6-yl thiazole heterocycles against human HePG2 and MCF7 cell lines. *Der Pharma Chemica* 2(5), 507-521.
- Ertas, M., Sahin, Z., Berk, B., Yurttas, L., Biltekin, S. N., & Demirayak, S. (2018). Pyridine-substituted thiazolylphenol derivatives: Synthesis, modeling studies, aromatase inhibition, and antiproliferative activity evaluation. *Archiv der Pharmazie*, 351(3-4), 1700272.
- Gellatly, S. L., & Hancock, R. E. W. (2013). Pseudomonas aeruginosa: new insights into pathogenesis and host defenses. *Pathogens and Disease*, 67(3), 159–173.
- Gowda, B. T., Jyothi, K., & D'Souza, J. D. (2002). Infrared and NMR spectra of arylsulfonamides. *Zeitschrift für Naturforschung A*, 57a, 967-973.
- Hamada, Y. (2018). Role of Pyridines in Medicinal Chemistry and Design of BACE1 Inhibitors Possessing a Pyridine Scaffold. *Pyridine*, doi:10.5772/intechopen.74719.
- Kashyap, S. J., Garg, V. K., Sharma, P. K., Kumar, N., Dudhe, R., & Gupta, J. K. (2011). Thiazoles: having diverse biological activities. *Medicinal Chemistry Research*, 21(8), 2123-2132.
- Russo, T. A., & Marr, C. M. (2019). Hypervirulent Klebsiella pneumoniae. *Clinical Microbiology Reviews*, doi:10.1128/cmr.00001-19.
- Sun, S., Jia, Q., Zenova, A. Y., Chafeev, M., Zhang, Z., Lin, S., & Oballa, R. M. (2014). The discovery of benzenesulfonamide-based potent and selective inhibitors of voltage-gated sodium channel Na v 1.7. *Bioorganic & Medicinal Chemistry Letters*, 24(18), 4397–4401.
- Supuran, C. (2017). Special Issue: Sulfonamides. *Molecules*, 22(10), 1642. doi:10.3390/molecules22101642.

The effects of vanadyl sulfate on glutathione, lipid peroxidation and nonenzymatic glycosylation levels in various tissues in experimental diabetes

Sevim Tunalı¹ , Refiye Yanardağ¹ 

¹Istanbul University-Cerrahpasa, Faculty of Engineering, Department of Chemistry, Istanbul, Turkey

ORCID IDs of the authors: S.T.0000-0003-3363-1290; R.Y. 0000-0003-4185-4363

Cite this article as: Tunalı, S., & Yanardag, R. (2021). The effects of vanadyl sulfate on glutathione, lipid peroxidation and nonenzymatic glycosylation levels in various tissues in experimental diabetes. *Istanbul Journal of Pharmacy*, 51(1), 73-78.

ABSTRACT

Background and Aims: Diabetes mellitus is characterized by hyperglycemia which over time leads to serious damage of several body systems. Vanadium ions and their complexes have been demonstrated to have various insulin-mimetic and antidiabetic effects. The object of the present work was to investigate the effect of vanadyl sulfate (VS) on serum total lipid and protein parameters, glutathione, lipid peroxidation and nonenzymatic glycosylation levels in cardiac, lens, lung and skeletal muscle tissues of STZ diabetic rats.

Methods: Randomly selected 6.0 - 6.5 month old Swiss Albino rats were separated into two diabetic and two control groups. A single intraperitoneal injection of 65 mg/kg streptozotocin (STZ) in 0.01 M citrate buffer (pH 4.5) was used to induce diabetes. 100 mg/kg VS was administered daily to one of the controls and one of the diabetic groups. On the 60th day of the experiment, serum total lipid and total protein levels were determined.

Results: Tissue samples were taken and used for determination of glutathione (GSH), lipid peroxidation (LPO) and nonenzymatic glycosylation (GSH) and protein levels.

Conclusion: According to the results, treatment with VS reversed the effects of diabetes by exerting antioxidant properties and preventing damage caused by diabetes on various tissues along with some serum parameters.

Keywords: Diabetes mellitus, vanadyl sulfate, oxidative stress, cardiac, lens, lung, skeletal muscle

INTRODUCTION

Diabetes mellitus (DM), caused by ineffectiveness or deficiency in the production of insulin by the pancreas, is one of the most serious chronic diseases. The expectations that 366 million people will be diabetic by 2030 shows that this disease is of tremendous importance (Li & Lian, 2016). Two main types of diabetes stand out. Type I diabetes (DM1), in which the beta cells in the pancreas have lost ability to produce the required quantities of insulin and type II diabetes (DM2), also known as non-insulin dependent diabetes mellitus (NIDDM), in which although pancreatic beta cells produce insulin, the secretion is impaired and hyperglycemia and insulin resistance develops (Domingo & Gómez, 2016). Chronic hyperglycemia in DM causes different morphological and functional changes in various tissues (Akgun-Dar, Bolkent, Yanardag, & Tunalı, 2007; Tunalı & Yanardag, 2013; Yilmaz-Ozden et al., 2014). Diabetes, like other metabolic diseases, is associated with the development of oxidative stress and chronic inflammation. The overproduction of reactive oxygen species (ROS) in cells and tissues, is the result of the release of free radicals caused by the disruption of the oxidative and antioxidative balance. Dysfunctions in insulin secretion which occur in diabetes are closely related

Address for Correspondence:

Sevim TUNALI, e-mail: stunalı@istanbul.edu.tr

Submitted: 10.04.2020
Revision Requested: 16.05.2020
Last Revision Received: 27.06.2020
Accepted: 03.07.2020

This work is licensed under a Creative Commons Attribution 4.0 International License.



with chronic oxidative stress and impaired signaling pathways and metabolism. This leads to decreased inflammation and immunity. Therefore, insulin resistance contributes primarily to the development of diabetes and cardiovascular diseases (Newsholme, Cruzat, Keane, Carlessi, & Bittencourt, 2016).

Vanadium is an important transition element in the fifth group of the periodic system and found in many organisms and mammalian tissues (Pal, Mani, Tripathi, & Datt, 2018). The insulin mimetic effect of vanadium salts was first discovered in the second half of the 20th century. According to the recommendation, vanadium salts and various vanadium compounds can replace insulin injections by administering orally at the appropriate dose in patients with DM (Heyliger, Tahiliani, & McNeill, 1985). This has led to the development of various vanadium-based compounds and a new field of research in the treatment of diabetes (Irving & Stoker, 2017).

The purpose of our study was to research the antidiabetic properties of VS on total lipid parameters and total protein levels of normal and STZ diabetic rats. Also, this study explored the effect of VS on glutathione, lipid peroxidation and nonenzymatic glycosylation levels on the cardiac, lens, lung and skeletal muscle tissues of STZ diabetic rats.

MATERIALS AND METHODS

Animals

6.0 - 6.5 month old male Swiss Albino rats were examined in this research. The experiments were examined and confirmed by the Local Institute's Animal Care and Use Committees of Istanbul University. All animals were healthy and fed with the experimental animal pulp and tap water.

Experimental diabetic model design

The animals were made diabetic with a single dose of streptozotocin (STZ) (65 mg/kg) dissolved in a freshly prepared citrate buffer solution (0.01 M pH=4.5) intraperitoneally (Jound, Lambert, Stauffacher, & Renold, 1969). Four groups were randomly created; group I untreated, nondiabetic controls (n=13); group II nondiabetic control animals administered VS (n=5); group III diabetically induced animals with STZ (n=11); group IV STZ-induced diabetic animals administered with VS (n=11). VS was administered at a dose of 100 mg/kg/day for 60 days without interruption by gavage technique.

Biochemical study and oxidative stress markers

After STZ injection, all tail vein blood samples were regularly collected from the rats on 0, 1, 30 and 60 days (Bolkent, Bolkent, Yanardag, & Tunali, 2005). Fasting blood glucose concentration above 200 mg/dL was considered diabetic. On the 60th day of the experiment, the animals were fasted overnight and then anesthetically sacrificed. Blood and tissue samples were taken from all groups. Blood samples were centrifuged to obtain serum for total lipid levels and protein contents were determined by the method of Frings, Fendley, Dunn, & Queen, (1972) and the method of Lowry, Rosebrough, Farr, & Randal, (1951) respectively. Cardiac, lens, lung, and skeletal muscle tissues were removed and frozen until the working day. The tissues were homogenized with a glass homogenizer in cold

0.9 % saline to make up 10% (w/v) homogenate. After centrifugation, the clear upper phase was used for determination of glutathione (GSH), lipid peroxidation (LPO), nonenzymatic glycosylation (NEG) and total protein levels by the methods of Ledwozyw, Michalak, Stepien, & Kadziolka, (1986), Beutler (1975), Parker, England, Casto, Hessel, & Goldstein, (1981) and Lowry et al., (1951) respectively.

Statistical analysis

The unpaired t test and analysis of variance (ANOVA) were used to analyze biochemical results calculated with a statistical computer package (NCSS). The results were performed as mean±SD. P<0.05 values were accepted as significant.

RESULTS

Considerable differences in serum total lipids levels and serum total protein contents were observed as shown in Table 1. Serum total lipids levels were significantly higher in diabetic groups when compared to the control group (P<0.0001). Oral administration of VS considerably decreased serum total lipids levels in the diabetic rats (P<0.0001). Serum total protein levels were lower in diabetic groups in comparison with non treated controls (P<0.0001). Oral VS application elevated the serum total protein levels in diabetic rats (P<0.005).

Table 1. Mean levels of serum lipids and protein for all groups*.

Groups	Total Lipid (% mg)	Total Protein (% mg)
Control	180.35±17.85	5.15±0.61
Control + VS	207.74±20.63	5.41±0.34
Diabetic	309.19±38.18 ^a	3.81±0.38 ^c
Diabetic + VS	210.28±40.52 ^b	4.68±0.32 ^d
P _{ANOVA}	0.0001	0.0001
*Mean ± SD; ^a P<0.0001 comparing to control group; ^b P<0.0001 comparing to diabetic group; ^c P<0.0001 comparing to control group; ^d P<0.005 comparing to diabetic group.		

Cardiac tissue

Figure 1 shows the effect of VS on GSH level of cardiac tissue. Cardiac tissue GSH level in the diabetic group was significantly decreased compared to the control group (^aP<0.05). Administration of VS caused a significant increase in GSH levels in the diabetic group (^bP<0.005).

The mean levels of LPO and NEG parameters are shown in Figures 2 and 3, respectively. There were remarkable increases in LPO and NEG levels in the STZ induced animals compared to untreated rats (^aP<0.005, ^aP<0.005). It was observed that administration of VS significantly decreased both LPO and NEG levels in diabetic rats (^bP<0.05, ^bP<0.05).

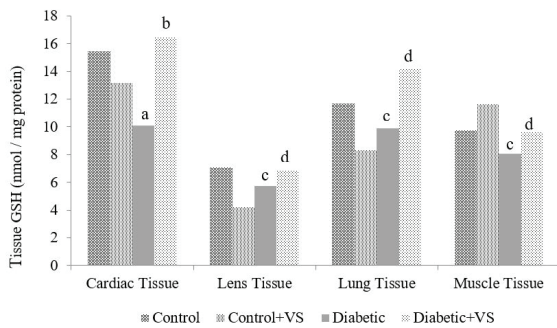


Figure 1. Effects of vanadyl sulfate on GSH levels of cardiac, lens, lung and muscle tissues for all groups. ^a*P*<0.05 comparing to control group; ^b*P*<0.005 comparing to diabetic group; ^c*P*<0.0001 comparing to control group; ^d*P*<0.0001 comparing to diabetic group.

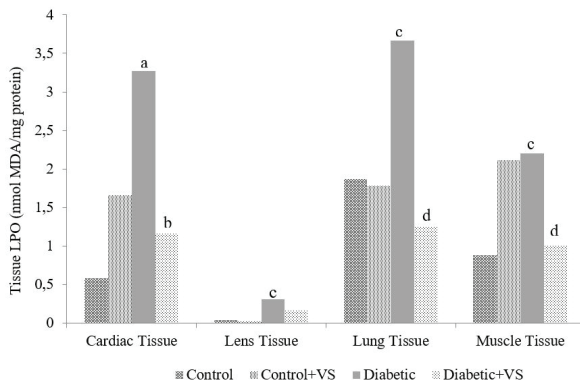


Figure 2. Effects of vanadyl sulfate on LPO levels of cardiac, lens, lung and muscle tissues for all groups. ^a*P*<0.005 comparing to control group; ^b*P*<0.05 comparing to diabetic group; ^c*P*<0.0001 comparing to control group; ^d*P*<0.0001 comparing to diabetic group.

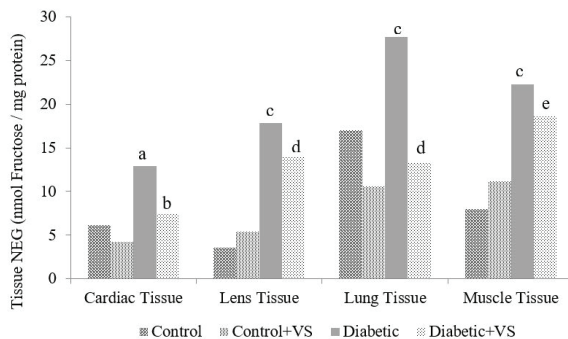


Figure 3. Effects of vanadyl sulfate on NEG levels of cardiac, lens, lung and muscle tissues for all groups. ^a*P*<0.005 comparing to control group; ^b*P*<0.05 comparing to diabetic group; ^c*P*<0.0001 comparing to control group; ^d*P*<0.0001 comparing to diabetic group; ^e*P*<0.001 comparing to diabetic group.

Lens tissue

The GSH levels of lens tissue for all groups are also given in Figure 1. The GSH was significantly lowered in diabetic groups when compared to controls (*P*<0.0001). The administration of VS to the diabetic groups increased the lens GSH levels (*P*<0.0001). Lens LPO levels in the diabetic group was significantly increased (*P*<0.0001). On the other hand, there was no significant decrease in LPO levels in the VS given diabetic group compared to the diabetic rats (Figure 2). The NEG level was

significantly increased in diabetic groups when compared to controls (*P*<0.0001). Oral administration of VS significantly decreased the level of NEG in the diabetic lens tissue (*P*<0.0001).

Lung tissue

The mean lung tissue GSH levels for all four groups are given in Figure 1. The lung GSH levels were significantly reduced in diabetic animals when compared to controls (*P*<0.0001). Oral application of VS significantly increased the GSH level on the 60 day. (*P*<0.0001). This situation is opposite for lung LPO and NEG levels as seen in Figure 2 and Figure 3. There was a significant increase in LPO and NEG values in the diabetic group compared to the control group (*P*<0.0001; *P*<0.0001). Upon the administration of VS to the diabetic group, both LPO and NEG values decreased in the VS treated diabetic rats (*P*<0.0001, *P*<0.0001).

Skeletal muscle tissue

As seen in Figure 1, a meaningful decrease in the muscle tissue GSH levels was seen in STZ-induced diabetic animals when compared to controls (*P*<0.0001). Administration of VS to diabetic rats restored the elevated GSH level in muscle tissue (*P*<0.0001). As shown in Figures 2 and 3, muscle LPO and NEG levels increased in the diabetic groups compared to that of the control groups (*P*<0.0001, *P*<0.0001).

Oral vanadium solution caused decreased LPO and NEG levels in diabetic rats (*P*<0.0001, *P*<0.001).

DISCUSSION

DM is a major risk factor for cardiovascular, corneal, respiratory and skeletal muscle diseases. Oxidative stress is known to precipitate the improvement of diabetes and its pathological events (Hajarnavis & Bulakh, 2019). Increased oxidative injury impairs the enzymatic defense system against reactive oxygen species. This is evidenced by the significant decrease of various antioxidant parameters in experimental diabetic models of various tissues.

According to the oxidative stress hypothesis, chronic complications of diabetes leads to the imbalance between antioxidant defense capacity and the rate of formation of reactive oxygen species and free radicals. In other words, hyperglycemia induces oxidative stress (Cayir et al., 2015).

Vanadium helps the antioxidant system by restoring oxidative conditions and inhibiting lipid peroxidation. This improved oxidative status is a result of reduced superoxide, hydroxyl radicals and free radicals and intracellular reactive oxygen spaces by vanadium ions. Vanadium also has the capability to restore insulin susceptibility in different types of diabetes (Tariq et al., 2020). In our previous studies, it was reported that VS and oxovanadium (IV) complex based on S-methylthiosemicarbazone have protective effects on pancreatic islet β cells via insulin-mimetic activity (Bolkent, Bolkent, Yanardağ, & Tunali, 2005; Yanardağ et al., 2009). In the light of these findings, this study was aimed to investigate the effects of VS on a large increase in oxidative stress of different tissues and serum parameters in diabetic rats.

The lipid profile and protein degradation of diabetic patients is changed strongly compared to non diabetics. The changes in cholesterol and triglyceride levels partially cause increase in the levels of atherosclerotic disease and myocardial infarction in diabetic individuals. Our data shows that diabetic oxidative injury increased serum total lipid and total protein levels in the diabetic group. The antidiabetic effects of vanadium via oral administration in rats lowered these parameters. The present finding is in agreement with previous studies which involved long term vanadate treatments in diabetic animals. According to these studies, vanadium treatment improved various serum lipid parameters along with its antidiabetic properties (Sekar & Govindasamy, 1991; Gupta, Raju, Prakash, & Baquer, 1999; Ding et al., 2001).

Diabetes is the main reason of cardiovascular morbidity and mortality. Today, it is known that the risk of heart failure increases in diabetic patients even if there is an improvement in coronary artery disease and hypertension (El Hadi, Vettor, & Rossato, 2019). The increases of ROS generation and even their accumulation, plays a crucial role in cardiomyocyte apoptosis (Cai et al., 2002). This causes antioxidant defense systems such as GSH - a major intracellular antioxidant that plays a key role in reducing the effects of oxidative stress - to be depleted in the atrium of diabetic hearts (Townsend, Tew, & Tapiero, 2003; Lutchmansingh et al., 2018). Cayir et al. (2015) demonstrated that there is a significant reduction in GSH level in diabetes related pulmonary injury. According to Yang et al. (2020), GSH level is an important indicator of antioxidant capacity, and GSH level in the lens tissue of four week STZ induced diabetic rats decreased. In our research, all tissues of the hyperglycemic group showed significantly decreased GSH levels when compared to control groups. In response to oral administration of VS, a positive role of VS to the antioxidant system by increasing GSH level was observed in all tissues. The ameliorative effects of vanadium against oxidative stress may be due to its influential power on cellular GSH level and up regulated mRNA. Protein expression of a catabolytic subunit of glutamate cysteine ligase is directly related to the synthesis of this tripeptide (Kim et al., 2011).

Diabetes induces disturbances of lipid profiles, especially an increased susceptibility to lipid peroxidation, which is responsible for major complication in various tissues of DM (Lu, 1999; Akgun-Dar, Bolkent, Yanardag, & Tunali, 2007; Tunali & Yanardag, 2013). In chronic diseases, such as DM2 and its complications, there is usually excessive formation of MDA (Rehman & Akash, 2017). Djelić et al. (2019) reported that lipid peroxidation may also be an important mediator of DNA damage related to oxidative stress caused by reactions of adrenaline and a higher level of glucose. In human cortical and nuclear cataract, MDA has been found to increase by 3.5 and 2.5 times respectively than the normal levels (Anderson, Rapp, & Wiegand, 1984; Griesmacher et al., 1995). Lung and muscle are also target organs in patients with either type 1 or type 2 DM (Li, Song, Wang, Meng, & Cui, 2018). Previous studies have indicated that diabetic hyperglycemia damages the respiratory system causing physiological and structural pulmonary alterations (Messner, Lundberg, & Wikström, 2003; Dennis et al.,

2010), and restrictive ventilatory dysfunction helps to facilitate the development of type 2 DM (Kim, Zhang, Kang, You, & Hyun, 2015). Szkudelska et al. (2019) demonstrated that accumulated lipid levels in Goto-Kakizaki diabetic rats significantly increased when compared to control rats. This was due to insulin dependent glucose uptake by skeletal muscles in physiological conditions. Moreover, insulin resistance in the skeletal muscle is thought to be the main failure in DM2, whereas reduced lipid accumulation in this tissue, with a concomitant improvement of intramuscular glucose carriage, shows a favorable effect on whole body glucose metabolism (Szkudelska et al., 2019).

In the present study, a significant difference was observed when the MDA (the final products of lipid peroxidation) levels of the groups were compared; MDA levels were higher in the diabetic groups of all studied tissues than in the control groups. This shows that MDA level is a priority marker of diabetic inflammatory and oxidative damage response. It decreased upon administration of VS and that suppressed inflammation and oxidative damage. The reversion of this process after treatment with VS is likely due to reduction in damage resulting from the oxidative stress demonstrated by cardiac, lens, lung and skeletal muscle lipid peroxidation.

Advanced glycation end products (AGEs) pathway is one of the four important pathways associated with chronic complications of DM (Naso et al., 2010). Formation of AGEs as a result of NEG, is a nonenzymatic reaction between the carbonyl group of reducing sugars and the free amino residues of proteins, lipids, or nucleic acids (Singh, Barden, Mori, & Beilin, 2001). These products are also complex heterogeneous compounds with fluorescent and non-fluorescent characters such as N ϵ -carboxymethyl lysine, N ϵ -carboxyethyl lysine, pentoside, argpyrimidine, glyoxal lysine dimer and methyl glyoxal lysine dimer (Bohlin et al., 2013; Lavelli, Sri Harsha, Ferranti, Scarafoni, & lametti, 2016; Chen et al., 2019). In our study, a significant alteration of cardiac, lens, lung and skeletal muscle tissues NEG levels were observed in diabetic rats. This is also an indicator of the oxidative stress damage caused by diabetes on these tissues. In the diabetic lens tissue, AGEs induces higher cross-linking of corneal collagen fibrils and proteoglycans thereby resulting in the development of cataract (Bao et al., 2017; Hajarnavis & Bulakh, 2019). Although lung tissue has evolved several mechanisms to attenuate oxidative stress (Otoupalova, Smith, Cheng, & Thannickal, 2020), they are the most affected in higher hyperglycemic conditions and uniquely exposed to a highly oxidizing environment. Abnormal glucose metabolism causes the production of AGEs which are primarily related with increased NEG level in this tissue. The increased NEG levels in cardiac and skeletal muscle tissues in diabetic rats are another important event for progression of DM pathogenesis. Crosslinking involving elastin and collagen can cause impaired relaxation and increased stiffness in myocardial and skeletal muscle tissues (Lee & Kim, 2017). In the present study, VS suppressed NEG levels of all the studied tissues in the diabetic group by acting as an antioxidant and effective insulin mimetic agent. These effects of vanadium sulfate on diabetic rats are in agreement with our previous studies (Tunali & Yanardag, 2006; Yanardag & Tunali, 2006).

CONCLUSION

Diabetic experimental animal models exhibit abrupt generation of free radical and oxidative stress due to persistent chronic hyperglycemia. The current study demonstrated that VS may exert potent protective functions against oxidative damage in tissues of STZ-induced diabetic rats with associated biochemical alterations. It was also observed that treatment with VS significantly restored some oxidative stress parameters and can be used as a more efficacious antioxidant and antidiabetic agent by suppressing the oxidative stress in oxidatively damaged diabetic rat tissues.

Peer-review: Externally peer-reviewed.

Author Contributions: Conception/Design of Study- S.T., R.Y.; Data Acquisition- S.T., R.Y.; Data Analysis/Interpretation- S.T., R.Y.; Drafting Manuscript- S.T., R.Y.; Critical Revision of Manuscript- S.T., R.Y.; Final Approval and Accountability- S.T., R.Y.

Conflict of Interest: The authors have no conflict of interest to declare.

Financial Disclosure: The Scientific Research Projects Coordination Unit of Istanbul University (Project number: T-936/06112000) supported this work.

REFERENCES

- Akgun-Dar, K., Bolkent, S., Yanardag, R., & Tunali, S. (2007). Vanadyl sulfate protects against streptozotocin-induced morphological and biochemical changes in rat aorta. *Cell Biochemistry & Function*, 25, 603-609.
- Anderson, R. E., Rapp, L. M., & Wiegand, R. D. (1984). Lipid peroxidation and retinal degeneration. *Current Eye Research*, 3, 223-227.
- Bao, F. J., Deng, M. L., Zheng, X. B., Li, N. A., Zhao, Y. P., Cao, S. Y., A., Wang, Q. M., Huang, J. H., & Elsheikh, A. (2017). Effects of diabetes mellitus on biomechanical properties of the rabbit cornea. *Experimental Eye Research*, 161, 82-88.
- Beutler, E. (1975). Glutathione in red blood cell metabolism; In A manual of biochemical methods, 2nd ed. Grune and Stratton, New York, pp. 112-114.
- Bohlin, C., Praestgaard, E., Baumann, M. J., Borch, K., Praestgaard, J., Monrad, R. N., & Westh, P. (2013). A comparative study of hydrolysis and transglycosylation activities of fungal α -glucosidases. *Applied Microbiology and Biotechnology*, 97, 159-169.
- Bolkent, S., Bolkent, S., Yanardag, R., & Tunali, S. (2005). Protective effect of vanadyl sulfate on the pancreas of streptozotocin-induced diabetic rats. *Diabetes Research and Clinical Practice*, 70, 103-109.
- Cai, L., Li, W., Wang, G., Guo, L., Jiang, Y., & Kang, Y. J. (2002). Hyperglycemia-induced apoptosis in mouse myocardium: mitochondrial cytochrome C-mediated caspase-3 activation pathway. *Diabetes*, 51, 1938-1948.
- Cayir, A., Ugan, R. A., Albayrak, A. D., Kose, E., Akpinar, Y., Cayir, H. T., Atmaca, Bayraktutan Z., & Kara M. (2015). The lung endothelin system: a potent therapeutic target with bosentan for the amelioration of lung alterations in a rat model of diabetes mellitus. *Journal of Endocrinological Investigation*, 38, 987-998.
- Chen, Y., Tanga, S., Chend, Y., Zhang, R., Zhou, M., Wang, C., Fenga, N., & Wu, Q. (2019). Structure-activity relationship of pro-cyanidins on advanced glycation end products formation and corresponding mechanisms. *Food Chemistry*, 279, 679-687.
- Dennis, R. J., Maldonado, D., Rojas, M. X., Aschner, P., Rondón, M., Charry, L., & Casas, A. (2010). Inadequate glucose control in type 2 diabetes is associated with impaired lung function and systemic inflammation: a cross-sectional study. *BioMed Central*, 10, 38.
- Djelić, N., Radaković, M., Borozan, S., Dimirijević-Srećković, V., Pajović, N., Vejnović, B., Borozan, N., Bankoglu, E. E., Stopper, H., & Stanimirović, Z. (2019). Oxidative stress and DNA damage in peripheral blood mononuclear cells from normal, obese, prediabetic and diabetic persons exposed to adrenaline in vitro. *Mutation Research - Genetic Toxicology and Environmental Mutagenesis*, 843, 81-89.
- Ding, W., Hasegawa, T., Hosaka, H., Peng, D., Takahashi, K., & Seko, Y. (2001). Effect of long-term treatment with vanadate in drinking water on KK mice with genetic non-insulin-dependent diabetes mellitus. *Biological Trace Element Research*, 80, 159-174.
- Domingo, J. L., & Gómez, M. (2016). Vanadium compounds for the treatment of human diabetes mellitus: A scientific curiosity? A review of thirty years of research. *Food and Chemical Toxicology*, 95, 137-141.
- El Hadi, H., Vettor R., & Rossato, M. (2019). Cardiomyocyte mitochondrial dysfunction in diabetes and its contribution in cardiac arrhythmogenesis. *Mitochondrion*, 46, 6-14.
- Frings, C. S., Fendley, T. W., Dunn, R. T. & Queen C. A. (1972). Improved determination of total serum lipids by the sulfo-phosphovanillin reaction. *Clinical Chemistry*, 18, 673-674.
- Griesmacher, A., Kindhauser, M., Andert, S. E., Schreiner, W., Toma, C., Knoebl, P., Pietschmann, P., Prager, R., Schnack, C., Schemthaler, G., & Mueller, M. M. (1995). Enhanced serum levels of thiobarbituric-acid-reactive substances in diabetes mellitus. *The American Journal of Medicine*, 98, 469-475.
- Gupta, D., Raju, J., Prakash, J., & Baquer, N. Z. (1999). Change in the lipid profile, lipogenic and related enzymes in the livers of experimental diabetic rats: effect of insulin and vanadate. *Diabetes Research and Clinical Practice*, 46, 1-7.
- Hajrnavis A. M., & Bulakh P. M. (2019). Anticataract effects of S. cumini and A. marmelos on goat lenses in an experimental diabetic cataract model, *Journal of Ayurveda and Integrative Medicine*, <https://doi.org/10.1016/j.jaim.2019.08.001>.
- Heyliger, C. E., Tahiliani, A. G., & McNeill, J. H. (1985). Effect of vanadate on elevated blood glucose and depressed cardiac performance of diabetic rats. *Science*, 227, 1474-1477.
- Irving E., & Stoker A. W. (2017). Vanadium compounds as PTP inhibitors. *Molecules*, 22, 2269.
- Jound, A., Lambert, E., Stauffacher, W., & Renold, A. E. (1969). Diabetogenic action of streptozotocin. Relationship of dose to metabolic response. *Journal of Clinical Investigation*, 48, 2129-2139.
- Kim, A. D., Zhang, R., Kang, K. A., You, H. J., & Hyun, J. W. (2011). Increased glutathione synthesis following Nrf2 activation by vanadyl sulfate in human Chang liver cells. *International Journal of Molecular Sciences*, 12, 8878-8894.
- Kim, C. H., Kim, H. K., Kim, E. H., Bae, S. J., Jung, Y. J., Choi, J., & Park, J. Y. (2015). Association of restrictive ventilatory dysfunction with the development of prediabetes and type 2 diabetes in Koreans. *Acta Diabetologica*, 52, 357-363.
- Lavelli, V., Sri Harsha, P. S. C., Ferranti, P., Scarafoni, A., & Iametti, S. (2016). Grape skin phenolics as inhibitors of mammalian α -glucosidase and α -amylase effect of food matrix and processing on efficacy. *Food & Function*, 7, 1655-1663.
- Ledwozyw, A., Michalak, J., Stepien, A., & Kadziolka, A. (1986). The relationship between plasma triglycerides, cholesterol, total lipids and lipid peroxidation products during human atherosclerosis. *Clinica Chimica Acta*, 155, 275-283.
- Lee, W. S., & Kim, J. (2017). Diabetic cardiomyopathy: where we are and where we are going. *The Korean Journal of Internal Medicine*, 32, 404-421.

- Li, D., Song, L. L., Wang, J., Meng, C. & Cui, X. G. (2018). Adiponectin protects against lung ischemia-reperfusion injury in rats with type 2 diabetes mellitus. *Molecular Medicine Reports*, 17, 7191-7201.
- Li, J., & Lian, H. (2016). Recent development of single preparations and fixed-dose combination tablets for the treatment of non-insulin-dependent diabetes mellitus. *Archives of Pharmacological Research*, 39, 731–746.
- Lowry, O. H., Rosebrough, W. I., Farr, A. L., & Randal R. J. (1951). Protein measurement with the folin phenol reagent. *Journal of Biological Chemistry*, 193, 265–275.
- Lu, S. C. (1999). Regulation of hepatic glutathione synthesis: current concepts and controversies. *Federation of American Societies for Experimental Biology Journal*, 13, 1169-1183.
- Lutchmansingh, F. K., Hsu J. W., Bennett, F. I., Badaloo, A. V., McFarlane-Anderson, N., Gordon-Strachan, G. M., Wright- Pascoe R. A., Jahoor, F., & Boyne M. S. (2018). Glutathione metabolism in type 2 diabetes and its relationship with microvascular complications and glycemia. *Public Library of Science One*, 13, e0198626.
- Messner, T., Lundberg, V., & Wikström, B. (2003). The Arctic Oscillation and incidence of acute myocardial infarction. *Journal of Internal Medicine*, 253, 666-670.
- Naso, F. C., Mello, R. N., Bona, S., Dias, A. S., Porawski, M., Ferraz, A. B. F., Richter, M. F. R., & Marroni N. P. (2010). Effect of *Agaricus blazei* Murill on the pulmonary tissue of animals with streptozotocin-induced diabetes. *Experimental Diabetes Research*, 2010, <https://doi.org/10.1155/2010/543926>.
- Newsholme, P., Cruzat, V.F., Keane, K.N., Carlessi R., & Bittencourt, P.I.H. (2016). Molecular mechanisms of ROS production and oxidative stress in diabetes. *Biochemical Journal*, 473, 4527–4550.
- Otoupalova, E., Smith, S., Cheng, G., & Thannickal, V. (2020). Oxidative stress in pulmonary fibrosis. *Comprehensive Physiology*, 10, 509-547.
- Pal, R.P., Mani, V., Tripathi, D., & Datt, C. (2018). Inorganic vanadium supplementation in crossbred calves: effects on antioxidant status, immune response and haemato-biochemical attributes. *Biological Trace Element Research*, 186, 154-161.
- Parker, K.M., England, J.D., Casto, J.D., Hessel, R., & Goldstein, P.E. (1981). Improved colorimetric assay for glycosylated hemoglobin. *Clinical Chemistry*, 27, 669–672.
- Rehman, K., & Akash, M. S. H. (2017). Mechanism of generation of oxidative stress and pathophysiology of type 2 diabetes mellitus: How are they interlinked? *The Journal of Cellular Biochemistry*, 118, 3577-3585.
- Sekar, N., & Govindasamy, S. (1991). Effects of vanadate on plasma lipoprotein profiles in experimental diabetic rats. *International Journal of Biochemistry*, 23, 935-940.
- Singh, R., Barden, A., Mori, T., & Beilin, L. (2001). Advanced glycation end products: a review. *Diabetologia*, 44, 129-146.
- Szkudelska, K., Deniziak, M., Hertig, I., Wojciechowicz, T., Tyczewska, M., Jaroszevska, M., & Szkudelski, T. (2019). Effects of resveratrol in goto-kakizaki rat, a model of type 2 diabetes. *Nutrients*, 11, 2488.
- Tariq H., Sharma, A., Sarkar, S., Ojha, L., Pal R. P., & Mani V. (2020). Perspectives for rare earth elements as feed additive in livestock — A review. *Asian-Australas The Journal of Animal Science*, 33, 373-381.
- Townsend, D. M., Tew, K. D., & Tapiero, H. (2003). The importance of glutathione in human disease. *Biomedicine & Pharmacotherapy*, 57, 145-155.
- Tunali, S., & Yanardag, R. (2006). Effect of vanadyl sulfate on the status of lipid parameters and on stomach and spleen tissues of streptozotocin-induced diabetic rats. *Pharmacological Research*, 53, 271-277
- Tunali, S., & Yanardag, R. (2013). Protective effect of vanadyl sulfate on skin injury in streptozotocin-induced diabetic rats. *Human and Experimental Toxicology*, 32, 1206-1212.
- Yanardag, R., & Tunali, S. (2006). Vanadyl sulfate administration protects the streptozotocin-induced oxidative damage to brain tissue in rats. *Molecular and Cellular Biochemistry*, 286, 153-159.
- Yanardag, R., Demirci, T.B., Ulküseven, B., Bolkent, S., Tunali, S., & Bolkent, S. (2009). Synthesis, characterization and antidiabetic properties of N(1)-2,4-dihydroxybenzylidene-N(4)-2-hydroxybenzylidene-S-methyl-thiosemicarbazidato-oxovanadium(IV). *European Journal of Medicinal Chemistry*, 44, 818–826.
- Yang, J. F., Gong, X., Bakh, N.A., Carr, K., Phillips, N.F.B., Ismail-Beigi, F., Weiss, M. A., & Strano, M. S. (2020). Connecting rodent and human pharmacokinetic models for the design and translation of glucose-responsive insulin. *Diabetes*, doi: 10.2337/db19-0879.
- Yilmaz-Ozden, T., Kurt-Sirin, O., Tunali, S., Akev, N., Can. A., & Yanardag, R. (2014). Ameliorative effect of vanadium on oxidative stress in stomach tissue of diabetic rats. *Bosnian Journal of Basic Medical Sciences*, 14, 105-109.

Short-term adaptive metabolic response of *Escherichia coli* to ciprofloxacin exposure

Engin Koçak¹ , Ceren Özkul² ¹Hacettepe University, Faculty of Pharmacy, Department of Analytical Chemistry, Ankara, Turkey²Hacettepe University, Faculty of Pharmacy, Department of Pharmaceutical Microbiology, Ankara, Turkey**ORCID IDs of the authors:** E.K. 0000-0002-1076-1300; C.Ö. 0000-0002-0921-5863**Cite this article as:** Kocak, E., & Ozkul, C. (2021). Short-term adaptive metabolic response of *Escherichia coli* to ciprofloxacin exposure. *Istanbul Journal of Pharmacy*, 51(1), 79-84.

ABSTRACT

Background and Aims: Antibiotic resistance is one of the most critical global health problems. Understanding the pathogen-antibiotic relationship at molecular level could lead to the discovery of new routes to overcome antibiotic resistance. In our present work, we evaluated early responses of *E. coli* against ciprofloxacin within 30 min by analyzing metabolome structure. Our main goal was to understand the initial steps of the adaptation and resistance process of pathogens under antibiotic stress.

Methods: Metabolomics analysis was performed by processing GC/MS and followed with the MS-DIAL metabolomics platform. In addition, Metaboanalyst 4.0 and the KEGG database were used for statistical and pathway analysis.

Results: In total, 207 metabolites were identified while 47 metabolites were significantly different under ciprofloxacin stress condition. Pathway analysis showed that amino acid, fatty acid, and aminoacyl-tRNA metabolisms were altered as an effect of ciprofloxacin at 30 min.

Conclusion: Our results suggest that the understanding of bacterial metabolism in early phase bacterial responses to antibiotics could be key to reducing the adaptation and resistance process.

Keywords: Metabolomics, GC/MS, ciprofloxacin, *E. coli*

INTRODUCTION

Antibiotic resistance is a global problem causing high morbidity and mortality rates. Increasing use and the inappropriate use of antibiotics are the major causes of antibiotic resistance (Ventola, 2015). There is an increasing effort to overcome the antibiotic resistance problem worldwide. However, classical antibiotic discovery approaches are not sufficient for this growing problem (Mills, 2006; Moloney, 2016). In recent years, researchers have focused on the antibiotic-bacteria relationship by using the omics approach to understand the mode of action of antimicrobial agents and the adaptation and resistance mechanisms of pathogens. This new approach has offered great opportunities in finding new routes to overcome antibiotic resistance. However, there is a long way ahead of us. Genomics, transcriptomics, proteomics, and metabolomics have drawn attention toward analyzing the cellular process at a molecular level. Metabolites are side or byproducts of biological reactions. A metabolome structure contains thousands of metabolites and is relatively dynamic when compared to a proteome structure. Metabolomics is the analysis of metabolome structures and has been used intensively for many biological systems. In microbiology, metabolomics techniques have gained popularity in analyzing cellular processes in experimental and clinical studies. It has been used to explain phenotypic resistances and adaptation processes (Pulido, Garcia-Quintanilla, Gil-Marques, & McConnell, 2016; Vranakis et al., 2014).

Address for Correspondence:

Engin KOÇAK, e-mail: kengin@hacettepe.edu.tr

Submitted: 31.08.2020

Revision Requested: 14.10.2020

Last Revision Received: 30.12.2020

Accepted: 31.12.2020

This work is licensed under a Creative Commons Attribution 4.0 International License.



Ciprofloxacin, which is a member of the fluoroquinolone group, has been used to treat urinary tract infections, including acute uncomplicated pyelonephritis (Irvani et al., 1995; Talan et al., 2004; Talan, Naber, Palou, & Elkharrat, 2004). In recent years, fluoroquinolone resistance has become a clinical problem as also encountered in many other antibiotic groups (Hooper & Jacoby, 2015; Piddock, 1998). Omics-based techniques have been used to understand fluoroquinolone resistance with various bacterial strains, mainly focusing on *E. coli* as a model microorganism. Li et al. analyzed the effect of ciprofloxacin on *E. coli* with proteomics and metabolomics analysis. They explored the middle-phase effect on metabolome within 3 hours (Li et al., 2018). Machuca et al. (2017) used transcriptomics analysis to observe the cellular response of *E. coli* to ciprofloxacin in a very early phase. In addition, other members of the fluoroquinolone group have been investigated by omics techniques focusing on bacterial response in different growth stages (Erickson, Otoupal, & Chatterjee, 2017; Lata et al., 2015).

Early-phase antibiotic response (within 0-1 hour) has recently become a promising approach in microbial-omics studies. This analysis could allow the observation of initial regulatory pathways of the adaptation process. Zampieri, Zimmermann, Claassen, & Sauer (2017) have recently used this approach for *E. coli* by using various antibiotics.

In our present work, we focused on the initial metabolic response (30 min) of *E. coli* against ciprofloxacin stress. We used a gas chromatography/mass spectroscopy (GC/MS) based metabolomics approach and evaluated altered pathways in early metabolic perturbation. We believe that our findings will contribute to the current literature in order to further understand the antibiotic-pathogen relationship in early phases.

MATERIAL AND METHODS

Bacterial culture and sample preparation

The standard bacterial strain used in this study was *E. coli* ATCC 25922. Overnight fresh cultures on Nutrient Agar were used for the experiments. The exact minimum inhibitory concentration of ciprofloxacin was determined by using the broth micro dilution method according to the Clinical Laboratory Standards Institute (CLSI) guidelines (CLSI, 2015). For metabolomics experiments, a sub-inhibitory concentration (MIC/2) of ciprofloxacin was used.

In order to determine growth rate of *E. coli* in our experimental conditions, a growth curve was constructed by plotting OD₆₀₀ nm values to time. Thus, we confirmed our sampling point.

A single colony was picked from fresh cultures and inoculated into 20 mL of nutrient broth (NB), incubated overnight. Late-stationary phase cells (OD₆₀₀=2.6) were then sub-cultured with or without a MIC/2 concentration of ciprofloxacin in 20 mL NB and incubated at 37°C for 30 min, which corresponds to late lag phase, in order to evaluate the initial adaptation of bacterial cells to antibiotic stress. The cultures were immediately centrifuged after the incubation period at 5000 g, 4°C for 10 min, followed by a washing step with phosphate buffered saline (PBS) 3 times. The pellet was re-suspended in PBS, and

cells were disrupted using a lysis buffer containing lysozyme in order to extract intracellular metabolites from cells.

Extraction of metabolites

In the extraction method, a methanol:water (9:1 v:v) co-solvent system was used to isolate metabolites from other biomolecules. A total of 1 mL of co-solvent was added to cell lysates, and they were incubated for 2 hours at 4°C. The mixtures were centrifuged 15000 g for 10 min at 4°C. Proteins were gathered at the bottom of the tube. Metabolites were taken, and the co-solvent was evaporated in a vacuum centrifuge. In the first step of derivation, 20 µL of a methoxyamine solution in pyridine (20 mg/mL) (Sigma, USA) was added to the dried extract and incubated at 70°C for 90 min. Then, 100 µL of MSTFA (Sigma, USA) was added and incubated at 37°C for 30 min.

Analysis of metabolites

Metabolites were separated and analyzed with a GC/MS system. Our GC/MS system was performed as described previously (Gonulalan et al., 2019). The Shimadzu GCMS-QP2010 Ultra GC/MS system was performed with a DB-5MS stationary phase column (30 m + 10 m DuraGuard × 0.25 mm i.d. and 0.25 µm film thickness). Samples were injected in a non-split mode. The injection volume was adjusted as 2 µL. A gradient system was used for metabolite separation. In the gradient system, the temperature was set at 70°C for one min and then increased up to 325°C. The total gradient time was 37.5 min. The MS detector was used in EI mode, and data acquisition was performed in full scan mode with a mass range between 50-650 m/z.

Data processing

The raw GC/MS data was analyzed in MS-DIAL (Lai et al., 2018) (version 3.96, http://prime.psc.riken.jp/Metabolomics_Software/MS-DIAL/). The minimum peak height was adjusted as 1000 amplitude, and the mass range was set for 0-650 m/z. The retention time tolerance was 2 min. In the identification process, the Kovats retention index database was used with 15302 records (http://prime.psc.riken.jp/Metabolomics_Software/MS-DIAL/). The peak area of metabolites were calculated and normalized according to total ion intensity. A metaboanalyst 4.0 platform (Chong et al., 2018) was used for statistical analysis. A volcano test was used with p-value <0.05 and fold change >1.5. Altered metabolites were evaluated with a pathway analysis (Pathway analysis module in metaboanalyst 4.0 and KEGG mapper system).

RESULTS AND DISCUSSION

The confirmed MIC of ciprofloxacin against *E. coli* ATCC 25922 was 0.015 µg/mL. The growth curve for the MIC/2 concentration and unexposed controls are presented in Figure 1. The doubling of cells started around 30 min, of which we collected samples for metabolomics analysis. There was no significant difference between the control and ciprofloxacin-exposed groups in terms of growth rate at our sampling time of 30 min (Mean OD₆₀₀ values were 0.071±0.0005 and 0.072±0.0005 for control and treated, respectively). We continued measuring until the 3 hour mark. The only significant decrease in the ciprofloxacin-exposed group (12.99% decrease when compared

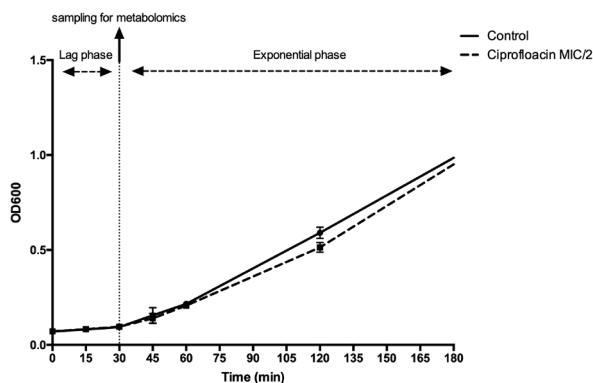


Figure 1. Growth curve for ciprofloxacin-exposed and -unexposed *E. coli* ATCC 25922.

to controls) was observed at 120 min (Mean OD600 values were 0.59 ± 0.03 and 0.51 ± 0.02 for control and treated, respectively; $p < 0.0001$).

Metabolites were separated and analyzed with a GC/MS system. The base peak chromatograms of the control and ciprofloxacin-treated groups are given in Figure 2. In the MS-DIAL platform, metabolites were identified with spectral similarity and retention index. In total, 1106 features were detected, and 207 of them were identified. The peak intensity of each metabolite was calculated and then normalized according to

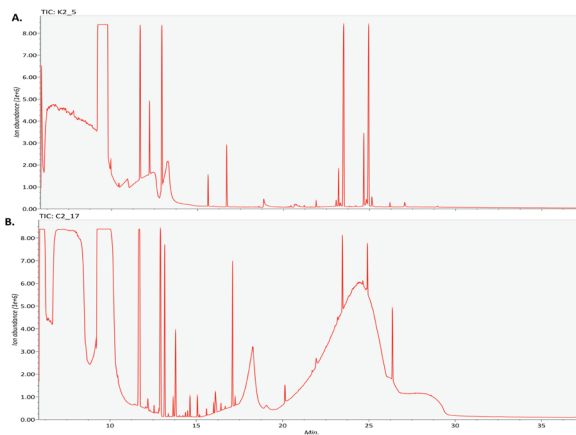


Figure 2. Total ion chromatograms of control (A) and ciprofloxacin treated (B) groups.

total ion intensity. Normalized MS-DIAL data was uploaded to a metaboanalyst 4.0 platform. A principal component analysis (PCA) was applied for all detected features in order to observe the changes of the general metabolome structure of *E. coli* under ciprofloxacin stress. The PCA results showed that there was a dramatic shift in the metabolome structure of *E. coli* in an early phase (Figure 3A). This result indicated that metabolic perturbation includes not only a few single targets but also various cellular processes simultaneously.

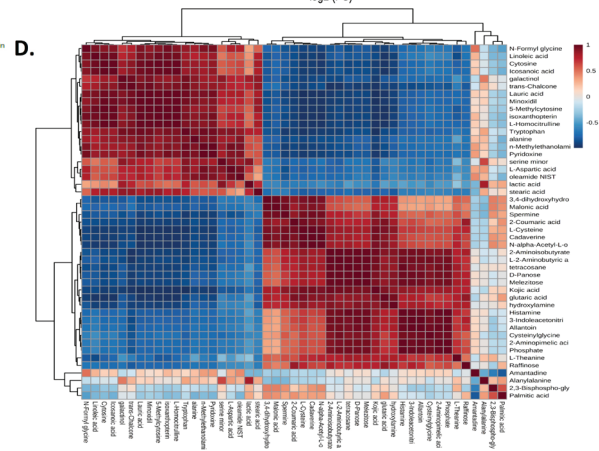
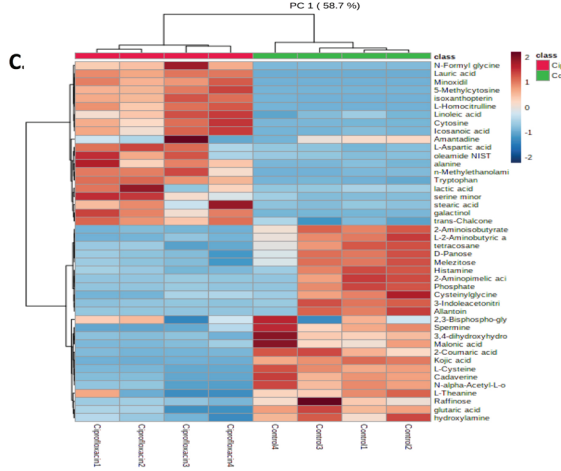
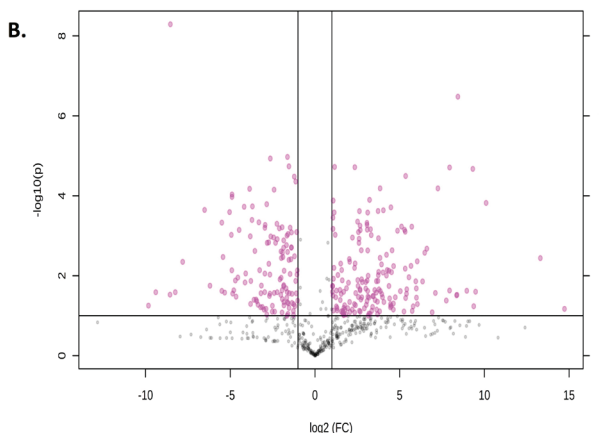
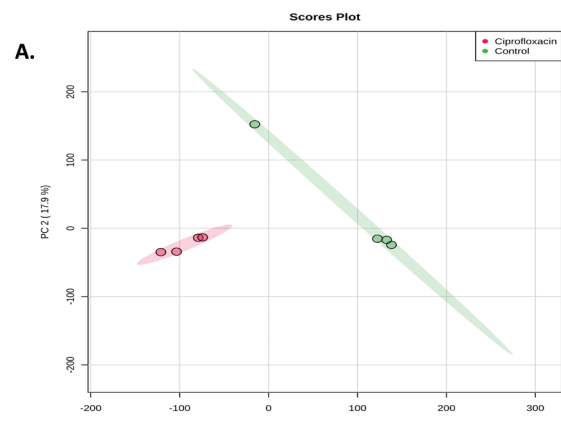


Figure 3. A) Principal component analysis of control and ciprofloxacin treated groups. B) Volcano plot analysis of detected metabolites with p value < 0.05 and fold change > 1.5 cut off value. C) Heat map of altered metabolites between two groups. D) Correlation matrix analysis.

Altered metabolites were determined by a volcano plot test with strict rules (p value <0.05 and fold change > 1.5) (Figure 3B). The results showed that 47 metabolites were altered under ciprofloxacin stress. Altered metabolites with fold change and p -value were given in supplementary information. A heat map and a correlation matrix are given in Figure 3C and 3D to visualize the relative abundance of metabolites with color intensity.

A pathway enrichment analysis is the key tool to understand the systematic effect of antibiotics over pathogens. In the present work, we used a metaboanalyst pathway analysis module (Figure 4A) and a KEGG mapper system (Figure 4B). The results showed that various metabolic pathways were altered significantly under a ciprofloxacin stress condition. The amino acid biosynthesis was the most affected metabolic process (Figure 5A). Amino acids play important roles in many cellular process, pathogenicity, and biofilm formation. In previous studies, it was shown that amino acid biosynthesis was changed under

antibiotic stress conditions. Moreover, amino acid biosynthesis could be one of the initial steps of the resistance mechanism (Dorries, Schlueter, & Lalk, 2014; Zampieri et al., 2017).

Alanine, aspartate, serine, tryptophan, and cysteine are involved in aminoacyl-tRNA biosynthesis and glycine, serine, and threonine metabolism. Aminoacyl-tRNAs play a central role in protein synthesis. Also, they are very important for the cell envelope that affects how the cell interacts with antibiotics (Kim, Lee, Choi, & Choi, 2003). Also, glycine, serine, and threonine metabolism is another important pathway for adaptation and resistance (Cheng et al., 2019; Ye et al., 2018). Our result on altered amino acid biosynthesis pathways may suggest an immediate transcriptional adaptation, which may be clarified with further transcriptomics studies.

Another critical point was the alteration of fatty acid metabolism (Figure 5B). Since fatty acid biosynthesis is essential for

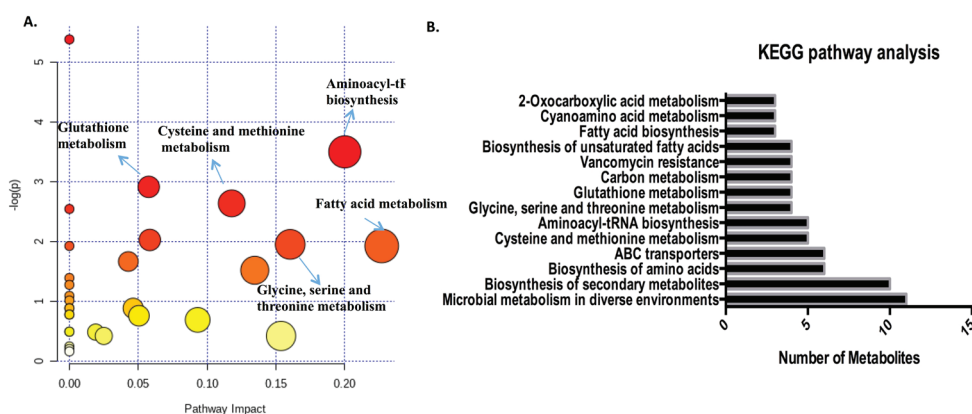


Figure 4. Pathway enrichment analysis; A) Metaboanalyst B) KEGG mapper platform.

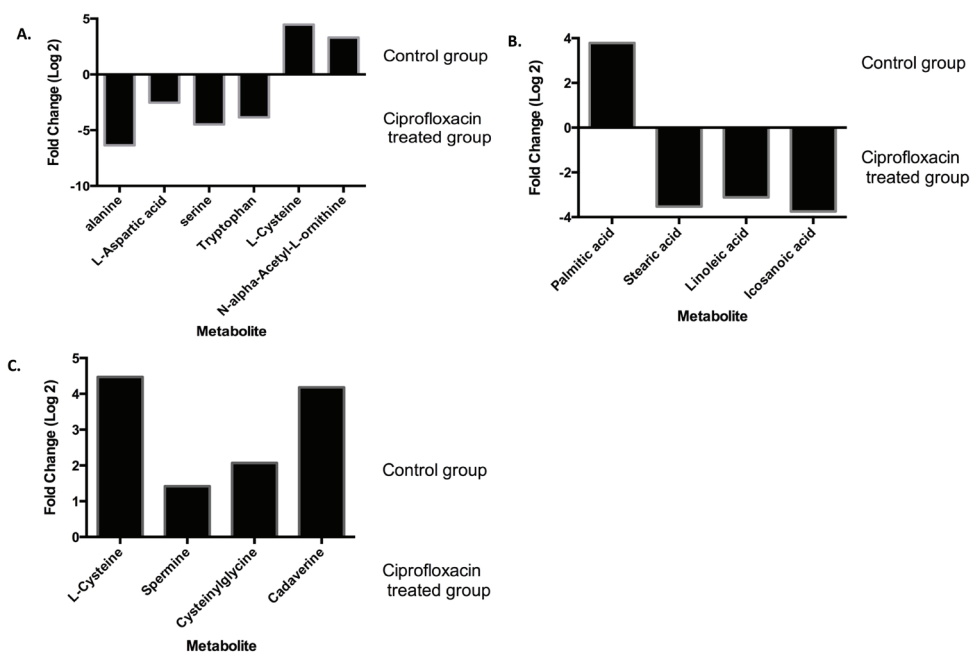


Figure 5. Differentially expressed metabolites in A) Amino acid biosynthesis B) Fatty acid metabolism C) Glutathione metabolism.

many bacterial pathogens, it has recently become a promising antimicrobial target (Yao & Rock, 2017). Some fatty acids are part of the phospholipid layer of the cell membrane, and their composition mostly depends on environmental conditions, which confirms their essential role in environmental adaptation (Yano, Nakayama, Ishihara, & Saito, 1998). Previous studies showed that fatty acid metabolism was different between antibiotic resistant and susceptible strains of various bacteria (Dunnick & O'Leary, 1970; Maifiah et al., 2017). Maifiah et al. (2017) showed that fatty acid composition was significantly changed in *Acinetobacter baumannii* under colistin stress within 15 min. In our work, we observed similar results in 30 min. Together, these results show that fatty acid metabolism is one of the most immediately affected cellular processes under stress.

Glutathione is mainly involved in bacterial redox regulation and adaptation to stress conditions (Smirnova & Oktyabrsky, 2005). In our present study, we found that various metabolites which are involved in glutathione metabolism decreased in ciprofloxacin-treated group (Figure 5C). Previous studies showed that glutathione metabolism up-regulated to protect cells against bactericidal antibiotics (Cameron & Pakrasi, 2010, 2011). However, the exposure timing was different from ours. They used 11 hours exposure time. Thus, it could be argued that the effect of ciprofloxacin was not sufficient to trigger glutathione metabolism in 30 min.

We acknowledge the following limitation of our study. We mainly focused on a fluoroquinolone antibiotic, ciprofloxacin in our present study, due to its widespread use in clinical settings. However, we cannot exclude the possibility that these early-phase metabolic differences may be a common stress response to various antibiotics or other chemical inducers. Indeed, Zampieri et al. (2017) showed that the patterns for selective metabolites were similar for antibiotic and hydrogen peroxide-exposed bacterial cells. Further studies with various antibiotic groups and chemicals are needed to clarify this issue.

CONCLUSION

Herein, we focused on the early phase response of *E. coli* against ciprofloxacin in order to determine the short-term adaptive metabolic response. We conclude that amino acid biosynthesis-related pathways and fatty acid metabolism are early immediate responses of *E. coli* cells to ciprofloxacin. In further experiments, we will focus on these pathways with targeted approaches. We believe that our findings will contribute to the current literature in understanding early pathogen-antibiotic interactions at the molecular level.

Peer-review: Externally peer-reviewed.

Author Contributions: Conception/Design of Study- E.K., C.Ö.; Data Acquisition- E.K., C.Ö.; Data Analysis/Interpretation- E.K., C.Ö.; Drafting Manuscript- E.K., C.Ö.; Critical Revision of Manuscript- E.K., C.Ö.; Final Approval and Accountability- E.K., C.Ö.

Conflict of Interest: The authors have no conflict of interest to declare.


Financial Disclosure: Authors declared no financial support.

REFERENCES

- Cameron, J. C., & Pakrasi, H. B. (2010). Essential role of glutathione in acclimation to environmental and redox perturbations in the cyanobacterium *Synechocystis* sp. PCC 6803. *Plant Physiology*, 154(4), 1672–1685. doi:10.1104/pp.110.162990
- Cameron, J. C., & Pakrasi, H. B. (2011). Glutathione facilitates antibiotic resistance and photosystem I stability during exposure to gentamicin in cyanobacteria. *Applied and environmental microbiology*, 77(10), 3547–3550. doi:10.1128/AEM.02542-10
- Cheng, Z. X., Guo, C., Chen, Z. G., Yang, T. C., Zhang, J. Y., Wang, J., Peng, X. X. (2019). Glycine, serine and threonine metabolites confound efficacy of complement-mediated killing. *Nature Communications*, 10(1), 3325. doi:10.1038/s41467-019-11129-5
- Chong, J., Soufan, O., Li, C., Caraus, I., Li, S., Bourque, G., Xia, J. (2018). MetaboAnalyst 4.0: towards more transparent and integrative metabolomics analysis. *Nucleic Acids Research*, 46(W1), W486–W494. doi:10.1093/nar/gky310
- CLSI. (2015). Methods for Dilution Antimicrobial Susceptibility Tests for Bacteria That Grow Aerobically; Approved Standard -Tenth Edition. CLSI document M07-A10. In: Wayne, PA: Clinical and Laboratory Standards Institute.
- Dorries, K., Schlueter, R., & Lalk, M. (2014). Impact of antibiotics with various target sites on the metabolome of *Staphylococcus aureus*. *Antimicrobial Agents and Chemotherapy*, 58(12), 7151–7163. doi:10.1128/AAC.03104-14
- Dunnick, J. K., & O'Leary, W. M. (1970). Correlation of bacteria lipid composition with antibiotic resistance. *Journal of Bacteriol*, 101(3), 892–900.
- Erickson, K. E., Otoupal, P. B., & Chatterjee, A. (2017). Transcriptome-Level Signatures in Gene Expression and Gene Expression Variability during Bacterial Adaptive Evolution. *mSphere*, 2(1). doi: 10.1128/mSphere.00009-17
- Gonulalan, E. M., Nemutlu, E., Bayazeid, O., Kocak, E., Yalcin, F. N., & Demirezer, L. O. (2019). Metabolomics and proteomics profiles of some medicinal plants and correlation with BDNF activity. *Phyto-medicine*, 152920. doi:10.1016/j.phymed.2019.152920
- Hooper, D. C., & Jacoby, G. A. (2015). Mechanisms of drug resistance: quinolone resistance. *Annals of New York Academy of Sciences*, 1354, 12–31. doi:10.1111/nyas.12830
- Iravani, A., Tice, A. D., McCarty, J., Sikes, D. H., Nolen, T., Gallis, H. A. et al. (1995). Short-course ciprofloxacin treatment of acute uncomplicated urinary tract infection in women. The minimum effective dose. The Urinary Tract Infection Study Group [corrected]. *Archives of Internal Medicine*, 155(5), 485–494.
- Kim, S., Lee, S. W., Choi, E. C., & Choi, S. Y. (2003). Aminoacyl-tRNA synthetases and their inhibitors as a novel family of antibiotics. *Applied Microbiol and Biotechnology*, 61(4), 278–288. doi:10.1007/s00253-003-1243-5
- Lai, Z., Tsugawa, H., Wohlgemuth, G., Mehta, S., Mueller, M., Zheng, Y., Fiehn, O. (2018). Identifying metabolites by integrating metabolome databases with mass spectrometry cheminformatics. *Nature Methods*, 15(1), 53–56. doi:10.1038/nmeth.4512
- Lata, M., Sharma, D., Deo, N., Tiwari, P. K., Bisht, D., & Venkatesan, K. (2015). Proteomic analysis of ofloxacin-mono resistant *Mycobacterium tuberculosis* isolates. *Journal of Proteomics*, 127(Pt A), 114–121. doi:10.1016/j.jprot.2015.07.031
- Li, W., Zhang, S., Wang, X., Yu, J., Li, Z., Lin, W., & Lin, X. (2018). Systematically integrated metabolomic-proteomic studies of *Escherichia coli* under ciprofloxacin stress. *Journal of Proteomics*, 179, 61–70. doi:10.1016/j.jprot.2018.03.002
- Machuca, J., Recacha, E., Briales, A., Diaz-de-Alba, P., Blazquez, J., Pascual, A., & Rodriguez-Martinez, J. M. (2017). Cellular Response to Ciprofloxacin in Low-Level Quinolone-Resistant *Escherichia coli*. *Frontiers Microbiology*, 8, 1370. doi:10.3389/fmicb.2017.01370

- Maifiah, M. H., Creek, D. J., Nation, R. L., Forrest, A., Tsuji, B. T., Velkov, T., & Li, J. (2017). Untargeted metabolomics analysis reveals key pathways responsible for the synergistic killing of colistin and doripenem combination against *Acinetobacter baumannii*. *Scientific Reports*, 7, 45527. doi:10.1038/srep45527
- Mills, S. D. (2006). When will the genomics investment pay off for antibacterial discovery? *Biochemical Pharmacology*, 71(7), 1096–1102. doi: 10.1016/j.bcp.2005.11.025
- Moloney, M. G. (2016). Natural Products as a Source for Novel Antibiotics. *Trends in Pharmacological Sciences*, 37(8), 689–701. doi: 10.1016/j.tips.2016.05.001
- Piddock, L. J. (1998). Fluoroquinolone resistance: overuse of fluoroquinolones in human and veterinary medicine can breed resistance. *British Medicinal Journal*, 317(7165), 1029–1030. doi: 10.1136/bmj.317.7165.1029
- Pulido, M. R., Garcia-Quintanilla, M., Gil-Marques, M. L., & McConnell, M. J. (2016). Identifying targets for antibiotic development using omics technologies. *Drug Discovery Today*, 21(3), 465–472. doi: 10.1016/j.drudis.2015.11.014
- Smirnova, G. V., & Oktyabrsky, O. N. (2005). Glutathione in bacteria. *Biochemistry (Moscow)*, 70(11), 1199–1211. doi:10.1007/s10541-005-0248-3
- Talan, D. A., Klimberg, I. W., Nicolle, L. E., Song, J., Kowalsky, S. F., & Church, D. A. (2004). Once daily, extended release ciprofloxacin for complicated urinary tract infections and acute uncomplicated pyelonephritis. *Journal of Urology*, 171(2 Pt 1), 734–739. doi:10.1097/01.ju.0000106191.11936.64
- Talan, D. A., Naber, K. G., Palou, J., & Elkharrat, D. (2004). Extended-release ciprofloxacin (Cipro XR) for treatment of urinary tract infections. *International Journal of Antimicrobial Agents*, 23 Suppl 1, S54–66. doi:10.1016/j.ijantimicag.2003.12.005
- Ventola, C. L. (2015). The antibiotic resistance crisis: part 1: causes and threats. *PT*, 40(4), 277–283.
- Vranakis, I., Goniotakis, I., Psaroulaki, A., Sandalakis, V., Tselentis, Y., Gevaert, K., & Tsiotis, G. (2014). Proteome studies of bacterial antibiotic resistance mechanisms. *Journal of Proteomics*, 97, 88–99. doi:10.1016/j.jprot.2013.10.027
- Yano, Y., Nakayama, A., Ishihara, K., & Saito, H. (1998). Adaptive changes in membrane lipids of barophilic bacteria in response to changes in growth pressure. *Applied Environmental Microbiology*, 64(2), 479–485.
- Yao, J., & Rock, C. O. (2017). Bacterial fatty acid metabolism in modern antibiotic discovery. *Biochimica et Biophysica Acta- Molecular and Cell Biology of Lipids*, 1862(11), 1300–1309. doi:10.1016/j.bbalip.2016.09.014
- Ye, J. Z., Lin, X. M., Cheng, Z. X., Su, Y. B., Li, W. X., Ali, F. M., Peng, B. (2018). Identification and efficacy of glycine, serine and threonine metabolism in potentiating kanamycin-mediated killing of *Edwardsiella piscicida*. *Journal of Proteomics*, 183, 34–44. doi:10.1016/j.jprot.2018.05.006
- Zampieri, M., Zimmermann, M., Claassen, M., & Sauer, U. (2017). Nontargeted Metabolomics Reveals the Multilevel Response to Antibiotic Perturbations. *Cell Reports*, 19(6), 1214–1228. doi:10.1016/j.celrep.2017.04.002

In vitro urease and trypsin inhibitory activities of some sulfur compounds

Eda Dağsuyu¹ , Refiye Yanardağ¹ ¹Istanbul University-Cerrahpasa, Faculty of Engineering, Department of Chemistry, Istanbul, Turkey**ORCID IDs of the authors:** E.D. 0000-0003-0395-1058; R.Y. 0000-0003-4185-4363**Cite this article as:** Dagsuyu, E., & Yanardag, R. (2021). *In vitro* urease and trypsin inhibitory activities of some sulfur compounds. *Istanbul Journal of Pharmacy*, 51(1), 85-91.

ABSTRACT

Background and Aims: Organosulfur compounds modulate the activities of plurality of metabolic enzymes, especially those that activate (cytochrome P_{450s}) or detoxify (glutathione-S-transferases) carcinogens. They also inhibit the formation of DNA adducts in different target tissues. The aim of the present study was to investigate the effect of some sulfur compounds on urease and trypsin activities *in vitro*.

Methods: In the present study, the inhibitory effect of sulfur compounds on the activities urease and trypsin were determined according to the method of Hanif et al. (2012) and Ribeiro et al. (2010), respectively.

Results: In comparison to the reference standard thiourea (IC₅₀= 53.81±0.68 µg/mL), S-allyl-L-cysteine (IC₅₀= 0.88±0.01 µg/mL) and D, L-methionine (IC₅₀= 0.91±0.02 µg/mL) had the highest urease inhibitor activity, corresponding to the lowest IC₅₀ values among the sulfur compounds. Among the sulfur compounds used in this study, D,L-methionine (IC₅₀= 0.13±0.01 mg/mL) exhibited the lowest IC₅₀ value for trypsin inhibitor, though its activity was less than that of tannic acid which was used as a standard (IC₅₀= 0.06±0.01 mg/mL).

Conclusion: The present outcome suggests that sulfur compounds are potential inhibitors of urease and trypsin activities, and may find importance in medicine and agriculture.

Keywords: Enzyme, inhibitors, sulfur compounds, urease, trypsin

INTRODUCTION

Urease (urea amidohydrolase, EC 3.5.1.5) is an enzyme that catalyzes the hydrolysis of urea to ammonia and carbon dioxide or carbamate. This enzyme contains nickel ion in its active center (Saeed et al., 2017). Ureasases are found in soil, higher plants, algae, fungi, bacteria and in invertebrates (Krajewska, 2009). The enzymes are important in the pathogenesis of many clinical conditions that are harmful to humans, animals, and crops. Increasing urease activity in agriculture causes important environmental and economic challenges. The ammonia released by the enzyme damages plants and soil (Amtul et al., 2006). Urease is a virulence factor found in a variety of pathogenic bacteria. *Helicobacter pylori* urease, one of the most studied bacterial ureases, causes gastritis, peptic ulceration and gastric cancer (Cox, Mukherjee, Cole, Casadevall, & Perfect 2000). Additionally, urease causes kidney stones formation and contributes to the pathogenesis of urolithiasis, hepatic coma, urinary catheter, encrustation, pyelonephritis, ammonia and hepatic encephalopathy, as well as reactive arthritis (Mobley, Island, & Hausinger, 1995; Ragsdale, 2009). Urease inhibitors are therapeutically important anti-ulcer drugs and are used to subdue microbial virulence (Onoda, Takido, Magaribuchi, & Tamaki, 1990). Since urease plays a key role in medicine and agriculture, its inhibitors are paramount for reducing the increased activity of the enzyme. Several classes of compounds have been shown to be urease inhibitors. Hydroxamate complex (Cheng, Zhang, You, Wang & Hai-Hua, 2014), homoserine lactone derivatives (Czerwonka et al., 2014), quinolones, oxadiazoles derivatives (Akhtar, Khan, Iqbal, Jones, & Hameed, 2014), oxindole derivatives (Taha et al., 2015), thiobarbituric acid derivatives

Address for Correspondence:

Refiye YANARDAĞ, e-mail: yanardag@istanbul.edu.tr

Submitted: 21.12.2020

Revision Requested: 14.01.2021

Last Revision Received: 14.01.2021

Accepted: 15.01.2021

This work is licensed under a Creative Commons Attribution 4.0 International License.



(Khan et al., 2014a), pyrogallol and catechol (Xiao, Ma & Zhu, 2010), 1,2,4-triazole and 1,3,4-thiadiazole derivatives (Khan et al., 2010), 3,4,5-trihydroxybenzohydrazone (Taha et al., 2019), benzophenone semicarbazones/thiosemicarbazones (Arshia et al., 2016), and thioureas (Khan et al., 2014b) have already been investigated. However, current inhibitors are inefficient and may have toxic effects. For this reason, the search for new and effective inhibitors continues.

Trypsin (EC 3.4.21.4) is a digestive enzyme produced by pancreatic acinar cells and belongs to a class of enzymes called serine proteases. Serine proteases are involved in processes such as food digestion, blood coagulation, fibrinolysis, blood pressure control, protein maturation, and immune response. These enzymes also play important roles in a wide variety of important pathological processes such as atherosclerosis, inflammation and cancer (Borg, 2004). The pancreatic serine endoprotease activity of trypsin is involved in protein digestion, specifically by cleaving peptidic bonds on the C-terminal group of lysine or arginine (Kang, Kana, Yeung & Liu, 2006). It acts in the duodenum by hydrolyzing peptide bonds and breaking down proteins into smaller peptides, after which the peptide products are hydrolyzed to amino acids via the action of other proteases (Rawlings & Barrett, 1994; Byrne, et al., 2002).

Trypsin inhibitors are used in the treatment of pancreatitis shock and disseminated intravascular coagulation (Inoue & Takano, 2010). Plants have been good sources of trypsin inhibitors (VanderJagt, et al., 2000). For example, high concentrations of trypsin inhibitors are found in Fabaceae seeds as well as other plant tissues (Mosolov & Valueva, 2005; Ruan, Chen, Shao, Wu, & Han, 2011). More so, different inhibitors have been synthesized for trypsin and trypsin-like enzymes (Mares-Guia & Shaw, 1965; Markwardt, Landman, & Walsmann, 1968; Evans, Olson, & Shore, 1982; Toyota, Chinen, Sekizaki, Itoh, & Tanizawa, 1996; Liu, Jiang, Luo, Yan, & Shen, 1998; Venkatesin & Sundanam, 1998; Toyota, et al., 2001). Unfortunately, the synthesized compounds have side effects, therefore prompting continual studies in search for new and safer antitrypsin compounds/inhibitors. The aim of this study was to examine the inhibitory potential of some sulfur compounds on urease and trypsin activities.

MATERIALS AND METHODS

In vitro urease inhibitory activity

Urease inhibitory activity was assayed spectrophotometrically by the method of Hanif et al. (2012). In brief, phosphate buffer (0.1 M, pH 7.50, and containing 0.1 M urea), test compound and enzyme (5 Unit/mL) were incubated for 10 minutes at 37°C. Solutions of phenol reagent and alkali reagent were thereafter added to each well. Then, the reaction mixture was incubated for 10 minutes at 37°C again. Absorbance levels were read at 625 nm. Thiourea was used as standard. Percentage inhibition was calculated using the following formula:

$$\text{Urease inhibitory activity (\%)} = \left[\left(\frac{A - B}{A} \right) \times 100 \right]$$

A is the enzyme activity without inhibitor.

B is the activity in presence of inhibitor.

In vitro trypsin inhibitory activity

Trypsin inhibitory activity was determined by the method of Ribeiro et al., which depends on the hydrolysis of N- α -benzoyl-DL-arginine-p-nitroanilide (BAPNA) by trypsin (Ribeiro, Cunha, & Sales, 2010). The test reaction mixture comprised of a sample at varying concentrations, trypsin solution (0.3 mg/mL from bovine pancreas), 2.5 mM HCl and 50 mM potassium phosphate buffer (pH 7.50). The reaction mixture was incubated at 37°C for 10 minutes, followed by the addition of BAPNA (2.5 mM) solution to the reaction mixture and further incubation for 15 minutes at 37°C. The reaction was stopped by adding 30% acetic acid solution. The absorbance of the samples was measured at 410 nm and tannic acid was used as positive control. The percentage of trypsin inhibitory activity was determined according to the following equation:

$$\text{Trypsin inhibitory activity (\%)} = \left[\left(\frac{A - B}{A} \right) \times 100 \right]$$

A is the enzyme activity without inhibitor.

B is the activity in presence of inhibitor.

The IC₅₀ was determined as the concentration of sulfur compounds required to inhibit urease and trypsin activity by 50%. Percentage enzyme inhibition activities of the inhibitors were used to calculate half maximum inhibitions (IC₅₀) for individual enzymes, via regression analysis data. The lower the IC₅₀ values, the higher the inhibition activity.

RESULTS AND DISCUSSION

The inhibitory effects of some sulfur compounds on urease and their respective (IC₅₀) values are shown in Table 1.

The urease inhibitory activity of sulfur compounds were investigated *in vitro*, in comparison with thiourea. In order to quantify the urease inhibitory activity, the half maximal inhibitory concentration (IC₅₀) values were calculated as shown in Table 1. All the sulfur compounds used in the present study inhibited urease activity (Table 1), in a dose-dependent manner. Low IC₅₀ values indicate that the enzyme is highly inhibited. Among the sulfur compounds used, S-allyl-L-cysteine (IC₅₀= 0.88±0.01 µg/mL) and D, L-methionine (IC₅₀= 0.91±0.02 µg/mL) demonstrated higher urease inhibitory activity than that of the reference standard thiourea (IC₅₀= 53.81±0.68 µg/mL). N-acetyl-L-cysteine (IC₅₀= 65.55±0.89 µg/mL), S-benzyl-L-cystine (IC₅₀= 93.17±3.54 µg/mL) and L-cystine (IC₅₀= 120.96±7.55 µg/mL) also showed promising inhibitions against urease enzyme activity. The urease inhibitory activities of the sulfur compounds used in the present study decreased in the order of: S-allyl-L-cysteine > D,L-methionine > thiourea > N-acetyl-L-cysteine > S-benzyl-L-cysteine > L-cystine > D,L-homocysteine > L-cysteine hydrochloride > S-methyl-L-cysteine > taurine > L-alliin > vitamin U > S-phenyl-L-cysteine (Table 1).

Table 1. Inhibitory activities of sulfur compounds on urease.

Compounds/Standard	Concentration ($\mu\text{g/mL}$)	Inhibition (%)*	IC ₅₀ ($\mu\text{g/mL}$)*
N-Acetyl-L-cysteine	500	97.42 \pm 1.55	65.55 \pm 0.89
	100	76.29 \pm 1.03	
	10	35.05 \pm 3.09	
	1	23.71 \pm 0.01	
	0.1	14.95 \pm 0.52	
L-Alliin	5000	96.56 \pm 1.15	562.16 \pm 7.08
	2500	83.21 \pm 0.76	
	1000	74.43 \pm 1.15	
	500	45.04 \pm 0.01	
	250	32.82 \pm 3.05	
S-Allyl-L-cysteine	1000	97.29 \pm 0.96	0.88 \pm 0.01
	500	74.77 \pm 0.46	
	1	57.02 \pm 0.88	
	0.01	45.87 \pm 0.92	
	0.001	31.31 \pm 3.78	
S-Benzyl-L-cysteine	5000	87.07 \pm 1.36	93.17 \pm 3.54
	2500	75.85 \pm 1.70	
	500	62.93 \pm 0.34	
	100	53.74 \pm 2.04	
	10	41.16 \pm 0.34	
L-Cysteine hydrochloride	1000	95.45 \pm 1.14	290.22 \pm 28.57
	500	69.89 \pm 0.57	
	100	46.02 \pm 5.11	
	10	34.09 \pm 0.01	
	1	15.34 \pm 2.84	
L-Cystine	100	42.16 \pm 1.96	120.96 \pm 7.55
	50	30.88 \pm 2.45	
	25	25.49 \pm 1.96	
	10	19.12 \pm 2.45	
	1	10.29 \pm 1.47	
D,L-Homocysteine	500	92.13 \pm 0.46	226.82 \pm 6.78
	250	68.52 \pm 1.85	
	100	21.30 \pm 0.93	
	10	12.96 \pm 1.85	
	1	6.94 \pm 1.39	
D,L-Methionine	1000	98.60 \pm 0.01	0.91 \pm 0.02
	500	84.27 \pm 0.35	
	100	67.83 \pm 0.01	
	1	55.24 \pm 1.40	
	0.001	30.07 \pm 3.50	
S-Methyl-L-cysteine	500	62.00 \pm 1.00	339.19 \pm 22.37
	1	38.00 \pm 1.00	
	0.1	26.50 \pm 4.50	
	0.01	19.00 \pm 3.00	
	0.001	14.00 \pm 4.00	
S-Phenyl-L-cysteine	5000	70.86 \pm 0.01	3263.57 \pm 46.26
	2500	39.07 \pm 1.32	
	500	24.17 \pm 0.33	
	250	16.56 \pm 0.66	
	100	3.97 \pm 0.66	
Taurine	2500	90.08 \pm 0.83	509.30 \pm 21.40
	1000	69.42 \pm 0.83	
	500	49.17 \pm 2.07	
	100	30.17 \pm 0.41	
	10	15.70 \pm 1.65	

Table 1. Continue.

Compounds/Standard	Concentration ($\mu\text{g/mL}$)	Inhibition (%)*	IC ₅₀ ($\mu\text{g/mL}$)*
Thiourea **	250	84.12 \pm 0.59	53.81 \pm 0.68
	100	54.71 \pm 4.12	
	50	46.47 \pm 0.59	
	10	38.24 \pm 0.59	
	1	22.94 \pm 1.76	
Vitamin U	10000	97.75 \pm 0.01	899.82 \pm 27.27
	5000	70.79 \pm 2.25	
	1000	55.62 \pm 1.69	
	10	36.52 \pm 1.69	
	0.1	21.35 \pm 0.01	

* Mean \pm SD of triplicate values; ** It means standard.

Urease has the potential to be used in anti-ulcer drugs (Krajewska, 2009). Sulfur containing compounds such as thiourea, thiosemicarbazone, and thiocarbonyl compounds can form chelate with transition metal ions. Some thiosemicarbazone and thiourea derivatives have been reported to be efficient urease inhibitors (Pervez, Chohan, Ramzan, Nasim & Khan, 2009; Arshia et al., 2016; Pervez et al., 2018; Islam, et al., 2019; Li et al., 2020; Shehzad et al., 2020). Thiosemicarbazone derivatives strongly inhibit the enzyme. This is because the sulfur atom in the structure of the compound binds two nickel ions of the enzyme's active site, thereby hindering its activity. Many thiourea derivatives are known to be urease inhibitors. This is also due to their ability to chelate nickel ions at the enzyme's active sites (Kanwal et al., 2019; Kumar & Kayastha, 2010; Li et al., 2018). Islam et al. (2019) demonstrated that thiosemicarbazone derivatives highly inhibited the urease enzyme. The strong urease inhibition effect of methionine and S-allyl-L-cysteine as seen in the present study may be linked to the ability of the compounds sulphur ion to easily and strongly bind to the nickel ion of the urease enzyme active site and thus inhibiting the enzyme.

The percentage inhibitory effect and half maximal inhibitory concentration (IC₅₀) values effects of some sulfur compounds on trypsin activity are presented in Table 2.

The *in vitro* trypsin inhibitory effect of sulfur compounds, in comparison with tannic acid, are presented in Table 2. Lower (IC₅₀) values indicate greater trypsin inhibitory activity. All the tested compounds exhibited trypsin inhibition activities, except S-benzyl-L-cysteine and S-phenyl-L-cysteine. D,L-methionine (IC₅₀= 0.13 \pm 0.01 mg/mL) exhibited the highest trypsin inhibition activity among the sulfur compounds used in the present study. The trypsin inhibitory activities of the sulfur compounds decreased in the order of: tannic acid > D,L-methionine > taurine > S-allyl-L-cysteine > N-acetyl-L-cysteine > L-alliin > L-cysteine hydrochloride > D,L-homocysteine > vitamin U > S-methyl-L-cysteine > L-cystine. D,L-methionine (IC₅₀= 0.13 \pm 0.01 mg/mL), taurine (IC₅₀= 0.55 \pm 0.08 mg/mL), S-allyl-L-cysteine (IC₅₀= 1.27 \pm 0.21 mg/mL), N-acetyl-L-cysteine (IC₅₀= 2.60 \pm 0.17 mg/mL) and L-alliin (IC₅₀= 7.45 \pm 0.22 mg/mL) showed better inhibitions against trypsin activity.

Excessive activity of trypsin is strongly implicated in many diseases such as acute pancreatitis, inflammation and tumour formation. The balanced activity of trypsin is necessary for different physiological functions. The abnormal activity of proteolytic enzymes causes disorders such as pulmonary emphysema, arthritis, muscle dysentery, pancreatitis and cancer (Shahwar, Raza, Rehman, Abbasi & Rahman, 2012). Managing

Table 2. Inhibitory activities of sulfur compounds on trypsin.

Compounds/Standard	Concentration (mg/mL)	Inhibition (%)*	IC ₅₀ (mg/mL)*
N-Acetyl-L-cysteine	5	91.26 \pm 2.20	2.60 \pm 0.17
	2.5	38.25 \pm 2.36	
	1	33.06 \pm 3.65	
	0.1	22.95 \pm 1.29	
	0.01	4.10 \pm 0.45	
L-Alliin	5	37.66 \pm 0.60	7.45 \pm 0.22
	3.75	21.63 \pm 1.18	
	2.5	13.14 \pm 3.34	
	1	6.89 \pm 1.13	
	0.1	2.73 \pm 0.98	
S-Allyl-L-cysteine	0.25	16.58 \pm 1.43	1.27 \pm 0.21
	0.1	13.11 \pm 0.45	
	0.05	10.38 \pm 1.55	
	0.01	9.47 \pm 1.29	
	0.00001	7.83 \pm 1.36	

Table 2. Continue.			
Compounds/Standard	Concentration (mg/mL)	Inhibition (%)*	IC₅₀ (mg/mL)*
S-Benzyl-L-cysteine	5		
	2.5		
	1	N.D.	N.D.
	0.1		
	0.01		
L-Cysteine hydrochloride	25	98.78±1.44	
	10	72.26±1.04	
	1	41.16±3.74	8.00±0.66
	0.0001	26.52±2.35	
	0.000001	3.96±0.50	
L-Cystine	0.1	30.33±4.83	
	0.09	15.85±2.11	
	0.08	9.56±1.34	155.51±14.13
	0.07	4.10±1.34	
	0.06	1.37±0.45	
D,L-Homocysteine	5	26.50±1.05	
	4	20.85±2.69	
	1	14.70±2.72	12.32±1.00
	0.25	10.94±1.28	
	0.01	6.67±0.73	
D,L-Methionine	0.1	40.00±1.95	
	0.01	30.81±1.08	
	0.005	15.86±1.56	0.13±0.01
	0.0025	11.35±2.16	
	0.0001	7.21±2.67	
S-Methyl-L-cysteine	50	49.74±1.21	
	1	37.69±4.78	
	0.5	19.74±2.93	51.37±1.93
	0.25	10.77±1.67	
	0.01	1.54±0.24	
S-Phenyl-L-cysteine	5		
	1		
	0.5	N.D.	N.D.
	0.1		
	0.01		
Tannic acid**	0.1	85.50±0.71	
	0.075	51.50±0.71	
	0.05	47.83±0.62	0.06±0.01
	0.025	41.17±1.55	
	0.01	7.67±0.24	
Taurine	1	69.82±2.49	
	0.01	43.60±5.77	
	0.0001	34.15±1.75	0.55±0.08
	0.00001	31.71±1.72	
	0.0000001	5.49±1.75	
Vitamin U	50	99.36±0.23	
	25	78.21±0.60	
	10	39.10±2.67	16.07±1.11
	1	29.81±3.49	
	0.01	12.66±0.48	

* Mean ± SD of triplicate values; ** It means standard; N.D. means not detected.

or treating such diseases with protease inhibitors obtained from natural sources provides an important goal in pharmaceutical research (Freder, Maliar, & Miertus, 2000; Maliar, Jedinak, Kadračová, & Sturdik, 2004; Tossi, Bonin, & Anthceva, 2000). Studies on the inhibitory effects of plant polyphenols and other phytochemicals on trypsin activity have been ongoing

(Rohn, Rawel, & Kroll, 2002; Klomklao, Benjakul, Kishimura & Chaijan, 2011; Shahwar et al., 2012). The various inhibitors bind to the amino acids (serine, histidine and aspartate) at the active center of the enzyme, therefore causing inhibition of the enzyme. Among the sulfur compounds examined in the present study, methionine, taurine and S-allyl-L-cysteine, which are the

sulfur amino acids, were the most active inhibitors of trypsin. These substances make the enzyme inactive by binding to the serine amino acid in the active site of the enzyme.

Methionine, a precursor of succinyl-CoA, homocysteine, cysteine, creatine, and carnitine, is an essential sulfur-containing amino acid. It is also known to inhibit oxidative damage in various tissues. It prevents DNA damage, cancer, cardiovascular diseases, neuropsychiatric disorders and neurodegenerative diseases. In addition, it plays an important role in detoxification, since it removes sulfur containing sections by chelation (Patra, Swarup, & Dwivedi, 2001; Martinez et al., 2017). Therefore, its aforementioned medical significance coupled with its strong trypsin inhibition may go a long way in managing and subsiding degenerative diseases if properly exploited.

CONCLUSIONS

The results of the present study indicate that sulfur-containing compounds are effective inhibitors of urease and trypsin activities. The highest inhibitory effect was exhibited by methionine. Therefore, methionine can be suggested to have an important role in enzyme inhibition, as well as in preventing diseases that may arise due to hyper activities of these enzymes.

Peer-review: Externally peer-reviewed.

Author Contributions: Conception/Design of Study- E.D., R.Y.; Data Acquisition- E.D., R.Y.; Data Analysis/Interpretation- E.D., R.Y.; Drafting Manuscript- E.D., R.Y.; Critical Revision of Manuscript- R.Y.; Final Approval and Accountability- E.D., R.Y.

Conflict of Interest: The authors have no conflict of interest to declare.

Financial Disclosure: Authors declared no financial support.

REFERENCES

- Akhtar, T., Khan, M. A., Iqbal, J., Jones, P. G. & Hameed, S. (2014). A facile one-pot synthesis of 2-arylamino-5-aryloxyalkyl-1,3,4-oxadiazoles and their urease inhibition studies. *Chemical Biology & Drug Design*, 84, 92-98. <https://doi.org/10.1111/cbdd.12297>
- Amtul, Z., Kausar, N., Follmer, C., Rozmahel, R. F., Atta-Ur-Rahman, Kazmi, S. A. ... Choudhary, M. I. (2006). Cysteine based novel non-competitive inhibitors of urease(s)—Distinctive inhibition susceptibility of microbial and plant ureases. *Bioorganic & Medicinal Chemistry*, 14, 6737-6744. <https://doi.org/10.1016/j.bmc.2006.05.078>
- Arshia, A., Khan, A., Khan, K. M. Saad, S. M., Siddiqui, S. J., Perveen, S., & Choudhary, M. I. (2016). Synthesis and urease inhibitory activities of benzophenone semicarbazones/thiosemicarbazones. *Medicinal Chemistry Research*, 25, 2666-2679. <https://doi.org/10.1007/s00044-016-1673-0>
- Borg T. K. (2004). It's the matrix! ECM, proteases, and cancer. *The American Journal of Pathology*, 164, 1141-1142. [https://doi.org/10.1016/S0002-9440\(10\)63201-4](https://doi.org/10.1016/S0002-9440(10)63201-4)
- Byrne, M. F. Mitchell, R. M., Stiffler, H., Jowell, P. S., Branch, M. S., Pappas, T. N... Baillie J. (2002). *Canadian Journal of Gastroenterology and Hepatology*, 16, 849-854.
- Cheng, X. S., Zhang, J. C., You, Z. L., Wang, X., & Hai-Hua Li. (2014). Synthesis, structures, and Helicobacter Pylori urease inhibition of hydroxamate-coordinated oxovanadium complexes with benzohydrazone ligands. *Transition Metal Chemistry*, 39, 291-297. <https://doi.org/10.1007/s11243-014-9802-4>
- Cox, G. M., Mukherjee, J., Cole, G. T., Casadevall, A., & Perfect, J. R. (2000). Urease as a virulence factor in experimental cryptococcosis. *Infection and Immunity*, 68, 443-448. <https://doi.org/10.1128/iai.68.2.443-448.2000>
- Czerwonka, G., Arabski, M., Wąsik, S., Jabłońska-Wawrzycka, A., Rogala, P., & Kaca, W. (2014). Morphological changes in Proteus mirabilis O18 biofilm under the influence of a urease inhibitor and a homoserine lactone derivative. *Archives of Microbiology*, 196, 169-177. doi: 10.1007/s00203-014-0952-8
- Evans, S. A., Olson, S. T., & Shore, J. (1982). p-Aminobenzamidine as a fluorescent probe for the active site of serine proteases. *Journal of Biological Chemistry*, 257, 3014-3017.
- Frečer, V., Maliar, T. & Miertus, S. (2000). Protease inhibitors as anticancer drugs: Role of molecular modelling and combinatorial chemistry in drug design. *International Journal of Medicine, Biology and the Environment*, 28, 161-173.
- Hanif, M., Shoaib, K., Saleem, M., Hasan Rama, N., Zaib, S., & Iqbal, J. (2012). Synthesis, urease inhibition, antioxidant, antibacterial, and molecular docking studies of 1,3,4-oxadiazole derivatives. *International Scholarly Research Notices: Pharmacology*, 928901. <https://doi.org/10.5402/2012/928901>
- Inoue, K. I., Takano, H. (2010). Urinary trypsin inhibitor as a therapeutic option for endotoxin-related inflammatory disorders. *Expert Opinion on Investigational Drugs*, 19, 513-520. <https://doi.org/10.1517/13543781003649533>
- Islam, M., Khan, A., Shehzad, M. T., Hameed, A., Ahmed, N., Halim, S. A. ... Al-Harrasi, A. (2019). Synthesis and characterization of new thiosemicarbazones, as potent urease inhibitors: In vitro and in silico studies. *Bioorganic Chemistry*, 87, 155-162. <https://doi.org/10.1016/j.bioorg.2019.03.008>
- Kang, K., Kana, C., Yeung, A., & Liu, D. (2006). The immobilization of trypsin on soap-free P(MMA-EA-AA) latex particles. *Materials Science and Engineering: C*, 26, 664-669. <https://doi.org/10.1016/j.msec.2005.07.020>
- Kanwal, -, Khan, M., Arshia, -, Khan, K. M., Parveen, S., Shaikh, M., Fatima, N., Choudhary, M. I. (2019). Syntheses, in vitro urease inhibitory activities of urea and thiourea derivatives of tryptamine, their molecular docking and cytotoxic studies, *Bioorganic Chemistry*, 83, 595-610. <https://doi.org/10.1016/j.bioorg.2018.10.070>
- Khan, I., Ali, S., Hameed, S., Rama, N. H., Hussain, M. T., Wadood, A. ... Choudhary, M. I. (2010). Synthesis, antioxidant activities and urease inhibition of some new 1,2,4-triazole and 1,3,4-thiadiazole derivatives. *European Journal of Medicinal Chemistry*, 45, 5200-5207. <https://doi.org/10.1016/j.ejmech.2010.08.034>
- Khan, M. K., Rahim, F., Khan, A., Shabeer, M., Hussain, S., Rehman, W. ... Choudhary, M. I. (2014a). Synthesis and structure-activity relationship of thiobarbituric acid derivatives as potent inhibitors of urease, *Bioorganic & Medicinal Chemistry*, 22, 4119-4123. <https://doi.org/10.1016/j.bmc.2014.05.057>
- Khan, K. M., Naz, F., Taha, M., Khan, A., Perveen, S., Choudhary, M. I., & Voelter, W. (2014b). Synthesis and in vitro urease inhibitory activity of N,N'-disubstituted thioureas, *European Journal of Medicinal Chemistry*, 74, 314-323. <https://doi.org/10.1016/j.ejmech.2014.01.001>
- Klomkloa, S., Benjakul, S., Kishimura, H., & Chaijan, M. (2011). Extraction, purification and properties of trypsin inhibitor from Thai mung bean (*Vigna radiata* (L.) R. Wilczek), *Food Chemistry*, 129, 1348-1354. <https://doi.org/10.1016/j.foodchem.2011.05.029>
- Kumar, S., & Kayastha, A.M. (2010). Soybean (Glycine max) urease: significance of sulfhydryl groups in urea catalysis. *Plant Physiology and Biochemistry*, 48, 746-750. doi: 10.1016/j.plaphy.2010.05.007
- Krajewska, B. (2009). Ureases I. Functional, catalytic and kinetic properties: A review. *Journal of Molecular Catalysis B: Enzymatic*, 59, 9-21. <https://doi.org/10.1016/j.molcatb.2009.01.003>

- Li, C., Huang, P., Wong, K., Xu, Y., Tan, L., Chen, H. ... Xie, J. (2018). Coptisine-induced inhibition of *Helicobacter pylori*: elucidation of specific mechanisms by probing urease active site and its maturation process. *Journal of Enzyme Inhibition and Medicinal Chemistry*, 33, 1362–1375. <https://doi.org/10.1080/14756366.2018.1501044>
- Li, W. Y., Ni, W. W., Ye, Y. X., Fang, H. L., Pan, X. M., He, J. L. ... Zhu, H. L. (2020). N-monoarylaceto thioureas as potent urease inhibitors: synthesis, SAR, and biological evaluation. *Journal of Enzyme Inhibition and Medicinal Chemistry*, 35, 404–413. doi: 10.1080/14756366.2019.1706503
- Liu, J. Q., Jiang, M. S., Luo, G. M., Yan, G. L., & Shen, J. C. (1998). Conversion of trypsin into a selenium containing enzyme by using chemical mutation. *Biotechnology Letters*, 20, 693–696. <https://doi.org/10.1023/A:1005378709179>
- Maliar, T., Jedinak, A., Kadrabova, J., & Sturdik, E. (2004). Structural aspects of flavonoids as trypsin inhibitors. *European Journal of Medicinal Chemistry*, 39, 241–248. doi: 10.1016/j.ejmech.2003.12.003
- Mares-Guia, M. & Shaw, E. J. (1965). Studies on the active center of trypsin. The binding of amidines and guanidines as models of the substrate side chain. *Journal of Biological Chemistry*, 240, 1579–1585.
- Markwardt, F., Landman, H., & Walsmann, P. (1968). Comparative studies on the inhibition of trypsin, plasmin and thrombin by derivatives of benzylamine and benzamidine. *European Journal of Biochemistry*, 6, 502–506. doi: 10.1111/j.1432-1033.1968.tb00473.x
- Martínez, Y., Li, X., Liu, G., Bin, P., Yan, W., Más, D. ... Yin, Y. (2017). The role of methionine on metabolism, oxidative stress, and diseases. *Amino Acids*, 49, 2091–2098. doi: 10.1007/s00726-017-2494-2
- Mobley, H. L., Island, M. D., & Hausinger, R. P. (1995). Molecular biology of microbial ureases. *Microbiological reviews*, 59, 451–480.
- Mosolov, V. V. & Valueva, T. A. (2005). Proteinase inhibitors and their function in plants: a review. *Applied Biochemistry and Microbiology*, 1, 227–246. <https://doi.org/10.1007/s10438-005-0040-6>
- Onoda, Y., Takido, M., Magaribuchi, T., & Tamaki, H. (1990). Effects of 12-sulfodehydroabietic acid monosodium salt (ta-2711), a new anti-ulcer agent, on gastric mucosal lesions induced by necrotizing agents and gastric mucosal defensive factors in rats. *The Japanese Journal of Pharmacology*, 52, 631–638. <https://doi.org/10.1254/jjp.52.631>
- Patra, R. C., Swarup, D., Dwivedi, S. K. (2001). Antioxidant effects of a tocopherol, ascorbic acid and L-methionine on lead induced oxidative stress to the liver, kidney and brain in rats. *Toxicology*, 162, 81–88. doi: 10.1016/s0300-483x(01)00345-6
- Pervez, H., Chohan, Z. H., Ramzan, M., Nasim, F. H., & Khan, K. M. (2009). Synthesis and biological evaluation of some new N4-substituted isatin-3-thiosemicarbazones. *Journal of Enzyme Inhibition and Medicinal Chemistry*, 24, 437–446. <https://doi.org/10.1080/14756360802188420>
- Pervez, H., Khan, N., Iqbal, J., Zaid, S., Yaqub, M., Tahir, M. N., & Naseer, M. M. (2018). Synthesis, crystal structure, molecular docking studies and bio-evaluation of some N4-benzyl-substituted isatin- 3-thiosemicarbazones as urease and glycation inhibitors. *Heterocyclic Communications*, 24, 51–58. doi: <https://doi.org/10.1515/hc-2017-0148>
- Ragsdale S. W. (2009). Nickel-based enzyme systems. *Journal of Biological Chemistry*, 284, 18571–18575. doi: 10.1074/jbc.R900020200
- Rawlings, N. D. & Barrett, A. J. (1994). Families of serine peptidases. *Methods in Enzymology*, 24, 19–61. doi: 10.1016/0076-6879(94)44004-2
- Ribeiro, J. K., Cunha, D. D., Fook, J. M., & Sales, M. P. (2010). New properties of the soybean trypsin inhibitor: Inhibition of human neutrophil elastase and its effect on acute pulmonary injury. *European Journal of Pharmacology*, 644, 238–244. doi: 10.1016/j.ejphar.2010.06.067
- Rohn, S., Rawel, H. M., Kroll, J. (2002). Inhibitory effects of plant phenols on the activity of selected enzymes. *Journal of Agricultural and Food Chemistry*, 50, 3566-3571. doi: 10.1021/jf011714b
- Ruan, J. J., Chen, H., Shao, J. R., Wu, Q. & Han, X. Y. (2011). An antifungal peptide from *Fagopyrum tataricum* seeds. *Peptides*, 32, 1151-1158. <https://doi.org/10.1016/j.peptides.2011.03.015>
- Saeed, A., Ur-Rehman, S., Channar, P., Larik, F., Abbas, Q., Hassan, M. ... Seo, S. Y. (2017). Jack bean urease inhibitors, and antioxidant activity based on palmitic acid derived 1-acyl-3- arylthioureas: synthesis, kinetic mechanism and molecular docking studies. *Drug Research*, 67, 596–605. doi: 10.1055/s-0043-113832
- Shahwar, D., Raza, M. A., Rehman, S. U., Abbasi, M. A., & Rahman, A. U. (2012). An investigation of phenolic compounds from plant sources as trypsin inhibitors. *Natural Product Research: Formerly Natural Product Letters*, 26, 1087–1093.
- Shehzad, M. T., Khan, A., Islam, M., Hameed, A., Khiat, M., Halim, S. A. ... Shafiq, Z. (2020). Synthesis and urease inhibitory activity of 1,4-benzodioxane-based thiosemicarbazones: Biochemical and computational approach. *Journal of Molecular Structure*, 1209, 127922. <https://doi.org/10.1016/j.molstruc.2020.127922>
- Taha, M., Ismail, N. H., Baharudin, M. S., Lalani, S., Mehboob, S., Khan, K. M. ... Choudhary, I. (2015). Synthesis crystal structure of 2-methoxybenzoylhydrazones and evaluation of their α -glucosidase and urease inhibition potential. *Medicinal Chemistry Research*, 24, 1310–1324. <https://doi.org/10.1007/s00044-014-1213-8>
- Taha, M., Shah, S. A. A., Khan, A., Arshad, F., Ismail, N. H., Afifi, M., & Choudhary, M. I. (2019). Synthesis of 3,4,5-trihydroxybenzohydrazone and evaluation of their urease inhibition potential. *Arabian Journal of Chemistry*, 12, 2973–2982. <https://doi.org/10.1016/j.arabjc.2015.06.036>
- Tossi, A., Bonin, I. & Anthceva, N. (2000). Aspartic protease inhibitors. An integrated approach for the design and synthesis of diaminodiol-based peptidomimetics. *European Journal of Biochemistry*, 267, 1715–1722. <https://doi.org/10.1046/j.1432-1327.2000.01164.x>
- Toyota, E., Chinen, C., Sekizaki, H., Itoh, K., & Tanizawa, K. (1996). Application of spontaneous Schiff base copper chelates formation process to the design of a trypsin inhibitor. *Chemical and Pharmaceutical Bulletin*, 44, 1104–1106. <https://doi.org/10.1248/cpb.44.1104>
- Toyota, E., Ng, K. K., Sekizaki, H., Itoh, K., Tanizawa, K., & James, M. N. G. (2001). X-ray crystallographic analyses of complexes between bovine b-trypsin and schiff base copper(II) or iron(III) chelates. *Journal of Molecular Biology*, 305, 471–479. doi: 10.1006/jmbi.2000.4303
- VanderJagt, D., Freiberger, C., Vu, H. T., Mounkaila, G., Glew R. S. & Glew R. H. (2000). The trypsin inhibitor content of 61 wild edible plant foods of Niger. *Plant Foods for Human Nutrition*, 55, 335–346. <https://doi.org/10.1023/A:1008136100545>
- Venkatesin, R. & Sundanam, R. V. (1998). Modulation of stability properties of bovine trypsin after in vitro structural changes with a variety of chemical modifiers. *Protein Engineering*, 11, 691–698. doi: 10.1093/protein/11.8.691
- Xiao, Z., Ma, T. W., Fu, W. C., Peng, X. C., Zhang, A. H., Zhu, H. L. (2010). The synthesis, structure and activity evaluation of pyrogallol and catechol derivatives as *Helicobacter pylori* urease inhibitors. *European Journal of Medicinal Chemistry*, 45, 5064–5070. <https://doi.org/10.1016/j.ejmech.2010.08.01>

Quality of turmeric powder in herbal stores: pharmacognostical investigations on turmeric powders obtained from herbal stores in Istanbul, Turkey

Ebru Kuruldak¹ , Fatmanur Yılmaz² , Gizem Gülsoy Toplan^{1,3} , Berna Özbek Çelik² , Afife Mat¹ 

¹Istanbul University, Faculty of Pharmacy, Department of Pharmacognosy, Istanbul, Turkey

²Istanbul University, Faculty of Pharmacy, Department of Microbiology, Istanbul, Turkey

³Istinye University, Faculty of Pharmacy, Department of Pharmacognosy, Istanbul, Turkey

ORCID IDs of the authors: E.K. 0000-0003-2041-8810; F.Y. 0000-0001-8442-8538; G.G.T. 0000-0002-0544-2532; B.Ö.Ç. 0000-0001-8909-8398; A.M. 0000-0002-9225-8572

Cite this article as: Kuruldak, E., Yılmaz F., Gulsoy Toplan, G., Ozbek Celik, B., & Mat A. (2021). Quality of turmeric powder in herbal stores: Pharmacognostical investigations on turmeric powders obtained from herbal stores in Istanbul, Turkey. *Istanbul Journal of Pharmacy*, 51(1), 92-97.

ABSTRACT

Background and Aims: *Curcuma longa* L., known as Turmeric, has been traditionally used in Asian culture since ancient times to treat several disorders. With the increase in studies on turmeric and its major compounds, it became popular. The study aims to investigate the safety and efficacy of powdered samples collected from 15 different herbal stores in Istanbul.

Methods: Macroscopical, microscopical, bacteriological, and some physicochemical methods were used to evaluate the turmeric powder samples and the extracts of the samples. Additionally, the qualitative determination of curcumin in extracts was carried out by thin-layer chromatography (TLC).

Results: The results of the study show that the powdered samples contain curcuminoids and are also of a moderate quality. The microbiological assay showed us the existence of high levels of pathogens.

Conclusion: Turmeric powder should be consumed carefully, the storage period, and also the origin of the Turmeric is significant in consumption.

Keywords: *Curcuma longa*, turmeric, curcuminoids, TLC, antibacterial activity, ash content

INTRODUCTION

Plants have been used to protect from disorders, treat many illnesses, and also for wellbeing, throughout human history. Today, many of them are still used in phytotherapy, while their secondary metabolites are increasingly gaining attention in the preparation of standardised herbal products or drugs. *Curcuma longa* L., known as Turmeric, has been traditionally used in Asian culture since ancient times to treat several disorders and also as a spice. Turmeric is the most commonly used plant in Ayurvedic medicine and has become popular all over the world by crossing the borders of Asia, with recent studies on its chemical composition and biological activities (Prasad & Aggarwal, 2011). With the growing interest, it is easy to reach turmeric products via pharmacies, the internet, and herbal stores.

Curcuma longa is one of 133 species of *Curcuma* which belong to the Zingiberaceae family. This perennial herb is native to India and Southeast Asia. Its rhizomes and oil have significant value (Prasad & Aggarwal, 2011). Ayurvedic remedies are used for many disorders such as: the improvement of digestion problems, irritable bowel syndrome, some liver diseases and the dissolution

Address for Correspondence:
Afife MAT, e-mail: afifemat@gmail.com

Submitted: 10.11.2020
Revision Requested: 23.01.2021
Last Revision Received: 30.01.2021
Accepted: 05.02.2021

This work is licensed under a Creative Commons Attribution 4.0 International License.



of gallbladder stones, some respiratory diseases such as runny noses, coughs, and sinusitis. They are also used for increasing the general energy of the body, regulating the menstrual cycle, the treatment of asthma, relieving arthritis, the calming of allergies and the treatment of diabetic wounds. Turmeric is also commonly used as a spice in South Asian and Middle Eastern food culture (Prasad & Aggarwal, 2011). Additionally, it is used as a dyeing agent in the textile and cosmetic industries due to possessing a bright yellow colour.

In recent years, several studies showed that the extracts and secondary metabolites of *Curcuma longa* possess remarkable anti-microbial, antifungal, antiviral, anti-inflammatory, anti-diabetic, neuroprotective, cardioprotective, gastroprotective, and especially anti-cancer effects (Aamon & Wahi, 1991; Labban, 2014; Gounder, & Lingamallu, 2012). Although some mechanisms for its biological activity have been elucidated, many mechanisms are not yet known and studies need to be conducted (Aamon & Wahi, 1991). The main mechanisms of these biological activities are based on increasing the level of antioxidant enzymes in the blood, the inhibition of lipid peroxidation, the scavenging effect of oxygen radicals, stimulation of COX2 activation, inhibition of TNF-alpha and nitric oxide secretion, and increasing collagen secretion (Araújo & Leon, 2001; Becit, Aydın, & Başaran, 2017)

In previous studies, more than 235 compounds, primarily phenolic compounds, and terpenoids were identified in *Curcuma* species (Li et. al., 2011). The chemical composition of *Curcuma longa* has been extensively studied revealing two major groups, curcuminoids and volatile oil, which are explored as essential components for biological activities. Curcumin, demethoxycurcumin, and bisdemethoxycurcumin are the major curcuminoids isolated from turmeric (Jayaprakasha, Rao & Sakariah, 2005). These curcuminoid pigments are responsible for the yellow colour in plants. The essential oil of Turmeric shows variety in its chemical composition which gives its aromatic odor and taste. According to studies, the major components of essential oil were determined as *ar*-turmerone, alpha-turmerone, beta-turmerone, zingiberene, zingiberone, and curlone (Jayaprakasha, Rao & Sakariah, 2005; Singh et. al., 2010). The essential oil also contains germacrone, sabinene, eucalyptol, borneol, and sesquiphellandrene (Jayaprakasha, Rao & Sakariah, 2005, Raina et al., 2002). As a result of many studies, having the great potential of anti-inflammatory and anti-cancer activities of turmeric is attributed to curcuminoids and volatile oil.

Due to the increase in scientific studies on turmeric and understanding of its potential, the demand for its products has increased around the world (Pothitirat & Gritsanapan, 2006). Today, it is easy to find turmeric products such as powdered and fresh rhizomes, tablets, capsules, and also liquid forms. The usage of powdered turmeric is quite popular and also easily accessible in Turkey. It is commercially available and is sold in open or packed forms, both in herbal stores and in markets, but without quality, safety, and also bacteriological control.

This study aims to investigate the safety and efficacy of powdered turmeric samples by macroscopical, microscopical, bacteriological, chemical, and some physical methods. 15 differ-

ent powdered turmeric samples were collected from several herbal stores in both Asian and European sides of Istanbul and their quality was evaluated according to Turkish pharmacopeia (Turkish Pharmacopoeia Journal, 2016).

MATERIALS AND METHODS

Plant material

Turmeric samples were purchased from different herbal stores in Istanbul. The analysis was conducted on 15 different samples.

Macroscopical evaluation

Evaluations were made for each turmeric sample in terms of colour, odour, taste, and appearance. The expected colour of the powder is orange-yellow. Spicy is described as scented. It tastes an aromatic, slightly bitter taste of turmeric. In terms of appearance, it should not contain macro particles.

Microscopical evaluation

When examined with the Sartur reagent under a microscope, it usually contains starch grains gelatinised and collected in starch paste; rarely it is possible to observe ovoid starch granules. When examined with chloral hydrate solution, specific characteristics of turmeric can be observed. These are as follows:

- a. Fragments of parenchyma containing secretory cells containing brown-yellow lipid masses
- b. Reticulated or dimpled xylem
- c. Rare pieces of the epidermis, traces of cover hairs covering the walls with light and irregular thickened cells; rarely long and warped, thick-walled, single-celled trichomes shredded or attached to free or epidermal cells
- d. Rarely long and curved, thick-walled, single-celled trichomes; shredded, free, or attached to epidermal cells
- e. Rare periderma pieces, sometimes covered with the epidermis (Turkish Pharmacopoeia Journal, 2016).

Physicochemical analysis methods

Preparation of the extracts

10 mL of ethanol (96%) was added to 1 g of a powdered sample, shaken in the ultrasonic water bath which was allowed to stand for 30 minutes at room temperature. It was then filtered by cotton. The filtrate was used for the analysis (Turkish Pharmacopoeia Journal, 2016).

Reference solution

Novasol Curcumin Licaps (liquid-filled encapsulation) capsule was used as a reference. The liquid capsule containing 20 mg of curcuminoids is diluted with 10 mg of ethanol (96%) (check again) .

Thin-layer chromatography

The thin-layer chromatographic method was used to determine the existence of curcuminoids in the samples. The turmeric samples and diluted reference solutions were applied to the silica gel plate in 10 mm bands. The combination of glacial acetic acid and toluene (20:80) was used as a mobile phase. Af-

ter the saturation of the chromatogram tank with the solvent system at least 30 min. TLC plates were developed until the solvent front was ± 1 cm from the top of the plate. Later, the plate is allowed to dry on the fume hood. Dry plaque is examined at 245 and 365 nm under ultraviolet light. It is then treated with anisaldehyde solution and heated at 100-105°C for 10 minutes; afterward, it is examined under ultraviolet light again (Turkish Pharmacopoeia Journal, 2016).

Determination of water content

A glass weighing container for each sample was passed through ethanol and allowed to dry in the etuve. Weighing dried vessels were left in the desiccator for 30 minutes. Then, each container is weighed first empty, and then with 1 g of substance. Each weighed sample was left to the desiccator to wait until it is taken to the oven. After the weighing of all samples has been completed, it was left in the oven at 100-105°C for 2 hours. At the end of 2 hours, the samples are taken and left to desiccate again for 30 minutes. Then each sample is weighed again. Yield calculation is made. As a result of the determination of the amount of water with 15 gr of the powdered herbal drug is detected at a maximum of 120 mL/kg (Baytop T., 1980).

Determination of ash content

For each sample, a porcelain crucible is passed through ethanol and allowed to dry in the oven. The crucible dried in the oven is left in the desiccator for 30 minutes. Each crucible is then weighed empty and with 1 g of sample. Each weighed crucible is taken to the oven. It is left in the oven for 1 hour at 200°C and then for 3 hours at 600°C. At the end of 4 hours, the samples in the oven are left in the desiccator again for 30 minutes to cool down. Weigh the cooled samples and calculate the yield. As a result of ash determination, total ash should be at most 7.0% (Baytop T., 1980).

Bacteriological tests

Antimicrobial activities of the extracts

Microorganisms: The American Type Culture Collection (ATCC) standard strains of *Staphylococcus aureus* ATCC 29213, *Enterococcus faecalis* ATCC 29212, *Pseudomonas aeruginosa* ATCC 27853, *Escherichia coli* ATCC 25922, *Klebsiella pneumoniae* ATCC 4352 and as a representative of fungi, the yeast, *Candida albicans* ATCC 10231 were used in the experiments. Inoculums of bacteria and *C. albicans* were prepared with overnight cultures, for producing a concentration of 1×10^8 colony-forming units (cfu/ml) and 1×10^7 cfu/ml, respectively.

Media: Cation-adjusted Mueller-Hinton broth (CAMHB, Difco Laboratories) and RPMI-1640 medium (Sigma) buffered to pH 7.0 with morpholine propane sulfonic acid (MOPS, Sigma) were used to determine the minimum inhibitory concentration (MIC) of bacteria/spore suspension and yeast, respectively, and tryptic soy agar (TSA, Difco Laboratories) was used for colony counts.

Determination of minimum inhibitory concentrations

(MIC): *In vitro* antibacterial activities of 14 different turmeric extracted samples against *S. aureus* ATCC 29213, *E. faecalis* 29212, *P. aeruginosa* ATCC 27853, *E. coli* ATCC 25922, *K. pneumoniae*

ATCC 4352; antifungal activities against *C. albicans* ATCC 10231 were investigated. MICs of compounds were determined by the micro broth dilution technique as described by the Clinical and Laboratory Standards Institute (CLSI 2000 & 2006). Molecules were dissolving in Dimethyl sulfoxide (DMSO, Sigma), and serial two-fold dilutions of molecules ranging from finally 5000 to 5 µg/mL or 500 to 0.5 µl/mL were prepared in Mueller-Hinton broth (MHB) for bacteria or spores, and RPMI-1640 medium for yeast. Each well was inoculated with 50 µL of a 4-6 h broth culture that gave a final concentration of 5×10^5 cfu/mL for bacteria or spores, and 5×10^3 cfu/mL for yeast in the test tray. The trays were covered and placed in plastic bags to prevent evaporation. The trays containing MHB were incubated at 37°C for 18-24 h, those containing RPMI-1640 medium at 37°C for 48 h. The MIC was defined as the lowest concentrations of compounds producing complete inhibition of visible growth. DMSO was used as a negative control in assays. Levofloxacin and fluconazole were used as reference antibiotics for bacteria and yeast, respectively.

Microbiological content determination

Turmeric samples collected from various transfers and numbered from 1 to 15 were weighed 1 gram and dissolved with 10 ml sterile distilled water. Then, ten-fold dilutions were made using sterile saline. 10 µl of dilutions were made, the Tryptic Soy Agar (TSA) for bacteria and Saboroud Dextrose Agar (SDA) for fungi spread on the solid broth surface and was left for incubation at 37°C for bacteria and 25°C for fungi in the oven. The colonies formed the following day were counted to determine the total number of live bacteria, and the number of total aerobic bacteria and fungi in one gram of turmeric was calculated in terms of the colony-forming unit (CFU) taking into account the dilution factor (Omurtag, 1966).

RESULT AND DISCUSSION

Macroscopical evaluation

The samples, which is shown in Figure 1 are numbered from 1 to 15. The appearance, odor, aromatic taste, and colour were determined for each sample. All turmeric samples possess an orange-yellow colour, aromatic, slightly bitter taste. The visible particles were not detected in most of the samples, only four samples (3, 9, 12, 14) contained minor black dirties.

Microscopical evaluation

Microscopical characters of each sample were evaluated by Sartur reagent and chloral hydrate solution. Examination under the microscope showed us the presence of gelatinised starch grains, reticulated or dimpled xylem, and fragments of parenchyma containing secretory cells containing brown-yellow lipid masses. Additionally, phelloderm pieces covered with epidermis were identified in some samples. The microscopical appearance of samples is shown below.

Physicochemical analysis results

TLC profiles of the extracts

Thin-layer chromatography plaque was examined under daylight and also 245 nm and 365 nm ultraviolet light. Consequently, three different curcumin compounds were identified

in each sample. Comparing the reference solution and extracts it is revealed that all samples contain significant curcuminoids which are generally used for standardising turmeric products (Figure 2).

Determination of water content

The percentage of total water was calculated from the amount of the sample before drying and the remaining amount after drying. The percentage of total water for turmeric is 15 g. for the sample it should be a maximum of 120 mL/kg. This corresponds to 10.71%. It was observed that all of the samples gave results below the maximum value (Table 1).

Determination of ash content

The total ash percentage was calculated over the amount of the sample before burning and the remaining amount after burning. The total ash percentage for turmeric should be a maximum of 7.0%. When evaluated according to this, it was observed that five samples (2, 3, 6, 11 and 14) left ash more than this percentage.

Sample No	Macroscobical Assessment	Microscobical Assessment
1		
2		
3		
4		
5		
6		
7		
8		
9		
10		
11		
12		
13		
14		
15		

Figure 1. The macroscobical and microscobical appearances of 15 powdered turmeric samples. a. parenchyma pieces including brown-yellow lipids, b. reticulated or dimpled xylem, c. single-celled trichomes attached to epidermis, d. periderma pieces, sometimes covered with parenchyma.

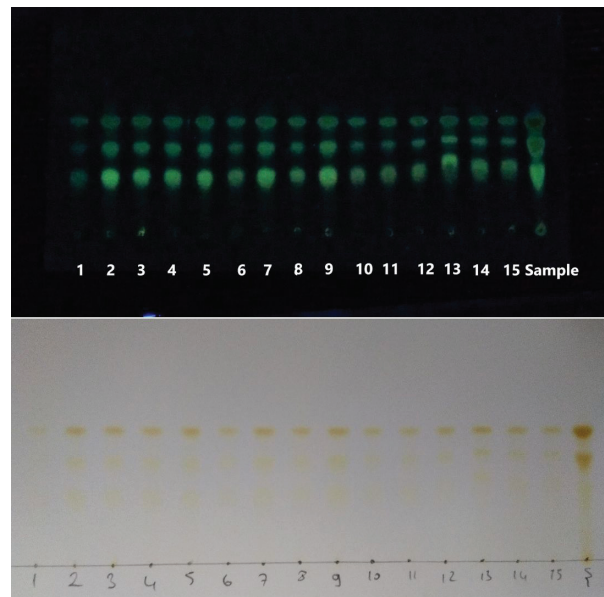


Figure 2. TLC chromatograms of samples under daylight (below) and 365 nm ultraviolet light (above).

Anti-microbiological activity

The MIC values of the extracted samples against the microorganisms which are representative for common infectious agents were obtained from susceptibility testing using the micro broth dilution technique, and they are summarised in Figure 3 below. The MIC values of the levofloxacin and fluconazole were within the accuracy range (CLSI, 2014) throughout the study.

Microorganisms	1	2	3	4	5	6	7	8	9	10	11	12	14	15
<i>S. aureus</i> ATCC 29213	312,5	312,5	312,5	625	625	312,5	312,5	312,5	312,5	312,5	312,5	156,25	156,25	312,5
<i>E. faecalis</i> ATCC 29212	625	625	312,5	156,2	312,5	78	156,2	156,2	78	78	625	625	1250	625
<i>E. coli</i> ATCC 25922	312,5	625	312,5	312,5	1250	625	625	625	312,5	312,5	312,5	625	625	156,2
<i>K. pneumoniae</i> ATCC 4352	625	625	312,5	312,5	625	312,5	312,5	156,2	312,5	312,5	625	625	625	312,5
<i>P. aeruginosa</i> ATCC 27853	625	312,5	312,5	312,5	625	312,5	625	312,5	312,5	312,5	312,5	625	312,5	625
<i>C. albicans</i> ATCC 10231	625	312,5	312,5	625	312,5	312,5	625	625	312,5	625	312,5	625	625	625
<i>S. epidermidis</i> ATCC 12228	1250	1250	1250	625	1250	1250	625	625	625	1250	625	625	1250	625

Figure 3. Antimicrobial activities of substances (µg/mL).

Microbiological content determination evaluation

Microbial count results are calculated. The number of bacteria in 1 gram of turmeric should not exceed 10⁴ CFU/gr and the amount of mould should not exceed 10³ CFU/gr (USP DSC, 2012). Only two samples were in the normal range for the fungi count results, and the rest of the samples had values above normal. All samples had shown above-normal results in bacterial count results.

CONCLUSION

Recently, turmeric has gained attention all around the world and that makes its products quite popular and accessible. However, determinations of the quality of these turmeric

Table 1. Ash content determination, water content determination, bacterial count and fungi count values of 15 samples.

Sample no	Ash content determination values	Water content determination values	Fungi count values (CFU/gr)	Bacterial count values (CFU/gr)
1	4,86 %	9,02 %	2,6*10 ⁴	3,1*10 ⁸
2	% 7,65 %	9,43	1,75*10 ⁴	9,5*10 ⁷
3	7,22	8,92 %	4*10 ³	2,85*10 ⁶
4	6,12 %	8,89 %	6*10 ³	2,7*10 ⁶
5	6,91 %	9,19 %	5*10 ²	1,15*10 ⁶
6	7,55 %	9,16 %	2,2*10 ⁵	2,95*10 ⁷
7	5,91 %	9,56 %	5*10 ³	3,2*10 ⁶
8	6,01 %	7,91 %	0	1,2*10 ⁶
9	5,64 %	9,76 %	6*10 ³	4,3*10 ⁶
10	2,51 %	9,60 %	1,7*10 ⁴	1,35*10 ⁶
11	7,59 %	9,11 %	5*10 ³	1,35*10 ⁶
12	5,18 %	8,80 %	4,5*10 ³	2,4*10 ⁶
13	4,90 %	9,54 %	1,05*10 ⁴	1,95*10 ⁶
14	7,80 %	9,02 %	4*10 ³	1,15*10 ⁷
15	4,79 %	8,37 %	1,5*10 ⁴	3,5*10 ⁷

products are insufficient, hence pharmacognostical studies on these samples should be carried out to evaluate the reliability and effectiveness.

The most used form of turmeric in Turkey is the powdered form due to its cheap price and easy consumption. The most important factors determining the medicinal effect are the source of the plant, usage form (fresh or dried), and its chemical composition. The macroscopical and microscopical evaluations confirm the powdered samples belong to the rhizome of turmeric. The presence of major curcuminoids is also detected by TLC. According to total ash and water content value, samples were found almost within acceptable limits, no adulteration or foreign materials were observed. Although physicochemical evaluations have confirmed that the powdered samples contain curcuminoids and are also of medium quality, microbiological tests have shown us the presence of high levels of bacteria and fungi. Our microbiological identification studies have shown that these microorganisms are spore bacteria belonging to *Bacillus* species from saprophytic bacteria. The fungi that cause microbial contamination in plant samples were determined as mould fungi. For products offered in open packaging, this pollution is an expected result. Turmeric is not cultivated in our country; the contamination might have consisted of import stages or storage conditions in herbal stores.

As a result of this study in which 15 different samples were evaluated, a big question mark has occurred about the consumption of the open turmeric powders neither as a spice nor for medicinal purposes.

In conclusion, we may say that it is recommendable to buy turmeric rhizomes and to powder it before using it at home.

Peer-review: Externally peer-reviewed.

Author Contributions: Conception/Design of Study-A.M., G.G.T.; Data Acquisition- E.K., F.Y.; Data Analysis/Interpretation- G.G.T., B.Ö.Ç.; Drafting Manuscript- E.K., G.G.T.; Critical Revision of Manuscript- A.M., B.Ö.Ç., G.G.T.; Final Approval and Accountability- E.K., F.Y., G.G.T., B.Ö.Ç., A.M.

Conflict of Interest: The authors have no conflict of interest to declare.







Financial Disclosure: Authors declared no financial support.

REFERENCES

- Araujo, C. A. C., & Leon, L. L. (2001). Biological activities of *Curcuma longa* L. *Memórias do Instituto Oswaldo Cruz*, 96(5), 723-728.
- Baytop. T., (1980), *Farmakognozi Ders Kitabı* [Pharmacognosy Text-book], Fatih Yayınevi Matbaası, 220-224.
- BECİT, M., AYDIN, S., & BAŞARAN, N. (2017). Kurkuminin terapötik ve toksik etkilerinin değerlendirilmesi. *Literatür Eczacılık Bilimleri Dergisi*, 6(2), 126-142.
- Clinical and Laboratory Standards Institute (CLSI), (2000). Reference Method for Broth Dilution Antifungal Susceptibility Testing of Yeasts; Approved Standard M27-A NCCLS, Wayne, Pennsylvania.
- Clinical and Laboratory Standards Institute (CLSI), (2006). Methods for dilution antimicrobial susceptibility tests for bacteria that grow aerobically: Approved Standard M7-A5. Wayne, PA: CLSI.
- Clinical and Laboratory Standards Institute (CLSI), (2014). Performance standards for antimicrobial susceptibility testing; 2nd informational supplement. M100-S24. Wayne, PA: CLSI
- Gounder, D. K., & Lingamallu, J. (2012). Comparison of chemical composition and antioxidant potential of volatile oil from fresh, dried, and cured turmeric (*Curcuma longa*) rhizomes. *Industrial crops and products*, 38, 124-131.
- Hermann, P. T. Ammon and M A. Wahi '. 1991. *Pharmacology of Curcuma longa. Planta Med*, 57, 1-7.

- Jayaprakasha, G. K., Rao, L. J. M., & Sakariah, K. K. (2005). Chemistry and biological activities of *C. longa*. *Trends in Food Science & Technology*, 16(12), 533-548.
- Labban, L. (2014). Medicinal and pharmacological properties of Turmeric (*Curcuma longa*): A review. *Int J Pharm Biomed Sci*, 5(1), 17-23.
- Li, S., Yuan, W., Deng, G., Wang, P., Yang, P., & Aggarwal, B. (2011). Chemical composition and product quality control of turmeric (*Curcuma longa* L.), *Pharmaceutical Crops*, 2, 28-54.
- Omurtag, C., 1966, Genel Mikrobiyoloji Yayın Kılavuzu, Ankara Üniversitesi Eczacılık Fakültesi Yayınları, 208-215.
- Pothitirat, W., & Gritsanapan, W. (2006). Variation of bioactive components in *Curcuma longa* in Thailand. *Current Science*, 1397-1400.
- Prasad, S., & Aggarwal, B. B. (2011). Turmeric, the golden spice. *Herbal Medicine: Biomolecular and Clinical Aspects*. 2nd edition, 263-288.
- Prasad, S., Gupta, S. C., Tyagi, A. K., & Aggarwal, B. B. (2014). Curcumin, a component of golden spice: from bedside to bench and back. *Biotechnology advances*, 32(6), 1053-1064.
- Raina, V. K., Srivastava, S. K., Jain, N., Ahmad, A., Syamasundar, K. V., & Aggarwal, K. K. (2002). The essential oil composition of *Curcuma longa* L. cv. Roma from the plains of northern India. *Flavour and Fragrance Journal*, 17(2), 99-102.
- Singh, G., Kapoor, I. P. S., Singh, P., De Heluani, C. S., De Lampasona, M. P., & Catalan, C. A. (2010). Comparative study of chemical composition and antioxidant activity of fresh and dry rhizomes of turmeric (*Curcuma longa* Linn.). *Food and chemical toxicology*, 48(4), 1026-1031.
- (2012), USP Dietary Supplements Compendium, Rockville, (978-1-936424-07-8)
- (2016), *Türk Farmakopesi*, [Journal of Turkish Pharmacopeia]. Ankara, Turkey: Anıl Reklam Matbaa Ltd. Şti, Volume II, 3498-3499.
- (06.11.2020), Retrieved from <http://powo.science.kew.org/taxon/urn:lsid:ipni.org:names:796451-1>

Isolation of potential liver x receptor alpha agonist and antioxidant compounds from *Hypericum microcalycinum* Boiss. & Heldr.

Seçil Sarıkaya Aydın¹ , Vahap Murat Kutluay¹ , Toshiaki Makino² , Makoto Inoue³ , Ümmühan Şebnem Harput⁴ , İclal Saraçoğlu¹ 

¹Hacettepe University, Faculty of Pharmacy, Department of Pharmacognosy, Ankara, Turkey

²Nagoya City University, Graduate School of Pharmaceutical Sciences, Nagoya, Japan

³Aichi Gakuin University, School of Pharmacy, Laboratory of Medicinal Resources, Nagoya, Japan

⁴Freelance Scientist, Previous address: Hacettepe University, Faculty of Pharmacy, Department of Pharmacognosy, Ankara, Turkey

ORCID IDs of the authors: S.S.A. 0000-0003-4692-9117; V.M.K. 0000-0003-4135-3497; T.M. 0000-0002-2524-8745; M.I. 0000-0003-0116-320X; Ü.Ş.H. 0000-0002-2641-3263; İ.S. 0000-0003-0555-6262

Cite this article as: Sarıkaya Aydın, S., Kutluay V. M., Makino, T., Inoue, M., Harput, U. S., & Saracoglu, I. (2021). Isolation of potential liver x receptor alpha agonist and antioxidant compounds from *Hypericum microcalycinum* Boiss. & Heldr. *İstanbul Journal of Pharmacy*, 51 (1), 98-104.

ABSTRACT

Background and Aims: *Hypericum microcalycinum* Boiss. & Heldr. is used for inflammatory diseases in Anatolia. The involvement of liver X receptors (LXRs) and free radicals in inflammatory diseases, activation of LXRs, and high radical contents in cancerous tissue and organs prompted us to determine the radical scavenging and LXR α agonist activity of aqueous fraction of methanol extract and fractions of *H. microcalycinum* along with the isolation studies from active fractions.

Methods: Isolation studies were carried out on chromatographic techniques. DPPH, NO, and SO radical scavenging activity methods were used for the determination of antioxidant activity, and a LXRE reporter gene assay was used for the determination of LXR α agonist activity.

Results: While the extract showed weak LXR α agonist activity, phenolic compounds- rich fractions showed moderate activity. DPPH radical scavenging capacities of the extract and some fractions seemed to be very high as well as some isolated compounds. Bioactivity- guided studies resulted in the isolation of catechin (1), epicatechin (2), apigenin-8-C-(2-O-acetyl)-glucopyranoside (3), quercetin-3-O- β -glucopyranoside (4), quercetin-3-O- β -arabinopyranoside (5), kaempferol-3-O- β -arabinopyranoside (6), luteolin-8-C- β -glucopyranoside (orientin) (7).

Conclusion: According to our results, compounds 1, 2, 4, and 5 may be responsible for the anti-inflammatory effects of *H. microcalycinum* as a function of LXR α agonist and free radical scavenging effects.

Keywords: *Hypericum microcalycinum*, phenolic compounds, free radical scavenging, LXR α agonist activity

INTRODUCTION

Natural products or therapeutic agents derived from natural sources have an important role in human health. In a continuation of our studies to find new bioactive compounds from herbal sources, we have focused on the *Hypericum* species, which are well known for their antidepressant, anti-inflammatory, antiproliferative and antimicrobial activities (Boga et al., 2016; Fobofou et al., 2015). In Anatolia, *Hypericum* species are used as an antispasmodic, sedative, and antihelmintic internally; antiseptic and for wound healing externally (Baytop, 1984). The constituents of the genus have been previously investigated, and several types

Address for Correspondence:

Vahap Murat KUTLUAY, e-mail: muratkutluay@hacettepe.edu.tr

Submitted: 06.07.2020

Revision Requested: 26.08.2020

Last Revision Received: 19.10.2020

Accepted: 03.12.2020

This work is licensed under a Creative Commons Attribution 4.0 International License.



of compounds were determined mainly naphthodianthrones, flavonoids, acylphloroglucinol derivatives, tannins, xanthones, and essential oils (Eroglu, Aksu, & Mat, 2008; Zorzetto et al., 2015). As part of our continuing research for bioactive metabolites from herbal medicines, we carried out chemical and biological investigations on the aerial parts of *H. microcalycinum* Boiss. & Heldr since detailed biological activity studies on this plant are lacking in the literature. *H. microcalycinum* has different synonyms which are *H. elongatum* C. A. Mey. var. *microcalycinum* (Boiss.& Heldr.) A. Ramos (Nunez, 1985) and *H. hyssopifolium* Chaix. subsp. *elongatum* (Ledeb.) Woron var. *microcalycinum* (Boiss.& Heldr.) (Robson, 1980).

The role of free radicals and reactive oxygen in the species is becoming increasingly important in the pathogenesis of diabetes, arteriosclerosis, cardiovascular diseases, cancer, and several neurodegenerative disorders (Aktas, Genc, Gozcelioglu, Konuklugil, & Harput, 2013). Nuclear receptors are one of the major targets for the development of new potential agents in diseases like inflammation, rheumatoid arthritis, obesity, diabetes, and cancer (Vedin, Gustafsson, & Steffensen, 2013). Since nuclear receptor signaling has an important function during the burying of dead cells and suppression of inflammation, nuclear receptors such as glucocorticoid receptors, PPAR (peroxisome proliferator activated receptors), and liver X receptors (LXR), are important therapeutic targets in inflammatory diseases (Szondy, Garabuczi, Joos, Tsay, & Sarang, 2014).

Liver X receptors were first identified in the mid-1990s (Fessler, 2018). The LXRs, LXR α (NR1H3), and LXR β (NR1H2) form a heterodimer with the retinoid x receptor (RXR), and its activity can be regulated by ligands for either LXR or RXR (Willy, 1995; Wang, Nakashima, Hirai, & Inoue, 2019). While LXR α and LXR β have similar DNA and ligand binding domains in humans, their distribution differs in tissues. LXR α is found predominantly in liver, intestine, kidney, spleen, macrophages, and adipose tissues, whereas LXR β is found more ubiquitously (Viennois et al., 2012). Previous studies have shown that both isoforms of LXR play a role in the inhibition of some inflammatory genes such as iNOS, COX2, IL6, the chemokines monocyte chemoattractant protein-1 (MCP-1) and MCP-3, and matrix metalloproteinase-9 (MMP9) (Joseph, Castrillo, Laffitte, Mangelsdorf, & Tontonoz, 2003).

It has been shown that LXR α has also a role in preventing oxidative stress and can affect oxidative stress response by regulating the expression of antioxidant genes (Gong et al., 2009). Nuclear receptors are one of the major targets for the development of new potential agents in diseases like inflammation, rheumatoid arthritis, obesity, diabetes, and cancer (Vedin et al., 2013).

Natural products and nature-derived compounds attract more attention day by day in the treatment of human and animals' diseases. The members of the *Hypericum* genus have been used in the treatment of various diseases worldwide and have been traded in the global marketplace. In this study, we focus on *H. microcalycinum*, which has not been studied in detail, to determine the potential antioxidant and anti-inflammatory activities. We aimed to identify the anti-inflammatory potential of the extract and to determine the bioactive compounds. For this purpose, the LXR response element (LXRE) reporter gene

assay (to determine LXR α agonist activity) and DPPH, NO, and SO radical scavenging activities (to determine antioxidant activity) for the aqueous fraction of methanol extract and different polyamide column fractions of *H. microcalycinum* were tested. As *Hypericum* species have been shown to be involved in inflammatory mechanisms, we hypothesized that it could be a function of the plant as a nuclear receptor activator and/or the extract's antioxidant activity.

MATERIALS AND METHODS

General

Fractionation and isolation studies were carried out on chromatographic techniques such as silica gel (Kieselgel 60, 60–230 mesh, Merck, Darmstadt, Germany), polyamide (Sigma Aldrich, St. Louis, MI, USA). In medium pressure liquid chromatography (MPLC) LiChroprep C18 (40–63 μ m, Merck) was used as an adsorbent. The system was equipped with a Büchi column (3,5 x 45 cm). 5–15 bar pressure and 5 ml/min flow rates were used. Silica gel 60 F254 plates (Merck) were used during isolation studies and CHCl₃–MeOH–H₂O (61:32:7, 70:30:3, 80:20:2) was used as the solvent system.

NMR spectra were recorded on an Agilent Varian VNS500 spectrometer (Agilent, Santa Clara, CA, USA). Positive-mode ESITOFMS was obtained on a JEOL JMS-T100LP AccuTOF LC-plus 4G spectrometer (JEOL, Tokyo, Japan) using a sample dissolved in MeOH.

3-(4,5-dimethylthiazol-2-yl)-2,5-diphenyltetrazolium bromide (MTT), DPPH, nitro blue tetrazolium (NBT), sodium nitroprusside, Folin–Ciocalteu reagent, gallic acid, ascorbic acid (AA) were obtained from Sigma–Aldrich. 3-*t*-butyl-4-hydroxyanizole (BHA) was purchased from Nacalai Tesque (Kyoto, Japan). Sulfanilamide and naphthylethylenediamine dihydrochloride were obtained from Merck.

HEK293 (Human embryonic kidney) cell line was obtained from Riken Bioresource Center Cell Bank (Japan). Minimum Essential Medium Earle's salts (MEM's Earle), trypsin were obtained from Sigma-Aldrich. Fetal bovine serum (FBS) was purchased from Biowest (Nuaille, France). Penicillin, streptomycin, and MEM non-essential amino acid solution were obtained from Fujifilm Wako Pure Chemical Industries (Osaka, Japan). T0901317 was purchased from Cayman Chemical (Ann Arbor, MI, USA).

Plant material

The aerial parts of *H. microcalycinum* were collected from Ağrı-Doğubeyazıt in July 2011 and identified by Prof. Dr. Hayri Duman (Gazi University, Faculty of Science, Department of Botany, Ankara, Turkey). A voucher specimen has been deposited in the Herbarium of the Faculty of Pharmacy, Hacettepe University, Ankara, Turkey (HUEF 11006).

Extraction and isolation

The air-dried aerial parts of the plant (90.8127 g) were extracted with MeOH at 40°C for 12 h (4 x 400 mL). A rotary equipped with a water bath and a 2 L flask was used for the extraction. The MeOH solutions were evaporated under vacuum to yield MeOH extract and it was dissolved in water and partitioned with petroleum ether to remove chlorophylls and other lipophilic compounds.

The aqueous fraction was lyophilized to yield 12.85 g dry weight. The aqueous fraction was applied to polyamide column chromatography to get four sub-fractions using increasing concentrations of methanol (0–25–50–75–100%). The aqueous fraction of methanol extract and polyamide column fractions were tested for radical-scavenging and LXRA agonist activities. Further isolation studies were continued on the active and phenolic compound rich fraction (Fraction D; 795 mg). Fr. D was applied to MPLC using 0–100% methanol as a solvent system. Five sub-fractions were obtained, and the fraction of 27% methanol was applied to silica gel column chromatography using different concentrations of CHCl_3 : CH_3OH as a mobile phase to give compounds **1** and **2** as a mixture (22.6 mg). The fraction of 45 % methanol was applied to silica gel column chromatography using different concentrations of CHCl_3 : CH_3OH as a mobile phase to give compound **3** in pure form (18.0 mg) and two of MPLC fractions were applied to preparative TLC to get compound **4** (20.3 mg) and compound **5** (70.8 mg) in pure form. MPLC fraction of 45% methanol was applied to preparative TLC to get compound **6** (3.4 mg) in pure form. MPLC fraction of 40% methanol was applied to preparative TLC to get compound **7** (5.1 mg) in pure form.

Antioxidant activity

DPPH radical scavenging activity

The DPPH radical scavenging effect was assessed by the discoloration of methanol solution of DPPH spectroscopically; AA and BHA were used as positive controls (Hatano et al., 1989; Jensen, Gotfredsen, Harput, & Saracoglu, 2010). DPPH (1 mM) solution was added to the MeOH solution of the extract, fractions, or compounds at various concentrations. The reaction mixture was shaken vigorously, and the absorbance of the remaining DPPH was measured at 517 nm after 30 min.. All the analyses were done in triplicate. Radical scavenging activity was expressed as the inhibition percentage.

SO radical scavenging activity by alkaline DMSO method

The method of Kunchandy and Rao was used to detect SO radical-scavenging activity of the samples, with slight modification. In brief, a SO radical was generated in a nonenzymatic system. The reaction mixture containing nitro blue tetrazolium (1 mg/mL solution in DMSO) and the sample or standard compounds was dissolved in DMSO. A total of 100 μL of alkaline DMSO (1 mL DMSO containing 5 mM NaOH in 0.1 mL water) was added to yield a final volume of 140 μL . The absorbance was measured at 560 nm by using a microplate reader (Kunchandy & Rao, 1990; Srinivasan, Chandrasekar, Nanjan, & Suresh, 2007).

NO radical scavenging activity

To determine NO radical scavenging activity of the samples, a serial diluted sample was added to a 96-well flat-bottomed plate. 10 mM sodium nitroprusside, dissolved in phosphate-buffered saline, was added to each well and the plate was incubated under light at room temperature for 150 minutes. Finally, an equal volume of the Griess reagent (1% sulfanilamide, 0.1% naphthylethylenediamine dihydrochloride, 2.5% H_3PO_4) was added to each well to measure the nitrite content. After chromophore was formed at room temperature in 10 minutes, absorbance at 577 nm was measured on a microplate reader (Tsai, Tsai, Yu, & Ho, 2007).

LXRA agonist activity

The LXRE reporter gene assay was used to determine LXRA agonist activity. HEK293 cells were cultured in MEM (Minimum Essential Medium) supplemented with 10% FBS, 1% nonessential amino acids, 50 U/ml penicillin, and 50 $\mu\text{g}/\text{ml}$ streptomycin at 37 °C in a humidified atmosphere of 5% CO_2 in the air.

The calcium phosphate co-precipitation method was used for transfection. For LXR luciferase reporter assay, pBApo-CMW-hLXR- α (30 ng), pGL4.1-DR4-Luc (120 ng), pCMX- β -gal expression vector (30 ng), and carrier DNA pUC18 were used to yield a total of 600 ng of DNA per well. After 6 hours, the cells were treated with test samples for 36 hours of incubation. The luciferase and β -galactosidase activities were analyzed from cell lysates using a luminescence reader and a spectrophotometer, respectively. The results were given in fold induction values relative to vehicle-treated cells after normalization of luciferase activity by β -galactosidase (Kotani, Tanabe, Mizukami, Makishima, & Inoue, 2010; Nakashima, Murakami, Tanabe, & Inoue, 2014).

RESULTS AND DISCUSSION

The methanol extract of *H. microcalycinum* aerial part was suspended in water and partitioned with petroleum ether. The aqueous fraction was used for the phytochemical and biological analysis. The aqueous fraction was subjected to polyamide column chromatography to afford four main fractions.

To evaluate LXRA agonist activity, the aqueous fraction of *H. microcalycinum* extract and its main polyamide column fractions were tested at a concentration of 100 $\mu\text{g}/\text{mL}$. In this study, an LXRA agonist, T09011317, was used as a positive control at the concentrations of 1, 10 and 100 nM. The results were given as fold induction values normalized by β -galactosidase. While the extract showed weak LXRA agonist activity, Fr. D, the phenolic compound-rich fraction, showed moderate activity with a fold value of 1.37 (Figure 1, Table 1).

Table 1. LXRA agonist activities of the *Hypericum microcalycinum* extract and fractions* Effects of *Hypericum microcalycinum* (aerial parts) and fractions on LXRE reporter gene transcription at 100 $\mu\text{g}/\text{ml}$ concentration were given as fold values.

Samples	Fold Value
Aqueous extract	0.96±0.02
Fr. A	1.15±0.06
Fr. B	1.6±0.06
Fr. C	2.22±0.07
Fr. D	1.37±0.08
T0901317 1 nM	1.22±0.11
T0901317 10 nM	2.91±0.13
T0901317 100 nM	5.49±0.34
Control	1±0.03

*Three independent test results were considered, averages and standard error means were given in the table.

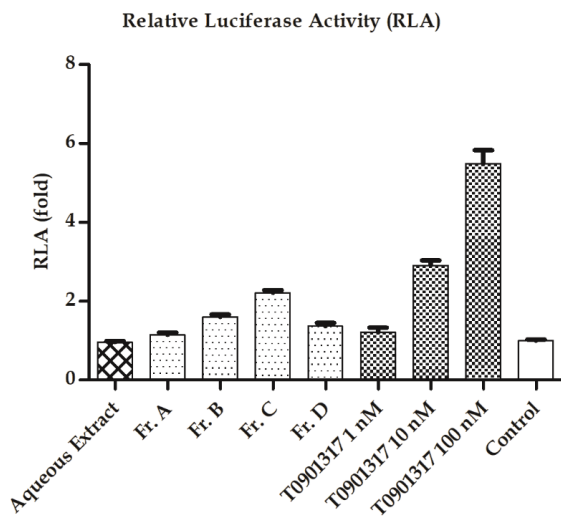


Figure 1. Effects of *Hypericum microcalycinum* (aerial parts) on LXRE reporter gene transcription at 100 $\mu\text{g}/\text{mL}$ concentration. Three independent test results were considered, averages and standard error means were given in the figure.

The aqueous *H. microcalycinum* extract and fractions of polyamide column were tested against 2,2-diphenyl-1-picrylhydrazyl (DPPH), NO, and SO radicals for antioxidant activity. Results were evaluated with the known antioxidants ascorbic acid (AA), butyl-4-hydroxyanizole (BHA), and quercetin. Tested fractions showed radical scavenging activity depending on their phenolic contents. Fr. A is the non-phenolic fraction of the polyamide column that showed the lowest radical scavenging activity. Fr. D, the phenolic-rich fraction, was found to possess high radical scavenging activity against the tested radicals. Its radical scavenging activity was comparable to that of known antioxidants AA, BHA, and quercetin. Radical scavenging activity (inhibition %) of Fr. D at a concentration of 200 $\mu\text{g}/\text{mL}$ against DPPH, NO and SO radicals were found as 90.5, 59.9, and 65.5 respectively, whereas radical scavenging activity (inhibition %) of Fr. A at a concentration of 200 $\mu\text{g}/\text{mL}$ against DPPH, NO and SO radicals were found as 0.8, 24.4, and 42.1 respectively.

Repeated chromatographies of the flavonoid fraction (Fr. D), which was eluted with 75–100% methanol, resulted in the isolation of seven compounds. The spectroscopic data (1D and 2D-NMR, and ESITOFMS) of the isolated compounds were compared to the data of the compounds that were given in the references and their structures were identified as follows: Catechin (**1**) and epicatechin (**2**) (Donovan, Luthria, Stremple, & Waterhouse, 1999), apigenin-8-C-(2-O-acetyl)-glucopyranoside (**3**) (Zhang & Xu, 2003), quercetin-3-O- β -glucopyranoside (**4**) (Islam et al., 2012), quercetin-3-O- α -arabinopyranoside (**5**) (Kadota et al., 1990), kaempferol-3-O- β -arabinopyranoside (**6**) (Nicollier & Thompson, 1983), luteolin-8-C- β -glucopyranoside (orientin) (**7**) (Almahy & Fouda, 2013) (Figure 2). All data is provided in the Supplementary document. Catechin and epicatechin were obtained as a mixture (ratio 1:3). Apigenin-8-C-(2-O-acetyl)- β -glucopyranoside was isolated for the first time from a *Hypericum* species in this study.

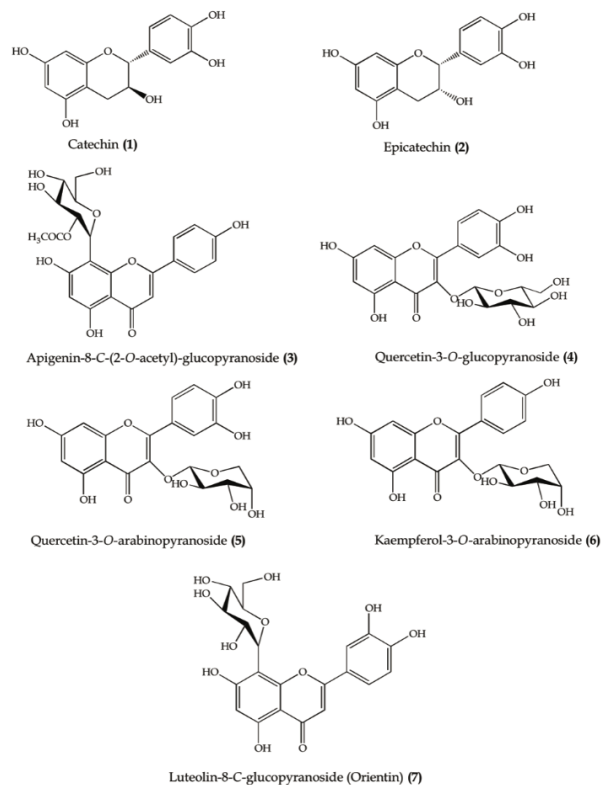


Figure 2. Isolated compounds from *Hypericum microcalycinum* Boiss.&Heldr.

Catechin (**1**): ^1H NMR (500 MHz, CD_3OD): 6.87 (1H, d, $j = 1.9$, H-2'), 6.80 (1H, dd, $j = 8.0$ Hz, H-5'), 6.76 (1H, dd, $j = 8.2/1.3$, H-6'), 5.96 (1H, d, $j = 2.31$ Hz, H-8), 5.89 (1H, d, $j = 2.31$ Hz, H-6), 4.59 (1H, d, $j = 7.5$ Hz, H-2), 4.00 (1H, ddd, H-3), 2.54–2.90 (2H, dd, H-4), ^{13}C NMR (125 MHz, CD_3OD): 157.86 (C-7), 157.59 (C-9), 156.93 (C-5), 146.26 (C-3'), 146.24 (C-4'), 132.30 (C-1'), 120.04 (C-6'), 116.08 (C-5'), 115.27 (C-2'), 100.82 (C-10), 96.29 (C-8), 95.50 (C-6), 82.87 (C-2), 68.83 (C-3), 28.54 (C-4)

Epicatechin (**2**): ^1H NMR (500 MHz, CD_3OD): 7.01 (1H, d, $j = 1.9$, H-2'), 6.84 (1H, dd, $j = 8.4/1.8$, H-6'), 6.79 (1H, dd, $j = 8.1$ Hz, H-5'), 5.98 (1H, d, $j = 2.37$ Hz, H-8), 5.95 (1H, d, $j = 2.29$ Hz, H-6), 4.85 (1H, s, H-2), 4.21 (1H, m, H-3), 2.77–2.88 (2H, dd, H-4), ^{13}C NMR (125 MHz, CD_3OD): 158.02 (C-7), 157.69 (C-9), 157.38 (C-5), 145.96 (C-3'), 145.80 (C-4'), 132.24 (C-1'), 119.40 (C-6'), 115.89 (C-5'), 115.33 (C-2'), 100.07 (C-10), 96.39 (C-6), 95.87 (C-8), 79.90 (C-2), 67.50 (C-3), 29.27 (C-4)

Apigenin-8-C-(2-O-acetyl) glucopyranoside (**3**): ^1H NMR (500 MHz, CD_3OD): 8.07 (1H, d, $j = 8.8$ Hz, H-2'/6'), 6.99 (1H, d, $j = 8.8$ Hz, H-3'/5'), 6.64 (1H, s, H-3), 6.25 (1H, s, H-6), 5.57 (1H, dd, $j = 4.5/10.2$ Hz, H-2''), 5.11 (1H, d, $j = 10.2$ Hz, H-1''), 4.02 (1H, dd, $j = 2.1/12.1$, H-6''a), 3.86 (1H, dd, $j = 5.7/12.1$, H-6''b), 3.74 (1H, d*, H-3''), 3.74 (1H, d, H-4''), 3.54 (1H, m, H-5''), 1.70 (3H, s, CH₃); ^{13}C NMR (125 MHz, CD_3OD): 184.15 (C=O), 166.71 (C-2), 163.90 (C-7), 162.99 (C-5), 162.76 (C-4'), 158.58 (C-9), 130.13 (C-2'/6'), 123.66 (C-1'), 116.97 (C-3'/5'), 105.75 (C-10), 103.66 (C-3), 103.60 (C-8), 98.97 (C-6), 83.14 (C-5''), 77.74 (C-3''), 74.08 (C-2''), 73.00 (C-1''), 72.24 (C-4''), 62.93 (C-6''), 20.52 (CH₃).

Quercetin-3-O-glucopyranoside (**4**): ¹H NMR (500 MHz, CD₃OD): 7.75 (1H, d, j = 2.1 Hz, H-2'), 7.61 (1H, dd, j = 2.1/8.4 Hz, H-6'), 6.88 (1H, d, j = 8.4 Hz, H-5'), 6.26 (1H, d, j = 1.8 Hz, H-8), 6.11 (1H, d, j = 1.8 Hz, H-6), 5.15 (1H, d, j = 7.8 Hz, H-1''), 3.74 (1H, dd, j = 2.3/11.9 Hz, H-6''a), 3.62 (1H, dd, j = 5.2/11.9 Hz, H-6''b), 3.52 (1H, dd, j = 7.8/9.0 Hz, H-2''), 3.45 (1H, m, H-3''), 3.39 (1H, m, H-4''), 3.25 (1H, m, H-5''), ¹³C NMR (125 MHz, CD₃OD): 178.60 (C-4), 170.30 (C-7), 162.59 (C-5), 158.99 (C-2), 158.13 (C-9), 150.45 (C-4'), 146.06 (C-3'), 135.39 (C-3), 123.07 (C-6'), 122.96 (C-1'), 117.30 (C-2'), 116.05 (C-5'), 105.09 (C-1''), 103.65 (C-10), 102.20 (C-6), 96.33 (C-8), 78.33 (C-5''), 78.20 (C-3''), 75.02 (C-2''), 71.14 (C-4''), 62.53 (C-6'').

Quercetin-3-O-arabinopyranoside (**5**): ¹H NMR (500 MHz, CD₃OD): 7.78 (1H, d, j = 2.1 Hz, H-2'), 7.61 (1H, dd, j = 2.1/8.5 Hz, H-6'), 6.91 (1H, d, j = 8.5 Hz, H-5'), 6.44 (1H, d, j = 2.1 Hz, H-8), 6.24 (1H, d, j = 2.1 Hz, H-6), 5.20 (1H, d, j = 6.5 Hz, H-1''), 3.94 (1H, dd, j = 6.5/8.4 Hz, H-2''), 3.89 (1H, m, H-5''a), 3.88 (1H, brs, H-4''), 3.68 (1H, dd, j = 3.2/8.4, H-3''), 3.48 (1H, d, j = 10.4, H-5'' b); ¹³C NMR (125 MHz, CD₃OD): 179.49 (C-4), 164.07 (C-7), 163.07 (C-5), 158.71 (C-9), 158.44 (C-2), 149.96 (C-4'), 145.99 (C-3'), 135.65 (C-3), 123.03 (C-6'), 122.89 (C-1'), 117.45 (C-2'), 116.17 (C-5'), 105.65 (C-10), 104.62 (C-1''), 99.87 (C-6), 94.69 (C-8), 74.12 (C-3''), 72.87 (C-2''), 69.10 (C-4''), 66.94 (C-5'').

Kaempferol-3-O-arabinopyranoside (**6**): ¹H NMR (500 MHz, CD₃OD): 6.15 (1H, d, j = 2.0 Hz, H-6), 6.02 (1H, d, j = 2.0 Hz, H-8), 8.05 (1H, d, j = 8.8 Hz, H-2'/H-6'), 6.85 (1H, d, j = 8.7 Hz, H-3'/H-5'), 4.95 (1H, d, j = 6.5, H-1''), 3.92 (1H, dd, j = 8.4/6.5, H-2''), 3.65 (1H, dd, j = 3.4/8.3, H-3''), 3.81 (1H, m, H-4''), 3.46 (1H, dd, j = 12.5/1.0, H-5''b), 3.83 (1H, d, j = 12, H-5''a); ¹³C NMR (125 MHz, CD₃OD): 158.5 (C-2 j), 135.5 (C-3), 170.29 (C-4), 159.31 (C-5), 97.40 (C-6), 162.36 (C-7), 103.62 (C-8), 154.81 (C-9), 102.50 (C-10), 122.1 (C-1'), 131.97 (C-2'), 116.89 (C-3'), 163.2 (C-4'), 116.89 (C-5'), 131.97 (C-6'), 105.40 (C-1''), 72.80 (C-2''), 74.33 (C-3''), 69.12 (C-4''), 66.92 (C-5'').

Luteolin-8-C-glucopyranoside (Orientin) (**7**): ¹H NMR (500 MHz, CD₃OD): 7.56 (1H, brs, H-2'), 7.51 (1H, dd, j = 8.2, H-6'), 6.92 (1H, d, j = 8.2, H-5'), 6.51 (1H, s, H-3), 6.23 (1H, s, H-6), 5.05 (1H, d, j = 9.9, H-1''), 4.15 (1H, t, H-2''), 3.97 (1H, d, j = 10.6, H-6''a), 3.86* (1H, H-6''b), 3.69 (1H, m, H-4''), 3.60 (1H, m, H-3''), 3.53 (1H, m, H-5''); ¹³C NMR (125 MHz, CD₃OD): 183.68 (C-4), 166.30 (C-7), 166.30 (C-2), 162.49 (C-5), 158.0 (C-9), 151.72 (C-4'), 147.34 (C-3'), 123.72 (C-1'), 120.73 (C-6'), 116.80 (C-5'), 114.53 (C-2'), 104.48 (C-3), 104.0 (C-10), 103.62 (C-8), 97.40 (C-6), 82.83 (C-5''), 80.48 (C-3''), 75.5 (C-1''), 72.90 (C-2''), 72.50 (C-4''), 63.10 (C-6'').

As seen in Table 2, five of the isolated compounds were tested for their radical scavenging activity because of their adequate amount for testing. While four of them showed strong scavenging activity, compounds **1** and **2**, which were a 1:3 mixture of catechin-epicatechin, exhibited the strongest free radical scavenging activity. Its activity was found to be more potent or very close to that of AA, BHA, and quercetin in the case of nitric oxide and superoxide radicals.

Catechin and epicatechin have shown high antioxidant activity due to their high number of hydroxyl groups (Prochazkova, Bousova, & Wilhelmova, 2011). In previous studies have report-

Table 2. Radical scavenging activities of the Hypericum microcalycinum extract and isolated compounds*.

Samples	Radical scavenging IC ₅₀ (µg/ml) ^a		
	DPPH	NO	SO
Aqueous extract	51.8±0.86	>1000	134.5±3.57
Compounds 1 and 2 ^b	23.1±0.26	38.9±5.71	33.5±1.11
Compound 3	358.8±6.36	85.5±1.04	>800
Compound 4	53.2±3.00	69.6±6.78	121.2±6.48
Compound 5	25.5±0.18	61.8±4.33	72.7±4.59
AA	9.1±0.08	66.6±4.49	25.2±0.81
BHA	6.7±0.17	310.7±10.34	>800
Quercetin	6.2±0.04	55.3±1.89	14.3±0.73

^a Radical scavenging activities of the isolated compounds and the references on DPPH, NO and SO radicals (BHA: butyl-4-hydroxy-anizole; AA: ascorbic acid); ^b Compounds **1** and **2** were isolated as a mixture (ratio 1:3); * Compounds **6** and **7** were not assessed because of the limited amount of sample; Three independent test results were considered, averages and standard deviations were given in table.

ed that the *o*-dihydroxy group in the B ring of flavonoids and the functional hydroxyl groups in the 3- and 5- positions also mediated antioxidant activity. Glycosylation at position 3 also decreases the radical scavenging (Prochazkova et al., 2011). The results of our study supported these data. According to the present research, it was found that compounds 1, 2, 4, and 5 show higher antioxidant activity. Comparison results of compounds 4 and 5 with quercetin support that glycosylation reduces the antioxidant effect. The results of DPPH radical scavenging assay in this study were compared to results obtained from previous literature. The IC₅₀ values of compounds 1 and 2 (catechin-epicatechin mixture), compound 4 (quercetin-3-O-glucopyranoside), compound 5 (quercetin-3-O-arabinopyranoside), and the positive control (quercetin) were found as 23.1, 53.2, 25.5, and 6.2 µg/mL, respectively. These data were similar to those in previous literature, in which IC₅₀ values of catechin, epicatechin, quercetin-3-O-glucopyranoside, quercetin-3-O-arabinopyranoside, and quercetin were reported as 14.3, 9.9, 22, 27.9, and 7.7 µg/mL, respectively (Razavi, Zahri, Zarrini, Nazemiyeh, & Mohammadi, 2009; Sarian et al., 2017; Zhang et al., 2005).

Previous studies on the structure-activity relationship studies of flavonoids suggested that hydroxyl group at position 3 could be important to activate LXRα. For example, while quercetin acts as an agonist, luteolin shows antagonist activity for LXRα (Fouache et al., 2019; Francisco et al., 2016). The hydroxyl group at the positions 5,7 and 4' are also necessary to show agonist activity (Fouache et al., 2019). The studies also revealed that not only aglycons, but also flavonoid glycosides could also activate LXRα (Hiebl, Ladurner, Latkolik, & Dirsch, 2018). Kaempferol-3-O-β-glucopyranoside also showed potent activity for LXRα with an EC₅₀ value of 1.8 µM. Quercetin-3-O-gluc-

uronide was also shown to activate LX α (Ohara et al., 2013). These findings suggest that compounds **4**, **5**, and **6** might be responsible for the LX α agonist activity of the extract.

CONCLUSION

Hypericum species has widespread use in traditional and contemporary medicine for its antidepressant, anti-inflammatory, antiproliferative and antimicrobial activities. According to our results, isolated compounds, particularly compounds **1**, **2**, **4** and **5** from active fractions may be responsible for the anti-inflammatory effects of *H. microcalycinum* as a function of LX α agonist and free radical scavenging effects.

Also, this is the first study for the isolation of apigenin-8-C-(2-O-acetyl)- β -glucopyranoside, **3** from a *Hypericum* species.

Peer-review: Externally peer-reviewed.

Author Contributions: Conception/Design of Study- S.S.A., V.M.K., Ü.Ş.H., İ.S.; Data Acquisition- S.S.A., V.M.K.; Data Analysis/Interpretation- S.S.A., V.M.K., T.M., M.I., Ü.Ş.H., İ.S.; Drafting Manuscript- S.S.A., V.M.K., Ü.Ş.H.; Critical Revision of Manuscript- V.M.K., T.M., M.I., Ü.Ş.H., İ.S.; Final Approval and Accountability- S.S.A., V.M.K., T.M., M.I., Ü.Ş.H., İ.S.

Conflict of Interest: The authors have no conflict of interest to declare.







Financial Disclosure: Authors declared no financial support.

REFERENCES

- Aktas, N., Genc, Y., Gozcelioglu, B., Konuklugil, B., & Harput, U. S. (2013). Radical scavenging effect of different marine sponges from mediterranean coasts. *Records of Natural Products*, 7(2), 96-104.
- Almahy, H. A., & Fouda, H. A. R. (2013). Isolation of Luteolin-8-C- β -D-glucopyranoside from the roots of *Salvadora persica* (Rutaceae). *Journal of Current Chemical and Pharmaceutical Sciences*, 3, 49-53.
- Baytop, T. (1999). *Türkiye'de Bitkilerle Tedavi: Geçmişte ve Bugün*, (pp. 166-167). Istanbul, Turkey: Istanbul Üniversitesi Yayınları.
- Boga, M., Ertas, A., Eroglu-Ozkan, E., Kizil, M., Ceken, B., & Topcu, G. (2016). Phytochemical analysis, antioxidant, antimicrobial, anticholinesterase and DNA protective effects of *Hypericum capitatum* var. *capitatum* extracts. *South African Journal of Botany*, 104, 249-257. doi: 10.1016/j.sajb.2016.02.204
- Donovan, J. L., Luthria, D. L., Stremple, P., & Waterhouse, A. L. (1999). Analysis of (+)-catechin, (-)-epicatechin and their 3'- and 4'-O-methylated analogs - A comparison of sensitive methods. *Journal of Chromatography B-Analytical Technologies in the Biomedical and Life Sciences*, 726(1-2), 277-283. doi: 10.1016/S0378-4347(99)00019-5
- Eroglu, E., Aksu, B. Z., & Mat, A. (2008). An overview on *Hypericum* species of Turkey. *Planta Medica*, 74(9), 1139-1139.
- Fessler, M. B. (2018). The challenges and promise of targeting the Liver X Receptors for treatment of inflammatory disease. *Pharmacology & Therapeutics*, 181, 1-12. doi: 10.1016/j.pharmthera.2017.07.010
- Fobofou, S. A., Franke, K., Sanna, G., Porzel, A., Bullita, E., La Colla, P., & Wessjohann, L. A. (2015). Isolation and anticancer, anthelmintic, and antiviral (HIV) activity of acylphloroglucinols, and regioselective synthesis of empetrifranzins from *Hypericum roeperianum*. *Bioorganic & Medicinal Chemistry*, 23(19), 6327-6334. doi: 10.1016/j.bmc.2015.08.028
- Fouache, A., Zabaïou, N., De Jossineau, C., Morel, L., Silvente-Poirot, S., Namsi, A., . . . Trousson, A. (2019). Flavonoids differentially modulate liver X receptors activity—Structure-function relationship analysis. *The Journal of Steroid Biochemistry and Molecular Biology*, 190, 173-182. doi: https://doi.org/10.1016/j.jsbmb.2019.03.028
- Francisco, V., Figueirinha, A., Costa, G., Liberal, J., Ferreira, I., Lopes, M. C., . . . Batista, M. T. (2016). The flavone luteolin inhibits liver X receptor activation. *Journal of Natural Products*, 79(5), 1423-1428. doi: 10.1021/acs.jnatprod.6b00146
- Gong, H., He, J., Lee, J. H., Mallick, E., Gao, X., Li, S., . . . Xie, W. (2009). Activation of the liver X receptor prevents lipopolysaccharide-induced lung injury. *The Journal of Biological Chemistry*, 284(44), 30113-30121. doi: 10.1074/jbc.M109.047753
- Hatano, T., Edamatsu, R., Hiramatsu, M., Mori, A., Fujita, Y., Yasuhara, T., . . . Okuda, T. (1989). Effects of the interaction of tannins with co-existing substances. 6. Effects of tannins and related polyphenols on superoxide anion radical, and on 1,1-diphenyl-2-picrylhydrazyl radical. *Chemical & Pharmaceutical Bulletin*, 37(8), 2016-2021.
- Hiebl, V., Ladurner, A., Latkolik, S., & Dirsch, V. M. (2018). Natural products as modulators of the nuclear receptors and metabolic sensors LX α , FX α and RX α . *Biotechnology Advances*, 36(6), 1657-1698. doi: https://doi.org/10.1016/j.biotechadv.2018.03.003
- Islam, M., Al-Amin, M. D., Siddiqi, M. M. A., Akter, S., Haque, M. M., Sultana, N., & Chowdhury, S. (2012). Isolation of quercetin-3-O- β -D-glucopyranoside from the leaves of *Azadirachta indica* and antimicrobial and cytotoxic screening of the crude extracts. *Dhaka University Journal of Science*, 60, 11-14.
- Jensen, S. R., Gotfredsen, C. H., Harput, U. S., & Saracoglu, I. (2010). Chlorinated iridoid glucosides from *Veronica longifolia* and their antioxidant activity. *Journal of Natural Products*, 73(9), 1593-1596. doi: 10.1021/np100366k
- Joseph, S. B., Castrillo, A., Laffitte, B. A., Mangelsdorf, D. J., & Tontonoz, P. (2003). Reciprocal regulation of inflammation and lipid metabolism by liver X receptors. *Nature Medicine*, 9(2), 213-219. doi: 10.1038/nm820
- Kadota, S., Takamori, Y., Nyein, K. N., Kikuchi, T., Tanaka, K., & Eki-moto, H. (1990). Constituents of the leaves of *Woodfordia fruticosa* Kurz. I. Isolation, structure, and proton and carbon-13 nuclear magnetic resonance signal assignments of woodfruticocin (woodfordin C), an inhibitor of deoxyribonucleic acid topoisomerase II. *Chem Pharm Bull (Tokyo)*, 38(10), 2687-2697. doi: 10.1248/cpb.38.2687
- Kotani, H., Tanabe, H., Mizukami, H., Makishima, M., & Inoue, M. (2010). Identification of a naturally occurring retinoid, honokiol, that activates the retinoid X receptor. *Journal of Natural Products*, 73(8), 1332-1336. doi: 10.1021/np100120c
- Kunchandy, E., & Rao, M. N. A. (1990). Oxygen radical scavenging activity of curcumin. *International Journal of Pharmaceutics*, 58(3), 237-240. doi: 10.1016/0378-5173(90)90201-E
- Nakashima, K., Murakami, T., Tanabe, H., & Inoue, M. (2014). Identification of a naturally occurring retinoid X receptor agonist from Brazilian green propolis. *Biochimica et Biophysica Acta-General Subjects*, 1840(10), 3034-3041. doi: 10.1016/j.bbagen.2014.06.011
- Nicollier, G., & Thompson, A. C. (1983). Flavonoids of *Desmanthus illinoensis*. *Journal of Natural Products*, 46(1), 112-117. doi: 10.1021/np50025a011
- Nunez, A. R. (1985). Taxonomia de *Hypericum hyssopifolium* Chaix Y Species Relacionadas. *Lagascalia*, 13(2), 173-185.
- Ohara, K., Wakabayashi, H., Taniguchi, Y., Shindo, K., Yajima, H., & Yoshida, A. (2013). Quercetin-3-O-glucuronide induces ABCA1 expression by LX α activation in murine macrophages. *Biochemical and Biophysical Research Communications*, 441(4), 929-934. doi: https://doi.org/10.1016/j.bbrc.2013.10.168

- Prochazkova, D., Bousova, I., & Wilhelmova, N. (2011). Antioxidant and prooxidant properties of flavonoids. *Fitoterapia*, 82(4), 513-523. doi: 10.1016/j.fitote.2011.01.018
- Razavi, S. M., Zahri, S., Zarrini, G., Nazemiyeh, H., & Mohammadi, S. (2009). Biological activity of quercetin-3-O-glucoside, a known plant flavonoid. *Russian Journal of Bioorganic Chemistry*, 35(3), 376-378. doi: 10.1134/S1068162009030133
- Robson, N. K. B. (1980). Hypericum L. . In P. H. Davis (Ed.), *Flora of Turkey and East Aegean Islands* (pp. 355-401). Edinburgh: Edinburgh University.
- Sarian, M. N., Ahmed, Q. U., So'ad, S. Z. M., Alhassan, A. M., Murugesu, S., Perumal, V., . . . Latip, J. (2017). Antioxidant and Antidiabetic Effects of Flavonoids: A Structure-Activity Relationship Based Study. *Biomed Research International*, 2017. doi: Artn 8386065 doi: 10.1155/2017/8386065
- Srinivasan, R., Chandrasekar, M. J. N., Nanjan, M. J., & Suresh, B. (2007). Antioxidant activity of *Caesalpinia digyna* root. *Journal of Ethnopharmacology*, 113(2), 284-291. doi: 10.1016/j.jep.2007.06.006
- Szondy, Z., Garabuczi, E., Joos, G., Tsay, G. J., & Sarang, Z. (2014). Impaired clearance of apoptotic cells in chronic inflammatory diseases: therapeutic implications. *Frontiers in Immunology*, 5, 354. doi: 10.3389/fimmu.2014.00354
- Tsai, P. J., Tsai, T. H., Yu, C. H., & Ho, S. C. (2007). Comparison of NO-scavenging and NO-suppressing activities of different herbal teas with those of green tea. *Food Chemistry*, 103(1), 181-187. doi: 10.1016/j.foodchem.2006.08.013
- Vedin, L. L., Gustafsson, J. A., & Steffensen, K. R. (2013). The oxysterol receptors LXRalpha and LXRbeta suppress proliferation in the colon. *Molecular Carcinogenesis*, 52(11), 835-844. doi: 10.1002/mc.21924
- Viennois, E., Mouzat, K., Dufour, J., Morel, L., Lobaccaro, J. M., & Baron, S. (2012). Selective liver X receptor modulators (SLiMs): What use in human health? *Molecular and Cellular Endocrinology*, 351(2), 129-141. doi: 10.1016/j.mce.2011.08.036
- Wang, W., Nakashima, K., Hirai, T., & Inoue, M. (2019). Anti-inflammatory effects of naturally occurring retinoid X receptor agonists isolated from *Sophora tonkinensis* Gagnep. via retinoid X receptor/liver X receptor heterodimers. *Journal of Natural Medicines*, 73(2), 419-430. doi: 10.1007/s11418-018-01277-1
- Willy, P. J., Umeson, K., Ong, E. S., Evans, R. M., Heyman, R. A., & Mangelsdorf, D. J. (1995). Lxr, a Nuclear Receptor That Defines a Distinct Retinoid Response Pathway. *Genes & Development*, 9(9), 1033-1045. doi: 10.1101/gad.9.9.1033
- Zhang, P. C., & Xu, S. X. (2003). C-glucoside flavonoids from the leaves of *Crataegus pinnatifida* Bge. var. *major* N.E.Br. *Journal of Asian Natural Products Research*, 5(2), 131-136. doi: 10.1080/1028602021000054982
- Zhang, X. F., Thuong, P. T., Jin, W., Su, N. D., Sok, D. E., Bae, K., & Kang, S. S. (2005). Antioxidant activity of anthraquinones and flavonoids from flower of *Reynoutria sachalinensis*. *Archives of Pharmacal Research*, 28(1), 22-27. doi: 10.1007/Bf02975130
- Zorzetto, C., Sanchez-Mateo, C. C., Rabanal, R. M., Lupidi, G., Petrelli, D., Vitali, L. A., . . . Maggi, F. (2015). Phytochemical analysis and in vitro biological activity of three *Hypericum* species from the Canary Islands (*Hypericum reflexum*, *Hypericum canariense* and *Hypericum grandifolium*). *Fitoterapia*, 100, 95-109.

In vitro evaluation of antimicrobial activity of *Distemonanthus benthamianus* chewing stick extract mouthwash

Mbang Nyong Femi-Oyewo¹ , Olutayo Ademola Adeleye¹ , Caroline Olufunke Babalola¹ ,
Olufemi Babatunde Banjo¹ , Modupe Nofisat Adebowale² , Florence Olubola Odeleye³ 

¹Olabisi Onabanjo University, Department of Pharmaceutics and Pharmaceutical Technology, Ago -Iwoye, Ogun State, Nigeria

²Olabisi Onabanjo University, Department of Pharmacognosy, Ago Iwoye, Ogun State, Nigeria

³Olabisi Onabanjo University, Department of Pharmaceutical Microbiology, Ago Iwoye, Ogun State, Nigeria

ORCID IDs of the authors: M.N.F. 0000-0003-0025-2227; O.A.A. 0000-0001-8716-4064; C.O.B. 0000-0002-1742-8762; O.B.B. 0000-0002-6970-516X; M.N.A. 0000-0002-0944-0702; F.O.O. 0000-0002-1783-1463

Cite this article as: Femi-Oyewo, M. N., Adeleye, O. A., Babalola, C. O., Banjo, O. B., Adebowale, M. N., & Odeleye, F. O. (2021). *In vitro* evaluation of antimicrobial activity of *Distemonanthus benthamianus* chewing stick extract mouthwash. *Istanbul Journal of Pharmacy*, 51(1), 105-110.

ABSTRACT

Background and Aims: Mouthwashes are oral home care product used to treat mouth infections and to maintain satisfactory oral hygiene. The use of effective mouthwash is a reasonable means to prevent dental caries and oro-dental infections. The aim of this study was to evaluate the antimicrobial potential of *Distemonanthus benthamianus* chewing stick extract formulated as a mouthwash against some microorganisms associated with oro-dental infections in comparison with two commercial brand mouthwashes.

Methods: The chewing stick was extracted with methanol and used to formulate mouthwash. Phytochemical screening was done to test for the presence of secondary metabolites. Antimicrobial activity of the crude extract and the formulated mouthwash on *Staphylococcus aureus*, *Streptococcus mutans* and *Candida albicans* was evaluated. The physical characteristics, pH and the stability of the mouthwashes were determined.

Results: The extract contains alkaloids, saponins flavonoids, steroids and tannins. The crude extract and the formulated mouthwashes showed significant difference in activity against the test microorganisms in the following order *Candida albicans* > *Staphylococcus aureus* > *Streptococcus mutans*. At high concentrations of the extract (0.3%W/V and 0.5%W/V) in formulations, antibacterial activities were significantly higher against *Streptococcus mutans* and *Staphylococcus aureus* when compared with the commercial brands. The pH of the mouthwashes ranged from 5.2 - 7.4. The stability of formulation F5 was maintained for 12 weeks.

Conclusion: The use of *Distemonanthus benthamianus* chewing stick extract mouthwash is safer, cheaper, and more effective in preventing dental caries and oro-dental infections compared to the commercial brand mouthwashes.

Keywords: Antimicrobial activity, chewing stick, microorganisms, mouthwash

Address for Correspondence:

Olutayo Ademola ADELEYE, e-mail: olutayo.adeleye@oouagoiwoye.edu.ng

This work is licensed under a Creative Commons Attribution 4.0 International License.



Submitted: 14.06.2020
Revision Requested: 22.06.2020
Last Revision Received: 06.09.2020
Accepted: 21.09.2020

INTRODUCTION

Mouthwashes are oral home care products. They are clear non-sterile aqueous solution termed medicated liquid intended to deodorize, clean and treat mouth infections. They are used to treat mouth infections and to ensure or maintain satisfactory oral hygiene to enhance oral health (Khirtika, Ramesh, & Muralidharan, 2017). Thus, the use of effective mouthwash is a reasonable means to prevent dental caries and oro-dental infections. This is achieved by the presence of chemical antimicrobial agents such as cetylpyridinium chloride, triclosan or chlorhexidine and essential oils in many of the commercially available mouthwash brands (Masadeh, Gharaibeh, Alzoubi, Al-Azzam, & Obeidat, 2013; Dabholkar, Shah, Kathariya, Bajaj, & Doshi, 2016; Kunte, Kadam, Patel, Shah, Lodaya, & Lakde, 2018).

The use of chewing sticks have been encouraged by the WHO since 1987 due to their enormous oral health benefits such as the elimination of bad odour, good cleansing properties and wide spectrum antimicrobial activities which they possess in the general maintenance of oral hygiene (Malik, Shaukat, Qureshi, & Abdur, 2014). They are less toxic because of their natural source. They are abundant in nature which makes them readily available and cheap. For people of low economic stature, they are a cheaper and safer alternative of mouth cleansing to commercial mouthwashes with side effects such as tooth staining and vomiting (Yadav & Yadav, 2013; Parkar, Thakkar, & Shah, 2013).

Distemonanthus benthamianus Baill. is a semi-deciduous tree which belongs to the family Leguminosae. It is commonly known as African satinwood in English and as movingui in French. It is widespread in Ghana and Nigeria, and known as "bonsamdua" and "ayan", respectively (Adeniyi, Obasi, & Lawal, 2011; Asamoah, Frimpong-Mensah, & Antwi-Boasiako, 2014). It is used traditionally in the treatment of different skin conditions, rheumatism, pains, fever, uro-genital and gastrointestinal infections (Saha et al., 2014; Shittu, Aliyu, David, Njinga, & Ishaq, 2019). The root is used in Western Nigeria as a chewing stick for oro-dental hygiene. There are experimental evidences which show that *D. benthamianus* possesses teeth cleansing properties and antimicrobial activity against a wide range of microorganisms associated with dental caries and oro-dental infections such as *Streptococcus mutans*, *Staphylococcus aureus*, *Candida albicans* etc. (Adeniyi & Odumosu, 2012; Aworinde, Eri-noso, & IbukunOluwa, 2016; Mebude, Adeniyi, & Lawal, 2017; Shittu et al., 2019). In view of these assertions, this study was carried out to investigate the antimicrobial potentials of the methanol extract of *D. benthamianus* chewing sticks against microorganisms associated with oro-dental infections and also to formulate and evaluate the antimicrobial activity of mouthwash containing different concentrations of the extract in comparison with two commercial brand mouthwashes.

MATERIALS AND METHODS

Plant collection

D. benthamianus chewing sticks (freshly uprooted root of the plant) were bought same day from Oke-Aje, Ijebu Ode, Ogun state, Nigeria in August 2019 and identified at the Forest Research Institute of Nigeria (FRIN) Ibadan, Oyo State by Mr. Sam-

uel Odewo. The plant was air dried, cut into pieces and ground into powder using an electric blender.

Test microorganisms

The test microorganisms used in this study were clinical isolates of *S. aureus*, *S. mutans* and *C. albicans* collected from the Microbiology Department of Olabisi Onabanjo University Teaching Hospital, Sagamu, Ogun State.

Preparation of plant extract

Five hundred grams of the powdered chewing sticks were extracted by the method of Adeleye, Babalola, Femi-Oyewo, & Balogun, (2019) with 75% methanol for 72 hours at room temperature. It was filtered; the filtrate was concentrated with a rotary evaporator at 40°C and stored in a refrigerator at 4°C.

Phytochemical analysis of extract

The extract was screened for the presence of phytochemicals according to the methods of Trease & Evans, (1989).

Antimicrobial sensitivity screening

The antimicrobial sensitivity of the test microorganism to different concentrations of *D. benthamianus* extract prepared with distilled water was evaluated by the agar well diffusion method (Hood, Wilkinson, & Cavanagh, 2003). The bacterial test isolates were inoculated into Nutrient Broth and incubated for 24 hours at 37°C while the fungal test isolate was inoculated into Sabouraud Dextrose Broth and incubated for 48 hours at 37°C. The inoculated broths were standardized to 0.5 McFarland standards (Hood et al., 2003). A 6 mm cork borer was used to bore wells in an agar plate inoculated with microorganisms (Nutrient Agar for bacterial and Sabouraud Dextrose Agar for fungi) and filled with 0.5 mL of different concentrations of the extracts, gentamicin or ketoconazole (positive control) and distilled water (negative control). The plates were incubated at 37±2°C for 24 hours and 48 hours for Nutrient Agar Sabouraud Dextrose Agar respectively. Zones of inhibition were measured in millimeters (mm).

Preparation of *Distemonanthus benthamianus* mouthwash

Each formulation (F1 - F5) was prepared according to Table 3. Sodium bicarbonate was dissolved in water and added to the mixture of chloroform water, peppermint oil and propylene glycol in a calibrated bottle. The extract *D. benthamianus* was dissolved in water and strained through a whatman paper to remove particles before being added to the mixture in the bottle.

Evaluation of mouthwash

Evaluation of physical characteristics of the mouthwashes

Physical characteristics (appearance, colour, taste, odour and flavour) of the mouthwashes were determined by visual inspection and sensory evaluation.

Evaluation of pH of the mouthwashes

The pH of the mouthwashes was determined in triplicate using a pH meter.

Antimicrobial assay of the mouthwashes

The antimicrobial assay of the mouthwashes was performed by the agar diffusion method similar to the previous method used for antimicrobial sensitivity screening.

Panelist perception

The physical characteristics of the mouthwashes were characterized by subjective physical and sensory assessment by 70 panelists, 10 for each formulation. The panelists were instructed to rate the appearance, taste, flavour, colour, smoothness and acceptability of the mouthwash as they perceived them on two scales of either good or bad and accepted or rejected.

Stability studies of the mouthwash

The stability of formulation F5 was evaluated by taking samples at specific intervals from the product stored at 4±1°C, 25±1°C and 50±1°C for 12 weeks (Almekhlafi, Thabit, Alwossabi, Awadth, Thabe, & Algaadari, 2014; Adeleye et al., 2019). The physical characteristics (appearance, colour, taste, odour and flavour) and antimicrobial properties of the samples were analyzed.

Statistical analysis

Significant difference in data obtained was analyzed with GraphPad Prism 5.01 using t-test and one-way ANOVA. P-values less than 0.05 were considered statistically significant.

RESULTS

The phytochemical constituents of the extract are shown in Table 1. The extract contains low concentrations of alkaloids and saponins with moderate concentrations of flavonoids, steroids and tannin.

Table 1. Phytochemicals of *Distemonanthus benthamianus* extract.

Test	Result
Alkaloids	+
Flavonoids	++
Saponins	+
Tannins	++
Steroids	++

+ = Low concentration; ++ = Moderate concentration

The antimicrobial assay of different concentrations of the crude extract is presented in Table 2. The crude extract showed a significant difference in activity against the test microorganism with the highest activity at 250 mg/mL concentration on *C. albicans* (27.1±0.20mm) followed by *S. aureus* (22.5±0.10mm) and *S. mutans* (16.3±0.22mm). The positive control 1 (gentamicin) had activities on *S. aureus* (28.5±0.10mm) and *S. mutans* (25.2±0.02mm), and the positive control 2 (ketoconazole) had activity on *C. albicans* (22.8±0.06mm) while the negative control (distilled water) showed no activity against the test microorganisms.

The composition of the formulated mouthwashes is shown in Table 3, and the physical characteristics and the pH of the mouthwashes are presented in Table 4. All the mouthwashes are clear solutions in appearance with a minty flavour and with colours ranging from light red to light blue. The formulated mouth-

Table 2. Antimicrobial assay of *Distemonanthus benthamianus* extract.

Extract (mg/ml)	Zone of Inhibition(mm)		
	<i>Streptococcus mutans</i>	<i>Staphylococcus aureus</i>	<i>Candida albicans</i>
250	16.3±0.22	22.5±0.10	27.1±0.20
125	14.9±0.14	20.8±0.20	24.7±0.07
62.5	12.7±0.06	18.1±0.04	22.3±0.16
31.25	10.1±0.21	16.0±0.21	17.8±0.10
15.625	8.4±0.10	12.8±0.14	12.0±0.42
Positive control 1	25.2±0.02	28.5±0.10	-
Positive control 2	-	-	22.8±0.06
Negative control	-	-	-

Positive control 1 = Gentamicin, Positive control 2 = Ketoconazole, Negative control = Distilled water

Table 3. Composition of *Distemonanthus benthamianus* extracts mouthwash.

Ingredients	F1	F2	F3	F4	F5
<i>D. benthamianus</i> extract (g)	-	0.1	0.2	0.3	0.5
Sodium bicarbonate (g)	1.0	1.0	1.0	1.0	1.0
Propylene glycol (mL)	1.0	1.0	1.0	1.0	1.0
Peppermint oil (mL)	1.5	1.5	1.5	1.5	1.5
Chloroform water (mL)	5.0	5.0	5.0	5.0	5.0
Amaranth solution (mL)	5.0	5.0	5.0	5.0	5.0
Water to (mL)	100.0	100.0	100.0	100.0	100.0

washes are odourless and neutral in taste while the commercial brand mouthwashes have a pleasant odour and a sweet taste. The pH of the mouthwashes ranges from 5.2 to 7.4.

The antimicrobial assay of the mouthwashes is presented in Table 5. All the test microorganisms are susceptible to the mouthwashes but at significantly different degrees except F1 which showed zero activity. Formulation F5 had the highest activity against all the test microorganisms with *C. albicans* showing the highest susceptibility (24.6±0.08mm), followed by *S. aureus* (17.8±0.20mm) then *S. mutans* (10.5±0.12mm).

The physical characterization and sensory assessment of the mouthwashes by panelists indicates that commercial brands generally had better physical and sensory characteristics, and were better accepted than the formulated mouthwashes (Table 6).

Table 4. Physical characteristics and pH.

Characteristics	F1	F2	F3	F4	F5	F6	F7
Appearance	Clear solution	Clear solution	Clear solution	Clear solution	Clear solution	Clear solution	Clear solution
Colour	Light red	Light red	Light red	Light red	Light red	Light blue	Light blue
Odour	Odourless	Odourless	Odourless	Odourless	Odourless	pleasant	pleasant
Taste	Neutral	Neutral	Neutral	Neutral	Neutral	Sweet	Sweet
Flavour	Minty	Minty	Minty	Minty	Minty	Minty	Minty
pH	7.4	7.2	7.1	6.8	6.6	6.8	5.2

F1 = mouthwash without herbal extract, F2 - F5 = formulated mouthwash containing 0.1%, 0.2%, 0.3%, and 0.5% *Distemonanthus benthamianus* extract respectively, F6 & F7 = commercial brand mouthwash; F6 mouthwash composition = triclosan sorbitol, alcohol, sodium saccharin, sodium lauryl sulfate, polyvinyl methyl ether/maleic acid copolymer, flavouring agents; F7 mouthwash composition = thymol, eucalyptol, methyl salicylate, menthol, sodium benzoate, benzoic acid, sorbitol, ethanol.

Table 5. Antimicrobial assay of mouthwashes.

Microorganisms	Zone of Inhibition (mm)						
	F1	F2	F3	F4	F5	F6	F7
<i>Streptococcus mutans</i>	-	5.2±0.02	6.6±0.10	8.3±0.03	10.5±0.12	9.5±0.04	6.3±0.04
<i>Staphylococcus aureus</i>	-	9.2±0.24	13.5±0.06	15.1±0.21	17.8±0.20	16.2±0.05	14.7±0.10
<i>Candida albicans</i>	-	15.5±0.15	18.2±0.20	20.7±0.24	24.6±0.08	14.3±0.21	11.7±0.02

Table 6. Panelist rating of physical characteristics.

Characteristics	F1	F2	F3	F4	F5	F6	F7
Appearance	80	70	80	70	70	80	80
Colour	80	80	80	60	80	80	80
Odour	60	60	60	50	50	90	80
Flavour	50	40	40	50	40	100	80
Taste	40	30	40	40	30	100	80
Smoothness	100	80	80	80	60	100	100
Acceptability	50	40	40	50	40	100	80

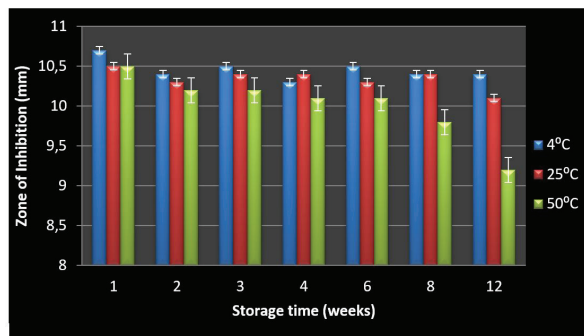


Figure 2. Antimicrobial stability of F5 mouthwash on *Streptococcus mutans* over time.

Figures 1, 2 and 3 show the antimicrobial stability of formulation F5 for 12 weeks. The stability was maintained at all experimental temperatures for 12 weeks.

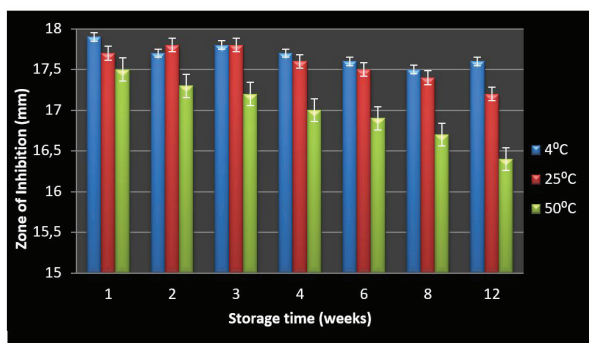


Figure 1. Antimicrobial stability of F5 mouthwash on *Staphylococcus aureus* over time.

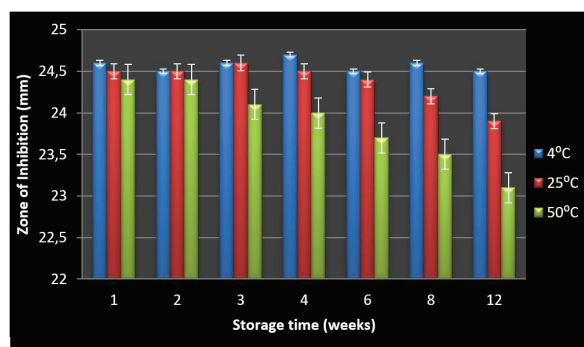


Figure 3. Antimicrobial stability of F5 mouthwash on *Candida albicans* over time.

DISCUSSION

A phytochemical test was performed to find the phytochemical constituents (bioactive secondary metabolites) present in *D. benthamianus* extract. Table 1 shows that the extract contains alkaloids, steroids, flavonoids, saponins and tannins as highlighted by other researchers (Aiyegoro, Akinpelu, Afolayan, & Okoh, 2008; Shittu et al., 2019; Obiang, Misso, Atome, Ondo, Engonga, & Emvo, 2019). The presence of some of these compounds has been linked to the antimicrobial activity of the extract. Adeniyi, Adeonipekun, & Omotayo, (2014); Aworinde et al., (2016); Mebude et al., (2017), reported that the presence of tannins, alkaloids, flavonoids and steroids in plants are responsible for their antimicrobial activities.

The antimicrobial assay of the crude extract revealed activity against the three test microorganisms and the susceptibility of the microorganisms to the extract was in the following order: *C. albicans*>*S. aureus*>*S. mutans*. The antimicrobial activity increased significantly ($P<0.05$) as the concentration of the extract increased. This indicates that the activity of the extract is concentration-dependent. As discussed above, the presence of tannins, alkaloids, flavonoids and steroids in the extract could be the reason for the antimicrobial activity of the extract. Physical characteristics (appearance, colour, odour, taste and flavor) of the formulated mouthwashes (F1–F5) and the commercial brand mouthwashes (F6–F7) showed that the formulations are clear solutions without particulate matters. The light red colouration and the minty flavour of the formulated mouthwashes were due to the inclusion of amaranth solution and peppermint oil respectively in the composition of the mouthwash. F1–F5 are odourless and neutral in taste but the commercial brands are pleasant in odour with a sweet taste.

The ideal pH range of saliva is 6.2–7.6 with an average pH of 6.7 (Baliga, Muglikar, & Kale, 2013), which helps maintain the pH of the mouth, including keeping the pH of the gum and teeth within a range of 6.7–7.3 so as to prevent proliferation of cariogenic bacteria, tooth demineralization, tooth decay and gum diseases (Zhao, Tsoi, Wong, Chu, & Matinlinna, 2017). When the mouth pH falls below the critical pH value of 5.5, various oral health complications could arise. As a result of low oral pH, incidences of tooth decay, enamel erosion, cariogenic bacterial growth, dental caries etc. have been reported (Takahashi, 2005; Van Zyk, & Van Heerden, 2010; Belardinelli, Morelato, Benavidez, Baruzzi, & López de Blanc, 2014; Dave, Gurunathan, & Vasantharajan, 2018). For pH compatibility with saliva, formulations should be within the mouth pH range (Baliga et al., 2013). The pH of the mouthwashes in this study ranged from 5.2–7.4. Only F7 fell below the pH range of the mouth, which could reduce saliva pH below the critical value. The implication is that if used over a long period of time it could further aggravate incidences of oro-dental infections. So, it is important to ensure that mouthwashes are buffered to be in the alkaline region to maintain the optimum saliva pH.

The three test microorganisms were susceptible to the mouthwashes at significantly various degrees depending on

concentration and type, except F1 which showed no activity. The zero antimicrobial profile of F1 was expected since it is a placebo product without extract. For the formulated mouthwashes, *C. albicans* was the most sensitive followed by *S. aureus* and *S. mutans*. These activities occur in a concentration-dependent manner with a significant increase in activity, with an increase in the concentration of the extract in the formulations. Mouthwashes containing the extract had significant activity on *C. albicans* ($P<0.0001$) at all concentrations employed in this study when compared to the commercial brands. At high concentrations of the extract in formulations F4 (0.3%^{w/v}) and F5 (0.5%^{w/v}), the antibacterial activity of these formulations were significantly higher against *S. mutans* and *S. aureus* ($P < 0.0001$) when compared with the commercial brands, except F6, which had a significantly higher activity against *S. aureus* than formulation F4 (0.3%^{w/v}). However, at low concentrations of the extract in formulations F2 (0.1%^{w/v}) and F3 (0.2%^{w/v}), the antibacterial activity of these formulations were significantly lower against *S. mutans* and *S. aureus* ($P<0.0001$) when compared with the commercial brands.

The rating of the physical characteristics of the mouthwashes from the assessment of panelists indicated generally that more than 50% of the panelists perceived all the mouthwashes as being good in appearance, colour, odour and smoothness, without a gritty taste. Generally, more than 50% of the panelists perceived the formulated mouthwashes to have a poor flavour and taste, unlike the commercial brands, which over 70% of the panelist perceived as having a good flavour and taste. More than 70% of the panelist accepted the commercial brands while less than 50% of panelists generally rejected the formulated mouthwashes. The rejection of the formulated mouthwashes was based on its palatability in which the flavour and sweetener in the formulation was a determining factor. Sweetener was not included in the formulated mouthwash, hence its high rejection rate. However, the commercial brand mouthwashes gained a high rate of acceptance due to the presence of sweeteners: sodium saccharin and sorbitol. The acceptability of the formulated mouthwashes can be improved upon by enhancing its palatability with the inclusion of a suitable sweetener.

The physical characteristics (appearance, colour, taste, odour and flavour) of the mouthwash were stable at the selected temperature for 12 weeks. There was a slight reduction in the antimicrobial activity of the mouthwash against the test microorganisms with an increase in the storage temperature and time duration. However, statistical analysis revealed no significant difference in antimicrobial activity. So, it can be said that the antimicrobial stability of the mouthwash was maintained at the selected temperature for 12 weeks. This finding is an indication that the mouthwash can be stored on shelves at room temperatures without becoming compromised.

Further research is necessary to isolate and evaluate the compound in the plant responsible for the antimicrobial activity *in vivo*. Also, toxicological evaluation of the formulated mouthwash is necessary to ascertain its safety.

CONCLUSION

The test microorganisms were sensitive to the mouthwashes but at various degrees depending on the concentration of the extract. The formulated mouthwashes showed more remarkable activity than the commercial brands. The formulated mouthwashes were stable in physical attributes and activity but were poor in acceptability and need to be improved to be considered for commercial production. This study concludes that the use of *Distemonanthus benthamianus* chewing stick extract mouthwash would be an effective, cheap and safe means to prevent dental caries and oro-dental infections compared to the commercial brand mouthwashes.

Acknowledgement: The authors are grateful to Mr King, Miss Tawa Lawal and Mrs Olupe, the laboratory technologists in the Faculty of Pharmacy, Olabisi Onabanjo University, Ago Iwoye, Nigeria for providing laboratory assistance.

Peer-review: Externally peer-reviewed.

Author contributions: Conception/Design of Study- M.N.F., O.A.A., C.O.B., M.N.A.; Data Acquisition- O.A.A., O.B.B., M.N.A., F.O.O.; Data Analysis/Interpretation- M.N.F., O.A.A., C.O.B., M.N.A., F.O.O.; Drafting Manuscript- O.A.A., O.B.B., M.N.A.; Critical Revision of Manuscript- M.N.F., O.A.A., C.O.B., F.O.O.; Final Approval and Accountability- M.N.F., O.A.A., C.O.B., O.B.B., M.N.A., F.O.A.






Conflict of Interest: The authors have no conflict of interest to declare.

Financial Disclosure: Authors declared no financial support.

REFERENCES

- Adeleye, O.A., Babalola, C.O., Femi-Oyewo, M.N., & Balogun, G.Y. (2019). Antimicrobial activity and stability of *Andrographis paniculata* cream containing shea butter. *Nigerian Journal of Pharmaceutical Research*, 15, 9-18.
- Adeniyi, B.A., Obasi, O.J., & Lawal, T. (2011). *In vitro* antifungal activity of *Distemonanthus benthamianus* stem. *International Journal of Pharmacy and Pharmaceutical Sciences*, 3, 52-56.
- Adeniyi, C.B., & Odumosu, B.T. (2012). Antibacterial and antifungal properties of *Distemonanthus benthamianus* (Fabaceae) crude extract. *Global Journal of Pharmaceutical Research*, 1, 567-574.
- Adeniyi, T.A., Adeonipekun, P.A., & Omotayo, E.A. (2014). Investigating the phytochemicals and antimicrobial properties of three sedge (Cyperaceae) species. *Notulae Scientia Biologicae*, 6, 276-281.
- Aiyegoro, O.A., Akinpelu, D.A., Afolayan, A.J., & Okoh, A.I. (2008). Antibacterial activities of crude stem bark extracts of *Distemonanthus benthamianus*. *Journal of Biological Sciences*, 8, 356-361.
- Almekhlafi, S., Thabit, A.M., Alwossabi, M.I., Awadth, N., Thabe, A.M., & Algaadari, Z. (2014). Antimicrobial activity of Yemeni myrrh mouthwash. *Journal of Chemical and Pharmaceutical Research*, 6, 1006-1013.
- Asamoah, A., Frimpong-Mensah, K., & Antwi-Boasiako, C. (2014). Efficacy of *Erythroleum suaveolens* (potrodom) and *Distemonanthus benthamianus* (bonsamdua) water extractives on the durability of five Ghanaian less used timber species. *Journal of Indian Academy of Wood Science*, 11, 72-81.
- Aworinde, D.O., Erinoso, S.M., & IbukunOluwa, M.R. (2016). Mineral compositions, phytochemical constituents and *in vitro* antimicrobial screening of some chewing sticks from Ibadan, Nigeria. *Journal of Applied Bioscience*, 101, 9589-9597.
- Baliga, S., Muglikar, S., Kale, R. (2013). Salivary pH: A diagnostic biomarker. *Journal of Indian Society of Periodontology*, 17, 461-465.
- Belardinelli, P.A., Morelato, R.A., Benavidez, T.E., Baruzzi, A.M., & López de Blanc, S.A. (2014). Effect of two mouthwashes on salivary pH. *Acta Odontologica Latinoamericana*, 27, 66-71.
- Dabholkar, C.S., Shah, M., Kathariya, R., Bajaj, M., & Doshi, Y. (2016). Comparative evaluation of antimicrobial activity of pomegranate-containing mouthwash against oral-biofilm forming microorganisms. *Advances in Human Biology*, 6, 99-103.
- Dave, P.H., Gurunathan, D., Vasantharajan, M.S. (2018). Comparison of pH levels of the saliva before and after the consumption of cough syrups in children. *Biomedical and Pharmacology Journal*, 11, 1443-1448.
- Hood, J.R., Wilkinson, J.M., & Cavanagh, H.M.A. (2003). Evaluation of common antibacterial screening methods utilized in essential oil research. *Journal of Essential Oil Research*, 15, 428-433.
- Khirtika, S.G., Ramesh, S., & Muralidharan, N.P. (2017). Comparative evaluation of antimicrobial efficacy of 0.2% Chlorhexidine, 2% iodine and homemade mouthrinse as an anti-carries agent. *Journal of Pharmaceutical Science Research*, 9, 2114-2116.
- Kunte, S., Kadam, N., Patel, A., Shah, P., Lodaya, R., & Lakde, L. (2018). Comparative evaluation of antimicrobial properties of pomegranate peel extract against *Streptococcus mutans* and *Lactobacillus*. *International Dental and Medical Journal of Advanced Research*, 4, 1-6.
- Malik, A.S., Shaukat, M.S., Qureshi, A.A., & Abdur, R. (2014). Comparative effectiveness of chewing stick and toothbrush: a randomized clinical trial. *North American Journal of Medical Sciences*, 6, 333-337.
- Masadeh, M.M., Gharaibeh, S.F., Alzoubi, K.H., Al-Azzam, S.I., & Obeidat, W.M. (2013). Antimicrobial activity of common mouthwash solutions on multidrug-resistance bacterial biofilms. *Journal of Clinical Medical Research*, 5, 389-394.
- Mebude, O.O., Adeniyi, B.A., & Lawal, T.O. (2017). *In vitro* antimicrobial activities of ethanol extract of *Distemonanthus benthamianus* (Aayan) Baillon (Fabaceae) on *Streptococcus mutans*. *Journal of Advances in Medicine and Medical Research*, 22, 1-8.
- Obiang, C.S., Misso, R.L., Atome, G.R., Ondo, J.P., Engonga, L.C., & Emvo, E.N. (2019). Phytochemical analyses, antimicrobial and antioxidant activities of stem bark extracts of *Distemonanthus benthamianus* H. Baill. and fruit extracts of *Solanum torvum* Sw. from Gabon. *Asian Pacific Journal of Tropical Biomedicine*, 9, 209-216.
- Parkar, S.M., Thakkar, P., & Shah, K. (2013). Antimicrobial activity of four commercially available mouthwashes against *Streptococcus Mutans*: An *in vitro* study. *Universal Research Journal of Dentistry*, 3, 108-112.
- Saha, J.B., Pétrissans, A., Molina, S., Ndikontar, M.K., Mounquengui, S., Dumarçay, S., & Gérardin, P. (2014). Study of the feasibility of a natural dye on cellulosic textile supports by red padouk (*Pterocarpus soyauxii*) and yellow movingui (*Distemonanthus benthamianus*) extracts. *Industrial Crops and Products*, 60, 291-297.
- Shittu, O.A., Aliyu, A., David, M.S., Njinga, N.S., & Ishaq, H.I. (2019). Potential antibacterial activity of two important local chewing sticks "*Fagara zanthoxyloides* and *Distemonanthus benthamianus*" along with antioxidant capacities. *Dhaka University Journal of Pharmaceutical Sciences*, 18, 223-232.
- Takahashi, N. (2005). Microbial ecosystem in the oral cavity: Metabolic diversity in an ecological niche and its relationship with oral diseases. *International Congress Series*, 1284, 103-112.
- Trease, A., & Evans, W.C. (1989). *Pharmacognosy*. 13th (ed). London: Balliere Tindall. Pp. 345-6, 535-6, 772-3.
- Van Zyk, A.W., & Van Heerden, W.F. (2010). Mouthwash: A review for South African health care workers. *South African family practice. Research Journal of Pharmaceutical, Biological and Chemical Sciences*, 5, 121-127.
- Yadav, R., & Yadav, S.K. (2013). Dental disease and its cure: A review. *Asian Journal of Pharmaceutical and Clinical Research*, 6, 16-20.
- Zhao, D., Tsoi, J.K., Wong, H.M., Chu, C.H., & Matinlinna, J.P. (2017). Pediatric over-the-counter (OTC) oral liquids can soften and erode enamel. *Dentistry Journal*, 5, 17-24.

Phytochemical screening, phenolic content and antioxidant activity of *Lavandula* species extracts from Algeria

Farah Haddouchi¹ , Tarik Mohammed Chaouche¹ , Meriem Saker² , Imane Ghellai¹ ,
Ouhiba Boudjemai¹ 

¹Abou Bekr Belkaïd University, Department of Biology, Laboratory of Natural Products, Tlemcen, Algeria

²Abou Bekr Belkaïd University, Department of Biology Laboratory of Physiology, Physiopathology and Biochemistry of Nutrition, Tlemcen, Algeria

ORCID IDs of the authors: F.H. 0000-0002-1204-3337; T.M.C. 0000-0002-8631-2587; M.S. 0000-0003-3194-5616; I.G. 0000-0003-3229-7147; O.B. 0000-0003-2899-2323

Cite this article as: Haddouchi, F., Chaouche T.M., Saker M, Ghellail, I., & Boudjemai, O. (2021). Phytochemical screening, phenolic content and antioxidant activity of *Lavandula* species extracts from Algeria. *Istanbul Journal of Pharmacy*, 51(1), 111-117.

ABSTRACT

Background and Aims: We are interested in the comparison of phytochemical screening, the estimation of the phenolic content and the antioxidant activity of the leaves and flowers of three species of *Lavandula* (*L. dentata*, *L. multifida*, and *L. stoechas*) from the Tlemcen region (Algeria).

Methods: The preparations of the hydro-methanolic extracts were carried out by maceration. The latter in order to quantify the phenolic compounds and to evaluate the antioxidant activity *in vitro* by trapping the DPPH^o radical and iron reducer.

Results: Phytochemical tests reveal the presence of tannins and flavonoids in all extracts with varying intensities. The determination of total phenols by the Folin ciocalteu method shows that the extract from the leaves of *L. multifida* is the richest in total phenols (23.11 mg EAG/g DW) and has the most important important reducing power (EC50= 343±10 µg/ml) and inhibition of DPPH radical activity (IC50= 7.43 µg/mL).

Conclusion: In this context, the results presented deduce that these plants are a promising source of phenolic compounds. Biological studies are needed to elucidate and conclude the effectiveness of these plants, which can be a challenge for new food and cosmetic products.

Keywords: *Lavandula*, Phytochemical screening, phenolic compounds, Antioxidant activity

INTRODUCTION

Investigations of medicinal plants are still under development. Because they have been recognised as an essential supply for healthcare treatments; so, it can be stated with all certainty that in recent years, there is a growing interest in the subject of natural active substances contained in herbs (Kala 2015; Adaszyńska-Skwirzyńska & Dziecioł 2017). The efficacy of the plants in the treatment of different human diseases has been attributed to the presence of different active compounds, principally phenolic derivatives. These compounds have been well-reported to exert antioxidant properties. They may prevent the damage caused by reactive oxygen species (Algieri et al., 2016). Lamiaceae is one of the largest families of flowering plants comprising about 250 genera and over 7,000 species (Napoli, Siracusa, & Ruberto, 2020). The *Lavandula* genus is an important member of this family (Canlı, Yetgin, Benek, Bozyl, & Murat Altuner, 2019), it is native to the Mediterranean region and grows as high as 1-2m with ever-

Address for Correspondence:

Farah HADDOUCHI, e-mail: farah.haddouchi@univ-tlemcen.dz

Submitted: 31.05.2020
Revision Requested: 30.07.2020
Last Revision Received: 01.11.2020
Accepted: 08.11.2020

This work is licensed under a Creative Commons Attribution 4.0 International License.



green leaves (Soheili & Salami, 2019). *Lavandula* is rich in a wide variety of secondary metabolites, such as essential oils, coumarins and phenolic compounds (Panuccio, Fazio, Papalia, & Barreca, 2016). It is used to treat superficial wounds and burns and has sedative, antibacterial, anti-fungal, antidepressant and anti-inflammatory effects (Soheili & Salami, 2019). The flowers and leaves of lavender either in the form of essential oil mostly, or different forms of extracts are extensively used in cosmetics, hygiene products, food industry, perfumery and pharmaceutical preparations with high industrial value (Panuccio et al., 2016; Canli et al., 2019; Soheili & Salami, 2019). This genus consists of 47 species of small green shrubs having aromatic foliage and flowers (Canli et al. 2019).

This work based its interest on three species of lavender used in traditional medicine in Algeria. *Lavandula multifida* L., which is often used to treat rheumatism, also has hypoglycemic and anti-inflammatory properties (El-Hilaly, Hmammouchi, & Lyoussi, 2003; Sosa et al. 2005). *L. stoechas* L. is a species applied to treat epilepsy and headaches, it has antimicrobial, analgesic, antiseptic and antispasmodic effects (Amara et al. 2017; Bousta & Farah 2020). Another species *L. dentata* L. has carminative and nervous properties; its essential oils have been used as a tonic against vertigo, nervous trembling, weakness, spasms and colic (Dif, Benyahia, Benali, Rahmani, & Bouazza, 2017). The present study aimed to quantify the phenolic compounds contained in the hydromethanolic extracts of *L. dentata*, *L. multifida*, and *L. stoechas*, and to evaluate their antioxidant capacities by DPPH° assay and iron reduction, in order to show possible differences in antioxidant content and improve the knowledge of bioactive compounds, which may be helpful for therapeutic and pharmaceutical applications.

MATERIALS AND METHODS

Plant material

Lavandula dentata, *L. stoechas* and *L. multifida*, were harvested in February 2020 in the Ghazaouet region, wilaya of Tlemcen (North-West of Algeria). They were identified in the Laboratory of Natural Products, the Department of Biology, in the University of Tlemcen, Algeria. Voucher specimens were deposited at the Herbarium of the Laboratory. The leaves and flowers of each plant were separated and dried in a dark and dry place. The samples were transformed into powder using an electric mill.

Preparation of hydro-methanolic extracts

The preparations of the hydro-methanolic extracts were carried out by maceration for 24 hours of 10g of the plant powder in 200 mL of methanol-water (70-30). After filtration, the extracts were evaporated at 45°C under reduced pressure.

The yield of the plants in dry extract was determined by calculating the following ratio: Yield% = $[P1 - P2 / P3] \times 100$

P1: Weight of the flask after evaporation, P2: Weight of the empty flask, P3: Weight of the starting dry plant material.

The dry extracts were taken up in a few millilitres of methanol for phytochemical tests, dosages and assessments of antioxidant activity.

Phytochemical tests of flavonoids and tannins

In order to highlight the presence or absence of certain compounds belonging to the chemical families of secondary metabolites, specific phytochemical tests were carried out based on color, turbidity or precipitation reactions, using the methods described in the literature (Haddouchi, Chaouche, & Nourdinne, 2018).

Detection of flavonoids

Ten drops of concentrated hydrochloric acid (HCl) and a few milligrams of magnesium turnings were added to 0.5 mL of each extract. The pink red or yellow coloration, after 3 min of incubation at room temperature, indicates the presence of flavonoids.

Detection of tannins

Eight drops of a dilute solution of ferric chloride (FeCl₃) at 1% were added to 0.5 mL of each extract. After a few minutes of incubation at room temperature, the ferric chloride develops a greenish coloration, which indicates the presence of catechic tannins or a blue-blackish one, which reveals the existence of gallic tannins.

Determination of total phenol contents

One hundred µL of each extract at a concentration of 1 mg/ml, and mixed with 2 mL of a sodium carbonate (2 %) solution were freshly prepared, the whole was agitated with a vortex. After 5 min, 100 µL of the Folin-Ciocalteu diluted reagent (1/20) was added, the mixture was incubated in total darkness for 30 min at room temperature, the absorbance was read at 700 nm. Different concentrations of gallic acid were used to prepare a calibration curve. The results were expressed as milligram gallic acid equivalents (GAE)/g DW (Chaouche, Haddouchi, Boudjemai, & Ghellai, 2020).

In vitro evaluation of antioxidant activity

Scavenging of the free radical DPPH°

At different concentrations, 50 µL of each extract was added to 1950 µL of a methanolic solution of 2,2-diphenyl-1-picrylhydrazyl (DPPH°) at 6.34 10⁻⁵ M. For each concentration, a blank was prepared. A negative control was prepared, in parallel, while mixing 50 µL of methanol with 1950 µL of a methanolic solution of DPPH° at the same used concentration. After incubation in the dark for 30 minutes and at room temperature, the reduction in DPPH° was accompanied by a change of color from purple to yellow in the solution. The absorbances were read at 515 nm using a spectrophotometer. The positive control used was butylated hydroxyanisole (BHA), and the radical scavenging activity was calculated as a percentage of DPPH° discoloration using the equation: DPPH° radical scavenging (%) = $[(A0 - A1) / A0] \times 100$ Where A0 and A1 are the absorbance at 30 min of the positive control and the extract, respectively. The anti-radical activity was expressed as IC₅₀ (µg/mL), this was the extract concentration required to cause a reduction of 50% to absorbance at 517 nm. A lower IC₅₀ value corresponds to the extract effectiveness (Chaouche et al. 2015).

Ferric reducing antioxidant potential (FRAP)

After adding 1 mL of each extract at different concentrations with 2.5 mL of 0.2 M phosphate buffer at pH= 6.6 and 2.5 mL

of a 1% potassium ferricyanide solution, the obtained mixture was incubated for 20 minutes at 50°C, and then 2.5 mL of 10% trichloroacetic acid was added to stop the reaction. The mixture was centrifuged at 650g for ten minutes at room temperature and 2.5 mL of the supernatant were added to 2.5 mL of distilled water and 0.5 mL of 0.1% iron chloride. The absorbance was read at 700 nm against a blank. The results make it possible to calculate the effective concentration (EC_{50}), which is the extract concentration corresponding to an absorbance equal to 0.5, the linear regression curve (optics density as a function of the different concentrations). The extract activity was finally compared with that of the positive control (BHA) (Chaouche et al. 2015).

Statistical analysis method should be written

Values shown in tables were means±standard deviations of three parallel measurements. IC50 and EC 50 values were calculated from linear regression analysis.

RESULTS

Yields of hydro-methanolic extracts

The extracts were prepared by maceration for 24 hours in methanol-water (70/30); the yields of dry extracts are shown in Table 1.

Phytochemical tests

Specific phytochemical tests were carried out based on staining reactions to highlight the presence or absence of two families of compounds belonging to polyphenols, which are flavonoids and tannins. The results obtained are presented in Table 2.

Phytochemical tests carried out on the extracts of the two parts, leaves and flowers of each studied plant, revealed the

presence of tannins and flavonoids in all the extracts with varying intensities. For flavonoids, the richest extracts are those of the leaves of *L. dentata* and *L. multifida*, with medium intensities. These tests also reveal that all the extracts contain catechic tannins with medium to high intensities, except the extract from the leaves of *L. multifida*, which contains gallic tannins with a very intense blue-black color.

Total polyphenol content

The estimation of total polyphenol contents was carried out by the Folin-Ciocalteu spectrophotometric method. The results obtained are expressed in milligrams of gallic acid equivalent per gram of dry matter (mg GAE/g DW) (Table 3).

Variable contents are found in the numerous hydro-methanolic extracts of the plants studied. The highest content was recorded for the extract of the leaves of *L. multifida* (23 ± 1.1 mg EAG/g DW). Significant contents have been observed in extracts of leaves of *L. stoechas* (18 ± 1.4 mg EAG/g DW), *L. dentata* (15.8 ± 0.9 mg EAG/g DW) and in extracts of flowers of *L. stoechas* (17.8 ± 1.6 mg EAG/g DW) and *L. dentata* (16.4 ± 0.5 mg EAG/g DW). The extract from the flowers of *L. multifida* has lower polyphenol content (7.9 ± 0.2 mg EAG/g DW).

Assessment of antioxidant activity

The evaluation of the antioxidant power of the extracts of our plants was determined by two *in vitro* methods, the trapping of the free radical DPPH° and iron reduction.

Trapping of the free radical DPPH°

The results obtained for the positive control, BHA and for the extracts are expressed as a percentage of inhibition of the free radical DPPH° as a function of the concentrations of extracts (Fig. 1).

The results obtained show that the inhibition percentages increase as a function of the concentration of extracts. The best inhibition percentages are obtained from the extracts of the leaves and flowers of *L. multifida*, 96.66% and 90.18% respectively, at a concentration of 1000 mg/ml. The extracts of *L. stoechas* and *L. dentata* have interesting inhibition percentages, which are between 64.39% and 75.45%. The antioxidant activity of the leaves of *L. multifida* are very close to that of BHA and the flowers are slightly (Statistics should be made, this is not a scientifically relevant comparison) lower. However, the other extracts are significantly lower to that of BHA.

Table 1. The yields obtained from the two parts of the plants studied.

	Plants	Yields (%)
Leaves	<i>L. dentata</i>	21.52±0.9
	<i>L. multifida</i>	12±0.6
	<i>L. stoechas</i>	18.69±0.8
Flowers	<i>L. dentata</i>	14.96±0.6
	<i>L. multifida</i>	10.76±0.6
	<i>L. stoechas</i>	15.54±0.5

Table 2. Results of phytochemical tests.

	Plants	Flavonoids		Tannins	
		Intensity	Colour	Intensity	Colour
Leaves	<i>L. dentata</i>	++	Yellow	+++	Green
	<i>L. multifida</i>	++	Yellow	+++	Dark blue
	<i>L. stoechas</i>	+	Yellow	++	Green
Flowers	<i>L. dentata</i>	+	Yellow	++	Green
	<i>L. multifida</i>	+	Yellow	+++	Green
	<i>L. stoechas</i>	+	Yellow	+++	Green

Very positive reaction: +++, Positive reaction: ++. Moderately positive reaction: +, Negative reaction: -

Table 3. Total phenol content in the hydro-methanolic extracts of the plants studied, expressed in (mg EAG/g DM) and in (mg EAG/g extract).

	Plants	Polyphenols (mg EAG/g DW)
Leaves	<i>L. dentata</i>	15.8±0.9
	<i>L. multifida</i>	23±1.1
	<i>L. stoechas</i>	18±1.4
Flowers	<i>L. dentata</i>	16.4±0.5
	<i>L. multifida</i>	7.9±0.2
	<i>L. stoechas</i>	17.8±1.6

mg EAG/g DW: mg of gallic acid equivalents per gram of dry weight

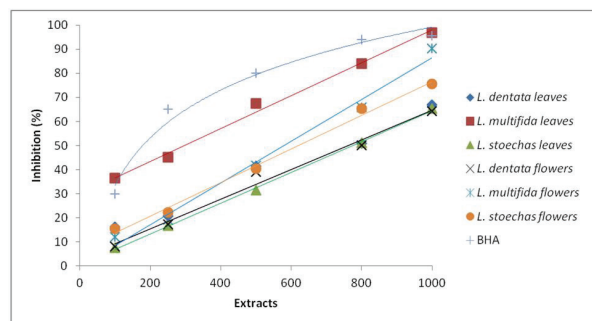


Figure 1. Percentages of inhibition of the DPPH^o radical as a function of the different concentrations of the extracts.

The antioxidant power of the different extracts was determined from the inhibitory concentration IC₅₀ (Table 4). This is the necessary concentration to inhibit 50% of the DPPH^o radical. The smaller its value, the greater the activity.

For comparative purposes, BHA, which is a standard antioxidant, has significant anti-free radical activity with an IC₅₀ value of 150 mg/mL.

According to the IC₅₀ values, the classification of the capacity of the extracts to trap the DPPH^o radical is as follows:

BHA > *L. multifida* leaves > *L. multifida* flowers > *L. stoechas* flowers > *L. dentata* leaves > *L. dentata* flowers > *L. stoechas* leaves.

Table 4. DPPH^o assay expressed as IC50 values (g/ml) for the hydro-methanolic extracts studied.

	Extracts	IC ₅₀ (g/ml)
Leaves	<i>L. dentata</i>	708±12
	<i>L. multifida</i>	300±8
	<i>L. stoechas</i>	758±14
Flowers	<i>L. dentata</i>	746±11
	<i>L. multifida</i>	571±9
	<i>L. stoechas</i>	612±10
BHA		150±7

IC₅₀: inhibition concentration 50%; DPPH: 2,2-diphenyl picrylhydrazyl; BHA: Butylated hydroxyanisole

Therefore, extracts from the leaves of *L. multifida* have the best anti-free radical activity with an IC₅₀ value of 300±8 mg/ml, followed by the extract of the flowers of this same plant. This activity remains lower than that of the positive control BHA.

Iron reduction

This method is based on the reduction capacity of Fe³⁺ present in the K₃Fe (CN)₆ complex into Fe²⁺. Figure 2 represents the reducing capacity of BHA and hydromethanolic extracts. This capacity increases as a function of the concentration of the extracts. At a concentration of 1 mg/ml, it is observed that the extract from the leaves of *L. multifida* has the highest absorbance (1.48).

The values of the optical densities obtained made it possible to calculate EC₅₀ of each extract (Table 5). It is the concentration at which the absorbance is equal to 0.5. The effectiveness of iron reduction is inversely proportional to the EC₅₀ concentration.

For comparative purposes, BHA used as a positive control has an EC₅₀ value of 300 mg/ml.

The classification of the efficiency of iron reduction is as follows: BHA > *L. multifida* leaves > *L. multifida* flowers > *L. stoechas* flowers > *L. dentata* flowers > *L. stoechas* leaves > *L. dentata* leaves. The most active extracts with the lowest EC₅₀ concentrations were found to be these of *L. multifida* leaves (EC₅₀ 343 mg/ml) and flowers (EC₅₀ 396 mg/ml).

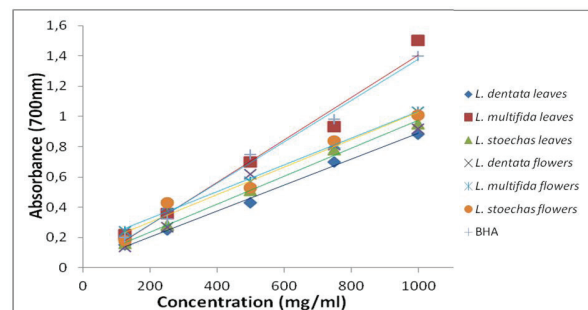


Figure 2. Reducing powers as a function of different concentrations of the extracts.

Table 5: The iron reducing power, expressed as EC50 values (g/ml) for the hydro-methanolic extracts studied.

	Extracts	EC ₅₀ (g/ml)
Leaves	<i>L. dentata</i>	508±14
	<i>L. multifida</i>	343±10
	<i>L. stoechas</i>	485±12
Flowers	<i>L. dentata</i>	467±12
	<i>L. multifida</i>	396±13
	<i>L. stoechas</i>	415±11
BHA		300±10

EC₅₀: effective concentration at which the absorbance was 0.5; BHA: Butylated hydroxyanisole

DISCUSSION

Our work is part of the evaluation of the antioxidant activity of the three aromatic plants of the genus *Lavandula*. The yields of hydromethanolic extracts, obtained by the maceration of the leaves and flowers in methanol-water are different from those found in the two previous works. One was made on the ethanolic-water extracts of *L. multifida* and *L. stoechas* (Bouharb et al. 2014) and the other on the crude aqueous extracts of *L. dentata* and *L. stoechas* (Bachiri, Echchegadda, Ibjibjen, & Nassiri, 2016), and both obtained using the same extraction method. However, it is difficult to compare our results with those of the bibliography, because the method, the solvents and the conditions of extraction, the geographical origin, the conditions of storage and the period of harvest are different.

Phytochemical screening was carried out in order to qualitatively determine the presence of tannins and flavonoids, two important groups of polyphenols, which are present according to the results, obtained in the hydromethanolic extracts of the studied plants with varying intensities. Our results are in agreement with the study carried out by Dif et al. (2017) on the leaves of the three species of *Lavandula* which provides an important presence of tannins in the leaves of *L. dentata* and *L. multifida*, and a weak presence in the leaves of *L. stoechas*. While flavonoids are moderately present in the leaves of the three plants studied. Other work carried out on the aerial parts of *L. dentata* and *L. stoechas*, shows that the extracts contain tannins and flavonoids with variable intensity (Ramchoun et al. 2009).

The quantitative study of polyphenols revealed that the polyphenol contents are close for the hydromethanolic extracts of the leaves and flowers of *L. dentata* (15.8 ± 0.9 and 16.4 ± 0.5 mg EAG/g DW, respectively) and for those of *L. stoechas* (18 ± 1.4 and 17.8 ± 1.6 mg EAG/g DW, respectively). However, the extract from the leaves of *L. multifida* has a higher content than that of the flowers. It is the richest extract in total polyphenols among the six studied. The total phenol content calculated in mg EAG/g extracted throughout the aerial part of *L. multifida*, studied by Ramchoun et al. (2009), is 199.16 mg EAG/g extract. This content is very close to that obtained, only, in the leaves of our plant of the same species (192 ± 3.6 mg EAG/g extract).

The polyphenol contents are higher than those found by Dif et al. (2017) in extracts from the leaves of *L. multifida* (74.74 mg EAG/g extract) and *L. stoechas* (67.58 mg EAG/g extract) and *L. dentata* (60.84 mg EAG/g extract). Another study shows that the respective contents of total phenols in methanolic extracts of *L. stoechas* is 25.2 mg GAE/g and of *L. multifida* is 30.8 mg GAE/g (Messaoud, Chograni, & Boussaid, 2012). In another study, they estimated 184.02 mg EAG/g for *L. dentata* extract and 64.54 mg EAG/g for *L. stoechas* extract, these results cannot be compared with ours (Bachiri et al. 2016). More recently, work carried out on the leaves of *L. dentata* reveals the presence of a higher amount of total polyphenols (39.58 mg EAG/g DW) than ours (Bettaieb Rebey, Bourgou, Saidani Tounsi, Faconnier, & Ksouri, 2017), in another work, the polyphenol content found in the flowers is higher than our results 20.58 ± 0.18 (El Hassouni, El Bachiri, & Belbachir, 2019).

It is difficult to compare our results with this work, because the use of different extraction techniques, different extraction solvents and calibration curves (quercetin, rutin, catechin) reduce the reliability of the comparison between studies. Studies have shown that the content of phenolic compounds varies considerably from one species to another and within the same species, due to extrinsic factors (temperature, climate, etc.) (Ksouri et al. 2019), genetics (the variety and origin of the species) (Ebrahimzadeh, Pourmorad, & Bekhradnia, 2008), physiological factors (the degree of maturation of the plant, the nature of the organs) (Maisuthisakul, Pongsawatmanit, & Gordon, 2007) and the duration of storage.

The antioxidant activity of polyphenols is mainly due to their ability to act as hydrogen donors, reducing agents and radical scavengers. Generally this activity is attributed to the total phenol content and its chemical structure (Messaoud et al. 2012). Consequently, the variation of antioxidant capacity between extracts, observed in our study, can be explained by their polyphenolic content and composition differences. The study by Ramchoun et al. (2009), on the extract from the aerial part of *L. multifida*, the IC_{50} value is 2.6 mg/mL. A value greater than that of the leaves and flowers of *L. multifida*, studied in this work. Similarly, the IC_{50} values, obtained by Dif et al. (2017) from the leaves of the three *Lavandula* species, are 2.15 mg/mL for *L. dentata*, 17.36 mg/mL for *L. multifida* and 25.52 mg/mL for *L. stoechas*, significantly higher values than ours. However, the study by Bettaieb et al. (2017) on the leaves, stems and roots of *L. dentata*, reveals IC_{50} values of: 200.8; 178.70 and 50.36 mg/mL, respectively. Therefore a more important activity in flowers, than that of our plant, the IC_{50} is 508.10 (El Hassouni et al. 2019). In methanolic extracts of *L. multifida* and *L. stoechas* the IC_{50} are 19.03 ± 12 IC_{50} , mg/mL and 34.2 ± 3.1 have proved to be more effective than our results (Messaoud et al. 2012). In another work, hydromethanolic extracts of *L. stoechas* showed a higher *in vitro* antioxidant activity against the DPPH free radical, than ours (Karabagias, Karabagias, & Riganakos, 2019).

For the reduction of iron, the EC_{50} recorded for the extracts of the of *L. multifida*, *L. stoechas* and *L. dentata* leaves and flowers, was very highly active compared to BHA, and the extracts of *L. multifida* were more active compared to the other extracts, it is probably linked to its high phenolic composition. In a study by Ramdan et al. (2017), the aqueous extract of *L. dentata* has less activity compared to the hydromethanolic extracts of the same species studied, on the other hand the ethanolic extract (EC_{50} 346.5mg/mL) has more activity than that found in our work. This activity depended mainly on the type of solvent used for extraction (Nguyen et al. 2017), the extraction method as well as the geographical location of the plant and the harvest season (Chaouche et al. 2020).

CONCLUSION

In recent years, natural substances have seen an increasing interest in the medical field, in the pharmaceutical areas and food industries. In this context we were interested in the quantification of total phenols and in the antioxidant power of hydromethanolic extracts of the leaves and flowers of three species of *Lavandula* (*L. dentata*, *L. multifida* and *L. stoechas*).

From the results obtained during this study, we noticed the presence of flavonoids and tannins in two parts of the three plants studied. The assay results of total polyphenols and the antioxidant activities in these extracts, show that the extract of the leaves *L. multifida* have a high level of polyphenols (23 ± 1.1 mg EAG/g DW) and a significant antioxidant power compared to other extracts (DPPH^o assay the leaves: IC₅₀ 300 ± 8 µg/ml), this activity remains low by comparing the IC₅₀ values of the extracts with those of the positive controls (BHA). This may be due to the fact that the concentrations necessary to exert an antioxidant activity are higher for crude plant extracts than for pure and synthetic molecules.

Finally, these results obtained, *in vitro*, constitute only a first step in the search for natural substances which have antioxidant activity. It would be interesting to carry out other techniques and methods such as: Testing the antioxidant effect by other *in vitro* and *in vivo* methods, isolating and identifying chemical compounds responsible for the antioxidant activity of *L. multifida*.

Peer-review: Externally peer-reviewed.

Author Contributions: Conception/Design of Study- F.H.; Data Acquisition- F.H., T.M.C., I.G., O.B.; Data Analysis/Interpretation- F.H., T.M.C., I.G., O.B.; Drafting Manuscript- T.M.C., I.G.; Critical Revision of Manuscript- F.H.; Final Approval and Accountability- F.H., T.M.C., M.S., I.G., O.B.

Conflict of Interest: The authors have no conflict of interest to declare.









Financial Disclosure: Authors declared no financial support.

REFERENCES

- Adaszyńska-Skwirzyńska, M., & Dzięcioł, M. (2017). Comparison of phenolic acids and flavonoids contents in various cultivars and parts of common lavender (*Lavandula angustifolia*) derived from Poland. *Natural product research*, 31(21), 2575-2580.
- Algieri, F., Rodriguez-Nogales, A., Vezza, T., Garrido-Mesa, J., Garrido-Mesa, N., Utrilla, M. P., González-Tejero, M.R., Casares-Porcel, M., Molero-Mesa, J., Del Mar Contreras, M., Segura-Carretero, A., Pérez-Palacio, J., Díaz, C., Vergara, N., Vicente, F., Rodríguez-Cabezas, M.E., & Galvez, J. (2016). Anti-inflammatory activity of hydroalcoholic extracts of *Lavandula dentata* L. and *Lavandula stoechas* L. *Journal of Ethnopharmacology*, 190, 142-158.
- Amara, N., Boukhatem, M. N., Ferhat, M. A., Kaibouche, N., Laisaoui, O., & Boufridi, A. (2017). Applications potentielles de l'huile essentielle de lavande papillon (*Lavandula stoechas* L.) comme conservateur alimentaire naturel. *Phytothérapie*, 4, 1-9.
- Bachiri, L., Echchegadda, G., Ibbijben, J., & Nassiri, L. (2016). Etude phytochimique et activité antibactérienne de deux espèces de Lavande Autochtones Au Maroc: «*Lavandula stoechas* L. et *Lavandula dentata* L.». *European Scientific Journal*, 12(30), 313-333
- Bettaieb Rebey, I., Bourgou, S., Saidani Tounsi, M., Fauconnier, M. L., & Ksouri, R. (2017). Etude de la composition chimique et de l'activité antioxydante des différents extraits de la Lavande dentée (*Lavandula dentata*). *Journal of New Sciences Agriculture and Biotechnology*, 39(2), 2096-2105.
- Bouharb, H., El Badaoui, K., Zair, T., El amri, J., Chakir, S., & Alaoui, T. (2014). Sélection de quelques plantes médicinales du Zerhoun (Maroc centrale) pour l'activité antibactérienne contre *Pseudomonas aeruginosa*. *Journal of Applied Biosciences*, 78(1), 6685-6693.
- Boust, D., & Farah, A. (2020). A Phytopharmacological review of a Mediterranean plant: *Lavandula stoechas* L. *Clinical Phytoscience*, 6(1), 9.
- Canlı, K., Yetgin, A., Benek, A., Bozyel, M. E., & Murat Altuner, E. (2019). *In Vitro* Antimicrobial Activity Screening of Ethanol Extract of *Lavandula stoechas* and Investigation of Its Biochemical Composition. *Advances in Pharmacological and Pharmaceutical Sciences*, 2019, 1-6.
- Chaouche, T. M., Haddouchi, F., Boudjemai, O., & Ghellai, I. (2020). Antioxidant and hemolytic activity of *Ziziphus jujuba* Mill and *Rhamnus alaternus* L (Rhamnaceae) extracts from Algeria. *Bulletin de la Société Royale des Sciences de Liège*, 89, 1-14
- Chaouche, T.M., Haddouchi, F., Atik-Bekara, F., Ksouri, R., Azzi, R., Boucherit, Z., Tefiani, C., & Larbat, R. (2015). Antioxidant, haemolytic activities and HPLC–DAD–ESI–MSn characterization of phenolic compounds from root bark of *Juniperus oxycedrus* subsp. *oxycedrus*. *Industrial Crops and Products*, 64, 182-187
- Dif, M. M., Benyahia, M., Benali, F. T., Rahmani, M., & Bouazza, S. (2017). Phenolic content and antioxidant activity of three Algerian species of lavenders. *Phytothérapie*, 15(6), 367-372.
- Ebrahimzadeh, M. A., Pourmorad, F., & Bekhradnia, A.R. (2008). Iron chelating activity screening, phenol and flavonoid content of some medicinal plants from Iran. *African Journal of Biotechnology*, 7(18), 3188-3192
- El Hassouni, A., El Bachiri, A., & Belbachir, C. (2019). *Lavandula dentata* Solid Residue from Essential Oil Industry. *Journal of Essential Oil Bearing Plants*, 22(6), 1601-1613.
- El-Hilaly, J., Hmammouchi, M., & Lyoussi, B. (2003). Ethnobotanical studies and economic evaluation of medicinal plants in Taounate province (Northern Morocco). *Journal of Ethnopharmacology*, 86(2-3), 149-158.
- Haddouchi, F., Chaouche, T.M., & Nourdinne, H. (2018). Screening phytochimique, activités antioxydantes et pouvoir hémolytique de quatre plantes sahariennes d'Algérie. *Phytothérapie*, 16(1), 254-262.
- Kala, C.P. (2015). Medicinal and aromatic plants: boon for enterprise development. *Journal of Applied Research on Medicinal and Aromatic Plants*, 2(4), 134-139.
- Karabagias, I.K., Karabagias, V.K., & Riganakos, K.A. (2019). Physico-Chemical Parameters, Phenolic Profile, *In Vitro* Antioxidant Activity and Volatile Compounds of Ladastacho (*Lavandula stoechas*) from the Region of Saidona. *Antioxidants*, 8(4), 80.
- Ksouri, R., Falleh, H., Megdiche, W., Trabelsi, N., Hamdi, B., Chaieb, K., Bakhrouf, A., Magné, C., & Abdely, C. (2009). Antioxidant and antimicrobial activities of the edible medicinal halophyte *Tamarix g allica* L and related polyphenolic constituents. *Food and Chemical Toxicology*, 47(8), 2083-2091.
- Maisuthisakul, P., Pongsawatmanit, R., & Gordon, M. H. (2007). Assessment of phenolic content and free radical scavenging capacity of some Thai indigenous plants. *Food Chemistry*, 100(4), 1409-1418.
- Messaoud, C., Chograni, H., & Boussaid, M. (2012). Chemical composition and antioxidant activities of essential oils and methanol extracts of three wild *Lavandula* L. species. *Natural Product Research*, 26(21), 1976-1984.
- Napoli, E., Siracusa, L., & Ruberto, G. (2020). New Tricks for Old Guys: Recent Developments in the Chemistry, Biochemistry, Applications and Exploitation of Selected Species from the Lamiaceae Family. *Chemistry & Biodiversity*, 17(3), e1900677.
- Nguyen, T. Q., Schmitz, A., Nguyen, T. T., Orlov, N. L., Böhme, W., & Ziegler, T. (2011). Review of the genus *Sphenomorphus* Fitzinger, 1843 (Squamata: Sauria: Scincidae) in Vietnam, with description of a new species from northern Vietnam and southern China and the first record of *Sphenomorphus mimicus* Taylor, 1962 from Vietnam. *Journal of Herpetology*, 45(2), 145-154.
- Panuccio, M. R., Fazio, A., Papalia, T., & Barreca, D. (2016). Antioxidant properties and flavonoid profile in leaves of Calabrian *Lavandula multifida* L., an autochthon plant of Mediterranean Southern regions. *Chemistry & Biodiversity*, 13(4), 416-421

- Ramchoun, M., Harnafi, H., Alem, C., Benlyas, M., Elrhaffari, L., & Amrani, S. (2009). Study on antioxidant and hypolipidemic effects of polyphenol-rich extracts from *Thymus vulgaris* and *Lavandula multifida*. *Pharmacognosy Research*, 1(3), 106.
- Ramdan, B., Amakran, A., Bakrim, N., Vannier, B., Greche, H., & Nhiri, M. (2017). Anti-glycation and radical scavenging activities of hydro-alcohol and aqueous extracts of nine species from Lamiaceae family. *Journal of Medicinal Plants*, 5(1), 331-345.
- Soheili, M., & Salami, M. (2019). *Lavandula angustifolia* biological characteristics: An *in vitro* study. *Journal of Cellular Physiology*, 234(9), 16424-16430.
- Sosa, S., Altinier, G., Politi, M., Braca, A., Morelli, I., & Della Loggia, R. (2005). Extracts and constituents of *Lavandula multifida* with topical anti-inflammatory activity. *Phytomedicine*, 12(4), 271-277.

Antimicrobial activities of some narrow endemic gypsopyhte

Esma Ocak¹ , Şule İnci² , Derviş Öztürk³ , Sanem Akdeniz Şafak⁴ , Ebru Özdeniz⁵ , Sevda Kırbağ² , Ahmet Harun Evren² , Latif Kurt⁵ 

¹Osmangazi University, Faculty of Science and Literacy, Department of Chemistry, Eskişehir, Turkey

²Firat University, Faculty of Science, Department of Biology, Elazığ, Turkey

³Osmangazi University, Mahmudiye Horse Breeding Vocational School, Eskişehir, Turkey

⁴Aksaray University, Faculty of Science and Lireracy, Department of Biology, Aksaray, Turkey

⁵Ankara University, Faculty of Science, Department of Biology, Ankara, Turkey

ORCID IDs of the authors: E.O.0000-0002-9085-4151; Ş.İ. 0000-0002-4022-5269; D.Ö. 0000-0001-7189-7407; S.A.Ş. 0000-0002-7660-9109; E.Ö. 0000-0003-4082-3071; S.K.0000-0002-4337-8236; A.H.E.0000-0003-1598-3065; L.K. 0000-0003-1598-3065

Cite this article as: Ocak, E., İnci, S., Öztürk, D., Akdeniz Şafak, S., Özdeniz, E., Kırbağ, S. ... Kurt, L. (2021). Antimicrobial activities of some narrow endemic gypsopyhte. *Istanbul Journal of Pharmacy*, 51(1), 118-122.

ABSTRACT

Background and Aims: In this study, antimicrobial activities of extracts obtained from narrowly dispersed local endemic gypsophytes grown in extreme habitats were investigated for the first time. The aim of this study was to analyze antimicrobial effects of narrow endemic plants that are *Thymus ekimii* Yildirimli, *Verbascum gypsicola* Vural & Aydogdu, *Glaucium secmenii* Yildirimli and *Psephellus erzincani* Wagenitz & Kandemir.

Methods: Antimicrobial activity of *T. ekimii*, *V. gypsicola*, *G. secmenii* and *P. erzincani* were determined according to the disk diffusion method. The microorganisms used for the present investigation; gram positive bacteria, gram negative bacteria and yeasts (*Bacillus megaterium* DSM32, *Escherichia coli* ATCC25922, *Candida albicans* FMC17).

Results: According to the results obtained, *P. erzincani* showed the best antimicrobial activity against *B. megaterium* DSM32 (23 mm), *E. coli* ATCC25922 (15 mm) and *C. albicans* FMC17 (23mm), respectively.

Conclusion: This study showed that extracts of these endemic plants have the potential for use as antimicrobial agents, especially *P. erzincani*.

Keywords: *Thymus ekimii*, *Verbascum gypsicola*, *Glaucium secmenii*, *Psephellus erzincani*, antimicrobial activity, gypsopyhte

INTRODUCTION

The increasing resistance of bacteria to clinical antibiotics necessitates the development of new agents in the treatment of diseases. Therefore, antibacterial and antifungal effects of herbal preparations are very important due to the high incidence of antibiotic resistance in treatment (Mummed, Abraha, Feyera, Nigusse, & Assefa, 2018). Some studies showed that plants can be successful in overcoming antibiotic resistance with combinatorial approaches (Van Vuuren & Viljoen, 2011; Hutchings & Cock, 2018; Blonk & Cock, 2019). Today, 80% of the active substances used in the treatment of infectious diseases are thought to be vegetable-oriented (Özdek, Seçkin, & Çibuk, 2020). Therefore, the use of plant extracts as an antioxidant and antimicrobial agent has been expanded in recent years.

Among the leading countries of the temperate zone, Turkey has a lot of floristic diversity and endemism. Therapeutic uses of plants are based on ancient times. It has been found mainly by trial and error in Anatolia as well as all over the world and medi-

Address for Correspondence:

Esma OCAK, e-mail: eocak@ogu.edu.tr

Submitted: 14.09.2020

Revision Requested: 31.10.2020

Last Revision Received: 04.11.2020

Accepted: 03.12.2020

This work is licensed under a Creative Commons Attribution 4.0 International License.



cally important plants have been widely used in traditional folk medicine for many centuries. It is known that some widespread endemic species have different antimicrobial effects (Yiğit, Kandemir, & Yiğit, 2002; Buruk, Sokmen, Aydin, & Erturk, 2006; Dulger, 2006; Benli, Güney, Bingöl, Geven, & Yiğit, 2007; Benli, Yiğit, Geven, Güney, & Bingöl, 2009; Türker, Birinci Yıldırım, Pehlivan Karakaş, & Köylüoğlu, 2009). While recent studies on antimicrobial activity are mostly concentrated on widespread endemic species, in this study, the antimicrobial effects of the gypsophyte species developing in gypseous soils, which are extremely arid habitats, were examined (Wagenitz, & Kandemir, 2008; Yıldırım, 2012).

T. ekimii is a member of the Lamiaceae family and it is known that this family species is used in food and cosmetics as well as in the pharmaceutical industry (Bekut et al., 2018). It is known that *Thymus* L. (thyme) is used as a spice in meals and facilitates digestion. It is used by local people for cramps, disinfection, and as an expectorant. In studies, it has been determined that there are biological activities such as antioxidant, antiseptic, and antimicrobial (Benli & Yiğit, 2005).

Some species of the genus *Verbascum* L., including *V. gypsicola*, have been used extensively for centuries to treat internal and external infections. It is traditionally used by local people as a tea, and is believed to have a chest loosening and expectorant effect. In addition, some species of the *Verbascum* L. genus have biological effects such as antimalarial, antiviral, antitumor, antihepatotoxic, antihyperlipidemic, antioxidant, anti-inflammatory, antinociceptive, wound-healing, antimicrobial, anthelmintic, sedative, pre-anesthetic, and anxiolytic (Civelek, 2018).

The genus *Glaucium* Mill., which includes the species *G. secmenii*, has been used by local people for food and medical purposes. Some species' seeds, green parts, and petals are used. It is stated in some studies that it is effective in colds, bronchitis, and in conditions such as expectorant and for insomnia (Saraç et al., 2018).

There are not many studies on the antimicrobial activities of taxa belonging to the genus *Psephellus* Cass., which also includes the *P. erzincani* species, and some species have been examined for their cytotoxic, antioxidant and anti-inflammatory activities (Korkmaz et al., 2019; Demiroz, Nalbantsoy, Aydin, & Baykan, 2020).

The genus *Psephellus* has been separated from *Centaurea*, and some *Centaurea* species are used for fever, diabetes, hemorrhoids, and peptic ulcers for therapeutic purposes among people. In pharmacological and phytochemical studies, antioxidant, antimicrobial, and antipyretic properties have been determined in many different *Centaurea* species (Korkmaz et al., 2019).

In this study, it was aimed to determine the antimicrobial activities of the extracts obtained from a methanol solvent of local gypsophyte endemics *T. ekimii*, *V. gypsicola*, *G. secmenii* and *P. erzincani*.

MATERIALS AND METHODS

Collection and identification of plant material

The common feature of plants is that they are local endemic species spread on gypsum soils, which are extremely excavated arid habits for plant life. Plant materials were diagnosed using Flora of Turkey and East Aegean Islands (Ekim 2000). Identified plant samples were checked in the ANK Herbarium, and the doublet of the plants was preserved in the ANK Herbarium (Table 1).

Extract of plant material

T. ekimii, *G. secmenii*, *V. gypsicola*, *P. erzincani* were dried and after milling added to the 40 mL 98% methanol by weighing 1 g for each sample.

Each sample was kept on a rotary shaker at 100 rpm for 72 hours to obtain the extract. It was then filtered using Whatman filter paper and stored at 4°C for further study. Then 20 µL (500 µg/L) extracts were injected into 6 mm diameter empty antibiotic discs (Ereçevit Sönmez, Kirbağ, & İnci, 2019).

Test microorganisms

In this study; *Escherichia coli* ATCC 25322 and *Bacillus megaterium* DSM32 as bacteria, and *Candida albicans* FMC17 as fungi were used. Microorganism cultures were obtained from the Firat University, Faculty of Science, Department of Biology, Microbiology Laboratory culture collection.

Preparation of microorganism cultures and testing of antimicrobial effect

The antimicrobial activity of extracts of plant samples obtained using methanol was determined according to the disk diffusion method (Collins & Lyne, 1989).

Table 1. The location and GPS coordinates and elevation of species extracted

Species	Locality, Collector and Number of plants	Elevation (m)
<i>Thymus ekimii</i> Yıldırımli	Between Aşağıkepen and Keven villages / Eskişehir 39°22'10.0" N 031°29'09.1" E, 05.06.2020 Kurt, L., 15214	938
<i>Glaucium secmenii</i> Yıldırımli	Ankara-Eskişehir road side / Eskişehir 39°33'51.4" N 031°48'27.9" E, 05.06.2020 Kurt, L., 14938	988
<i>Verbascum gypsicola</i> Vural & Aydogdu	Beypazarı-Nallıhan road, near Çayırhan / Ankara 40°06'24.3" N 031°43'45.5" E, 06.06.2020 Kurt, L., 15583	611
<i>Psephellus erzincani</i> Wagenitz & Kandemir	İlic-Dirvigi road, near Bağistas village / Erzincan 39°27'02.1" N 038°28'52.4" E, 12.06.2020 Kurt, L., 14701	889

Bacterial strains (*E. coli* ATCC25322, *B. megaterium* DSM32), were incubated in Nutrient Buyyon (Difco) for 24 hours at $35\pm 1^\circ\text{C}$ and the yeast strain (*C. albicans* FMC17) was incubated at $25\pm 1^\circ\text{C}$ for 48 hours in Malt Extract Buyyon (Difco). Cultures grown in broth medium were adjusted to the 0.5 McFarland standard. The culture of prepared bacteria and yeast in broth are as follows; Mueller Hinton Agar and Yeast Malt Extract Agar were inoculated with 1% (10^6 cells/mL of bacteria, 10^4 cells/mL yeast and cells/mL as per Mc Farland standard) and after shaking well, 25 ml were placed in sterile petri dishes with a diameter of 9 cm and homogeneous dispersion was provided.

Six mm diameter antimicrobial discs (Oxoid), each of which was absorbed 20 μl of different extracts, were placed in the solidified agar medium aseptically.

After the petri dishes prepared in this way were kept at 4°C for 1.5-2 hours, the bacteria grafted plates were incubated at $37\pm 0.1^\circ\text{C}$ for 24 hours, and the yeast-grafted plates at $25\pm 0.1^\circ\text{C}$ for 72 hours.

As a control, different standard discs were used for bacteria (Piperacillin/Tozabactam 110 μg /disk) and yeasts (Mycostatin 30 μg /disk).

Inhibition zones formed on the medium at the end of the period were evaluated in mm.

RESULTS AND DISCUSSION

The antimicrobial effects of *T. ekimii*, *G. secmenii*, *V. gypsicola*, *P. erzincani* methanol extracts against *B. megaterium* DSM32, *E. coli* ATCC25322 and *C. albicans* FMC17 are shown in Table 2. Mycostatin (30 μg /disk) used for yeasts created a 15 mm inhibition zone against *C. albicans* FMC17. Piperacillin/Tozabactam (110 μg /disk) prevented the growth of tested bacteria at different rates (25-38 mm inhibition zone).

	Diameter of Inhibition Zone (mm)		
	<i>Bacillus megaterium</i> DSM32	<i>Escherichia coli</i> 25322ATCC	<i>Candida albicans</i> FMC17
<i>Thymus ekimii</i>	11	10	14
<i>Glaucium secmenii</i>	11	10	12
<i>Verbascum gypsicola</i>	8	7	7
<i>Psephellus erzincani</i>	23	15	23
Control	25	38	15

Against *B. megaterium* DSM32 *T. ekimii*, *G. secmenii* and *V. gypsicola* formed a 11 mm and 8 mm zone diameter respectively, while the inhibition zone of *P. erzincani* was measured at 23 mm (Figure 1). It has been determined that *T. ekimii*, *G. secmenii*, *V. gypsicola*, *P. erzincani* prevent the development of *E. coli* ATCC25322 at different rates (7-15 mm) (Figure 2). *T. ekimii*, *G. secmenii*, *V. gypsicola* and *P. erzincani* species formed 14 mm, 12 mm, 7 mm and 23 mm inhibition zones against *C. albicans* FMC17, respectively (Figure 3). According to the results obtained, the *P. erzincani* extract showed the best antimicrobial activity against *B. megaterium* DSM32 (23 mm), *E. coli* ATCC25322 (15 mm) and *C. albicans* FMC17 (23 mm).

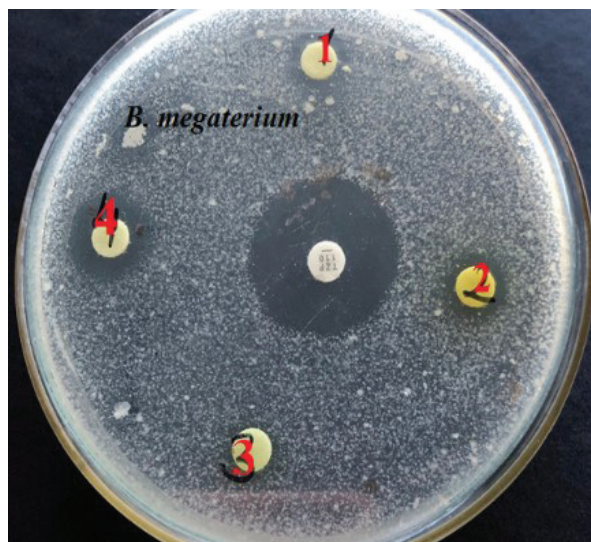


Figure 1. Antimicrobial effects of narrow endemic gypsopyhte against *B. megaterium* (numbers in petri; 1- *T. ekimii*; 2- *G. secmenii*; 3- *V. gypsicola*; 4- *P. erzincani*).

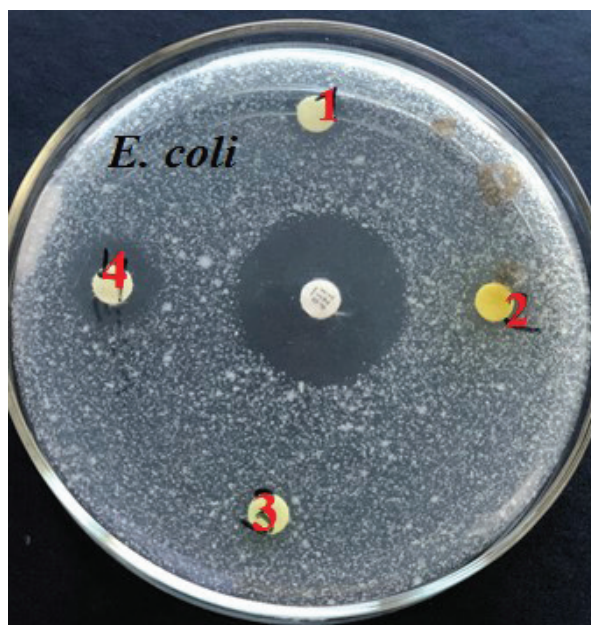


Figure 2. Antimicrobial effects of narrow endemic gypsopyhte *E. coli* (numbers in petri; 1- *T. ekimii*; 2- *G. secmenii*; 3- *V. gypsicola*; 4- *P. erzincani*).

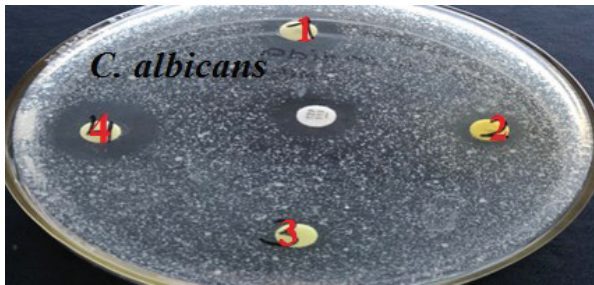


Figure 3. Antimicrobial effects of narrow endemic gypsophyte against *C. albicans* (numbers in petri; 1- *T. ekimii*; 2- *G. secmenii*; 3- *V. gypsicola*; 4- *P. erzincani*).

The antimicrobial activity of some *Thymus* species have been shown in other previous studies. In the studies conducted, it was determined that essential oils obtained from *Thymus algeriensis* prevent the development of *S. aureus* ATCC25923, *B. subtilis* 166, *S. enteridis* ATCC502, *E. coli* GM109, *P. aeruginosa* and *L. monocytogenes* at different rates (9-74 mm inhibition zone) (Guesmi, Mouna, Mondher, & Ahmed, 2014). In a different study, the antimicrobial effect of essential oils of *T. vulgaris* L. against different strains of *E. coli* 25922 was determined as 22.7-2.8 $\mu\text{l ml}^{-1}$, and antimicrobial effect against different strains of *S. aureus* ATCC25923, ATCC6538 as 11.4-45.4 $\mu\text{l ml}^{-1}$. It has been reported that essential oils of the same species show 0.11 $\mu\text{l ml}^{-1}$ antimicrobial activity against different strains of *C. albicans* ATCC10231 (Bogavac et al., 2015). The essential oils of *Thymus longicaulis* subsp. *longicaulis* were found to have an antimicrobial effect of 0.781 $\mu\text{g/ml}$ against *S. aureus* ATCC25923 and 0.098 $\mu\text{g/ml}$ against *E. coli* and *C. albicans* DSMZ1386 (Demiryapan, 2020). It was determined that *Thymus serpyllum* ethanol, methanol, and water extracts did not prevent the development of *E. coli* ATCC11229 at a concentration of 150 mg/ml, and the ethanol and methanol extract prevent the development of *C. albicans* RSKK02029 (8 mm inhibition zone) (Ökmen, Arslan, Vurkun, Mammadkhanli, & Ceylan, 2017). The essential oils of *Thymus vulgaris* have been reported to have 49.27 \pm 7.26 mm against *S. aureus* NCTC8530 and 39.55 \pm 0.52 mm against *E. coli* BL21 (Kılıç, 2019).

The antimicrobial effects of methanol, ethanol, and water extracts of *Verbascum degenii* against some hospital pathogens were investigated. In the results obtained, while methanol extract formed an inhibition zone of 20 \pm 1.6 mm against *S. aureus*, ethanol extract formed an inhibition zone of 21 \pm 1.5 mm, and no inhibition zone was observed in water extract (Avşar, Keskin, & Berber, 2016).

While the water extract of *Glaucium grandiflorum* Boiss. & Huet var. *grandiflorum* has antimicrobial effects >5 mg/ml against *E. coli* ATCC25922, 0.625 mg/ml against *S. aureus* ATCC29213 and >5 mg/ml against *C. albicans* ATCC10231; ethanol extract against the same microorganisms showed antimicrobial effects >5 mg/ml, 5 mg/ml and 1.25 mg/ml, respectively (Saraç et al., 2018).

Many microorganisms that harm human health show resistance to drugs due to using unnecessary and wrong antibiotics. Therefore, there is a need to discover new substances from

natural sources, including plants. In this study, the antimicrobial activity of gypsophytes grown in gypsiferous soils, which are extreme habitats for plants, were investigated. The species discussed in this study are local endemic gypsophytes and their antimicrobial activities were examined for the first time. It has been predicted that species growing in extreme habitats may have high antimicrobial activities.

Among the four gypsophytes examined in this study, *P. erzincani* extract showed the best antimicrobial activity against *B. megaterium* DSM32 (23 mm), *E. coli* ATCC25322 (15 mm) and *C. albicans* FMC17 (23 mm). Investigating the antimicrobial activities of species grown in extreme habitats may lead to new antibiotic research.

The results obtained show that antimicrobial effects of *T. ekimii*, *V. gypsicola*, *G. secmenii* and *P. erzincani* are different from *Thymus algeriensis*, *T. vulgaris*, *T. longicaulis* subsp. *longicaulis*, *T. serpyllum*, *Glaucium grandiflorum* var. *grandiflorum* in literature. As a result of the adaptation of these plants (*T. ekimii*, *V. gypsicola*, *G. secmenii* and *P. erzincani*) to extreme habitats (gypsum soils etc.), their defense systems are well developed and have a high resistance against drought, bacteria, viruses, and other pathogens. Therefore, it is very important that research of the antimicrobial effects of plant species living in these extreme conditions and their use as an antimicrobial agent against microorganisms receive further investigation and study.

In conclusion, these four narrow endemic plants, especially *P. erzincani*, have the potential for use as antimicrobial agents. Endemic plant species as antimicrobial agents are substantial in pharmacology and more investigation is necessary in terms of contributing to the literature.

Peer-review: Externally peer-reviewed.

Author contributions: Conception/Design of Study- E.O., S.K., L.K.; Data Acquisition-L.K., E.Ö.; Data Analysis/Interpretation-Ş.İ., S.K., A.H.E.; Drafting Manuscript- E.O., L.K., E.Ö., Ş.İ.; Critical Revision of Manuscript-E.O.; Final Approval and Accountability- E.O., Ş.İ., D.Ö., S.A.Ş., E.Ö., S.K., A.H.E., L.K.

Conflict of Interest: The authors have no conflict of interest to declare.

Financial Disclosure: Authors declared no financial support.

REFERENCES

- Avşar, C., Keskin, H., & Berber, İ. (2016). Hastane infeksiyonlarından izole edilen mikroorganizmalara karşı bazı bitki ekstraktlarının antimikrobiyal aktivitesi. [Antimicrobial Activity of Some Plant Extracts against Microorganisms Isolated from Hospital Infections]. *International Journal of Pure and Applied Sciences*, 2(1), 22-29.
- Bekli, M., Brkic, S., Kladar, N., Dragovic, G., Gavarić, N., & Božin, B. (2018). Potential of selected Lamiaceae plants in anti(retro)viral therapy. *Pharmacological Research*, 133, 301–314. <https://doi.org/10.1016/j.phrs.2017.12.016>
- Benli, M., & Yiğit, N. (2005). Ülkemizde yaygın kullanımı olan kekik (*Thymus vulgaris*) Bitkisinin Antimikrobiyal Etkisi. *Orlab On-Line Mikrobiyoloji Dergisi*, 3(8), 1-8.
- Benli, M., Güney, K., Bingöl, Ü., Geven, F., & Yiğit, N. (2007). Antimicrobial activity of some endemic plant species from Turkey. *African Journal of Biotechnology*, 6(15), 1774-1778.

- Benli, M., Yiğit, N., Geven, F., Güney, K., & Bingöl, Ü. (2009). Antimicrobial activity of endemic *Digitalis lamarckii* Ivan from Turkey. *Indian Journal of Experimental Biology*, 47(3), 218-21.
- Bogavac, M., Karaman, M., Janjusevic, L., Sudji, J., Radovanovic, B., Novakovic, Z. ... Bozin, B. (2015). Alternative treatment of vaginal infections – in vitro antimicrobial and toxic effects of *Coriandrum sativum* L. and *Thymus vulgaris* L. essential oils. *Journal of Applied Microbiology*, 119, 697-710. <https://doi.org/10.1111/jam.12883>
- Blonk, B., & Cock, I.E. (2019). Interactive antimicrobial and toxicity profiles of *Pittosporum angustifolium* Lodd. extracts with conventional antimicrobials. *Journal of Integrative Medicine*, 17, 261–272. <https://doi.org/10.1016/j.joim.2019.03.006>
- Buruk, K., Sokmen, A., Aydin, F., & Erturk, M. (2006). Antimicrobial activity of some endemic plants growing in the Eastern Black Sea Region, Turkey. *Fitoterapia*, 77, 388–391. <https://doi.org/10.1016/j.fitote.2006.03.002>
- Civelek, ED. (2018). *Verbascum pyramidatum* Bieb. Üzerinde Farmakognozik Araştırmalar in Hacettepe University, (Master's Thesis). Retrieved from <http://www.openaccess.hacettepe.edu.tr>
- Collins, C.H., Lyne, P.M., Grange, J.M. & Flkinham III, J.O. (2004). *Microbiological Methods*, (p. 140), London, Arnold. .
- Demiroz, T., Nalbantsoy, A., Aydin, K., & Baykan, S. (2020). Phytochemical composition and antioxidant, cytotoxic and anti-inflammatory properties of *Psephellus goeksunensis* (Aytaç & H. Duman) Greuter & Raab-Straube. *South African Journal of Botany*, 130, 1-7. <https://doi.org/10.1016/j.sajb.2019.11.021>
- Demiryapan, A. (2020). *Teucrium polium* L. ve *Thymus longicaulis* subsp. *longicaulis* C. Presl Bitkilerinden Elde Edilen Uçucu Yağların GC-MS Analizi Ve Antimikrobiyal Aktiviteleri in Kastamonu University, (Master's Thesis). Retrieved from <http://tez.yok.gov.tr/UlusalTezMerkezi/tezSorguSonucYeni.jsp>
- Dulger, B. (2006). Antimicrobial Activity of Some Endemic Scrophulariaceae from Turkey. *Pharmaceutical Biology*, 44(9), 672–676. <https://doi.org/10.1080/13880200601009099>
- Ekim, T. (2000). *Verbascum* In Güner, A., Özhatay, N., Ekim, T., & Başer, K.H.C. (eds.). *Flora of Turkey and the East Aegean Islands, Vol. XI (Supplement 2)*. (p. 193). Edinburgh, UK: Edinburgh University Press
- Erecevit Sönmez P, Kirbağ S., & İnci Ş. (2019). Antifungal and Antibacterial Effect of Dodder (*Cuscuta campestris*) Used for Hepatitis Treatment of Mothers and Newborn Infants in Province Mardin in Turkey. *Yüzüncü Yıl Üniversitesi Tarım Bilimleri Dergisi*, 29(4), 722-730. <https://doi.org/10.29133/yyutbd.605970>
- Guesmi, F., Mouna, B.F., Mondher, M., & Ahmed, L. (2014). In-vitro assessment of antioxidant and antimicrobial activities of methanol extracts and essential oil of *Thymus hirtus* sp. *algeriensis*. *Lipids in Health and Disease*, 13, 114. <https://doi.org/10.1186/1476-511X-13-114>
- Hutchings, A., & Cock, I.E. (2018). An interactive antimicrobial activity of *Embellica officinalis* Gaertn. fruit extracts and conventional antibiotics against some bacterial triggers of autoimmune inflammatory diseases. *Pharmacognosy Journal*, 10(4), 654–62. <https://doi.org/10.5530/pj.2018.4.108>
- Kılıç, Ö. (2019). *Bazı Bitkilerde Uçucu Yağların Biyoaktif ve Antimikrobiyal Özelliklerinin Araştırılması in Ordu University*, (Master's Thesis). Retrieved from <http://earsiv.ordu.edu.tr>
- Korkmaz, N., Ozlem Sener, S.O., Balturk, N., Kanbolat, S., Badem, M., Aliyazicioglu, R. ... Alpay Karaoglu, S. (2019). Determination of Phenolic Contents by HPLC, and Antioxidant, Antimicrobial, Antityrosinase, and Anticholinesterase Activities of *Psephellus hubermorathii*. *Journal of Pharmaceutical Research International*, 26(1), 1-10. <https://doi.org/10.9734/JPRI/2019/v26i130125>
- Mummied, B., Abraha, A., Feyera, T., Nigusse, A., & Assefa, S. (2018). In Vitro Antibacterial Activity of Selected Medicinal Plants in the Traditional Treatment of Skin and Wound Infections in Eastern Ethiopia, *BioMed Research International*, Volume 2018, 8, Article 1862401. <https://doi.org/10.1155/2018/1862401>
- Ökmen, G., Arslan, A., Vurkun, M., Mammadkhanli, M., & Ceylan, O. (2017). Farklı Baharatların Antimikrobiyal ve Antioksidan Aktiviteleri. *Elektronik Mikrobiyoloji Dergisi*, 15(1): 16-28.
- Özdek, U., Seçkin, H., & Çibuk, S. (2020). Investigation of Antimicrobial Effects of *Amygdalus trichamygdalus* (Sweet Almond) and *Amygdalus nana* L. (Bitter Almond) Plants. *Van Veterinary Journal*, 31(1), 22-26. <https://doi.org/10.36483/vanvetj.651515>
- Saraç, H., Daştan, T., Durukan, H., Durna Daştan, S., Demirbaş, A., & Karaköy, T. (2018). Kırmızı Gelincik (Fam: Papaveraceae, *Glaucium grandiflorum* Boiss. & Huet var. *grandiflorum*) Bitkisinin Farklı Özütlelerinin Besin Elementi İçeriğinin ve In Vitro Antiproliferatif Etkilerinin Değerlendirilmesi. *Süleyman Demirel Üniversitesi Ziraat Fakültesi Dergisi*, 1. *Uluslararası Tarımsal Yapılar ve Sulama Kongresi Özel Sayısı*, 417-428.
- Türker, H., Birinci Yıldırım, A., Pehlivan Karakaş, F., & Köylüoğlu, H. (2009). Antibacterial Activities of Extracts from Some Turkish Endemic Plants on Common Fish Pathogens. *Turkish Journal of Biology*, 33, 73-78. <https://doi.org/10.3906/biy-0805-18>
- Van Vuuren, S., & Viljoen, A. (2011). Plant-based antimicrobial studies—methods and approaches to study the interaction between natural products. *Planta Medica*, 77(11), 1168–82. <http://dx.doi.org/10.1055/s-0030-1250736>
- Wagenitz, G., & Kandemir, A. (2008). Two new species of the genus *Psephellus* (*Compositae*, *Cardueae*) from eastern Turkey. *Willdenowia*, 38, 521-526.
- Yıldırım, Ş. (2012). The heaven of gypsophilous phytodiversity of Turkey: Kepen, Sivrihisar, Eskişehir, Turkey, 13 taxa as new. *The Herb Journal of Systematic Botany*, 19(2), 1-51.
- Yiğit, D., Kandemir, A., & Yiğit, N. (2002). Antimicrobial Activity of Some Endemic Plants (*Salvia cryptantha*, *Origanum acutidens*, *Thymus sipyleus* ssp. *sipyleus*). *Erzincan Eğitim Fakültesi Dergisi*, 4(2), 77-81.

Chelidonium majus L. (Papaveraceae) morphology, anatomy and traditional medicinal uses in Turkey

Golshan Zare , Neziha Yağmur Diker , Zekiye Ceren Arituluk , İffet İrem Tatlı Çankaya 

Hacettepe University, Faculty of Pharmacy, Department of Pharmaceutical Botany, Ankara, Turkey

ORCID IDs of the authors: G.Z. 0000-0002-5972-5191; N.Y.D. 0000-0002-3285-8162; Z.C.A. 0000-0003-3986-4909; İ.İ.T.Ç. 0000-0001-8531-9130

Cite this article as: Zare, G., Diker, N. Y., Arituluk, Z. C., & Tatlı Çankaya, İ. İ. (2021). *Chelidonium majus* L. (Papaveraceae) morphology, anatomy and traditional medicinal uses in Turkey. *İstanbul Journal of Pharmacy*, 51(1), 123-132.

ABSTRACT

Background and Aims: *Chelidonium majus* is known as "kırlangıç otu" in Turkey and the different plant parts, especially the latex and aerial parts have been used as folk medicines for different purposes such as digestion, hemorrhoids, jaundice, liver, eye, and skin diseases. Despite the traditional uses of *Chelidonium*, there have been no detailed anatomical studies related to this species.

Methods: The description and distribution map of *C. majus* was expended according to herbarium materials and an anatomical study was made using fresh materials. The information related to traditional uses and local names of this species was evaluated from ethnobotanical literature in Turkey. For anatomical studies freehand sections were prepared using razor blades and sections were double-stained with Astra blue and safranin.

Results: In the anatomical study, epidermal sections containing trichome and stomata characters were elucidated. The leaves are bifacial and hypostomatic. The stomata are anomocytic in the paradermal section. The cross-section of the stem showed multi-layered parenchymatous cells in the cortex and a single-layered endodermis with simple eglandular trichomes. The cross-section of the root showed that the epidermis was replaced with the periderm. Under the phloem, which had few layers, the xylem was composed of tracheary elements surrounded by sclerenchymatous cells.

Conclusion: Our results indicated that the morphological and anatomical characters alongside articulated laticifers and latex properties provide useful tools for the identification of this taxon from the other genera in the Papaveraceae family.

Keywords: Anatomy, *Chelidonium majus*, morphology, traditional uses, Turkey

INTRODUCTION

Papaveraceae Juss. is a medicinally important family comprising 23 genera and ca. 240 species found mainly in the Northern Hemisphere (Kadereit, 1993). All the family members are lactiferous with a well-developed duct system that produces a different kind of latex, from milky or watery white to yellow or red juice in all parts of the plant.

Chelidonium L. (greater celandine) from the Chelidoneiae tribe is a world-wide distributed genus from temperate Eurasia to Northwest Africa and the Atlantic coasts of America (Cullen, 1965). Although this genus has been considered a monotypic genus for a long time, Krahulcová (1982) divided it into two separate species according to their different chromosome numbers and distribution areas: *Chelidonium majus* L. ($2n=12$) distributed in Europe, Siberia and China and *C. asiaticum* (H. Hara) Krahulc. ($2n=10$) distributed in East Asia and Japan. *C. majus* is one of the oldest medicinal plants, having been in use since ancient times, and Dioscorides and Pliny describe its uses to treat different diseases (Zielinska et al., 2018).

Address for Correspondence:

Golshan ZARE, e-mail: golshanzare@gmail.com

Submitted: 30.07.2020
Revision Requested: 11.09.2020
Last Revision Received: 15.09.2020
Accepted: 14.10.2020

This work is licensed under a Creative Commons Attribution 4.0 International License.



Chelidonium, also known as greater celandine or devil's milk, has been used in various complementary and alternative medicine (CAM) systems including homeopathy and Traditional Chinese Medicine (TCM) to treat various skin disorders such as papillae, warts, condylomas, as well as ulcers, cancer, oral infection, liver disorders, chronic bronchitis, asthma, and general pain (EMA, 2010; Aljuraissy Mahdi & Al-Darraj, 2012; Maji & Pratim, 2015; Hao, Gu & Xiao, 2015; Nawrot et al., 2017).

The latex of this species has been used externally for the treatment of skin conditions such warts, calluses, wounds, herpes, and cons in Iran (Miraldi, Ferri & Mostaghimi, 2001) and in European countries including Croatia (Prieroni et al., 2003; Varga, Solic, Dujakovic, Luczaj & Grdisa, 2019), Georgia (Bussman et al. 2017), Portugal (Gaspar et al., 2002; Novais, Santos, Mendes & Pinto-Gomes, 2004; Neves, Matos, Moutinho, Queiroz & Gomes, 2009), Slovenia (Lumpert & Krefl, 2017), Albania (Pieroni, Dibra, Grishaj, Grishaj, Maçai, 2015), Romania (Papp, Birkas-Frendl, Farkas & Pieroni, 2013), Italy (Leporatti & Ivancheva, 2003; Bellia & Pieroni, 2015; Guarrera, Forti & Marignoli, 2005; Dei Cas et al., 2015; Menale et al., 2006; Passalacqua, Guarrera & De Fine, 2007; Cornara, La Rocca, Terrizzano, Dente, F. & Mariotti, 2014; Fortini, Marzio, Guarrera & Iorizzi, 2016), Bosnia and Herzegovina (Redzic, 2007; Saric-Kundalic, Dobes, Klatte-Asselmeyer & Saukel, 2010; 2011; Savic Macukanovic-Jocic & Jaric, 2019), Kosovo (Mustafa et al. 2012), Spain (Blanco, Macia & Morales, 1999; Gonzalez-Hernandez Romero, Rodriguez-Guitian & Rigueiro, 2004; Benitez, Gonzalez-Tejero & Molero-Mesa, 2010; Calvo, Akerreta & Cavero, 2011; Rigat et al., 2015;), and Montenegro (Menkovic et al., 2011) (Figure 1). However, the leaves, flowers or aerial parts of *C. majus* are used internally in liver and gallbladder complaints in several countries (Ivancheva & Statcheva, 2000; Leporatti & Ivancheva, 2003; Pieroni, Dibra, Grishaj, Grishaj & Maçai, 2005; Jaric et al., 2007; Menkovic et al., 2011; Savikin et al. 2013; Jaric et al., 2015). Besides these, it is used for the treatment of bronchitis, lithontriptic, stomach ulcers in Kosovo (Mustafa et al., 2012), for lung cancer in Bosnia and Herzegovina (Redzic, 2007), for diarrhea, asthma, and gastric disorders in Iran (Miraldi, Ferri & Mostaghimi, 2001), for cold, asthma, bronchitis, and pneumonia in Spain (Menendez-baceta et al. 2014), as abortifacient in Italy (Idolo, Motti & Mazzoleni, 2009), against cancer, for hemorrhoids and blood cleansing in Ukraine, as well as for kidney problems in Romania (Soukand & Pieroni, 2016) (Figure 1).



Figure 1. Distribution map of countries with traditional use of *Chelidonium*.

In Turkey, *C. majus* is called "kırlangıç otu" (Güner, Aslan, Ekim, Vural & Babaç, 2012) and it has been used as a traditional medicinal plant for 26 different purposes in ten provinces mainly located in the Northwestern parts of Turkey.

The aerial parts, leaves and flowers of the plant are used both externally and internally, while the latex is used only externally for the treatment of skin diseases. Applying the latex directly to remove warts is the most common medicinal use of the plant (Uzun et al., 2004; Kültür, 2007; Ünsal, Vural, Sarıyar, Özbek & Ötük 2010; Kızılarıslan & Özhatay, 2012; Akbulut & Özkan, 2014; Sargın, Akçicek & Selvi, 2013; Saraç, Özkan & Akbulut, 2013; Sargın, Selvi & Lopez, 2015; Polat, Cakilcioglu, Kaltalıoğlu, Uluslan & Türkmen, 2015; Mumcu & Korkmaz, 2018). The traditional medicinal uses of *C. majus* in Turkey are presented in Table 1.

The greater celandine herb has been approved by both the European Pharmacopoeia and Turkish Pharmacopoeia. In addition, it has also been included in Commission E monographs for its use in spastic discomfort of the bile ducts and gastrointestinal tract, gall bladder and skin diseases (EMA, 2010; WHO, 2010; Görsöz, 2018). Pharmacological studies indicated *Chelidonium* extracts have anti-viral (Zuo, 2008; Gilca, Gamana, Pannaita, Stoian & Atanasiu 2010), anti-microbial (Kokoska, 2002), anti-tumor, anti-inflammatory (Lee, 2007) and analgesic properties (Huang, 1999).

Chelidonium is a particularly well-known genus because of the presence of numerous therapeutically important alkaloids located in the different parts of the plant, especially in the latex. More than forty alkaloids including phenanthridine (3,4-benzylisoquinoline), protoberberine, protopine, quinolizidine, aporphine) have been isolated from *Chelidonium* (Kedzia, Łozykowska, & Gryszczynska, 2013; Hao, Gu & Xiao, 2015; Zielinska et al., 2018). Isoquinoline alkaloids are pharmacologically relevant substances of this taxon (Grosso et al., 2014; Zielinska et al., 2018).

According to the therapeutic potential and traditional uses of *C. majus* and its hepatotoxic effect in chronic administration (EMA, 2010; WHO, 2010; Pantano et al., 2017), it is important to conduct morphological and anatomical studies to provide reliable diagnostic characters for the identification of raw material and commercial samples to avoid any unwanted toxic harm.

Despite the medicinal uses of *Chelidonium* species, there has not been any detailed research on the anatomical and morphological properties of the genus in Turkey. In this study, we provide detailed anatomical properties of *C. majus*, expanded morphological information and a distribution map based on Turkish samples. In addition, the traditional uses of this plant in Turkey are discussed in detail.

MATERIAL AND METHODS

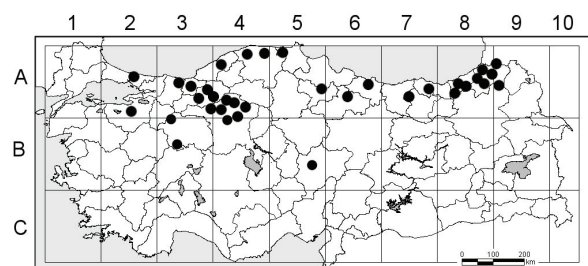
Fresh plant materials at the flowering period were collected from Ankara, Turkey in June 2019 by Golshan Zare (GZ1309). Voucher specimens were deposited in the Hacettepe University Faculty of Pharmacy Herbarium under the classification code HUEF20008. For morphological investigation, 44 speci-

Table 1. Traditional medicinal uses of *C. majus* in Turkey.

Province	Local name	Parts Used	Preparation	Administration*	Use	Literature
Afyonkarahisar	Kırlangıç otu	Aerial parts	Infusion	Int.	Digestion, hemorrhoids, jaundice, liver, eye disease, skin diseases	Arı et al., 2015
Bilecik	Kırlangıç otu	Latex	Raw	Ext.	Warts	Unsal et al., 2010
Giresun	Kına otu	Flowers Leaves	Decoction	Ext.	Warts	Polat et al., 2015
Izmit	Temre otu	Aerial parts	Infusion	Int.	Diuretic	Kızılarşlan and Özhatay, 2012
		Latex	Raw	Ext.	Wounds, eczema	
Kırklareli	Sarılık otu, Sultan otu, yara otu, temra otu, mayasıl otu	Herba	Decoction	Ext.	Hepatitis	Kültür, 2007
		Latex	Raw	Ext.	Inflamed wounds, wounds, warts, itching, hemostatic	
		Leaves	Decoction	Ext.	Rheumatism, sciatica	
Manisa	Siğil otu, Bostan otu	Aerial parts	Infusion	Int.	Spasm, dyspepsia, gastrointestinal diseases	Sargin et al., 2013; Sargin et al., 2015
			Raw	Ext.	Carminative, costiveness, warts, corns	
		Leaves	Mash	Ext.	Warts	
Rize	Mecmenük çayırı	Aerial parts	Raw	Ext.	Eczema, warts, acne	Saraç et al., 2013
Sakarya	---	Aerial parts	Infusion	Int.	Eczema	Uzun et al., 2004
Samsun	Kırlangıç otu	Aerial parts	---	Int.	Diuretic, purgative, caustic	Mumcu and Korkmaz, 2018
		Latex	---	Ext.	Warts, ringworm	
Trabzon	Temre	Latex	Raw	Ext.	Skin diseases	Akbulut and Ozkan, 2014

*Int.: Internal; Ext: External

mens of *C. majus* from the Ankara University Faculty of Science Herbarium (ANK), Hacettepe University Faculty of Science Herbarium (HUB), Ankara University Faculty of Pharmacy Herbarium (AEF), Hacettepe University Faculty of Pharmacy Herbarium (HUEF) and Edinburgh (E) Virtual Herbarium were studied and Flora of Turkey and the East Aegean Islands (Cullen, 1965) were followed for terminology and description order. The distribution information related to herbarium samples, records of flora in Turkey and the East Aegean Islands and the collected fresh materials of *C. majus* were plotted on a map (Figure 2). Determination and measurement of microscopic characters were done by means of direct observation under Leica Stereo Microscopes (Model EZ4) and photographed.

**Figure 2.** Distribution map of *C. majus* in Turkey.

Fresh specimens (GZ1309) were used for the anatomical investigations and cross-sections were prepared from leaves (at middle), stems (basal and top), pedicels and roots. Paradermal

sections were also performed for leaves. Freehand sections were prepared using razor blades and sections were cleared with sodium hypochlorite and then stained by double stain with Astra blue and safranin. Slides were observed with a Leica CME light microscope and photographed.

RESULTS AND DISCUSSION

Morphology

Chelidonium majus L., Sp. Pl. 505 (1753).

Kırlangıç otu (Güner, Aslan, Ekim, Vural & Babaç, 2012).

Type: Described from Europe (Hb. Linn. 668/1).

Synonyms: *C. laciniatum* Mill., Gard. Dict., ed. 8. n. 2 (1768). *C. majus* var. *grandiflorum* DC., Syst. Nat. 2: 99 (1821). *C. laciniatum* var. *fumariifolium* DC., Syst. Nat. 2: 100 (1821). *C. umbelliferum* Stokes, Bot. Mat. Med. 3: 180 (1812).

Perennial herb, 30–70(–100) cm, branched at the base. Rhizome thick, fleshy, reddish-brown. Stem erect, branched with bright orange sap, sparsely pubescent, especially on the nodes, woody stock covered by persistent leaf. Basal leaves petiole 2–14 (18) cm, blade glaucous abaxially with conspicuous veins, green adaxially, obovate-oblong or broadly obovate, 8–20 cm, abaxially sparsely pubescent especially on the veins, adaxially glabrous, bipinnatifid or pinnatisect, lobes 2–4 pairs, obovate-oblong, irregularly parted or lobed; lobe margin crenate. Cauline leaves alternate, petiole 5–18 mm; blade 2–12 (–15) x 1–8 cm, leaves pinnate with 5–7 broad leaflets, the terminal leaflet often 3-fid, ovate to oblong. Inflorescence nearly umbellate with flowers (2) –5–7 (8). Pedicel tenuous, 2–8 cm, pubescent when young, later glabrous. Flowers 2–2.5 cm across. Sepals 2, free, caducous, ovoid, 5–8 mm, glabrous or sparsely pubescent. Petals 4, yellow, obovate, 10 x 8–15 mm, entire. Stamens 8 mm numerous. Filaments yellow, anthers oblong. Style short, with 2 spreading stigma-lobes (Figure 3). Ovary

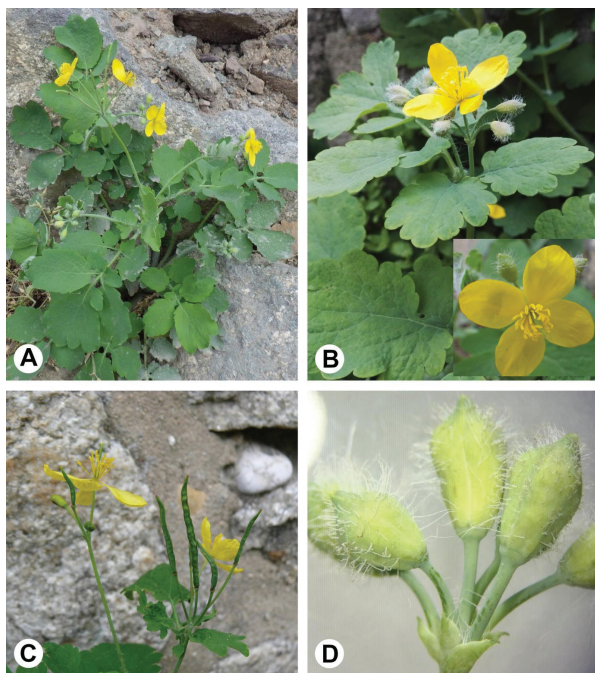


Figure 3. A, Habitus; B, flower and inflorescence; C, capsule fruit; D, flower buds with trichomes.

linear, 1 cm, glabrous. Fruit slender siliqua-like capsule (2) 30–60 x 2–4 mm, torulose, glabrous, monolocular, without a septum, basipetal, opening from below by 2 valves, many seed, pedicel the same as or usually shorter than fruit. Seeds 1–2 mm, dark brown or black, shiny in fresh material, reticulate patterned, with a white appendage, ovoid, alveolate (Figure 4).

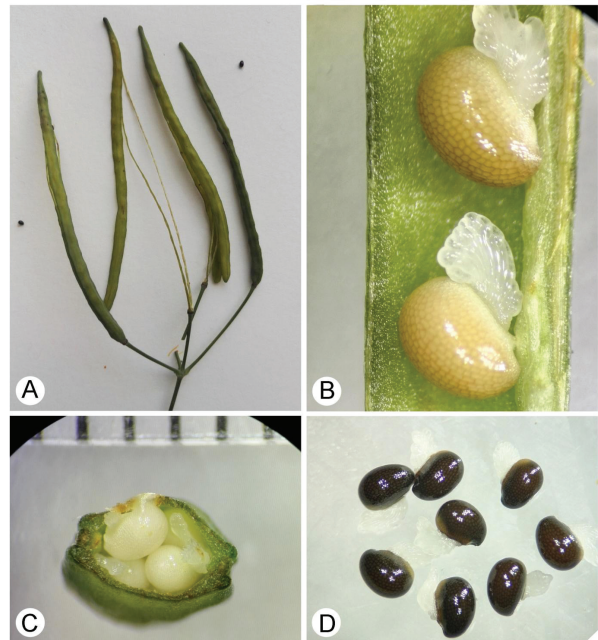


Figure 4. A, Fruit; B, fruit longitudinal sections; C, fruit Transverse sections; D, seed.

Flowering time: April–August.

Habitat: Shaded ground in woods and thickets, sea level–2000 m.

Phytogeographic region: Euro-Siberian element.

World distribution: Widespread in Asia, North America and whole Europe, Northwest Africa; it grows in forests and open shrubby areas, shady, ruderal sites.

Turkey distribution: West and Black Sea regions (Figure 2).

Examined specimens: A2(E) Istanbul: Kestanesou, 22.06.1895 Aznavour (E!); Bursa: Uludağ to Soğukpınar, 500-1000 m, 16.05.1962, *Dudley* 34741 (E!). A3 Bolu: Karadere to Yedigöl, 650 m, 18.06.1962, *P.H.Davis & Coode*, 37688 (E!); Bolu to Abant lake, 800-900 m, 14.07.193, *S. Fehmi* (ANK!); Yedigöller National Park, 1000 m, 13.06.1977, *R. İlarıslan* 102 (ANK!); Düzce: Aşağıkaraköy, Çilimli, 2000 m, 16.05.2009, *A. Mine Gençler Özkan, İ. Gürbüz, G. Akaydin, E. Miser* 26472 (AEF!); Akçakoca, Küpler village, 350-370 m, 22.07.2002, *A. Dođru Koca* 1864 (HUB!); Ankara: between Bepazarı and Kırısak, around Yiğenler village, 1050-1300 m 01.06.2001, *Ali A. Dönmez* 8953 (HUB!); Ankara: Çankaya, Bülbülderesi, by the road, 945 m, 20.06.2019, *G. Zare* 1309 (HUEF!); A4 Zonguldak: Amasra, 14.04.1985, *Venter* (HUB!); Ankara: Bepazarı, Dereli, 1300 m, 02.07.1978, *Y. Akman* 75 (ANK!); Ankara: Çubuk, Karagöl, around the lake, 1500 m, 23.05.1973,

S. Erik 423 (HUBI); Kızılcahamam, around Güven, 1200 m, 13.06.1992, M. Koyuncu 9792 (AEFI); ibid., 22.07.2002, H. Duman 2291 (AEFI); Seyhamamı, stone pit, 1000 m, 27.07.1975, B. Kasaplıgil, S. Başaran (AEFI); Maden suyu, 1000 m, 17.07.1977, K. Karamanoğlu, M. Coşkun 14513 (AEFI); Kızılcahamam, Çamları village, 02.07.1948, K. Karamanoğlu 522 (ANKI); Kastamonu: Azdavay to Cide, 800 m, 31.07.1962, P.H.Davis 38690 (EI); between Cide-Kızılca, 900 m, 12.06.1979, O. Ketenoğlu 1387 (ANKI); İnebolu, 18.04.1932, W. Katte (ANKI). A5 Kastamonu: Yağalar village, 1500 m, 12.06.1975, M. Kılıç 3324 (ANKI); Ayancık, Çangal, 1100 m, 11.08.1945, Bakı Kasaplıgil (ANKI); Amasya, 30.06.1893, A. Manissadjian 754 (EI). A6 Tokat: Artova, Aktaş, Çal Tepe, ca. 1300-1400 m, 16.07.19, R. İlarıslan 588 (ANKI). A7 Giresun: Gengene village, 700 m, 24.06.1977, Y. Akman 702 (ANKI); Gümüşhane: Harava village, 1100 m, 17.08.1983, Ş. Yıldırım 5736 (HUBI). A8 Trabzon: Sürmene, around Köprübaşı, 700 m, 29.04.1982, A. Güner 4292, B. Yıldız (ANKI AEFI); Uzungöl castel, 28.07.1994, N. Tanker, M. Koyuncu, M. Yıldız, S. Kuruas (AEFI); Rize: Çamlıhemşin, near Zilkale, c. 700 m, 16.08.1980, A. Güner 3061 (HUBI); Salarha, Kömürçüler village, 200 m, 21.04.1985, A. Güner 6282, M. Bilgin (HUBI); 2. km from Güneyce to İkizdere, 320 m, 26.03.1983, A. Güner 4610, B. Yıldız, M. Bilgin (HUBI); Artvin: Arhavi, around Ortacalar, 750 m, 21.04.1984, M. Koyuncu 6782, T. Ekim, A. Güner, M. Bilgin (AEFI); Dikyamaç village, 750 m, 22.04.1997, M. Coşkun 19870 (AEFI); Alaca (Tiryal) southeast slope, 163 m, 14.06.1978, A. Düzenli 895 (ANKI); Artvin: Dikyamaç village, 05.06.1993, M. Coşkun 184 (AEFI); Borçka, 50 m, 18.05.1985, Ş. Yıldırım 7876 (HUBI); Çoruh, 1100 m, 28.04.1960, Stainton 8301 (EI). A9 Artvin: Çoruh, Ardanuç to Kordevan mountain, 1450 m, 27.06.1957, D. 30140 (EI); Kars: Posof, 1600-1750 m, 29.06.1986, N. Demirkuş 3658 (HUBI). B3 Afyonkarahisar: Şuhut, Koçyatağı village, 28.05.2003, 1200 m, Ahmet Sezgin 03048 (HUEFI); Eskişehir: Türkmen mountain, 1400 m, 07.06.1985, T. Ekim 2550 (ANKI). B5 Kayseri: Hisarak, 14.06.1944, H. Bağda (ANKI).

Anatomy

The anatomical structures of the specimen were determined by examination of the root, stem, pedicel and leaf cross-sections. Additionally, the stomatal index of the species is presented in Figures 5-8.

Trichome: The surfaces of all parts of this species contain simple, uniseriate (4-6 cell) and eglandular trichomes whose density show variation in different parts of individuals and among the population (Figures 5 A-C). On the leaf surface, trichomes are dorsiventral and density is higher on the veins and nodes.

Leaves: Cross-sections of the leaf blades in both surfaces contain epidermal cells with sinuous anticlinal walls covered by a thin layer of cuticula. The superior epidermis of the leaf consists of 4-6 angled, rectangular, anisodiametric cell layers and stomata are absent. Mature epidermis cell size is $79.16 \pm 16.35 \times 26.66 \pm 5.77 \mu\text{m}$. Leaves are hypostomatous and stomata are confined to the lower surface (abaxial). Stomata type is ranunculaceous (anomocytic) and guard cells are surrounded with 4-6 cells which are not distinct from the remaining cells in the mature epidermis (Figure 5 D-E). Upper epidermis have slightly larger cells than lower epidermis. These cells are significantly wavy in anticlinal walls, with $21 \pm 4.0 \mu\text{m}$ width in narrow the

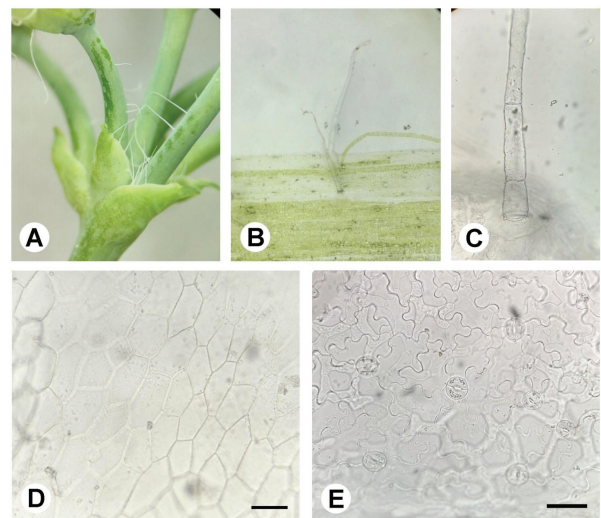


Figure 5. Transverse sections of the epidermis, A-C, uniseriate hairs; D, adaxial epidermis; E, abaxial epidermis with ranunculaceous type stomata. Scale bars: (D, E) 50 μm .

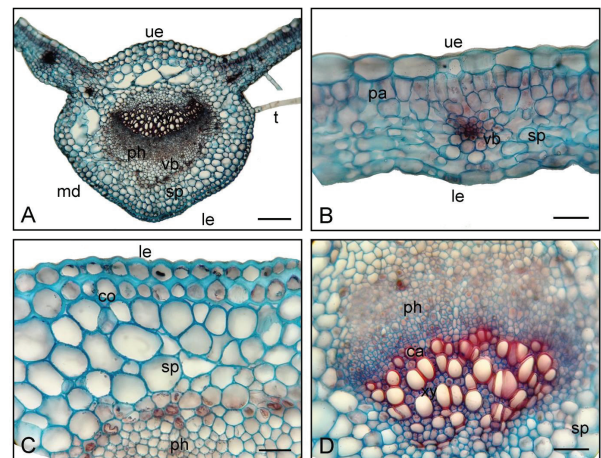


Figure 6. Transverse sections of Leaf. A, C, and D, midrib; B, blade; ca, cambium; ue, upper epidermis; le, lower epidermis; pa, palisade cell; sp, spongy parenchyma cell; ph, phloem; t, trichome; xy, xylem. Scale bars: (A), 200 μm , (B, C, D) 50 μm .

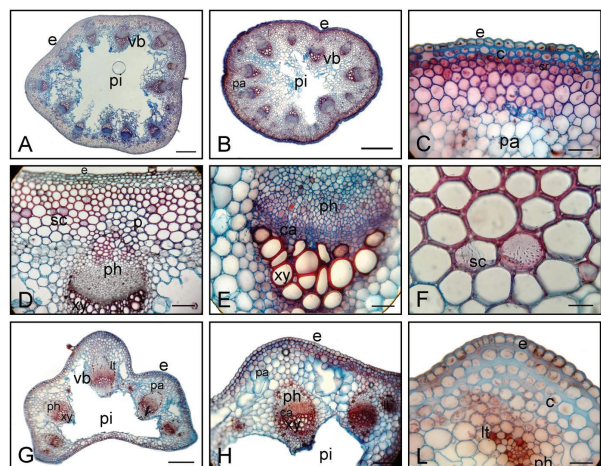


Figure 7. Transverse sections of stem and pedicel. A-F Stem; G-L, pedicel. ca, cambium; co, cortex; ue, upper epidermis; le, lower epidermis; pa, palisade cell; sp, spongy parenchyma cell; ph, phloem; pi, pith region; vb, vascular bundle; sc, secretory cell; xy, xylem. Scale bars: (A, B, G) 500 μm , (D, H), 200 μm , (C, E, F, L) 50 μm .

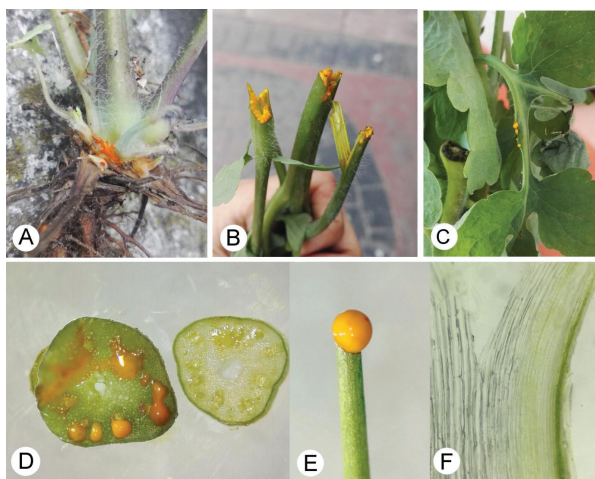


Figure 8. A-C, Orange latex in root, stem and leaves of the *Chelidonium*; D cross section of stem; E and F, Transverse and longitudinal section of stem and articulated laticiferous tubes.

part, $73.00 \pm 9.2 \mu\text{m}$ width in the large part of the cells and $42.36 \pm 3.98 \mu\text{m}$ length. The inferior epidermis consists of numerous stomata whose rounded shape and stomata index is $19.66 \pm 1.61 (\text{mm}^2)$. Stomata size is $21.5 \pm 2.1. \times 21.13 \pm 2.0 \mu\text{m}$. In leaf cross-section slides indicated leaves have bifacial (dorsiventral) structure and the palisade layer is restricted to the upper side (Adaxial). Leaf thickness is between 180–200 μm and the mesophyll structure generally includes one or several layers of palisade parenchyma cells under the upper epidermis and thin-walled spongy parenchyma cells with wide intercellular spaces. However, the transverse region is sometimes not distinctly differentiated into palisade and spongy regions (Figures 6). The leaf main vein thickness is 800-1100 μm , contains 1-3 layers of collenchyma under the epidermis and 3-5 layers of thin-walled parenchyma cells with different sizes between the collenchyma layer and the arc-shaped vascular bundles. In this area, a few calcium oxalate crystals were seen in the cells. Veins contain numerous collateral vascular bundles, with the xylem located on the upper side and phloem located on the lower side, and in main vein latex cells found in the vascular region (Figure 6).

Stem: The stem transverse section in the young part is circular and in the old part tends to show a pentagonal shape with rounded corners. The outer part is covered with a single layer of epidermal cells with a thin cuticula. Multicellular simple trichomes are seen on the epidermis. Immediately under the epidermis single or multi-layered collenchymatous cells were detected. The cortex consists of multi-layered parenchymatous cells that have various shapes and sizes. Vascular bundles are collateral and 12-14 bundles are arranged in a single ring with concentric zones. The xylems generally tend to be V-shaped. In vascular bundles, 2-6 cambium layers between phloem and xylem are distinguishable. The xylem part is larger than the phloem part. The pith consists of parenchymatous cells that are large and polygonal in shape. This tissue is torn in the lower part of the stem and these tears form a pith cavity (Figure 7A-B). Latex is generally present throughout all parts of the plant and is found in articulated laticiferous tubes. Laticiferous tubes are placed in vascular bundles close to the phloem. In some of

the cross-section slides, sieve plates related to the transverse or lateral walls of these tube cells were found (Figures 8). Calcium oxalate crystals occur in the parenchymatous cells.

Petiole: The petiole cross-section is triangular and its anatomical structure is similar to the stem structure. It contains a single layer of epidermis, one to several layers of collenchyma in the corners, and commonly exhibits an arc of vascular bundles without sclerenchyma. Also, there are articulated laticiferous latex tubes and cells and crystals of calcium oxalate in the cortex cells (Figures 7 G-L).

Root: The root structure indicates that this plant is annual. The periderm is generally scratched from the cortex and the cortex is multi-layered with 20-35 layers. Endodermis cannot be distinguished and borders are not clear. The primary structure in the central vascular bundle is diarch and xylem places under phloem (Figures 9).

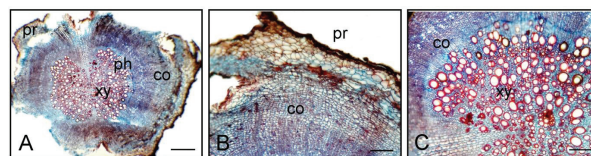


Figure 9. Transverse sections of root. a, cambium; co, cortex; pr, periderm; ph, phloem; pi, pith region; vb, vascular bundle; xy, xylem. Scale bars: (A) 500 μm , (B, C), 200 μm .

DISCUSSION

In this study, we investigated the distribution area, morphological and anatomical properties of *C. majus* as one of the traditional medicinal plants in Turkey. There are lots of studies on the phytochemical and therapeutic perspective of the genus *Chelidonium* (Kedzia Łozykowska & Gryszczynska, 2013; Grosso et al. 2014; Zielinska et al. 2018) but the distribution area, morphological and anatomical features of this species have not been taken into consideration, especially in Turkey.

The distribution area of *Chelidonium* in Flora of Turkey (Cullen 1965) is restricted to the Black Sea region and this taxon is known as the Euro-Siberian element. Our findings indicated this species grows abundantly in the transition area from Euro-Siberian to Irano-Turanian phytogeographic area. There are two records from Afyonkarahisar and Kayseri that are far from the natural distribution area of this species (Figure 2). This can be caused by anthropogenic impact or seeds being carried by animals. The habitats of this plant are forests and shady rural areas. We also found lots of individual plants in parks and roadsides in the cities.

Our results on morphological features are in agreement with the description of the taxon in the Flora of Turkey (Cullen, 1965). We also expended morphological characters according to 44 examined samples from fresh material and herbarium mentioned specimens. The shape of the leaves, umbellate inflorescence, small, yellow flowers, basipetal dehiscence capsule shaped fruits with deciduous valves and arillate seeds can be used to differentiate this species from other members of the family.

Although latex secretion in many unrelated families decreases its diagnostic value, whatever the chemical nature of its contents, it can be helpful in the taxonomy of taxa (Metcalf & Chalk, 1957). In the Papaveraceae family, the presence of latex is a predominant character among members that shows the variation in colour and chemical component (Metcalf & Chalk, 1957; Kadereit, 1993). The shiny orange latex found in all organs of the plant is peculiar to *C. majus* and is placed in articulated non anastomosing laticifers (Figure 8). Also, in agreement with Kadereit (1993), this tube significantly associated with the phloem of the vascular bundle and these structures can easily be distinguished even in broken or powdered herbal drugs (Pallag, Pasca, Taichiş, Honiges & Moisa, 2015; İşcan, Köse & Demirci, 2019). Kadereit (1993) indicated latex tends to disappear from the older parts of the plant; however, we found it in the old parts but the amount was low.

While the trichome types provided an important diagnostic character among the species of Papaveraceae family, the results indicated that uniseriate trichomes are diagnostic for the whole tribe Chelidoniae. In addition, considering the diagnostic value of epidermal cell shape, the presence of stomata just in the adaxial side of leaves, in contrast with other genera such as *Papaver* and *Roemeria* (Metcalf & Chalk, 1957) and the stomata index can provide confirmatory evidence in the identification of this taxon.

These results can help to facilitate the identification of material for use by people, detecting contamination of this taxon with other herbal drugs and providing identified raw material for scientific research in the medicinal field.

C. majus is one of the oldest medicinal species, having been in use since ancient times. This plant was cited by Dioscorides to treat jaundice and dermatologic disorders and Pliny the Elder for the preparation of eye lotion (Jones, 1966; Dioscorides, Osbaldeston & Wood, 2000). *C. majus* has been extensively used to treat eye diseases, ulcers and skin disorders as well as against colic and jaundice in Europe (Mayer, Uehleke & Saum, 2003). In Turkey, especially in the Black Sea region, a distribution area of *Chelidonium*, the different parts of this plant, commonly latex and the aerial parts of the plant have been used as folk medicines for the treatment of different diseases (Table 2). The latex is externally as hemostatic and for the treatment of skin diseases such as wounds, eczema, warts, ringworm, and itching (Kültür, 2007; Ünsal Vural, Sariyar, Özbek & Ötük, 2010; Kızılarşlan & Özhatay, 2012; Akbulut & Özkan, 2014; Mumcu & Korkmaz, 2018). The infusions of aerial parts are used internally to treat hepatitis (Kültür, 2007), hemorrhoids, jaundice, liver, eye and skin diseases (Arı et al. 2015). In addition, it is used for gallbladder, (Mumcu & Korkmaz, 2018), and gastrointestinal diseases such as digestion, spasm, dyspepsia (Sargin, Akçiçek & Selvi, 2013; Sargin, Selvi & Lopez, 2015; Mumcu & Korkmaz, 2018) and used as purgative and diuretic (Kızılarşlan & Özhatay, 2012; Mumcu & Korkmaz, 2018). It is also used externally to treat warts, corns, acne (Sargin, Akçiçek & Selvi, 2013; Saraç, Ozkan & Akbulut, 2013; Sargin, Selvi & Lopez, 2015), eczema (Uzun et al., 2004; Saraç, Ozkan & Akbulut, 2013; Polat, Cakilcioglu, Kaltalioglu, Ulsan & Türkmen, 2015), and rheumatism (Kültür, 2007).

In traditional medicine different parts of the plant are used for several therapeutic purposes. Nawrot et al (2017) suggest protein content of the *Chelidonium* can be affected by the biological activity of this taxa. They calm changes in the plant's needs at different developmental life stages from intense biosynthetic processes to defence against different environmental factors such as pathogens can affect latex composition. These changes in phytochemical composition could explain the biological activity alteration and subsequently divergent medicinal use of the plant extracts in the different developmental stages. The skin treatment properties of *C. majus* might be related to antibacterial, antifungal, antiviral and anti-inflammation activities of these taxa. It seems that these activities are attributed mostly to the alkaloids and flavonoids present in *Chelidonium* (Zuo et al., 2008; Zeileska et al. 2018). Stickl (1928) proved that the bactericidal properties are related to chelerythrine (Taborska Bochorakova, Dostal & Paulova, 1995) and sanguinarine (Hadaruga & Hadaruga, 2009). Also, the glycosaminoglycan present in the latex beside alkaloids containing chelidonine (Monavari, Shahrabadi, Keyvani, Bokharaei-Salim, 2012), chelerythrine (Taborska, Bochorakova, Dostal & Paulova, 1995), sanguinarine (Hadaruga & Hadaruga, 2009), coptisine (Bodalski, Pelezarskaund & Ujec, 1958) and berberine is able to inhibit the development of human immunodeficiency virus (HIV) (Gerencer et al., 2006) and human papilloma virus (HPV) (Etxenagusia et al., 2000). The antifungal activity of *Chelidonium* is attributed to alkaloidal compounds such as dihydrochelerythrine and dihydrosanguinarine which inhibit spore germination and the growth of mycelium in fungi (Maji & Pratim, 2015).

The other most reported indications of *C. majus*, both in European/Mediterranean and East Asian (TCM) traditions were for various liver complaints (Zielinska et al., 2018). Some of the hepatoprotective and choleric/cholagogue activities might be explained by the presence of hydroxycinnamic (caffeic acids' esters and dihydrochelerythrine (Weiskirchen, 2016). The *in vivo* research indicated that the phenolic components and alkaloids contain chelidonine, berberine and theprotopine showed choleric activity and caused an increase in the bile acid flow. It seems this effect is responsible for their hepatoprotective activity (Vahlensieck et al., 1995).

The main concern in *Chelidonium* is a possible hepatotoxicity of the plant because of the presence of alkaloids (Maji & Pratim, 2015; Zeileska et al. 2018). Research points out dose-dependent toxicity and according to EMA the toxicity of using dried parts of *Chelidonium* in a normal dose is low but severe and irreversible hepatotoxicity can happen in a high dose or chronic uptake (EMA, 2010). Nevertheless, further investigation is needed to determine possible toxic effects in daily administration and term of use.

CONCLUSION

C. majus is most commonly used for the treatment of skin diseases and liver disorders in Turkey and other countries. Considering the toxicity of this species alongside its traditional uses and common commercial materials, detailed morphological and anatomical structures can provide a useful tool to avoid contamination of this taxon with other drugs.

Our results indicated that the morphological characters such as leaf and flower shape, seed-specific morphology provided useful tools for the identification of this taxon from the other genera in the Papaveraceae family. Also, the presence of orange latex in all parts of the fresh materials or articulated laticifers with remaining latex content can be used as authentication diagnostic characters in powdered herbal drugs or broken plant materials. The other anatomical structures such as the stem and root cross-section, trichomes and stomata type share common structures across all taxa of the family and provided a limited opportunity to support the identification of this taxon.

Peer-review: Externally peer-reviewed.

Author Contributions: Conception/Design of Study- G.Z., N.Y.D., Z.C.A., İ.İ.T.Ç.; Data Acquisition- G.Z., N.Y.D.; Data Analysis/Interpretation- G.Z., N.Y.D.; Drafting Manuscript- G.Z.; Critical Revision of Manuscript- G.Z., N.Y.D., Z.C.A., İ.İ.T.Ç.; Final Approval and Accountability- G.Z., N.Y.D., Z.C.A., İ.İ.T.Ç.

Conflict of Interest: The authors have no conflict of interest to declare.

Financial Disclosure: Authors declared no financial support.

REFERENCES

- Akbulut, S., & Ozkan, Z. C. (2014). Traditional Usage of Some Wild Plants in Trabzon Region (Turkey). *Kastamonu Uni., Orman Fakültesi Dergisi*, 14(1), 135–145.
- Aljuraissy, Y. H., Mahdi, N. K., & Al-Darraj, M. N. J. (2012). Cytotoxic effect of *Chelidonium majus* on cancer cell. *Al-Anbar Journal of Veterinary Sciences*, 5(1), 85–90.
- An, S., Temel, M., Kargoğlu, M., & Konuk, M. (2015). Ethnobotanical survey of plants used in Afyonkarahisar-Turkey. *Journal of Ethnobiology and Ethnomedicine*, 11(84), 2015.
- Bellia, G., & Pieroni, A. (2015). Isolated, but transnational: the local nature of Waldensian ethnobotany, Western Alps, NW Italy. *Ethnobiology and Ethnomedicine*, 11, 37.
- Benitez, G., Gonzalez-Tejero, M. R., & Molero-Mesa, J. (2010). Pharmaceutical ethnobotany in the Western part of Granada province (Southern Spain): Ethnopharmacological synthesis *Journal of Ethnopharmacology*, 129, 87–105.
- Blanco, E., Macia, M. J., & Morales, R. (1999). Medicinal and veterinary plants of El Caurel (Galicia, Northwest Spain). *Journal of Ethnopharmacology*, 65, 113–124.
- Bodalski, T., Pelezarskaund, H., & Ujec, M. (1958). Action of some alkaloids of *Chelidonium majus* on *Trichomonas vaginalis* in vitro. *Archivum Immunologiae et Therapiae Experimentalis*, 6,705–711.
- Bussman R.W., Paniagua Zambrana, N.Y., Sikharulidze, S., Kikvidze, Z., Kikodze, D., Tchelidze, D.B.K., & Robbie, E. (2017). Ethnobotany of Samtskhe-Javakheti, Sakartvelo (Republic of Georgia), Caucasus. *Indian Journal of Traditional Knowledge*, 16(1), 7–24.
- Calvo, M. I., Akerreta, S., & Cavero, R.Y. (2011). Pharmaceutical ethnobotany in the Riverside of Navarra (Iberian Peninsula). *Journal of Ethnopharmacology*, 135, 22–23.
- Cavero, R.Y., Akerreta, S., & Calvo, M. I. (2011). Pharmaceutical ethnobotany in the Middle Navarra (Iberian Peninsula). *Journal of Ethnopharmacology*, 137, 844–855.
- Cornara, L., La Rocca, A., Terrizzano, L., Dente, F., & Mariotti, M.G. (2014). Ethnobotanical and phytomedicine knowledge in the North-Western Ligurian Alps. *Journal of Ethnopharmacology*, 155(1), 463–484.
- Cullen, J. (1965). *Chelidonium*. In: Davis PH (ed.) *Flora of Turkey and the east Aegean Islands* (vol.1, pp. 213–214). UK: Edinburgh University Press.
- Dei Cas, L., Pugni, F., & Fico, G. (2015). Tradition of use on medicinal species in Valfurva (Sondrio, Italy). *Journal of Ethnopharmacology*, 163, 113–134.
- Dioscorides, P., Osbaldeston, T. A., & Wood, R. P. A. (2000). *Dioscorides de Materia Medica, Being a Herbal with Many other Materials Written in Greek in the First Century of the Common Era*. An Indexed Version in Modern English. Johannesburg: Ibis Press.
- European Medicines Agency (EMA). (2011, September 13) Committee on Herbal Medicinal Products (HMPC): Public statement on *Chelidonium majus* L., herba EMA/HMPC/743927/2010. Retrieved from https://www.ema.europa.eu/en/documents/public-statement/final-public-statement-chelidonium-majus-l-herba_en.pdf.
- Etxenagusia, M. A., Anda, M., Gonzalez-Mahave, I., Fernandez, E., & Fernandez de Corres, L., (2000) Contact dermatitis from *Chelidonium majus* (greater celandine). *Contact Dermat*, 43, 47.
- Fortini, P., Di Marzio, P., Guarrera, P. M., & Iorizzi, M. (2016). Ethnobotanical study on the medicinal plants in the Mainerde Mountains (Central-Southern Apennine, Italy). *Journal of Ethnopharmacology*, 184, 208–218.
- Gaspar, N., Godinho, J., Vasconcelos, T., Caldas, D., Mendes, P., & Barros, O. (2002). Ethnobotany in the center of Portugal (Santarém) In: Rauter A.P., Palma F.B., Justino J., Araújo M.E., dos Santos S.P. (eds) *Natural Products in the New Millennium: Prospects and Industrial Application. Proceedings of the Phytochemical Society of Europe*, (vol. 47, pp.271–284) Springer, Dordrecht.
- Gerencer, M., Turecek, P. L., Kistner, O., Mitterer, A., Savidis-Dacho, H., & Barrett, N.P. (2006) *In vitro* and *in vivo* anti-retroviral activity of the substance purified from the aqueous extract of *Chelidonium majus* L. *Antiviral Research*, 72(2),153–156.
- Gilca, M., Gamana, L., Panaita, E., Stoian, I., & Atanasiu, V. (2010). *Chelidonium majus* – an Integrative Review: Traditional Knowledge versus Modern Findings, *Forsch Komplementmed*, 17, 241–248.
- Gonzalez-Hernandez, M. P., Romero, R., Rodriguez-Guitian, M., & Rigueiro, A. (2004). Medicinal use of some plants in Galicia (NW-Spain). *Acta horticulture*, 629, 63–75.
- Görsöz, H. (2018). *Türk Farmakopesi-2017*. Ankara, Turkey: Artı 6 Reklam Matbaa.
- Grosso, C., Ferreres, F., Gil-Izquierdo, A., Valentão, P., Sampaio, M., Lima, J., & Andrade, P. B. (2014). Box-Behnken factorial design to obtain a phenolic-rich extract from the aerial parts of *Chelidonium majus* L. *Talanta*, 130, 128–136. <https://doi.org/10.1016/j.talanta.2014.06.043>
- Guarrera, P. M., Forti, G., & Marignoli, S. (2005). Ethnobotanical and ethnomedicinal uses of plants in the district of Acquapendente (Latium, Central Italy). *Journal of Ethnopharmacology*, 96, 429–444.
- Güner, A., Aslan, S., Ekim, T., Vural, M., & Babaç, M.T. (Eds). (2012). *Türkiye Bitkileri Listesi (Damarlı Bitkiler)* (pp. 281–282). İstanbul, Turkey: N. Gökyiğit Botanik Bahçesi & Flora Araştırmaları Derneği Yayınları.
- Hadaruga, D. I., & Hadaruga, N. G. (2009) Antioxidant activity of *Chelidonium majus* L. extracts from the Banat county. *Journal of Agroalimentary Processes and Technologies*, 15(3), 396–402.
- Hao, D., Gu, X., & Xiao, P. (2015) *Medicinal Plants Chemistry, Biology and Omics* (pp.171–216). UK: Woodhead Publishing.
- Huang, C. K. (1999). *The Pharmacology of Chinese Herbs* (2nd ed.). USA: CRC Press.
- Idolo, M., Motti, R., & Mazzoleni, S. (2009). Ethnobotanical and phytomedicine knowledge in a long-history protected area, the Abruzzo, Lazio and Molise National Park (Italian Apennines). *Journal of Ethnopharmacology*, 127, 379–395.

- İşcan, G., Köse, Y. B. & Demirci, F. (2019) *Bitkisel Drogların Makroskobik ve Mikroskobik Özellikleri* (pp 88-89). Türkiye: Antalya Eczacı Odası Yayını No :1.
- Ivancheva, S. & Statcheva, B. (2000). Ethnobotanical inventory of medicinal plants in Bulgaria. *Journal of Ethnopharmacology*, 69, 165–172.
- Jaric, S., Macukanovic-Jocic, M., Djurdjevic, L., Mijatovic, M., Kostic, O., Karadzic, B. & Pavlovic, P. (2015). An ethnobotanical survey of traditionally used plants on Suva planner mountain (Southeastern Serbia). *Journal of Ethnopharmacology*, 175, 93–108.
- Jaric, S., Popovic, Z., Macukanovic-Jocic, M., Djurdjevic, L., Mijatovic, M., Karadzic, B. & Pavlovic, P. (2007). An ethnobotanical study on the usage of wild medicinal herbs from Kopaonik Mountain (Central Serbia). *Journal of Ethnopharmacology*, 111, 160–175.
- Jones, W.H.S. (1966). Pliny Natural History with an English Translation in Ten Volumes, Vol. VII, Libri XXIV–XXVII. London: Harvard University Press.
- Kadereit, J.W. (1993). Papaveraceae. In: K. Kubitzki, J.G. Rohwer & V. Bittrich (eds.) *The families and genera of vascular plants* (vol.2, pp. 494–506). Berlin: Springer-Verlag.
- Kedzia, B., Łozkowska, K. & Gryszczynska, A. (2013). Chemical composition and contents of biological active substances in *Chelidonium majus* L. *Postepy Fitoterapii*, 3, 174–181.
- Kızıllarlan, Ç. & Özhatay, N. (2012). Wild Plants Used as Medicinal Purpose in the South Part of Izmit (Northwest Turkey), *Turkish Journal of Pharmaceutical Science*, 9(2), 199–218.
- Kokoska, L., Polensky, Z., Rada, V., Nepovim, A. & Vanek, T. (2002) Screening of some Siberian medicinal plants for antimicrobial activity. *Journal of Ethnopharmacology*, 82(1), 51–53.
- Krahulcova A. (1982). Cytotaxonomic study of *Chelidonium majus* L. s. l. *Folia Geobotanica et Phytotaxonomica*, 17, 237–268.
- Kültür, Ş. (2007). Medicinal plants used in Kırklareli Province (Turkey). *Journal of Ethnopharmacology*, 111, 341–364.
- Lee, Y.C., Kim, S.H., Roh, S.S., Choi, H.Y. & Seo, Y.B. (2007) Suppressive effects of *Chelidonium majus* methanol extract in knee joint, regional lymph nodes, and spleen on collagen-induced arthritis in mice. *Journal of Ethnopharmacology*, 112(1), 40–48.
- Leporatti, M.L. & Ivancheva, S. (2003). Preliminary comparative analysis of medicinal plants used in the traditional medicine of Bulgaria and Italy. *Journal of Ethnopharmacology*, 87, 123–142.
- Linnaeus, C. (1753) *Chelidonium*, *Species Plantarum*, vol. 1. (pp.505). Stockholmiae.
- Lumpert, M. & Kreft, S. (2017). Folk use of medicinal plants in Karst and Gorjanci, Slovenia. *Journal of Ethnobiology and Ethnomedicine*, 13,16.
- Maji, A., K. & Pratim, B. (2015). *Chelidonium majus* L. (Greater celandine) – A Review on its Phytochemical and Therapeutic Perspectives. *International Journal of Herbal Medicine*, 3(1), 10–27. <https://doi.org/10.22271/flora.2015.v3.i1.03>.
- Mayer, J. G., Uehleke, B. & Saum, K. (2003). *Handbuch der Klosterheilkunde* (pp.213–221). Muenchen: Verlag Zabert Sandmann.
- Menale, B., Amato, G., Di Prisco, C. & Muoio, R. (2006). Traditional uses of plants in North-Western Molise (Central Italy). *Delpinoa*, 48, 29–36.
- Menendez-baceta, G., Aceituno-mata, L., Molina, M., Reyes-garcia, V., Tardio, J. & Pardo-de-santayana, M. (2014). Medicinal plants traditionally used in the Northwest of the Basque Country (Biscay and Alava), Iberian Peninsula. *Journal of Ethnopharmacology*, 152, 113–134.
- Menkovic, N., Savikin, K., Tasic, S., Zdunic, G., Stesevic, D., Milosavljevic, S. & Vincek, D. (2011). Ethnobotanical study on traditional uses of wild medicinal plant in Prokletije Mountains (Montenegro). *Journal of Ethnopharmacology*, 133, 97–107.
- Metcalfe, C.R. & Chalk, L. (1957). *Anatomy of the Dicotyledons* (vol. 1., pp.74–78). London: Oxford Univ. Press. <https://doi.org/10.1111/j.2042-7158.1950.tb13008.x>
- Miraldi, E., Ferri, S. & Mostaghimi, V. (2001). Botanical drugs and preparations in the traditional medicine of West Azerbaijan (Iran) *Journal of Ethnopharmacology*, 75, 77–87.
- Monavari, S.H., Shahrabadi, M.S., Keyvani, H., Bokharaei- Salim, F. (2012) Evaluation of *in vitro* antiviral activity of *Chelidonium majus* L. against *Herpes simplex virus* type-1. *African Journal of Microbiology Research*, 6(20), 4360–4364.
- Mumcu, Ü. & Korkmaz, H. (2018) Ethnobotanical uses of alien and native plant species of Yeşilirmak Delta, Samsun, Turkey, *Acta Biologica Turcica*, 31(3), 102–113.
- Mustafa, B., Hajdari, A., Krasniqi, F., Hoxha, E., Ademi, H., Quave, C.L., Pieroni, A. (2012). Medical ethnobotany of the Albanian Alps in Kosovo. *Journal of Ethnobiology and Ethnomedicine*, 8:6.
- Mustafa, B., Hajdari, A., Pajazita, Q., Sylva, B., Quave, C.L. & Pieroni, A. (2012). An ethnobotanical survey of the Gollak region, Kosovo. *Genetic Resources and Crop Evolution*, 59, 739–754.
- Nawrot, R., Jozefiak, D., Sip, A., Kuzma, D., Musidlak, O., Gozdzicka-Józefiak, A. (2017). Isolation and characterization of a non-specific lipid transfer protein from *Chelidonium majus* L. latex. *International Journal of Biological Macromolecules*, 104(Pt A), 554–563. <https://doi.org/10.1016/j.ijbiomac.2017.06.057>
- Neves, J.M., Matos, C., Moutinho, C., Queiroz, G. & Gomes, L.R. (2009). Ethnopharmacological notes about ancient uses of medicinal plants in Tras-os-Montes (Northern of Portugal) *Journal of Ethnopharmacology*, 124, 270–283.
- Novais, M.H., Santos, I., Mendes, S. & Pinto-Gomes, C. (2004). Studies on pharmaceutical ethnobotany in Arrabida Natural Park (Portugal) *Journal of Ethnopharmacology*, 93, 183–195.
- Pallag, A., Pasca, B., Taichiş, D. I., Honiges, A., Moisa, C., (2015) Microscopic studies of some *Chelidonium majus* L. populations. *Analele Universităţii din Oradea, Fascicula: Ecotoxicologie, Zootehnie şi Tehnologii de Industrie Alimentară*, 14B, 391–396.
- Pantano, F., Mannocchi, G., Marinelli, E., Gentili, S., Graziano, S., Busarò, F.P. & Di Luca, N.M. (2017). Hepatotoxicity induced by greater celandine (*Chelidonium majus* L.): a review of the literature. *European Review for Medical and Pharmacological Sciences*, 21(1), 46–52.
- Papp, N., Birkas-Frendl, K., Farkas, A. & Pieroni, A. (2013). An ethnobotanical study on home gardens in a Transylvanian Hungarian Csango village (Romania). *Genetic Resources and Crop Evolution*, 60, 1423–1432.
- Passalacqua, N.G., Guarrera, P.M. & De Fine, G. (2007). Contribution to the knowledge of the folk plant medicine in Calabria region (Southern Italy). *Fitoterapia*, 78, 52–68.
- Pieroni, A., Dibra, B., Grishaj, G., Grishaj, I. & Maçai, S.G. (2005). Traditional phytotherapy of the Albanians of Lepushe, Northern Albanian Alps. *Fitoterapia*, 76, 379–399.
- Pieroni, A., Ibraliu, A., Abbasi, A.M. & Papajani-Toska, V. (2015). An ethnobotanical study among Albanians and Armenians living in the Rraice and Mokra area of Eastern Albania. *Genetic Resources and Crop Evolution*, 62, 477–500.
- Polat, R., Cakilcioglu, U., Kaltalioglu, K., Ulsan, M.D. & Türkmen, Z. (2015). An ethnobotanical study on medicinal plants in Espiye and its surrounding (Giresun-Turkey). *Journal of Ethnopharmacology*, 163, 1–11.
- Prieroni, A., Giusti, M.E., Münz, H., Lenzarini, C., Turkovic, G. & Turkovic, A. (2003). Ethnobotanical knowledge of the Istro-Romanians of Zejane in Croatia. *Fitoterapia*, 74, 710–719.
- Redzic, S.S. (2007). The ecological aspect of ethnobotany and ethnopharmacology of population in Bosnia and Herzegovina. *Collegium Antropologicum*, 31(3), 869–890.

- Rigat, M., Valles, J., D'Ambrosio, U., Gras, A., Iglesias, J. & Garnatje, T. (2015). Plants with topical uses in the Ripelles district (Pyrenees, Catalonia, Iberian Peninsula): Ethnobotanical survey and pharmacological validation in the literature. *Journal of Ethnopharmacology*, 164, 162–179.
- Saraç, D.U., Ozkan, Z.C. & Akbulut, S. (2013). Ethnobotanic features of Rize/Turkey province. *Biological Diversity and Conservation*, 6(3), 57–66.
- Sargin, S.A., Selvi, S. & Lopez, V. (2015). Ethnomedicinal plants of Sarigöl district (Manisa), Turkey. *Journal of Ethnopharmacology*, 171, 64–84.
- Sargin, S.A., Akçiçek, E. & Selvi, S. (2013). An ethnobotanical study of medicinal plants used by the local people of Alaşehir (Manisa) in Turkey. *Journal of Ethnopharmacology*, 150(3), 860–874.
- Saric-Kundalic, B., Dobes, C., Klatter-Asselmeyer, V. & Saukel, J. (2010). Ethnobotanical study on medicinal use of wild and cultivated plants in middle, South and West Bosnia and Herzegovina. *Journal of Ethnopharmacology*, 131, 33–55.
- Saric-Kundalic, B., Dobes, C., Klatter-Asselmeyer & V. & Saukel, J. (2011). Ethnobotanical survey of traditionally used plants in human therapy of east, North and Northeast Bosnia and Herzegovina. *Journal of Ethnopharmacology*, 133, 1051–1076.
- Savic, J., Macukanovic-Jocic, M. & Jaric, S. (2019). Medical ethnobotany on the Javor Mountain (Bosnia and Herzegovina). *European Journal of Integrative Medicine*, 27, 52–64.
- Savikin, K., Zdunic, G., Menkovic, N., Zivkovic, J., Cujic, N., Terescenko, M. & Bigovic, D. (2013). Ethnobotanical study on traditional use of medicinal plants in South-Western Serbia, Zlatibor district. *Journal of Ethnopharmacology*, 146, 803–810.
- Soukand, R. & Pieroni, A. (2016). The importance of a border: Medical, veterinary, and wild food ethnobotany of the Hutsuls living on the Romanian and Ukrainian sides of Bukovina. *Journal of Ethnopharmacology*, 185, 17–40.
- Stickl, O. (1928) Die bactericide Wirkung der Extrakte und Alkaloide des Schöllkrautes (*Chelidonium majus*) auf gram positive. *Pathogene Mikroorganismen. Zeitschrift für Hygiene und Infektionskrankheiten*, 108, 567–577. <https://doi.org/10.1007/BF02201625>
- Taborska, E., Bochorakova, H., Dostal, J. & Paulova, H. (1995) The greater celandine (*Chelidonium majus* L.) - review of present knowledge. *Ceska a Slovenska Farmacie*, 144(2), 71–75.
- Ünsal, Ç., Vural, H., Sariyar, G., Özbek, B. & Ötük, G. (2010) Traditional Medicine in Bilecik Province (Turkey) and Antimicrobial Activities of Selected Species. *Turkish Journal of Pharmaceutical Science*, 7(2), 139–150.
- Uzun, E., Sariyar, G., Adersen, A., Karakoc, B., Ötük, G., Oktayoğlu, E. & Pirildar, S. (2004) Traditional medicine in Sakarya province (Turkey) and antimicrobial activities of selected species. *Journal of Ethnopharmacology*, 95, 287–296.
- Vahlensieck, U., Hahn, R., Winterhoff, H., Gumbinger, H.G., Nahrstedt, A. & Kemper, F.H. (1995) The effect of *Chelidonium majus* herb extract on choleresis in the isolated perfused rat liver. *Planta Medica*, 61(3), 267–271.
- Varga F., Solic, I., Dujakovic, M.J., Luczaj, L. & Grdisa, M., (2019) The first contribution to the ethnobotany of inland Dalmatia: medicinal and wild food plants of the Knin area, Croatia. *Acta Societatis Botanicorum Polonaise*, 88(2), 3622.
- Weiskirchen, R., (2016) Hepatoprotective and anti-fibrotic agents: it's time to take the next step. *Frontiers in Pharmacology*, 6(303), 1–40. <https://doi.org/10.3389/fphar.2015.00303>
- World Health Organization. (2010) *WHO Monographs on medicinal plants commonly used in the Newly Independent States (NIS)* (pp.73–91). Geneva: WHO Press.
- Zielinska, S., Jezierska-Domaradzka, A., Wójciak-Kosior, M., Sowa, I., Junka, A. & Matkowski, A.M. (2018). Greater Celandine's Ups and Downs—21 Centuries of Medicinal Uses of *Chelidonium majus* From the Viewpoint of Today's. *Pharmacology. Frontiers Pharmacology*, 9, 299. <https://doi.org/10.3389/fphar.2018.00299>
- Zuo, G.Y., Meng, F.Y., Hao, X.Y., Zhang, Y.L., Wang, G.C. & Xu, G.L. (2008) Antibacterial alkaloids from *Chelidonium majus* Linn (Papaveraceae) against clinical isolated of methicillin resistant *Staphylococcus aureus*. *Journal of Pharmacy and Pharmaceutical Science*, 11(4), 90–94. <https://doi.org/10.18433/J3D30Q>

The anatomical properties of endemic *Hypericum kotschyianum* Boiss.

Onur Altınbaşak , Gülay Ecevit Genç , Şükran Kültür 

Istanbul University, Faculty of Pharmacy, Pharmaceutical Botany, Istanbul, Turkey

ORCID IDs of the authors: O.A. 0000-0002-7167-7663; G.E.G. 0000-0002-1441-7427; Ş.K. 0000-0001-9413-5210

Cite this article as: Altınbaşak, O., Ecevit Genç, G., & Kültür, S. (2021). The anatomical properties of endemic *Hypericum kotschyianum* Boiss. *Istanbul Journal of Pharmacy*, 51(1), 133-136.

ABSTRACT

Background and Aims: This study reveals the anatomical features of *Hypericum kotschyianum* Boiss. species and compares them with previous studies. The anatomical characteristics of stem, leaf, and root were studied using a light microscope. In addition, anatomical structures were measured.

Methods: The studied material was collected from Arslanköy, Mersin. The collected specimens were identified. Dried specimens were kept in Istanbul University Faculty of Pharmacy Herbarium (ISTE) and filed using the ISTE number system (ISTE 98173). Also, some plant materials were kept in 70% ethanol for anatomical examination. All sections from plants were cut by hand using a blade. Samples were examined in SARTUR reagent. Photographs were taken using a light microscope.

Results: When we examined the cells around the stomata in the light of the neighboring cells, we observed that the stomata is an anomocytic type in leaf superficial section. The number of cells that radially surround the bottom of the trichomes on the leaf surface is 9. This can be specified as a characteristic feature of this type. In the stem cross-section of *H. kotschyianum* species, secretory canals were observed. In *H. kotschyianum* stem cross-section, irregular ridges were present and wing structure was not observed. The existence of secretory canals was observed in *H. kotschyianum* root cross-section.

Conclusion: We examined *Hypericum kotschyianum* anatomically for the first time. Therefore, this study is important in providing information that will be the source of other studies on this plant.

Keywords: *Hypericum kotschyianum*, plant anatomy, Turkey

INTRODUCTION

Hypericum L. genus is spreading all over the world and includes 460 species of trees, shrubs, and herbaceous plants (Perrone et al., 2013b). Approximately 100 species grow naturally in Turkey, of which 46 are endemic (Davis et al., 1967; Özhatay et al., 2009; Özhatay et al., 2011; Özhatay et al., 2015; Güner et al., 2000; Güner, 2012).

The secretory structures of the genus *Hypericum* are highly specialized for the synthesis and deposition of biologically active compounds and it has great potential. These secretory structures are found in vegetative and generative organs. Their phytochemical diversity has been revealed by taxonomic and anatomical studies (Perrone et al., 2013a; Ciccarelli et al., 2001; Nahrstedt, 1997).

Other studies worldwide have also concentrated on *Hypericum perforatum* L which has traditionally been used to heal wounds, burns, and swellings, and also used as an anti-inflammatory. In addition, it has been used internally for stomach diseases, ulcers, enteritis, and diabetes (Özkan & Mat, 2013). Moench's study on extracts of *Hypericum* species such as *H. perforatum*, *H. calycinum* L., and *H. confertum* Moench demonstrates that especially *H. calycinum* extracts are potential agents to use in cosmeceuticals for anti-aging and skin-whitening purposes (Ersoy et al., 2019). Experimental studies on the inhibition of the inflammatory pathway

Address for Correspondence:

Onur ALTINBAŞAK, e-mail: oaltinbasak@gmail.com

This work is licensed under a Creative Commons Attribution 4.0 International License.



Submitted: 22.06.2020
Revision Requested: 30.07.2020
Last Revision Received: 03.09.2020
Accepted: 14.10.2020

and recovery of DNA damage for *H. olympicum* L. species have also been carried out. (Kurt-Celep et al., 2020).

There are some features which are characteristic of the anatomy of *Hypericum*. According to Metcalfe et al. (1957) pith rays are uniseriate, and the xylem and phloem are somewhat narrower. Pith development is greater in herbaceous *Hypericum*. Also, stomata of *Hypericum* species are generally surrounded by three or more cells.

Another characteristic feature of the anatomy of *Hypericum* is secretory canals' distribution. Secretory canals are always present in the secondary phloem, however sometimes there are also found in the pith, pericycle, and outer part of the primary cortex. In the root, secretory canals are present in the pericycle and secondary phloem of *Hypericum* (Metcalfe et al., 1957).

H. kotschyanum is an endemic species that was recorded as growing naturally only in Konya and Niğde provinces (Davis et al., 1967). The stem is 10-30 cm long, branched from the base, and has woolly hairs. Leaves are on the main stem, 5-15 mm, hairy. Inflorescence shapes are pyramidal or cylindric. There are glands like black dots on the petals. They usually grow on calcareous and rocky lands at an altitude of 1800-2000 m (Duman & Sevimli, 2008).

H. kotschyanum is known to local people by its vernacular name "Kantaron, Antoron, Antoryon" in Arslanköy, Mersin province. Anatomical studies were not found in the literature review of the *H. kotschyanum*. In this study, the stem, leaf, and root parts of the endemic species were examined and the anatomical structure was revealed for the first time.

MATERIAL AND METHODS

The studied material was collected from Arslanköy, Mersin, by Prof. Dr. Şükran Kültür in June 2012. The collected specimens were identified by Şükran Kültür. Dried specimens were kept and filed using an ISTE number (ISTE 98173) in Istanbul University Faculty of Pharmacy Herbarium (ISTE). Some plant materials were stored in 70% ethanol for anatomical examination. All sections from the plants were cut by hand using a blade. Samples were examined in SARTUR reagent. Photographs were taken using a light microscope (Olympus BH-2 and Canon A640 digital camera).

RESULTS

Leaf

On the cross-section of the leaf, there is a thick cuticle layer on the outer surface. Trichome derived from epidermis are found on the lower and upper surface of the leaf. Below the cuticle layer, there is a single-layer epidermal. In the leaf mesophyll cross-section, palisade parenchyma cells are located under the upper epidermis and there are spongy parenchyma cells under this parenchyma layer. The mesophyll is bifacial. Also, schizogenous secretory canals with a large gap are distinguished (Figure 1). These gaps are $0,575\pm 0,159$ μm in diameter. The leaf thickness is between 1,483-2,287 μm and the average is $1,883\pm 0,317$ μm .

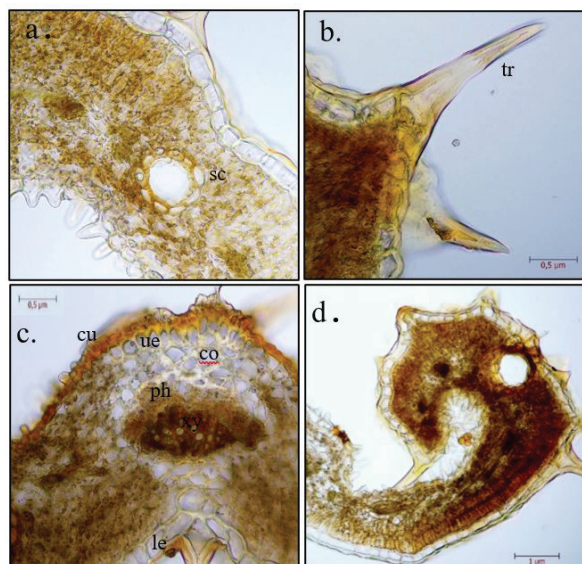


Figure 1. The cross-sections of leaf of *H. kotschyanum*; (a) sc: secretory canal, (b) tr: trichome, (c) ue: upper epidermis, le: lower epidermis, cu: cuticle, co: collenchyma, ph: phloem, xy: xylem, (d) mesophyll general view.

In the cross-section of the main vein, 3-4 layers of collenchyma are observed under the upper epidermis. Xylem is on the lower side of the main vein and phloem is located on the upper; the veins are collateral (Figure 1). The leaf's main vein thickness average is 3,47 μm .

When the superficial cross-section of the leaf was examined, it was observed that the cover hairs were derived from the middle of 9 epidermal cells. Stoma was found only on the lower surface of the leaf. The leaf is hypostomatic. Stomata are the anomocytic type, but 3-5 cells are adjacent to the stoma (Figure 2). The stomatal index for the lower surface is 25.

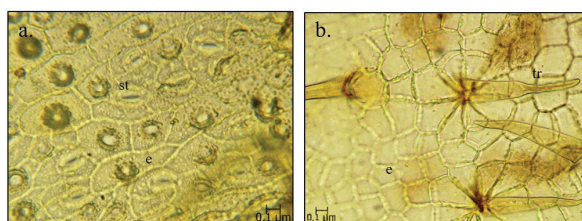


Figure 2. The surface sections of the leaf of *H. kotschyanum*; (a) lower surface of the leaf (b) the upper surface of the leaf; e: epidermis, st: stomata, tr: trichome.

Stem

In the cross-section of the stem, there is one epidermal layer under the thick-walled cuticle. There are many one-celled eglandular trichomes on the epidermal layer. Under this epidermal layer, collenchyma cells are located as 7-8 layers (Figure 3). The phloem layer extends under the collenchyma cells and the width of the phloem layer is about $0,639 \pm 0,073$ μm . Also, large secretory canals are observed on the phloem layer. Between the phloem and xylem layer, there is a thin cambium layer. The xylem has gaps that expand towards the pith. The pith is composed of parenchymatic cells that vary in diameter (Table 1).

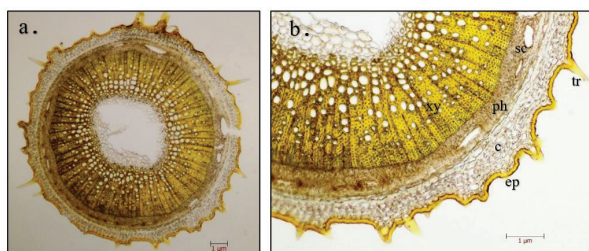


Figure 3. The cross-sections of the stem of *H. kotschyanum*; (a) general view, (b) cortex and vascular bundles; ep: epidermis, c: cortex, sc: secretory canal, fl: phloem, tr: trichomes, xy: xylem.

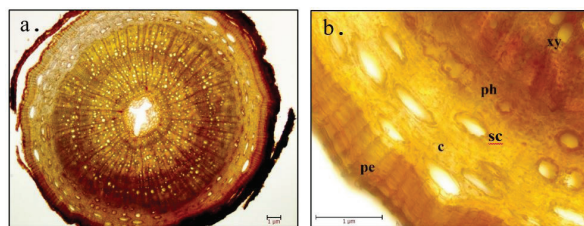


Figure 4. The cross-sections of root of *H. kotschyanum*; (a) general view, (b) cortex and vascular bundles; pe: periderm, c: cortex, sc: secretory canal, ph: phloem, xy: xylem.

	Width (μm)		Number
	Min.-Max.	Avr. \pm Sd	
Stem			
Pith cell (diameter)	0,143-0332	0,203 \pm 0,056	
Trachea (diameter)	0,158-0,311	0,232 \pm 0,044	
Floem layer	0,552-0,751	0,639 \pm 0,073	
Leaf			
Secretory pockets (diameter)	0,462-0,687	0,575 \pm 0,159	
Lower stomata			8
Lower epidermis cell			32
Stomatal index			25
Mesophyll thickness	1,483-2,287	1,883 \pm 0,317	
Root			
Cortex thickness	1,299-1,501	1,395 \pm 0,063	
Phloem thickness	0,328-0,542	0,443 \pm 0,075	
Trachea (diameter)	0,165-0,269	0,202 \pm 0,034	

Root

In the cross-section of the root, there are 4-5 layers of periderm on the outside. Just below this layer, there is cortex tissue with a large number of secretory canals (Figure 4). Cortex tissue thickness is $1,395 \pm 0,063 \mu\text{m}$. The phloem layer is located outside the xylem and the average thickness is of this tissue is about $0,443 \pm 0,075 \mu\text{m}$. Xylem tissue is located in the innermost layer. There is a large width of traches. These traches are about $0,202 \pm 0,034 \mu\text{m}$ in width. The pith layer has parenchymatic cells.

DISCUSSION

The stem, leaf, and root anatomy of *H. kotschyanum* were examined for the first time with this study.

When we examined the stomata according to its neighboring cells, we observed that the stomata is an anomocytic type in the superficial section of the leaf. These observations on the Hypericaceae family properties correspond to other studies (Metcalfe & Chalk, 1957). In studies carried out by Tekin (2017) and Altınbaşak (2019) the leaves of *H. thymopsis* Boiss. are bifacial, without hypodermis and stomata are anisocytic and anomocytic. In our study we observed that *H. kotschyanum* stomata are anomocytic and the leaves are bifacial. Also *H. perforatum*, *H. perforatum* L., *H. tetrapterum* Fr., *H. androsaemum* L., and *H. hircinum* L., leaves are bifacial but the leaves of *H. pubescens* Boiss., *H. triquetrifolium* Turra, and *H. aegypticum* L. are isobilateral (Perrone et al., 2013a). Yaylacı et al. (2013) studied the anatomical characteristics of *H. sechmenii* Ocağ & Koyuncu. Study showed that *H. sechmenii* has equifacial leaves, anomocytic stomata.

The thick cuticle layer and stomata on the leaf only on the lower surface indicate that the plant grows in an environment that requires the use of water more efficiently. Hence, the features of this species confirm that *H. kotschyanum* has a xeromorphic structure.

Ciccarelli et al. (2001) stated in their study that there is a translucent secretion canal in the leaf of *Hypericum perforatum*. Secretion canals of the same type were observed in the *H. kotschyanum* mesophyll layer. Also in the studies of Tekin (2017) and Altınbaşak (2019), *H. scabrum* L. and *H. thymopsis* have the same secretion canals. But *H. spectabile* Boiss does not have these features. The number of the cells that radially surround the bottom of the trichomes on the leaf surface is 9. This can be specified as a characteristic feature of *H. kotschyanum*.

In the stem cross-section of *H. kotschyanum*, secretory canals were observed just like in the *H. perforatum* species in Lotocka & Osińska's (2010) studies. In the study by Altınbaşak (2019) *H. spectabile* has large secretion canals in the phloem layer like *H. kotschyanum*. As in other studies with *Hypericum* species, collenchyma tissue was observed in the stem cross-section (Erkara & Tokur, 2004; Lotocka & Osińska, 2010). The presence of wings on the stem is an important feature for *Hypericum* species. Perrone et al. (2013a), Altınbaşak (2019), and Tekin (2017) showed the presence of wings in the species in their

studies and used these structures in the differentiation of species. However, in *H. kotschyianum* stem cross-section, irregular ridges are present and wing structure is not observed.

In the studies by Erkara & Tokur (2004) and Altınbaşak (2019), it was stated that there are 4-5 rows of periderm layers in the roots of *H. montbretii* Spach, *H. origanifolium* Willd., *H. spectabile* and *H. perforatum* species. Also, *H. kotschyianum* has the same number of periderm layers in the roots. In the study conducted on *H. montbretii*, *H. origanifolium*, and *H. perforatum* species, the existence of secretion canals in the roots are not mentioned (Erkara & Tokur, 2004). Unlike these species, the existence of secretory canals was observed in *H. kotschyianum* root cross-section.

We examined *Hypericum kotschyianum* anatomically for the first time. Therefore, this study is important in providing information that will be the source of other studies on the plant. Anatomical studies on the genus *Hypericum* can be used to distinguish the species more prominently.

Peer-review: Externally peer-reviewed.

Author Contributions: Conception/Design of Study- O.A., G.E.G., Ş.K.; Data Acquisition- O.A., G.E.G., Ş.K.; Data Analysis/Interpretation- O.A., G.E.G., Ş.K.; Drafting Manuscript- O.A., G.E.G., Ş.K.; Critical Revision of Manuscript- O.A., G.E.G., Ş.K.; Final Approval and Accountability- O.A., G.E.G., Ş.K

Conflict of Interest: The authors have no conflict of interest to declare.

Financial Disclosure: Authors declared no financial support.

REFERENCES

- Altınbaşak, O. (2019). Pharmaceutical Botany Research On Some Natural Spreading Hypericum L. Species In Turkey. (Master dissertation). Retrieved from <https://tez.yok.gov.tr/UlusalTezMerkezi/tezSorguSonucYeni.jsp>.
- Ciccarelli, D., Andreucci, A. C., & Pagni, A. M. (2001). Translucent glands and secretory canals in *Hypericum perforatum* L. (Hypericaceae): Morphological, anatomical and histochemical studies during the course of ontogenesis. *Annals of Botany*, 88(4), 637–644. <https://doi.org/10.1006/anbo.2001.1514>
- Davis, P., Cullen, J., & Codde, M. J. E. (Eds.). (1967). *Flora of Turkey and the East Aegean Islands Vol. 2*. Edinburgh: Edinburgh University Press.
- Duman, R., & Sevimli, A. (2008). *H. perforatum* L., *H. scabrum* L. ve *H. kotschyianum* Boiss. Ekstrelerinin Antibakteriyel Aktivitelerinin Belirlenmesi. [Determination of Antibacterial Activities *H. perforatum* L., *H. scabrum* L. and *H. kotschyianum* Boiss. Extracts]. *Selçuk Üniversitesi Fen Edebiyat Fakültesi Dergisi*, 31, 27–33.
- Ersoy, E., Eroglu Ozkan, E., Boga, M., Yilmaz, M. A., & Mat, A. (2019). Anti-aging potential and anti-tyrosinase activity of three *Hypericum* species with focus on phytochemical composition by LC–MS/MS. *Industrial Crops and Products*, 141(August). <https://doi.org/10.1016/j.indcrop.2019.111735>
- Güner, A., Özhatay, N., Ekim, T., & Başer, K. (Eds.). (2000). *Flora of Turkey and the East Aegean Islands. Vol. 11 (Supplement II)*. Edinburgh: Edinburgh University Press.
- Güner, A. (Eds.). (2012). *Türkiye Bitkileri Listesi-Damarlı Bitkiler*. [Turkey Plants List-Vascular Plants]. Istanbul: Nezahat Gökyiğit Botanik Bahçesi.
- Kurt-Celep, İ., Celep, E., Akyüz, S., İnan, Y., Barak, T. H., Akaydin, G., Yesilada, E. (2020). *Hypericum olympicum* L. recovers DNA damage and prevents MMP–9 activation induced by UVB in human dermal fibroblasts. *Journal of Ethnopharmacology*, 246(August). <https://doi.org/10.1016/j.jep.2019.112202>
- Lotocka, B., & Osińska, E., (2010). Shoot anatomy and secretory structures in *Hypericum* species (Hypericaceae). *Botanical Journal of the Linnean Society*, 163(1), 70–86. <https://doi.org/10.1111/j.1095-8339.2010.01046.x>
- Metcalfe, C. R., & Chalk, L. (1957). *Anatomy of the Dicotyledons Volume 1*. London: Oxford University Press.
- Nahrstedt, A. (1997). Biologically active and other chemical constituents of the herb of *Hypericum perforatum* L. *Pharmacopsychiatry*, 30(SUPPL. 2), 129–134. <https://doi.org/10.1055/s-2007-979533>
- Özhatay, F. N., Kültür, Ş., & Gürdal, M. B. (2011). Check-list of additional taxa to the supplement Flora of Turkey V. [*Turkish Journal of Botany*, 35(5), 589–624. <https://doi.org/10.3906/bot-1101-20>
- Özhatay, N., Kültür, Ş., & Aslan, S. (2009). Check-list of additional taxa to the Supplement Flora of Turkey IV. *Turkish Journal of Botany*, 33(3), 191–226. <https://doi.org/10.3906/bot-0805-12>
- Özhatay, N., Kültür, Ş., & Gürdal, B. (2015). Check-list of additional Taxa to the supplement flora of Turkey VII. *Journal of Pharmacy of Istanbul University*, 45(1), 61–86. <https://doi.org/10.5152/istanbuljpharm.2017.006>
- Özkan, E. E., & Mat, A. (2013). An overview on *Hypericum* species of Turkey. *Journal of Pharmacognosy and Phytotherapy*, 5(3), 38–46. <https://doi.org/10.5897/JPP2013.0260>
- Perrone, R., De Rosa, P., De Castro, O., & Colombo, P. (2013a). A further analysis of secretory structures of some taxa belonging to the genus *Hypericum* (Clusiaceae) in relation to the leaf vascular pattern. *Turkish Journal of Botany*, 37(5), 847–858. <https://doi.org/10.3906/bot-1206-22>
- Perrone, R., De Rosa, P., De Castro, O., & Colombo, P. (2013b). Leaf and stem anatomy in eight *Hypericum* species (Clusiaceae). *Acta Botanica Croatica*, 72(2), 269–286. <https://doi.org/10.2478/botcro-2013-0008>
- Potoğlu Erkara, I., Tokur, S. (2004). Morphological and anatomical investigations on some *Hypericum* L., species growing naturally in and around Eskisehir. *Trakya Univ J Sci*, 5, 97–105.
- Tekin, M. (2017). Pharmacobotanical study of *Hypericum thymopsis*. *Revista Brasileira de Farmacognosia*, 27, 143–152
- Yaylacı, Ö. K., Özgis, İ. K., Sezer, O., Orhanoğlu, G., Öztürk, D., Koyuncu, O. (2013). Anatomical studies and conservation status of rare endemic *Hypericum sechmenii* Ocak & Koyuncu (Sect. *Adenosepalum*) from Eskişehir-Turkey. *J. Selçuk Univ Nat Appl Sci*, 2, 1–11.

Fungal homoserine transacetylase: A potential antifungal target

Esra Seyran¹ ¹International Centre for Genetic Engineering and Biotechnology, Trieste, Italy**ORCID IDs of the authors:** E.S. 0000-0002-0384-4300**Cite this article as:** Seyran, E. (2021). Fungal homoserine transacetylase: A potential antifungal target. *Istanbul Journal of Pharmacy*, 51(1), 137-140.

ABSTRACT

We are facing a significant challenge due to the tremendous rise in drug resistant fungal pathogen populations. The number of antifungal drugs is limited, as are the known targets they inhibit. The limited number of drugs and targets that have been successfully exploited in antifungal drug discovery is in part due to the eukaryotic nature of these organisms, which is shared with mammalian cells. An ideal antifungal substance is one that targets an indispensable pathway for pathogenic fungal survival that is not present in mammals or plants. Methionine is an essential amino acid for fungi and inhibition of its biosynthesis is deleterious for the pathogen. The biochemical pathways that produce methionine do not exist in mammals as they acquire it from their diet. Homoserine transacetylase, which catalyses the first committed step in methionine biosynthesis, therefore represents an attractive drug target. This enzyme is absent in mammals and unique to fungi and bacteria, suggesting that drugs targeting it would be of low toxicity, if any, to mammals, while having a lethal effect against the fungal pathogen. Homoserine transacetylase, based on its role in the production of methionine and its absence in mammals and plants could be a potential antifungal target.

Keywords: Antifungal, Homoserine Transacetylase, Methionine

INTRODUCTION

Fungal infections in general accounted for 40% of deaths due to hospital acquired infections. Several fungal pathogens, such as *Coccidioides immitis*, can infect healthy individuals, however, the majority of fungal infections are caused by opportunistic pathogens that attack immunosuppressed patients of HIV, chemotherapy or organ transplant (Pfaller & Diekema, 2007). Developments in the treatments against HIV and cancer are leading to longer survival of immunocompromised individuals but, unfortunately, aggressive immunosuppressive therapy for organ transplant recipients and exposure to a broad spectrum antibiotics are also predisposing patients to fungal infections. Fungal infections in immunocompromised individuals are often life threatening. Mortality rates of hospitalized patients with candidiasis are approximately 50% (Low & Rotstein, 2011). Increased prevalence of *Candida albicans* clinical isolates resistant to traditional therapies calls for the need for novel agents containing higher specificity for fungal cells over mammalian cells (Ashman et al., 2004; Whaley et al., 2016). There is an urgent need for novel agents containing higher specificity for fungal cells over mammalian cells.

The novel fungal specific agents could potentially be identified by targeting unique biochemical activities that are present in *C. albicans* and other pathogenic fungi but which are absent in mammalian systems. The mechanism of action of conventional antifungal drugs can be broadly classified as those acting on fungal membrane permeability or on the enzymes of the ergosterol biosynthetic pathway. The selectivity of these antifungal agents is obtained by their ability to bind to sterols that are unique to fungal

Address for Correspondence:

Esra SEYRAN, e-mail: esraseyran@gmail.com

This work is licensed under a Creative Commons Attribution 4.0 International License.

Submitted: 19.07.2020
Revision Requested: 26.06.2020
Last Revision Received: 19.07.2020
Accepted: 04.09.2020

cells or by their ability to target fungus specific enzymes that are required for the production of the fungal cell membrane. The major class of antifungal agents in clinical use against candidiasis today are azoles. The azole class of antifungals act by inhibiting the biosynthesis of ergosterol and have a broad spectrum of fungistatic activity. Inhibition of cytochrome P450 dependent sterol 14 α -demethylase by azoles leads to a depletion of ergosterol and an accumulation of 14 α -methyl sterols, leading to disruption of the fungal cell membrane (Mazu, Bricker, Flores-Rozas, & Ablordepey, 2016). The azoles, fluconazole, itraconazole and ketoconazole are used frequently against invasive mucocutaneous candidiasis and cryptococcal meningitis (Chang, Yu, Heitman, Wellington, & Chen, 2017).

Fungal resistance to azoles is currently a problem in both medicine and agriculture. Azole resistance initially appeared in barley powdery mildew isolates in the early 1980s, soon after azole resistance became prevalent in other important plant pathogens (Hollomon, 1993). Clinically, azole resistance is increasing in frequency, especially among HIV patients with *C. albicans* infections (Vandeputte et al., 2005). Resistance is often a consequence of treatment or prevention of mucocutaneous candidiasis with low doses of fluconazole over a long period of time. In the case of immunocompromised patients, infections often reoccur, and patients are often less responsive to azoles. Moreover, resistance to one azole drug can usually lead to cross-resistance to other azoles (Panackal et al., 2006). In *C. albicans*, azole resistance is mediated through more than one mechanism. Resistance can be the result of an alteration of the target enzyme, the cytochrome P-450 lanosterol 14 α demethylase, either by overexpression or as a result of point mutations in the gene that encodes it. The former requires the need for a higher intracellular azole concentration to complex all the enzyme molecules present in the cells, and the latter leads to amino acid substitutions, resulting in a decreased affinity for azole derivatives. A second major mechanism is the failure of azole antifungal agents to accumulate inside the fungal cell as a consequence of enhanced drug efflux (Warrilow et al., 2019). The Polyene class of antifungals are macrolide antibiotics made up of alternating conjugated double bonds. The polyene drugs interact with ergosterol in fungal membranes and induce channels in the fungal membrane, resulting in the loss of membrane selective permeability. Cholesterol is a building block in human cell membranes with a similar in structure to ergosterol, and as a result there is some toxicity associated with the use of polyene class antifungals (Omura & Tanaka, 1984). The other problem in hand is the high potential of current antifungal compounds for drug-drug interactions. For example, azoles are both a substrate and inhibitor of several cytochrome P450 enzymes, with CYP3A4 being the major enzyme involved. Other classes of antifungal drugs such as echinocandins may lead to pharmacodynamic interaction on the level of renal toxicity (Zager, 2000).

Amino acid biosynthesis pathways as antifungal targets

The development of new antifungal drugs with new and different mechanism of actions is critical in order to provide treatment to life threatening fungal diseases. The yeast genome study revealed that approximately 1,100 genes are required

for fungal viability and around 350 of these genes have no homologues in the human genome (Ho et al., 2002). Amino acid biosynthesis has been considered as a potential target for antimicrobial drug development. Certain amino acids are not produced by mammals. The aspartic acid pathway is involved in the biosynthesis of a quarter of all amino acids required for protein synthesis and produces several critical metabolic intermediates. In particular, methionine, threonine and isoleucine are synthesized as branches off the aspartic acid biosynthesis pathway. The aspartic acid pathway is highly conserved in bacteria, fungi and plants but is not found in mammals, making key enzymes of this pathway attractive targets for drug discovery (Nazi et al., 2007).

Several molecules that affect microbial growth and infection by interfering with the aspartic acid pathway have been reported in the past few years. For example, the amino acid analog (S)-2-amino-5-hydroxynuc-4-oxopentanoic acid validates the idea of consideration of this pathway as a target. This compound inhibits homoserine dehydrogenase of the aspartic acid biosynthetic pathway. This compound hinders *C. albicans* infections in mice with no toxic effect to the host (Yamaki et al., 1990). Another example, azoxybacillin, produced by *Bacillus cereus*, is effective against the biosynthesis of sulphur containing amino acids. Rhizoctin A, from *Bacillus subtilis*, disrupts threonine biosynthesis (Yamaguchi et al., 1988). In the first step of the aspartic acid pathway, aspartate kinase phosphorylates aspartate to give aspartyl-phosphate. Aspartyl-phosphate is reduced in an NADPH-dependant manner to give aspartate 4-semialdehyde by the enzyme aspartate semialdehyde dehydrogenase. This reaction involves a nucleophilic attack followed by a hydride transfer from NADPH resulting in the formation of aspartate 4-semialdehyde. At this stage in plants and bacteria the pathway branches to synthesize either lysine or methionine, threonine, and isoleucine through homoserine, which is the only possible intermediate for fungi. In yeast, homoserine biosynthesis is achieved through the NADPH/NADH-dependent reduction of aspartate 4-semialdehyde by the action of homoserine dehydrogenase. The final common precursor of this pathway is homoserine, before the pathway branches in two different directions, the first to produce methionine and the second to produce threonine or isoleucine. In the methionine biosynthetic branch of the Asp pathway, the hydroxyl group of homoserine is activated by acylation. Two crucial acylating enzymes that convert homoserine to methionine are homoserine transacetylase and homoserine transsuccinylase. Both enzymes activate the hydroxyl group of homoserine for displacement of the corresponding acid by the thiol of cysteine to form cystathionine by the pyridoxal phosphate dependent enzyme cystathionine synthase.

Homoserine transacetylase as a target for new antifungal drug development

Fungal homoserine transacetylases are approximately 450 amino acids long and belong to the α/β hydrolase fold superfamily of enzymes that includes various esterases, lipases, and peptidases. This family is characterized by an eight-stranded sheet connected by helices with an active site catalytic triad plug. The nucleophilic residues in the catalytic triad can be serine, cysteine or glutamic acid (Born, Franklin, & Blanchard,

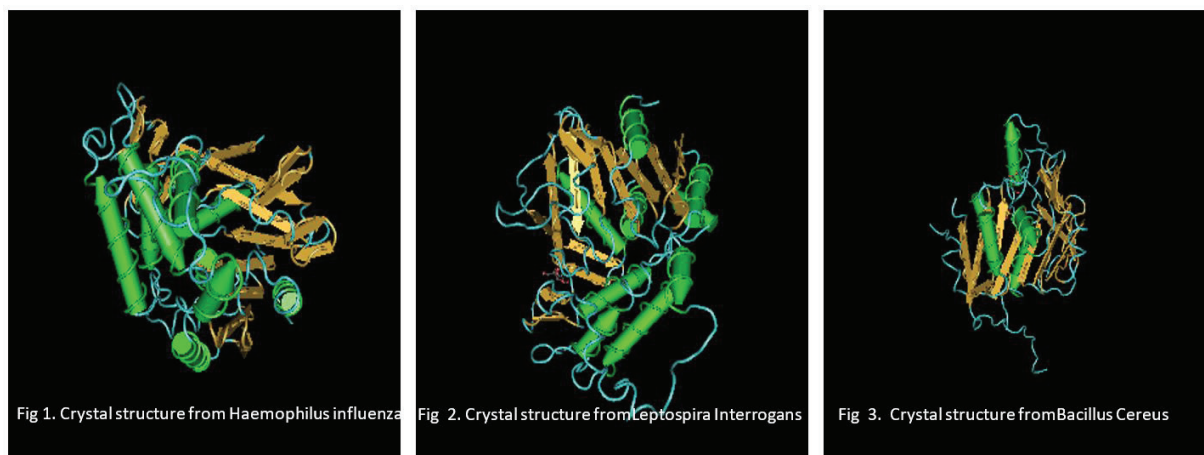


Figure 1-3. Clear differences exist between structurally characterized examples of homoserine transacetylase.

2000; Ollis et al., 1992). Homoserine transacetylase catalyses the first committed step in the synthesis of methionine from aspartic acid. The enzyme catalyses the transfer of the acetyl group from acetyl coenzyme A to the hydroxyl group of homoserine. Early efforts were focused on isolation and purification of the enzyme. Homoserine transacetylase was initially purified from *Bacillus polymyxa*. Early kinetic studies revealed that the enzyme catalyses the transfer of the acetyl group through a ping-pong mechanism in which the acyl group of acetyl CoA is first transferred to an active site residue before subsequent transfer to the hydroxyl moiety of homoserine (Wyman & Paulus, 1975). A ping-pong reaction is where in a two-substrate, two-product system an enzyme reacts with one substrate to form a product and a modified enzyme, the latter then reacts with a second substrate to form a second product and regenerates the original enzyme (Cleland, 1977). Born *et al.* showed that homoserine transacetylase from *Haemophilus influenzae* also undergoes a reaction with a ping-pong kinetic mechanism; an initial acyl-enzyme intermediate is formed with acetyl-coA then the acetate is transferred to the hydroxyl group of homoserine (Born, et al., 2000). Homoserine transacetylase from the fission yeast *Schizosaccharomyces pombe* follows a covalent catalytic strategy to acetylate homoserine through an active site serine residue. Steady-state kinetic parameters provide evidence that enzyme from *S. pombe* also follows a ping-pong mechanism. Using site directed mutagenesis, site-specific mutants of the enzyme were constructed. Steady state kinetics study of the mutants demonstrated that Ser163, Asp403, and His432 are the likely active-site residues of a catalytic triad (Nazi, & Wright, 2005). Crystal structures of prokaryotic forms of enzyme have been solved (Zager, 2000). Figures 1, 2 and 3 are generated using the Protein Structure Data Base. The overall detailed topology of these three proteins obviously differs from each other.

The details of the active site and how it might bind a drug are likely significantly different. In order to exploit the potential of homoserine transacetylase as an antifungal target, the structural basis of catalytic activation of homoserine transacetylase needs to be determined from *C. albicans* or from a phylogenetically closely related human pathogenic fungi.

CONCLUSIONS

The first step for drug discovery is target identification. A potent drug should have low host toxicity, ideally should not be found in host cells, and should be essential for the life of the pathogen while presenting the desired activity for inactivating targets. The conserved subset fungal amino acid biosynthetic enzymes which are absent in human presents an underexploited realm as antifungal drug targets. Particularly, the biosynthesis of methionine has been suggested to be susceptible to small molecule inhibition in fungi. Methionine is synthesized in bacteria, fungi, and plants. The first committed step in methionine biosynthesis is identified as the acetylation of homoserine by the enzyme homoserine transacetylase, a promising drug-susceptible target for new antifungal drug development.

Peer-review: Externally peer-reviewed.

Author Contributions: Conception/Design of Study- E.S.; Data Acquisition- E.S.; Data Analysis/Interpretation- E.S.; Drafting Manuscript- E.S.; Critical Revision of Manuscript- E.S.; Final Approval and Accountability- E.S.

Conflict of Interest: The authors have no conflict of interest to declare.

Financial Disclosure: Authors declared no financial support.

REFERENCES

- Ashman, R. B., Farah, C. S., Wanasangkul, S., Hu, Y., Pang, G., & Clancy, R. L. (2004). Innate versus adaptive immunity in *Candida albicans* infection. *Immunology and Cell Biology*, 82(2), 196–204. <https://doi.org/10.1046/j.0818-9641.2004.01217.x>
- Born, T. L., Franklin, M., & Blanchard, J. S. (2000). Enzyme-catalyzed acylation of homoserine: mechanistic characterization of the *Haemophilus influenzae* met2-encoded homoserine transacetylase. *Biochemistry*, 39(29), 8556–8564. <https://doi.org/10.1021/bi000462p>
- Chang, Y. L., Yu, S. J., Heitman, J., Wellington, M., & Chen, Y. L. (2017). New facets of antifungal therapy. *Virulence*, 8(2), 222–236. <https://doi.org/10.1080/21505594.2016.1257457>
- Cleland W. W. (1977). Determining the chemical mechanisms of enzyme-catalyzed reactions by kinetic studies. *Advances in Enzymology and Related Areas of Molecular Biology*, 45, 273–387. <https://doi.org/10.1002/9780470122907.ch4>

- Hollomon D. W. (1993). Resistance to azole fungicides in the field. *Biochemical Society Transactions*, 21(4), 1047–1051. <https://doi.org/10.1042/bst0211047>
- Low, C. Y., & Rotstein, C. (2011). Emerging fungal infections in immunocompromised patients. *F1000 Medicine Reports*, 3, 14. <https://doi.org/10.3410/M3-14>
- Mazu, T. K., Bricker, B. A., Flores-Rozas, H., & Ablordepey, S. Y. (2016). The Mechanistic Targets of Antifungal Agents: An Overview. *Mini Reviews in Medicinal Chemistry*, 16(7), 555–578. <https://doi.org/10.2174/1389557516666160118112103>
- Nazi, I., & Wright, G. D. (2005). Catalytic mechanism of fungal homoserine transacetylase. *Biochemistry*, 44(41), 13560–13566. <https://doi.org/10.1021/bi0514764>
- Nazi, I., Scott, A., Sham, A., Rossi, L., Williamson, P. R., Kronstad, J. W., & Wright, G. D. (2007). Role of homoserine transacetylase as a new target for antifungal agents. *Antimicrobial agents and chemotherapy*, 51(5), 1731–1736. <https://doi.org/10.1128/AAC.01400-06>
- Ollis, D. L., Cheah, E., Cygler, M., Dijkstra, B., Frolow, F., Franken, S. M., Schrag, J. (1992). The alpha/beta hydrolase fold. *Protein Engineering*, 5(3), 197–211. <https://doi.org/10.1093/protein/5.3.197>
- Omura S., & Tanaka H. (1984). Production, structure, and antifungal activity of polyene macrolides, , In S. Omura (Ed.), *Macrolide Antibiotics: Chemistry, Biology, and Practice* (pp. 351–405). New York, USA: Academic Press.
- Panackal, A. A., Gribskov, J. L., Staab, J. F., Kirby, K. A., Rinaldi, M., & Marr, K. A. (2006). Clinical significance of azole antifungal drug cross-resistance in *Candida glabrata*. *Journal of Clinical Microbiology*, 44(5), 1740–1743. <https://doi.org/10.1128/JCM.44.5.1740-1743.2006>
- Pfaller, M. A., & Diekema, D. J. (2007). Epidemiology of invasive candidiasis: a persistent public health problem. *Clinical Microbiology Reviews*, 20(1), 133–163. <https://doi.org/10.1128/CMR.00029-06>
- Vandeputte, P., Larcher, G., Bergès, T., Renier, G., Chabasse, D., & Bouchara, J. P. (2005). Mechanisms of azole resistance in a clinical isolate of *Candida tropicalis*. *Antimicrobial Agents and Chemotherapy*, 49(11), 4608–4615. <https://doi.org/10.1128/AAC.49.11.4608-4615.2005>
- Warrilow, A. G., Nishimoto, A. T., Parker, J. E., Price, C. L., Flowers, S. A., Kelly, D. E., Kelly, S. L. (2019). The Evolution of Azole Resistance in *Candida albicans* Sterol 14 α -Demethylase (CYP51) through Incremental Amino Acid Substitutions. *Antimicrobial Agents and Chemotherapy*, 63(5), e02586-18. <https://doi.org/10.1128/AAC.02586-18>
- Whaley, S. G., Berkow, E. L., Rybak, J. M., Nishimoto, A. T., Barker, K. S., & Rogers, P. D. (2016). Azole Antifungal Resistance in *Candida albicans* and Emerging Non-*albicans* *Candida* Species. *Frontiers in Microbiology*, 7, 2173. <https://doi.org/10.3389/fmicb.2016.02173>
- Wyman, A., & Paulus, H. (1975). Purification and properties of homoserine transacetylase from *Bacillus polymyxa*. *The Journal of Biological Chemistry*, 250(10), 3897–3903.
- Yamaguchi, H., Uchida, K., Hiratani, T., Nagate, T., Watanabe, N., & Omura, S. (1988). RI-331, a new antifungal antibiotic. *Annals of the New York Academy of Sciences*, 544, 188–190. <https://doi.org/10.1111/j.1749-6632.1988.tb40403.x>
- Yamaki, H., Yamaguchi, M., Imamura, H., Suzuki, H., Nishimura, T., Saito, H., & Yamaguchi, H. (1990). The mechanism of antifungal action of (S)-2-amino-4-oxo-5-hydroxypentanoic acid, RI-331: the inhibition of homoserine dehydrogenase in *Saccharomyces cerevisiae*. *Biochemical and Biophysical Research Communications*, 168(2), 837–843. [https://doi.org/10.1016/0006-291x\(90\)92397-i](https://doi.org/10.1016/0006-291x(90)92397-i)
- Zager R. A. (2000). Polyene antibiotics: relative degrees of in vitro cytotoxicity and potential effects on tubule phospholipid and ceramide content. *American Journal of Kidney Diseases : the official journal of the National Kidney Foundation*, 36(2), 238–249. <https://doi.org/10.1053/ajkd.2000.8967>

Bioavailability of berberine: challenges and solutions

Asha Thomas¹ , Seema Kamble¹ , Sanjeevani Deshkar² , Lata Kothapalli¹ , Sohan Chitlange² 

¹Patil Institute of Pharmaceutical Sciences and Research, Department of Pharmaceutical Chemistry, Pimpri, Pune, MS, India

²Patil Institute of Pharmaceutical Sciences and Research Department of Pharmaceutics, Pimpri, Pune, MS, India

ORCID IDs of the authors: A.T. 0000-0003-1058-8779; S.K. 0000-0003-0967-1225; S.D. 0000-0002-3393-717X; L.K. 0000-0002-7412-5805; S.C. 0000-0002-9355-3303

Cite this article as: Thomas, A., Kamble, S., Deshkar, S., Kothapalli, L., & Chitlange, S. (2021). Bioavailability of berberine: Challenges and solutions. *Istanbul Journal of Pharmacy*, 51(1), 141-153.

ABSTRACT

Berberine is a quaternary benzyloquinoline alkaloid with multiple pharmacological effects used for the treatment of hypertension, tumors, bacterial infections, inflammation, HIV, and cardiac diseases. In phase I clinical trials, berberine is safe at excessive doses but manifests poor bioavailability. Major challenges like poor absorption, rapid metabolism, and rapid systemic elimination are responsible for low plasma and tissue levels of berberine. Various strategies have been undertaken by several researchers to overcome this issue and enhance the bioavailability of berberine. This includes the design of new formulation strategies; novel drug delivery systems (NDDS) like liposomes, nanosized dosage forms, phospholipid complexes, mucoadhesive microparticles, and microemulsions; the use of adjuvants; and the design of structural analogues of berberine. This review focuses on the occurrence of berberine in numerous plants and its pharmacological activities as evidenced through numerous preclinical and clinical studies. The later part of this review highlights the bioavailability issue of berberine which arises due to its poor absorption, elevated rate and extent of metabolism, and quick elimination and clearance from the body. A systematic effort has been made to analyze the various formulation strategies, including the design of newer berberine analogues and derivatives. These strategies can be further explored to increase the bioavailability, medicinal value, and application of this promising molecule.

Keywords: Berberine, bioavailability improvement, metabolism, pharmacokinetics

INTRODUCTION

Berberine (5,6-dihydro-9,10-dimethoxybenzo[g]-1,3-benzodioxolo[5,6-a]quinolizinium) (Figure 1) is an isoquinoline alkaloid with a molar mass of 336.3612 g/mol. It is present as a non-basic and quaternary protoberberine in several herbs, including European barberry, goldenseal, goldthread, Oregon grape, phellodendron, and tree turmeric (Neag et al., 2018). The reported uses of berberine-containing species are summarized in Table 1. Berberine (BBR) is a yellowish crystalline powder with a faint characteristic odor and sour taste. It is moderately soluble in methanol, with marginally solubility in ethanol and water (Battu et al., 2010). Berberine is reactive to light and heat; when exposed to high temperature and light, it undergoes degradation and thus affects its stability (Neag et al., 2018). Several pharmacological effects of BBR are reported in literature, which includes anti-depressant (Sun et al., 2014), anti-atherosclerosis (Sarna, Wu, Hwang, Siow, & O, 2010), anti-diarrheal (Zhang et al., 2012b), anti-osteoporosis (Lee et al., 2008), anti-hypercholesterolemia (Kong et al., 2008), and neuroprotective effects (Zhang et al., 2012a). Reports on the extraction of different BBR-employing techniques (classical and conventional methods) using different solvents like methanol, ethanol, and aqueous or acidified methanol/ethanol are available in literature. Conventional methods enhance the extraction efficiency and reduce extraction times and solvent volumes used in the extraction process when compared to the classical methods. BBR in plant extracts and in biological fluids have been quantified using analytical techniques like Ultra Violet spectroscopy (UV), High Performance Liquid Chromatography (HPLC), High Performance Thin Layer Chromatography (HPTLC), Thin Layer Chromatography (TLC), Capillary

Address for Correspondence:

Asha THOMAS, e-mail: asha.thomas@dypvp.edu.in

Submitted: 03.07.2020

Revision Requested: 04.09.2020

Last Revision Received: 03.10.2020

Accepted: 18.11.2020

This work is licensed under a Creative Commons Attribution 4.0 International License.



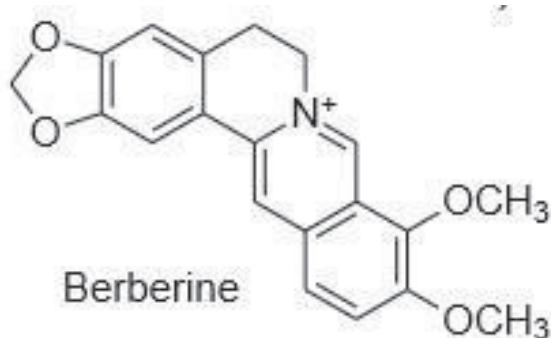


Figure 1. Structure of Berberine.

Electrophoresis (CE), and Liquid Chromatography coupled with Mass Spectrometry (LC-MS) (Neaget et al., 2018).

BBR is present in several plants and is also reported to be responsible for numerous biological activities. Table 1 summarizes the plant species, content of berberine in plant parts, and their reported biological activities. BBR is also present in several marketed herbal preparations, either in pure chemical form as berberine or as plant extracts (ex. berberine in raw herb *Daruharidra* (*Berberis aristata* DC) (Neag et al., 2018). However the major drawback of BBR is its low bioavailability and poor pharmacokinetics, which is majorly responsible for its reduced efficacy. The foremost objective of this review is to discuss in detail the bioavailability, factors controlling bioavailability, and means to improve the bioavailability of BBR.

Method of data collection

A methodical collection of scientific literature, reports, experiments, case studies, and examination of work reported was performed with the help of data available from various sources, using several electronic literature databases such as Google Scholar, PubMed, Medline and Science direct databases. The information was searched up to April 2020. The search phrases used included: physicochemical, phytochemical and pharmacological properties, pharmacokinetics, metabolism, preclinical & clinical studies, bioavailability, strategies reported for bioavailability enhancement of berberine, and preparations containing berberine.

Selection criteria

The data collected was further sorted on the basis of specific principles: articles based on the pharmacological screening of berberine for various activities; articles based on preclinical and clinical studies written with emphasis on the dose requirement of berberine and the bioavailability issues thereof; articles on problems of bioavailability of berberine; and papers on pharmacokinetics, tissue distribution, metabolism, and half-life were all included in the study. This review elaborates the varied strategies that were undertaken till date, with the objective to improve the bioavailability of berberine thereby enhancing its efficacy.

Preclinical studies

Preclinical case studies have reported that BBR is safe at higher doses but exhibits poor bioavailability. Deng et al., in their study, demonstrated that BBR was rapidly absorbed but eliminated very slowly in rat bodies after oral administration of

combinations of *Coptis* (*Coptidis rhizoma*) and *Evodia* (*Evodiae fructus*) (1.086 g/kg). The maximum plasma drug concentration achieved was 121.1 ± 11.9 ng/ml, appearing at 90min of the study (Deng et al., 2008). In another study, BBR showed the maximum plasma concentration of 2.31 μ g/ml at 0.5h with slow elimination (5h) from rat bodies after administration of the Xiexin-Tang decoction at a dose of 20ml/kg (Yi, Jian-Ping, Xu, & Lixin, 2006). The pharmacokinetics of BBR (200 mg/kg) and lysergol (20 mg/kg) in plasma after oral administration in rats was compared and reported by Patil et al. (2012). The findings of this study indicated that the pharmacokinetic profile of lysergol (C_{max} -316.54 \pm 26.83 ng/ml, T_{max} -2.25h, $t_{1/2}$ -21.3 \pm 1.75h) was higher than BBR (C_{max} -112.30 \pm 12.07 ng/ml, T_{max} -2.5h, $t_{1/2}$ -5.23 \pm 0.41h). However, the oral bioavailability of BBR was enhanced on concomitant administration with lysergol. Following oral administration of 90 mg/kg/d of BBR to rats, improved lipid-lowering efficacy (46.2%) was observed in comparison to BBR monotherapy (26.8%) (Kong et al., 2008).

A study provided the first preclinical evidence of effect of BBR loaded into chitosan nanoparticle (NP), and their surface modification induced neurodegenerative changes and hepatotoxicity in rats. BBR-NPs formulation (4 mg/kg, intraperitoneal, i.p.) was administered for 14 days, and on the 15th-day lipopolysaccharide (LPS), BBR- NPs showed significant implication on the neuroprotective and hepatoprotective effects (Soudi et al., 2019). Another study demonstrated the pharmacokinetic parameters of BBR, following intragastric administration at a dose of 25 mg/kg in normal and diseased rats (post inflammatory irritable bowel syndrome). The findings showed that the C_{max} in the diseased animal group (18.53 \pm 0.61 ng/ml at 15 min), when compared to the normal control group (16.74 \pm 4.47 ng/ml at 15 min) was increased significantly while CL/F was decreased (Gong et al., 2014a).

The mean plasma concentration vs. time profile after intragastric (i.g.) administration of *Rhizoma coptidis* extract (96 mg/kg) containing 22 mg/kg berberine was also studied. It was observed that BBR was absorbed quickly in the body within 15 min of the study in both the normal control and the diseased groups (post inflammatory irritable bowel syndrome). It was noteworthy that the plasma drug concentration of BBR remarkably increased in diseased model group (39.2 \pm 7.9 ng/ml at 15 min) compared to the normal control group (20.0 \pm 12.1 ng/ml at 15 min). However, compared to the normal control group (198.6 \pm 75.4 L/h/kg), the diseased model group (124.3 \pm 27.4 L/h/kg) demonstrated slower elimination of BBR (Gong et al., 2014a). The pharmacokinetics of BBR following oral administration (20 mg/kg) to normal and Type-2 diabetes mellitus (T2DM)-induced rats (model group) exhibited increase in C_{max} and T_{max} in T2DM group (34.41 \pm 4.25 μ g/ml at 2.24h) when compared to the normal group (17.35 \pm 3.24 μ g/ml at 2.04h) (Jia, Xu and Xu, 2017).

Clinical studies

A clinical study, carried out in 50 patients with hypercholesterolemia on short-term administration of oral nutraceutical combination (NC) consisting of 500 mg BBR, 200 mg red yeast rice, and 10 mg policosanols daily for 6 weeks, decreased

Table 1. Uses of Berberine containing species.

Biological name	Berberine content (%)	Activity	Reference
<i>Berberis aristata</i>	Root - 4%	Antimicrobial activity Anti-osteoporotic activity Antidiarrheal activity Antihyperglycemic activity Cytotoxic activity	Singh, Srivastava and Rawat, 2007; Yogesh et al., 2011; Joshi, Shirkhedkar, Prakash, & Maheshwari, 2011; Semwal, Gupta, Singh, Kumar, & Giri, 2009; Das, Das, Mazumder, Das and Basu, 2009
<i>Berberis asiatica</i>	Root - 2.09% Steam- 1.29%	Antimicrobial activity Antibacterial activity Anti-diabetic activity Anticancer activity	Bhandari, Nath, Ray, & Tewari, 2000; Singh, Vishnoi, Dhingra, & Kishor, 2012; Singh, & Jain, 2010
<i>B. chitria</i> Buch-Ham. ex. Lindl	5.0 - 4.2%	Antimicrobial activity Wound healing activity	Eto, Inoue, & Kadowaki, 2012; Biswas & Mukherjee, 2003
<i>B. lycium</i> Royle	2.3%	Antimicrobial activity Antihyperglycemic activity Anti-diabetic activity Wound healing activity	Hussain, Khan, Habib, & Hussain, 2011; Jigneshkumar, 2011; Gulfraz, 2008; Pirbalouti, Azizi, Koohpayeh, & Hamed, 2010
<i>B. vulgaris</i> L.	5%	Antibacterial activity Antioxidant activity Hepatoprotective activity Antimicrobial activity	Villinski et al., 2003; Tomosaka et al., 2008; Agarwal, Srivastava, Saxena, & Kumar, 2006; Owokotomo & Owoeye, 2011
<i>Coscinium fenestratum</i> (Goetgh.) Colebr.	Stem 3.5%	Antidiabetic activity Antibacterial effect Antihyperglycemic activity	Shirwaikar, Rajendran and I. S.R. Punitha, 2005a; Nair, Narasimhan, Shiburaj, & Abraham, 2005; Shirwaikar, Rajendran and I. S.R. Punitha, 2005b.
<i>Mahonia napaulensis</i> DC.	Root 0.5%	Antifungal activity Anti-inflammatory activity	Bajpai and Vankar, 2007; Andreicut et al., 2018
<i>Thalictrum foliolosum</i> DC.	Rhizome 0.35%	Anti-gastric ulcer activity Antiplasmodial activity	Malairajan, Gopalakrishnan, Narasimhan, & Veni, 2008; Das, Rabha, Talukdar, Goswami, & Dhiman, 2016;
<i>Berberis aquifolium</i>	Rhizome 8-9%	Antimicrobial activity Antiradical and antioxidant	Cernakova and Košťálová, 2002; Rackova, Majekova, Kost, & Stefek, 2004
<i>Berberis thunbergii</i>	Rhizome 8-9%	Antioxidant and Anti-Inflamantory activity	Zhang, Schutzki and Nair, 2013
<i>Coptis teeta</i>	Rhizome 8-9%	Antibacterial activity Inhibitors of topoisomerase	Kong et al., 2009; Kobayashi et al., 1995
<i>B.lyceum</i>	Steam - 4%	Antimicrobial activity	Ali, Uddin and Jalal, 2015
<i>Palmatine</i>	0.30%	Antifungal activity Inhibition of tyrosine hydroxylase	Li et al., 2015; Lee, Zhang and Kim, 1996
<i>Goldenseal</i>	0.5 - 6%	Antibacterial activity Inhibits human CYP3A activity Human cytochrome p450 inhibition	Ettefagh, Burns, Junio, Kaatz, & Cech, 2011; Gurley et al., 2008; Chatterjee and Franklin, 2003,
<i>Goldthread</i>	8-12%	Hair growth-promoting activity Inhibit prostate cancer cell proliferation and NF-Kbsignaling	Zhao, Collier, Huang, & Whelan, 2014

the atherogenic profile and lipid levels in the hypercholesterolemic patients (Affuso, Ruvolo, Micillo, Saccà, & Fazio, 2010). Another study showed that 40 hyperlipidemic patients on administration of BBR alone (500 mg/day) against BBR (500mg/day) combined with 10 mg policosanol and 3 mg/day red yeast extract for 4 weeks exhibited decreased TG (triglyceride) and LDL-C (low density lipoprotein cholesterol) in the combination group by 26% and 25% respectively when compared to BBR alone (22% and 20% respectively) (Cicero, Rovati and Setnikar, 2007). Another clinical study in 97 T2DM patients (type-2 diabetes mellitus) suggested the insulin receptor (InsR)-up-regulating and glucose-lowering activities of BBR (1g/d for 2 months). In these patients, the FBG (fasting blood glucose), HbA1c (Hemoglobin A1c), and TG (triglyceride) levels were significantly reduced by 25.9%, 18.1%, and 17.6%, respectively, as compared to their levels prior to the treatment. In patients affected with chronic hepatitis B and C, the FBG and TG levels were significantly lowered after treatment with berberine (Zhang et al., 2010). In another study, which observed the effect of either placebo or a proprietary nutraceutical combination consisting of BBR, policosanol, and red yeast rice in 64 patients with metabolic syndrome after 18 weeks of treatment, a significant reduction in the homeostasis model assessment of insulin resistance (HOMA-IR) index and low density lipoprotein-cholesterol (LDL-C) in the nutraceutical combination group compared with placebo was observed (HOMA: -0.6 ± 1.2 vs 0.4 ± 1.9 ; $p < 0.05$ and LDL-C: -0.82 ± 0.68 vs -0.13 ± 0.55 mmol/L; $p < 0.0001$). In addition, significant reduction in blood

glucose and insulin levels and increase in endothelial-dependent FMD (flow mediated vasodilation) (1.9 ± 4.2 ; $p < 0.05$) were also observed (Affuso et al., 2012). A trial carried out on women affected by polycystic ovary syndrome showed that, in the treatment with BBR when compared to metformin treatment, similar decrease in waist circumference and waist-to-hip ratio ($p < 0.01$), FPG (fasting plasma glucose) and FPI (fasting plasma insulin), insulin area under the curve, and HOMA-IR ($p < 0.05$) were recorded (Wei et al., 2012). Table 2 shows the comparative plasma and tissue levels of berberine in animals and humans through different routes of administration.

Challenges in the bioavailability of berberine

The bioavailability of any agent within the body is foreshortened owing to its short inherent activity, poor absorption, elevated rate of metabolism, the formation of metabolic products, and/or the quick elimination and clearance from the body. Studies to date have suggested the utility of BBR as a therapeutic agent for the treatment of various ailments. However, several previous studies related to the absorption, distribution, metabolism, and excretion of BBR indicate poor absorption with rapid metabolism of BBR that significantly affects its bioavailability. Studies of BBR in rats have reported low oral bioavailability of $< 1\%$ (0.68% and 0.36%) (Chen et al., 2011; Liu et al., 2010) due to extensive intestinal first-pass elimination, interaction with P-glycoprotein (Pg-P) efflux pumps, and the high distribution in the liver. In this section, problems of BBR bioavailability such as low plasma levels, limited tissue distribution, apparent rapid metabolism, and short half-life are described in detail.

Table 2. Plasma and Tissue levels of berberine in animals and human through different routes of administration.

Species	Route	Dose	Plasma/Tissue	Time	Conc. level	Ref.
Rat	Intragastric	96 mg/kg	Plasma	15 min	20.04 ± 12.14 ng/mL	Gong et al., 2014b
Rat	Intravenous	3 mg/kg	Hippocampus	3.6 h	272 ± 12 ng/g	Wang et al., 2005b
Rat	Oral	200 mg/kg	Tissue	1.33 h	25.85 ± 7.34 μ g/mL	Tan et al., 2013
			Liver	8 h	68.19 ng/g	
			Kidney	12 h	13.92 ng/g	
			Lung	4 h	11 ng/g	
			Muscle	12 h	5 ng/g	
			Brain	12 h	8 ng/g	
			Heart	24 h	9.5 ng/g	
			Pancreas	2 h	9.8 ng/g	
			Fat	2 h	10 ng/g	
Rat	Oral	4 mg/kg	Plasma	0.083 h	1205.3 ± 270.9 ng/mL	Liu, et al., Hao, Xie, Lv, Liu, & Wang, 2009
Rat	Oral	200 mg/kg	Plasma	2.5 h	112.30 ± 12.07 ng/mL	Wang et al., 2005a
Human	Oral	400 mg	Plasma	9.8 ± 6.6 h	0.4356 ± 0.2792 ng/mL	Inbaraj, kukielczak, Bilski, Sandvik, & Chignell, 2001
Mice	Intravenous	2.5 mg	Plasma	0.083 h	0.712 μ g/mL	Wang et al., 2011
Rabbits	Intragastric	50 mg/kg	Plasma	1.09 ± 0.37 h	129.49 ± 24.54 ng/mL	Hu et al., 2013
Rat	Intragastric	25 mg/kg	Plasma	15.0 min	18.53 ± 0.61 ng/mL	Yu et al., 2017

Plasma concentration

One of the major problems associated with BBR is its extremely low plasma levels. The low plasma concentration of BBR is mainly related to the following pharmacokinetic causes: 1. extensive metabolism in the gut and/or liver, 2. marked excretion to intestinal lumen, bile, and urine, as well as enterohepatic circulation, 3. poor absorption, 4. predominant tissue distribution.

When BBR was given orally at a dose of 20 mg/kg to rats, a maximum plasma concentration of 2.31 µg/mL was observed at 0.5 h of the study and high concentration until 5 h; BBR was slowly eliminated from the rat bodies. Following intravenous administration of 3 mg/kg of BBR to rats, the concentration of BBR in plasma and hippocampus was found to be 38.5 ng/mL at 4 h and 30.7 ng/mL at 48 h, respectively, with fast elimination (1.13 h) from the body (Wang et al., 2005). The elimination phase of BBR in the liver was significantly slower than that in blood. When BBR at a dose of 20 mg/kg was administered via femoral vein by i.v. bolus injection, it was detected in the liver up to 80 min post administration. BBR in bile was detected for up to 6 h; the disposition of BBR in bile is higher as compared to that of the liver and blood (Tsai & Tsai, 2004).

Tissue distribution

Uptake and distribution of BBR in body tissues is very important for its biological activity, yet only a limited number of studies have been addressed this issue. Although BBR is present at a very low level in blood and its bioavailability was reported to be less than 1%, the pharmacological effect of BBR can be correlated with its high tissue distribution. BBR at a dose of 200 mg/kg via oral route showed a maximum amount in the liver (68.19 ng/g) 8h after dosing. A maximum concentration of BBR was observed at 24 h in the heart; 12 h in the kidneys, muscles, and brain; 4h in the lungs; and 2 h in the pancreas (Tan et al., 2013). BBR can easily penetrate the blood-brain barrier, with rapid accumulation in the hippocampus region after intravenous administration, followed by slow elimination (Tsai & Tsai, 2004). Tissue distribution of BBR in rats after oral administration of 6 g/kg for 1 week was determined by a HPLC method. Repeated administration of BBR dose increased its concentration in the heart, liver, and kidneys, with lower concentration in the spleen and lungs (Xiao et al., 2018). When BBR and 8-cetylberberine (8-BBR-C16) was given orally at a dose of 80 mg/kg to rats, the plasma concentration increased 2.8 times. Tissue distribution was determined by RP-HPLC; a maximum concentration (3731.82 ng/g) was found in the lungs (Hu, Chen, Zou, Li, & Ye, 2014).

Metabolites

Numerous studies have assessed the metabolism of berberine in rats and in humans. Once absorbed, BBR is subjected to conjugations like sulfation and glucuronidation at various tissue sites. BBR was reported to undergo extensive metabolism when administered orally to rats. The liver was indicated as the major organ responsible for the metabolism of BBR. Following oral administration of BBR to rats (100 mg/kg) and humans (300 mg/kg), the urinary metabolites analyzed indicated that BBR undergoes similar bio-transformations in both rats and humans. Nine metabolites were isolated, demethyleneberberine-2-sulfate (HM1 and HM3), jatrorrhizine-3-O-sulfate (HM5), thalifendine

(RM5), jatrorrhizine-3-O-β-D-glucuronide (HM2), thalifendine-10-O-β-D-glucuronide (HM3), berberrubine-9-O-β-D-glucuronide (HM4 and HM2), 3,10-demethylpalmatine-10-O-sulfate (HM6 and RM4), columbamin-2-O-β-D-glucuronide (HM7), and demethyleneberberine-2,3-di-O-β-D-glucuronide (RM1), by HPLC (Qiu et al., 2008). After the oral administration of BBR (40 mg/kg), the rat liver tissues and bile samples collected and evaluated showed the presence of four main metabolites (berberrubine, thalifendine, demethyleneberberine, and jatrorrhizine), detected in liver after 0.5 h and in bile 1h after the study (Wang, Feng, Chai, Cao, & Qiu, 2017). Liquid chromatography coupled to ion trap time-of-flight mass spectrometry (LC/MS-IT-TOF) was used for the identification of major metabolites of BBR, thalifendine (M1), berberrubine (M2), and jatrorrhizine (M4), in the liver and kidney, respectively. The level of AUC (area under the concentration-time curve) for metabolites of BBR in the liver was 40 times higher and in kidney seven times higher than that in plasma (Tan et al., 2013). The LC/MS analysis of the plasma samples of BBR identified berberrubine, demethyleneberberine, and their glucuronide analogous as the important metabolites seen after oral administration (4 mg/kg, berberine) to rats (Liu et al., 2009). After oral administration of BBR (200 mg/kg) to rats, a total of 16 berberine related metabolites including 10 phase-I metabolites and six phase-II metabolites were identified and clarified by LC-IT-TOF/MS system (Ma et al., 2013). Figure 2 represents the *in vivo* phase I metabolites of berberine.

Half-life

The systemic elimination or clearance of BBR from the body is also an important factor which determines its relative biological activity. With the lower dose of BBR (3 mg/kg) administered intravenously to rats, the elimination half-life in thalamus was found to be 14.6 h, which indicates that BBR quickly distributes itself in the thalamus and can pass through the blood-brain barrier (Wang et al., 2005). The kinetic characteristics of BBR are different in the hippocampus and plasma. In the *in vivo* study, after 3 mg/kg i.v. doses were given to rats, BBR was eliminated from plasma in 1.13 h and from the hippocampus in 12 h (Wang et al., 2005). Another study reported that, with the higher dose of BBR (150 mg/kg) by oral gavage in groups i.e. G1 (untreated), G2 (Biofield treated berberine), and G3 (Biofieldtreated animals who received biofielduntreated berberine) groups, plasma clearance of BBR decreased to 81% (G2) and 50% (G3) as compared to the control group (Inbaraj, Kukielczak, Bilski, Sandvik, & Chignell, 2001). After oral administration of BBR at a dose of 200 mg/kg in rats, 83% of BBR was excreted mainly as thalifendine from bile (24 h) and as thalifendine and berberrubine (78%) on urinary excretion (48 h) (Ma et al., 2013).

Solutions to improve the bioavailability of berberine

The low oral bioavailability of berberine is one of the prime hurdles for market approval of BBR. The absorption, biodistribution, metabolism, and elimination studies of BBR have unfortunately shown poor absorption, rapid metabolism, and elimination of BBR as major reasons for its poor bioavailability. One of the approaches to overcome the low gastrointestinal absorption due to extensive intestinal first-pass effect resulting in low plasma levels of BBR involves effective modulation of the P-gp mediated efflux of BBR. Studies have focused on

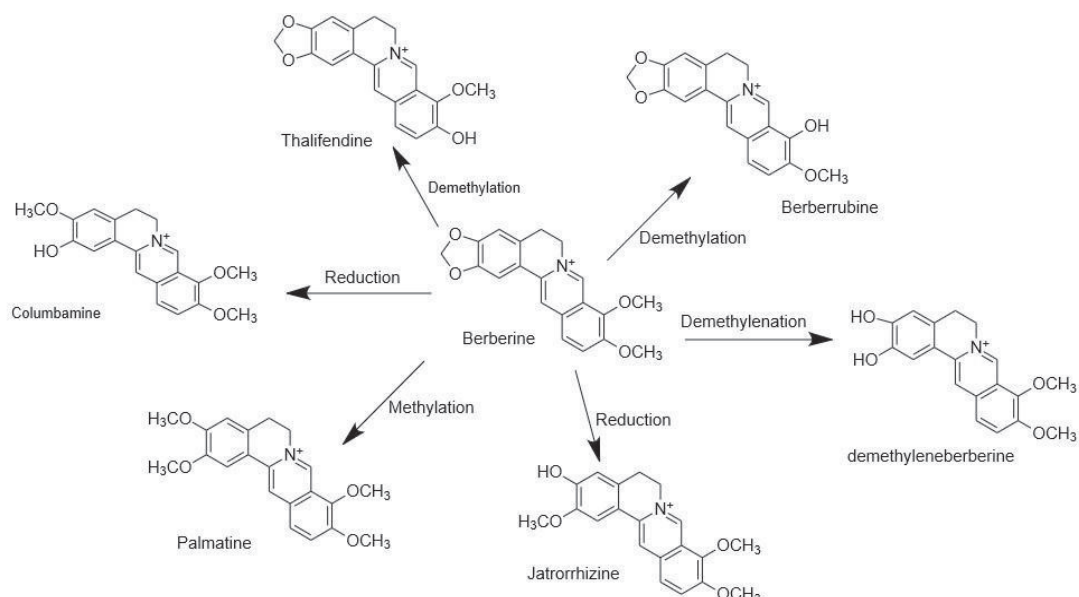


Figure 2. Phase -1 metabolites of berberine *in vivo*.

the effective utilization of pharmaceutical excipients that have P-gp inhibitory effects. Several novel dosage forms like nano-sized dosage forms, liposomes, micelles, and phospholipid complexes are optimistic formulations which overcome the problems of BBR by imparting longer circulation, better permeability, and resistance to metabolic processes (Chen et al., 2011). The strategies to improve the bioavailability of BBR are summarized in Table 3.

Nano-sized dosage forms

Presently, nano-sized technology is an important solution for bioavailability enhancement of therapeutic agents. BBR has been incorporated in nanoparticle-based delivery systems to circumvent the pitfalls of its poor bioavailability. The synthesis, physicochemical characterization, and antimicrobial activity of nanoparticles of BBR with sizes less than 110 nm has been reported. Antimicrobial activity of berberine nanoparticles prepared by evaporative precipitation of nanosuspension (EPN) and anti-solvent precipitation with a syringe pump (APSP) method have shown two-to-four-fold increase in activity against gram-negative bacteria (Sahibzada et al., 2018). Berberine-loaded solid lipid nanoparticles (BBR-SLNs) for topical application were developed and characterized as having a 76.8 nm particle size. Single doses of BBR-SLNs (50 mg/kg) compared to BBR alone showed substantial enhancement in the peak plasma concentration, area under the curve, and mean residence time after oral administration to rats. BBR-SLNs at a high dose (100 mg/kg) showed more significant effect when compared to an equivalent dose of BBR (Xue et al., 2013). Polymer-lipid hybrid nanoparticles (PEG-lipid-PLGA NPs) loaded with BBR phospholipid complex and BBR-soybean phosphatidylcholine complex (BBR-SPC) enhanced the oral BBR efficiency and can be used to enhance the liposolubility of BBR and improve the affinity with the biodegradable polymer in order to increase the drug-loading capacity and controlled/sustained release. The PEG-lipid-PLGA NPs/BBR-SPC enhanced the oral relative bioavailability (approximately 343%) when compared with the free BBR suspension group after administration at a dose of 50 mg/

kg via intragastric gavage in rats (Yu et al., 2017). The selenium-coated nanostructured lipid carriers (SeNLCs), 160 nm in particle size, were formulated, which enhanced the oral bioavailability with an entrapment efficacy (EE) of 90% of BBR. An *in vivo* study in rats (50 mg/kg, BB-SeNLCs) by oral route demonstrated enhanced oral bioavailability (approximately 6.63 times) when compared to a BBR solution. The plasma concentration of BBR was quantified by ultra-performance liquid chromatography-quadrupole time-of-flight mass spectrometry (UPLC-QTOF/MS) (Yin, Hou, Yin, & Song, 2017). Development of novel nanosystems shelled with heparin for BBR delivery increased the suppressive effect of BBR on *H. pylori* growth while efficiently reducing the cytotoxic effects in *H. pylori*-infected cells. In this research, the nanosystem was prepared by the simple ionic gelation method (Chang et al., 2011).

Nanocrystals dosage form

Nanocrystals are a major alternative for enhancing the poor oral bioavailability of water-soluble drugs as compared to other nanocarrier drug delivery systems. Formation of nanocrystals enhances the solubility and dissolution rate of poorly soluble drugs (Liu, Tu, Cheng, Feng, & Jin, 2020). Semi-crystalline nanoparticles (NPs) prepared by evaporative precipitation of nanosuspension (EPN) and anti-solvent precipitation with a syringe pump (APSP) were prepared to overcome the poor solubility of BBR and improve the dissolution rate and bioavailability of BBR. NPs prepared by the EPN method showed better results than those prepared by the APSP method in terms of solubility and dissolution rate (Sahibzada et al., 2018). Another study showed improved oral bioavailability using Brij-S20 (BS20)-modified nanocrystal formulation (BBR-BS20-NCs). A significant improvement in the maximum concentration (C_{max}) and area under the curve (AUC_{0-t}) in the pharmacokinetic studies were observed (Xiong et al., 2018).

Liposomes, micelles, and phospholipid complexes

Liposome is an excellent drug delivery system as it can be used to incorporate both hydrophilic and hydrophobic mol-

Table 3. Formulation development strategies for bioavailability enhancement of berberine.

Type of dosage form	Methodology used	Improved PK/Bioavailability parameters	Reference
Nano sized dosage form	Berberine loaded solid lipid nanoparticles (BBR-SLNs)	Substantial enhancement in the peak plasma concentration, area under the curve, and mean residence time.	Xue et al., 2013
	Polymer-lipid hybrid nanoparticles loaded with BBR phospholipid complex (PEG-lipid-PLGA NPs/BBR-SPC)	Enhanced the oral relative bioavailability	Yu et al., 2017
	Selenium-coated nanostructured lipid carriers (SeNLCs)	Enhanced the oral bioavailability with an entrapment efficacy (EE) of 90%.	Yin, Hou, Yin, & Song, 2017
Nanocrystals dosage form	Berberine -Brij-S20 -modified nanocrystal formulation (BBR-BS20-NCs)	Significant improvement in the maximum concentration (C_{max}) and area under the curve (AUC_{0-t})	Xiong et al., 2018
Liposomes	Berberine-loaded solid proliposomes	Higher blood plasma concentration (227.08 $\mu\text{g/ml}$). <i>In vitro</i> drug release study indicated sustained release of berberine-proliposomes.	Jia et al., 2019
	Chitosan-coated nano-liposome	<i>In vitro</i> study showed improved stability and delayed BH release in the simulated gastrointestinal (GI) environment	Nguyen et al., 2014
Micelles	Berberine loaded anhydrous reverse micelle (ARMs) formulation	Significantly increased plasma level of active BBR in rats	Wang et al., 2011
	Berberine-mixed 1,2-distearoyl-sn-glycero-3-phosphoethanolamine-N-[methoxy(polyethyleneglycol)-2000] (PEG-PE) and d- α -tocopheryl polyethylene glycol 1000 succinate (TPGS) micelle system (mMic)	Intestinal absorption enhancement effect of approximately 3-5 fold (maximum plasma concentration of 1.22 mg/kg)	Shen, Kim, Yao, & El-bayoumi, 2016
Microemulsion	Berberine-loaded microemulsion formulation	Improved the bioavailability 6.47 times greater than that of the berberine tablet	Gui et al., 2008
	Berberine hydrochloric nanometer microemulsion	Improved the efficiency of antibacterial activity	Wu, Zhu, & Zhu, 2009
	Self-microemulsifying drug delivery system (SMEDDS)	<i>In vitro</i> study showed that the release of BBR from SMEDDS was faster (5h) than the commercial tablet. In the <i>in vivo</i> study plasma concentration was 163.4% higher than the commercial tablet.	Zhu et al., 2013
	Cremonophore- integrated chylomicron "cremochylomicrons" loaded with berberine	Inhibited the BBR absorption (43%) and confirmed the lymphatic targeting ability of cremochylomicrons.	Elsheikh, Elnaggar, Hamdy, & Abdallah, 2018
	Berberine-loaded chylomicron	10.5-fold enhancement in intestinal permeability over free berberine	Godugu, Patel, Dodapaneni, Somagani, & Singh, 2014

Table 3. Continue.

Type of dosage form	Methodology used	Improved PK/Bioavailability parameters	Reference
Mucoadhesive Microparticle	Novel duodenum-specific drug delivery system for duodenal application, based on thiolated chitosan and hydroxypropyl methylcellulose acetate maleate (HPMCAM)	90% of the drug released within 6h	Liu et al., 2011
	Mucoadhesive microparticle formulation prepared using the dual channel spray gun technology	Increased plasma concentration by 6.98 folds and decreased the tumor volume by 49.8-53.4% when compared to untreated control groups	Godugu, Patel, Dodapaneni, Somagani, & Singh, 2014
Adjuvant	Nanosystem-based adjuvants with Baicalin or berberine loaded ultra-deformable vesicles	<i>In vitro</i> study showed antioxidant effect (baicalin vesicle) and photoprotective effects (berberine vesicle)	Mir-Palomo et al., 2019
	<i>Coptidis rhizome</i> and berberine	<i>In vitro</i> study, showed correlation of <i>Coptidis rhizome</i> and berberine with the ECC line which decreased the S phase and accumulation of cells in the G0/G1 phase in esophageal cancer.	Iizuka et al., 2000
	BBR and <i>palmatine</i>	<i>In vitro</i> study showed that a combination of BBR and <i>palmatine</i> inhibits the acetylcholinesterases using the recombinant human acetylcholinesterases.	Mak et al., 2014

ecules. Polymerized, microencapsulated, and polymer-coated liposome systems have been employed to increase the potential of oral drug delivery. A recent study reported the preparation of BBR-loaded solid proliposomes using water as the solution enhanced dispersion by using supercritical CO₂ (SEDS) with an 80 nm size and high entrapment efficacy of 90.3% of BBR. *In vivo* study results indicated that the oral bioavailability of BBR-proliposomes was significantly improved following oral administration of a 150 mg/kg dose to rats. It was observed that the BBR-proliposomes resulted in higher blood plasma concentration (227.08 µg/mL) than that of the plain BBR (23.50 µg/mL). The *in vitro* drug release study indicated sustained release of BBR-proliposomes (Jia et al., 2019). *In vitro* and *in vivo* study for the chitosan-coated nano-liposome for the oral delivery of berberine hydrochloride (BH) carried out in rabbits demonstrated a marked improvement in the pharmacokinetic parameters after oral administration when compared to the uncoated nano-liposome. Also, the *in vitro* study showed improved stability and delayed BH release in the simulated gastrointestinal (GI) environment (Nguyen et al., 2014). 3²-full factorial design was employed for the preparation of liposome. It was observed that the formulated liposome system increased the lipid concentration with the highest entrapment efficiency (78.43%). By increasing the plasma concentration levels and lowering the kinetics of elimination, micelles and phospholipid complexes are reported to enhance the gastrointestinal absorption of natural drugs thereby improving their bioavailability (Sailor, Seth, Parmar, Chauhan, & Javia,

2015). A significant improvement in BBR bioavailability was reported due to berberine-loaded anhydrous reverse micelle (ARMs) formulation. In this study, BBR (100 mg/kg) was administered orally to diabetic rats, and berberine anhydrous reverse micelle (ARM) exhibited a maximum plasma concentration of 0.628 µg/mL at 4 h after oral administration as compared to that of berberine solution (a maximum plasma concentration of 0.298 µg/mL at 2 h after oral dosing). About a 2.4-fold increase in oral bioavailability of berberine from the BBR-loaded ARMs in rats was observed over the free BBR. The results of the study indicated that the BBR-loaded ARMs can significantly increase the plasma level of active BBR in rats (Wang et al., 2011). The *in vitro* and *in vivo* anticancer activity of polymeric phospholipid micelles containing BBR was studied. In the *in vitro* study, faster release of berberine-mixed 1,2-distearoyl-sn-glycero-3-phosphoethanolamine-N-[methoxy(polyethyleneglycol)-2000] (PEG-PE) mixed with D-α-tocopheryl polyethylene glycol 1000 succinate (TPGS) was observed (61% berberine release after 24 h). In the *in vivo* part of this study, the effect of berberine-mixed 1,2-distearoyl-sn-glycero-3-phosphoethanolamine-N-[methoxy (polyethyleneglycol)-2000] (PEG-PE) and d-α-tocopheryl polyethylene glycol 1000 succinate (TPGS) micelle system (mMic) was evaluated in comparison to free berberine; enhancement of the intestinal absorption of approximately 3-to-5-fold (maximum plasma concentration of 1.22 mg/kg) was observed after a 300 mg/kg oral dose (Shen, Kim, Yao, & Elbayoumi, 2016).

Microemulsion

As a potentially excellent vehicle candidate, microemulsions can increase the solubility of bioactive materials and can also improve the absorption through human gut membrane because of their extremely low surface tension. Drugs can directly contact the GI epithelium cell; consequently, the bioavailability can be significantly improved (Swenson & Curatolo, 1992; O'Driscoll, 2002). Gui et al. have prepared and evaluated the oral microemulsion formulation of BBR (24.0 nm size) which was found to be stable at room temperature. An *in vivo* study with male Sprague-Dawley rats (50 mg/kg oral dose) demonstrated improved bioavailability of the oral berberine-loaded microemulsion formulation, which was 6.47 times greater than that of the berberine tablet suspension at 7.3 h of the study (Gui et al., 2008). Berberine hydrochloric microemulsion for antibacterial activity was developed and characterized by Sun and Ouyang (2007). The formulated microemulsion (56.8 nm size) was found to be stable under high temperatures and strong light conditions and gave a prolonged *in vitro* release of berberine. The *in vivo* study in rats resulted in improved antibacterial activity employing the microemulsion when compared to the other dosage forms. Zhu et al. developed self-microemulsifying drug delivery system (SMEDDS) to improve the oral bioavailability of BH. The *in vitro* study indicated faster release of BBR from SMEDDS (5h) as compared to the commercial tablet formulation, with improved stability. In the *in vivo* study in rats, the effect of SMEDDS was evaluated in comparison to commercial tablet formulation; the plasma concentration was found to be 163.4% higher than the commercial tablet following the administration of a 25 mg/kg oral dose (Zhu et al., 2013). A previous study demonstrated that the cremophore-integrated chylomicron, "cremochylomicrons," loaded with BBR inhibited the BBR absorption (43%) and confirmed the lymphatic targeting ability of the cremochylomicrons. In the *in vivo* part of this study, the effect of the formulated cremochylomicron was evaluated in comparison to free BBR in rat model. The comparison of the effect of cremochylomicron with free BBR gave a significant enhancement (>2 fold) in rate and extent of absorption of BBR (Elsheikh, Elnaggar, Hamdy, & Abdallah, 2018). Another study showed that the berberine-loaded chylomicron increased the intracellular fluorescence 2-fold, using confocal microscopy analysis with a 10.5-fold enhancement in intestinal permeability over free BBR. Therefore, berberine-loaded chylomicron is considered as an attractive bioactive-nanocarrier for berberine lymphatic targeting and bioavailability improvement (Godugu, Patel, Doddapaneni, Somagoni, & Singh, 2014).

Mucoadhesive microparticles

Chen et al. developed and optimized a novel mucoadhesive drug delivery system (drug-resin complex core loaded with BHberberine hydrochloride) which influences the gastric retention of berberine (85% at 300 min of the study) (Chen et al., 2008). A novel duodenum-specific drug delivery system for duodenal application, based on thiolated chitosan and hydroxypropyl methylcellulose acetate maleate (HPMC-AM), which is used for the coating of thiolated chitosan microspheres, was also reported. The *in vitro* study showed that 90% of the BBR was released within 6h after transferring into simulated patho-

logical duodenal fluid (SPDF) (Liu et al., 2011). Mucoadhesive microparticle formulation prepared using the dual channel spray gun technology significantly increased the oral bioavailability and anticancer effects of BBR. The *in vivo* study in Sprague Dawley rats demonstrated increased plasma concentration of BBR by 6.98-fold and decreased the tumor volume by 49.8-53.4% when compared to the untreated control group (Godugu et al., 2014).

Adjuvant

SilviaA previous study formulated and characterized nano-system-based adjuvants with baicalin/berberine-loaded ultradeformable vesicles for the treatment of vitiligo. The *in vitro* study showed the antioxidant effect (baicalin vesicle) and photoprotective effects (berberine vesicle) through the stimulation of melanin production and tyrosinase activity in melanocytes (Mir-Palomo et al., 2019). *Coptidis rhizome* and BBR, a known inhibitor of the proliferation of human esophageal cancer cell (ECCs) lines, were administered in human volunteers. The *in vitro* study showed a good correlation of the treatment with *Coptidis rhizome* and BBR on the ECC line, which decreased the S phase and the accumulation of cells in the G0/G1 phase, proving to be useful alternative therapies for oesophageal cancer (Iizuka et al., 2000). BBR and palmatine, when used in combination, exhibited synergistic effect. The *in vitro* study showed that the combination of BBR and palmatine inhibits the acetylcholinesterases, using the recombinant human acetylcholinesterases. The drug-reducing index of BBR and palmatine were found to be 2.98 and 2.66, respectively, which might be beneficial in the treatment of patients with Alzheimer disease (Mak et al., 2014). The antimicrobial activity of BBR against Methicillin-resistant *Staphylococcus aureus* (MRSA) (90%), the synergistic effect between BBR and oxacillin against MRSA, and the additive effect between BBR and ampicillin were observed. BBR (1-50 µg/mL), compared with the vehicle-treated control group, decreased MRSA adhesion and intracellular invasion in human gingival fibroblasts (Yu et al., 2005). Thus, overall, these studies indicated that the activity of BBR can be modulated both at the cellular level and at the organismic level, and we can expect surprising types of regulations when different agents are used simultaneously with BBR.

Derivatives and analogues

The chemical structure of BBR plays a crucial role in its biological activity. For example, isomerization has proved to have a significant influence on the antioxidant activity of BBR. Thus, several researchers are working on the effective structural modification of BBR with the aim to achieve a better biological response. Numerous studies dealing with the improved biological activity of BBR derivatives and/or analogues can be found in the literature. Shan et al., in their study, designed the BBR analogue, designated IMB-Y53, which was reported to display improved glucose-lowering efficacy both in the *in vitro* and *in vivo* studies in comparison to BBR. In this study, the maximum tolerable dose of IMB-Y53 following oral administration to male wistar rats was 200 mg/kg. IMB-Y53 absorption was rapid after oral administration. The maximum plasma concentration of nearly 5.84 ng/ml was detected 2h after the oral

dose. In the *in vitro* study, when IMB-Y53 (40 μ M) was orally administered, in the C2C12 cells, IMB-Y53 up-regulated InsR mRNA by 2.3-fold and protein expression levels by 1.9-fold. IMB-Y53 (20 μ M-40 μ M) stimulated the glucose consumption by 1.5-1.7 fold in the muscle cells. Another strategy to improve the biological activity of BBR involved the synthesis of new 13-diphenylalkyl analogues of BBR. The presence of the diphenylalkyl chain at the 13-position of BBR significantly improved the binding ability to the DNA (Shan et al., 2013). BBR is a novel cholesterol-lowering agent acting through a mechanism different from that of statins; the two methoxyl groups in an ortho-distribution (10- and 11-position) on the benzene ring increased the low-density-lipoprotein receptor (LDLR) up-regulatory activity (Kawanishi et al., 2006). Another group of researchers also designed, synthesized, and evaluated new BBR analogues that can up-regulate the low-density-lipoprotein receptor (LDLR). Accordingly, BBR analogues with the methylene dioxy group at the 2-and 3-position were reported to be the essential requirements for the activity. The *in vivo* study in hyperlipidemic rats (100mg/kg/day) decreased the blood cholesterol by 42.6% and LDL-c by 49.4% (Li et al., 2009). Although many BBR analogues are found to show improved biological activity over BBR, specific evaluation of structural analogues and/or derivatives of BBR demonstrated no significant improvement in the tissue and plasma distribution. However, the promising biological effects of the modified BBR derivatives/ analogues compared to BBR throws light onto the possibility of modulating the bioavailability of BBR through such structural modifications.

CONCLUSIONS

Berberine is a quaternary ammonium salt from the protoberberine group of benzylisoquinoline alkaloids which has been used for centuries as a remedy for many ailments. Extensive scientific research over the past decade has shown the ability of this compound to modulate multiple cellular targets and hence display favorable preventive and therapeutic action for the treatment of a wide variety of diseases. BBR acts on a diverse range of molecular targets like transcription factors, growth factors and their receptors, cytokines, enzymes, and genes regulating cell proliferation and apoptosis, and inflammatory factors. As detailed in this review, tissue levels of BBR, irrespective of the route of administration, exhibited rapid metabolism and elimination, which are the major factors limiting its bioavailability. Effective modulation of the route and the medium of BBR administration, the blocking of metabolic pathways by the concomitant administration with other agents, and structural modifications are the main strategies that are now being explored to improve the bioavailability of BBR. Attempts to enhance the *in vitro* and *in vivo* efficacy of BBR through structural modifications of the molecule and/or new formulations have been recently reported and explored. This review outlines the challenges in the bioavailability improvement of BBR and the various solutions being researched to tackle this issue. Varied novel delivery strategies, including those of nanosized dosage forms, liposomes, and phospholipid complexes, offer significant promise and are worthy of further exploration in attempts to enhance the bioavailability,

medicinal value, and application of this interesting molecule from Mother Nature.

Acknowledgements: The authors would like to thank Dr. D. Y. Patil Institute of Pharmaceutical Sciences and Research, Pune, Maharashtra, India for providing the necessary infrastructural facilities to carry out this work.

Peer-review: Externally peer-reviewed.

Author Contributions: Conception/Design of Study- A.T., S.D.; Data Acquisition- A.T., S.K., S.D., L.K., S.C.; Data Analysis/Interpretation- A.T., S.K., S.D., L.K., S.C.; Drafting Manuscript- A.T., S.K.; Critical Revision of Manuscript- A.T., S.K., S.D., L.K., S.C.; Final Approval and Accountability- A.T., S.K., S.D., L.K., S.C.

Conflict of Interest: The authors have no conflict of interest to declare.

Financial Disclosure: Authors declared no financial support.

REFERENCES

- Affuso, F., Ruvolo, A., Micillo, F., Saccà, L., & Fazio, S. (2010). Effects of a nutraceutical combination (berberine, red yeast rice and policosanols) on lipid levels and endothelial function randomized, double-blind, placebo-controlled study. *Nutrition, Metabolism and Cardiovascular Diseases*, 20(9), 656-661.
- Affuso, F., Mercurio, V., Ruvolo, A., Pirozzi, C., Micillo, F., Carlomagno, G., ... & Fazio, S. (2012). A nutraceutical combination improves insulin sensitivity in patients with metabolic syndrome. *World journal of cardiology*, 4(3), 77.
- Agarwal, M., Srivastava, V. K., Saxena, K. K., & Kumar, A. (2006). Hepatoprotective activity of *Beta vulgaris* against CCl₄-induced hepatic injury in rats. *Fitoterapia*, 77(2), 91-93.
- Ali, H., Uddin, S., & Jalal, S. (2015). Chemistry and biological activities of *Berberis lycium* Royle. *Journal of Biologically Active Products from Nature*, 5(5), 295-312.
- Andreicut, A. D., Parvu, A. E., Moț, A. C., Parvu, M., Fischer-Fodor, E. V. A., Feldrihan, V., ... & Irimie, A. (2018). Anti-inflammatory and antioxidant effects of *Mahonia aquifolium* leaves and bark extracts. *Farmacologia*, 66(1).
- Bajpai, D., & Vankar, P. S. (2007). Antifungal textile dyeing with mahonianapaulensis dc leaves extract based on its antifungal activity. *Fibers and Polymers*, 8(5), 487.
- Battu, S. K., Repka, M. A., Maddineni, S., Chittiboyina, A. G., Avery, M. A., & Majumdar, S. (2010). Physicochemical characterization of berberine chloride: a perspective in the development of a solution dosage form for oral delivery. *Aaps Pharmscitech*, 11(3), 1466-1475.
- Bhandari, D. K., Nath, G., Ray, A. B., & Tewari, P. V. (2000). Antimicrobial activity of crude extracts from *Berberis asiatica* stem bark. *Pharmaceutical Biology*, 38(4), 254-257.
- Biswas, T. K., & Mukherjee, B. (2003). Plant medicines of Indian origin for wound healing activity: a review. *The International Journal of Lower Extremity Wounds*, 2(1), 25-39.
- Čerňáková, M., & Košťálová, D. (2002). Antimicrobial activity of berberine—A constituent of *Mahonia aquifolium*. *Folia Microbiologica*, 47(4), 375-378.
- Chang, C. H., Huang, W. Y., Lai, C. H., Hsu, Y. M., Yao, Y. H., Chen, T. Y., ... & Lin, Y. H. (2011). Development of novel nanoparticles shelled with heparin for berberine delivery to treat *Helicobacter pylori*. *Acta Biomaterialia*, 7(2), 593-603.
- Chatterjee, P., & Franklin, M. R. (2003). Human cytochrome p450 inhibition and metabolic-intermediate complex formation by goldenseal extract and its methylenedioxyphenyl components. *Drug Metabolism and Disposition*, 31(11), 1391-1397.

- Chen, F., Zhang, Y., Liu, Q., Pang, M. Z., Yang, X. G., & Pan, W. S. (2008). Optimization of a novel mucoadhesive drug deliver system with ion-exchange resin core loaded with berberine hydrochloride using central composite design methodology. *Yao xuexue bao=Acta Pharmaceutica Sinica*, 43(9), 963-968.
- Chen, W., Miao, Y. Q., Fan, D. J., Yang, S. S., Lin, X., Meng, L. K., & Tang, X. (2011). Bioavailability study of berberine and the enhancing effects of TPGS on intestinal absorption in rats. *Aaps Pharm-sci-tech*, 12(2), 705-711.
- Cicero, A. F., Rovati, L. C., & Setnikar, I. (2007). Eulipidemic effects of berberine administered alone or in combination with other natural cholesterol-lowering agents. *Arzneimittelforschung*, 57(01), 26-30.
- Das, N. G., Rabha, B., Talukdar, P. K., Goswami, D., & Dhiman, S. (2016). Preliminary in vitro antiplasmodial activity of Aristolochiagriffithii and Thalicttrum foliolosum DC extracts against malaria parasite Plasmodium falciparum. *BMC Research Notes*, 9(1), 51.
- Das, S., Das, M. K., Mazumder, P. M., Das, S., & Basu, S. P. (2009). Cytotoxic activity of methanolic extract of Berberis aristata DC on colon cancer. *Global Journal of Pharmacology*, 3(3), 137-140.
- Deng, Y., Liao, Q., Li, S., Bi, K., Pan, B., & Xie, Z. (2008). Simultaneous determination of berberine, palmatine and jatrorrhizine by liquid chromatography–tandem mass spectrometry in rat plasma and its application in a pharmacokinetic study after oral administration of coptis–evodia herb couple. *Journal of Chromatography B*, 863(2), 195-205.
- Elsheikh, M. A., Elnaggar, Y. S., Hamdy, D. A., & Abdallah, O. Y. (2018). Novel cremochylomicrons for improved oral bioavailability of the antineoplastic phytomedicine berberine chloride: Optimization and pharmacokinetics. *International Journal of Pharmaceutics*, 535(1-2), 316-324.
- Eto, T., Inoue, S., & Kadowaki, T. (2012). Effects of once-daily teneligliptin on 24-h blood glucose control and safety in Japanese patients with type 2 diabetes mellitus: a 4-week, randomized, double-blind, placebo-controlled trial. *Diabetes, Obesity and Metabolism*, 14(11), 1040-1046.
- Ettefagh, K. A., Burns, J. T., Junio, H. A., Kaatz, G. W., & Cech, N. B. (2011). Goldenseal (*Hydrastis canadensis* L.) extracts synergistically enhance the antibacterial activity of berberine via efflux pump inhibition. *Planta Medica*, 77(08), 835-840.
- Godugu, C., Patel, A. R., Doddapaneni, R., Somagoni, J., & Singh, M. (2014). Approaches to improve the oral bioavailability and effects of novel anticancer drugs berberine and betulinic acid. *PLoS one*, 9(3), e89919.
- Gong, Z., Chen, Y., Zhang, R., Wang, Y., Guo, Y., Yang, Q., ... & Zhu, X. (2014a). Pharmacokinetic comparison of berberine in rat plasma after oral administration of berberine hydrochloride in normal and post inflammation irritable bowel syndrome rats. *International journal of molecular sciences*, 15(1), 456-467.
- Gong, Z., Chen, Y., Zhang, R., Wang, Y., Yang, Q., Guo, Y., ... & Wang, Y. (2014). Pharmacokinetics of two alkaloids after oral administration of Rhizoma Coptidis extract in normal rats and irritable bowel syndrome rats. *Evidence-Based Complementary and Alternative Medicine*, 2014.
- Gulfraz, M., Mehmood, S., Ahmad, A., Fatima, N., Praveen, Z., & Williamson, E. M. (2008). Comparison of the antidiabetic activity of Berberis lycium root extract and berberine in alloxan-induced diabetic rats. *Phytotherapy Research*, 22(9), 1208-1212.
- Gui, S. Y., Wu, L., Peng, D. Y., Liu, Q. Y., Yin, B. P., & Shen, J. Z. (2008). Preparation and evaluation of a microemulsion for oral delivery of berberine. *Die Pharmazie-An International Journal of Pharmaceutical Sciences*, 63(7), 516-519.
- Gurley, B. J., Swain, A., Hubbard, M. A., Hartsfield, F., Thaden, J., Williams, D. K., ... & Tong, Y. (2008). Supplementation with goldenseal (*Hydrastis canadensis*), but not kava kava (*Piper methysticum*), inhibits human CYP3A activity in vivo. *Clinical Pharmacology & Therapeutics*, 83(1), 61-69.
- Hu, Y. L., Chen, C., Zou, Z. Y., Li, X. G., & Ye, X. L. (2014). Comparative study of pharmacokinetics and tissue distribution of 8-cetylberberine and berberine in rats. *Acta Pharmaceutica Sinica*, 49(11), 1582.
- Hussain, M. A., Khan, M. Q., Habib, T., & Hussain, N. (2011). Antimicrobial activity of the crude root extract of Berberis lycium Royle. *Advances in Environmental Biology*, 5(4), 585-588.
- Iizuka, N., Miyamoto, K., Okita, K., Tangoku, A., Hayashi, H., Yosino, S., ... & Oka, M. (2000). Inhibitory effect of Coptidis Rhizoma and berberine on the proliferation of human esophageal cancer cell lines. *Cancer Letters*, 148(1), 19-25.
- Inbaraj, J. J., Kukielczak, B. M., Bilski, P., Sandvik, S. L., & Chignell, C. F. (2001). Photochemistry and photocytotoxicity of alkaloids from Goldenseal (*Hydrastis canadensis* L.) 1. Berberine. *Chemical Research in Toxicology*, 14(11), 1529-1534.
- Jia, J., Zhang, K., Zhou, X., Ma, J., Liu, X., Xiang, A., & Ge, F. (2019). Berberine-loaded solid liposomes prepared using solution enhanced dispersion by supercritical CO₂: Sustained release and bioavailability enhancement. *Journal of Drug Delivery Science and Technology*, 51, 356-363.
- Jia, Y., Xu, B., & Xu, J. (2017). Effects of type 2 diabetes mellitus on the pharmacokinetics of berberine in rats. *Pharmaceutical Biology*, 55(1), 510-515.
- Jigneshkumar, P. R. (2011). *Evaluation of the Antihyperglycemic, Cardio protective and Antihyperlipidemic activity of flowers of Sesbania grandiflora (Linn)* (Doctoral dissertation, RGUHS).
- Joshi, P. V., Shirkhedkar, A. A., Prakash, K., & Maheshwari, V. L. (2011). Antidiarrheal activity, chemical and toxicity profile of Berberis aristata. *Pharmaceutical Biology*, 49(1), 94-100.
- Kawanishi, N., Sugimoto, T., Shibata, J., Nakamura, K., Masutani, K., Ikuta, M., & Hirai, H. (2006). Structure-based drug design of a highly potent CDK1, 2, 4, 6 inhibitor with novel macrocyclic quinoxalin-2-one structure. *Bioorganic & Medicinal Chemistry Letters*, 16(19), 5122-5126.
- Kobayashi, Y., Yamashita, Y., Fujii, N., Takaboshi, K., Kawakami, T., Kawamura, M., ... & Nakano, H. (1995). Inhibitors of DNA topoisomerase I and II isolated from the Coptis rhizomes. *Planta Medica*, 61(05), 414-418.
- Kong, W. J., Wei, J., Zuo, Z. Y., Wang, Y. M., Song, D. Q., You, X. F., ... & Jiang, J. D. (2008). Combination of simvastatin with berberine improves the lipid-lowering efficacy. *Metabolism*, 57(8), 1029-1037.
- Kong, W. J., Wei, J., Zuo, Z. Y., Wang, Y. M., Song, D. Q., You, X. F., ... & Jiang, J. D. (2008). Combination of simvastatin with berberine improves the lipid-lowering efficacy. *Metabolism*, 57(8), 1029-1037.
- Kong, W. J., Zhao, Y. L., Xiao, X. H., Wang, J. B., Li, H. B., Li, Z. L., ... & Liu, Y. (2009). Spectrum–effect relationships between ultra performance liquid chromatography fingerprints and anti-bacterial activities of Rhizoma coptidis. *Analytica Chimica Acta*, 634(2), 279-285.
- Lee, H. W., Suh, J. H., Kim, H. N., Kim, A. Y., Park, S. Y., Shin, C. S., ... & Kim, J. B. (2008). Berberine promotes osteoblast differentiation by Runx2 activation with p38 MAPK. *Journal of Bone and Mineral Research*, 23(8), 1227-1237.
- Lee, M. K., Zhang, Y. H., & Kim, H. S. (1996). Inhibition of tyrosine hydroxylase by palmatine. *Archives of Pharmacal Research*, 19(4), 258.
- Li, Y. H., Yang, P., Kong, W. J., Wang, Y. X., Hu, C. Q., Zuo, Z. Y., ... & Du, N. N. (2009). Berberine Analogues as a novel class of the low-density-lipoprotein receptor up-regulators: synthesis, structure–activity relationships, and cholesterol-lowering efficacy. *Journal of Medicinal Chemistry*, 52(2), 492-501.

- Li, Y., Wang, H., Si, N., Ren, W., Han, L., Xin, S., ... & Bian, B. (2015). Metabolic profiling analysis of berberine, palmatine, jatrorrhizine, coptisine and epiberberine in zebrafish by ultra-high performance liquid chromatography coupled with LTQ Orbitrap mass spectrometer. *Xenobiotica*, 45(4), 302-311.
- Liu, Y., Hao, H., Xie, H., Lv, H., Liu, C., & Wang, G. (2009). Oxidative demethylation and subsequent glucuronidation are the major metabolic pathways of berberine in rats. *Journal of Pharmaceutical Sciences*, 98(11), 4391-4401.
- Liu, Y. H., Zhu, X., Zhou, D., Jin, Y., Zhao, C. Y., Zhang, Z. R., & Huang, Y. (2011). pH-sensitive and mucoadhesive microspheres for duodenum-specific drug delivery system. *Drug Development and Industrial Pharmacy*, 37(7), 868-874.
- Liu, Y. T., Hao, H. P., Xie, H. G., Lai, L., Wang, Q., Liu, C. X., & Wang, G. J. (2010). Extensive intestinal first-pass elimination and predominant hepatic distribution of berberine explain its low plasma levels in rats. *Drug Metabolism and Disposition*, 38(10), 1779-1784.
- Liu, J., Tu, L., Cheng, M., Feng, J., & Jin, Y. (2020). Mechanisms for oral absorption enhancement of drugs by nanocrystals. *Journal of Drug Delivery Science and Technology*, 101607.
- Ma, J. Y., Feng, R., Tan, X. S., Ma, C., Shou, J. W., Fu, J., ... & He, W. Y. (2013). Excretion of berberine and its metabolites in oral administration in rats. *Journal of Pharmaceutical Sciences*, 102(11), 4181-4192.
- Mak, S., Luk, W. W., Cui, W., Hu, S., Tsim, K. W., & Han, Y. (2014). Synergistic inhibition on acetylcholinesterase by the combination of berberine and palmatine originally isolated from Chinese medicinal herbs. *Journal of Molecular Neuroscience*, 53(3), 511-516.
- Malairajan, P., Gopalakrishnan, G., Narasimhan, S., & Veni, K. J. K. (2008). Evaluation of anti-ulcer activity of *Polyalthia longifolia* (Sonn.) Thwaites in experimental animals. *Indian Journal of Pharmacology*, 40(3), 126.
- Mir-Palomo, S., N  cher, A., Bus  , M. O. V., Caddeo, C., Manca, M. L., Manconi, M., & Diez-Sales, O. (2019). Baicalin and berberine ultra-deformable vesicles as potential adjuvant in vitiligo therapy. *Colloids and Surfaces B: Biointerfaces*, 175, 654-662.
- Nair, G. M., Narasimhan, S., Shiburaj, S., & Abraham, T. K. (2005). Antibacterial effects of *Coscinium fenestratum*. *Fitoterapia*, 76(6), 585-587.
- Neag, M. A., Mocan, A., Echeverr  , J., Pop, R. M., Bocsan, C. I., Cri  an, G., & Buzoianu, A. D. (2018). Berberine: Botanical occurrence, traditional uses, extraction methods, and relevance in cardiovascular, metabolic, hepatic, and renal disorders. *Frontiers in Pharmacology*, 9, 557.
- Nguyen, T. X., Huang, L., Liu, L., Abdalla, A. M. E., Gauthier, M., & Yang, G. (2014). Chitosan-coated nano-liposomes for the oral delivery of berberine hydrochloride. *Journal of Materials Chemistry B*, 2(41), 7149-7159.
- O'Driscoll, C. M. (2002). Lipid-based formulations for intestinal lymphatic delivery. *European Journal of Pharmaceutical Sciences*, 15(5), 405-415.
- Owokotomo, I. A., & Owwoeye, G. (2011). Proximate analysis and antimicrobial activities of *Bambusa vulgaris* L. leaves' beverage. *African Journal of Agricultural Research*, 6(21), 5030-5032.
- Patil, S., Dash, R. P., Anandjiwala, S., & Nivsarkar, M. (2012). Simultaneous quantification of berberine and lysergol by HPLC-UV: evidence that lysergol enhances the oral bioavailability of berberine in rats. *Biomedical Chromatography*, 26(10), 1170-1175.
- Pirbalouti, A. G., Azizi, S., Koohpayeh, A., & Hamed, B. (2010). Wound healing activity of *Malva sylvestris* and *Punica granatum* in alloxan-induced diabetic rats. *Acta Poloniae Pharmaceutica*, 67(5), 511-516.
- Qiu, F., Zhu, Z., Kang, N., Piao, S., Qin, G., & Yao, X. (2008). Isolation and identification of urinary metabolites of berberine in rats and humans. *Drug Metabolism and Disposition*, 36(11), 2159-2165.
- Rockova, L., Majekova, M., Kost, D., & Stefek, M. (2004). Antiradical and antioxidant activities of alkaloids isolated from *Mahonia aquifolium*. *Structural Aspects Bioorganic & Medicinal Chemistry*, 12, 4709-4715.
- Sahibzada, M. U. K., Sadiq, A., Faidah, H. S., Khurram, M., Amin, M. U., & Haseeb, A. (2018). Berberine nanoparticles with enhanced in vitro bioavailability: characterization and antimicrobial activity. *Drug Design, Development and Therapy*, 12: 303-12.
- Sailor, G., Seth, A. K., Parmar, G., Chauhan, S., & Javia, A. (2015). Formulation and in vitro evaluation of berberine containing liposome optimized by 32 full factorial designs. *Journal of Applied Pharmaceutical Science*, 5(7), 023-028.
- Sarna, L. K., Wu, N., Hwang, S. Y., Siow, Y. L., & O, K. (2010). Berberine inhibits NADPH oxidase mediated superoxide anion production in macrophages. *Canadian Journal of Physiology and Pharmacology*, 88(3), 369-378.
- Semwal, B. C., Gupta, J., Singh, S., Kumar, Y., & Giri, M. (2009). Anti-hyperglycemic activity of root of *Berberis aristata* DC in alloxan-induced diabetic rats. *International Journal of Green Pharmacy (IJGP)*, 3(3).
- Shan, Y. Q., Ren, G., Wang, Y. X., Pang, J., Zhao, Z. Y., Yao, J., ... & Jiang, J. D. (2013). Berberine analogue IMB-Y53 improves glucose-lowering efficacy by averting cellular efflux especially P-glycoprotein efflux. *Metabolism*, 62(3), 446-456.
- Shen, R., Kim, J. J., Yao, M., & Elbayoumi, T. A. (2016). Development and evaluation of vitamin E D- -tocopheryl polyethylene glycol 1000 succinate-mixed polymeric phospholipid micelles of berberine as an anticancer nanopharmaceutical. *International Journal of Nanomedicine*, 11, 1687.
- Shirwaikar, A., Rajendran, K., & Punitha, I. S. R. (2005a). Antidiabetic activity of alcoholic stem extract of *Coscinium fenestratum* in streptozotocin-nicotinamide induced type 2 diabetic rats. *Journal of Ethnopharmacology*, 97(2), 369-374.
- Shirwaikar, A., Rajendran, K., & Punitha, I. S. R. (2005b). Antihyperglycemic Activity of the Aqueous Stem Extract of *Coscinium fenestratum*. in Non-insulin Dependent Diabetic Rats. *Pharmaceutical Biology*, 43(8), 707-712.
- Singh, M., Srivastava, S., & Rawat, A. K. S. (2007). Antimicrobial activities of Indian *Berberis* species. *Fitoterapia*, 78(7-8), 574-576.
- Singh, P., & Jain, S. (2010). Antidiabetic activity of *Berberis asiatica* (DC) roots. *International Journal of Pharmaceutical Sciences and Research*, 1, 109-112.
- Singh, S. K., Vishnoi, R., Dhingra, G. K., & Kishor, K. (2012). Antibacterial activity of leaf extracts of some selected traditional medicinal plants of Uttarakhand, North East India. *Journal of Applied and Natural Science*, 4(1), 47-50.
- Soudi, S. A., Nounou, M. I., Sheweita, S. A., Ghareeb, D. A., Younis, L. K., & El-Khordagui, L. K. (2019). Protective effect of surface-modified berberine nanoparticles against LPS-induced neurodegenerative changes: a preclinical study. *Drug Delivery and Translational Research*, 9(5), 906-919.
- Sun, S., Wang, K., Lei, H., Li, L., Tu, M., Zeng, S., ... & Jiang, H. (2014). Inhibition of organic cation transporter 2 and 3 may be involved in the mechanism of the antidepressant-like action of berberine. *Progress in Neuro-Psychopharmacology and Biological Psychiatry*, 49, 1-6.
- Swenson, E. S., & Curatolo, W. J. (1992). Intestinal permeability enhancement for proteins, peptides and other polar drugs: mechanisms and potential toxicity. *Advanced Drug Delivery Reviews*, 8(1), 39-92.
- Tan, X. S., Ma, J. Y., Feng, R., Ma, C., Chen, W. J., Sun, Y. P., ... & He, W. Y. (2013). Tissue distribution of berberine and its metabolites after oral administration in rats. *PLoS one*, 8(10), e77969.

- Tomosaka, H., Chin, Y. W., Salim, A. A., Keller, W. J., Chai, H., & Kinghorn, A. D. (2008). Antioxidant and cytoprotective compounds from *Berberis vulgaris* (barberry). *Phytotherapy Research*, 22(7), 979-981.
- Tsai, P. L., & Tsai, T. H. (2004). Hepatobiliary excretion of berberine. *Drug Metabolism and Disposition*, 32(4), 405-412.
- Villinski, J., Dumas, E., Chai, H. B., Pezzuto, J., Angerhofer, C., & Gafner, S. (2003). Antibacterial activity and alkaloid content of *Berberis thunbergii*, *Berberis vulgaris* and *Hydrastis canadensis*. *Pharmaceutical Biology*, 41(8), 551-557.
- Wang, K., Feng, X., Chai, L., Cao, S., & Qiu, F. (2017). The metabolism of berberine and its contribution to the pharmacological effects. *Drug Metabolism Reviews*, 49(2), 139-157.
- Wang, T., Wang, N., Song, H., Xi, X., Wang, J., Hao, A., & Li, T. (2011). Preparation of an anhydrous reverse micelle delivery system to enhance oral bioavailability and anti-diabetic efficacy of berberine. *European Journal of Pharmaceutical Sciences*, 44(1-2), 127-135.
- Wang, X., Wang, R., Xing, D., Su, H., Ma, C., Ding, Y., & Du, L. (2005). Kinetic difference of berberine between hippocampus and plasma in rat after intravenous administration of *Coptidis rhizoma* extract. *Life Sciences*, 77(24), 3058-3067.
- Wang, X., Xing, D., Wang, W., Su, H., Tao, J., & Du, L. (2005). Pharmacokinetics of berberine in rat thalamus after intravenous administration of *Coptidis rhizoma* extract. *The American Journal of Chinese Medicine*, 33(06), 935-943.
- Wei, W., Zhao, H., Wang, A., Sui, M., Liang, K., Deng, H., ... & Guan, Y. (2012). A clinical study on the short-term effect of berberine in comparison to metformin on the metabolic characteristics of women with polycystic ovary syndrome. *European Journal of Endocrinology*, 166(1), 99.
- Sun, H. W., & OUYANG, W. Q. (2007). The preparation and antibacterial activity in vitro of berberine hydrochloric nanometer microemulsion. *Journal of Northwest A & F University (Natural Science Edition)*, 1.
- Xiao, L., Xue, Y., Zhang, C., Wang, L., Lin, Y., & Pan, G. (2018). The involvement of multidrug and toxin extrusion protein 1 in the distribution and excretion of berberine. *Xenobiotica*, 48(3), 314-323.
- Xiong, W., Sang, W., Linghu, K. G., Zhong, Z. F., San Cheang, W., Li, J., ... & Wang, Y. T. (2018). Dual-functional Brij-S20-modified nanocrystal formulation enhances the intestinal transport and oral bioavailability of berberine. *International Journal of Nanomedicine*, 13, 3781.
- Xue, M., Yang, M. X., Zhang, W., Li, X. M., Gao, D. H., Ou, Z. M., ... & Yang, S. Y. (2013). Characterization, pharmacokinetics, and hypoglycemic effect of berberine loaded solid lipid nanoparticles. *International Journal of Nanomedicine*, 8, 4677.
- Yi, L., Jian-Ping, G., Xu, X., & Lixin, D. (2006). Simultaneous determination of baicalin, rhein and berberine in rat plasma by column-switching high-performance liquid chromatography. *Journal of Chromatography B*, 838(1), 50-55.
- Yin, J., Hou, Y., Yin, Y., & Song, X. (2017). Selenium-coated nanostructured lipid carriers used for oral delivery of berberine to accomplish a synergic hypoglycemic effect. *International Journal of Nanomedicine*, 12, 8671.
- Yogesh, H. S., Chandrashekar, V. M., Katti, H. R., Ganapaty, S., Raghavendra, H. L., Gowda, G. K., & Gopalkrishna, B. (2011). Anti-osteoporotic activity of aqueous-methanol extract of *Berberis aristata* in ovariectomized rats. *Journal of Ethnopharmacology*, 134(2), 334-338.
- Yu, F., Ao, M., Zheng, X., Li, N., Xia, J., Li, Y., ... & Chen, X. D. (2017). PEG-lipid-PLGA hybrid nanoparticles loaded with berberine-phospholipid complex to facilitate the oral delivery efficiency. *Drug Delivery*, 24(1), 825-833.
- Yu, H. H., Kim, K. J., Cha, J. D., Kim, H. K., Lee, Y. E., Choi, N. Y., & You, Y. O. (2005). Antimicrobial activity of berberine alone and in combination with ampicillin or oxacillin against methicillin-resistant *Staphylococcus aureus*. *Journal of Medicinal Food*, 8(4), 454-461.
- Zhang, C. R., Schutski, R. E., & Nair, M. G. (2013). Antioxidant and anti-inflammatory compounds in the popular landscape plant *Berberis thunbergii* var. *atropurpurea*. *Natural Product Communications*, 8(2), 1934578X1300800207.
- Zhang, H., Wei, J., Xue, R., Wu, J. D., Zhao, W., Wang, Z. Z., ... & Pan, H. N. (2010). Berberine lowers blood glucose in type 2 diabetes mellitus patients through increasing insulin receptor expression. *Metabolism*, 59(2), 285-292.
- Zhang, Y., Wang, X., Sha, S., Liang, S., Zhao, L., Liu, L., ... & Wu, K. (2012a). Berberine increases the expression of NHE3 and AQP4 in sennosideA-induced diarrhoea model. *Fitoterapia*, 83(6), 1014-1022.
- Zhang, Q., Qian, Z., Pan, L., Li, H., & Zhu, H. (2012b). Hypoxia-inducible factor 1 mediates the anti-apoptosis of berberine in neurons during hypoxia/ischemia. *Acta Physiologica Hungarica*, 99(3), 311-323.
- Zhao, Y., Collier, J. J., Huang, E. C., & Whelan, J. (2014). Turmeric and Chinese goldthread synergistically inhibit prostate cancer cell proliferation and NF- κ B signaling. *Functional Foods in Health and Disease*, 4(7), 312-339.
- Zhu, J. X., Tang, D., Feng, L., Zheng, Z. G., Wang, R. S., Wu, A. G., ... & Zhu, Q. (2013). Development of self-microemulsifying drug delivery system for oral bioavailability enhancement of berberine hydrochloride. *Drug Development and Industrial Pharmacy*, 39(3), 499-506.

Evaluation of toxic effects of statins and their possible role in treatment of cancer

Aysun Ökçesiz¹ , Ülkü Ündeğer Bucurgat² 

¹Erciyes University, Faculty of Pharmacy Department of Toxicology, Kayseri, Turkey

²Hacettepe University, Faculty of Pharmacy Department of Toxicology, Ankara, Turkey

ORCID IDs of the authors: A.Ö. 0000-0001-9130-2853; Ü.Ü.B. 0000-0002-6692-0366

Cite this article as: Okcesiz, A., & Undeger Bucurgat, U. (2021). Evaluation of toxic effects of statins and their possible role in treatment of cancer. *Istanbul Journal of Pharmacy*, 51(1), 154-160.

ABSTRACT

Hydroxymethyl glutaryl CoA (HMG-CoA) reductase inhibitors (statins) are drugs that show hypolipidemic effect via inhibition of hydroxymethyl glutaryl CoA reductase (HMG CoA R), a rate-limiting step in the synthesis of cholesterol. The effects of statins, independent of lipid-lowering ones, are termed pleiotropic effects and these have gained importance in recent years. Potential anticancer effect, one of the pleiotropic effects of statins, is remarkable. In this review we aim to summarize the possible use of statins in the treatment of cancer. Pleiotropic effects include antioxidant and antiinflammatory activities due to inhibition of new vessel formation in cancer cells, reduction of resistance to chemotherapeutic agents and inhibition of the production of reactive oxygen species (ROS) with the induction of apoptosis. The potential anticancer activity of statins against different tumor models is emphasized *in vitro* and *in vivo* conditions. For this reason, current efforts are directed to providing therapeutic benefits from statins in the treatment of cancer. This study shows that statins can be effective in preclinical models in advanced or recurrent metastatic diseases when administered alone or in combination with molecularly targeted agents. Future studies may shed further light on this topic.

Keywords: Cancer, statin, toxicity

INTRODUCTION

Statins are the first choice of drugs in the treatment of cardiovascular diseases and have been used in clinical practice for a long time (Bedi, Dhawan, Sharma, & Kumar, 2016; Sodero & Barrantes, 2020). Statins have been prescribed effectively and extensively for the therapy of hypercholesterolemia. Examples of the effects of statins are atheroma plaque stabilization, improvement in endothelial dysfunction, decrease in platelet aggregation and anti-inflammatory effects regardless of their antilipidemic effects. Statins are therefore used for primary and secondary prevention of cardiovascular diseases (Sabuncu et al., 2016). Several statins have more recently begun to be used, including atorvastatin, fluvastatin, lovastatin, pitavastatin, pravastatin, rosuvastatin and simvastatin (Shuhaili, Samsudin, Stanslas, Hasan, & Thambiah, 2017). As with many drugs, statins have side effects. The most important of these appear to be the variability of liver enzymes and muscle-related complaints which may occur from myalgia to severe fatal rhabdomyolysis. When these side effects are investigated, the underlying molecular mechanism which is seen is that of mitochondrial damage due to the depletion of ubiquinone. Although genetic factors play a part in the development of side effects of these well-tolerated drugs, they are largely dose-dependent. Therefore, clinicians need to be more careful in this regard (Margaritis, Channon, & Antoniadis, 2014; Shuhaili et al., 2017). Statins are drugs that show hypolipidemic effects by inhibition of the hydroxymethyl glutaryl CoA reductase (HMG CoA R) enzyme, which is the rate-limiting step in mevalonate pathway (Crescencio et al., 2009; Margaritis et al., 2014). The mevalonate pathway is closely related to the formation and pro-

Address for Correspondence:

Ülkü ÜNDEĞER BUCURGAT, e-mail: uundeger@hacettepe.edu.tr

This work is licensed under a Creative Commons Attribution 4.0 International License.



Submitted: 20.01.2020
Revision Requested: 26.06.2020
Last Revision Received: 19.07.2020
Accepted: 04.09.2020

gression of cancer, as it is responsible for cholesterol synthesis and protein prenylation (Gruenbacher & Thurnher, 2015). The end products of this pathway, such as cholesterol, dolichol, and ubiquinone, are vital. Also, cell functions are significantly affected by inhibition of mevalonate synthesis (Osmak, 2012). Statins inhibit the mevalonate synthesis step which is shown in (Figure 1) (Osmak, 2012; Margaritis et al., 2014). The end products of this pathway cannot be formed, thereby stopping the production of sterols, which are essential cholesterol for membrane integrity, as well as blocking isoprenylation of basic oncoproteins regulating proliferation, migration, invasion, cell cycle, cell proliferation and cell fate (Osmak, 2012; Pisanti, Ciaglia, & D'Alessandro, 2014).

In this way, statins have become a promising drug group in cancer treatment since they reduce both cholesterol and isoprenoid levels in the blood. Numerous data have shown that the probable anticancer mechanisms of statins depend on many factors. The toxicity of statins is thought to be due to cell cycle arrest, inhibition of cell proliferation/angiogenesis and metastasis, promotion of apoptosis, or changes in molecular pathways. These changes may vary depending on the kind of cancer cell, the duration that these cells are exposed, and the type and dose of statin used (Gauthaman, Fong, & Bongso, 2009; Matusiewicz, Meissner, Toporkiewicz, & Sikorski, 2015). Although significant anticancer effects have been observed in all statins, the available data propose that there are some differences in the antitumor effects of each statin derivative. Besides, statins have shown differences in pharmacokinetics, potency, and therapeutic efficacy.

Physical & chemical properties and toxicokinetics

Aspects that increase statin concentrations (e.g drug-drug interactions) may raise the risk of adverse effects. These interactions rely on the pharmacokinetic properties of statins: simvastatin, lovastatin, and atorvastatin are metabolized via cytochrome P450 (CYP) 3A, but others are metabolized independently of this pathway (Ho & Walker, 2012). Statins are excreted in feces, urine, bile or through renal clearances in the form of metabolites or unchanged (Çetin & Özgüneş, 2017). From a pharmacological perspective, statins are hypolipidemic drugs with inhibition of hydroxymethyl glutaryl CoA reductase (HMG CoA R), a rate-limiting step in cholesterol synthesis (Stancu & Sima, 2001).

These drugs are divided into two classes: hydrophilic and lipophilic. The lipophilicity of statins enables them to access different tissues. More lipophilic statins get higher levels of exposure in non-hepatic tissues, whereas hydrophilic statins are more hepatoselective. Thus, different effects of statins in hepatic and nonhepatic tissues can be predicted (Kato et al., 2010).

The pharmacokinetics of statins alter depending on their hydrophilic or lipophilic properties and appropriate membrane carriers. Hydrophilic statins have been shown to initially accumulate in the liver where they are taken up by the organic anion-bearing polypeptide OATP1B1, which is one of the membrane carriers. OATP1B1 is also the most important carrier of lipophilic character pitavastatin uptake. Hydrophilic pravastatin and rosuvastatin undergo little metabolism through cytochromes and are commonly excreted unchanged (Matusiewicz et al., 2015). The pharmacologic properties of statins are shown below in (Table 1) (Wong, Dimitroulakos, & Minden, 2002).

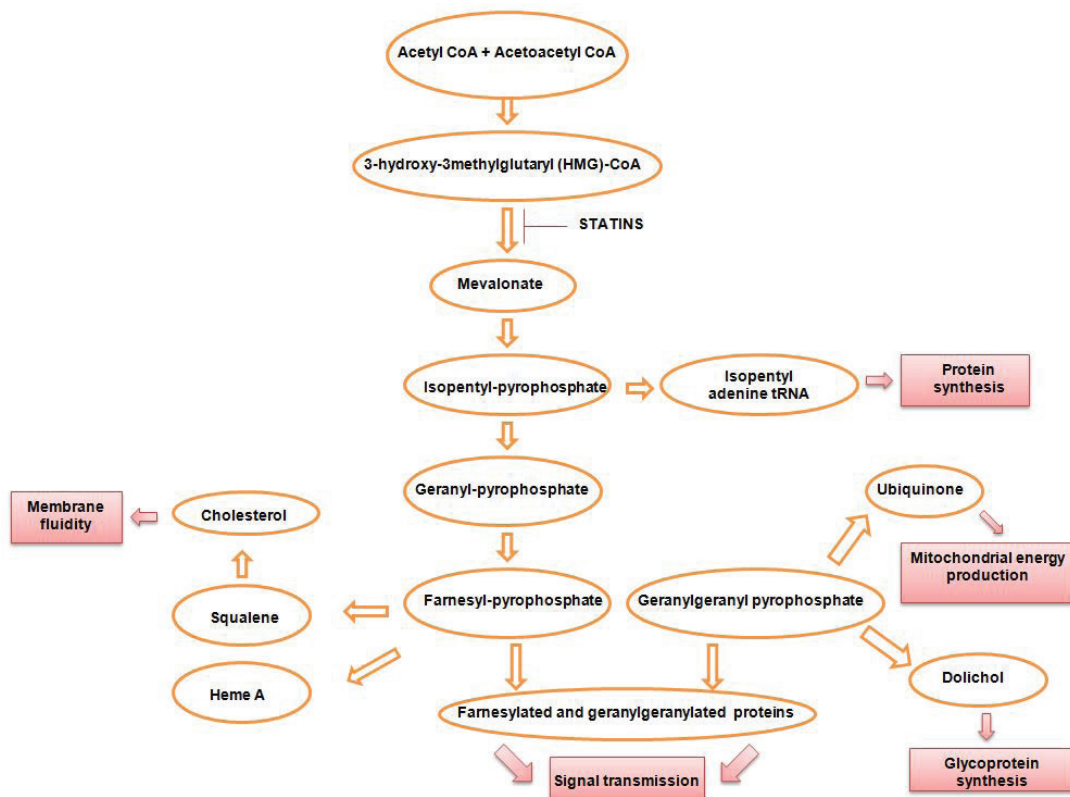


Figure 1. Statins inhibit the mevalonate synthesis step.

Table 1. Pharmacologic properties of statins.

Statins	Features				
	Lipophilicity	Structure	Source	Metabolism via cytochrome system	Daily Dose for Cholesterol Treatment (mg/day)
Lovastatin	+	Lactone	Fungal	CYP3A4	20-80
Simvastatin	+	Lactone	Fungal	CYP3A4	10-80
Pravastatin	-	Acid	Fungal	Minimum	10-40
Fluvastatin	+	Acid	Synthetic	CYP2C9, CYP2D6	20-80
Atorvastatin	+	Acid	Synthetic	CYP3A4	10-80
Rosuvastatin	-	Acid	Synthetic	CYP2C9, CYP2C19	5-80
Pitavastatin	+	Acid	Synthetic	CYP2C9, CYP2C18	4

It is known that there is no significant difference between the activities of fungal or synthetic statins. It should also be noted that lipophilic statins are substantially more effective than hydrophilic ones (Matuszewicz et al., 2015).

Effects on cell cycle

Cell homeostasis depends on the balance between cell proliferation and death. (Vermeulen, Berneman, & Van Bockstaele, 2003). The complex process involving cell growth and proliferation, organism development, DNA damage and repair, tissue hyperplasia in response to damage, and diseases is called cell cycle. It is also defined as the interval between two successive mitotic divisions to reveal two cells. (Schafer, 1998; Vermeulen, Van Bockstaele, Berneman, 2003). The cell cycle is conventionally divided into two stages; interphase and mitosis. Interphase includes G₀, G₁, Synthesis phase (S) and G₂ phases. (Gap=G) (Vermeulen, Berneman, & Van Bockstaele, 2003; Foster, 2008). The G₁ phase is the stage in which preparations are made for the division of the cell by metabolic changes. At this stage growth in size of the cell occurs. DNA synthesis occurs in the S phase, and in the G₂ phase, it is the period when rapid cell growth occurs and becomes ready for mitosis. Mitosis and cytokinesis occur in the mitotic (M) phase. This cycle is provided by critical checkpoints such as the G-S, G-M and the metaphase anaphase checkpoints. The cell cycle progression is regulated by several families of proteins known as cyclins (Fan, Sanyal, & Bruzzone, 2018). *In vitro* studies have shown that statins arrest cells by affecting these proteins that regulate the cell cycle. (Matuszewicz et al., 2015). Cell cycle arrest is caused in G₁/S and G₂/M by the effect of statins on the expression of these proteins (Ahmadi et al., 2020).

There are numerous studies about this subject on the statin family. One such study evaluated the potential anticancer effect of fluvastatin in three hepatocellular cancer cell lines. (Zhang, Wu, Zhou, Xie, & Zheng, 2010). Fluvastatin was observed to induce apoptosis in a dose-dependent manner and to inhibit cell proliferation by stopping the cell cycle in the G₂/M phase. As a result of the study, it was shown that fluvastatin significantly reduced the invasion potency of these cells. In another study on fluvastatin, cell cycle progression in the cervical cancer cell line was performed by flow cytometry (Campos-Lara & Mendoza-Espinoza, 2011). A moderate G₁

phase arrest was observed with 48 hours of exposure to these cells with a significant decrease in the S phase percentage compared to the control. Furthermore, a significant increase in the percentage of apoptotic cells was observed. In another study on cell cycle analysis of embryonal carcinoma, ovarian cancer and colorectal cancer cells which had been exposed to simvastatin, lovastatin or mevastatin for 48 hours showed a decrease in the number of cells, such as the decrease in S phase compared to control groups (Gauthaman, Richards, Wong, & Bongso, 2007). The presence of small peaks in the sub G₁ phase indicating apoptosis was significant in these three cell lines exposed with simvastatin and lovastatin. In another study, researchers emphasized that the antiproliferative effect caused by statins may be related to the increase in the percentage of cells in the G₁ and G₂/M phases in the cell cycle (Sánchez et al., 2008). Fluvastatin, simvastatin, and atorvastatin inhibited breast cancer cell proliferation. It has been reported that antiproliferation is related to a decrease in DNA synthesis and a cell cycle arrest in the G₁ and G₂/M phases, and that fluvastatin leads to a decrease in mitochondrial membrane potential. Another test was conducted to discover whether pitavastatin has an anticancer effect on the glioblastoma cell line (Jiang et al., 2014). The effects of statins on cell cycle in tumor cells were analyzed and shown to inhibit G₁ / S growth in glioblastoma and breast cancer cell lines. Pitavastatin was shown to trigger the cell cycle 12 hours after treatment, and tumor cells in the S phase were significantly reduced, while the cell population in the G₀ / G₁ phase increased. It was also reported in this study that a high dose of pitavastatin was not able to inhibit tumor growth significantly in the glioblastoma cell line when oral gavage was administered to mice. As shown in the said study, it is important to optimize the dosage and modification of the formulation in the use of statins for anti-cancer therapy.

Anticancer effect

Cancer is a disease caused by uncontrolled division and proliferation of cells under the influence of genetic and environmental conditions. There are more than 100 types of known cancer. Cancer is a personal dependent disease, although standard approaches have been developed for certain types of cancer. Today, in addition to existing treatments, new meth-

ods continue to be developed with the advance of technology (Baykara, 2016). Statins are well tolerated despite their side effects. With the support of epidemiological studies and clinical data in the last 20 years, it has been emphasized that statins may play an important role in the prevention and treatment of cancer. The anticancer effect that statins can produce has not yet been fully understood. The possible anticancer effect of statins depends largely on the type of tumor and type of statin (De Wolf, De Wolf & Richardson, 2018). Studies evaluating the cytotoxic effects of many drugs in the statin family in the liver, skin, colon, pancreas and ovarian cancer cells are included in the literature, and in these studies it was found that the combination of statins with chemotherapeutic drugs in multiple drug resistance tumor cells was effective in overcoming drug resistance (You et al., 2016; Villarino et al., 2017; Yasui et al., 2007; Zhang, Zheng, Yang, Yang, & Yuan, 2017; De Wolf et al., 2018). The use of statins as anticancer drugs or as adjuvant combined with conventional chemotherapeutic drugs has been proven (Pisanti et al., 2014). Some studies have shown that co-administration of statins and antineoplastics causes synergistic cytotoxicity (De Wolf, et al., 2018; Al-Qatati, & Aliwaini, 2017). A group of scientists demonstrated that when fluvastatin, a lipophilic statin, and cisplatin were administered together synergistic cytotoxicity occurred. Combined treatment of fluvastatin and cisplatin compared to a drug administration alone led to significantly more inhibition of cell proliferation (Taylor-Harding, Orsulic, Karlan, & Li, 2010).

It seems to be useful to understand the link between statins and the inhibition of cell proliferation to suggest new approaches in cancer treatment. The data obtained in the light of the studies supported the finding that high concentration and accumulation of statins in plasma and tumors will provide significant benefit to their anticancer effect (Jiang et al., 2014). Data are demonstrating that statins arrest the cell cycle in healthy cells and cancer cells at certain stages and stimulate cell death. Cell death is closely related to oxidative stress and the formation of reactive oxygen species (ROS) because these formations seriously damage vital macromolecules such as lipids, proteins, and nucleic acids. It is known that the resulting ROS and oxidative stress can damage cellular DNA, oxidize specified macromolecules, and inactivate certain enzymes and their cofactors. Oxidation leads to loss of biological properties and ultimately cell death (Sánchez et al., 2008; Tong, Chuang, Wu, & Zuo, 2015). It has been stated that statins can also contribute to cell damage by causing increased ROS production within the cell. It is considered that statins cause mitochondrial dysfunction and this results in an increase in ROS production (Li, et al., 2019).

In a study investigating the effects of statins on human breast adenocarcinoma cell line (MCF-7), cell death, production of ROS and mitochondrial membrane potential were observed. Statins have been shown to provoke both apoptosis and necrotic cell death. To determine whether statin-induced cell death is based on oxidative stress, researchers studied breast cancer cells with statins and N-acetyl cysteine, a potent antioxidant. At the end of the said study, N-acetyl cysteine was shown to stop statin-induced cell death. Researchers also

noted that cell death caused by statins in MCF-7 cells was due to oxidative stress. It was emphasized that the administration of statins alone or in combination with antineoplastic agents such as doxorubicin or cisplatin may be an effective alternative in the therapy of breast cancer (Sánchez et al., 2008). There are currently more than 30 ongoing clinical trials, but there is insufficient information on the use of statins in cancer treatment (Gu, Saha, Thomas, & Kaur, 2019). Most clinical studies on statins have shown that no significant results have been achieved for the treatment of many types of cancer. Although statins with antiproliferative effects have been made with interest in *in vitro* and *in vivo* studies on breast cancer, one study reported that statins did not yield the expected results and these results were not clear (May & Glode, 2016).

Another essential mechanism that causes cell death is thought to occur through the mevalonate pathway. In this way, statins inhibit cholesterol synthesis and many molecules, for example, coenzyme Q10 (CoQ10). CoQ10 is one of the electron transport chain components known as ubiquinones. CoQ10 plays a role in the production of adenosine triphosphate (ATP) energy. Therefore, the decrease in the concentration of CoQ10 is an important issue observed especially in the regulation of mitochondrial dysfunction. Studies have shown that statins may lead to a reduction in ATP production due to the effect on CoQ10, and this effect can cause cytotoxicity (Berber, Celik, & Aksoy, 2014).

In a study of colon cancer stem cells and *in vivo* mouse tumor xenografts, a group of researchers concluded that pitavastatin inhibits these stem cells and induces cell apoptosis. In that study, it was determined that pitavastatin inhibits the growth of mouse tumor xenografts and pitavastatin has a potential role in inhibiting the proliferation of stem cells in colon carcinoma (Zhang et al., 2017).

In another study suggesting that statins have a positive effect on liver cancer, a group of scientists reported that statin use causes a 40% reduction in liver cancer risk, regardless of their exposure time, according to a meta-analysis. It was also reported that this use was inversely proportional to the risk of liver cancer (Pradelli et al., 2013). In another study, the effect of fluvastatin in the statin family on pediatric tumor treatment was explored. The patients who were due to undergo metronomic chemotherapy with thalidomide were treated with fluvastatin, carboplatin and vincristine. In that study, it was observed that the survival of pediatric patients was significantly increased in the treatment with fluvastatin and thalidomide-related carboplatin, and vincristine. It was emphasized that there was a significant decrease in tumor volume in patients with increased quality of life (López-Aguilar et al., 2008).

Numerous human clinical trials have demonstrated the anticancer effects of statins. The overall evaluation of these studies showed that the combination of statins with other agents yielded more promising results than the trials performed alone. It is clear that further studies are needed to investigate and confirm potential synergies in these combined therapies (Chae et al., 2015).

Antioxidant / oxidant effect

It is known that statins used for hypolipidemic purposes are also used in the antioxidant aspect of cardiovascular diseases by reducing oxidative stress. Many studies conducted with *in vitro* and *in vivo* models support the use of statins as protective agents in cardiac disorders by reducing ROS production. However, the effect of statins on oxidative stress varies in different tissues and organs (Liu et al., 2019). Oxidative stress is increasingly recognized as a significant cause of cancer (Schupp, Schmid, Heidland, & Stopper, 2008). In many studies, one of the mechanisms underlying statin-induced toxicity is thought to be due to oxidative stress. Lack of antioxidant defense or the overproduction of free radicals is known to cause oxidative stress (Liu et al., 2019). One of the studies that analyzed the relationship between statins and oxidative stress, showed that statins increased ROS production in freshly isolated rat hepatocytes. In the said study, researchers investigated the effect of three different statins on the cell using different concentrations. They reported an increase in lipid peroxidation in addition to ROS formation after statin administration. They observed that there was also an increase in cellular mitochondrial membrane potential. Additionally, it was shown that L-carnitine administration could be evaluated as a preventive agent by causing a decrease in these statin-induced toxicity markers (Abdoli, Azarmi, & Eghbal, 2015). Similar studies have been recorded in *in vitro* studies confirming that increased oxidative stress is caused by statins as observed in this study. A group of researchers set out to clarify the role of oxidative stress in simvastatin cytotoxicity in murine colon carcinoma and melanoma cells and they demonstrated that simvastatin induced cell death by increasing intracellular oxidative damage and promoting apoptosis (Qi et al., 2010).

Genotoxic effect

One of the most important targets of oxidative attacks is known to be DNA. It is known that if repair mechanisms cannot eliminate oxidative DNA damage, sequencing may occur in cells, including age-related functions and subsequent development of malignancy. Therefore, the effects of statins on DNA are important (Schupp et al., 2008). There are several studies about the genotoxic/antigenotoxic effects of statins. Potential genotoxic effects of statins were evaluated in *in vivo* and *in vitro* mutagenicity experiments. As an example of these studies a group of researchers observed the genotoxic potential of lovastatin examined by comet assay and repaired DNA fractures caused by doxorubicin (Damrot et al., 2006). In this study, they showed that the resistance to topoisomerase II inhibitors causes a reduction in DNA damage with lovastatin. This could be clinically useful to relieve the side effects of anticancer drugs. The possible genotoxic effect of atorvastatin, a lipophilic statin such as lovastatin on human lymphocytes was investigated by comet, chromosome aberration, and sister chromatite exchange assays (Gajski & Garaj-Vrhovac, 2007). According to the results, it was noted that human lymphocytes exposed to atorvastatin showed more genotoxic damage compared to the control for all three methods used, and statistically significant results were obtained. In the comet assay, DNA damage in human lymphocytes exposed to atorvastatin was shown to be higher than in the control

cells at 24, 48 and 72 hours of exposure time for tail length, whereas the damage at 72 hours exposure time was higher for the tail moment compared to the control cells. Another group investigated the possible genotoxic effects of atorvastatin in human lymphocytes in *in vitro* conditions at 6, 24 and 48 hours exposure times (Gajski, Garaj-Vrhovac & Oreščanin, 2008). In the study, it was determined that the DNA damage caused by atorvastatin is due to oxidative stress measured by formamidopyrimidine DNA glycosylase (fpg)-modified comet assay. In addition, the researchers observed basal DNA damage in the results of the standard comet assay. Due to this determination, they emphasized that the genotoxic effect was not only due to oxidative stress, but also to other mechanisms of genotoxicity which may be involved. In another study on human lymphocytes, the genotoxic potential of rosuvastatin was evaluated by the micronucleus test, chromosome aberration, and comet assay (Gajski et al., 2008). The frequency of chromosomal aberration was shown to increase at 24 and 48 hours of exposure time and showed a significant increase in stimulation of micronucleus formation compared to the negative control. In the comet assay, tail length, tail moment and tail intensity were evaluated, and it was reported that the tail intensity increased significantly at all concentrations except one (0.0625 µg/mL). The researchers showed that rosuvastatin has cytotoxic and genotoxic potential in human lymphocyte cells. It was also recommended that patients treated with this drug should be monitored.

CONCLUSION

Some studies highlight the anticancer aspect of statins in various cancer types. According to the above studies statins have been suggested as a genotoxic agent by using standard and fpg-modified alkaline comet assay, micronucleus test, chromosome aberration, and sister chromatite exchange assays. The difference between comet parameters in the presence and absence of the fpg enzyme suggested that the DNA damage caused by statins is mediated by oxidative stress. It was emphasized that detailed studies should be carried out in mammalian systems.

The results from the studies emphasize that statins can be used alone, and there are also possible combination therapies with standard chemotherapeutics. Accordingly, in order to get benefit from cancer treatment from statins, the type of statin, dose, duration of exposure, and the type of cancer to be treated are very important. Further studies to clarify the status of statins in cancer treatment are crucial.

Peer-review: Externally peer-reviewed.

Author Contributions: Conception/Design of Study- A.Ö., B.Ü.B.; Data Acquisition- A.Ö., B.Ü.B.; Data Analysis/Interpretation- A.Ö., B.Ü.B.; Drafting Manuscript- A.Ö., B.Ü.B.; Critical Revision of Manuscript- A.Ö., B.Ü.B.; Final Approval and Accountability- A.Ö., B.Ü.B.

Conflict of Interest: The authors have no conflict of interest to declare.

Financial Disclosure: Authors declared no financial support.

REFERENCES

- Abdoli, N., Azarmi, Y., & Eghbal, M. A. (2015). Mitigation of statins-induced cytotoxicity and mitochondrial dysfunction by L-carnitine in freshly-isolated rat hepatocytes. *Research in Pharmaceutical Sciences*, 10(2), 143–151.
- Ahmadi, M., Amiri, S., Pecic, S., Machaj, F., Rosik, J., Łos, M. J., ... & Shojaei, S. (2020). Pleiotropic effects of statins: a focus on cancer. *Biochimica et Biophysica Acta (BBA)-Molecular Basis of Disease*, 1866(12):165968.
- Al-Qatati, A., & Aliwaini, S. (2017). Combined pitavastatin and dactarbazine treatment activates apoptosis and autophagy resulting in synergistic cytotoxicity in melanoma cells. *Oncology letters*, 14(6):7993-7999.
- Baykara, O. (2016). Kanser tedavisinde güncel yaklaşımlar [Current modalities in treatment of cancer]. *Balikesir Sağlık Bilimleri Dergisi*, 5(3), 154-165.
- Bedi, O., Dhawan, V., Sharma, P. L., & Kumar, P. (2016). Pleiotropic effects of statins: new therapeutic targets in drug design. *Naunyn-Schmiedeberg's archives of pharmacology*, 389(7), 695-712.
- Berber, A. A., Celik, M., & Aksoy, H. (2014). Genotoxicity evaluation of HMG CoA reductase inhibitor rosuvastatin. *Drug and chemical toxicology*, 37(3), 316-321.
- Campos-Lara, M., & Mendoza-Espinoza, J. A. (2011). Cytotoxic evaluation of fluvastatin and rosuvastatin and effect of fluvastatin in the hela cell cycle. *African Journal of Pharmacy and Pharmacology*, 5(2), 189-193.
- Chae, Y. K., Yousaf, M., Malecek, M. K., Carneiro, B., Chandra, S., Kaplan, J., ... & Giles, F. (2015). Statins as anti-cancer therapy; Can we translate preclinical and epidemiologic data into clinical benefit?. *Discovery medicine*, 20(112), 413-427. Retrieved from <https://www.discoverymedicine.com>
- Crescencio, M. E., Rodríguez, E., Páez, A., Masso, F. A., Montaña, L. F., & López-Marure, R. (2009). Statins inhibit the proliferation and induce cell death of human papilloma virus positive and negative cervical cancer cells. *International journal of biomedical science: IJBS*, 5(4), 411-420.
- Çetin, T., & Özgüneş, H. (2017). Statinlerin Toksikolojik Açından Değerlendirilmesi [Toxicological evaluation of statins]. *Hacettepe Üniversitesi Eczacılık Fakültesi Dergisi*, (1), 18-28.
- Damrot, J., Nübel, T., Epe, B., Roos, W. P., Kaina, B., & Fritz, G. (2006). Lovastatin protects human endothelial cells from the genotoxic and cytotoxic effects of the anticancer drugs doxorubicin and etoposide. *British journal of pharmacology*, 149(8), 988-997.
- De Wolf, E., De Wolf, C., & Richardson, A. (2018). ABT-737 and picilisib synergistically enhance pitavastatin-induced apoptosis in ovarian cancer cells. *Oncology letters*, 15(2), 1979-1984.
- Fan, Y., Sanyal, S., & Bruzzone, R. (2018). Breaking bad: how viruses subvert the cell cycle. *Frontiers in cellular and infection microbiology*, 8, 396.
- Foster, I. (2008). Cancer: A cell cycle defect. *Radiography*, 14(2), 144-149.
- Gajski, G., & Garaj-Vrhovac, V. (2007). Application of cytogenetic endpoints and comet assay on human lymphocytes treated with atorvastatin in vitro. *Journal of Environmental Science and Health, Part A*, 43(1), 78-85.
- Gajski, G., Garaj-Vrhovac, V., & Oreščanin, V. (2008). Cytogenetic status and oxidative DNA-damage induced by atorvastatin in human peripheral blood lymphocytes: standard and Fpg-modified comet assay. *Toxicology and applied pharmacology*, 231(1), 85-93.
- Gauthaman, K., Fong, C. Y., & Bongso, A. (2009). Statins, stem cells, and cancer. *Journal of cellular biochemistry*, 106(6), 975-983.
- Gauthaman, K., Richards, M., Wong, J., & Bongso, A. (2007). Comparative evaluation of the effects of statins on human stem and cancer cells in vitro. *Reproductive biomedicine online*, 15(5), 566-581.
- Gruenbacher, G., & Thurnher, M. (2015). Mevalonate metabolism in cancer. *Cancer letters*, 356(2), 192-196.
- Gu, L., Saha, S. T., Thomas, J., & Kaur, M. (2019). Targeting cellular cholesterol for anticancer therapy. *The FEBS journal*, 286(21), 4192-4208.
- Internet source 1. U.S. National Library of Medicine. (2020, October 16). Pitavastatin: Human Toxicity Excerpts. Retrieved from <https://pubchem.ncbi.nlm.nih.gov/compound/5282452#section=Human-Toxicity-Excerpts>
- Jiang, P., Mukthavaram, R., Chao, Y., Nomura, N., Bharati, I. S., Fogal, V., ... & Kapoor, S. (2014). In vitro and in vivo anticancer effects of mevalonate pathway modulation on human cancer cells. *British journal of cancer*, 111(8), 1562-1571. <https://dx.doi.org/10.1038/bjc.2014.431>
- Ho, C. K., & Walker, S. W. (2012). Statins and their interactions with other lipid-modifying medications: safety issues in the elderly. *Therapeutic advances in drug safety*, 3(1), 35-46.
- Kato, S., Smalley, S., Sadarangani, A., Chen-Lin, K., Oliva, B., Branes, J., ... & Cuello, M. (2010). Lipophilic but not hydrophilic statins selectively induce cell death in gynaecological cancers expressing high levels of HMGCoA reductase. *Journal of cellular and molecular medicine*, 14(5), 1180-1193. <https://dx.doi.org/10.1111/j.1582-4934.2009.00771.x>
- Li, L. Z., Zhao, Z. M., Zhang, L., He, J., Zhang, T. F., Guo, J. B., ... & Peng, S. Q. (2019). Atorvastatin induces mitochondrial dysfunction and cell apoptosis in HepG2 cells via inhibition of the Nrf2 pathway. *Journal of Applied Toxicology*, 39(10), 1394-1404.
- Liu, A., Wu, Q., Guo, J., Ares, I., Rodríguez, J. L., Martínez-Larañaga, M. R., ... & Martínez, M. A. (2019). Statins: Adverse reactions, oxidative stress and metabolic interactions. *Pharmacology & therapeutics*, 195, 54-84. <https://dx.doi.org/10.1016/j.pharmthera.2018.10.004>
- López-Aguilar, E., Sepúlveda-Vildósola, A. C., Betanzos-Cabrera, Y., Rocha-Moreno, Y. G., Gascón-Lastiri, G., Rivera-Márquez, H., ... & de la Cruz-Yañez, H. (2008). Phase II study of metronomic chemotherapy with thalidomide, carboplatin-vincristine-fluvastatin in the treatment of brain stem tumors in children. *Archives of medical research*, 39(7), 655-662. <https://dx.doi.org/10.1016/j.arcmed.2008.05.008>
- Margaritis, M., Channon, K. M., & Antoniades, C. (2014). Statins as regulators of redox state in the vascular endothelium: beyond lipid lowering. *Antioxidants & redox signaling*, 20(8), 1198-1215.
- Matuszewicz, L., Meissner, J., Toporkiewicz, M., & Sikorski, A. F. (2015). The effect of statins on cancer cells. *Tumor Biology*, 36(7), 4889-4904.
- May, M. B., & Glode, A. (2016). Novel uses for lipid-lowering agents. *Journal of the advanced practitioner in oncology*, 7(2), 181-187.
- Osmak, M. (2012). Statins and cancer: current and future prospects. *Cancer letters*, 324(1), 1-12.
- Pisanti, S., Picardi, P., Ciaglia, E., D'Alessandro, A., & Bifulco, M. (2014). Novel prospects of statins as therapeutic agents in cancer. *Pharmacological research*, 88, 84-98.
- Pradelli, D., Soranna, D., Scotti, L., Zambon, A., Catapano, A., Mancina, G., ... & Corrao, G. (2013). Statins and primary liver cancer: a meta-analysis of observational studies. *European journal of cancer prevention*, 22(3), 229-234. <https://dx.doi.org/10.1097/CEJ.0b013e328358761a>
- Qi, X. F., Kim, D. H., Yoon, Y. S., Kim, S. K., Cai, D. Q., Teng, Y. C., ... & Lee, K. J. (2010). Involvement of oxidative stress in simvastatin-induced apoptosis of murine CT26 colon carcinoma cells. *Toxicology letters*, 199(3), 277-287. <https://dx.doi.org/10.1016/j.toxlet.2010.09.010>
- Sabuncu, T., Sönmez, A., Bayram, F., Cesur, M., Aydoğdu, A., İzol Torun, A. N. (2016). Lipid metabolizma bozuklukları tani ve tedavi kılavuzu [Guide to diagnosis and treatment of lipid metabolism disorders]. Ankara, Turkey: Miki Matbaacılık.

- Sánchez, C. A., Rodríguez, E., Varela, E., Zapata, E., Paez, A., Massó, F. A., ... & Lopez-Marure, R. (2008). Statin-induced inhibition of MCF-7 breast cancer cell proliferation is related to cell cycle arrest and apoptotic and necrotic cell death mediated by an enhanced oxidative stress. *Cancer investigation*, 26(7), 698-707. <https://dx.doi.org/10.1080/07357900701874658>
- Schafer, K. (1998). The cell cycle: a review. *Vet Pathol*, 35(6):461-478.
- Schupp, N., Schmid, U., Heidland, A., & Stopper, H. (2008). Rosuvastatin protects against oxidative stress and DNA damage in vitro via upregulation of glutathione synthesis. *Atherosclerosis*, 199(2), 278-287.
- Shuhaili, M. F. R. M. A., Samsudin, I. N., Johnson Stanslas, S. H., & Thambiah, S. C. (2017). Effects of different types of statins on lipid profile: a perspective on Asians. *International journal of endocrinology and metabolism*, 15(2), e43319.
- Sodero, A. O., & Barrantes, F. J. (2020). Pleiotropic effects of statins on brain cells. *Biochimica et Biophysica Acta (BBA)-Biomembranes*, 1862(9),183340.
- Stancu, C., & Sima, A. (2001). Statins: mechanism of action and effects. *Journal of cellular and molecular medicine*, 5(4), 378-387.
- Taylor-Harding, B., Orsulic, S., Karlan, B. Y., & Li, A. J. (2010). Fluvastatin and cisplatin demonstrate synergistic cytotoxicity in epithelial ovarian cancer cells. *Gynecologic oncology*, 119(3), 549-556.
- Tong, L., Chuang, C. C., Wu, S., & Zuo, L. (2015). Reactive oxygen species in redox cancer therapy. *Cancer letters*, 367(1), 18-25.
- Vermeulen, K., Berneman, Z. N., & Van Bockstaele, D. R. (2003). Cell cycle and apoptosis. *Cell proliferation*, 36(3), 165-175.
- Vermeulen, K., Van Bockstaele, D. R., & Berneman, Z. N. (2003). The cell cycle: a review of regulation, deregulation and therapeutic targets in cancer. *Cell proliferation*, 36(3), 131-149.
- Villarino, N., Signaevskaia, L., van Niekerk, J., Medal, R., Kim, H., Lahmy, R., ... & Itkin-Ansari, P. (2017). A screen for inducers of bHLH activity identifies pitavastatin as a regulator of p21, Rb phosphorylation and E2F target gene expression in pancreatic cancer. *Oncotarget*, 8(32), 53154. <https://dx.doi.org/10.18632/oncotarget.18587>
- Wong, W. W., Dimitroulakos, J., Minden, M. D., & Penn, L. Z. (2002). HMG-CoA reductase inhibitors and the malignant cell: the statin family of drugs as triggers of tumor-specific apoptosis. *Leukemia*, 16(4), 508-519.
- Yasui, Y., Suzuki, R., Miyamoto, S., Tsukamoto, T., Sugie, S., Kohno, H., & Tanaka, T. (2007). A lipophilic statin, pitavastatin, suppresses inflammation-associated mouse colon carcinogenesis. *International journal of cancer*, 121(10), 2331-2339.
- You, H. Y., Zhang, W. J., Xie, X. M., Zheng, Z. H., Zhu, H. L., & Jiang, F. Z. (2016). Pitavastatin suppressed liver cancer cells in vitro and in vivo. *OncoTargets and therapy*, 9, 5383-5388.
- Zhang, W., Wu, J., Zhou, L., Xie, H. Y., & Zheng, S. S. (2010). Fluvastatin, a lipophilic statin, induces apoptosis in human hepatocellular carcinoma cells through mitochondria-operated pathway. *Indian J Exp Biol*, 48(12), 1167-1174.
- Zhang, Z. Y., Zheng, S. H., Yang, W. G., Yang, C., & Yuan, W. T. (2017). Targeting colon cancer stem cells with novel blood cholesterol drug pitavastatin. *Eur Rev Med Pharmacol Sci*, 21(6), 1226-1233.